Mechanisms involved in chronic neuropathic pain after avulsion injury

Chew, Daniel John

Mechanisms involved in chronic neuropathic pain after avulsion injury

Daniel John Chew

Centre for Neuroscience and Trauma
Bart's and The London School of Medicine and Dentistry
Queen Mary University of London

A thesis submitted in accordance with the regulations for the degree of PhD.

March 2010

To my mother and sister,

and the memory of my father

Abstract

Motor vehicle accidents are the most common cause of injuries involving avulsion of spinal roots from the brachial or lumbosacral plexuses. This results in chronic intractable pain that is refractory to pharmacotherapy. This is largely due to lack of information on underlying mechanisms, and lack of an established animal model to test drug treatments.

This thesis has: 1) compared the neuroanatomical effects of dorsal root rhizotomy (DRR) and avulsion (DRA) in the spinal cord. DRR is commonly used to model avulsion injury but unlike avulsion it does not damage the spinal cord, as often happens clinically. 2) Developed a behavioural model of spinal root avulsion injury (SRA). 3) Evaluated the behavioural effects of drugs prescribed to treat neuropathic pain or those used clinically to treat other conditions like motoneuron disease or spinal cord injury.

DRA produced a greater and prolonged glial, inflammatory, vascular response and cell loss than DRR. SRA produced thermal and mechanical hypersensitivity in the affected hind-paw. Neurodegenerative and neuroinflammatory responses were observed in both the avulsed and adjacent spinal segments, but produced no changes in the neuronal phenotype adjacent dorsal root ganglion neurons, suggesting that the evoked behaviour is mediated by central mechanisms.

Administration of amitriptyline or carbamazepine reduced behavioural hypersensitivity in SRA, confirming their limited clinical efficacy in treatment of avulsion injury. Minocycline and riluzole produced therapeutic efficacy. Both compounds prevented the establishment of behavioural hypersensitivity, which correlated histologically with microglial inhibition, although riluzole was transiently effective. Additionally, minocycline reversed the hypersensitivity, an effect that persisted beyond drug wash-out, whereas riluzole had a limited effect that only lasted whilst the drug was administered.

This thesis provides insight into the mechanisms of avulsion-induced neuropathic pain. The establishment of a behaviourally reproducible avulsion model provides a platform to test new pharmacological candidates for treatment, such as minocycline.

Acknowledgements

The funding of this thesis was via a Nathalie Rose Barr PhD grant (NRB080) from the U.K. charitable organisation Spinal Research, to which I am indebted for their substantial financial and administrative support.

I am most grateful to my supervisors Dr Peter Shortland and Professor Thomas Carlstedt, for their ongoing support and constructive critique, and the opportunity to participate in this project.

I am grateful to the School of Medicine and Dentistry, and the Blizard Institute for Cellular and Molecular Sciences, at Bart's and The London, for providing excellent laboratory space and equipment necessary to undertake this work.

Abbreviations

ADAM	A disintegrin and metalloproteinase domain
Aif	Allograft inflammatory factor
ALS	Amyotrophic lateral sclerosis
AMPA	A-amino-3-hydroxyl-5-methyl-4-isoxazole-propionate
ART	Artemin
ATF3	Activating transcription factor
ATP	Adenosine Triphosphate
BDNF	Brain-derived neurotrophic factor
BSA	Bovine serum albumin
BSF2	Fetal bovine serum
CaMK	Calcium/calmodulin-dependent protein kinase
CCl/r	Cysteine-cysteine chemokine ligand/receptor
CCI	Chronic constriction injury
CGRP	Calcitonin gene-related peptide
ChAT	Choline acetyltransferase
CNS	Central nervous system
COX	Cyclo-oxygenase
contra	Contralateral (uninjured side)
CREB	cAMP response element-binding protein
CSPG	Chondroitin sulphate proteoglycan
CSF	Cerebrospinal fluid
CTB	Cholera toxin B subunit
CX3C1	Fractalkine
DAPI	4’,6-diamidino-2phenylindole
DH	Dorsal horn
DRA	Dorsal root avulsion
DREZ	Dorsal root entry zone
DRG	Dorsal root ganglion
DRR	Dorsal root rhizotomy
EAA (T)	Excitatory amino acid (transporter)
EAE	Experimental Autoimmune Encephalomyelitis
Ex Av	Extra avidin
ERK	Extracellular signal-regulated kinases
FACS	Fluorescence-activated cell-sorting
FITC	Fluorescein isothiocyanate
FNE	Free nerve ending
FRAP	Fluoride-resistant acid phosphatase
FSC	Forward scatter

GABA	Gamma-aminobutyric acid
GAP43	Growth associated protein 43
GDNF	Glial cell line-derived neurotrophic factor
GFAP	Glial fibrillary acidic protein
GLAST	Glutamate aspartate transporter
GLT	Glutamate transporter (rodent)
HCl	Hydrochloric acid
HIV	Human Immunodeficiency Virus
HSP	Heat-shock protein
HTM	High threshold mechanoreceptor
IB4	Isolectin B4
Iba1	Ionized calcium binding adaptor molecule 1
IFNγ	Interferon gamma
IL (12/6/1β)	Interleukin
ipsi	Ipsilateral (injured side)
KCC2	Chloride-cotransporter/potassium chloride exporter 2 channel
LTM	Low threshold mechanoreceptor
MAG	Myelin associated glycoprotein
MAPK	Mitogen-activated protein kinase
MCP	Monocyte chemoattractant protein
MHC	Major histocompatibility complex
MPO	myeloperoxidase
MMP	Matrix metalloproteinase
MPTP	1-methyl-4-phenyl-1,2,3,6-tetrahydropyridine (neurotoxin)
NADPH	Nicotinamide adenine dinucleotide phosphate
NDS/NGS	Normal donkey/goat serum
NeuN	Neuronal nuclei
NF200/N52/SMI32	Heavy neurofilament (200 kD)
NGF	Nerve growth factor
NK1	Neurokinin 1
NMDA	N-methyl-D-aspartic acid
NO (S)	Nitric Oxide (Synthase)
NPY	Neuropeptide Y
NT3	Neurotrophin 3
NTN	Neurturin
OEC	Olfactory ensheathing cell
OMgp	Oligodendrocyte-myelin glycoprotein
P2Xr (4/7)	Purinoreceptor (4 and 7)
PBS	Phosphate buffered saline
PECAM	Platelet endothelial cell adhesion molecule

PFA	Paraformaldehyde
PGE	Prostagladin E
PI	Propidium iodide
PKC	Protein kinase C
PNI	Peripheral nerve injury
PNS	Peripheral nervous system
RECA1	Rat endothelial cell antigen (1)
ROS	Reactive oxygen species
SCI	Spinal cord injury
SNT/L	Spinal nerve transection/ligation
SP	Substance P
SPRR1A	*Gene that encodes* Cornifin A protein
SRA	Spinal root avulsion
SSC	Sodium chloride-sodium citrate buffer/ Side scatter
STT	Spinothalamic tract
TCA	Tricyclic antidepressant
TNFα	Tumour necrosis factor alpha
TLR	Toll-like receptor
Tol Blue	Toluidine blue
TRITC	Tetramethyl rhodamine iso-thiocyanate
TRPV1	Transient receptor potential cation channel, family V, member 1
TTX	Tetrodotoxin
TUNEL	Terminal deoxynucleotidyl transferase dUTP nick end labelling
VEGF	Vascular endothelial growth factor
VGLUT	Vesicular glutamate transporter
VH	Ventral horn
VIP	Vasoactive intestinal peptide
VRA	Ventral root avulsion
VREZ	Ventral root entry zone
VRR	Ventral root rhizotomy
WGA-HRP	Wheat germ agglutinin-horseradish peroxidase

List of Figures and Tables

Contents

Chapter 1: General Introduction

1.1: The peripheral nerves

The mammalian nervous system comprises a central nervous system (CNS), consisting of the brain and spinal cord, and peripheral nervous system (PNS), consisting of nerves outside the CNS that make up the autonomic, and somatic nervous systems. The somatic nervous system is responsible for voluntary control of skeletal muscle through motor output via upper motor neurones, such as the corticospinal tract, which innervate lower motor neurones in the spinal ventral horn that innervate muscles. It also is responsible for sensory processing from the external and internal environment, through sensory receptors and afferent fibres in the periphery, with final projections to the spinal cord. This somatic sensory system consists of neuronal endings of mainly exteroceptors, which provide information on the external body's interaction within the environment, such as cutaneous, auditory, olfactory, vestibular, and vision modalities. Some neuronal endings are interoceptive, located in visceral tissue, providing information on internal homeostatic environments of organs, such as the mesentery and gut wall. Other sensory information includes proprioception that, unlike extero- and interoception, is an unconscious sensory feedback mechanism of muscles and joints enabling quick responses to body movement and position in the environment. (Brodal, 2004)

The transmission of sensory information from skin, muscle, joints, and viscera to the spinal cord involves a process of axon potential propagation via peripheral nerves. These fibres are referred to as afferents, as they convey information *from* the periphery *to* the CNS. They are coupled with non-neuronal cells called Schwann cells, which provide structural and nutrient support of peripheral nerves, influence conduction properties through their myelin sheath, and are essential for axon targeting and regeneration. The peripheral nerves of the cutaneous somatic nervous system consist of a transducing/receptive terminal in the dermis or epidermis, a nerve fibre that conducts action potentials centrally, a cell body in the dorsal root ganglion, and synaptic endings in the spinal cord. (Brodal, 2004)

Peripheral nerves supply specific areas of skin called dermatomes. A dermatome is supplied by the sensory fibres of a single nerve root. There are 31 spinal nerve roots (8 cervical, 12 thoracic, 5 lumbar, 5 sacral, and 1 coccygeal) in the human (Gray et al., 1980) and each has a separate sensory pattern of distribution, referred to in the spinal cord as segmental and in the periphery dermatomal. By this organization dermatome areas are generally isolated; however, adjacent dermatomes do overlap slightly (Brodal, 2004).

The mechanism by which sensory neurones are activated by a stimulus, lies within specific end organs/receptors with the dermis and epidermis of the skin. Primary afferent modality is defined as the type of stimulus that will induce a response in the neurone. This can be thermal (cooling/warming), mechanical (depression, stretch, pressure, hair movement), and chemical (capsaicin, PH) stimuli (Loeser and Bonica, 2001). Afferents can exist in the periphery that respond to only one stimulus, or a mixture of many or all stimuli, referred to as 'polymodal' (Kumazawa, 1990). In some cases afferents have been shown to be totally inactive to natural stimuli, but these fibres become active under pathological conditions. These fibres are referred to as 'silent' nociceptors (Michaelis et al., 1996), and may be responsible for pain states. The intensity of the stimulus to which the end organ responds and therefore sets the primary afferent firing '*threshold*' is also an important factor that defines sensory subsets. Low-threshold mechanoreceptors (LTM) are activated by mechanical displacement of a low intensity, and high-threshold mechanoreceptors (HTM) are the opposite. This intensity 'graded' sensory system is essential in defining noxious from innocuous stimuli.

Primary afferents can be categorised by their anatomy and electrophysiological properties into A- and C- fibres (Djouhri and Lawson, 2004). Unmyelinated axons are classified as C-fibres, and are slowly conducting, in the order of <2m/s, and are thin with a diameter of 0.2-1.5µm. C-fibres typically innervate peripheral targets via unspecialised afferent endings called free nerve endings (FNE). Most FNEs are polymodal; therefore C-fibres can act as either thermoreceptors, mechanoreceptors, chemoreceptors and/or, polymodal nociceptors. Myelinated axons classified as A-fibres have a much greater rate of conduction, up to 120m/s, due to their capacity for 'saltatory' conduction, first described by Tasaki (Tasaki, 1939). The action potential propagates through areas of ionic insulation (myelin), interrupted by areas of

unmyelinated spaces (nodes of Ranvier) containing large numbers of ion channels allowing for ionic efflux and influx. The node of Ranvier produces an 'all-or-none' action potential, maintaining the same conductivity on each propogation. These channels and ionic movement across the axon membrane provide quick refraction of the axon current and repolarisation at that location, in preparation for further action potential propagation (Tasaki, 1939). The consistent frequency of action potential propagation, and therefore the extent of myelination and axon diameter, is what encodes for the intensity of a stimulus: A-fibres can be subclassified into α, β, and δ, depending on this principle (Loeser and Bonica, 2001). Aα fibres are the largest diameter (13-22um) primary afferent axons and have conduction velocities of 70-120m/s and have a substantial proprioceptive role (Brodal, 2004;Djouhri and Lawson, 2004). Aβ fibres have conduction velocities of 30-70m/s and range from 8-13μm in diameter, and make up the cutaneous mechanoreceptors and secondary muscle spindle proprioceptors, however they also have significant nociceptive properties (Djouhri and Lawson, 2004). Aδ fibres are thinly myelinated (1-5μm in diameter), with conduction velocity in the range of 3-30m/s, and comprise principally D-hair LTM units that respond to both stretch and cooling of the skin. They also have a substantial nociceptive role, conveying fast and sharp pain such as one would experience after a traumatic insult (Djouhri and Lawson, 2004).

The peripheral nerves or afferents, when travelling toward the CNS, converge from the back of the body and limbs into dorsal rami, and from the front of the body and limbs into ventral rami. These rami contain both sensory fibres with afferent trajectory, but also motor axons with efferent trajectory toward muscle targets. Both somatic rami converge with the sympathetic axons of the autonomic nervous system arising from the sympathetic ganglion chain, via the white and grey 'rami communicans' (Gray et al., 1980), and become a spinal nerve. The white rami, existing from T1-L2 spinal nerves, contain preganglionic axons from the intermediolateral cell column of the spinal cord, which innervate postganglionic sympathetic efferents. The grey rami, existing at all levels of the spinal cord, contain the postganglionic sympathetic efferent axons. At this point the spinal nerve enters the spinal column via the intervertebral foramina, somatic efferent and afferent projections separate into the ventral/anterior or dorsal/posterior root respectively. The dorsal root is where the cell bodies of the sensory neurones are located, bundled within ganglia. Dorsal root ganglion (DRG) cells are pseudo-unipolar

in anatomy. DRG cells are lined by a specific flattened Schwann cell called a satellite cell that supplies nutrients and structural support. DRG cell bodies can be sub-classified by their biochemical properties, which closely align with their electrophysiological properties (Priestley et al., 2002). Unmyelinated C-fibres can be divided into two classes: peptidergic and non-peptidergic neurones. Peptidergic neurones comprise 40% of the DRG population and express calcitonin gene-related peptide (CGRP) and substance P (Lawson et al., 1997), whereas non-peptidergic neurones, comprising another 40%, can be identified by the lectins they express, specifically Griffonia Simplicifolia Lectin-1 (IB4) (Streit et al., 1986), or by enzymes, such as fluoride resistant acid phosphatase (FRAP) (Carr et al., 1991;Carr et al., 1990) or LA4 antibody (Alvarez et al., 1991). However these two C-fibre populations are not mutually exclusive and overlap by approximately 8-30% depending on the markers used (Alvarez et al., 1991;Carr et al., 1990;Averill et al., 1995). Myelinated A-fibres, comprising the final 40% group can be identified by the heavy (200kDa) neurofilaments they contain, by several commercial antibodies (NF200, N52, and RT97) (Perry et al., 1991;Lawson et al., 1984).

1.2: The spinal cord

The DRG convey a central branch or root toward the central nervous system and provide the path for the sensory afferents to enter the spinal cord. The ventral root is where the motor efferents leave the spinal cord to join with the dorsal root at the spinal nerve level. One segment of the spinal cord is defined longitudinally by a pair of dorsal and ventral roots. Where the dorsal root crosses through the pia mater and enters the spinal cord, it no longer referred to as the PNS but rather now the CNS. The anatomical area for this is called the dorsal root entry zone (DREZ), and is situated between the external surface of the spinal cord and the apex of the dorsal horn grey matter. The DREZ is divided into a medial division of myelinated fibres involved in proprioception and mechanoreception, and a lateral division of mostly unmyelinated fibres involved in thermoreception, pressure reception, and nociception (Sindou et al., 1974;Light and Perl, 1977;Chung and Coggeshall, 1979;Chung et al., 1979). In this way somatic sensory modalities are beginning an anatomical separation before entering the CNS. The lateral division of the DREZ is usually referred to as Lissauer's Tract, and contains high threshold and nociceptive fibres (EARLE, 1952;Loeser and Bonica, 2001). Lissauer’s

tract does not contain cell bodies and for this reason is not defined as the one of the dorsal horn laminae, although it is located just dorsal to lamina I. The terminations of these sensory afferents, and some of those within the medial division, are distributed amongst the dorsal horn laminae. Small diameter axons (unmyelinated C and myelinated Aδ) branch after leaving Lissauer's Tract where they enter the dorsal horn directly, or branch and travel longitudinally for one or two spinal segments before synapsing (Sindou et al., 1974;LaMotte, 1977;Light and Perl, 1977). Large (Aαβ) myelinated fibres enter the dorsal columns directly where they ascend the spinal cord as the dorsal column-medial lemniscal pathway (main non-noxious pathway), synapsing with the dorsal horn nuclei at the level of the medulla, in the cuneate and gracile nuclei. Aαβ-fibres also send collateral branches into the dorsal horn. This division creates two distinct sensory pathways from one fibre type (Light and Perl, 1977;LaMotte, 1977;Traub and Mendell, 1988).

The terminations of the different classes of sensory afferents show lamina specificity (Light and Perl, 1977). The structure of the dorsal horn was first defined in the cat (REXED, 1952;REXED, 1954), and can be divided into a series of six stacked laminae (I-VI) and the ventral horn divided into four (VII-X) containing second order dorsal horn neurones that respond to afferent and supraspinal input, as well as lower motor neurone cell bodies. Lamina I is referred to as the marginal layer, and lamina II as the substantia gelatinosa. Collectively, these two laminae are referred to as the superficial dorsal horn, and are essentially the most important laminae involved in nociceptive processing of all sensory modalities and peripheral origins (LaMotte, 1977;Light and Perl, 1979;Light et al., 1979;Sugiura et al., 1989;Ling et al., 2003;Light and Perl, 2003). These laminae contain a very complex neurochemical organisation of neurotransmitters, neuropeptides, and receptors (Coggeshall and Carlton, 1997). Lamina I receives input from Aδ fibres and peptidergic C-fibres (Light and Perl, 1979;Light et al., 1979). Lamina II, which can be subdivided into inner (IIi) and outer (IIo), receives input from Aδ and peptidergic-C fibres in IIo, and Aβ and non-peptidergic-C fibres terminate in IIi (Light and Perl, 1979;Light et al., 1979). The deeper laminae (III-VI) deal with low threshold tactile information, proprioception, and nociception (lamina V). The beginning of lamina III can be distinguished by the larger numbers of myelinated axons in the latter, and extensive dendritic arbors, and is responsive to low threshold Aαβ

afferents (Loeser and Bonica, 2001). Lamina IV, which is also innervated by Aαβ fibres, can be distinguished by the appearance of large cell bodies that send dendritic processes to the superficial laminae and axons up the dorsal columns and the contralateral lateral white matter (Brown et al., 1977;Bennett et al., 1983;Loeser and Bonica, 2001). Laminae V (as well as lamina IV) contain cells of a wide dynamic range of activation, that are activated by cutaneous and visceral nociceptive afferents, such as Aδ-fibres and visceral C-fibres (Light and Perl, 1979), and send axons via the spinothalamic and spinomesencephalic tracts, that contribute the perception of pain (Loeser and Bonica, 2001). Lamina VI, is the base of the dorsal horn, and its borders are difficult to distinguish within the cervical and thoracic segments (Molander et al., 1989), and is usually only discernible in the lumbar enlargements (REXED, 1952;Molander et al., 1984). It is thought to consist of both motor and sensory neurones (Loeser and Bonica, 2001) innervated by Aαβs. Laminae VII to X are ventrally located and contribute a small percentage of axons to nociceptive ascending tracts namely the spinoreticular tract (Kevetter et al., 1982), but are mostly associated with motor activity, from reflex arcs of primary afferent-interneuronal segmental loops, as well as descending voluntary input. Lamina VII contains neurones that send projections up the dorsal-columns (Bennett et al., 1983), contains the intermediolateral cell column (preganglionic sympathetic neurones T1-L2), and the sacral autonomic nucleus (preganglionic parasympathetic neurones S2-S4) depending on the segmental level (REXED, 1954;Molander et al., 1984;Molander et al., 1989) and are innervated by A-αβ afferents. Medially to lamina VII is an area of neurones referred to as Clarke's nucleus; a proprioceptive clustering of interneurones that project axons within the lateral funiculus, giving rise to the posterior spinocerebellar tract (Mann, 1973). Laminae VIII and IX contain α and γ motor neurones responsible for extrafusal (skeletal movement) and intrafusal (proprioceptive control) muscle innervation. Little is known about the function of lamina X (also called the dorsal commissural nucleus) that is located around the central canal. Some evidence suggests a visceral (C-fibre innervation) nociceptive function (Miller and Seybold, 1987) as well as an autonomic function (Nicholas et al., 1999), but most neurones have convergent stimuli suggesting this lamina has multiple functions (Loeser and Bonica, 2001).

The somatotopy of the dorsal horn is similar to sensory cortex in that it has an ordering of neurones that represents a dermatomal pattern. A precise 'map' has been established in the cat and rat, within laminae I-IV of the dorsal horn, using electrical stimulation (Takahashi et al., 1995) and neurochemical tracing of cutaneous peripheral nerves from the hindlimb (Brown and Culberson, 1981;Swett and Woolf, 1985;Molander and Grant, 1985;Woolf and Fitzgerald, 1986;Molander and Grant, 1986;Shortland et al., 1989;Takahashi et al., 2003). The central terminals of afferents originating from the periphery form a reliable somatotopic map of overlapping terminals in the dorsal horn. There is extensive spread of termination of roots within the spinal segments, typically 1 or 2 segments rostrally and caudally from the corresponding segment (Brown and Culberson, 1981), but a distinct and separate somatotopy is found when labeling subdivisions of the sciatic nerve (Swett and Woolf, 1985;Molander and Grant, 1986). This distinct cutaneous-dorsal horn dermatomal somatotopy is conformed by intracutaneous wheat germ agglutinin-horseradish peroxidase (WGA-HRP) injections (Molander and Grant, 1985), with some degree of overlap due to overlapping peripheral fields. This overlap was confirmed by intra-axonal HRP injection of individual hair follicle afferents, with terminal collateral sprouting and arborisations noted in the laminae (Shortland et al., 1989). Further, different lamina distribution of A and C fibre projections was confirmed in the rat lumbar spinal cord (Woolf and Fitzgerald, 1986), suggesting not only location but also modality is distinguished by the organization of primary afferent termination. This dorsal horn somatotopy ensures sensory information is separated and ordered, before entering higher centres of the cortex. This provides the nervous system with a fast and efficient method to distinguish modality and location of stimulus.

1.3: From nociception to pain.

The second order dorsal horn neurones can be differentiated according to their responses to peripheral cutaneous stimuli, into classes numbered 1-4 (Cervero et al., 1976;Menetrey et al., 1977;Cervero and Tattersall, 1986). Class 1 cells can be activated by innocuous stimuli, and can be subdivided into 1A- responsive to hair movement and/or touch, and 1B- hair movement and/or touch and pressure, or pressure only. These neurones were unresponsive to noxious stimuli suggesting this class integrates purely

LTM information from A-αβ afferents, and predominate in laminae III and IV (Menetrey et al., 1977). Class 2 are a group of neurones that are driven by both noxious and innocuous stimuli, and are similarly divided into A and B subcategories depending on stimulus modality (Menetrey et al., 1977). They are most often referred to as 'wide dynamic range neurones' or 'multireceptive', and are most abundant in the dorsal horn predominating in laminae I, II, V, and X, and respond to A- and C-fibre afferents. These neurones receive most of the descending input to the dorsal horn from higher centres, and are involved in response to a stimulus chain (Menetrey et al., 1977;Cervero and Tattersall, 1986). Class 3 cells code purely noxious mechanical stimuli, such as pin prick (Menetrey et al., 1977) and referred to as nociceptor specific, and are found predominantly in lamina I (Cervero et al., 1976;Cervero and Tattersall, 1986). Class 4 neurones respond to joint and deep tissue pressure (Menetrey et al., 1977).

The second order neurones within lamina I, III, V-VII, and X send projections to higher centre structures such as the thalamus, periaqueductal grey, parabrachial region, bulbar reticular formation, hypothalamus, amygdaloid nucleus, septal nucleus, and many others, in anatomically defined tracts. Most projection tracts are anterolaterally located in the spinal cord associated with the perception of pain, with the exception of the dorsal column pathway, required mainly for non-noxious sensing and detecting precise location of stimulus (Willis and Coggeshall, 1991;Willis and Westlund, 1997;Almeida et al., 2004).

The Spinothalamic Tract (STT) is the major constituent of the anterolateral pathway, and is associated with directing information mainly of a noxious nature, but also crude touch. The tract has been mapped in monkeys, cats and rats, and originates from second order dorsal horn neurones mainly within laminae I and IV-VI, but some are also found in lamina X. The tract crosses the spinal cord through the anterior white commissure, and ascend contralaterally (located lateral to the ventral horn) eventually synapsing with the contralateral ventral posterolateral nucleus of the thalamus. This nucleus is subdivided for specific areas of the body, and each area projects to its own section of the primary sensory cortex. Two separate STT projections can be identified entering the thalamus and encode fast and slow pain: A bilateral medial-nuclear-group, called the ***paleo***spinothalamic tract, encodes slow pain and is involved in motivational-affective aspects of pain, and originates from the deep dorsal horn, ventral horn, and around the

central canal, and terminates within the intralaminar nuclear complex of the thalamus, namely the central lateral nucleus. The lateral-nuclear-group, called the ***neo***spinothalamic tract encodes fast pain and is involved in sensory-discriminative characterisation of pain, and originates from lamina I and V, and terminates within the ventrobasal complex, namely the posterior nuclei (Hodge, Jr. and Apkarian, 1990;Willis and Coggeshall, 1991;Ralston, III and Ralston, 1992;Willis and Westlund, 1997;Almeida et al., 2004).

The ***spinoreticular pathway*** from laminae V, VII and VIII**,** with smaller contribution from laminae I and X, ascends on both sides of the spinal cord, synapsing in the lateral reticular formation, involved in motor control, and the medial reticular formation involved in nociceptive mechanisms. Some fibres terminate bilaterally in the intralaminar nuclei of the thalamus. From there the next neuron in the chain takes the information to many areas of the brain, including the anterior part of the cingulate gyrus and amygdala (associated with memory and emotion), and hypothalamus (associated with autonomic responses). This complex pathway involves the integration of motivational-affective understanding of pain, and is also an essential modulator of descending inhibitory pathways (Willis and Westlund, 1997;Almeida et al., 2004).

The ***spinomesencephalic tract*** originates from cells that closely aligned with the STT, namely within laminae I and IV-VI, with some in the ventral horn and lamina X, and so also encode nociceptive infomation. These projection neurones also travel contralaterally in the anterolateral pathway, and terminate in the periaqueductal grey, nucleus cuneiformis, intercolliculus nucleus, superior colliculus, pretectal nucleus and many more areas of the midbrain. The functions of the spinomesencephalic tract are likely a contribution to aversive behaviour; involving locomotion, cardiovascular, orientation, motivational, and possibly acute analgesia to prime the body for quick retreat from the noxious stimulus (Willis and Coggeshall, 1991;Willis and Westlund, 1997;Almeida et al., 2004).

The ***spinoparabrachial tract*** originates in lamina I, is an exclusively nociceptive pathway, and travels to the parabrachial nucleus in the pons, which in turn projects to the amygdala, hypothalamus, and other limbic system structures in the forebrain. These

areas most likely participate in the emotional-affective responses to noxious events, such as memory, fear, and autonomic functions such as stress (Almeida et al., 2004).

The ***spinohypothalamic pathway*** originates from neurones of laminae I, V, X, the lateral spinal nucleus, and nucleus caudalis, carrying information of emotional significance from the skin, lips, sex organs, gastrointestinal tract, intracranial blood vessel tongue and cornea, directly to the medial and lateral hypothalamus, nucleus accumbens and the septal nucleus. The spinohypothalamic pathway is responsible for the integration of nociceptive input involved with autonomic, cardiovascular, and neuroendocrine responses to noxious stimuli, as well as some motivational aspects of pain (Willis and Westlund, 1997;Almeida et al., 2004).

The post-synaptic dorsal column pathway (***spinomedullary***), and ***spinocervical tract***, are not part of the anterolateral pathway and are essentially involved in transmitting tactile and non-noxious information to higher centres (Almeida et al., 2004). Neurones from laminae I, and a few originating in laminae V-VIII, project up the dorsal columns to the ventrolateral medulla (Andrew et al., 2003). Second order dorsal horn neurones from laminae III and IV send projections to the cervical nucleus (Brown, 1981;Willis and Coggeshall, 1991). These both have a major role in carrying information of a non-noxious somatic modality (Giesler, Jr. and Cliffer, 1985), however many spinocervical tract cells have wide dynamic range and could respond to noxious cutaneous stimulation (Cervero et al., 1977)**.**

1.4: Nerve plexi and limb innervation

External stimuli as well as motor coordination are processed initially within the spinal cord, in two anatomically distinct areas: the cervical and lumbar enlargements. These enlargements are responsible for the innervations of the upper and lower limbs respectively. Communication between these neuronal clusters and the periphery occur via intricate networks of roots and nerves, called the brachial and lumbosacral plexuses.

1.4.1: Anatomy of the brachial plexus in man

The human brachial plexus is an arrangement of branching nerve fibres responsible for cutaneous and muscular innervations of the hand, arm, forearm, and shoulder (Fig 1.1), (Gray et al., 1980), and is anatomically similar to the rat (Rodrigues-Filho et al., 2003).

Roots:

The brachial plexus begins at the level of the spinal cord as a collection of nerve roots: C5, C6, C7, C8, and T1 (Fig 1.1). The roots emerge from the spinal vertebral foramina, immediately posterior to the vertebral artery, and merge forming three main trunk divisions: superior/upper (C5-C6), middle (C7), and inferior/lower (C8-T1) (Fig 1.1), that proceed through the neck, the axilla, and into the arm. The trunks of the brachial plexus pass between the anterior and middle scalene muscles and branch extensively. The trunks divide and cross, turning into anterior and posterior divisions, each consisting of upper, middle, and lower trunks (Fig 1.1), which innervate the ventral and dorsal halves of the arm. The six divisions then regroup to become three cords, which are named by their position with respect to the axillary artery. The posterior cord, behind the artery, is formed from the three posterior divisions of the trunk (consisting of all roots), the lateral cord comprises the anterior divisions from the upper and middle trunks (consisting of C5-C7 roots), and the medial cord is the continuation of the anterior division of the lower trunk (consisting of C8-T1 roots) (Fig 1.1) (Gray et al., 1980).

Peripheral nerve:

The cord branches are the origins of the individual nerves that supply both innervation to the muscles controlling arm and hand movement, but also sensory cutaneous innervation to the arm and hand. A cutaneous nerve branch from the lateral cord, called the musculocutaneous (that later becomes the lateral cutaneous nerve of the forearm) (Fig 1.1), innervates portions of the forearm, wrist, and thumb. Cutaneous nerve branches from the posterior cord include, the axillary nerve (Fig 1.1) (that later becomes the superior lateral brachial cutaneous nerve) that innervates the skin above the deltoid and tricep brachii of the shoulder and top of the forearm, and the radial nerve (Fig 1.1) (that becomes the posterior brachial cutaneous nerve) that innervates most of the posterior surface of the arm. Cutaneous nerves branched from the medial cord include

the ulnar nerve (Fig 1.1) that innervates the skin of the medial side of the hand and fingers, the medial brachial and antebrachial cutaneous nerves (Fig 1.1) that innervate the front and medial skin of the forearm, arm, ending at the wrist, and lastly a limited innervation comes from the median nerve (Fig 1.1) that supplies regions of the hand not served by the ulna or radial nerve (Gray et al., 1980).

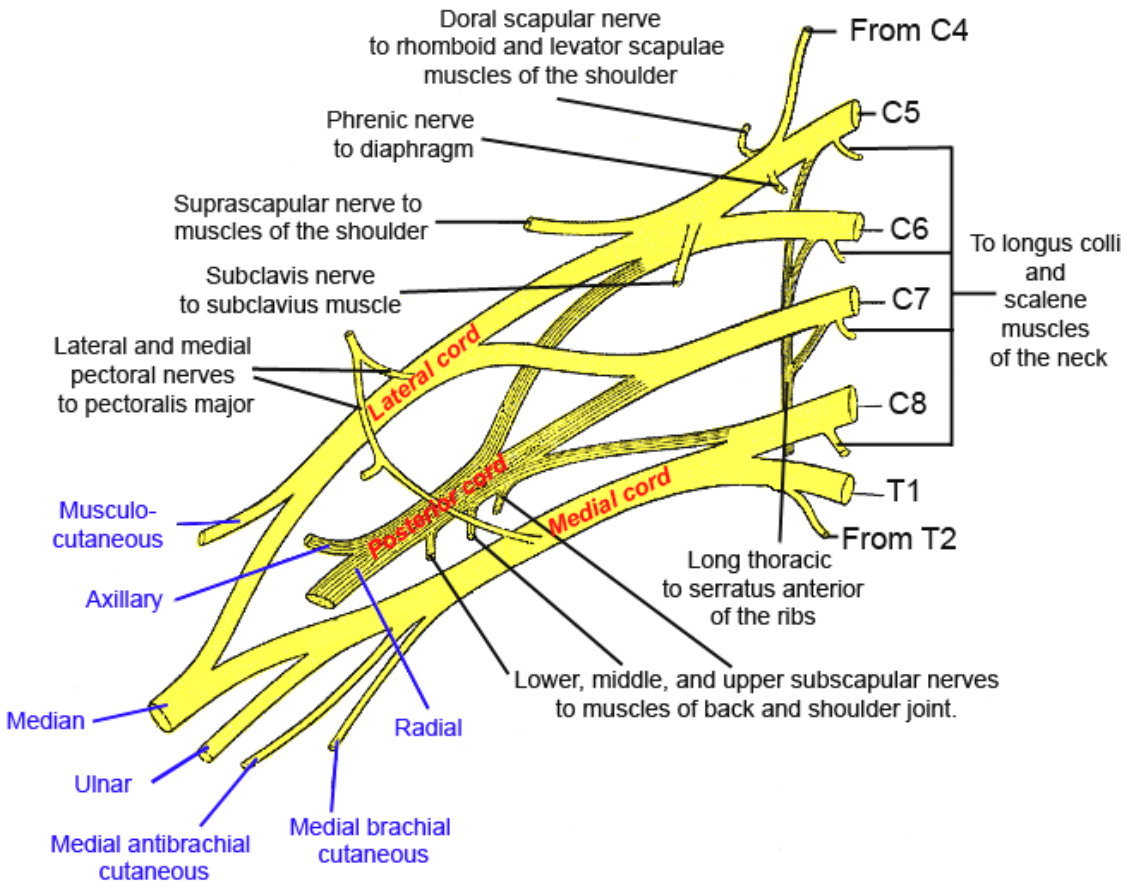

Figure 1.1: Brachial plexus and sensory system of the arm in human. Plexus constitutes C5-T1, with contributions from C4 and T2. These roots combine into 3 main cords: lateral, medial, and posterior. Sensory innervation comes from the nerves branched from these three cords (indicated in blue). These nerves also have motor function also, including other nerve branches (indicated in black) showed more proximally. Adapted from (Gray et al., 1980).

1.4.2: Anatomy of the lumbo-sacral plexus in man

The lumbo-sacral plexus is the network of nerves formed from the lumbar, sacral, and coccygeal roots, and provides motor and sensory innervations of the lower limbs, urogenital, and pelvic floor regions. It involves two main plexuses - the lumbar and sacral. The sacral plexus in turn contains two additional plexuses – the pudendal and the

coccygeal (Fig 1.2, (Gray et al., 1980). In contrast to the brachial plexus, the lumbosacral plexus anatomy varies between species, the details of which are discussed below. It is important to consider these anatomical inconsistencies when attempting to interpret dissimilar behavioural responses to nerve injuries, within different species and strains, compared to human conditions. Indeed cats, dogs and rats are used as in vivo models for peripheral nerve injury, neuropathic pain, and inflammatory pain extensively.

The Lumbar Plexus

Roots:

The spinal nerve roots of (T12), L1, L2, L3, and L4 form the beginning of the lumbar plexus in man. A division of L4 sends communicating branches to the sacral plexus via the L5 root (see later), and this region is referred to as the lumbosacral trunk (Fig 1.2). The rat in this context has an additional L6 root (Asato et al., 2000). The roots emerge from intervertebral foramina forming adjacent loops of communication, and are joined by gray rami communicans to the ganglia of the sympathetic trunk. The plexus passes obliquely in nerve branches outward behind the psoas major muscle of the vertebral column and down into the pelvic area, under the inguinal ligament and finally into and down the thigh (Gray et al., 1980).

Peripheral nerve:

The lumbar plexus differs from the brachial plexus in that it does not form an intricate interlacement of nerves, rather several nerve distributions arise from one or more of the spinal nerves, in the following manner: the first lumbar nerve (Fig 1.2), frequently supplemented by a branch from T12, splits into an upper and lower branch; the upper and larger branch divides into the iliohypogastric, supplying anterior and lateral cutaneous innervation of the gluteal region, and ilioinguinal nerves, supplying the anterior area of the groin; the lower and smaller branch unites with a branch of the L2 to form the genitofemoral nerve innervating the skin medially to the groin.

A large portion of L2 with a portion of L3 becomes the lateral femoral cutaneous nerve (Fig 1.2) that in turn branches into anterior and posterior regions after passing through the femoral triangle of the inner upper-thigh and down into the leg. The anterior branch

innervates the anterio-lateral thigh region, and the posterior branch innervates the posterior-lateral aspect of the thigh.

The remainder of L2 combines fully with the third and fourth lumbar nerves to become the femoral cutaneous nerve (Fig 1.2), the largest of the lumbar nerves. This has three branches: the anterior/intermediate cutaneous femoral nerve, supplying the anterior thigh region, the saphenous nerve, supplying the medial aspect of the calf and foot, and the medial cutaneous femoral nerve, supplying the medial aspect of the thigh.

L2-L4 join together and form a distinct nerve to the femoral, called the obturator nerve (Fig 1.2) that has an anterior and posterior branch that exits the pelvis through the obturator foramen, and innervates the upper half of the medial cutaneous area of the thigh. In 29% of cases there is a ventral branch of the obturator called the accessory obturator that provides sensory innervation to the hip joint (Gray et al., 1980).

The Sacral Plexus

Roots:

The sacral plexus is formed by the loops of communication between part of the L4, the lumbosacral trunk, the L5, and the first three sacral roots (S1-S3) (Fig 1.2). The sacral plexus innervates the skin on the back of the thigh, leg and around the anus and genitals (Gray et al., 1980).

Peripheral nerve:

A large majority of these nerve roots join together to form the largest nerve of the body, the sciatic nerve (L4, L5, S1, and S2, Fig 1.2), that emerges from below the piriformis muscle of the gluteal region and enters the leg. This nerve subdivides into the tibial, and the common peroneal nerve. The tibial further decussates into the sural nerve, medial and lateral plantar nerves, and the calcaneal nerve, further down in the leg and foot. The calcaneal nerve supplies the ball of the foot, the sural the lateral aspect of the foot and posterio-lateral leg, the medial and lateral plantar nerves (similar to the ulnar and median nerves in the brachial plexus) innervate the medial and lateral plantar surfaces of the plantar foot respectively. The common peroneal also branches further down the leg into the deep peroneal nerve that innervates the skin between the 1st and 2nd toe, the

superficial peroneal nerve that innervates the anterio-lateral shin region and foot dorsum, and the lateral sural cutaneous nerve that innervates the anterio-lateral calf just below the knee. The L6 root in rat has a variable contribution to the sciatic nerve (Asato et al., 2000;Rigaud et al., 2008;Shehab, 2009), with sometimes the L3 root contributing (Asato et al., 2000).

The posterior femoral cutaneous nerve (Fig 1.2), is part of the sacral plexus also and is served by S1, S2, roots S3, and innervates the whole posterior aspect of the thigh, from gluteal region to the popliteal fossa. (Gray et al., 1980).

The Pudendal Plexus

The pudendal plexus is located ventrally to the posterior wall of the pelvis and is formed from the medial part of the sacral plexus. It culminates in two nerves: the pudendal (S2, S3, and S4 nerve roots) and perforating cutaneous/inferior cluneal (S2 and S4 nerve roots) (Fig 1.2). This nerve/plexus divides down in the pelvis into the inferior rectal nerve, the perineal nerve and the dorsal nerve of the penis/clitoris. These innervate the peri-anal skin, scrotum/labia majora and penis/clitoris respectively.

The perforating cutaneous/inferior cluneal nerve also part of the pudendal plexus (Fig 1.2) innervates the skin covering the gluteal region above the region supplied by the posterior femoral cutaneous nerve. This nerve is absent in 33% of cases and its role can be taken by a branch from the posterior femoral cutaneous (Gray et al., 1980).

The Coccygeal plexus

The coccygeal plexus is the most caudal part of the spinal cord and sacral plexus. It consists of just one nerve: the anococcygeal nerve. It is formed from the coccygeal root with communicating filaments from the fourth and fifth sacral roots, uniting to form the coccygeal plexus (Fig 1.2). This consists of a few fine filaments which pierce the sacrotuberous ligament to supply the small amount of skin in the region of the coccyx (Gray et al., 1980).

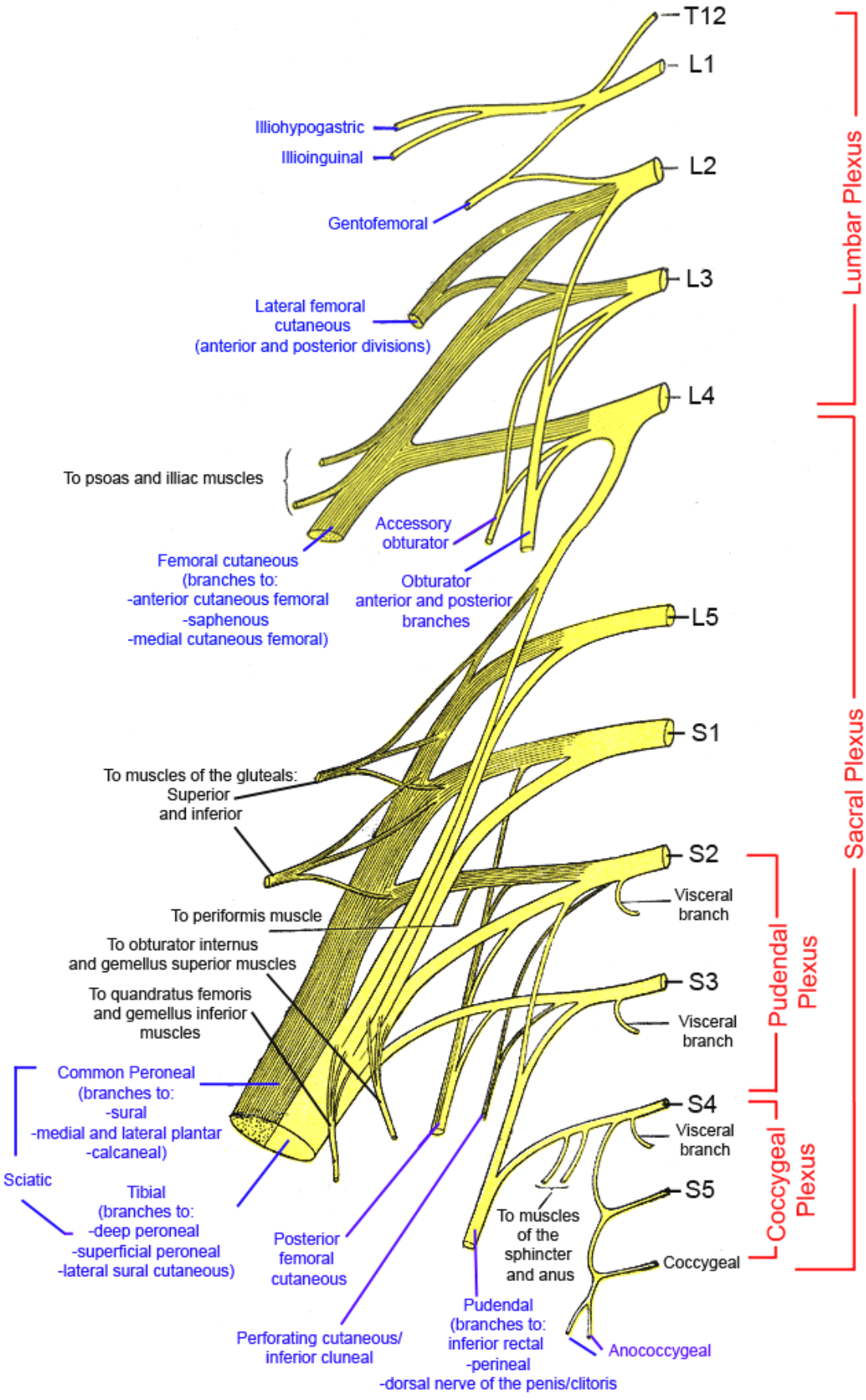

Figure 1.2: Lumbosacral plexus and sensory system of the leg, foot, pelvis, genitals, and anus in human. Plexus constitutes T12-Coc1. The major cutaneous sensory nerves consisting of lateral femoral cutaneous, femoral cutaneous, obturator, sciatic, posterior femoral cutaneous, perforating cutaneous, pudendal and anococcygeal (indicated in blue). These nerves also have motor function, including other nerve branches (indicated in black). Adapted from (Gray et al., 1980).

1.5: Brachial and lumbo-sacral plexus injuries

Ramon y Cajal (Ramon and May, 1928) first documented the characteristic of regeneration after injury within the peripheral nervous system, noting the appearance of 'ball-like appendages' (buds) at the central end of transected axons within the sciatic nerve, contrary to the limited capacity seen in the CNS (Ramon and May, 1928). In the case of spinal roots, he discovered that the dorsal component had a capacity to regenerate toward, but not through, the root entry zone after a central root injury. This is thought to be due to two main factors: firstly, the non-permissive environment of the CNS through the development of astrocytic glial scars and secretion of inhibitory molecules such as chondroitin sulphate proteoglycans (Fawcett, 2006;Yiu and He, 2006), and secondly the lack of intrinsic growth potential within the axon (Caroni, 1997). This growth potential relies on the formation of a growth-cone, by localized protein turn-over at the terminal end of transected axons, and is controlled by the upregulation of regeneration-associated genes such as small proline-rich repeat protein 1A (SPRR1A) and growth associated protein (GAP43) (Snider et al., 2002). This is regulated by extensive intracellular signalling pathways specifically within neurones of a certain age (embryonic/neonatal) and type (peripheral) (Chierzi et al., 2005;Verma et al., 2005). In contrast to the CNS, lesions to the mature sciatic nerve in animal models leads to Wallerian degeneration of the distal fibres, and a robust regenerative response in the proximal fibres of the transected nerve (Fawcett and Keynes, 1990).

Spinal root avulsions involve a lesion to the peripheral nervous system at the CNS transition zone, and can result in trauma to both CNS and PNS (Carlstedt, 2009). The extent of CNS disruption is dependent upon avulsion proximity to the root entry zone, and therefore a wide variety of neuropathology can be presented to the clinic. Also they have the potential to affect both ventral and dorsal root components, resulting in motor and/or sensory disruption initially, cell death of motor neurones (Koliatsos et al., 1994;Bergerot et al., 2004;Bigbee et al., 2007), and neuropathic pain (Berman et al., 1998). These neuropathies usually occur from high-energy traction forces to the limbs, and approximately 1000 new cases appeared in 2008. The injury most commonly, in 80-90% of avulsion cases (Flores, 2006), involves damage to the roots (C5-T1) of the brachial plexus (Terzis et al., 2001;Carlstedt, 2009), and are caused notably by motor bike accidents (Rosson, 1987) or obstetrical complications that involve shoulder

dystocia (Hoeksma et al., 2000). American and European studies show that 10-20% of all peripheral nerve lesions involved the brachial plexus (Flores, 2006). Brachial plexus avulsion can present as two main types: upper and lower (Carlstedt, 2009). Upper avulsions involving C5-C8 occurs from excessive lateral neck flexion away from the shoulder, leading to loss of rotation capacity in the shoulder muscles, arm flexors and hand extensor muscles and results in Erb's palsy. Lower avulsions involving C8 and T1 occurs through sudden traction force on the arm away from the shoulder with subsequent paralysis of intrinsic muscles of the hand and flexors of the wrist and fingers resulting in Klumpke's palsy.

Lumbosacral root avulsions commonly involve roots L4, L5, and S1 (Huittinen, 1972) and often result from lap-belt motor vehicle injuries (Tubbs et al., 2006), or trauma to the pelvis (Tung et al., 2005). Studies into the prevalence of lumbo-sacral neurological injury, showed an incidence rate of 30 to 46% in cases of unstable pelvic fractures (Huittinen, 1972), and that pain occurs in 10-25% of injuries to the nerve (Sindou et al., 2001).

Clinically, avulsion is diagnosed where the root is both stretched (neuropraxia) and torn (ruptured) from the cord. Root avulsions can be caused by central tensile force such as twisting of the head and neck, or an applied force of a lap belt against the momentum of the body, leading to the spinal cord being pulled cranially away from the roots. This results in avulsion with roots still held by attachments to the interverebral foramen. If the limb is pulled from the body in traction injuries, such as motor bike and obstetrical accidents, the nerve roots are pulled from the cord and in some cases leading to displacement of the roots outside the spinal canal requiring more complex surgical intervention (Carlstedt, 2009).

In humans, paralysis, muscle atrophy, and excruciating, intractable deafferentation pain occurs within 48 hours of brachial (Bruxelle et al., 1988;Berman et al., 1996;Uetani et al., 1997)}(Berman et al., 1998;Htut et al., 2006) and lumbosacral plexus/cauda equina avulsions (Sampson et al., 1995;Sindou et al., 2001;Stevanato et al., 2007). In cases of sacral avulsions such as conus medullaris and cauda equina injuries, a lower motor neurone autonomic dysfunction also occurs, including atonic bladder and flaccid anal sphincter control, and in males a loss of reflexogenic erection (Kingwell et al., 2008).

Accompanying pain is characterised as crushing with intermittent shooting pains down the deafferented limb (Berman et al., 1998) coupled with generation of border-zone hypersensitivity and allodynia across affected-unaffected dermatomes (Htut et al., 2006;Havton and Carlstedt, 2009). The pain is resistant to most pharmacotherapies (Parry, 1980), and can lead patients to suicidal behaviours (Zhang et al., 2008) or revert to amputation for therapy (Piva et al., 2003). The most widely accepted effective treatment for relief of this neuropathic pain is a DREZ lesion called DREZotomy (Nashold, Jr. and Ostdahl, 1979;Sampson et al., 1995;Sindou et al., 2005;Teixeira et al., 2007). However initial pain relief is variable (47.8%-90%), as is the follow-up prognosis (26.1%-73.9%) at 12 months (Sampson et al., 1995;Sindou et al., 2005) (Chen and Tu, 2006;Zhang et al., 2008), with a risk of low limb paralysis presenting (Piva et al., 2003). The DREZ lesion targets the ventro-lateral part of the central dorsal rootlets, medial Lissauers tract, and laminae I-V of the dorsal horn (Zhang et al., 2008), designed to selectively destroy the nociceptive fibres and terminations of the lateral bundle of the dorsal rootlet (Sindou et al., 2001). Nowadays, either DREZotomy or ventral root reconstructive surgery is used as therapy for alleviating neuropathic pain, with the later having the benefit of restoring functional motor recovery (Carlstedt et al., 1995). Recently high cervical spinal cord stimulation has been shown to be effective at pain relief after brachial plexus avulsion, which DREZotomy or antidepressant and anticonvulsant pharmacotherapy failed to relieve (Piva et al., 2003;Lai et al., 2009), by activating descending inhibitory pathways. However patients needed permanent implantation of the stimulator devise to maintain efficacy. Reconstructive surgery constitutes re-implantation of the root (Carlstedt, 2009;Havton and Carlstedt, 2009), via nerve transfers for pre-ganglionic transection and nerve grafts for post-ganglionic transection (Berman et al., 1998;Anand and Birch, 2002). This has had clinical success, with respect to recovery of motor function after spinal root avulsion in the brachial plexus (Carlstedt et al., 1995;Carlstedt et al., 2000;Carlstedt et al., 2004;Carlstedt et al., 2009), having been developed in pre-clincal models in primates and rodents (Carlstedt et al., 1986;Carlstedt et al., 1993;Bergerot et al., 2004;Nogradi et al., 2007). Similar reconstructive surgery for the lumbosacral plexus also yields some lower extremity functional improvement (Lang et al., 2004;Sivaraman et al., 2008). Importantly, this surgical procedure even when delayed by 1 year diminishes the severity of the pain prior to the onset of motor functional recovery (Berman et al., 1996;Berman et al., 1998;Carlstedt et al., 2004;Htut et al., 2006;Kato et al., 2006). Furthermore, patients

who have undergone reconstructive surgery are more likely to be effectively treated with carbamazepine and amitriptyline (Berman et al., 1998), drugs that previously were shown to have limited efficacy in avulsion pain (Parry, 1980;Berman et al., 1996;Piva et al., 2003). Successful functional motor recovery and the effectiveness of pain relief is directly related to age of patient and delay of surgical intervention (Carlstedt et al., 2000;Kato et al., 2006), and CNS plasticity is likely to be the overwhelming factor for this success. This plasticity does have its disadvantages. Avulsion of C5 root, the origin of the phrenic nerve, accompanied with surgical reimplantation, can lead to the phenomenon of the 'breathing arm': a spontaneous contraction of arm muscles in synchrony with inspiration, believed to be due to inappropriate regeneration and plasticity of the phrenic motor pool axons into the peripheral nerves of the arm (Carlstedt et al., 2004;Htut et al., 2006;Carlstedt, 2009).

In animal models it has been made clear that re-implantation alone will not bring about an optimal functional recovery, as motor neurones continue to die and axonal regeneration through the implanted root is poor (Bergerot et al., 2004;Nogradi et al., 2007), and additional therapy is required. One such intervention could be providing a medium for the motor axons to regenerate through before entering the more growth promoting environment of the peripheral nerve. Olfactory ensheathing cell (OEC) transplantation into the VREZ with ventral root re-implantation after rhizotomy (Li et al., 2007) has shown an improvement of axonal growth through the CNS-PNS transition zone by 4 fold; however, functional recovery was not found due to lack of peripheral muscle unit-axonal re-connection. In multiple lumbar ventral root avulsion (VRA) rat models, permanent motor deficit can be attributed to irreversible motor neurone cell death, where 50-80% of the motor pool is lost after 2 weeks (Koliatsos et al., 1994;Bergerot et al., 2004). In models of single lumbar ventral root avulsion, there is a loss of motor neurones in the affected segment but also an enhancement of the monosynaptic activity of reflex arcs of the adjacent uninjured motor neurones (Holmberg and Kellerth, 1996;Holmberg and Kellerth, 2000) after 12 weeks, suggesting a plastic compensatory mechanism that aims to maintain a functional locomotor activity in the limb.

Minocycline, riluzole, glial cell line-derived neurotrophic factor (GDNF), and brain derived neurotrophic factor (BDNF) administration post VRA have all shown improved

motor neurone survival (Bergerot et al., 2004;Blits et al., 2004;Parsadanian et al., 2006;Zhou and Wu, 2006;Hoang et al., 2008), with a 90% survival rate at 6 weeks (Wu et al., 2003). When combined with re-implantation better motor neurone survival occurs, and locomotor function can be restored (Bergerot et al., 2004;Nogradi and Vrbova, 2001;Nogradi et al., 2007), providing a critical window for therapeutic intervention into motor functional regeneration. This survival is associated with influencing anti-apoptotic intracellular signalling pathways involving c-Jun, and also the inhibition of nNOS expression (Novikov et al., 1995). However, withdrawal of neutrophic support directs motor neurones back to their original fate (Bergerot et al., 2004), suggesting only a life support mechanism of action in these cases. In a more extensive avulsion injury to multiple roots within a plexus, the death of motor neurones may require reconstitution of the motor neuronal pool if any functional recovery is to occur. Embryonic postmitotic motor neurone grafts (Nogradi and Vrbova, 1996) have been shown to survive and extend axons through re-implanted ventral roots after avulsion and reach target muscles, providing possible therapy for patients that may have missed the 'therapeutic window' of cell death prevention. Interestingly, these motor neurone grafts successfully survive and elongate axons, only if the host motor neurones themselves die (Nogradi and Vrbova, 2001), suggesting an association of donor cell rejection in injured spinal cord to successful clearance of injured or dying cells.

Avulsion injuries of cervical and lumbosacral dorsal roots, are a major challenge for rehabilitation, as these lesions result in an irreversible loss of sensory function (Havton and Carlstedt, 2009) and severe intractable pain (Sampson et al., 1995;Stevanato et al., 2007). Avulsion of brachial plexus dorsal roots in rat leads to severe impairment of successful forepaw grasping (Ibrahim et al., 2009b) as well as bilateral below-level hypersensitivity (Rodrigues-Filho et al., 2003). Experimental treatment techniques under investigation for regeneration involve DREZ OEC-transplantation with dorsal root re-implantation after rhizotomy (Li et al., 2004), improving axonal growth through the CNS-PNS transition into the dorsal horn and up the dorsal columns for 10mm, corresponding to improvement of lost forepaw grasping over several weeks (Ibrahim et al., 2009a). Immediate intrathecal neurotrophin administration after dorsal root crush injury leads to specific subpopulations of injured sensory afferents crossing the DREZ (McPhail et al., 2005). NGF, NT3, and GDNF treatment lead to re-growth of damaged sensory axons through the root entry zone into the cord. Reconnections to dorsal horn

neurones were also found to be functional, and nociceptive sensitivity to noxious heat and pressure were restored (Ramer et al., 2000). Clinically, however the situation is less optimistic. Effective therapeutics are still required after surgical intervention for treatment of ongoing neuropathic avulsion pain (Berman et al., 1998), DREZotomy is only partially effective (Sampson et al., 1995), and allodynia has been shown to accompany regeneration (Htut et al., 2006). At present it unclear what, if any, effects to the dorsal horn neuronal pool occur after avulsion of the dorsal roots and what mechanisms can contribute to the sensory changes seen after dorsal root avulsion.

1.6: Lumbosacral plexus injury *in vivo*

This thesis has attempted to more closely model human avulsion injury in the lumbosacral region of the rat by tearing rather than cutting the roots. Clinically lumbosacral avulsion is far rarer injury than brachial plexus avulsion (Stevanato et al., 2007;Carlstedt, 2009) as the plexus is protected within the bony pelvis, and the reason for designing animal models in the lumbosacral region needs to be made clear. So far in pre-clinical animal models of pain and peripheral nerve injury, quantitive sensory analysis techniques have been designed for assessing somatic behavioural changes in the hindpaw (lumbar region) and not forepaw (cervical region). These techniques are well established and used consistently in the literature for peripheral nerve injury models, and the assessment of neuropathic pain, and consist of von-Frey hair filaments (Seltzer et al., 1990), thermal probe assessments (Hargreaves et al., 1988), and other methods such as cold plates and chemical irritants (Bennett and Xie, 1988), and more recently an automated plantar asthesiometer (Dolan and Nolan, 2007), some of which are used in this thesis. In addition, and as described earlier, the detailed anatomy of the rat lumbosacral somatotopy, dermatomal innervation and physiology in the dorsal horn is far better understood than in the cervical/brachial region (Swett and Woolf, 1985;Molander and Grant, 1985;Woolf and Fitzgerald, 1986;Molander and Grant, 1986;Shortland et al., 1989;Takahashi et al., 1995;Takahashi et al., 2003). Surgery of the lumbar region is anatomically easier and less invasive than cervical surgery, with less muscle and surrounding tissue to dissect, and for lumbosacral avulsion injury there are less post-surgical implications, such as breathing difficulties.

In this thesis three models have been applied to model root avulsion: L3-L6 dorsal root avulsion, L3-L6 dorsal root rhizotomy, to fully injure the hind-paw, and L5 spinal root avulsion. Dorsal roots L3-L6 were avulsed or transected, affecting the two main hindlimb nerves: the sciatic nerve and the saphenous nerve, to compare the models. The sacral roots were not avulsed, as injury to these roots can result in post-surgical complications to parasympathetic autonomic function, such as bladder and bowel function. In addition, a single L5 ventral+dorsal root avulsion (spinal root avulsion) was chosen as the vast majority of lumbosacral avulsions involve mainly the L5 root (Maillard et al., 1992). This model also provides an opportunity to assess evoked behavioural responses produced by the adjacent L4 intact afferents as a way of modelling borderzone hypersensitivity shown in patients (Htut et al., 2006;Havton and Carlstedt, 2009).

1.7: Thesis aims

The first chapter of this thesis will aim to compare the *in vivo* model of avulsion currently in use in the literature, dorsal root rhizotomy (DRR), against a more direct injury to the spinal cord, dorsal root avulsion (DRA). The former model does not directly damage the dorsal horn of the spinal cord, a characteristic that often happens clinically. The spatial and temporal neuropathology of the dorsal cord after these different deafferentation injuries at early and late time points will be assessed to provide more information on the underlying consequences of root avulsion injury with possible mechanisms of the neuropathic pain.

There is, at present, a lack of established animal models to test drug treatments for avulsion-pain. The second chapter will describe a behavioural avulsion model (L5 SRA) enabling quantitative testing of the development and characterisation of evoked, at-level, neuropathic avulsion-pain. Behavioural sensory tests of both tactile and thermal modalities will be implemented, and histology of the adjacent (L4) and avulsed (L5) spinal segments and DRG will be analysed.

At present some therapy for avulsion-pain shows efficacy, including DREZotomy (Nashold, Jr. and Ostdahl, 1979;Sindou et al., 2005) and antidepressants and anticonvulsants (Berman et al., 1998;Flores, 2006), however this is limited due to the

re-occurance of pain after ablative therapy, and side-effects and tolerance with drugs. The third chapter will aim to determine whether the antidepressant amitriptyline, and the anticonvulsant carbamazepine, administered to SRA injured rats produces results similar to that seen for patients with respect to neuropathic pain treatment. Results will clarify the effectiveness of the drugs pre-clinically as well as providing further proof-of-concept of SRA-induced neuropathic behaviour.

The last results chapter will aim to provide evidence for potential efficacy of the drugs, minocycline and riluzole, at present prescribed for other clinical conditions such as amyotrophic lateral sclerosis (ALS), neuroprotection after SCI, and acne, in the treatment of avulsion-pain. Minocycline has shown effective neuroprotective qualities pre-clinically for SCI (Lee et al., 2003;Wells et al., 2003;Teng et al., 2004) and root avulsion (Hoang et al., 2008), and analgesic properties for PNI (Raghavendra et al., 2003;Ledeboer et al., 2005) and SCI (Hains and Waxman, 2006;Marchand et al., 2009). Riluzole has shown neuroprotective qualities in VRA models (Nogradi and Vrbova, 2001;Bergerot et al., 2004;Nogradi et al., 2007), and has shown analgesic properties in PNI (Sung et al., 2003;Coderre et al., 2007). Both drugs may therefore be effective at reducing SRA-induced pain through similar mechanisms. Evoked behaviour and histological effects will be assessed in an immediate and maintained treatment regime in the SRA model. A delayed treatment regime will assess the potential for these drugs to effectively reverse and prevent the return of avulsion-pain behaviour.

Chapter 2: Methodology

2.1: Animal housing and number

142 adult male Wistar rats (Charles River, U.K.) of weight 150-350g were used in this thesis and were kept in standard housing conditions with 12 hour light/dark cycle, and given water and a standard rat chow pellet diet *ad libertum.* All animal procedures were in accordance with the Animal Scientific Procedures Act 1986 and UK Home Office regulations.

- *Dorsal root avulsion and rhizotomy immunohistology groups:*

In total 50 rats were involved in the DRA and DRR comparative immunohistochemistry analysis. 20 rats underwent L3-L6 unilateral dorsal root avulsion (DRA), and were left for 1 day (N=4), 2 days (N=6), 14 days (N=6), and 28 days (N=4) post injury, before sacrifice. 20 rats underwent L3-L6 unilateral dorsal root rhizotomy (DRR), and were left for 1 day (N=4), 2 day (N=6), 14 day (N=6) and 28 day (N=4). 6 rats underwent laminectomy, for 1 day (N=3) and 14 day (N=3) for sham surgery comparisons. 4 rats were processed for naïve immunohistochemical comparison.

- *Flow Cytometry groups:*

28 rats also underwent surgery for flow cytometric analysis. Rats underwent DRA and were left for 2 days (N=8) or 2 weeks (N=4) post injury before sacrifice. A DRR group were sacrificed at 2 day (N=8) or 2 week (N=4). Rats underwent unilateral laminectomy, and sacrificed at 2 days (N=4). 6 rats were also sacrificed without surgery for naïve flow cytometric comparison.

- *Spinal root avulsion behavioural groups:*

64 rats were used for behavioural analysis of a spinal root avulsion injury.

Naïve (N=6), sham operated (N=6), and L5 unilateral spinal root avulsion (SRA) (N=6) rats were behaviourally tested daily for 14 days and then sacrificed. Additionally rats

underwent SRA and were administered (i.p daily for first week then every other day for second week) riluzole (N=6; 4mg/kg. Sigma-Aldrich, UK.), minocycline (N=6; 40mg/kg. Sigma-Aldrich, UK.), and HCl-vehicle (N=6; 0.1M identical volume) and were sacrificed on day 14. All tissue was then processed for immunohistochemical analysis.

SRA rats were also given 3 isolated doses (days 11, 18, and 21) of carbamazepine (N=6; 32mg/kg, and 64mg/kg. Sigma-Aldrich, UK.), amitriptyline (N=6; 30mg/kg, and 64mg/kg. Sigma-Aldrich, UK.), and 45% 2-hydroxypropyl-beta-cyclodextrin-vehicle (N=6, identical volume. Sigma-Aldrich, UK.) and behaviourally assessed for 30 days (for Carbamazepine and Amitriptyline). Delayed minocycline (N=5 40mg/kg) and riluzole (N=5 4mg/kg) treatment groups were assessed over a period of 4 weeks with treatment given in the second and third weeks of the study. Tissue was collected but not processed for presentation in this thesis.

2.2: Surgery

Dorsal root avulsion and dorsal root rhizotomy:

Male Wistar rats were deeply anaesthetised with 4% isofluorane (Abbott Animal Health, U.K.) in 1.5L/min of O_2, and a hemi-laminectomy of the lumbar L4-L6 region of the cord was performed involving incision of the dorsal skin surface, exposure of the L1-3 vertebrae, removal of the dorsal vertebral processes and incising the dura mater. A local anaesthetic application of 2% xylocaine (Abbott Animal Health, U.K.) was made to the exposed dorsal surface of the lumbar cord, before the corresponding L3-L6 dorsal roots were identified and isolated with fine jeweller forceps (Fine Science Tools, U.K.). These roots were then carefully pulled from the cord, modelling an avulsion injury, or transected (rhizotomised) with fine micro-scissors (Fine Science Tools, U.K.). Sham laminectomy surgery was also performed which included all of the above procedure, including exposing the dorsal surface of the cord and incising the dura, but excluding avulsion or rhizotomy of the roots. Overlying muscle and skin were resutured with 3.0 ethicon sutures, and topical auromycin antibiotic (Abbott Animal Health, U.K.) applied to the external surface.

Spinal Root avulsion:

For sensory behavioural analysis to be performed post injury, an injury paradigm of avulsion that allows for evoked responses was required. A single spinal root avulsion model was designed where only the L5 root is avulsed, leaving the L4 root and corresponding plantar paw dermatome intact. Male Wistar rats again were anaesthetised with 4% isoflurane in 1.5L/min of O_2. An incision was made ipsilaterally to the iliac crest, the L5 lateral vertebral process identified and removed exposing the L5 spinal root. The L5 spinal root is then isolated with curved watchmaker forceps distally from the DRG and then carefully pulled from the cord. In this way both the L5 dorsal and ventral roots are avulsed from the cord. Sham surgery included all of the above procedure, excluding avulsion of the L5 spinal root. Overlying muscle and skin were resutured with 3.0 ethicon sutures, and topical antibiotic applied to the external surface. A major benefit of this model over multiple DRA and DRR surgery is that a lumbar laminectomy is not required as a surgical control, and so that spinal column does not become distorted, and trauma is directed only to the nerve roots and entry zones, more closely mimicking the neuropathy seen clinically.

2.3: Behavioural analysis

Injury paradigm:

The benefits of the SRA injury model over multiple DRA and DRR is that it provides an opportunity for a deafferentation neuropathy to be analysed through evoked behavioural responses. The L4 and L5 spinal roots innervate the plantar surface of the rat hind paw, and the dermatome border runs diagonally along the rat hind paw plantar surface, from the middle digit through the distal surface of the heel. To test the development of evoked border-zone sensitivity, a condition seen clinically after brachial and/or lumbar plexus avulsion injury (Htut et al., 2006;Havton and Carlstedt, 2009), it is this area of the hindpaw that will be stimulated. The red circle in Figure 1 indicates the area of testing which best avoids pressure pads and is most central on the hindpaw for equal and consistent distribution of body weight through the paw. Three tests were used to analyse sensory and motor deficits after SRA; a horizontal ladder, mechanical stimulation, and thermal stimulation.

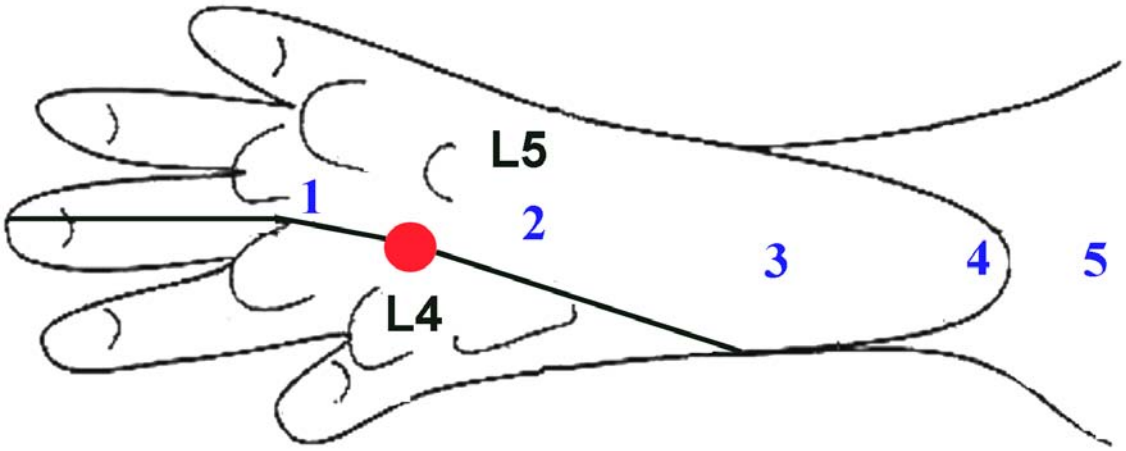

Figure 2.1: Behavioural testing of the rat plantar hind paw. Diagram modified from Takahashi *et al.*, 2003. The area for mechanical and thermal testing is at the border of the L4 and L5 dermatomes, avoiding paw pads as indicated by the red circle. Blue numbers indicate locomotor foot fault scoring. A 5-point system was designed and depended upon plantar foot placement on the ladder rung. Scoring was thus: 1 = normal plantar step with toe grip on rung, 2 = mid-plantar placement without toe grip on the rung, 3 = heel placement on rung, 4 = foot slips off rung and 5 = foot completely misses a rung either at the toe or heel.

Acclimatisation:

54 male Wistar rats of 150-175g were acclimatised to the animal unit and cages for 2 days before handling. After such time they were acclimatised to the behavioural room, ladder preparation, and Perspex test boxes (Ugo Basile, Italy) for 2 days before stimulus testing. Each test was performed in the morning (unless stated otherwise) at the same time before cages were cleaned to prevent external factors effecting behaviour (Vissers et al., 2003). Animals would always be tested from the least stressful and intensive test (ladder) first, and the most intensive stimulus (thermal) last, to prevent effects of one test interfering with another and to minimise stress. It was assumed that acclimatisation was reached when exploratory behaviour of the rats ceased and grooming began in the test boxes. Each animal was tested for no more than 2 hours before being placed back in home cages to minimise stress and to allow feeding. Animal groups were blinded throughout the experiment.

Horizontal ladder test:

To test the development of motor deficits after avulsion of the L5 ventral root a horizontal ladder set-up was used. A ladder was propped no more than 6 inches over a table and attached to a cardboard cylinder and dark box at one end (Figure 2).

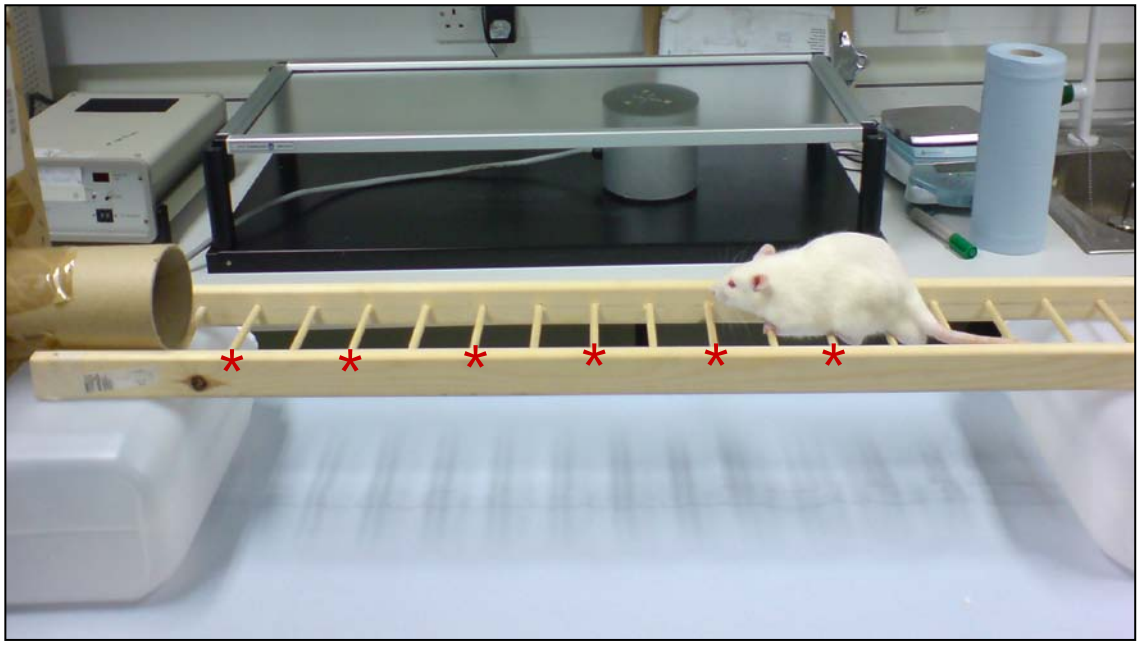

Figure 2.2: The horizontal ladder test for locomotor function. After a few days of exposure the animal voluntarily walks across the ladder into a tunnel at the far end. Red asterisks denote the rungs on which the injured hindlimb will be scored for foot faults in frame-by-frame video analysis.

Rats underwent 2 weeks training on the ladder every other day. Rungs were evenly spaced allowing the rat to remember rung spacing. This allows testing the ability of the animal to recruit spared lower motor units of the L4 ventral horn to perform a pre-trained task. This is opposed to changing the rung spacing every day. This tests a rats ability to accurately recruit, control, and alter coordination of higher motor neurone activity of the brainstem and spinal cord, for each rung spacing, and is used notably in spinal cord injury paradigms (Maier et al., 2008;Metz and Whishaw, 2002). After the training period each rat that was placed at one end of the ladder would naturally and independently walk across the ladder in a quadrupedal motion (each ipsilateral hind-paw placement occurs every other rung), rarely misplacing a step, and finally entering the cylinder. On the day of base-lining (day 0) the rats were set across the ladder three

times and video recorded from the left side from a raised position (Figure 2). Surgery was then performed either on the same day or next day. Post operative tests were performed on days 1, 3, 5, 7, 9, 11 and 14 for untreated groups: naïve, sham SRA, and SRA, and sacrificed on day 14. Drug treatment groups did not undergo locomotor testing.

Quantitative video analysis was only performed at the end of the experiment to prevent bias. Videos were slowed down for detailed frame-by-frame analysis of the ipsilateral hindpaw placement in two ways. The first type of analysis quantified the total number of rung missteps out of 6. The second answered the question of what type of foot placement is most prominent across 6 rungs (foot fault score). 6 rungs were assessed ipsilaterally (Figure 2.2). Figure 2.1 describes the score the rat will receive when balancing on a certain area of the plantar surface.

Mechanical plantar aesthesiometer ('Von Frey'):

For behavioural assessment of tactile hypersensitivity readings were taken using an automated plantar aesthesiometer (Ugo Basile, Italy). This consists of a movable actuator that lifts a blunt probe at a controlled force rate onto the plantar paw surface. This rate was set at 1.7 grams/second with a cut off weight of 50 grams and latency of 30 seconds. This experimental set-up benefits from the removal of observational bias, human error, and variable force applied by the investigator experienced with manual Von Frey hairs. The mechanical aesthesiometer has greater accuracy (to nearest 0.1 gram) and the weight incurred on the plantar paw increases at a linear rate from 0 to 50g, whereas manual hair numbers have an exponential force increase, with large force differences at higher hair values between adjacent hairs. Rats were acclimatised and baselined, and then tested post operatively, in a similar way to the manual hair investigation. The probe made contact with the same plantar area, and increased force until the foot was voluntarily withdrawn. A positive response was determined as a single voluntary flexion withdrawal of the foot, with or without foot licking or biting, from the meshed flooring during the increasing weight of the probe. Each limb was tested 3 times with an interval of 5 minutes to prevent habituation to the stimulus, and readings were taken ipsilaterally and contralaterally and averaged. Post operative tests were performed on days 1, 3, 5, 7, 9, 11 and 14 for untreated groups: naïve, sham SRA,

and SRA, and sacrificed on day 14. For post operative time points in treatment groups see section 2.1.4.

Thermal plantar test ('Hargreaves'):

The automated thermal plantar test in accordance with previous literature (Hargreaves et al., 1988) consists of a glass panel raised 8 inches above a table, on top of which are placed the Perspex test boxes. An infrared aesthesiometer probe (Ugo Basile, Italy) makes contact with the glass, and when active, heats up the glass and plantar paw surface of the rat above it providing a noxious heat stimulus. Infrared intensity was set at 50 units corresponding to 150mW of power applied per cm^2. A safety cut off was set at 20 seconds latency to prevent tissue damage, and indicated non-responsiveness. Rats were daily acclimatised to the test boxes for ten minutes prior to testing until exploratory behaviour stopped. Once baselined rats were then tested post operatively in an identical way to the automated mechanical aesthesiometer. A consistent withdrawal response was maintained at approximately 8 seconds at baseline. Post operative tests were performed on days 1, 3, 5, 7, 9, 11 and 14 for untreated groups: naïve, sham SRA, and SRA, and sacrificed on day 14. For post operative time points in treatment groups see section 2.1.4.

Weight measurements:

The marker of spontaneous neuropathic pain, autotomy, did not occur in the SRA model, as the hind-paw was only partially de-afferented. Instead weight loss or rate reduction (Willenbring et al., 1994) was analysed. A reduction in growth rate after surgery was taken as a sign of a loss of appetite or motivation to feed, indicative of a developing spontaneous and chronic pain state. Weight was measured every other day, before behavioural testing, for the duration of the training period and post-injury period. Attention was taken to make sure rats did not lose more than 15% of their original body weight and remained in a healthy condition. Weight changes were graphically represented as a histogram of mean daily weight gain.

2.4: Pharmacotherapy

Two treatment paradigms for neuropathic pain were assessed in this work. Firstly the prevention of hypersensitivity development by immediate pharmacological intervention, and secondly, the treatment or reversal of an established neuropathic pain state. These methods of treatment have translational possibilities in either acute or chronic root avulsion injured patients respectively. Antidepressant, anticonvulsant, neuroprotective, and anti-neuroinflammatory drugs were assessed. All drugs were administered to the animals intra-peritoneal and the experimenter was blinded throughout the experimental procedure.

Single dose treatment groups:

Conventional neuropathic pain treatments were explored as a treatment option for an established neuropathic deafferentation pain. Amitriptyline (Amitriptyline Hydrochloride, Sigma-Aldrich, UK.) dissolved in saline (30mg/ml), and carbamazepine (Sigma-Aldrich, UK.) dissolved in 45% 2-hydroxypropyl-beta-cyclodextrin (30mg/ml, Sigma-Aldrich, UK.) were administered at 32mg/kg on post operative days 11 and 13, and at 64 mg/kg on days 18 and 21, alongside a vehicle treatment group, after confirmation of the establishment of hypersensitivity at 5 and 7 days. One hour after treatment thermal and mechanical hypersensitivity was assessed in the way described in section 2.1.3. On days 14 and 20 animals were behaviourally assessed but without further treatment to ascertain whether hypersensitivity had returned in the absence of treatment. Animals were sacrificed on day 21.

Immediate treatment groups:

Two separate drugs were assessed for therapeutic efficacy immediately after injury as a treatment paradigm for prevention of neuropathic pain development. Minocycline hydrochloride (Sigma-Aldrich, UK.) was dissolved in saline (100mg/ml) and administered at 40mg/kg, and riluzole (Sigma-Aldrich, UK.) was dissolved in 0.1M HCl (10mg/ml) and administered at 4mg/kg, immediately after injury and every day for 7 days (days 0-6 p.o.), then every other day up to 14 days (days 7, 9, 11, and 13 p.o.), along with a vehicle group. Immunohistochemical effects were assessed in two

deafferentation models: DRA and SRA at day 14. Behavioural effects were assessed on post-injury days 1, 3, 5, 7, 9, 11 and 14, each time 24 hours after drug administration.

Delayed treatment groups:

In addition to pre-emptive treatment of minocycline and riluzole, a post-operative treatment regime was studied to ascertain efficacy of these drugs in ameliorating neuropathic pain during treatment, and permanently during drug withdrawal. Drugs were prepared and administered in accordance with the pre-emptive treatment, but given at day 7 every day for a week (days 7-13 p.o.), then every other day for a subsequent week (days 14, 16, 18, and 20 p.o.). Behavioural effects were assessed on post-injury days 3-27, each time 24 hours after drug administration.

2.5: Sacrifice and dissection

The animals were sacrificed by CO_2 asphyxiation until breathing ceased and responsiveness to toe pinch was not detectable. The skin over the sternum was gripped with forceps and incisions made in the abdomen until the diaphragm was fully exposed. The xiphoid process of the sternum was clamped and held up so the diaphragm could be cut. The ribcage was cut bi-laterally and xiphoid process clamped back in a position so as to expose the whole thoracic cavity, with the heart accessible and still beating. A small incision to the left ventricle was made with fine micro scissors and a perfusion-drip needle inserted and clamped into place. The right atrium was identified and an incision made with fine micro scissors, and 0.9% saline was flushed through the hepatic circulation. After 200ml of saline had passed through the circulation, and the exiting fluid from the right atrium and liver was clear of blood, the animal was perfused with 400-500ml of chilled 4% paraformaldehyde (Sigma-Aldrich, UK.) in 0.1M PBS at pH 7.4, until the tissue and limbs were rigid.

The animals were dissected and vertebrae carefully opened with curved malleus nippers (Fine Science Tools, Heidelburg. Germany). The L4-L6 dorsal root ganglia were identified from there location relative to the iliac crest (L6 closest, L5 and L4 rostrally). The DRG were isolated and dissected with fine micro scissors (Fine Science Tools, Heidelburg, Germany) and roots traced back to the DREZ at the corresponding

segmental level. In this way the lumbar cord, from L3 to L6, could be accurately removed. The cords and DRG were then 'post-fixed' (4% PFA in 0.1M PBS at pH 7.4.) for 2-3 hours to ensure full fixation. Tissue was then removed from the fixative and submerged in a graded sucrose solution (10%, 20%, then 30% in 0.1M PBS) for 12 hours in each concentration, or until the tissue had sunk to the bottom of the container indicating elimination of water from the tissue. The ventral and dorsal roots of the spinal cord were trimmed up to the DREZ, dural layer removed, the external surface of the cord dried on a paper towel, and vertically embedded in optimum cutting temperature (OCT) gel through freezing. The spinal cord was then sectioned on a Leica CM 1900 cryostat (Leica, Milton Keynes. U.K.) into 18μm thick transverse sections. Ten to fifteen sections were mounted per Superfrost slide (V.W.R. International, Lutterworth. U.K.), each adjacent section separated by approximately 340μm. L4 and L5 DRG were longitudinally sectioned into 8μm thick sections, with 6 sections sequentially presented on the slide. Slides were air dried for 2 hours and stored in a slide box containing cryoprotectant (120ml ethylene glycol, 200ml PBS, and 200ml sucrose) at -20°C until further use.

2.6: Cell suspension preparation for flow cytometry

After sacrifice and removal of the L3-L6 spinal cord (as described in section 2.1.5), the cord was placed in Ham's F12 medium (Gibco, Paisley. U.K.) on ice. The cord was then divided into ipsilateral and contralateral halves under a microscope through a scalpel incision through the posterior median sulcus and anterior median fissure.

Each half of the cord was placed in a 24 well plate at 37.5°C for 30 minutes with 800ul of F12 + 100ul of Type 1 Collagenase (Worthington. Reading. U.K.) added. The collagenase was diluted and filtered from powdered stock in the ratio 0.125g in 10ml of F12, after which the media was topped up with 100ul of fresh Type 1 collagenase and the cords left again for 30 minutes at 37.5°C. After this time the collagenase was removed by pipette and the tissue was twice washed in 1M Dulbeco's PBS (P.A.A. Yeovil. U.K.). 1ml of BSF2 was added to each well and the tissue carefully dissociated through manual pipette titration, maintaining the cellular integrity but ensuring cell separation. These suspensions were then centrifuged at 1000rpm for 30 minutes. After removal of the supernatant, the pellet was resuspended in 1ml of 1M Dulbeco's PBS

and centrifuged at 600rpm for 5 minutes in preparation for propidium iodide (PI. Invitrogen, Pailey, UK.) single staining and neurone-specific nuclear protein (donkey α-mouse NeuN, Chemicon, Chandlers Ford, Uk.) in conjunction with 4,6-diamidino-2-phenylindole (DAPI. Invitrogen, Paisley, UK.) double labelling.

2.6.1: Propidium Iodide staining for cell death analysis

After cell suspension preparation, the supernatant was removed with a manual pipette and 100µl of 5µg/ml PI (in 0.1M PBS) in 400µl of cell suspension was added to each sample tube in preparation for analysis with an LSR11 flow cytometer (BD Biosciences, Oxford. U.K.). PI is a DNA nuclear stain that is impermeable to unfixed-cells with intact membranes. It specifically labels cells with permeabilised membranes, or in other words, cells that have undergone (but not specifically undergoing) apoptotic or necrotic cell death. In this way, flow cytometry provides a count of dead cells per sample analysed.

2.6.2: NeuN and DAPI staining for identification of cell specific death

After cell suspension preparation, the supernatant was removed and 1ml of DAPI (1:15000) was then added to the pellet for 5 minutes at room temperature. After this incubation, the suspension was again centrifuged at 600rpm/5min, supernatant removed with a pipette controller pipetboy (Pipettboy Acu, Scientific Laboratory Supplies, Nottingham, U.K.) and the cells resuspended in 10ml of 1M PBS PH 7.4. After another centrifuge/wash cycle, and removal of supernatant, the cells were fixed in 1ml 70% ethanol (ETOH) + 2% glucose for 30 minutes at room temperature. After this time the suspension was centrifuged at 600rpm/5min, supernatant removed, resuspended in 1M PBS PH 7.4, again centrifuged at 600rpm/5min, and supernatant removed. 1ml of the primary antibody donkey α-mouse NeuN was added to the cells at a concentration of 1:1000. The suspension is incubated for 30 minutes at 37.5°C. After which time the suspension was centrifuged at 600rpm/5min supernatant removed, resuspended in 0.1M PBS PH 7.4, and centrifuged at 600rpm/5min. The remaining pellet was suspended in 1ml of donkey α-mouse fluorescein isothiocyanate (FITC 1:400) (Jackson ImmunoResearch Labs, Suffolk. U.K.), and again incubated for 30 minutes at 37.5°C. Two more centrifuge and PBS wash cycles (see above) occurred before the suspension

was placed on ice. 500µl of the suspension was then isolated for flow cytometric analysis with an LSR11 flow cytometer.

2.6.3: Preparation of controls for gating parameters

Negative staining controls were used for PI flow cytometry. 400µl samples of unstained cell suspension (see section 2.2.1) in 100µl 0.01M PBS were analysed. The scatter plot produced gives a gating parameter for positive against negative staining known as the P1 box (see section 3.4.1a), that can be kept constant throughout the experiment, and accurately divides stained and non-stained cells. Gating parameter controls were also prepared for NeuN/DAPI labelled cell suspensions. These consisted of unstained (see section 2.2.1), primary antibody only, secondary antibody only, and DAPI only cell suspensions (modified from section 2.2.1b). The resultant scatter plots classified the positive against negative fluorescent staining gate parameters of FITC and DAPI lasers within the flow cytometer. In this way focused analysis of the positively stained cell suspensions is performed (see section 3.4.1b).

2.7: Terminal deoxynucleotidyl transferase-mediated dUTP nick end (TUNEL) labelling

Slides were washed twice in 0.01M PBS-Tween20 for 15 minutes after removal from -20°C cryoprotective storage. The sections were then encircled with a hydrophobic PAP-pen prior to incubation in equilibrium buffer [potassium cacodylate 200mM, pH 6.6 at 25^{o}C, Tris-HCL 25mM, pH 6.6 at 25^{0}C, DTT 0.2mM, BSA 0.25mg/ml, and cobalt chloride 2.5mM (Promega. Wisconsin. U.S.A)], 100ml per slide for 10 minutes at room temperature. The equilibration buffer was then tapped off, and approximately 100µl of the freshly made incubation mix (98µl equilibrium buffer, 1µl of biotinylated nucleotide mix, and 1µl of TdT enzyme (Promega. Wisconsin. U.S.A) was applied to each slide. Parafilm (Promega. Wisconsin. U.S.A) was placed over the top of the slide to ensure direct and even distribution of the enzyme mix and the tissue through removal of any air-liquid interface. These slides were incubated for 1 hour at 37°C in a humid chamber, ensuring they did not dry out. The slides were then incubated twice in 2x Standard Sodium Citrate (SSC) buffer (diluted from 20x SSC (Promega. Wisconsin. U.S.A.) in distilled water) for 15 minutes each, denaturing the TdT enzyme and ending

the reaction. The SSC was removed through 3 washes in PBS for 5 minutes each. The slides were then incubated for 2 hours in extra-avidin conjugated FITC (Ex-Av FITC 1:400. Sigma, Poole, U.K.) at room temperature in a humidifier, after which time the slides were again washed 3 times in 0.01M PBS for 5 minutes and coverslip mounted with 0.01M PBS-glycerol (1:8) and nail varnish seal. These were then stored at 4°C in the dark until analysis.

2.8: Single immunohistochemical staining protocol

Slides were removed from cryoprotective storage, rinsed in two washes of PBS-Tween20 for 15 minutes each and prepared in the same manner as described above for TUNEL staining. 10% normal donkey or goat serum (NDS/NGS) was applied to the tissue for 1 hour in preparation for antibody incubation. NDS was used if the secondary was derived from donkey, and NGS used if the secondary was derived from goat. The excess serum was tapped off the slide, the primary antibodies were added. The primary antibodies used to label primary afferent terminals, glia, neurones, leukocytes, and vasculature are listed and described in Table 2.1. Detrimental effects of root injury apon the spinal cord and peripheral nerves will be ascertained using these immunohistochemical markers.

The dilutions indicated were made from stock antibody aliquots of 1:5 or 1:10, stored at -80°C, through serial dilutions with 0.01M PBS-0.2%TritonX-0.1%NaAzide. Primaries were incubated for 24 hours at room temperature in a humidifier to prevent the slides from drying out. After this time the slides were washed thrice for 5 minutes each in 0.01M PBS-Tween20, and the secondary antibody added.

For studies involving L3-L6 DRA and DRR spinal cord (Results 1) either donkey α-mouse, donkey α-rabbit specific tetramethylrhodamine-5 isothyocyanate (TRITC 1:400) (Jackson ImmunoResearch Labs, Suffolk. U.K.), or Ex-Av FITC (1:400) (Sigma, Poole. U.K.), were applied specific to the species of primary. The slides were incubated for 2 hours in a dark humidifier at room temperature, and then washed 3 times for 5 minutes each in 0.01M PBS, and mounted in accordance with Chapter 2.3.

For studies involving L5 SRA spinal cord and DRG (Results 2-3) either donkey α-rabbit Alexa Fluor 594 (1:1000), goat α-mouse Alexa Fluor 594 (1:000), or donkey α-rabbit Alexa Fluor 488 (1:1000) (Invitrogen, Paisley. U.K.), were used and correspond to a spectrum emission wavelength of TRITC (red-594) and FITC (green-488). In addition Ex-Av FITC (1:400) (Sigma, Poole, U.K.) was also used for IB4-biotin DRG staining.

The rhodamine and fluorescien secondaries were replaced by Alexa Fluors during the project due to laboratory centre preference, superior staining quality, and quicker incubation time (1 hour). However image analysis between old and new secondary antibodies was kept separate.

Table 2.1: Primary antibodies and lectins used

Primary antibody	*Abbreviation*	*Concentration and species*	*Distributor*	*Description of specificity*
Rat-CD68	ED-1	1:1000 Mouse	Serotec. Oxford. U.K.	Specific to activated microglia and the majority of tissue macrophages, and also weakly by blood granulocytes.
Rat Endothelial Cell Antigen	RECA-1	1:100 Mouse	Serotec. Oxford. U.K.	Specific to a cell surface antigen present on the endothelia of the vasculature.
Ionized calcium-binding adapter molecule-1	Iba1	1:1000 Rabbit	Wako. Neuss. Germany.	Specific for a Ca2+-binding peptide produced by activated monocytes and microglial cells.
Glial Fibrillary Associated Protein	GFAP	1:1000 Mouse	Chemicon. Chandlers Ford. U.K.	Specific to intermediate filament proteins within astrocytes processes, and satellite cells.
Calcium binding protein- S100	S100	1:1000 Mouse	Chemicon. Chandlers Ford. U.K.	Specific to glial and ependymal astrocyte cell bodies, including cytoplasm and nucleus.
Neurone-specific Nuclear Protein	NeuN	1:1000 Mouse Rabbit	Chemicon. Chandlers Ford. U.K.	Specific to mature neuronal cell bodies but not proliferative cells.
Calcitonin Gene-Related Peptide	CGRP	1:2000 Rabbit	Sigma. Poole.U.K.	Specific marker of the terminals of small unmyelinated peptidergic afferents in the dorsal horn.
Biotinylated-Griffonia (Bandeiraea) Simplicifolia Isolectin-B4	IB4-biotin	1:200 Lectin	Affiniti. Exeter. U.K.	Specific to unmyelinated non-peptidergic afferent terminals in lamina II-i. Also a marker for agglutinate B-type red blood cells, microglia, and blood vessels.
Rat neutrophils	Anti-neutrophil	1:1000 Rabbit	Gift from Prof H. Perry, Southampton University (Bolton and Perry 1998)	Raised against rat neutrophils, at Southampton University.
Heavy (200kDa) Neurofilament	N52/NF200	1:16000 Mouse	Sigma. Poole. U.K.	Specific marker for myelinated large A-fibre sensory afferents in the DRG.
Transient receptor potential cation channel, subfamily V, member 1	TRPV1	1:2000 Rabbit	Chemicon Chandlers Ford. U.K.	Specific marker for receptor present in small and medium sized sensory neurones, which is activated by heat, capsaicin, and vanilloid compounds.
Activating transcription factor 3	ATF3	1:200 Rabbit	Santa-Cruz Wembley. U.K.	Specific marker for cellular stress or injury.

2.9: Double immunohistochemical labelling protocol

For identification of sensory cell bodies within a DRG section, NeuN was applied alongside the specific subpopulation or injury marker, such that anti-mouse NeuN was used alongside biotin-IB4, anti-rabbit CGRP, anti-rabbit ATF3, and anti-rabbit TRPV1, and anti-rabbit NeuN was used alongside anti-mouse N52. The two primary antibodies

were made up in solution together whilst maintaining the dilution quoted in Table 1, and applied to the slide in an identical way as single labeling for 24 hours, then three 5 minute washes in 0.01M PBS+Tween20. The two corresponding Alexa Fluor secondary antibodies were applied separately for 1 hour each. Each secondary was applied for an hour and then washed off in three washes of 0.01M PBS+Tween20 for five minutes each and mounted as described in sections 2.3/2.4.

For cases of identifying cell specific cell death, a TUNEL assay in conjunction with cell specific immunohistochemistry was performed. Astrocytes, microglia, neutrophils and neurones were labelled and analysed in this way. In all cases TUNEL staining was undertaken first (see section 2.3), prior to normal donkey serum being applied, so as not to interfere with the sensitive TdT-fragmented DNA binding. Before the secondary antibody ExAv FITC (1:400) is added, after 3 sets of 5 minute washes in 0.01M PBS+Tween20, either α-mouse S100, α-rabbit Iba1, α-rabbit 'anti-neutrophil', α-mouse ED1, or α-mouse NeuN (all dilutions indicated in Table 1) were added to the slide. These were then incubated at room temperature in a humidifier for 24 hours. After which time the slides were washed 3 times for 5 minutes each in 0.01M PBS+Tween20, before Ex-Av FITC (1:400) and α-rabbit TRITC (1:400) or α-mouse TRITC (1:400) (dependent upon the primary antibody species) were sequentially applied to the slide. The slides were incubated with the first secondary antibody for 2 hours at room temperature in a humidifier, covered from light with foil for 2 hours. After such time, the slides were washed 3 times for 5 minutes each in 0.01M PBS+Tween20 and the next secondary applied to the slide and the process repeated. The coverslipping procedure is identical to the method for TUNEL (see section 2.3) and general immunohistochemistry (see section 2.4), and the slides were stored at 4°C in the dark prior to analysis.

2.10: Toluidine blue staining protocol

In many cases identification of cell types via immunofluorescence is dependent upon epitope expression within a cell. If this epitope is not available due to the fixation process, or is in low quantities in the cell, or the antibody has poor specificity, then staining will be variable. For identification of general morphological changes and neuronal and glial cell numbers within the dorsal horn after injury, independent of

antibody-epitope binding, a metachromatic dye called toluidine blue was used that stains cell cytoplasm. Slides were removed from cryoprotective storage and rinsed in two washes of 0.01M PBS-Tween20. The slides were then dipped into 0.1% (w/v) toluidine blue in 0.1 PB PH 7.4, and incubated for 30 seconds. After which they were dipped briefly in distilled-H2O. The slides were then dehydrated through the alcohols: 70%, 90%, and 100%, twice in each dilution for 2 minutes. The slides were than incubated in xylene, twice for 2 minutes, in fume cupboard. The slides were mounted with coverslips in synthetic resin Depex Polystyrene (DPX. Sigma-Aldrich, UK.) and allowed to dry in the fume cupboard.

2.11: Microscopy

Photography:

All fluorescence microscopy was undertaken 1-2 days after the immunohistochemical incubation, to reduce effects of faiding of fluorescence from the fluorochromes, but was not essential for toludine blue staining. Photographs of all immunohistochemical markers were taken with a digital camera (Hamamatsu Photonics. Welwyn Garden City. U.K.) connected to the microscope, at a constant exposure time of 1.223 seconds to allow comparison across groups in staining intensity. Areas of cord and segmental level were all kept consistent between animals and experimental groups. For L3-L6 DRA and DRR, 6 sections were selected randomly but with the intent of obtaining a range of segmental levels within the whole deafferented area, and the dorsal horn photographed. In the case of ED1 staining both dorsal horn and DREZ/dorsal columns were photographed as infiltration of blood borne macrophages occurs through the damaged DREZ in root injury models, as well as across microvascular endothelial tissue in the deeper dorsal horn. For L5 SRA, 3 to 4 sections were selected from both L5 and L4 regions for comparable analysis of injured versus uninjured segmental levels. Differences in segmental level were identified anatomically (Molander et al., 1984). Magnifications of photographs for analysis were either 10x or 20x optical zoom. For DRG images, photographs were taken of sections with equal distributions of neuronal bodies at either 10x or 20x optical zoom at a constant exposure time of 1.223 seconds.

Percentage staining:

For immunohistological staining that could not be accurately measured or represented by counts alone, a percentage positive staining was calculated for GFAP, IB4, CGRP, Iba1, ED1, and RECA-1. Each photograph was grey-scaled through Adobe Photoshop CS2, removing background staining intensity and non-specific staining, and cropped to isolate the entire area of interest. For CGRP and IB4 these were the medial portion of the superficial laminae. For GFAP and Iba1 the medial portion of the dorsal horn was analysed. For RECA, medial portions of the dorsal and ventral horns, as well as lamina X (central canal) were analysed. These photographs were manipulated by intensity gradient scaling with Qwin V3 (Leica, Milton Keynes. U.K.). This involves converting the grey scale into a binary pixel measure. All positively stained pixels, measuring above background levels, is set as 1 (positive), and staining below this is given 0 (negative), for the marker of interest. Areas of cavitation and necotic tissue that could give false positive and false negative staining could be cropped from the image before analysis. In the Q-win programme, a frame area of 200000 pixels^2 is placed in the area of interest for IBa1, GFAP, RECA-1 and ED1 and the area covered must be exclusively tissue. For IB4 and CGRP, this box is 10000 pixels^2 and all four corners must be in contact with positive staining, to prevent false negative calculation from incorrect placement. This box and the area of the cord are kept constant, examples of which are shown in figure 2.3 for each of the different markers. Sections with extensive cavitation or distortion are not analysed, and the adjacent section is taken instead. Positive staining quantity therefore, is given as number of positive pixels of the total pixel number in the given area; a percentage. This data manipulation allows easy comparison between injury groups.

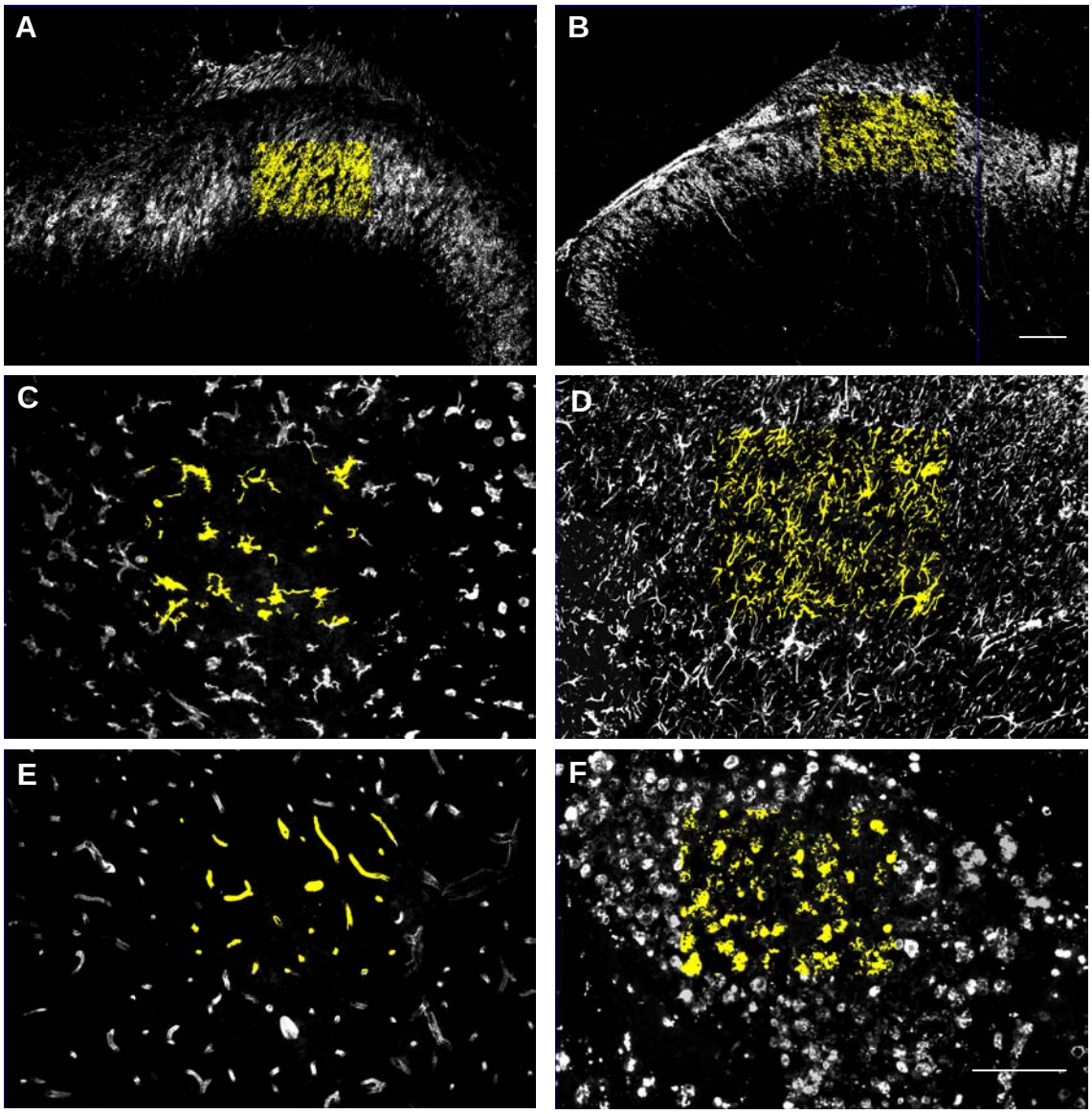

Fig 2.3: Method of Q-win percentage density staining calculation for CGRP, IB4, ED1, RECA-1, GFAP, and IBa1. In all cases photos have been greyscaled, removing background staining leaving only positive staining. Yellow boxes represent positive staining within the area of interest for each immunohistochemical marker. These boxes are kept constant in size and placement for each marker. *A*. Q-win analysis for IB4 staining in lamina II. A box of 10000 pixels^2 is placed within an area of positive staining. *B*. Q-win analysis for CGRP in lamina I. Similarly to IB4, a box of 10000 pixels^2 is placed. *C-E*. Q-win analysis for IBa1, GFAP, and RECA-1 staining in the dorsal horn respectively. A box of 200000 pixels^2 is used. *F*. Q-win analysis for ED1 staining in the dorsal columns, using a 200000 pixel box. Similar analysis was undertaken for the dorsal horn. Scale= 100μm

Counts:

Counts for DRG subpopulations using CGRP, IB4, N52, ATF3, and TRPV1 were taken directly from the microscope. Each section was counted sequentially until 400 NeuN

positive cells with a visible nucleus were identified. Within these sections the total number of DRG subpopulation was counted, providing a percentage of total cells recorded.

Positive cell counts for TUNEL nuclei and neutrophils were taken directly from the slide through a Leica DM-RB Fluorescence Microscope (Leica. Milton Keynes. U.K.). Counts were restricted to the dorsal horn and dorsal columns (including the dorsal root entry zone) for TUNEL and neutrophils. DAPI was used alongside TUNEL to prevent false positive counts. Counts were averaged from 5-6 sections per animal, to give a mean count for each animal throughout the injury zone. For NeuN counts within DRA, DRR, SRA, sham-SRA, and naive spinal cord, a magnification of x10 was used to take photographs of the dorsal horn, and total numbers of positive neurones were counted in lamina I to III (Figure 2.4) according to anatomical boundaries (Molander et al., 1984) for all time points. A line, parallel to the superficial laminae was drawn in the dorsal horn using photoshop (Adobe) approximately 270μm from the extremity of the dorsal grey matter to isolate the area of quantification. Total counts from lamina I-III were preferred to isolate boxed areas, as this method of quantification analyses the total neuronal pool. To clarify whether neurones were lost after root injury, or whether it is just the NeuN epitope being reduced within neurones, the general histological dye toluidine blue was used. A selection of neurones within the centre of the dorsal horn were counted rather than total number, as the dorsal horn could not be delineated in many cases, as glia are also label with this dye. A 263μm by 158μm box was drawn around the medial section of the dorsal horn incorporating a section of laminae I-III and kept consistent between sections, and neuronal numbers were counted. Neurones could be distinguished from glia due to their more rounded and larger appearance. Also Tol Blue counts within the dorsal horn could only be taken at 1 and 2 days, as staining intensity of glia around dorsal root entry zone and superficial dorsal horn after these early time points obscured neuronal identification. Counts were also taken in the ventral horn for SRA, sham-SRA, and naïve animals of motor neurones in L5 and L4, using NeuN and Tol Blue staining. Motor neurones are distinguishable from interneurones as much larger and distinctly located in ventro-lateral areas in the L4 and L5 segments (Fig 2.4). Few motor neurones are also found in the ventro-medial areas in L5 that are also counted, and become more numerous in L6 (Fig 2.4).

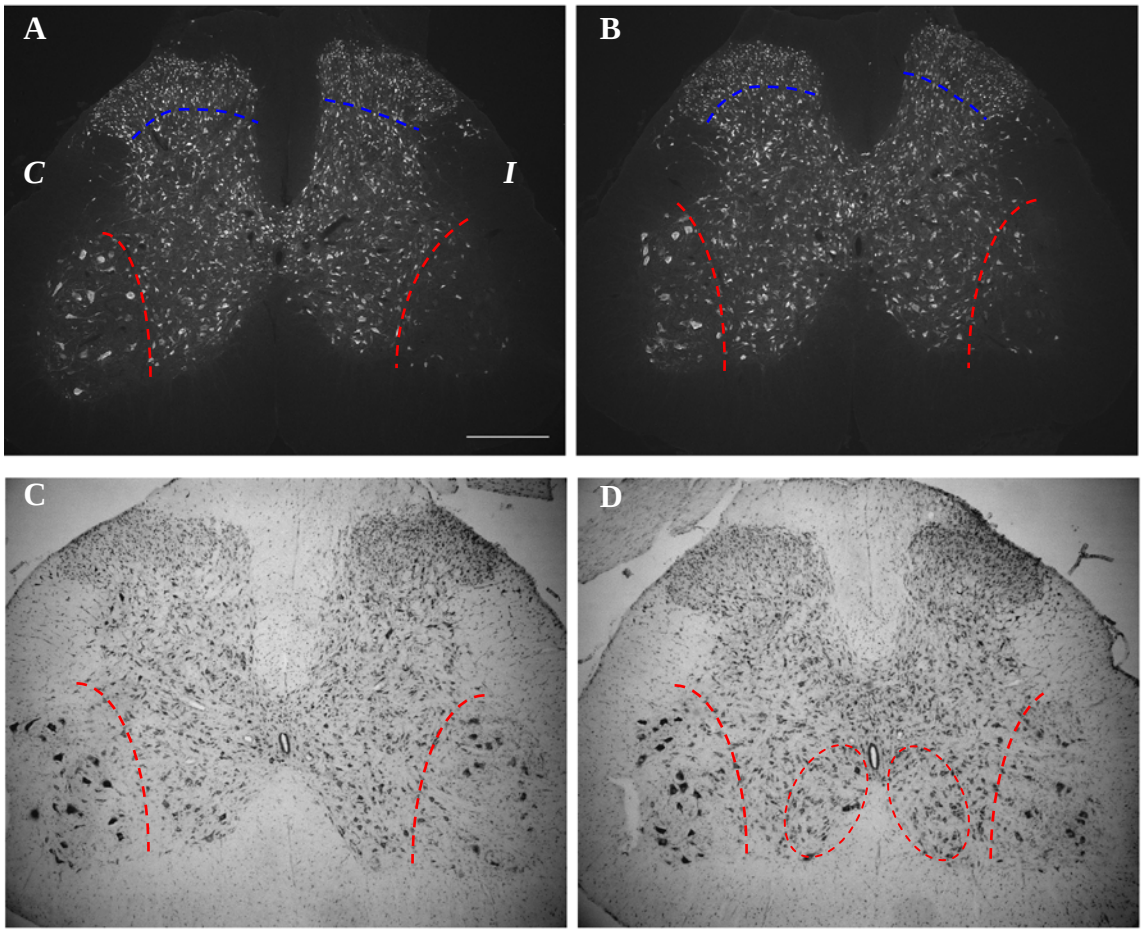

Fig 2.4: Method of dorsal horn and motor neurone selection. 2 week SRA spinal cord stained with NeuN at L4 (A) and L5 (B) segmental levels, and Tol Blue at L4 (C) and L5 (D) segmental levels. I and C represent ipsilateral and contralateral sides. Blue dotted lines represent the area of quantification of dorsal horn neurones. This line is placed parallel to extremity of superficial dorsal horn at 130µm. Motor neurones could be easily identified with NeuN and Tol Blue staining and were contained within the areas denoted by the red dotted lines. Scale= 400µm

2.12: Statistical analysis

All data is graphically presented as a time series after injury. Analysis was undertaken by the statistical method 'repeated measures' 'two-way analysis of variance' (ANOVA), using SPSS version 15.0 (SPSS UK Ltd. Woking. U.K.), due to the continued nature of data collection across time points within a group. The Shapiro-Wilks normality test was used to indicate a Gaussian distribution within groups. Fisher's Least Significant Difference (LSD) post-hoc test was used, as it is the most widely used and of medium conservativeness to differences in data, to identify significant difference amongst the data groups in question. All P-value significance is indicated within corresponding graphs, presented as an asterisk by the repective data

point using the notation: P<0.05 (*/#/x/+), P<0.01 (**/##/xx/++), and P<0.001 (***/###/xxx/+++).

For immunohistochemical analysis of DRA and DRR sham, and naïve groups, day zero is the naive group, and sham groups are presented as a comparison for the individual time points of 1 and 14 days post injury. Both ipsilateral and contralateral values are represented. Comparisons are made between ipsilateral vs contralateral (*), injury vs naïve (#), injury vs sham (x), and DRA vs DRR (+), above the respective data point.

For behavioural groups comparisons were made in several ways: *1) Untreated:* SRA-untreated, SRA-sham, and naïve; *2) Immediate treatment:* SRA-riluzole, SRA-minocycline, and SRA-HCl vehicle; *and Single dose treatment:* SRA-carbamazepine, SRA-amitriptalyine, and SRA-cyclodextrin-vehicle; and *3) Delayed and treatment withdrawal:* SRA-minocycline and SRA-riluzole.

1) The SRA group was compared against naïve and sham groups for specific time points and between injured and uninjured hindlimbs within groups, using significant difference notation: against baseline (#), ipsilateral vs contralateral (x), injury vs naïve (*), and injury vs sham (+) above the respective data point.

2) The immediate minocycline and riluzole drug treatment groups, and single dose treatment groups of amitriptyline and carbamazepine, were compared against vehicle their pre-operative baseline values and between injured and uninjured hindlimbs using significant difference notation: against vehicle (*), against baseline (#), ipsilateral vs contralateral (x).

3) The delayed minocycline and riluzole drug treatment groups were compared against their pre-operative baseline levels (#), and between injured and uninjured hindlimbs (x).

Chapter 3: Histological assessment of dorsal root avulsion and dorsal root rhizotomy, as rat models of root avulsion injury.

3.1: Introduction

3.1.1: Current models for avulsion

Rhizotomy is the surgical severance of spinal nerve roots between the DREZ and dorsal root ganglia (DRG), and unlike avulsion, is not a traction severance of the nerve root and does not lead to direct damage to the spinal cord. It is conducted experimentally and therapeutically rather than presenting in a pathophysiological setting. Clinical uses are to alleviate intractable pain from joints or other peripheral targets (Loeser, 1972), such as in cases of multiple sclerosis to alleviate trigeminal neuralgic neuropathic pain (Kondziolka et al., 1994), as well as treatment for radiation-induced plexopathy pain (Teixeira et al., 2007). It is also undertaken to alleviate symptoms of neuromuscular conditions, such as severe muscle spasms presented in cerebral palsy (Hodgkinson et al., 1997) and spastic diplegia (Tilton, 2009). However, this treatment can itself often lead to post operative neuropathic pain states (Hesselgard et al., 2007), and in some pre-clinical laboratories can induce neuropathic pain (Eschenfelder et al., 2000;Asato et al., 2000;Song et al., 2003), although this is controversial (Sukhotinsky et al., 2004). Due to the severity of this deafferentation, this treatment technique is now not used in isolation, and has been modified with the addition of stereotactic radiosurgery (Teixeira et al., 2007), intrathecal baclofen (Tilton, 2009), and deep brain and central nervous system stimulation (Patwardhan et al., 2006).

In preclinical research rhizotomy is often used as a model of dorsal root injury. When modeling fully deafferented limbs**,** due to the nature of the injury, hyperalgesic and allodynic responses cannot be elicited to evoked sensory tests. However, qualitative measures such as autotomy, including vigorous scratching of the deafferented limb, can be detected after unilateral brachial plexus rhizotomy (Kriz and Rokyta, 2000) and lumbosacral rhizotomy (Lombard et al., 1979). This extreme behaviour is thought to be due to false nociception from abnormal central activity of the dorsal horn and represent

spontaneous pain (Kauppila, 1998). However, this extreme behavior could be a response to an anethetised and flaccid limb (Rodin and Kruger, 1984). In this case, the animal does not recognize the limb as part of its body scheme and attacks it as a foreign object impeding locomotion. An aditional problem with this evaluation method is that there is no scale dictating the level of pain induced (Kauppila, 1998). Minor environmental factors such as stress and animal husbandry (Kauppila and Pertovaara, 1991) can affect the behavior, and ethical reasons prohibit extensive autotomy through the requirement of humane end points to experiments. Weight loss, grooming, and exploratory behavior (Vos et al., 1994) have also been used as measures of spontaneous pain. Both evoked sensory and observational qualitative methods are used as behavioural measures of neuropathic pain (Coderre and Melzack, 1986). However, the presence and extent of autotomy as well as other qualitative measures of pain are at best variable. Indeed autotomy has also been shown to be markedly reduced in animals with higher levels of serotonin and dopamine in the spinal cord (Feria et al., 1992). Autotomy also shows strain dependency (Rubinstein et al., 2003), and only occurs in adult rodents (Vaculin et al., 2005). This suggests an ontogenetical dependence in CNS maturity on the susceptibility for autotomy. However, the proposition that autotomy is a result of neuropathic pain has met with controversy, as adult brachial plexus injury patients do not show autotomy. In addition, autotomic presentations in non-human primate lumbar-avulsion models can be abolished by simple care of wounds (Pioli et al., 2003), and by altering simple housing conditions (Berman and Rodin, 1982).

As stated previously rhizotomy models are inconsistent when it comes to inducing behavioural hypersensitivity. Sheen and Chung ((Sheen and Chung, 1993)) first showed that DRR does not always lead to evoked neuropathic pain behaviour, and suggested afferent connections of the DRG cell body to cord are required for evoked pain sensations. This has been corroborated more recently (Sukhotinsky et al., 2004). Also in agreement, mechanical and cold allodynia, as well as spontaneous pain, induced by tight ligation of L5 and L6 spinal nerves, is completely attenuated by rhizotomy of these injured dorsal roots (Yoon et al., 1996). Contrary to this are studies showing that dorsal root crush, rhizotomy, ligation or partial dorsal root rhizotomy produces transient thermal and mechanical allodynia and hyperalgesia (Colburn et al., 1999;Eschenfelder et al., 2000;Nakamura and Myers, 2000;Song et al., 2003;Rothman et al., 2005), and other studies demonstrating that rhizotomy does not reverse spinal nerve ligation-

induced pain behaviour (Asato et al., 2000;Sheth et al., 2002). Infact neuropathic pain behaviour has been shown to be maintained for up to 4 weeks, with no difference in presentation between injuries distal to the DRG (PNI/SNT) or proximally to it (DRR) (Winkelstein et al., 2001a). In some cases groups have shown an acute development of allodynia after dorsal root transection, but returns to baseline after 7 days (Sheth et al., 2002;Rothman et al., 2005). The development of neuropathic pain behaviour after DRR in some models, gives reason as to why in some scenarios (Sheth et al., 2002) it cannot as a therapy relieve PNI-induced pain; as this is replacing one pain (PNI-induced) for another (rhizotomy-induced) (Sukhotinsky et al., 2004). The inconsistencies between DRR-induced pain outcomes between laboratories may be due to variable injury models, rat strains, or method of data collection, but at present it is unclear why DRR elicits tactile allodynia in some hands but not others. This variability suggests that dorsal root rhizotomy may be an unsuitable model for avulsion-pain, as the later injury consistently induces pain (Parry, 1980;Bonnard and Narakas, 1985;Bruxelle et al., 1988).

In the context of dorsal root injury, there are different sequences of events compared to SCI and PNI. This is most noticeable with respect to degeneration, with the latter injury leading to Wallerian degeneration of the distal nerve axons at much greater rate than with a central lesion (Vargas and Barres, 2007). This distinction is also applicable to regenerative properties of injured or severed nerve fibres, with the peripheral nerve having an ability for regrowth, reconnection and functional repair, due to intrinsic and extrinsic growth permitting factors (Johnson et al., 2005), that are not present in the CNS (Jackowski, 1995). There is also evidence (Colburn et al., 1999;Winkelstein et al., 2001a) suggesting the site of both root and nerve injury in relation to the DRG impacts on the magnitude of the subsequent spinal glial activation, cytokine expression, but interestingly not neuropathic pain behaviour (Winkelstein et al., 2001a). The most notable difference with rhizotomy and avulsion root injuries is the damage to the spinal cord, specifically the dorsal horn (Ovelmen-Levitt et al., 1984). The primary trauma to the dorsal horn, dorsal columns and DREZ after root injury, can be observed through histological analysis of toluidine blue staining. Damage is evident in the medial portion of Lissauer's tract with avulsion injury and subsequently gliosis in the substantia gelatinosa. In some cases the superficial laminae are absent and interneurones of lamina III have atrophied (Ovelmen-Levitt et al., 1984). This indicates a dramatic disruption to

post-synaptic neuronal populations and extensive necrotic and apoptotic cell death. Micro-vascular disruption and endothelial cell loss can also be observed after transection of the dorsal surface of the spinal cord (Imperato-Kalmar et al., 1997), accompanied by the activation and infiltration of monocytes and leukocytes (Fleming et al., 2006;Thacker et al., 2007). This infiltration generates acute lesion expansion and injury exacerbation as well as facilitating endogenous repair processes such as axonal sprouting and remyelination (Jones et al., 2005). Functionally on injury, damaged sensory terminals emit a barrage of action potentials, which lasts for many seconds, or even minutes, onto dorsal horn neurones (Seltzer et al., 1991). Several weeks after root transection however, extensive receptive field expansion is seen in the deep laminae to the spared input (Ovelmen-Levitt et al., 1984); deafferented cells show a spontaneous, repetitive and continuous patterning of axon potential propagation from extracellular recordings in the dorsal horn (Dalal et al., 1999). Lack of sensory innervation from a deafferented nerve, or an acute barrage of action potentials from transected roots, may evoke a change in the original pattern of neural processing within the dorsal horn and in its central projections (Melzack et al., 2001), leading to prolonged heightened neuronal responses. Indeed after dorsal rhizotomy in the cat (Loeser and Ward, Jr., 1967), unitary activity recordings of deep laminae neurones were found to be hyperactive compared to non-deafferented neurones. This hyperactivity was also found to be present in human patients (Guenot et al., 2003) and rats (Guenot et al., 2002) with brachial plexus avulsion, and this discharge pattern is abolished through DREZotomy (Guenot et al., 2003). This hyperactivity is thought to contribute to the maintenance of spontaneous deafferentation pain (Dalal et al., 1999) as well as neuropathic behaviour, such as autotomy, *in vivo* (Seltzer et al., 1991).

3.1.2: Secondary consequences to dorsal root avulsion

Consequences of injury to the spinal cord are not limited to the initial insult; be it from compression, root injury and peripheral nerve injury. Degeneration for example has been shown to continue for years after initial insult (Totoiu and Keirstead, 2005). Secondary injury within the CNS is the response of the intrinsic nervous system and extrinsic vascular system to the initial trauma. Both inflammatory and immune responses from non-neuronal cells in the blood, such as the recruitment of destructive neutrophils and macrophages (Popovich et al., 1997;Popovich and Jones, 2003), and

within the CNS, such as reactive microglia (Fleming et al., 2006;Milligan and Watkins, 2009) are believed to be involved. These cell types produce ‘zones’ of pathological change that spread out from the initial trauma, and also progress within the site of injury. Processes such as inflammation, gliosis, oxidative damage and excitotoxicity lead to necrosis and apoptosis, axonal swelling and damage, Wallerian degeneration, and the formation of cystic cavities (Hagg and Oudega, 2006). Many of these secondary processes have been characterised after SCI and PNI, and have been successfully manipulated therapeutically (Baptiste and Fehlings, 2006). However very little work has concentrated upon the understanding the progressive effects of root avulsion injury within the spinal cord, and as such therapeutic intervention at the cellular level is limited. Presented here is a review of secondary injury phenomena, some degenerative, others regenerative, and their possible involvement in dorsal root avulsion.

3.1.2.1: Glial changes

Glial cells are important players in the functioning of the nervous system both before and after injury. The main types of CNS glial cells are astrocytes, microglia and oligodendrocytes. Each has a distinct role: oligodendrocytes play a role in myelinating and supporting CNS axons, microglia provide innate immunity for the CNS by actively assessing the state of the spinal cord, excavating dead neurones, plaques and infectious antigens, and astrocytes provide structural support to neurons and regulate potassium and calcium ion concentration, and extracellular pH (Fawcett and Asher, 1999). Astrocytes also importantly regulate the amount of synaptic glutamate available to neurons through the expression of Na^+-dependent transporter proteins (Rat homologues: GLAST and GLT1. Human homologues: EAAT1 and EAAT2) on their surfaces, preventing excitotoxicity (Anderson and Swanson, 2000).

Upon damage, the central nervous system undergoes an injury response, called ‘reactive gliosis’ or glial scarring, the main function of which is neuroprotective by limiting the size of the injury. However this process is detrimental to recovery, due to the impedence of axon regrowth (Fawcett and Asher, 1999;Fawcett, 2006). The final structure of a glial scar, which takes 6 weeks to fully develop *in vitro* (Polikov et al., 2006), is predominantly astrocytic; however, nearly all non-neuronal cells of the CNS are involved (Ohlsson et al., 2004). The main players are oligodendrocytes, meningeal

cells, astrocytes, and microglia. Glia are actively recruited in response to injury through infiltration and/or migration to the injury site, and their numbers are greatly increased through proliferation of the resident population in the CNS (Liu et al., 2000a;Scholz and Woolf, 2007).

Astrocytes play the major role in creating and maintaining the integrity of the structure of the 'non-permissive' glial scar, forming a barrier to external or foreign matter. They can be identified by labelling proteins they express such as, glial fibrillary acidic protein (GFAP), a member of the class III intermediate filament protein family, or by the calcium binding protein, S100β. Upon root injury and spinal nerve transection astrocytes hypertrophy by 3-4 days within the ipsilateral dorsal horn (Murray et al., 1990;Colburn et al., 1999). Astocytes do not proliferate (Murray et al., 1990) but increase expression of GFAP across 28 days in direct comparison to microglia (Tanga et al., 2004;Tanga et al., 2006). Neonatal root injury shows less propensity for astrogliosis (Murray et al., 1990), and may provide rational as to why plasticity and indeed recovery after root re-implantation is more effective in infants (Carlstedt et al., 2000;Kato et al., 2006). As described the main role of reactive astrocytes is to maintain the structural and functional integrity of the scar (Fawcett, 2006). If astrocytes are prevented from becoming reactive (through administration of antiviral ganciclovir), SCI in rats leads to wide spread tissue disruption, pronounced cellular degeneration, failure of wound contraction, and motor impairment, far beyond that of equivalent untreated rats (Faulkner et al., 2004). To accomplish this essential scar formation astrocytes produce and express chondroitin sulphate proteoglycans (CSPG), cytotactin/tenascin, neurocan, brevican, and versican and may other extracellular matrix components (Beggah et al., 2005). However, these non-permissive proteins are adverse to natural growth-cone elongation and targeting (Yiu and He, 2006), and inhibitory to successful re-targeting and repair of transected axons after CNS lesioning (McKeon et al., 1991) or dorsal root crush (Chong et al., 1999). Chondroitinase ABC, an enzyme that breaks down CSPGs, has been shown to improve regenerative neuronal growth through scar tissue and functional recovery, in animal models of SCI (Bradbury et al., 2002) and root injury (Cafferty et al., 2008). In addition 7-14 days after PNI, glutamate transporters, GLT-1 and GLAST, downregulate their expression profiles on astrocytes (Xin et al., 2009). The vesicular glutamate transporter, VGLUT 1, found in neurones and astrocytes (Montana et al., 2004) are also downregulated by DRR and sciatic nerve transection by 12 days

(Brumovsky et al., 2007). This reduction in transporters increases extracellular glutamate, leaving dorsal horn neurones susceptible to excitotoxicity and cell death, and/or hyperexcitabilty resulting in neuropathic pain.

Other glia within the spinal cord, for example oligodendrocytes, also express important inhibitory molecules such as myelin inhibitory molecule N1-250/NogoA (GrandPre et al., 2000), myelin-associated glycoprotein (MAG) (Fawcett and Asher, 1999), oligodendrocyte myelin glycoprotein (OMgp), Semaphorin 4D and Tenascin-R (Yiu and He, 2006), proteoglycans (Beggah et al., 2005), and NG2 (Keirstead and Blakemore, 1999), to aid successful scarring but also impeding regeneration (Fawcett, 2006). Meningeal cells that cover the external surface of the CNS rapidly migrate to the site of trauma after a penetrating injury to neuronal tissue (Fawcett and Asher, 1999). They condense together to form a protective layer around the injury along side astrocytes, inhibitory to neurite outgrowth, called the glial limitans. This inhibition is likely to come from the production of NG2 and the multifunctional protein tenascin (Levine and Nishiyama, 1996) as well as the production of the chemorepellant, semaphorin 3A (Niclou et al., 2003). After dorsal root transection, a contributor to the growth inhibitory environment of the DREZ, as well as the deep grey matter and dorsal columns, is likely to be meningeal cell activity (Chong et al., 1999).

Microglia have a different role to astroytes within the CNS scar, and play an essential role in the spinal cord and brain as an active immune defence for the central nervous system. Under resting conditions they are quiescent, but continuously sample the local environment looking for signs of damage or infection, removing dead cells and pathogens (Rock et al., 2004). Microglia can be labelled with an antibody to ionized calcium adaptor binding protein-1 (Iba1), a protein product of the gene, allograft inhibitory factor-1 (Aif1). This protein is constituatively expressed in microglia, and is upregulated during activation of this cell type. Microglia become activated through a number of receptor-agonist signals from neurones or by other glial cells that include ATP-$P_2X_4/X_7/Y_6$ signalling, CX3C1 (fractalkine)-CX3CR1 signalling, and HSP (Heat shock protein)-TLR (Toll-like receptor) signalling (Tsuda et al., 2003;Obata et al., 2008;Milligan and Watkins, 2009;Inoue et al., 2009). When for example, spinal root damage occurs, microglia become activated and participate in phagocytosing degenerating debris (Hoffmann et al., 1993;Hashizume et al., 2000a;Liu et al., 2000a). Indeed, in the rhizotomised dorsal funiculus of the kitten, microglia have been shown to

contain myelin and lipids (Franson and Ronnevi, 1989), and astrocytes and microglia transport debris from the neuropil to the blood via endothelial cells (Holtzer et al., 1998). Microglia, identified by OX42 labelling, are upregulated through proliferation around primary afferent terminals and motor neurones 24 hours after sciatic nerve transection, dorsal root rhizotomy and spinal root avulsion, peaking around a week after (Eriksson et al., 1993;Colburn et al., 1999;Liu et al., 2000a;Penas et al., 2009). However after dorsal root rhizotomy microglia present much less compliment activity and reactivity than after PNI (Liu et al., 1998;Colburn et al., 1999). It has recently been concluded that the microglial/macrophage response after disease, injury, or inflammation to the nervous system is not a homogenous one (Cameron and Landreth, 2010), and can occur via a 'classical' pathway (M1) involved in inflammation and immune response, or an 'alternative' pathway (M2) for anti-inflammatory processes such as wound healing and phagocytosis (Kigerl et al., 2009). It is understood that microglia have the capacity for aiding neuroregeneration or collateral sprouting, perhaps through phagocytosis of myelin debris and growth factor expression (Aldskogius, 2001), and this could well occur through the M2 pathway (Kigerl et al., 2009). The M1 pathway however is neurotoxic (Kigerl et al., 2009), mediated via free radicals, cytokines, and complement component expression (Aldskogius and Kozlova, 1998). Functionally, after spinal cord injury in mice, activation of microglia via therapeutic administration of IL-12, assisted in remylination and lead to improved recovery (Yaguchi et al., 2008). However the ability of microglial-phagocytosis in the CNS is less than observed in the periphery; controlled by monocyte-macrophages (Aldskogius and Kozlova, 1998), taking 14 days to complete primary afferent terminal phagoctyosis after dorsal root rhizotomy (Liu et al., 1998). This slow clearance may explain the absence of effective regeneration in the CNS compared to the PNS. Complement-3 (C3) component expression strongly facilitates monocyte-macrophage phagocytosis in the PNS (Aldskogius and Kozlova, 1998). C3 is not induced in microglia-macrophages of the dorsal horn after rhizotomy (Liu et al., 1998) but is expressed in microglial-macrophages of the dorsal horn after sciatic nerve cut (Liu et al., 1998), suggesting anterograde degeneration is not a stimulus for the generation of a complement-induced fully-phagocytotic microglial (M2) phenotype; rather DRG cell body connectivity to the dorsal horn is the crucial difference. It may be this factor, among many others, that controls neuroregenerative capacity. It is suggested that if microglia can be pharmacologically influenced to undergo activation via the M2

pathway, this may provide a neuroprotective strategy and reducing neuroinflammation in SCI (Kigerl et al., 2009), and could also be applicable to root injury.

In recent years, a major role for microglia and astrocytes has emerged in the onset and maintenance of neuropathic pain (Raghavendra et al., 2003;Watkins and Maier, 2003;McMahon et al., 2005;Nesic et al., 2005;Tsuda et al., 2005;Tanga et al., 2006;Inoue and Tsuda, 2009). The roles of astrocytes and microglia may be slightly different in peripheral compared to spinal cord injury models. It is suggested that microglia are important for the onset of neuropathic pain in peripheral nerve injury (Raghavendra et al., 2003), with the development of a maintained chronic pain state, the result of a replacement of activated microglia with activated astrocytes. This is confirmed in sciatic nerve injury, where microglial activation preceeds astrogliosis (Cavaliere et al., 2007). An interesting point is dorsal root rhizotomy produces only transient microglial reactivity (Eriksson et al., 1993;Colburn et al., 1999) of much less magnitude than PNI, and leads to further scepticism over whether the injury leads to neuropathic pain behaviour (Sukhotinsky et al., 2004). Conversely, in spinal cord injury models, microglia have a much larger and prolonged role, having been shown necessary for the maintenance of chronic pain states (Hains and Waxman, 2006) alongside chronically ‘over-activated’ astocytes (Nesic et al., 2005). Noxious stimuli, disease or trauma to neurones can cause release of excitatory neurotransmitters like glutmate, and a milieu of neuroactive compounds like heat shock proteins (HSPs), fractalkine, prostaglandins (PGE-2), reactive oxygen species (ROS) such as nitric oxide (NO), pro-inflammatory cytokines (TNFα, IL1β, IL6), and ATP. These compounds activate glial cells in close proximity, which in turn generate and release more proinflammatory mediators which increase AMPA and NMDA receptor conductivity and number in neurones, contributing to the maintenance of the pain (Watkins et al., 2001;McMahon et al., 2005;Milligan and Watkins, 2009) and may induce cell death through excitotoxicity mechanisms. Although the glial reaction is largely confined to the sites of injury, activated microglia can migrate to areas of the spinal cord that are not directly affected by trauma and contribute to the sensitization of neurones, thereby contributing to evoked pain sensations like hyperalgesia and allodynia (Beggs and Salter, 2007). It is unclear however what role these glial cells have to play after dorsal root avulsion and corresponding neuropathic avulsion-pain.

3.1.2.2: Neuronal changes

The changes that occur to the neuronal population of the spinal cord will be catagorised into *presynaptic*, i.e. to primary afferents, and *postsynaptic*, i.e. to dorsal horn neurones.

Presynaptic

The time course of degeneration of the transected afferent nociceptor fibre terminals in the dorsal horn can be measured through substance-P (SP) labeling within lamina I, II, and V, with notable decrease by 7 days (Zhang et al., 1993), and is most marked at 10-11 days (Tessler et al., 1980) after complete DRR of the lumbosacral plexus. Neurofilament degeneration is prominent at 3-4 days post rhizotomy, and absent beyond 7 days (Ralston, III and Ralston, 1982) This terminal degeneration is not exclusive to root deafferentation, but also occurs prominently at 30 days post peripheral nerve transection within lamina I-IV, lissauers tract, dorsal funiculus, gracile nucleus, and to a less extent in lamina V and VI (Arvidsson et al., 1986), suggesting DRG connection is not enough to prevent primary afferent terminal degeneration in the long term, and most likely through loss of target derived growth factors is key. Interestingly at 2 weeks, ipsilateral loss of CGRP positive terminals is incomplete in the deafferented dorsal horn, even after rhizotomy of 5 lumbar segmental levels in the cat (Traub et al., 1989), suggesting the presence of a lengthy segmental collateral supply of peptidergic C fibres. This could also represent resident CGRP-positive second order dorsal horn neurones, that are know to be present in the rat lumbar cord (Conrath et al., 1989).

Alongside the loss of synaptic input from deafferented fibres, there is also evidence to suggest a gain of synapses through three charaterised pathways: plasticity of descending supraspinal circuits, local interneuronal circuits, and sprouting of adjacent spared root. This increase in synaptic densities has been shown after unilateral DRR within the ipsilateral dorsal horn, and described as an anatomical compensatory recovery mechanism (Murray and Goldberger, 1986;Zhang et al., 1993;Zhang et al., 1995) that may contribute to functional recovery of some reflexes and locomotion, but also central sensitization mechanisms and hypersensitivity of dorsal horn neurones (see chapter 4). More specifically some of the sprouting involves a proliferation of SP and serotonin (5HT) containing terminals in lamina I, II and Clarke's nucleus, usually 2 weeks after multiple unilateral rhizotomies (Tessler et al., 1980;Polistina et al., 1990;Wang et al.,

1991;Zhang et al., 1993). This compensatory form of sprouting originates from the terminals of supraspinally descending 5HT systems like the raphe nuclei and the reticular formation (Shapiro, 1997), or in the case of SP, interneuronal or propriospinal fibre sprouting segmentally at the level of lesion (Tessler et al., 1980;Tessler et al., 1981). Descending tracts from the raphe nucleus facilitates or inhibits nociceptive processing in lamina II via inhibitory 5HT-1A receptors present on interneurones, and rubrospinal tracts facilitates motor efferents. It may be via the latter tract sprouting by which the functional recovery of locomotion seen after extensive DRR could occur, through a mechanism of 'reactive reinnervation' (Zhang et al., 1993). There is also evidence to suggest adjacent intact roots may sprout into lamina II after dorsal root rhizotomy (Zhang et al., 1995) recovering the lost terminals. This occurs by 35 days post rhizotomy, with CGRP terminal densities increasing by 7 fold compared to the maximal loss seen at 5 days (McNeill et al., 1991). There is however some debate over whether deafferentation can induce spared root sprouting (Mannion et al., 1998), or if primary afferent sprouting even exists after injury (Shehab, 2009). Further evidence for primary afferent sprouting evidence will be covered in chapter 4.

Postsynaptic

One of the most notable effects of deafferentation injuries within the postsynaptic neuronal population is the amount and rate of cell death that occurs. Peripheral nerve injury models have shown cell death to occur in the superficial dorsal horn at 7 days but not 3 and 14 [(Azkue et al., 1998;Scholz et al., 2005) but see (Polgar et al., 2004) for contradictory data], and a much more delayed and progressive loss of DRG neurones across 32 weeks (Vestergaard et al., 1997;Tandrup et al., 2000). The mechanism of the transynaptic cell death in the dorsal horn is likely hyperactivity of peripheral nerves leading to glutamate excitotoxicity. Indeed increased activity of injured peripheral fibres induces activity-dependent apoptosis of dorsal horn neurones (Coggeshall et al., 2001). This cell loss can be prevented by caspase inhibitors, which reduces dorsal horn hyperexcitability and neuropathic pain associated through maintaining lamina II interneurones (Scholz et al., 2005). The effect upon the postsynaptic neurones of the dorsal horn is dramatic after dorsal root injuries, with spontaneous discharges of the dorsal horn neurones after unilateral brachial plexus rhizotomy (Dalal et al., 1999), possible 'umasking' of previously unresponsive neurones (Basbaum and Wall, 1976), correlating with the onset of neuropathic pain behaviour in the rat (Guenot et al., 2002).

This hyperactivity may lead to excitotoxcity of neurones. However, it is unclear whether dorsal horn neurones die after root transection. Indeed complete lumbosacral plexus dorsal rhizotomy does not lead to dorsal horn cell death, quantified in Clarke's nucleus, as measured by cresyl violet histological counts (Sanner et al., 1993). Interestingly, rhizotomy can prevent retrograde cell death in Clarke's Nucleus induced by hemisection of spinocerebellar tract axons (Sanner et al., 1993), suggesting in spinal cord injury, primary afferents could exacerbate an axotomy injury perhaps through glutamate excitotoxicity. In PNI models there is still debate as to whether cell loss is even specific to dorsal horn neurones, with TUNEL-positive cells being identified as microglia, or even if it is causal to the development of allodynia and hyperalgesia (Polgar et al., 2005). The above literature suggest apoptotic cell death in the dorsal horn, whether it is specifically glial or neuronal, is activity dependent, and an ectopically active spared nerve or DRG-dorsal horn neurone contact is required to induce it (Coggeshall et al., 2001;Scholz et al., 2005). Therefore it will be interesting to see if dorsal horn neurone apoptosis is present in a full lumbosacral plexus-avulsed dorsal horn, or if indeed neuronal loss even occurs.

Ventral root avulsion (Koliatsos et al., 1994;Carlstedt and Cullheim, 2000;Bergerot et al., 2004) leads to motor neurone death *in vivo* peaking by 14 days. This may well be a response to accumulation of free radicals and consequently oxidative damage (Martin et al., 1999). NO, produced in an enzyme reaction with L-arginine and nitric oxide synthase (NOS), regulates immune function, blood vessel dilation, as well as serving as a neurotransmitter/neuromodulator in the processment and nociceptive stimuli (Reuss and Reuss, 2001;Cizkova et al., 2002). It has been implicated in the development of neuronal plasticity and hyperactivity in dorsal horn neurones and DRG after PNI (Cizkova et al., 2002). In free-radical chemical configuration, and excess, NO leads to cellular oxidative stress responses, DNA damage, and apoptosis. Neuronal NOS (nNOS) can be used as a marker for the molecule NO in naïve tissue, and is concentrated in lamina I-III and autonomic regions of the rat dorsal horn (Reuss and Reuss, 2001). Its expression increases in both DRG and spinal neurones after SCI (Vizzard, 1997) or PNI (Ma et al., 2000;Cizkova et al., 2002;Keilhoff et al., 2002). After ventral root avulsion NOS expression increases in motor neurones, and is associated with cell death (Wu, 1993), and inhibition of NOS through nitroarginine administration reduces this cell loss (Wu and Li, 1993;Ayata et al., 1997). However

DRG, spinal interneurone, and motor neurone survival, regeneration, and revascularisation are severely compromised in peripheral nerve injured NOS (neuronal, endothelial and inducible isoforms) knock-out mice (Keilhoff et al., 2003). Further NOS-positive surviving motor neurones (35% of total pool) can be found 9 weeks post ventral root avulsion, colocalised with Heat Shock Protein 27 (HSP27) (He et al., 2003). HSP27 is a chaperone protein, and may assist radical scavenger systems from removing excess toxic NO. NO may control a fine balance of anti-apoptotic and pro-apoptotic actions depending on its oxidative state or presence of scavenger systems in certain cells, and may not be the underlying determinant of cell death in models of nerve injury. nNOS is upregulated in injured and intact DRGs after selective dorsal root rhizotomy (Qin et al., 2004), but is reduced in dorsal horn neurones 5 days after such an injury alongside Substance P terminals, suggesting its spinal expression is regulated by peripheral afferent connection (Reuss and Reuss, 2001). Little is known about the role of nNOS or NO in dorsal horn neurone specific cell death in dorsal root avulsion models however, or indeed if it contributes to neuropathic pain. Nitic Oxide's 'double edged sword' role in neuronal survival and death is confusing, and may not provide adequate assessment of dorsal horn neuronal population after rhizotomy or avulsion.

3.1.2.3: Vascular changes

CNS lesions, especially shearing and stretching, lead to direct mechanical damage to the microvasculature, especially in the grey matter. This direct disruption of the blood brain barrier, causes hemorrhaging of the vasculature (Maikos and Shreiber, 2007), altered blood flow and ischemia (Senter and Venes, 1978). For example after a spinal cord compression injury, endothelial cells of the vasculature are lost as early as 1 and 2 days in mice (Benton et al., 2008a;Benton et al., 2008b) and rat models (Imperato-Kalmar et al., 1997). An important regenerative response is observed after SCI, with increased vessel number and thickness 4 days post injury in the rat (Imperato-Kalmar et al., 1997), and 3 days in the mouse (Benton et al., 2008a), at both the injury site and at more rostral and caudal sites. This is associated with a unique IB4 intravascular binding surrounding the lesion site, and the up-regulation of ADAM8 in endothelial cells suggestive of neovascualture and angiogensis (Benton et al., 2008a;Mahoney et al., 2009). Matrix metalloproteinases (MMP) present in the extracellular matrix and on inflammatory cells activate and cause the release of VEGF and fetal growth factors that

lead to plasticity of endothelial cells (Mautes et al., 2000). In the mouse, expression levels of platelet/endothelial cell adhesion molecule-1 (PECAM-1) found on endothelial cells, consistently recovers across 14 days after spinal cord injury (Benton et al., 2008a), and this closely correlates with an accumulation of connective tissue in the primary injury cavity, and regeneration of ascending sensory fibres (Inman and Steward, 2003a) and descending corticospinal fibres (Steward *et al.,* 2008). However, in stark contrast, angiogenesis is not mainted in the rat or other mammals after SCI (Inman and Steward, 2003a;Inman and Steward, 2003b) and at 7 days the number of vessels declined and cystic caverns containing CSF form in the epicenter (Imperato-Kalmar et al., 1997). After ventral root avulsion in cats (Holtzer et al., 1998), endothelial cells contained vacuoles filled with fibrous-like substances, and microvasculature was surrounded by glia and phagosomes containing myelin, suggesting transport of necrotic debris from the neuropil to the blood occurs via endothelial cells after injury. This role of vasculature endothelial cells after injury must be beneficial for protective scarring; however, it is still unclear if vascular plasticity is benefitial or detrimental to the traumatized spinal cord (Mautes et al., 2000). It is clear that this biphasic response in the rat vasculature (Imperato-Kalmar et al., 1997), and maintained cavatiation in mammals of higher order than mice, suggests angiogenesis is incapable of counterbalancing chronic progressive degeneration of vasculature after SCI. So far rat models of dorsal root rhizotomy and sciatic nerve transection show no obvious reduction in vasculature staining by 7 days, suggesting direct trauma to the spinal cord is needed to induce a vascular response (Liu et al., 1998). Further work however is necessary to identify the effects of dorsal root avulsion on vasculature maintenance.

3.1.2.4: Inflammation

During the period of vascular disruption and endothelial cell loss, production of cytotoxic reactive species within the spinal cord neuropil can occur. This causes rapid activation of resident glial cells, but also infiltration of monocytes through extravasation via endothelial cells (Fawcett and Asher, 1999;Thacker et al., 2007) resulting in an inflammatory response (Fleming et al., 2006). This response is associated with endothelial degredation via MMPs expressed on inflammatory cells (Mautes et al., 2000). This causes an acute extravasation of mast cells, granulocytes, T-cells, monocytes, and neutrophils from the blood stream, peaking at 3 days (Popovich et al.,

1997;Thacker et al., 2007). This produces further upregulation of cell adhesion molecules, chemokines, cytokines (Morganti-Kossmann et al., 2002), and interleukins (Hashizume et al., 2000a). These inflammatory mediators can have detrimental effects on cell survival (Popovich and Longbrake, 2008), by the production of reactive oxygen species that damages healthy tissue (Carlson et al., 1998), and can cause neuropathic pain (Thacker et al., 2007). Conversely macrophages and resident microglial-derived macrophages have been shown to be beneficial to functional recovery and axon regeneration (Stoll, 2002;Gensel et al., 2009); both neutrophils and macrophages, for example, have a role in phagocytic debris clearance of necrotic tissue and myelin, which creates cystic caverns that are eventually walled off from healthy tissue by astrocytic processes containing the lesion site and preventing the spread of damage. Activated microglia and monoctyes release cytokines and growth factors that support neurone and oligodendrocyte survival and remyelination (Popovich and Longbrake, 2008), and are antibacterial and are important for adaptive immunity involving T and B lymphocytes (Ankeny and Popovich, 2009). For these reasons the neuroinflammatory response has been defined as a ‘double-edged sword’, with both positive and negative functions on the injured spinal cord. In mice and rats there is a distinctly different immune response to SCI (Inman and Steward, 2003b;Sroga et al., 2003). Mice have a delayed and prolonged T-cell infiltration beginning at 14 days, compared to the acute and transient infiltration seen in rat CNS lesions at 3-7 days. Mice have a greater MHC class II expression and fibrocytes in the injury site. These differences likely contribute to the greater propensity for wound healing, survival, and regenerative capacity in mice, than rats and higher mammals (Inman and Steward, 2003a), and indicates further the essential role the immune system plays in CNS recovery.

After SCI for example, leukocytes become tethered to the endothelial cells of the microvasculature of the spinal cord through selectins. Endothelial cell-adhesion molecules and MMPs then interact with leukocyte integrins to facilitate extravasation to the lesion site (Gris et al., 2004). After thoracic cord compression injury, myeloperoxidase activity has been shown to peak at 24 hours (Carlson et al., 1998) representing an acute neutrophil invasion. Ling (1979) was the first to observe, through intravenous colloidal carbon injection and light microscopy, monocyte-derived macrophages in blood vessel lumina, in the neuropil, and crossing the endothelial membrane between 3 and 7 days after DRR (Ling, 1979b), and stab injury to the brain

(Ling, 1979a). The author also described a substantial population of microglial-derived macrophages (Ling, 1979b). Recently both dorsal root rupture (a modified avulsion injury) and rhizotomy have been shown to induce aggregation of macropahges from the injury site at the dorsal root into the dorsal funiculus, with high expression of p38-MAPK and TNFα at 48 hours, suggesting active and inflammatory properties of these monocytes, that may aggrevate the injury (Nomura et al., 2005). Indeed after human brachial plexus avulsion injury and chronic constriction injury in the rat macrophages expressing the enzyme cycloxygenase-2 (COX-2), have been shown within the DRG, peripheral nerve and spinal cord, that induce PGE-2 production, contributing to inflammation and neuropathic pain (Durrenberger et al., 2004). As a therapeutic intervention against blood-borne inflammation, inhibitors of the endothelial-monocyte adhesion molecules P-selectin (Taoka et al., 1997) and CD11d/CD18 integrins (Gris et al., 2004;Oatway et al., 2005) administered after SCI, have been shown to improve motor and autonomic scores, reducing neuropathic pain behaviour, increasing neuroprotection, myelination and axonal sparing. These *in vivo* data provide direct evidence for the role of neutrophils and macrophages in the exasserbation of secondary neuronal injury (Carlson et al., 1998), as well as in the generation and maintenance of neuropathic pain (Thacker et al., 2007). However, in the case of root avulsion injuries, leukocyte inflammatory effects such as those described for SCI are yet to be characterized in the dorsal horn.

3.1.3: Aims

The secondary injury consequences described after dorsal root rhizotomy including reactive gliosis and vascular extravasion of cytokines and leukocytes, have the primary aim of isolating the lesion site, preventing further damage, clearing debris and preserving remaining neuronal function. However, the increased presence some of these components create a potential problem: they may contribute to neuropathic pain and further neuronal loss. Maintaining a fine balance between these neuroprotective and neurotoxic effects after dorsal root injury is therefore therapeutically essential. However, it is still unknown to what extent and across what time scale dorsal root avulsion can initiate neurodegeneration, inflammation, and dorsal horn neuronal loss, and whether rhizotomy as an *in vivo* model produces a similar spinal response.

The aims of this project are as follows:

- To compare the effects of tearing of the roots (avulsion injury) to a surgical cutting of the roots (rhizotomy), in terms of the effects in the spinal cord dorsal horn and dorsal columns. This comparison will extend to activity of glia subpopulations, including phagocytic leukocytes, disruption of the microvasculature, and degeneration of nociceptors. The aim is to see if a traumatic traction injury, which can damage the CNS, produces a more severe response in the dorsal horn than an artificial surgical root lesion that does not affect the spinal cord and does not occur naturally in patients. Avulsion injury may then be a more appropriate model to study mechanistic changes in brachial plexus injured patients.

- To establish if neuronal cell loss does indeed occur in the spinal cord due to deafferentation of the dorsal root, and to characterize which cellular subpopulations are preferentially affected. Cellular apoptotic cascades will be assessed through quantitative analysis of cell death using TUNEL analysis (Gavrieli et al., 1992) and fluorescence-assisted flow cytometric analysis, within specific regions of the spinal cord. The cellular origin of this apoptosis will be identified through double labeling immunohistochemistry to various markers associated with neuronal and non-neuronal populations.

3.2: Results

3.2.1: Quantitative loss of primary afferent connection within the dorsal horn after dorsal root deafferentation

CGRP and IB4 immunohistochemistry (ir) was used to analyse the time course of reduction in terminal afferent staining in the deafferented spinal cord. In this way comparisons with previous work on the time course of terminal degeneration (Ralston, III and Ralston, 1982) and deafferentation (Traub et al., 1989) in rhizotomy models can be compared.

3.2.1.1: Peptidergic (CGRP) afferent terminals

Naïve tissue (Fig 3.1) showed intense CGRP-positive granular-like staining uniformly within the superficial laminae (I and II). Immunostaining was also seen in the deep laminae (V) and around the central canal (X). Quantitative analysis was performed from only in the superficial laminae (Fig 3.2). Naïve tissue presented 32.7% (+/- 1.33) density staining in the superficial laminae (Fig 3.2).

CGRP-ir reduction from naïve levels is significant bilaterally at 1 day in all injury models (Fig 3.1). Density staining values are reduced in DRA [15.3% (+/-3.83) ipsilaterally and 21.0% (+/-0.88) contralaterally], DRR [16.5% (+/-1.15) ipsilaterally and 20.4% (+/-1.94) contralaterally], and sham [21.8% (+/-3.19) ipsilaterally and 24.5% (+/-2.50) contralaterally] (Fig 3.2). Ipsilaterally DRA is significantly lower than sham, but there is no difference between DRR and DRA, or between cord sides within injury models (Fig 3.2).

The loss at 1 day is maintained at 2 days in both injury groups (Figs 3.1 and 3.2). However, DRA ipsilateral levels [13.0% (+/-2.58)] are now significantly lower than the respective contralateral side [21.4 (+/-2.45)] (Fig 3.2). There is no significant difference between DRR and DRA CGRP-ir ipsilaterally or contralaterally (Fig 3.2).

The most extensive loss of CGRP-ir occurs at 14 days post injury (Fig 3.1). Both DRR and DRA show reduced ipsilateral CGRP-ir to 4.44% (+/-0.45) and 1.58% (+/-0.19)

respectively, with DRA significantly more reduced than DRR (Fig 3.2). Contralaterally no further reduction in CGRP-ir is observed (Figs 3.1 and 3.2). No significant difference was observed at 14 days between sham cord sides, with no further reduction from day 1 sham (Figs 3.1 and 3.2).

Only residual CGRP-ir remains ipsilaterally at 28 days post injury (Fig 3.1). Density staining is reduced to 0.43% (+/-0.13) and 1.9% (+/-0.80) within the ipsilateral superficial laminae of DRA and DRR tissue respectively. Significant difference between the two injury models is not found ipsilaterally (Fig 3.2). Further contralateral loss in DRA is present (Fig 3.1) with a density staining of 11.4% (+/-3.50) with notable scarring in the dorsal horn (Fig 3.1 and 3.2). Further contralateral loss in DRR is not seen (Figs 3.1 and 3.2). Contralaterally, DRA CGRP-ir is significantly lower than DRR (Fig 3.2).

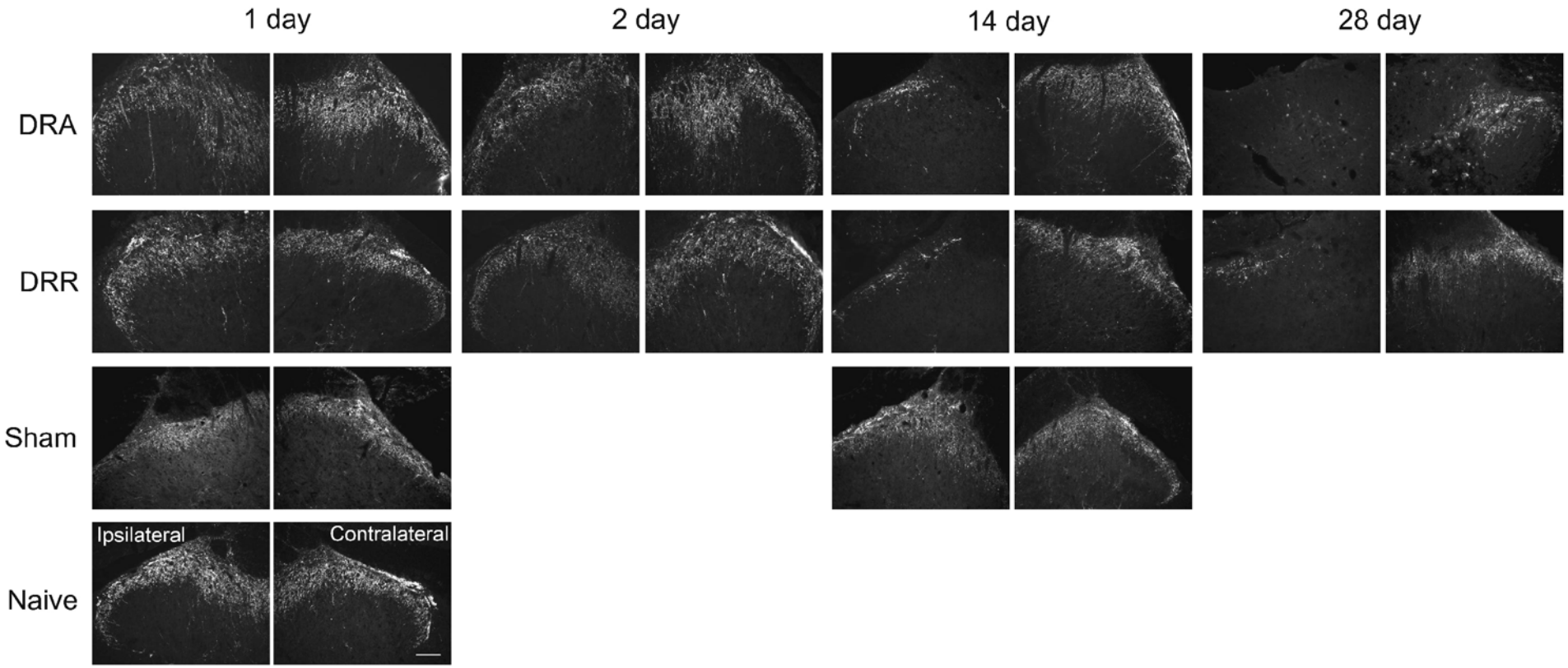

Fig 3.1: CGRP staining in the superficial laminae after root injury. Naïve CGRP staining is located within laminae I, II, V, and is granular in appearance. 1 day after DRA, DRR, and sham injury CGRP staining is reduced bilaterally. Further reduction is observed at 2 days post DRA and DRR, in the ipsilateral dorsal horn. 14 days post DRA and DRR CGRP staining is markedly reduced ipsilaterally in the dorsal horn. 14 day sham shows no further reduction in CGRP intensity from 1 day. laminae. At 28 days post DRA and DRR, only patchy and punctuate CGRP staining is observed ipsilaterally. Further loss of CGRP immunoreactivity is observed contralaterally after DRA, with the dorsal horn presenting scarring and damage itself. Ipsilateral images are shown to the left, and contralateral to the right. Scale = 100μm. Examples of L5 segmental level.

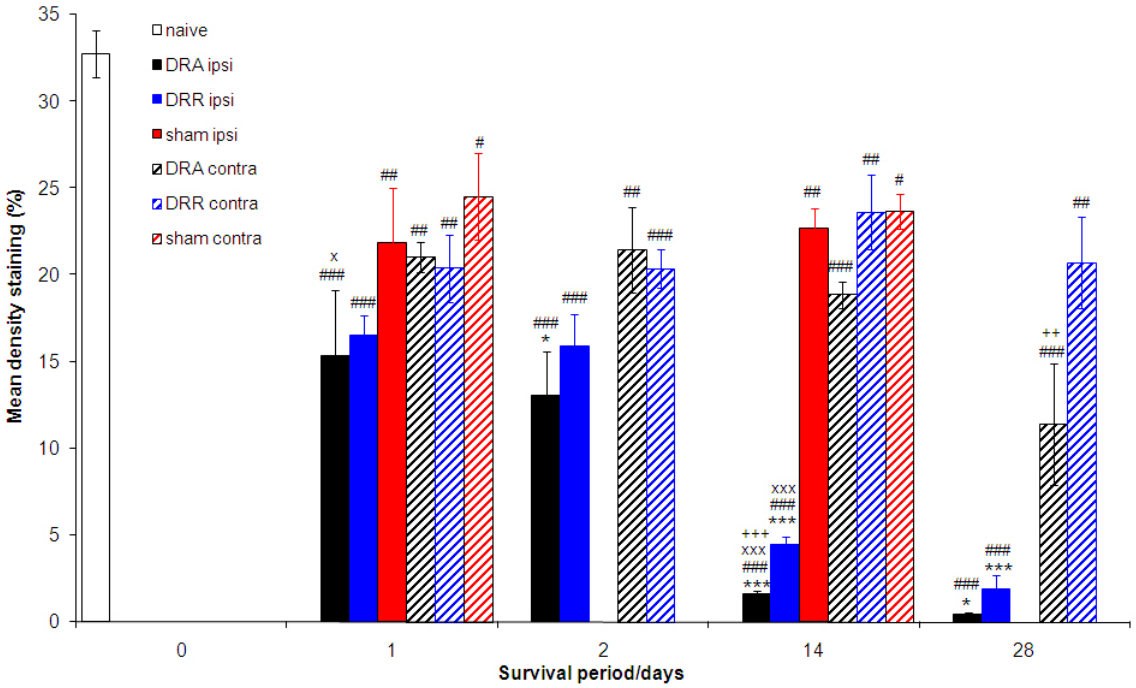

Fig 3.2: Quantitative analysis of CGRP density in the superficial dorsal horn. CGRP immunoreactivity is shown as mean percentage positive staining of analysed area, as measured by Q-win program, at 0, 1, 2, 14, and 28 days post dorsal root injury. Comparisons are made between ipsilateral vs contralateral **(*)**, injury vs naïve **(#)**, injury vs sham **(x)**, and DRA vs DRR **(+)**, shown above the respective data point. N. numbers: naïve (4), 1 day sham (3), 1 day DRA (4), 1 day DRR (4), 2 day DRA (6), 2 day DRR (6), 14 day sham (3), 14 day DRA (6), 14 day DRR (6), 28 day DRA (4), 28 day DRR (4).

3.2.1.2: Non-peptidergic (IB4) afferent terminals

Naïve tissue presented intense positive staining within lamina II and Lisseaur's Tract only, with a patchy non-granular appearance (Fig 3.3). No staining was observed in deeper laminae. Control groups presented 49.5% (+/- 2.14) density staining in the superficial lamina (Fig 3.4).

Similar to results from CGRP quantitative analysis, IB4-ir reduction is apparent and statistically different bilaterally at 1 day in all injury models including sham (Figs 3.3 and 3.4). IB4-ir for DRA, ipsilaterally, was significantly lower than sham (Fig 3.4). No difference between injury models, or between cord sides within injury models, was found at this time point.

IB4-ir reduction is maintained at 2 days (Fig 3.3). Only in DRA animals, was significant further ipsilateral reduction between 1 and 2 days (Fig 3.4). A significant difference was also observed between ipsilateral and contralateral IB4-ir in DRA at 2 days (Fig 3.4), but significance was not reached for DRR side comparison (P value = 0.089).

Similar to CGRP, the most significant ipsilateral reduction in IB4-ir in both deafferentation models compared to sham occurred at 14 days post injury (Figs 3.3 and 3.4). At this time point, both DRR and DRA had severely reduced ipsilateral IB4-ir (Fig 3.3) with values at 1.23% (+/-0.53) and 0.06% (+/-0.01) respectively (Fig 3.4), with no difference between these values. Contralaterally a significantly lower IB4-ir was apparent in DRA than DRR (Figs 3.3 and 3.4). No difference was observed at 14 days between sham cord sides, and no further reduction was presented from 1 day (Figs 3.3 and 3.4).

At 28 days post injury, ipsilateral staining was almost absent after deafferentation injury (Fig 3.3), with levels at 0.06% (+/-0.06) in DRA and 0.23% (+/-0.06) in DRR, with no significant difference between these values (Fig 3.4). Significant contralateral loss from 14 days is apparent in both models, and DRA is significantly less than DRR (Figs 3.3 and 3.4).

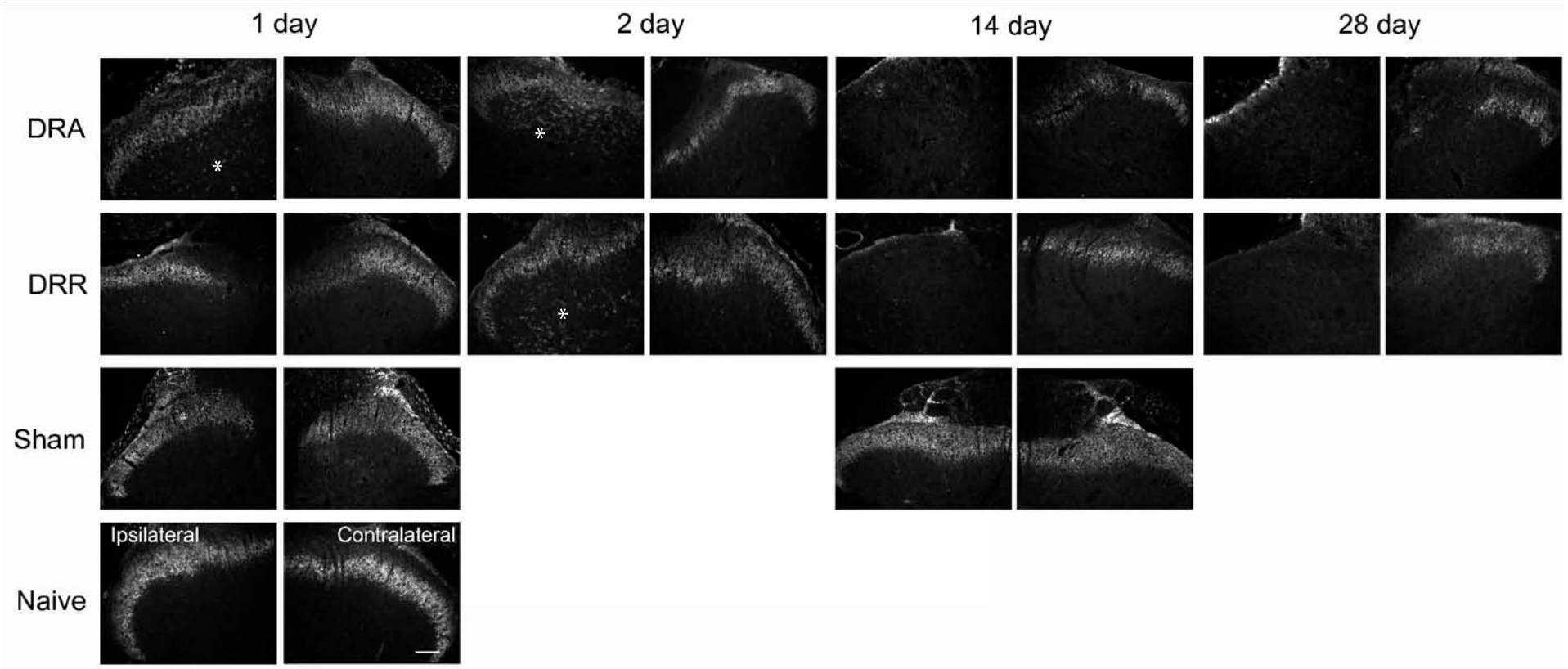

Fig 3.3: IB4 staining in the superficial laminae after root injury. Naïve IB4 staining is located within lamina II and Lisseaur's tract. 1 day after DRA, DRR, and sham injury, IB4 staining is reduced bilaterally, with greatest reduction observed ipsilaterally in DRA. Further reduction is observed at 2 days post DRA and DRR ipsilaterally. IB4-labelled microglia/macrophages are visible in DRA and DRR tissue (asterisk) at these early time points. 14 day post DRA and DRR IB4 staining is markedly reduced ipsilaterally with little to no staining remaining. A further reduction contralaterally is noted only with DRA. No further IB4 staining reduction is observed in sham tissue from 1 day. At 28 days post DRA and DRR marked reduction is noted contralaterally, prominently in DRA tissue. Ipsilaterally within the dorsal horn, scarring and damage in the DREZ and cord surface is observed. Ipsilateral images are shown to the left, and contralateral to the right. Scale = 100μm. Examples of L5 segmental level.

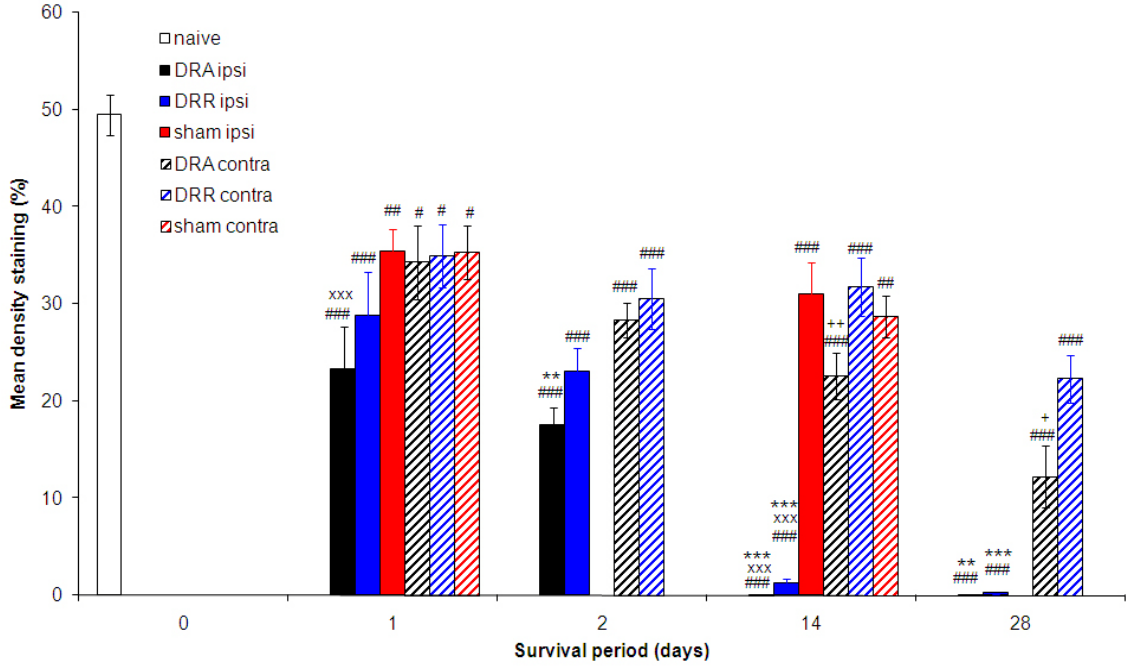

Fig 3.4: Quantitative analysis of IB4 density in the superficial dorsal horn. IB4 immunoreactivity is shown as a percentage positive staining of analysed area, as measured by Q-win program, at 0, 1, 2, 14, and 28 days post dorsal root injury. Comparisons are made between ipsilateral vs contralateral **(*)**, injury vs naïve **(#)**, injury vs sham **(x)**, and DRA vs DRR **(+)**, shown above the respective data point. N. numbers: naïve (4), 1 day sham (3), 1 day DRA (4), 1 day DRR (4), 2 day DRA (6), 2 day DRR (6), 14 day sham (3), 14 day DRA (6), 14 day DRR (6), 28 day DRA (4), 28 day DRR (4).

3.2.2: Quantification of glial activity within the dorsal horn after dorsal root injury

3.2.2.1: Microglia

In naïve lumbar cord, Iba1 staining of microglia was uniform throughout the entire transverse cord showing no preference for white or grey matter. The morphology of these cells was star shaped (ramified) in appearance. A cell body was clearly identifiable with dendritic processes radiating out in all directions (Fig 3.5). Through Q-win analysis of the dorsal horn mean percentage positive staining was 3.96% (+/-0.23) (Fig 3.6).

After injury these microglia undergo morphological changes, similar to developmental reactive microglia, as well as upregulation in number. Initially they lose their processes

(becoming amebiod), then multiply within, or migrate toward, the ipsilateral dorsal columns and dorsal horn (Fig 3.5), which is confirmed statistically as increased density (Fig 3.6).

At 1 day post injury there is no significant increase in intensity from naïve or sham (Fig 3.6) in microglia staining in either injury model. However in the case of DRA microglia have started to under reactivity, losing their multiple processes, becoming polarized and orientating their bodies towards the zone of injury, notably the superficial dorsal horn and the DREZ (Fig 3.5).

At 2 days post injury ipsilaterally, in DRA [9.57% (+/-0.75)] and DRR [7.90% (+/-0.86)] a significant increase in microglial staining is apparent (Fig 3.6), without contralateral changes. There is no statistical difference in Iba1 intensity between DRA and DRR injuries (Figs 3.5 and 3.6).

The most significant microglial effects occur at 14 days post injury, and bilaterally (Fig 3.5 and 3.6). The microglia take on a markedly different morphology: rounded, swollen, and absent of processes (Fig 3.5), which is more prominent in DRA [20.1% (+/-1.80)] than DRR [10.8% (+/-0.86)] (Fig 3.6). Sham ipsilateral Iba1-ir is significantly increased from naïve to 7.73% (+/-0.25) (Fig 3.6). Both injury models show statistically greater ipsilateral Iba1-ir than sham. A significant contralateral increase in Iba1-ir, from sham and naïve levels, is present in DRA [10.6% (+/-0.58)] (Fig 3.6). A significant contralateral increase is present in DRR [6.61% (+/-0.51)] compared to naïve; however this is not significantly different to sham (Fig 3.6).

At 28 days post injury no further increase in IBa1-ir is present ipsilaterally (Fig 3.5 and 3.6). Indeed DRR immunoreactivity shows a decrease in Iba1-ir ipsilaterally (7.16% +/-0.58) and contralaterally (3.99% +/-0.20). However in DRA a significant gain in contralateral immunoreactivity is observed at 14.4% (+/-0.62) such that a greater difference in microglial activity is present between injury models (Fig 3.6). Significant difference is maintained between cord sides and between deafferentation groups (Fig 3.6).

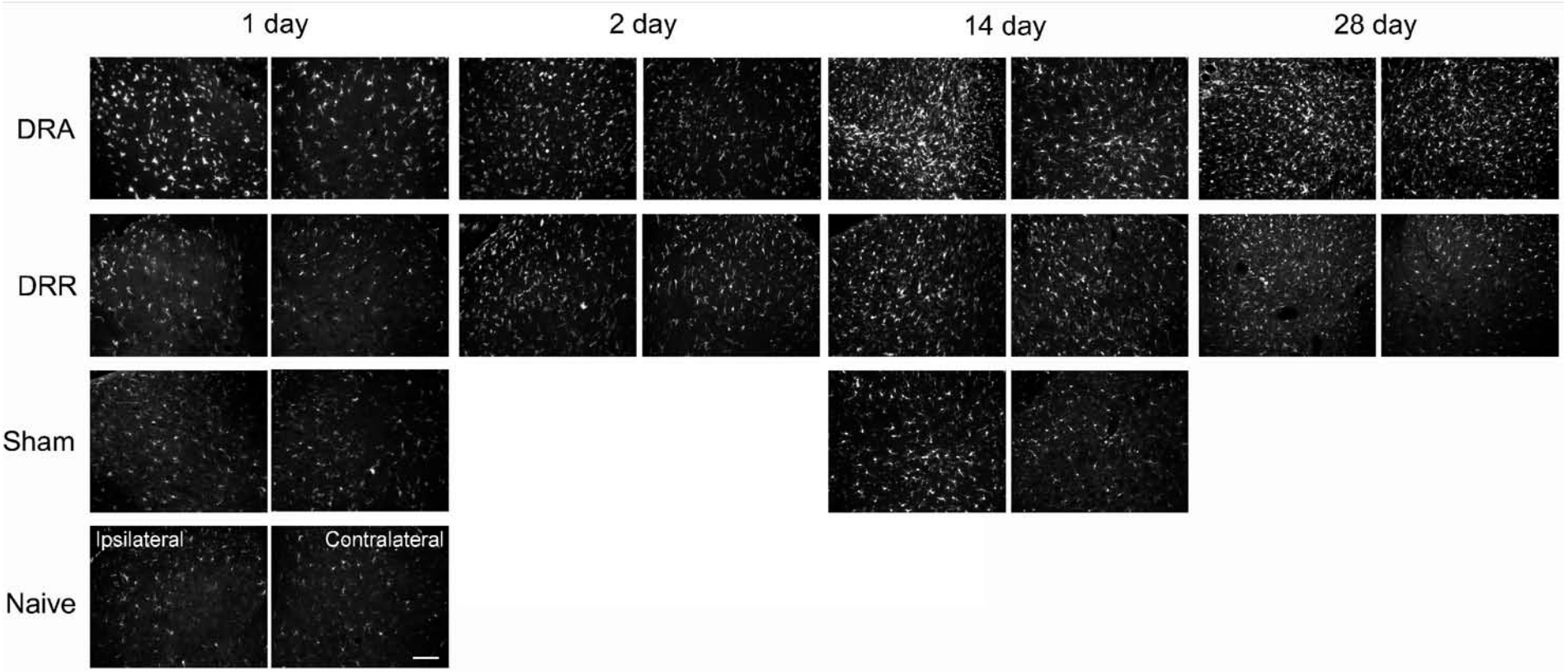

Fig 3.5: IBA1 staining in the dorsal horn after root injury. Naïve IBA1 staining shows a resting (ramified) microglial state, with a distinguishable cell soma and dendritric-like branches. 1 day sham and DRR injury presents no increase in microglial reactivity from naïve levels. Ipsilateral DRA injured tissue shows some activation of microglia with shortening of processes and swelling of soma, however this is not significant when analysed for immunoreactivity density. 2 day post DRR and DRA present significant microglial reactivity ipsilaterally but no effects contralaterally. After 14 days post DRR injury, microglial reactivity is maintained without further notable increase in density staining ipsilaterally, with a slight but significant increase in contralateral staining. 14 days post DRA shows much greater increase in microglial reactivity ipsilaterally, as well as a prominent contralateral effect. At 28 days post DRR no further change is noted in microglial populations, and the contralateral effect is lost. At 28 days post DRA microglial reactivity is maintained bilaterally in considerable contrast to DRR tissue. Reactivity of microglia is shown as an upregulation in number, and a morphological change into a typical phagocytic shape absent of processes. Ipsilateral images are shown to the left, and contralateral to the right. Scale = 100µm. Examples of L5 segmental level.

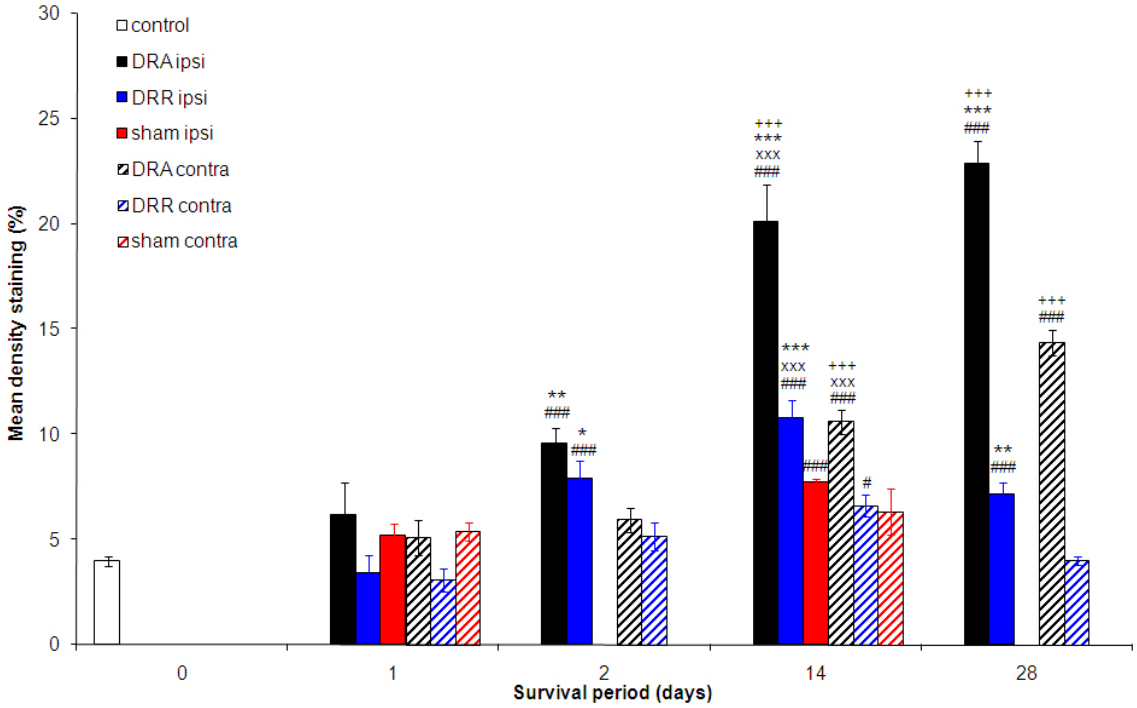

Fig 3.6: Quantitative analysis of Iba1 staining in the dorsal horn. IBA1 immunoreactivity is shown as a percentage positive staining of analysed area, as measured by Q-win program, at 0, 1, 2, 14, and 28 days post dorsal root injury. Significant differences from naïve and between groups are indicated by asterisks. Comparisons are made between ipsilateral vs contralateral **(*)**, injury vs naïve **(#)**, injury vs sham **(x)**, and DRA vs DRR **(+)**, shown above the respective data point. N. numbers: naïve (4), 1 day sham (3), 1 day DRA (4), 1 day DRR (4), 2 day DRA (6), 2 day DRR (6), 14 day sham (3), 14 day DRA (6), 14 day DRR (6), 28 day DRA (4), 28 day DRR (4).

3.2.2.2: Astrocytes

GFAP-positive astrocytes in the naïve tissue are uniformly distributed throughout the cord in both grey and white matter, and are star shaped in morphology with short processes (Fig 3.7). Q-win analysis of the dorsal horn produced an 8.77% (+/-1.37) mean positive staining for GFAP (Fig 3.8).

After injury to the roots, dorsal horn astrocytes respond rapidly by upregulating GFAP, undergoing hypertrophy, elongation and migration of processes towards the injury site, and finally forming a scar (Fig 3.7). They can undergo cell division and produce fine processes which migrate toward the locality of the lesion and interconnect via tight and gap junctions to form the eventual glial scar.

At 1 day post injury, a significant ipsilateral increase in GFAP-ir is present in DRA (Fig 3.8) compared to naïve and contralateral, with astrocyte processes polarised toward the DREZ (Fig 3.7). No significant increase in GFAP-ir is evident in DRR or sham (Figs 3.7 and 3.8).

At 2 days post injury, DRA shows significant bilateral increase in GFAP-ir from naive, and significantly greater than DRR (Fig 3.8). DRR shows a significant ipsilateral increase in GFAP-ir compared to contralateral and naïve levels (Fig 3.8), and polarisation and hypertrophy of processes is first observed (Fig 3.7).

At 14 days post injury there is a significant bilateral increase from 2 days, in both injury models (Fig 3.8). Astrocytes no longer have elongated and polarized processes, and resume their original star shapes, as well as forming notable structures around cavities (Fig 3.7). There is a significant bilateral GFAP-ir increase compared to naïve levels in sham tissue (Fig 3.7 and 3.8). DRA presents a significantly greater bilateral GFAP-ir to sham at 14 days, whereas in DRR tissue GFAP-ir is statistically greater than sham only ipsilaterally (Fig 3.8). There is significantly greater GFAP-ir in DRA than DRR, ipsilaterally [24.0% (+/-1.62) and 19.1% (+/-1.92) respectively] and contralaterally [20.7% (+/-0.52) and 13.5% (+/-1.83) respectively] (Fig 3.8).

At 28 days post injury no further increase in GFAP-ir is apparent. Levels are maintained at 24.3% +/-0.83 (DRA) and 15.1% +/-1.17 (DRR) ipsilaterally, and contralaterally at 19.7% +/-1.02 (DRA) and 8.65% +/-0.37 (DRR) respectively. Significant difference between deafferentation models is maintained bilaterally.

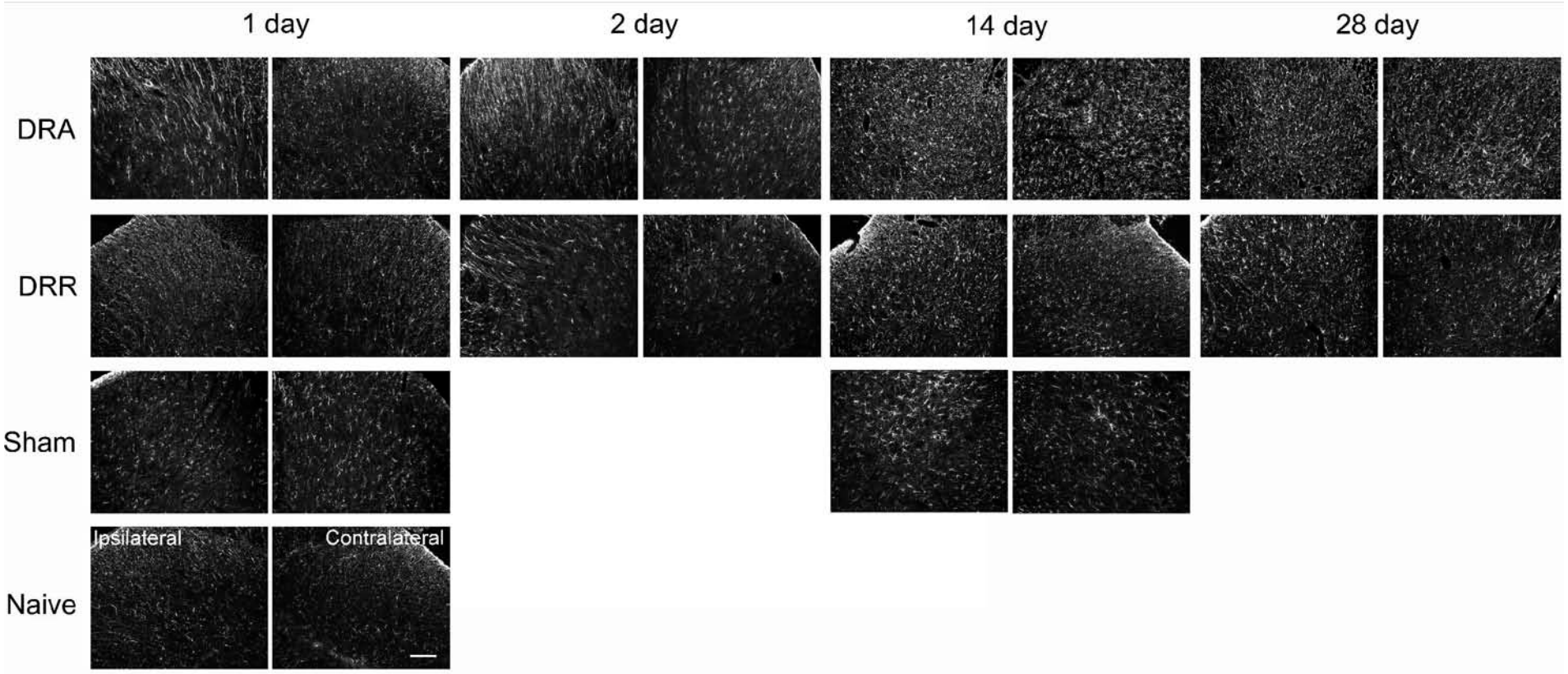

Fig 3.7: GFAP staining in the dorsal horn after root injury. In naïve tissue, GFAP-positive astrocytes are apparent throughout the ipsilateral dorsal horn, star shaped in appearance with short processes. 1 day after injury sham and DRR tissue show no increase in GFAP-ir, whereas DRA tissue presents astrocyte hypertrophy, elongation, and directional migration toward the ipsilateral DREZ. 2 days post injury shows further ordered elongation of astrocytes in DRA, and a contralateral increase in GFAP-ir, and for the first time astrocyte reactivity in DRR ipsilaterally. 14 days after sham injury the dorsal horns bilaterally show slight but significant increase in GFAP expression in astrocytes. At 14 days post DRR and DRA the ipsilateral dorsal horn shows an increase in gliosis compared to 2 days, with markedly different astrocyte morphology. There is also a contralateral effect. At 28 days no further increase in GFAP astrocyte reactivity is noted in the injury models, and in the case of DRR GFAP-ir decreases bilaterally. At the later time points a gliotic scar is notable in the DREZ and superficial dorsal horn and columns, where interconnecting astrocytic processes layer the dorsal columns and surround large necrotic cysts and vacuoles. Ipsilateral images are shown to the left, and contralateral to the right. Scale = 100μm. Examples of L5 segmental level.

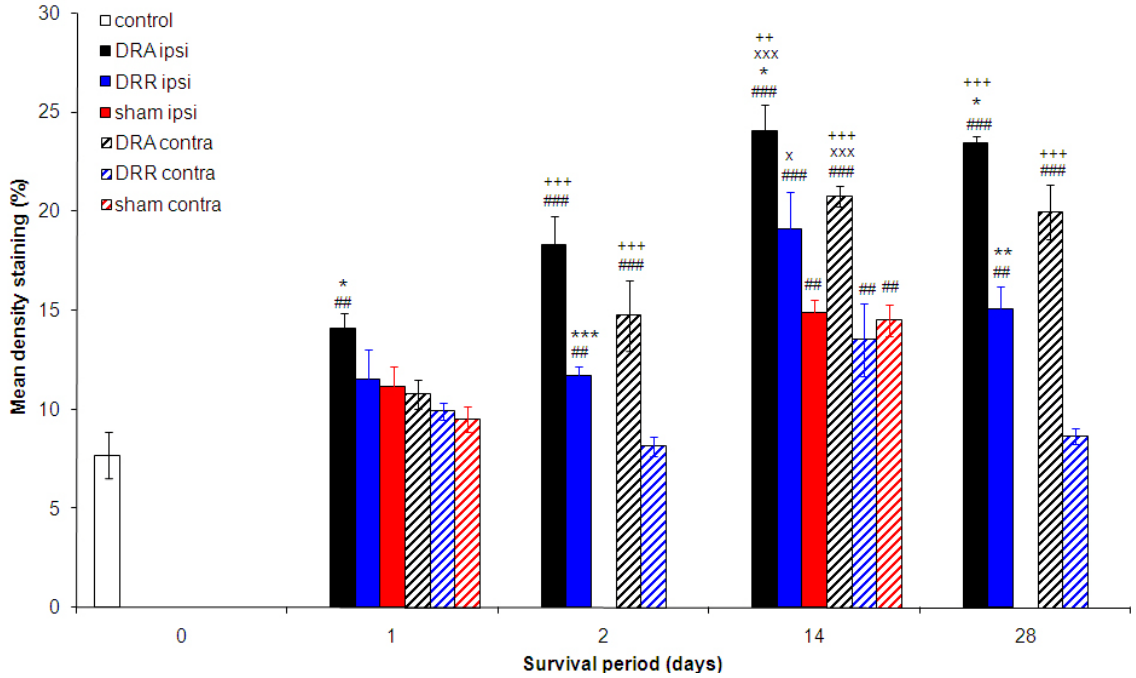

Fig 3.8: Quantitative analysis of GFAP staining in the dorsal horn. GFAP immunoreactivity is shown as a percentage positive staining of analysed area, as measured by Q-win program, at 0, 1, 2, 14, and 28 days post dorsal root injury. Significant differences are indicated by asterisks to the right of the data point or error bar. Comparisons are made between ipsilateral vs contralateral **(*)**, injury vs naïve **(#)**, injury vs sham **(x)**, and DRA vs DRR **(+)**, shown above the respective data point. N. numbers: naïve (4), 1 day sham (3), 1 day DRA (4), 1 day DRR (4), 2 day DRA (6), 2 day DRR (6), 14 day sham (3), 14 day DRA (6), 14 day DRR (6), 28 day DRA (4), 28 day DRR (4).

3.2.3: Blood borne infiltration within the dorsal horn and dorsal root entry zone

3.2.3.1: Macrophages

Macrophages can be identified using an antibody to ED1 (labels human CD68 glycoprotein). This complement factor is a lysosomal membrane antigen expressed in mononuclear phagocytes, both blood borne-derived and microglial-derived.

Naïve tissue revealed scarcely any macrophage staining within any areas of the cord (Fig 3.11). This was also the case for 1 and 14 day sham surgery (Figs 3.9 to 3.11). Some ED1 macrophages were present in 14 day sham ipsilateral dorsal horn (Fig 3.10), but when quantified did not reach significant difference from naïve tissue (Fig 3.11)

At 1 day post DRA some sparse macrophage staining is observed (Figs 3.9 and 3.10), however significantly increased ED1-ir is statistically reached only within the ipsilateral

dorsal horn compared to contralateral, with a mean percentage staining of 1.00% (+/-0.35) (Fig 3.11). Compared to naïve however, this does not reach statistical significance (P=0.063). No significant ED1-ir is found in DRR or sham tissue.

At 2 days post DRA increase in ED1-ir is significantly greater than naïve and contralateral values, in the ipsilateral dorsal horn [2.17% (+/-0.37)] and columns [2.66% (+/-0.49)] (Fig 3.11). DRR ED1-ir is also increased ipsilaterally in both dorsal horn [1.64% (+/-0.29)] and dorsal column [1.82% (+/-0.24)] compared to naïve and contralateral levels (Fig 3.11). The macrophages are granular in appearance, and are small, few in number, and irregularly dispersed between superficial and deep lamina, and the DREZ and dorsal columns (Figs 3.9 and 3.10).

A statistically significant ED1-ir expression increase occurs after 14 days in the ipsilateral dorsal horn, but more so in the ipsilateral dorsal columns of DRA (Figs 3.9 to 3.11). 14 day sham tissue shows no significant increase in ED1-ir. ED1-ir of DRA has significantly increased from 2 days, reaching 10.5% (+/-0.78) in the dorsal columns and 3.62% (+/-0.86) in the dorsal horn (Fig 3.11). DRR ED1-ir has significantly increased in the dorsal columns to 4.06% (+/-1.06) compared to sham, naïve, and contralateral values, and in the dorsal horn 1.65% (+/-0.42) compared to naïve and contralateral values, without significance from sham in this case (Fig 3.11).

At 28 days post DRA injury further increase is observed in the dorsal horn, ipsilaterally [5.46% (+/-1.40)] and contralaterally [1.78% (+/-0.54)], and more extensively in the dorsal columns, ipsilaterally [18.3% (+/-1.79)] and contralaterally [6.27% (+/-3.19)] (Figs 3.9 to 3.11). In DRR tissue no contralateral effect is observed (Figs 3.9 and 3.10), and further ED1-ir increase is observed only ipsilaterally in the dorsal columns [9.82% (+/-0.91)] (Figs 3.9 and 3.11). In all cases DRA initiates a far greater ED1-ir expression in the dorsal horn and columns than DRR at 28 days.

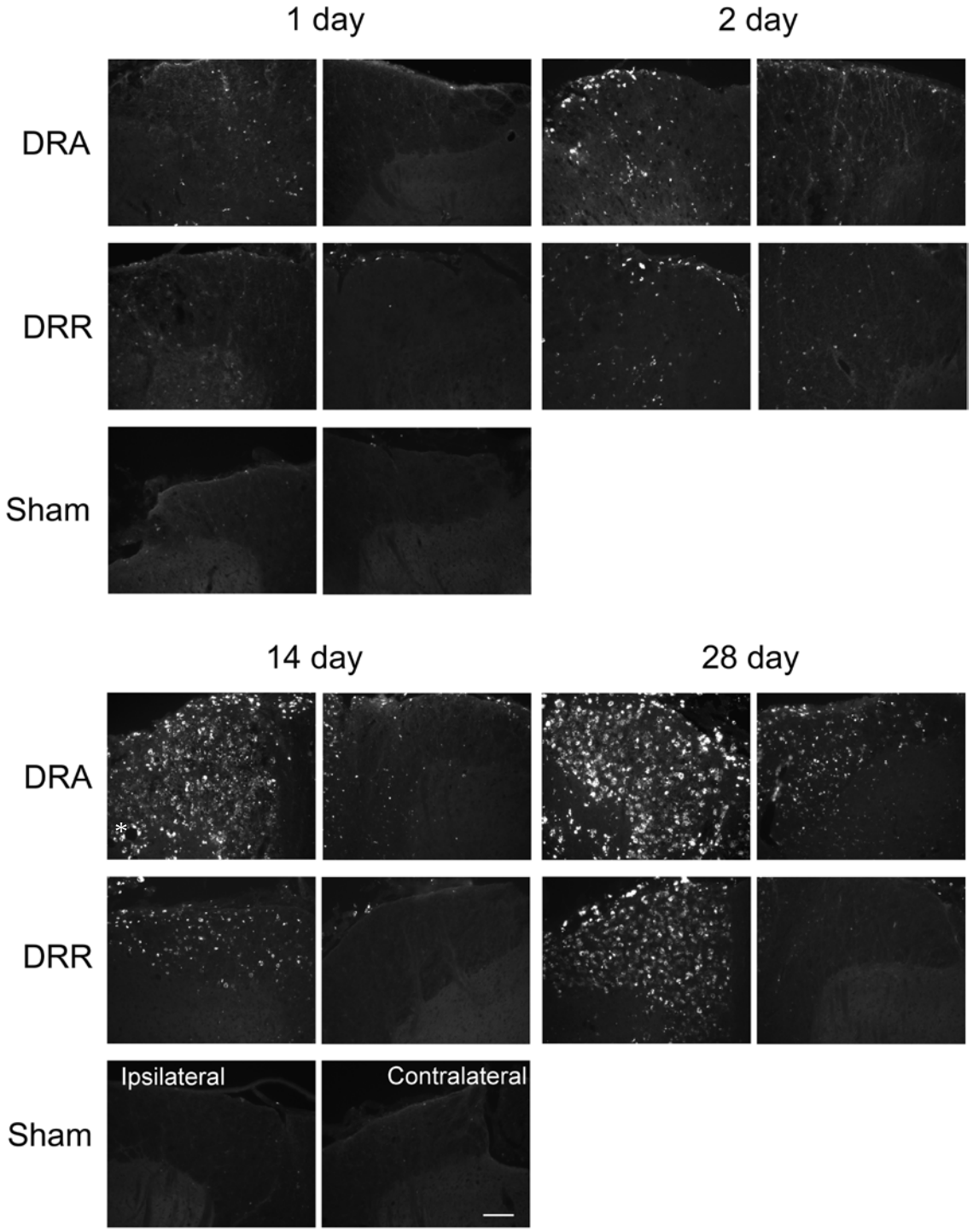

Fig 3.9: ED1 staining in the dorsal columns after root injury. ED1-positive macrophages are not found in 1 day sham tissue or naïve tissue (not shown). 1 day after DRA and DRR injury few macrophages are found in the DREZ. After 2 days in DRA and DRR ED1 is distributed as patches of staining throughout the dorsal columns, but mainly near the DREZ, with many macrophages found towards the pia mater. 14 day sham shows no ED1 positive macrophages. At 14 days in DRA tissue, swollen macrophages are clearly defined in the dorsal columns, and the tissue shows cavitation (white asterisk). At 14 days in DRR, ED1 positivity and tissue cavitation is also noted but not to the same extent as DRA. A few macrophages are found contralaterally in DRA tissue. 28 days post DRR and DRA tissue shows greatly increased ED1 immunoreactivity from previous time points, with ED1 staining throughout the dorsal columns. A significant contralateral ED1 staining is present in DRA tissue. There are significantly greater macrophages in the DRA than in the DRR tissue. Naïve tissue is not shown. Ipsilateral images are shown to the left, and contralateral to the right. Scale = 100μm. Examples of L5 segmental level.

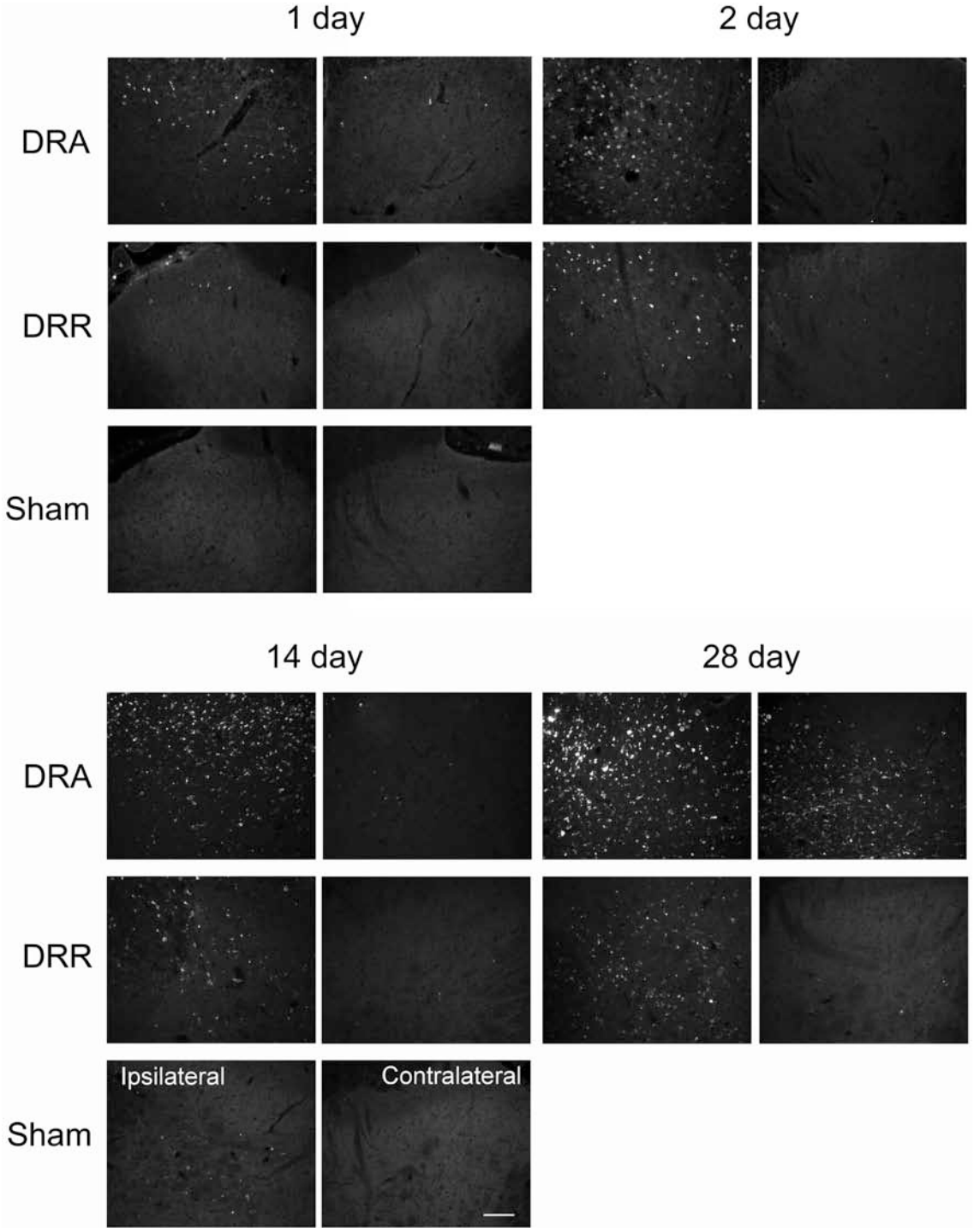

Fig 3.10: ED1 staining in the dorsal horn after root injury. ED1-positive macrophages are not found in 1 day sham tissue or naïve tissue (not shown). 1 day after DRA and DRR injury few macrophages are found in the dorsal horn, more so in the former. After 2 days in DRA and DRR ED1 is distributed in a punctuate fashion throughout the dorsal horn. No contralateral effect is noted at these early time points. 14 day sham shows few ED1 positive macrophages in the dorsal horn. At 14 days in DRA tissue, punctuate ED1 staining is clearly defined in the dorsal horn. At 14 days in DRR, ED1 positivity is also noted but not to the same extent as DRA. 28 days post DRR and DRA tissue shows greatly increased ED1 immunoreactivity from previous time points, with ED1 staining throughout the dorsal horn. A clear contralateral ED1 increase is noted in DRA tissue. There are significantly greater macrophages in the DRA than in the DRR tissue. Naïve tissue is not shown. Ipsilateral images are shown to the left, and contralateral to the right. Scale = 100μm. Examples of L5 segmental level.

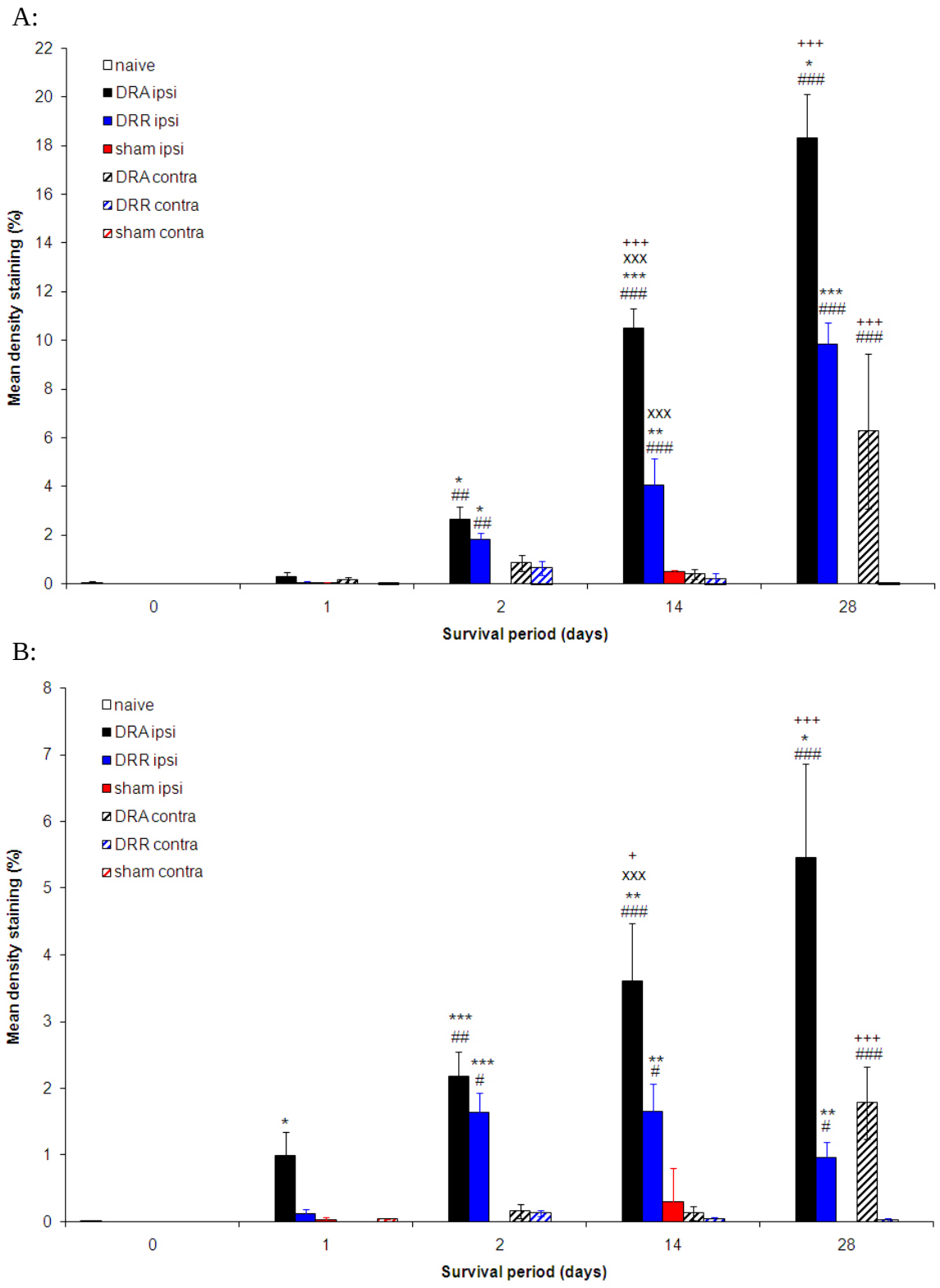

Fig 3.11: Quantitative analysis of ED1 in the dorsal columns (A) and dorsal horns (B). ED1 immunoreactivity is shown as a percentage positive staining of analysed area, as measured by Q-win program, at 0, 1, 2, 14, and 28 days post dorsal root injury. Comparisons are made between ipsilateral vs contralateral **(*)**, injury vs naïve **(#)**, injury vs sham **(x)**, and DRA vs DRR **(+)**, shown above the respective data point. N. numbers: naïve (4), 1 day sham (3), 1 day DRA (4), 1 day DRR (4), 2 day DRA (6), 2 day DRR (6), 14 day sham (3), 14 day DRA (6), 14 day DRR (6), 28 day DRA (4), 28 day DRR

3.2.3.2: Neutrophils

Naïve sections presented few, if any, neutrophils in the dorsal horn and columns. Neutrophils that were identified were almost exclusively associated with the microvasculature and were not within the grey or white neuronal matter. The mononuclear cells are typically rounded, 10-15μm in diameter, with intense staining of the cell membrane, with a weaker immunoreactivity in the cytoplasm (Fig 3.12). Mean numbers for neutophils within naïve tissue were 1.85 (+/-0.68) and 1.23 (+/-0.27) in the dorsal horn and columns respectively (Fig 3.13).

At 1 day post injury neutrophils were found throughout the dorsal horn and dorsal columns (Fig 3.12). After DRA a significant increase in neutrophil number was quantified in the dorsal horn [95.1 (+/-8.36)] and dorsal columns [41.7 (+/-5.32)] compared to sham and naïve tissue (Fig 3.13), where counts peak at this time point. Neutrophils were also found in DRA tissue within the contralateral dorsal column [12.9 (+/-2.15)] and dorsal horn [14.4 (+/-2.32)] at levels significantly greater than sham and naïve tissue (Fig 3.13). After 1 day post DRR significant neutrophil infiltration is found exclusively ipsilaterally, in the dorsal columns [17.0 (+/-2.10)] and dorsal horn [24.1 (+/-3.85)] compared to naïve and sham tissue (Fig 3.13). Neutrophil counts were were significantly greater after DRA than DRR in both dorsal horn and columns, bilaterally. A small but significant neutrophil infiltration was quantified in 1 day sham, within the ipsilateral dorsal horn [7.90 (+/-1.66)] (Figs 3.12 and 3.13).

At 2 days post injury no further increase in neutrophil number can be observed in DRA tissue, however further increase in infiltration occurs in DRR tissue (Fig 3.12). Neutrophil counts in DRR tissue reach 34.8 (+/-9.24) in the dorsal horn, and 37.9 (+/-3.48) in the dorsal columns, significantly greater than naïve and corresponding contralateral sides (Fig 3.13). DRA tissue shows significantly more neutrophils in the dorsal horn than DRR; however, similar numbers are noted in the dorsal columns of these two injuries (Figs 3.12 and 3.13). At 2 days in both injury models, a significant contralateral neutrophil infiltration is apparent in the dorsal columns after DRA [12.7(+/-3.33)] and after DRR [13.5 (+/-3.43)] compared to naïve neutrophil counts (Fig 3.13). A small but significant increase in neutrophils is observed in the

contralateral dorsal horn after DRA [6.36 (+/-1.35)] compared to naïve levels, that is absent in DRR (Figs 3.12 and 3.13).

At 14 days post injury, neutrophil number decreases dramatically in both models (Fig 3.12). However ipsilateral values for DRA [6.75 (+/-0.75)] and DRR [9.58 (+/-1.54)] are still significantly higher than sham and naïve neutrophil numbers in the dorsal horn at this time point (Fig 3.13). In the dorsal columns ipsilateral DRR neutrophil counts [3.47 (+/-1.70)] reach significance against naïve, but this is not significant against sham neutrophil counts (Fig 3.13). In the dorsal columns of DRA tissue, neutrophils are present (Fig 3.12); however, counts do not reach significance against naïve or sham levels (P=0.82, Fig 3.13). At this time point there is a large quantity of anti-neutrophil-ir staining present in the ipsilateral cord that is not associated with cellular morphology, but rather a particulate mater that is speckled in appearance (Fig 3.12), that was not quantified. Further analysis of neutrophil number at 28 days shows no significance difference from naïve levels (Fig 3.13), but the particulate anti-neutrophil-ir staining is still observed in the dorsal cord (Fig 3.12).

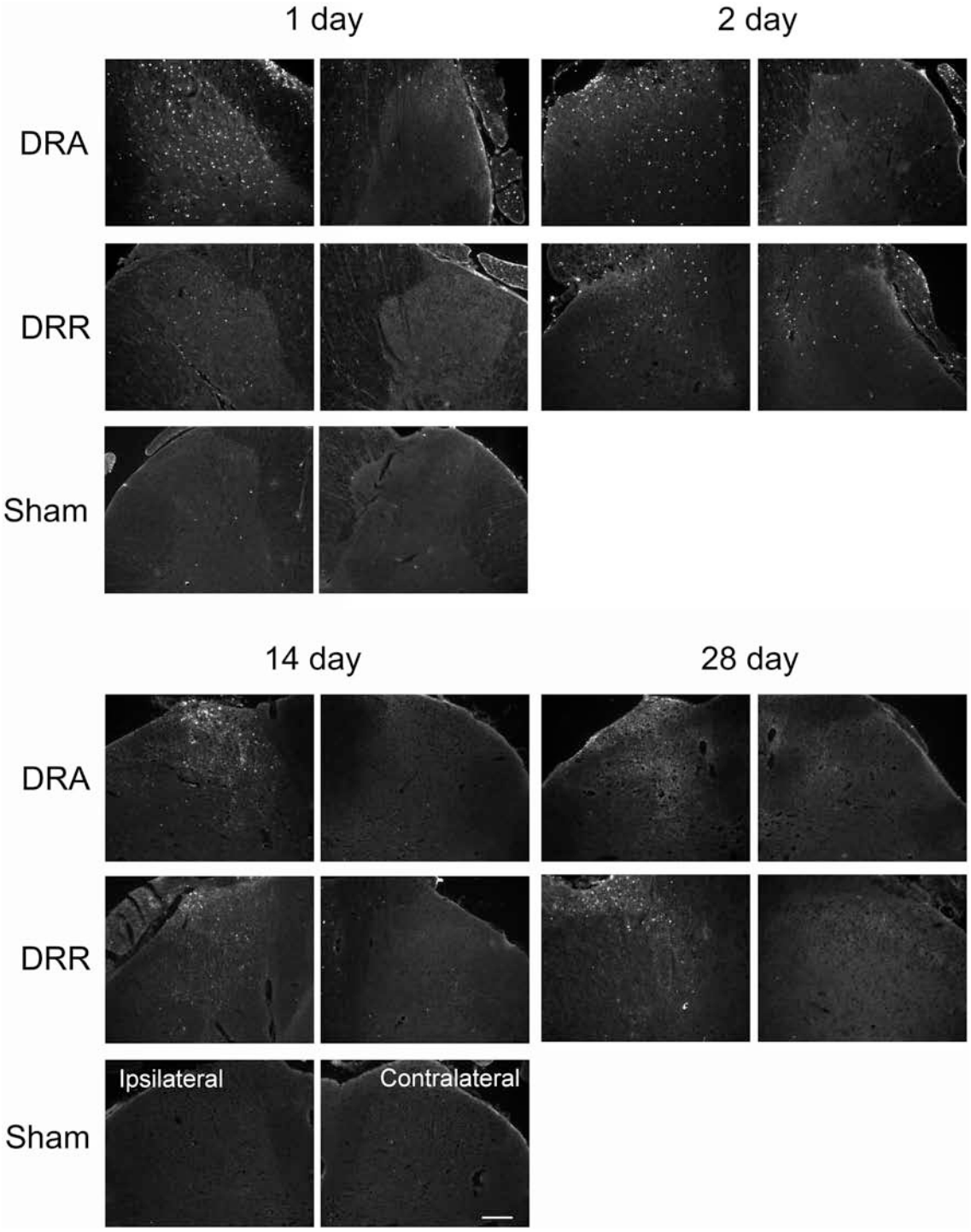

Fig 3.12: Neutrophils in the spinal cord after root injury. Neutrophils are spherical in appearance, with staining around the cell membrane. Few neutrophils are found in sham tissue either 1 day or 14 days post injury. 1 day after DRA, neutrophils are apparent throughout the entire dorsal cord, with a few present contralaterally. 1 day DRR tissue shows a smaller, but still significant, increase in neutrophil number in the dorsal horn and columns but with ipsilateral preference. 2 days after DRR a significant increase in neutrophils is noted in the dorsal columns, DREZ and within the degenerating root. At 2 days after DRA, neutophils have a similar concentration to 1 day levels. At 2 days post injury notable contralateral neutrophil infiltration is observed. At 14 days after injury the numbers of identifiable neutrophils is markedly reduced. However neutrophil-ir debris is found throughout the ipsilateral cord. In DRA tissue necrotic tissue and cystic cavities around the lesion site is notable. 28 day tissue is similar to 14 day injury in both models, with no significant identifiable neutrophils and only particulate staining present around the injury site. Naïve tissue is not shown as staining was not present. Ipsilateral images are shown to the left, and contralateral to the right. Scale = 200μm. Examples of L5 segmental level.

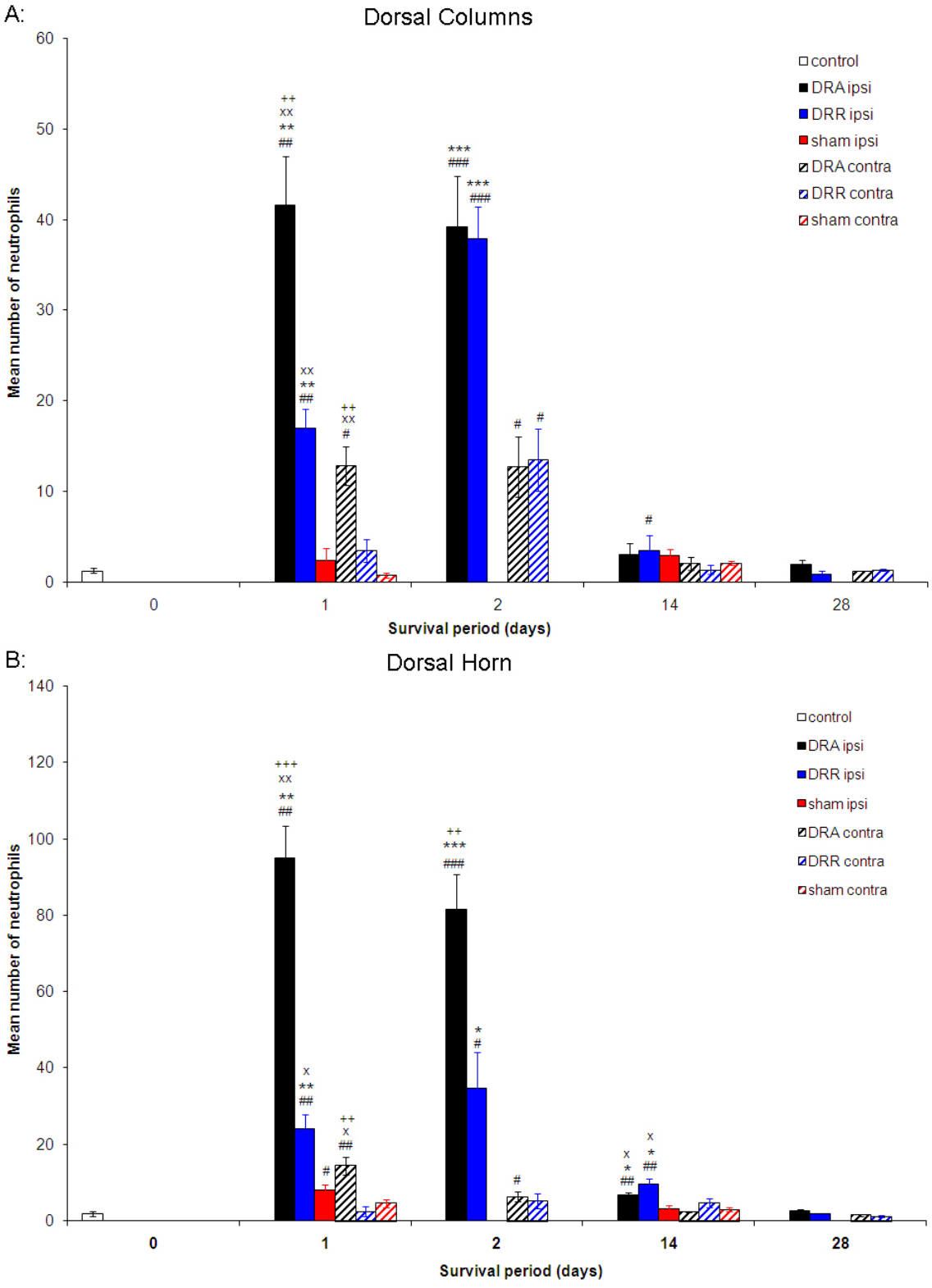

Fig 3.13: Neutrophil counts in the dorsal column (A) and dorsal horn (B) after injury. Neutrophil immunoreactivity is shown as mean number of positive cells per section at 0, 1, 2, 14, and 28 days post dorsal root injury. Similar time course of neutrophil infiltration occurs in the dorsal columns as in the dorsal horn. Contralateral neutrophil counts were also detected, however not significantly greater than naïve. Infiltration was maximal at 1 day in the avulsion model and 2 days in the rhizotomy model. Comparisons are made between ipsilateral vs contralateral **(*)**, injury vs naïve **(#)**, injury vs sham **(x)**, and DRA vs DRR **(+)**, shown above the respective data point. N. numbers: naïve (4), 1 day sham (3), 1 day DRA (4), 1 day DRR (4), 2 day DRA (6), 2 day DRR (6), 14 day sham (3), 14 day DRA (6), 14 day DRR (6).

3.2.4: The integrity of the microvascular system of the lumbar spinal cord

Damage to the dorsal horn microvasculature is shown histologically as a decrease in endothelial cell immunoreactivity as measured by RECA-1 antibody (Fig 3.14).

Naïve rat spinal cord, labelled with RECA-1 and Q-win analysed, provided percentage density staining values of 5.89% (+/-0.28) of the dorsal horn (Fig 3.15).

At 1 day after DRA a decrease in RECA-1-ir was observed ipsilaterally [3.49% (+/-0.35)] compared to naïve and contralateral levels (Fig 3.15). A RECA-1-ir reduction was found in 1 day DRR ipsilaterally [4.71% (+/-0.28)], significant only from naïve levels (Fig 3.15). No contralateral reduction was found at this time point (Figs 3.14 and 3.15). DRA tissue presents significantly less RECA-ir than DRR at 1 day (Fig 3.15). A significant reduction in RECA-ir was found in sham ipsilaterally [4.12% (+/-0.82)] compared to naïve (Fig 3.15).

A statistically significant ipsilateral reduction is apparent at 2 days post DRA [2.51% (+/-0.35)] and DRR [2.93% (+/-0.62)] (Fig 3.15). A delayed contralateral effect is also significant at this time point with values of RECA-ir at 2.77% (+/-0.50) for DRA and 4.01% (+/-0.37) for DRR (Fig 3.15). Difference between DRR and DRA RECA-ir at 2 days (Fig 3.14) do not reach statistical significance (P=0.074) (Fig 3.15).

At 14 days post injury a significant recovery in RECA-1-ir is presented in DRR animals (Fig 3.14), with staining reaching 5.18% (+/-0.53) ipsilaterally and 5.80% (+/-0.50) contralaterally, with no significant difference to sham or naïve levels. However there is no such improvement from 2 days in DRA [3.65% (+/-0.43) ipsilaterally and 3.55% (+/-0.51) contralaterally], and is still significantly less bilaterally than naïve and sham levels, and for the first time, DRR RECA-1-ir levels (Fig 3.15).

No change is seen in either deafferentation group at 28 days from 14 days (Fig 3.14). In DRA tissue RECA-1-ir [(3.36% +/-0.46 ipsilaterally) and (3.54% +/-0.29 contralaterally)] is significantly lower than naïve and DRR values bilaterally (Fig 3.15). DRR RECA-1-ir values are maintained from 14 days, and are not significantly different to naïve levels bilaterally (Fig 3.15).

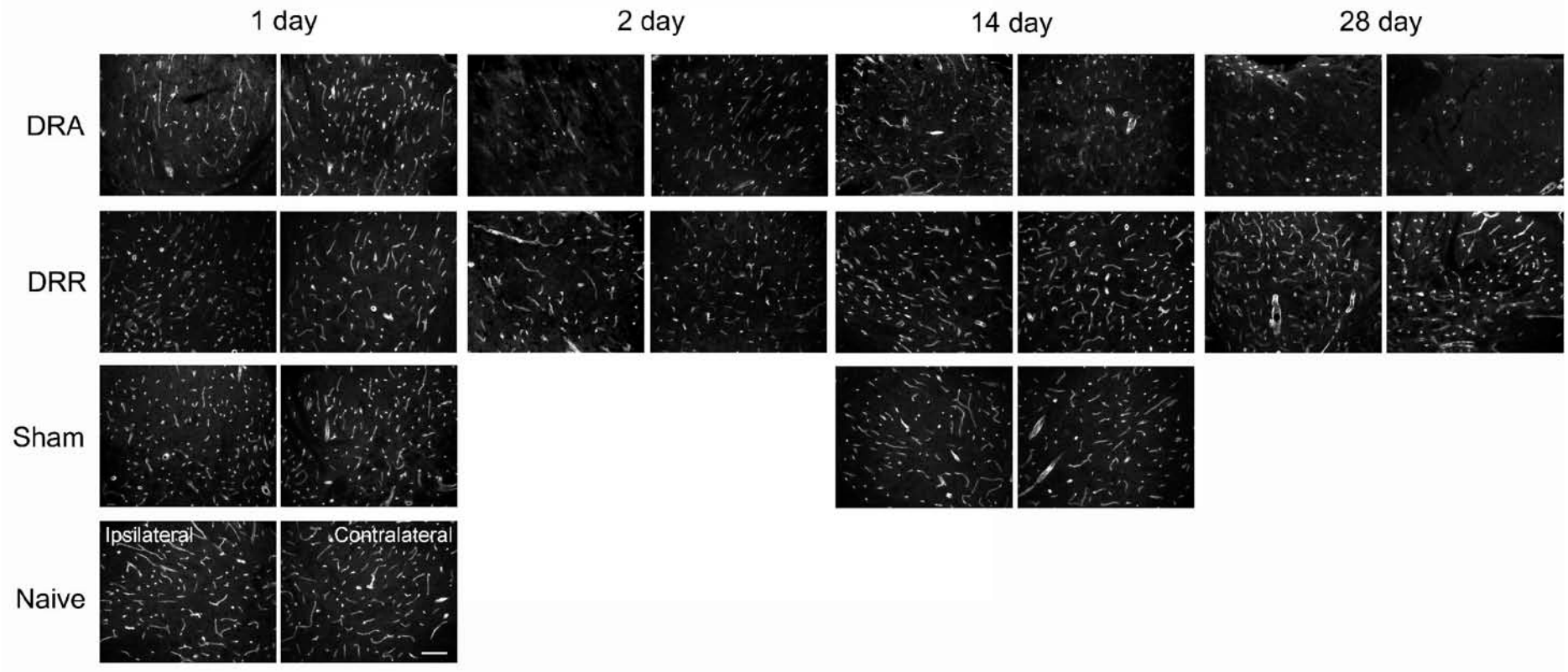

Fig 3.14: RECA-1 staining in the spinal cord and ipsilateral dorsal horn after injury. Naïve RECA-1 staining presents a heavily vascularised grey and white matter, with smooth and thick vessels travelling transversely and sagittally. 1 day sham, DRA, and DRR show ipsilateral reduction in RECA-1-ir. At 2 days in DRA and DRR tissue, blood vessel numbers are decreased as is vessel length within the section bilaterally. The vessels seem broken with sharp edges to their endings. After 14 days in DRR tissue, regeneration of the vasculature from 2 days is noted bilaterally, to that which resembles naïve and 14 sham tissue. Number, thickness, and staining have increased, and individual vessels are longer and smoother in appearance than at 2 days. After 14 days in DRA tissue however no such regeneration is noted within the microvasculature. At 28 days DRR tissue is revascularised resembling naïve tissue, however DRA tissue shows a maintained loss of vasculature bilaterally. Ipsilateral images are shown to the left, and contralateral to the right. Scale = 100μm. Examples of L5 segmental level.

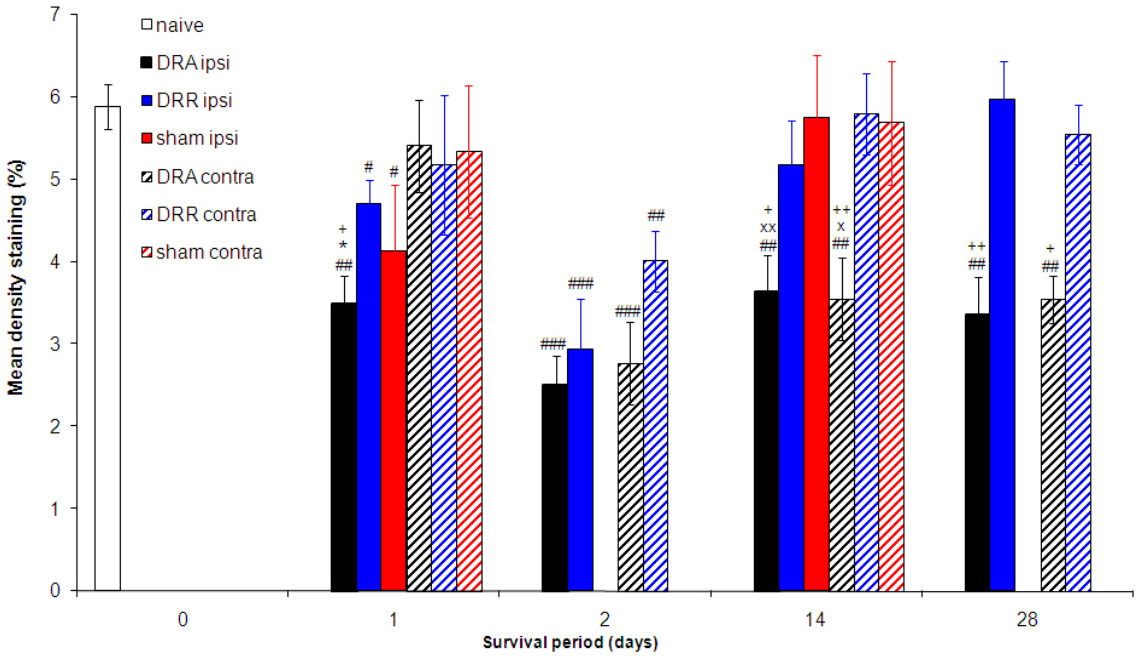

Fig 3.15. Quantitative analysis of RECA-1 in the dorsal horn. RECA-1 immunoreactivity is shown as a percentage positive staining of analysed area, as measured by Q-win program, at 0, 1, 2, 14, and 28 days post dorsal root injury. A significant decrease (~ 50%) in vasculature staining is evident at 2 days post DRA and DRR. which is maintained at 14 and 28 days post DRA only. DRR tissue shows significant vascular recovery at 14 days. No significant difference is found in RECA staining at 1 day compared to naïve. Comparisons are made between ipsilateral vs contralateral **(*)**, injury vs naïve **(#)**, injury vs sham **(x)**, and DRA vs DRR **(+)**, shown above the respective data point. N. numbers: naïve (4), 1 day sham (3), 1 day DRA (4), 1 day DRR (4), 2 day DRA (6), 2 day DRR (6), 14 day sham (3), 14 day DRA (6), 14 day DRR (6), 28 day DRA (4), 28 day DRR (4).

3.2.5: Cell death and neuronal loss

3.2.5.1: Fluorescence-activated cell-sorting (FACS) flow cytometry

Cytometry was used to quantitatively examine cell viability within the naïve, sham, and DRR/DRA spinal cord. Information was collected on the total L3-L6 spinal cord, through fluorescence analysis of a free suspension sample of dissociated cells.

Scattered light measurements determined the ratio of dead cells to live cells in the suspended sample of dissociated cells. As the cell suspension sample flowed through the cytometer each cell or cell particulate matter, was subjected to deflection by electric charge. This deflection can be forward or sideways, as is detected by the flow cytometer as events on a scatter plot. The extent of forward scatter (FSC) is dependent upon size of particle, and side scatter (SSC) is dependent upon cytoplasmic granulation (a cellular

marker for a dying or dead cell). In this way a detection of dead cells can be accomplished without fluorescence, described as flow cytometry (Fig 3.16A).

A selection of these events was taken in favour of isolating whole cell counts (represented by the P1 box [Fig 3.16B-F and Fig 3.17B-F]). After scattering, these events were subjected to laser excitation, and a series of dichroic mirrors and filters directed the emission into channels for detection. As more than one fluorophore was used in some cases, the mirrors separate the emission spectrum characterising the different staining, such as DAPI and FITC. Each fluorophore detected was measured as an event and plotted on a scatter graph, constituting the fluorescence-activated component of the analysis.

PI FACS:

Figure 3.16A is a scatter plot example of all events from a sample of injured cord. The 'P1' box represents a sample population of the largest events, typically whole cells rather than debris. This sample population can be divided into PI-positive (Red - dead/dying/broken membranes) and PI-negative (Black - alive/intact membranes) cells (Figs 3.16B-F). This provides a percentage of dead cells within this sample, representing the L3-L6 cord. The placement and size of the 'P1 box' (Fig 3.16A), as well as the grid-line dissectors (Figs 3.16B-F) are kept constant between experiments, and have been previously defined through adding the same dissociated spinal cord sample to the flow cytometer, absent of PI staining.

Naïve tissue and 2 day sham tissue (Fig 3.16B) showed 0.83% (+/-0.21) and 2.05% (+/-0.32) PI+ve cell percentages within samples of L3-L6 cord (Fig 3.18A).

At 2 days after injury, DRA [10.3% (+/-2.03%)] and DRR [13.4% (+/-5.39%)] tissue show significant increases in PI+ve cells in the scatter plots (Figs 3.16C-D), from naïve and sham levels, but werere not significantly different from one another (Fig 3.18A).

At 14 days post injury PI+ve cells decreased from 2 days (Fig 3.16E and 3.16F). PI+ve cells within tissue samples in both DRA [0.68% (+/-0.16)] and DRR [1.87% (+/-0.21)] were not significantly higher than naïve or sham PI+ve cell percentages (Fig 3.18A).

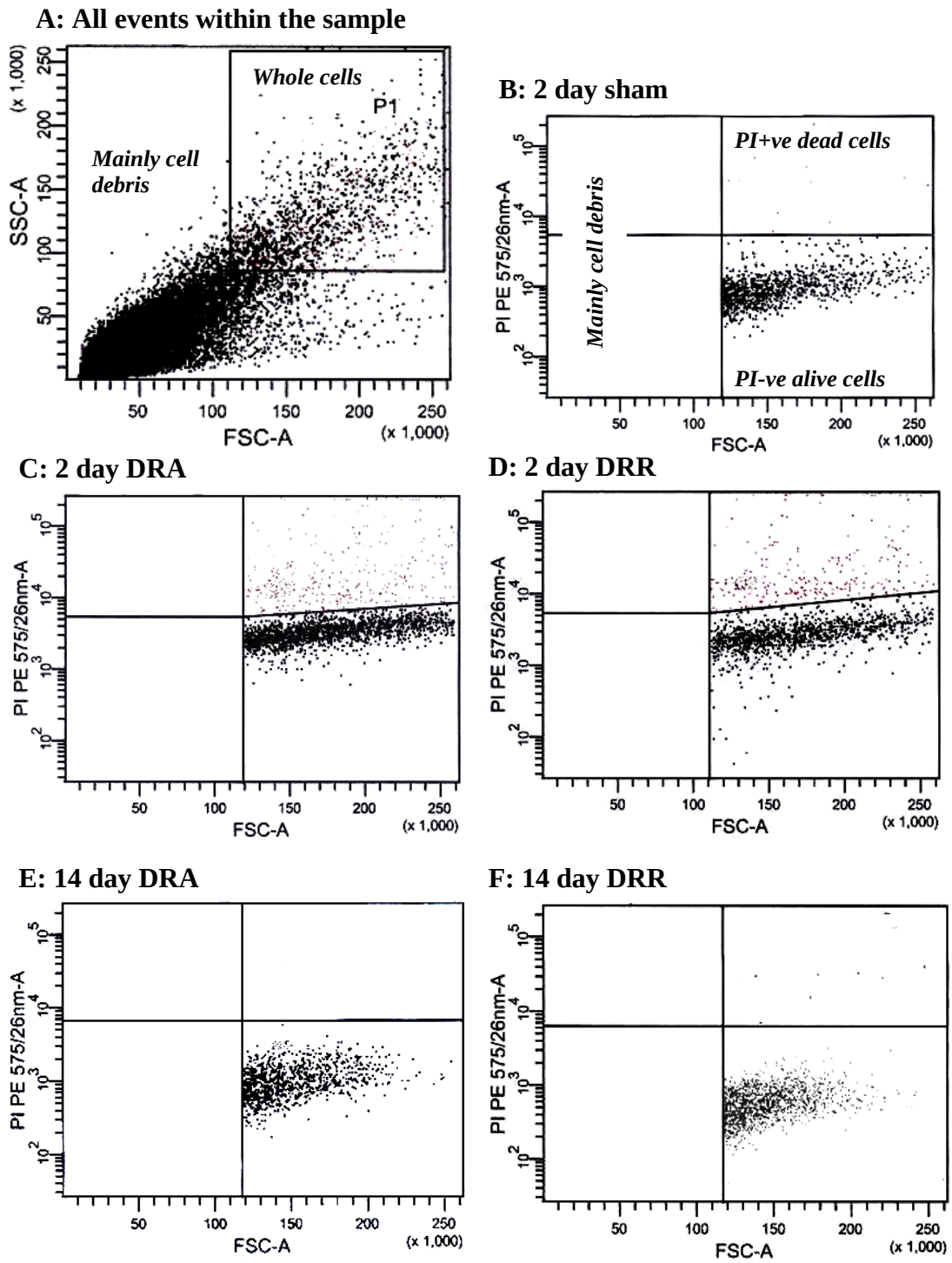

Fig 3.16: Sample of raw data read-out from flow cytometric analysis of PI within the L3-L6 spinal cord. A: Typical initial forward (FSC) and side scatter (SSC) plot of total events taken from 2 day DRA tissue. Event number represents whole cells, as well as cell debris. The box (P1) represents the population of largest sized events, i.e. whole cells. Cells at the top of this box are mainly apoptotic or dead. The P1 box is kept consistent throughout the experiment. **B:** P1 box of 2 day sham showing little dead cells (in red). Crossing lines represent the barriers between PI-positive and negative whole cells. Top right represents whole cell PI counts, and bottom right represents PI negative cells. **C:** 2 day DRA, P1 box showing dead cells. **D:** 2 day DRR, P1 box showing dead cells. **E:** 14 day DRA, P1 box showing little dead cells. **F:** 14 day DRR, P1 box showing little dead cells.

NeuN FACS:

Further analysis of the type of dead cells analysed by PI staining was accomplished. In this case DAPI was used in a similar way as PI to give the percentage of dead cells. However these cell types were further analysed with NeuN staining, to ascertain if the dead cells are neuronal.

Similarly to PI flow cytometry, unstained sample controls were used to determine DAPI and FITC positive staining (Fig 20a). After the initial scatter plot was formed these gates were kept constant throughout the experiment. These gating parameters divides the P1 boxes into 4 quadrants labelled Q(1-4)-2, with quadrant Q2-2 DAPI and FITC positive representing dead neurones. Quadrant Q4-2 represents live neurones. The remaining quadrants represent non-neuronal cells. Therefore a ratio of alive to dead neurones can be found within the sample through the equation (Q2-2/Q4-2) x 100.

Naïve tissue presented 12.1% (+/-1.00) and sham 7.23% (+/-1.30) NeuN/DAPI+ve cell percentages within the respective samples (Fig 3.18B). This figure is higher than that seen with PI and is most likely due to the greater damage caused by more mechanical dissociation steps in the procedure.

At 2 days post injury, NeuN/DAPI+ve colocalisation percentages rose significantly (Figs 3.17C-D) from naïve and sham values, to 36.8% (+/-2.55) in DRA tissue samples and 29.9% (+/-3.16) in DRR tissue samples (Fig 3.18B). DRA showed a significantly greater NeuN/DAPI+ve percentage staining than DRR (Fig 3.18B) in concurrence with immunohistochemical counts of NeuN (see section 3.2.5.2).

Similar to PI scatter plot data at 14 days, scatter plots of NeuN/DAPI showed decreases in positive cell percentages (Fig 3.17E and 3.17F). Levels decreased to 12.9% (+/-1.76) in DRA tissue samples and to 15.6% (+/-2.46) and were not significantly different to sham or naïve values, and were not significantly different between injury groups (Fig 3.18B).

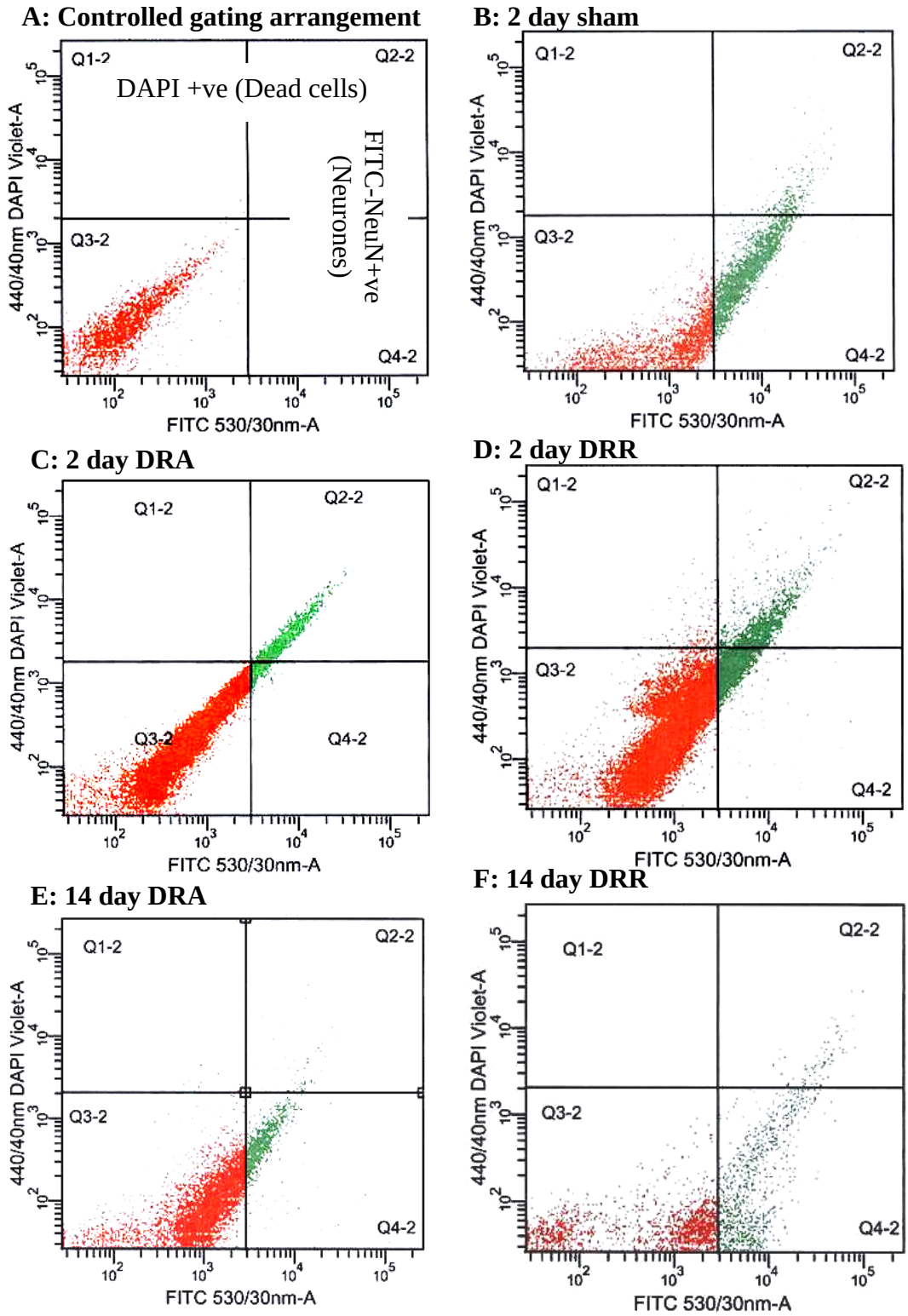

Fig 3.17: Sample of raw data from flow cytometric analysis of NeuN/DAPI within the L3-L6 spinal cord. Further analysis of P1 boxes from original forward and side scatter event plots. **A:** Control tissue sample absent of staining and subjected to fluorescent light of wavelength 440nm (DAPI excitation) and 530nm (FITC excitation). Quadrants can then be set as to a positive stain. Q1-2 represents positive DAPI and Q4-2 represents positive NeuN-FITC. Q2-2 represents colocalisation and population of dead neurones. Q2-2/Q4-2 gives the percentage dead neurones in P1 box within the spinal cord sample. **B:** Quadrant plot for 2 day sham showing a shift of the population toward DAPI positive. **C:** Quadrant plot for 2 day DRA showing a shift toward DAPI positive. **D:** Quadrant plot for 2 day DRR. **E:** Quandrant plot for 14 day DRA. The majority of events have shifted below the DAPI positive gate. **F:** Quadrant plot for 14 day DRR. The majority of events have, similarly to 14 day DRR, shifted to below the DAPI positive gate.

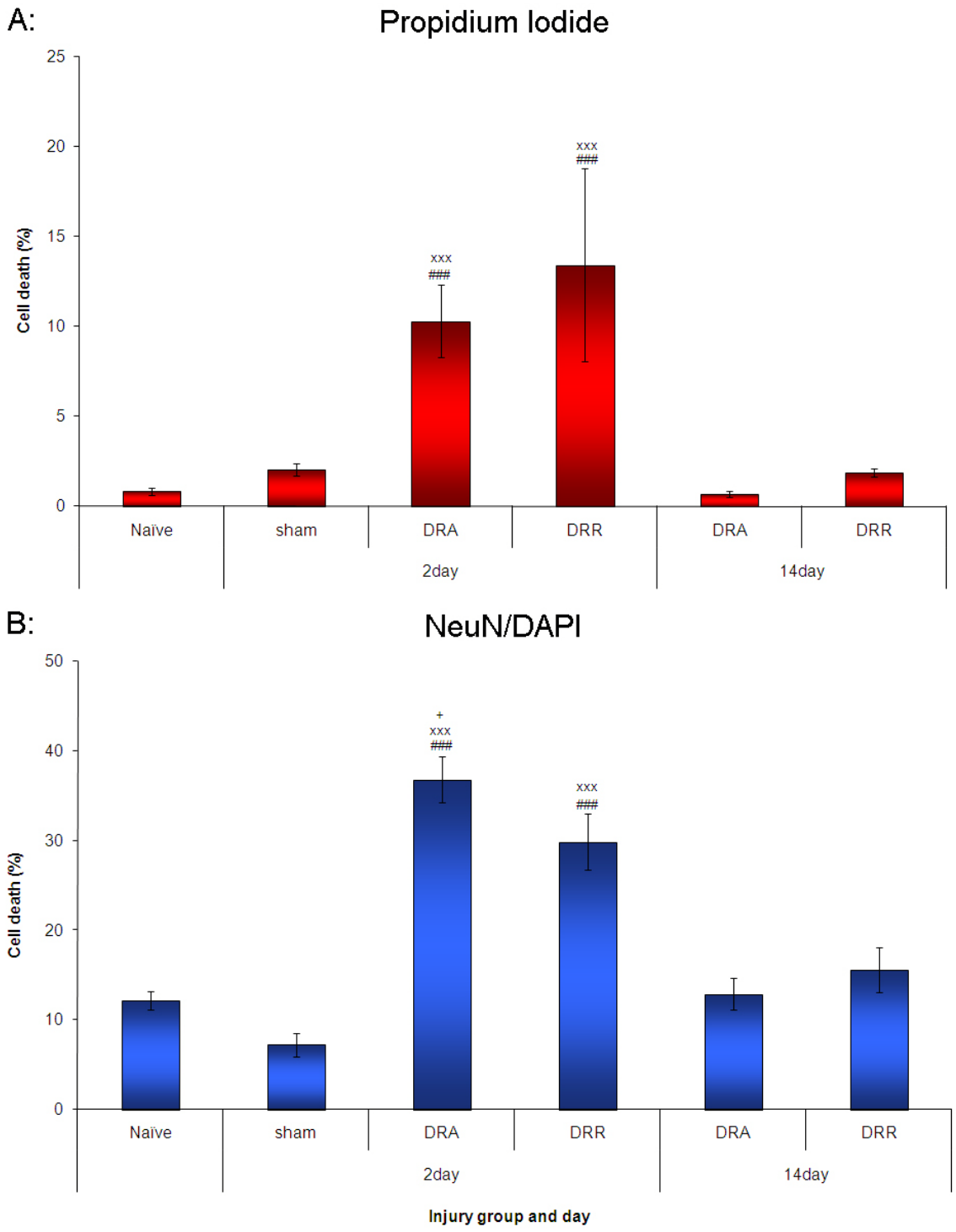

Figure 3.18: Flow cytometric analysis of cell death in the spinal cord using Propidium iodide (A) and NeuN/DAPI (B) colocalisation. Cell death is shown as a percentage of total count, at 0, 2, and 14 days post dorsal root injury. **A:** PI positive cell death of the L3-6 lumbar cord is significantly greater than sham and naïve tissue within the injury models at 2 days, with no difference between DRA and DRR, and no increase in cell death in sham. At 14 days percentage cell death returns to baseline levels. **B:** Percentage neuronal cell death of the L3-6 lumbar cord is significantly more than sham and naïve tissue within the injury models at 2 day, with DRA greater than DRR, with no increase in neuronal cell death in sham tissue. At 14 days, percentage cell death returns to naïve levels. Comparisons are made between injury vs naïve **(#)**, injury vs sham **(x)**, and DRA vs DRR **(+)**, shown above the respective data point. N numbers are: naïve (6), sham (4), 2 day DRA (8), 2 day DRR (8), 14 day DRA (4), and 14 day DRR (4)

3.2.5.2: Immunohistochemical analysis of NeuN neuronal loss

NeuN positive cell counts in the naïve dorsal horn averaged 410 (+/-11.4) per section (Fig 3.20), with staining located mostly in the cytoplasm, and in some cases the nucleus also. Neurones are organized in layers, or a lamina distribution, with clustering of small neurones in lamina I, fewer in lamina II, and larger neurones with dendritic-like processes in lamina III-V (Fig 3.19). Some neurones can be found outside the grey matter, and these constitute cells of the lateral spinal nucleus (Gwyn and Waldron, 1968; Molander *et al.,* 1984) that respond to noxious stimulation and are involved in pain processment (Menetry *et al.,* 1980; Dagci *et al.,* 2008) (Fig 3.19).

At 1 day post injury NeuN decreased significantly in the ipsilateral dorsal horn of DRA animals (Fig 3.19) compared to naïve and sham, with counts at 308.2 (+/-25.5) ipsilaterally (Fig 3.20). Contralateral levels [359.6 (+/-15.7)] showed a trend toward reduction (Fig 3.20). Significance was not reached between cord sides (P=0.058) (Fig 3.20). Significant decrease in NeuN counts bilaterally were calculated for DRR, at 322.7 (+/-4.70) ipsilaterally and 350.6 (+/-1.70) contralaterally against naïve, with ipsilateral significantly less than contralateral and sham (Fig 3.20). No significant differences were found between DRA and DRR injury models after 1 day (Fig 3.20).

At 2 days post injury NeuN counts were reduced to 285.7 (+/-18.8) in the ipsilateral dorsal horn of DRA, which was significantly less than naïve levels, the respective contralateral side, as well as ipsilateral DRR [334.6 (+/-20.2)] (Fig 3.20). DRR tissue does not show significant difference between cord sides at 2 days (Fig 3.20). Tissue cavities are apparent in the areas of NeuN loss in DRA, but not in DRR (Fig 3.19). Both injury models showed a small but significant contralateral loss of NeuN number compared to naïve tissue (Fig 3.19).

At 14 days post injury, no further decrease in NeuN is apparent in either injury, and sham tissue shows no NeuN reduction (Figs 3.19 and 3.20). Cavities within the dorsal horn that were observed in 2 day tissue, have become ‘walled off’ from neuronal populations most likely through tissue scaring (Fig 3.19). Ipsilateral NeuN counts in DRA [284.6 (+/-15.2)] and DRR [335.5 (+/-15.7)] are significantly less than sham and naïve levels, with DRA significantly less than DRR. Contralateral counts in DRA,

although showing some NeuN reduction (Fig 3.19) are not significantly reduced from sham or naïve (P=0.10) due to a large standard error. However contralateral DRR counts are significantly lower than both naïve and sham levels at 14 days (Fig 3.20).

At 28 days post injury further significant NeuN decrease occurs in DRA but not DRR (Fig 3.19 and 3.20). In DRA, both ipsilateral [143.6 (+/-22.6)] and contralateral [279.3 (+/-23.3)] NeuN counts are significantly lower than naïve and DRR, with ipsilateral DRA significantly lower than contralateral DRA levels (Fig 3.20). Mean NeuN positive neurone loss in laminae I-IV, over 28 days after DRA injury, is 56.4% ipsilaterally and 30.1% contralaterally, whereas in DRR it is 19.6% and 14.5% in respective cord sides. NeuN populations are greatly reduced in the superficial lamina and deeper laminae, leaving a band of NeuN+ve cells in the intermediate laminae. In some cases scarring has become so severe that neuronal groups have become separated and isolated from the main neuronal population. Patches of neurones can be observed, some of which appear isolated to the white matter (Fig 3.19).

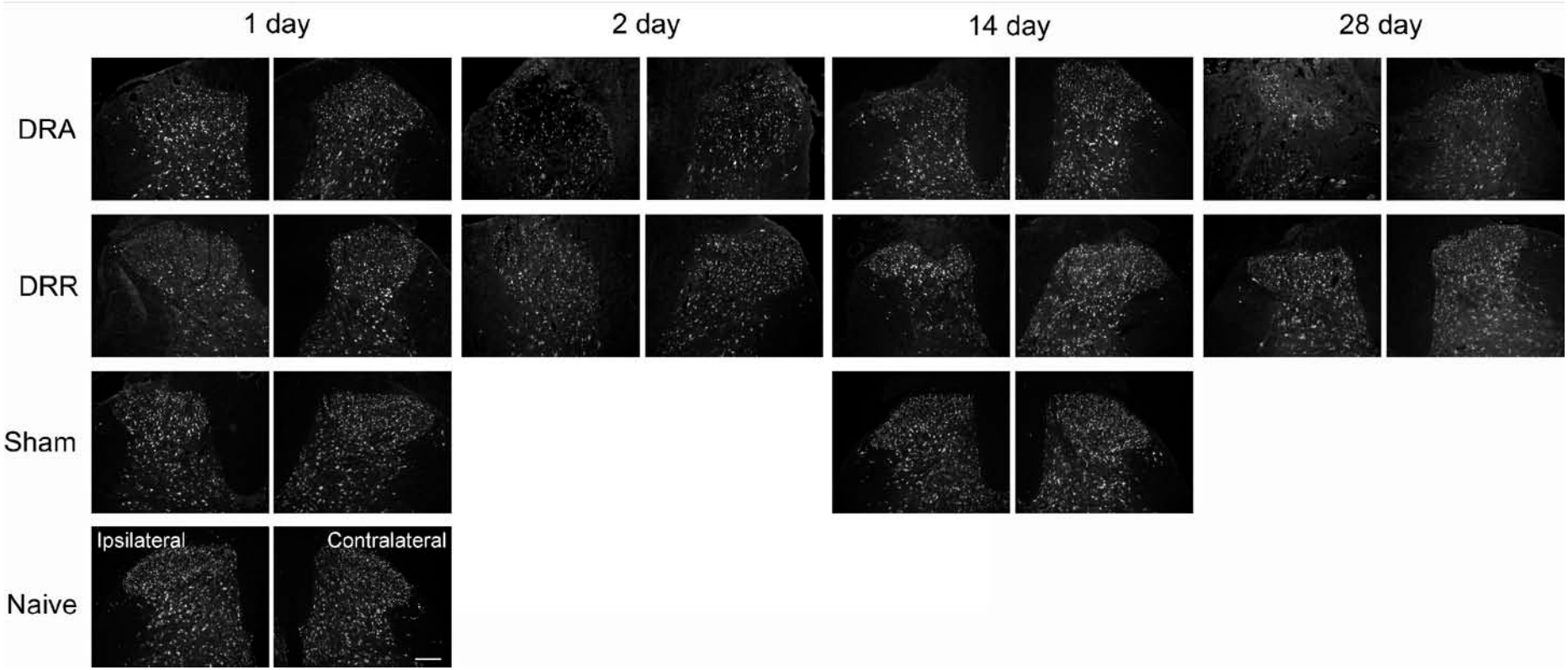

Fig 3.19: NeuN staining in the dorsal horn after dorsal root injury. 1 day sham injury does not lead to notable NeuN loss. 1 day DRA and DRR lead to ipsilateral NeuN loss. 2 day DRA tissue has large vacuolisation and cavitation in the dorsal horn, with notable NeuN loss. 2 day DRR shows partial cavitation and NeuN loss. In 14 day DRA tissue, no further cell loss is noted, and cavitation and vacuolisation is absent from the tissue presumably covered by scar tissue. In 14 day DRR scarring is also apparent, with no further loss from 2 days. In 28 day DRA, the trauma of root avulsion has severely reduced cell number from 14 days in superficial and deeper laminae. NeuN+ve cells can be seen in isolated patches, which have been walled off from the dorsal horn by the scar No further cell loss is noted in 28 day in DRR tissue. Ipsilateral images are shown to the left, and contralateral to the right. Scale = 200μm. Examples of L5 segmental level.

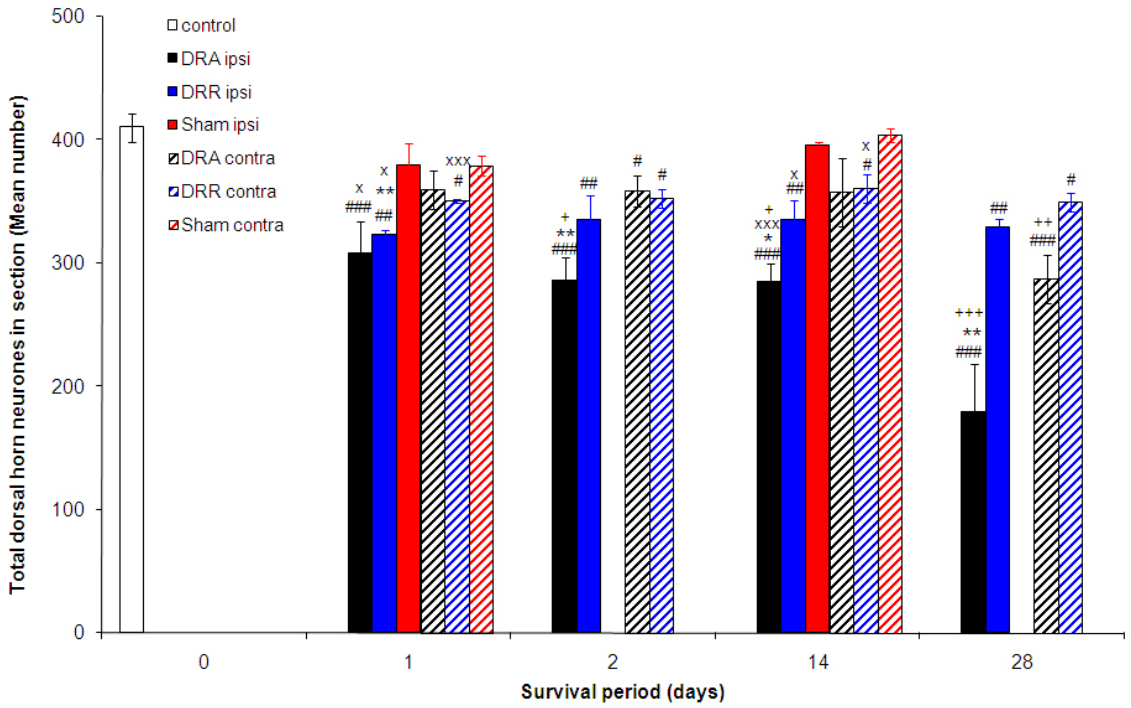

Fig 3.20: NeuN counts in the dorsal horn after injury. NeuN immunoreactivity is shown as a mean number of positive cells in laminae I-IV at 0, 1, 2, 14, and 28 days post dorsal root injury. NeuN staining decrease within the dorsal horn follows a 2 step process. Reduction is first apparent at 1 day, increasing to 2 days, with avulsion presenting a greater loss than rhizotomy. Significant further reduction is then only apparent in the avulsion model after 4 weeks, bilaterally. Comparisons are made between ipsilateral vs contralateral **(*)**, injury vs naïve **(#)**, injury vs sham **(x)**, and DRA vs DRR **(+)**, shown above the respective data point. N. numbers: naïve (4), 1 day sham (3), 1 day DRA (4), 1 day DRR (4), 2 day DRA (6), 2 day DRR (6), 14 day sham (3), 14 day DRA (6), 14 day DRR (6), 28 day DRA (4), 28 day DRR (4).

3.2.5.3: Histological analysis of toluidine blue neuronal loss

Toluidine blue staining of naïve cord showed cell bodies in the grey matter, but also lightly in the white matter, suggesting both glia and neurones are stained. In naïve tissue glia could be distinguished from neurones due to their smaller size and less intensity of staining (Fig 3.21); however, at later time points reactivity, hypertrophy, and swelling in size of many glia and leukocytes prevented easy identification.

In naïve tissue (Fig 3.21), toluidine blue positive cell counts within the boxed area of the dorsal horn averaged 100.7 (+/-4.97) cells (Fig 3.22).

At 1 day post injury a significant reduction in neuronal number was found in the dorsal horn of DRA (Fig 3.21) with 80.5 (+/-4.03) cells (Fig 3.22). Ipsilateral DRA tissue had significantly less cells than naïve, sham [96.9 (+/-5.15)], contralateral DRA [95.8 (+/-1.76)], and ipsilateral DRR [92.0 (+/-1.97)] at this time point (Fig 3.22). No significant reduction of toluidine blue stained cells was found in DRR or sham. No contralateral reduction in number was observed.

At 2 days post injury a significant decrease in toluidine blue counts from naïve levels was present bilaterally in DRA [80.2 (+/-2.41) ipsilaterally and 90.9 (+/-1.73) contralaterally], with statistical difference between cord sides. DRR was statistically lower than naïve bilaterally, with ipsilateral counts [81.8 (+/-3.60)] statistically lower than contralateral counts [92.0 (+/-2.68)]. No significant difference was found between injury models at this time point, and this reduction at 2 days was not significantly different from corresponding 1 day tissue in either case. Darker staining is notable around the pia mater in DRA tissue and dorsal horn (Fig 3.21).

At 14 days post injury, accurate counts of toluidine blue positive neurones were not able to be made, as neurones could not be clearly distinguished from glia. Glia surrounding the injury site within the dorsal horn, columns and root entry zone had become intensely stained for toluidine blue in both DRR and DRA so that the dorsal horn and neurones could no longer be distinguished. This glial staining was even more prominent at 28 days (not shown) preventing correct neuronal counts at this time point also.

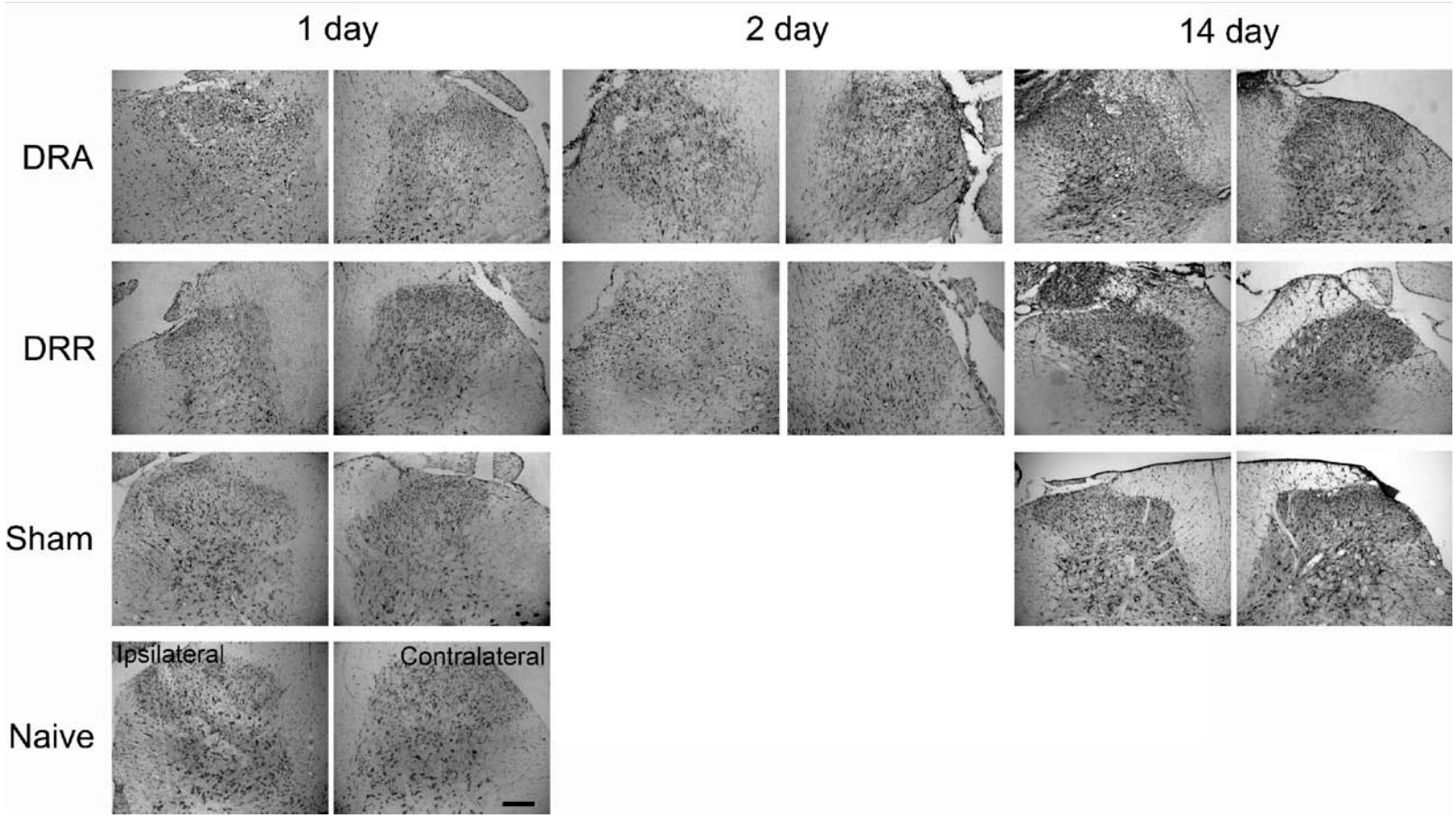

Fig 3.21: Toluidine blue staining in the ipsilateral dorsal horn after dorsal root injury. Naïve dorsal horn presents dark cellular staining in a lamina distribution. Faint staining of cells in the white matter is observed 1 day sham and DRR dorsal horn shows no change in toluidine blue cell population. 1 day DRA shows a reduced toluidine blue cell count as well as tissue disruption and cavitation. 2 day DRR tissue shows a small but significant reduction in toluidine blue cell count bilaterally. 2 day DRA shows further tissue disruption cell loss, however dark staining is presented in the dorsal horn bilaterally. 14 days post sham shows no toluidine cell loss. 14 days in DRR and DRA present dramatic tissue disruption and intense toluidine staining around the DREZ and superficial dorsal horn, masking the positive identifcation of neurones at this time point. Ipsilateral images are shown to the left, and contralateral to the right. Scale = 200μm. Examples of L5 segmental level.

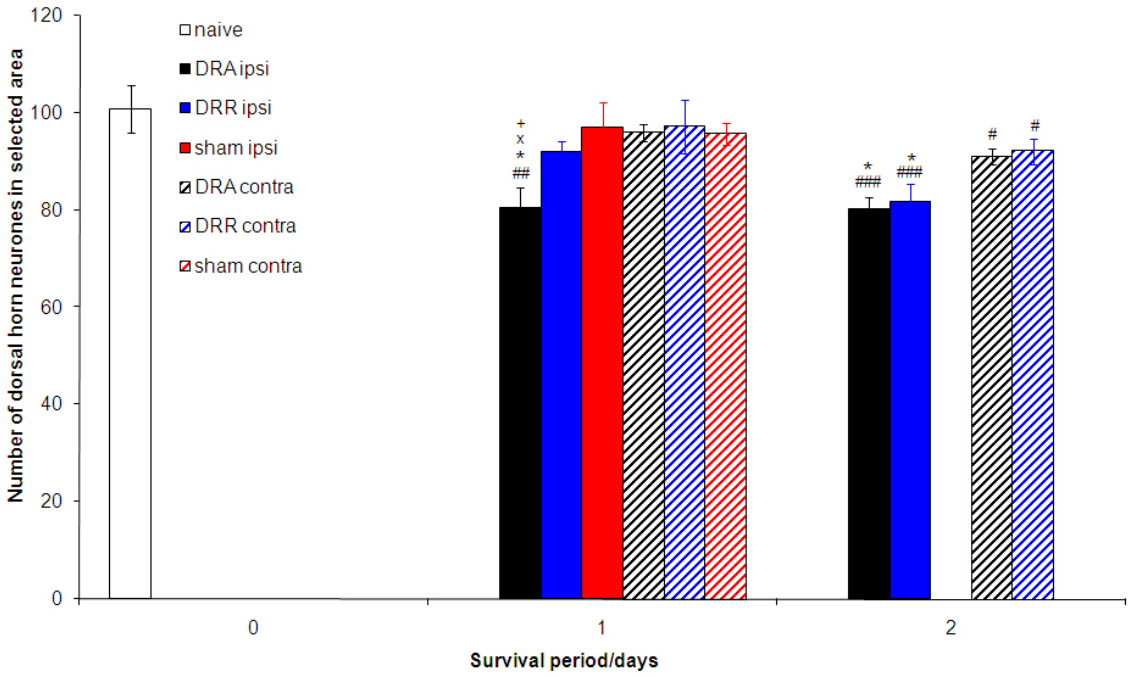

Fig 3.22: Toluidine blue counts in a sample of the dorsal horn after injury. Tol Blue counts are shown as a mean number of positive cells in a 4.16cm^2 boxed area in the superficial dorsal horn at 0, 1, and 2 days post dorsal root injury. Counts decreased within the dorsal at 1 and 2 day. Reduction is first significant at 1 day after DRA, maintaining after 2 days, with avulsion presenting a greater loss than rhizotomy. Significant reduction in counts is only found after 2 days in DRR. 14 day and 28 day tissue could not be accurately quantified. Comparisons are made between ipsilateral vs contralateral **(*)**, injury vs naïve **(#)**, injury vs sham **(x)**, and DRA vs DRR **(+)**, shown above the respective data point. N. numbers: naïve (4), 1 day sham (3), 1 day DRA (4), 1 day DRR (4), 2 day DRA (6), 2 day DRR (6).

3.2.5.4: Immunohistochemical analysis of cell death in the spinal cord

Single labelling

TUNEL staining was used to characterize the end stage apoptotic event of DNA fragmentation within cells of the spinal cord after DRA and DRR injury. TUNEL-positivity was confirmed with the nuclei counter stain DAPI, and counts were made in the dorsal horn and dorsal columns.

Very few TUNEL positive nuclei were found in naïve sham (1 or 14 days) tissue. Values for naïve were 0.8 (+/-0.37) in the dorsal columns and 0.8 (+/-0.2) in the dorsal horn (Fig 3.24). Values for ipsilateral sham were 1.13 (+/-0.13) in the dorsal columns and 1.33 (+/-0.66) in the dorsal horn (Fig 3.24).

An ipsilateral increase in TUNEL counts is observed by 1 day (Fig 3.24). TUNEL positive nuclei were small and round in appearance with granular staining in the centre (Fig 3.23). They were found throughout the dorsal horn, dorsal root entry zone and dorsal columns, preferentially ipsilaterally (Fig 3.23). 1 day DRA tissue showed a significant increase from naïve, ipsilateral sham, and DRA contralateral tissue, with 24.5 (+/-1.61) and 14.5 (+/-3.22) mean counts in the dorsal horn and column respectively (Fig 3.24). 1 day DRR tissue showed significantly much lower numbers of TUNEL-positive nuclei than DRA, with 6.76 (+/-2.89) and 4.02 (+/-1.07) in the ipsilateral dorsal horn and dorsal column respectively (Fig 3.24). This is statistically greater than contralateral DRR, ipsilateral sham, and naïve tissue. At this time point there is a significant difference between the injury models, with avulsion showing greater numbers of TUNEL-positive cells in the dorsal columns, but significant difference is not reached in the dorsal horn (Fig 3.24).

At 2 days, TUNEL numbers have significantly increased from 1 day. Levels now reach 28.1 (+/-2.30) and 40.6 (+/-6.32) per section in the avulsion model, and 16.0 (+/-1.90) and 18.2 (+/-3.37) per section in the rhizotomy model, for the dorsal columns and horns respectively. Within the dorsal columns, for both injury models, a significant contralateral effect is seen from naive, with counts at 5.42 (+/-1.50) for rhizotomy and 4.69 (+/-1.47) for avulsion; these are not significantly different from each other. Similar

to 1 day, the avulsion model showed significantly greater TUNEL counts than rhizotomy in the ipsilateral dorsal columns and dorsal horn, with greater tissue damage and cystic cavities (Fig 3.25c).

At 14 days no significant TUNEL staining was found in DRR or DRA injury models compared to naïve or sham (Fig 3.24).

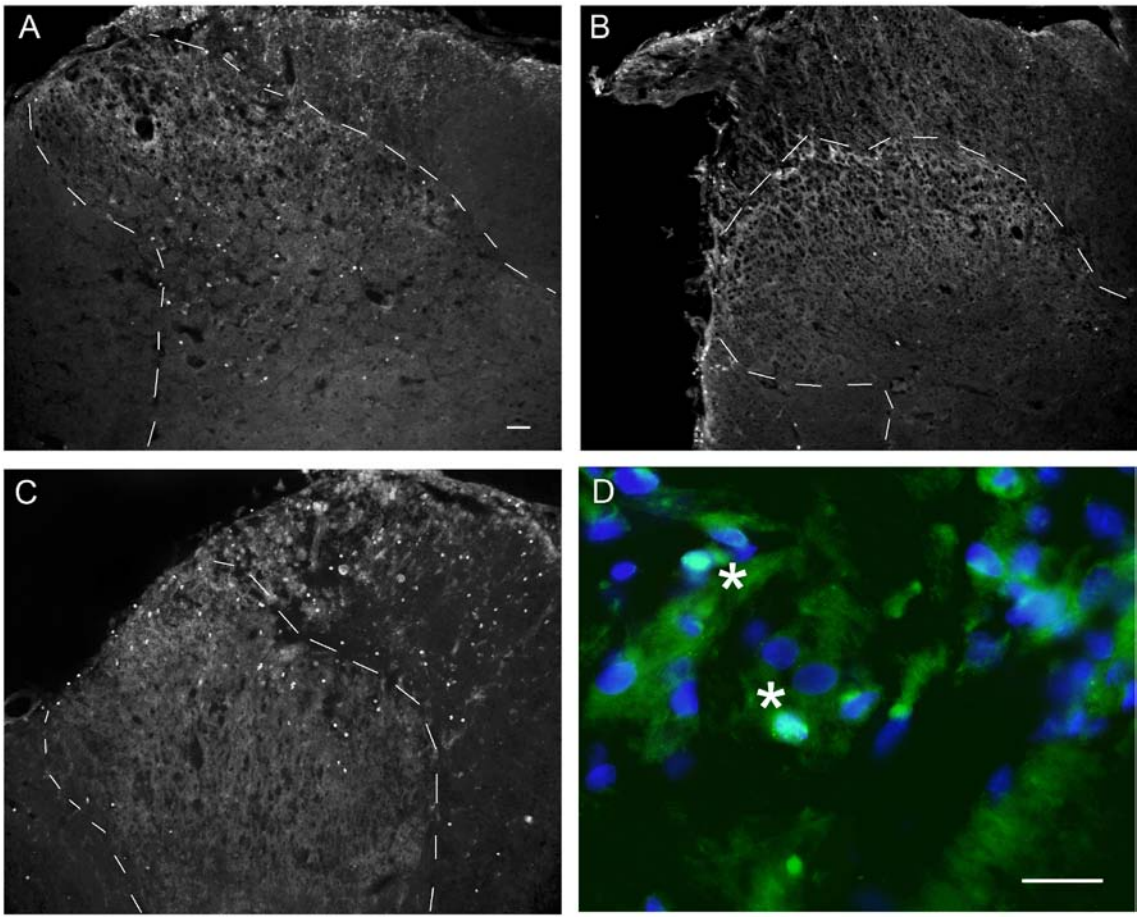

Figure 3.23: **TUNEL staining in the ipsilateral dorsal horn and dorsal columns. A:** 1 day DRA TUNEL positive cells are present in the ipsilateral dorsal horn, and column with tissue necrosis and cavity formation apparent. **B:** 1 day DRR presents few TUNEL counts in the dorsal horn and column. **C:** 2 days DRA shows TUNEL positive cells thoughout the superficial dorsal horn and dorsal columns. Ouline of dorsal horn is delineated by white lines. **D:** TUNEL positive nuclei (Green) double labelled with DAPI (Blue) for positive confirmation (asterisk). Scale = 50μm

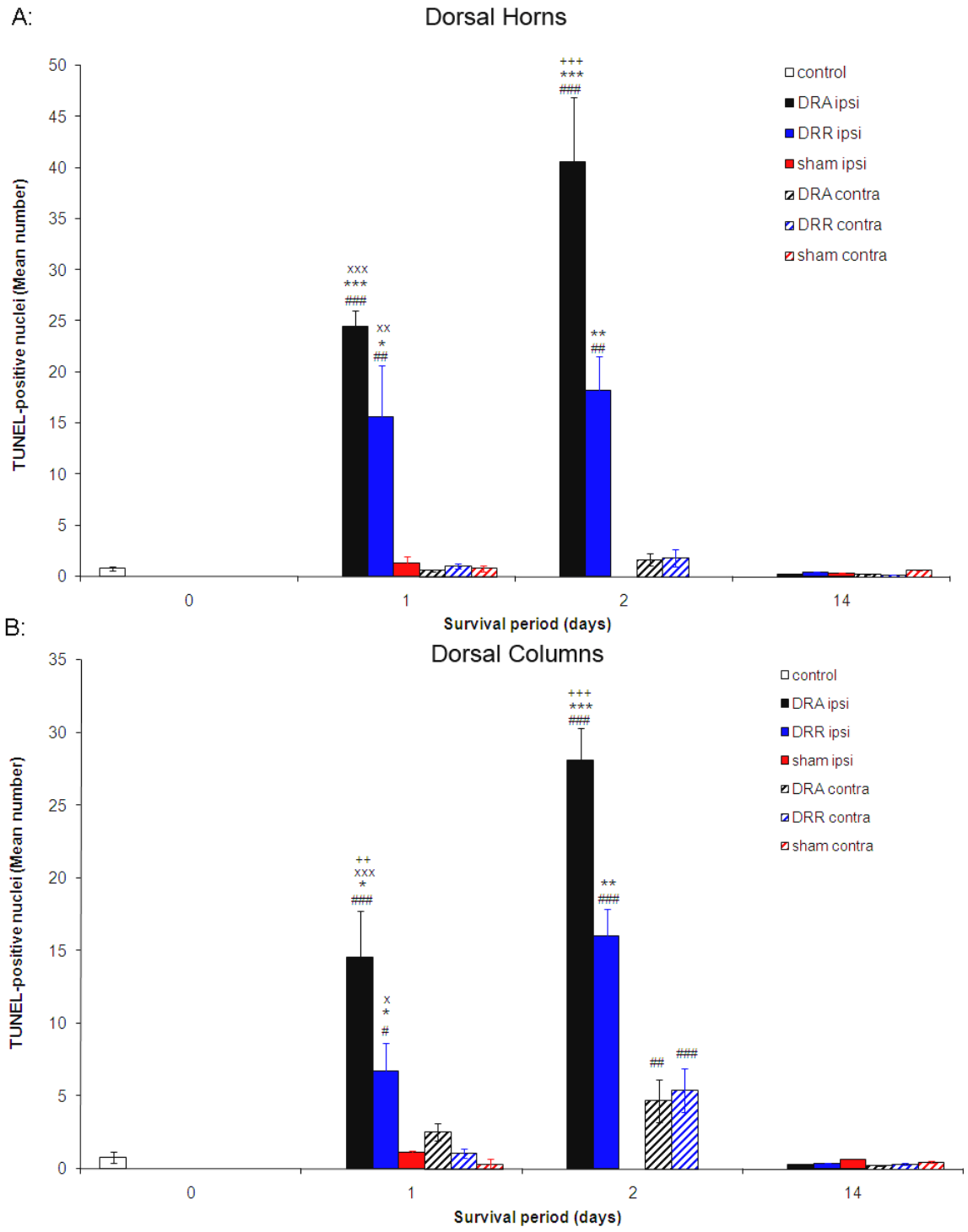

Figures 3.24: TUNEL-labelled cell counts in the dorsal columns and dorsal horn after injury respectively. TUNEL positive counts are shown as a mean number of positive cells per section at 0, 1, 2, and 14 days post dorsal root injury. TUNEL positive cells were found only at 1 and 2 days post injury, with 2 days significantly greater than 1 day. DRA presented significantly greater numbers of apoptotic nuclei than DRR at 1 and 2 days. Significant contralateral TUNEL labelling presented in both injury models only in the dorsal column, and only at 2 days. TUNEL labelling at 2 and 4 weeks (data not shown) showed no significant difference in counts from naïve baseline. Comparisons are made between ipsilateral vs contralateral **(*)**, injury vs naïve **(#)**, injury vs sham **(x)**, and DRA vs DRR **(+)**, shown above the respective data point. N. numbers: naïve (4), 1 day sham (3), 1 day DRA (4), 1 day DRR (4), 2 day DRA (6), 2 day DRR (6), 14 day sham (3), 14 day DRA (6), 14 day DRR (6).

Double labelling

To identify whether neurones, glial cells, or infiltrating leukocytes are dying by apoptosis after root injury, double labelling immunocytochemistry was performed with a variety of markers and TUNEL in 1 and 2 day DRA tissue.

Neuronal:

NeuN-TUNEL colocalisation was not apparent in the cord at either 1 or 2 day time points (Fig 3.25).

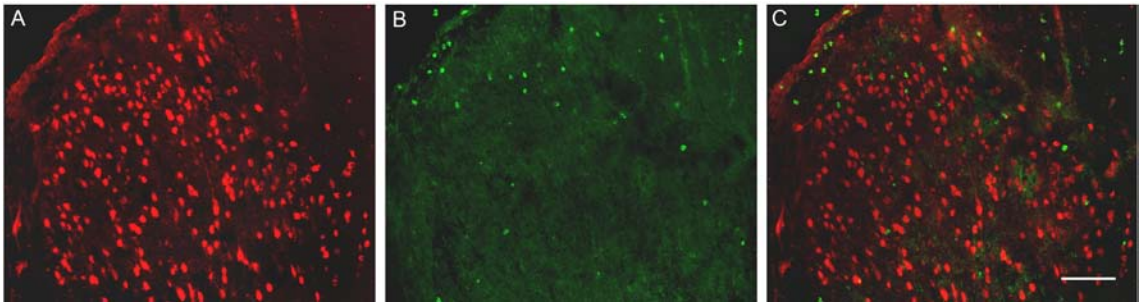

Figure 3.25: NeuN(red)–TUNEL(green) co-localisation in the ipsilateral dorsal horn. A: NeuN staining of 1 day DRA. **B:** TUNEL positivity. **C:** Merge shows no co-localisation. Scale = 200µm

Astroglial:

As astrocytes have been shown to undergo differentiation and proliferation during gliosis after injury to the CNS, it is possible that they may be undergoing apoptosis at these same time points to control the rate and extent of glial scarring within the lesion site of the DREZ and superficial laminae. TUNEL-S100 staining provided co-localisation of the apoptotic cell bodies and nucleus of astrocytes. However no apoptotic astrocytes were found in the cord at 1 or 2 days time points (Fig 3.26).

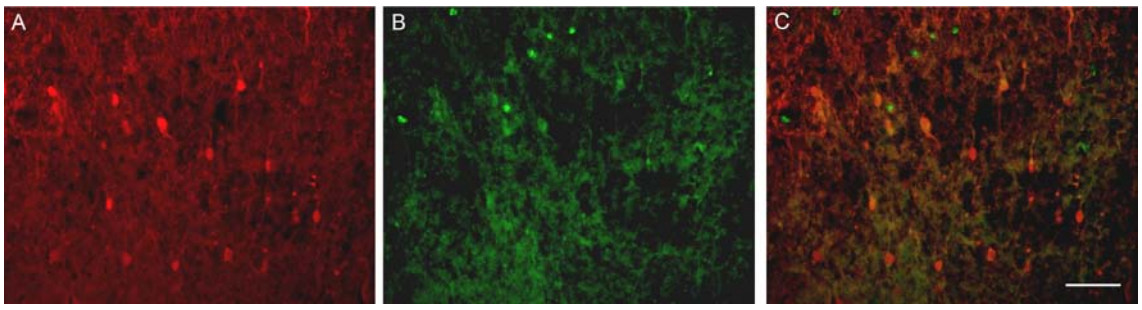

Figure 3.26: **S100(red)-TUNEL(green) co-localisation in the ipsilateral dorsal columns. A:** S100 staining of 1 day DRA. **B:** TUNEL positivity in the dorsal horn **C:** Merged image showing no double-labelled astrocytes. Scale = 100µm

Microglia:

Across 1 and 2 days of peak TUNEL expression in DRA tissue, many apoptotic nuclei co-localised with Iba1 for microglia. These nuclei were found almost exclusively within the lesion site in the dorsal column and superficial laminae, but only accounted for a small proportion of TUNEL positivity. Only the morphologically 'reactive' population of microglia, with a typical rounded appearance lacking processes which may also be ED1 positive, were TUNEL positive (Fig 3.27).

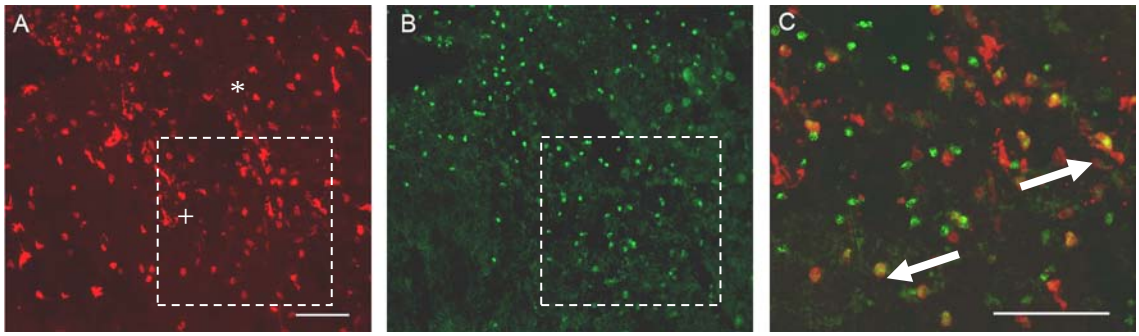

Figure 3.27: **Iba1 (red) -TUNEL (green) colocalisation in the ipsilateral dorsal horn. A:** Iba1 staining of dorsal horn (+) and dorsal columns (*) in 1 day DRA. **B:** TUNEL positivity. **C:** Merged image of the box regions outlined in **A** and **B**. Some double-labelled microglia are apparent (arrow). The majority of TUNEL positive cells do not co-localise with Iba-1. Scale = 100µm

Macrophage:

ED1-TUNEL colocalisation was also found at 1 and 2 day time points in both DRA and DRR (Fig 3.28). These were found within the lesion site and superficial dorsal horn and, similarly to Iba1, accounted for only a small proportion of TUNEL positive nuclei. They may be the same population as Iba1 as ED1 labels activated microglia.

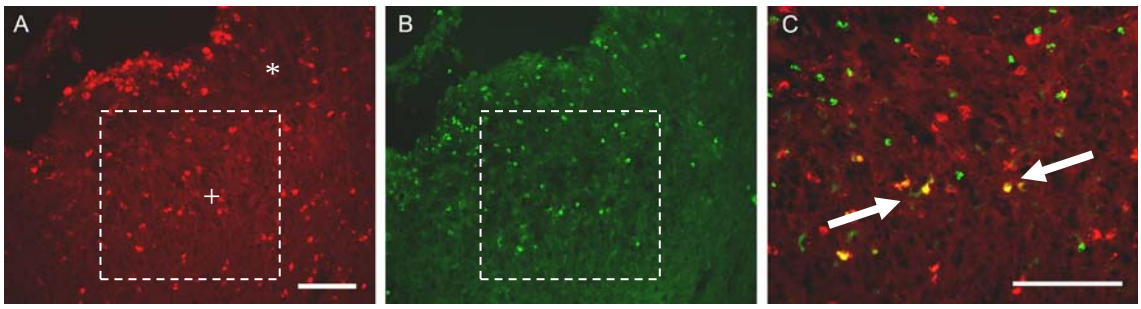

Figure 3.28: **ED1 (red) –TUNEL (green) colocalisation staining in the ipsilateral dorsal horn. A:** ED1 staining in dorsal horn (+) and dorsal columns (*) in 2 day DRA. **B:** TUNEL positivity in the dorsal horn. **C:** Merged image of the box regions outlined in **A** and **B**. Some double-labelled macropahges are apparent (arrow). The majority of TUNEL positive nuclei do not colocalise with ED1. Scale = 100µm

Neutrophil:

Anti-neutrophil-TUNEL co-localisation was also exclusive in 1 and 2 day DRA tissue, providing evidence that it is the neutrophil population of cells that are responsible for the TUNEL staining at 1 and 2 day time points after root transection injuries (Fig 3.29).

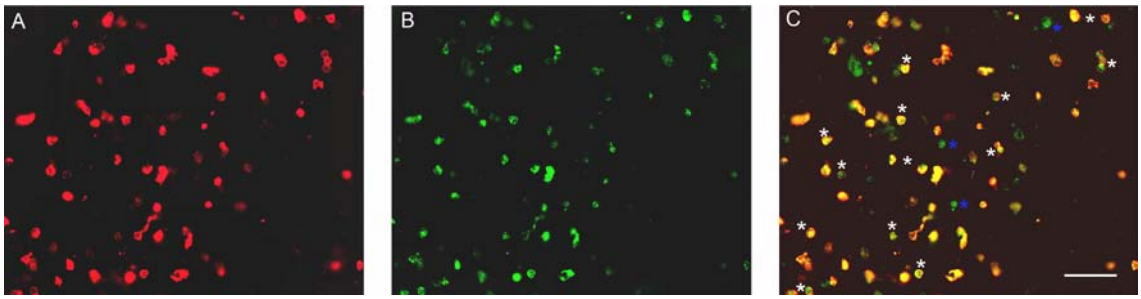

Figure 3.29: **Neutrophil(red)-TUNEL(green) co-localisation staining in the ipsilateral dorsal horn. A:** Neutrophil staining of 1 day DRA. **B:** TUNEL positivity in the dorsal horn. **C:** merged image showing almost all TUNEL positive cells are neutrophils (white asterisk) with very few single labelled TUNEL nuclei (blue astersik). Scale = 50μm

3.3: Discussion

3.3.1: Summary

The new findings of this study can be summarised as follows:

No difference is observed across 28 days ipsilaterally between DRA injury and DRR injury with respect to primary afferent terminal labelling with CGRP or IB4. However across 28 days a more severe contralateral loss of primary afferent terminal labelling occurs after DRA compared to DRR.

A more intense astrocytic reaction occurs ipsilaterally in the dorsal horn after DRA injury at 1 day increasing up to 14 days, and maintained up to 28 days bilaterally, compared to a delayed and significantly less severe astrogliosis in DRR and only ipsilaterally. Microglial effects are delayed compared to astocyte effects after root injury. Significant increases in microglial labelling in both models occurs at 2 days, with greatest microgliosis observed at the later time points of 14 and 28 days. A more intense microglial reaction occurs bilaterally at 14 and 28 days in DRA dorsal horn, compared to more modest effects in DRR.

An ipsilateral infiltration of both neutrophil and macrophage blood borne cells are present in both the dorsal horn and the dorsal column after both deafferentation injuries. A time and injury dependent increase in macrophage staining is shown within the ipsilateral dorsal regions, starting in DRA ipsilateral dorsal horn at 1 day compared to 2 days in DRR. Significant macrophage recruitment in the dorsal columns is delayed in both models to 2 days, but produces a more substancial infiltration than within the dorsal columns at the two later time points. Intense macrophage staining is observed in DRA dorsal horn and columns at 14 and 28 days, and is significantly greater than in corresponding DRR tissue. By direct comparison, the other leukocyte population analysed, neutrophils, infiltrate at 1-2 days with minimal numbers at 14 days, and none at 28 days. DRA injury leads a greater infiltration of neutrophils across 1 and 2 days than DRR.

Microvascular RECA-1 labelling is reduced bilaterally by 1 day in DRA dorsal horn, and is maintained up to 28 days. A similar reduction in RECA-1 staining occurs at 1 day post DRR, however a recovery of staining back to naïve levels of density staining is observed by 14 days.

There is a reduction in NeuN labelling beginning at 1 day in both DRA and DRR that is maintained up to 14 days. There is a more severe 'second wave' of NeuN-ir reduction by 28 days that is bilateral, but this is only found in the DRA model. DRA therefore leads to a more severe neuronal deterioration than DRR across this time period. This loss is confirmed by NeuN FACs and also toluidine blue counts, suggesting cells are indeed lost rather than a decrease in epitope for the anitbody.

At 1-2 days post DRA and DRR, apoptotic expression was found by TUNEL staining within the dorsal horn and columns (Chew *et al.,* 2008), that is absent at 14 days, and this was supported with PI flow cytometry. TUNEL staining was restricted ipsilaterally within the dorsal horn and column, and quantitative analysis showed that DRA is more severe at inducing apoptosis than DRR. Colocalisation studies showed apoptosis to be restricted to the non-neuronal cell population, mainly the neutrophils but also some microglia and macrophages.

Significant contralateral effects were shown to occur in all cell types and staining protocols. This contralateral effect was usually delayed, showing effect at 14 and 28 days predominantly, and of less magnitude than ipsilateral to injury. In all markers analysed, DRA lead to a greater contralateral effect than DRR.

These results suggest that DRR, commonly used as an *in vivo* model of avulsion, gives a milder representation of the traumatic state of the dorsal horn compared to true avulsion injury. This is true with respect to glial activity, the state of the vasculature, as well as amount of blood borne inflammatory and phagocytic infiltration. However primary afferent degeneration and neuronal reduction do not seem to differ. This is the first time neuronal loss after avulsion has been demonstrated, beginning at 1 day, and progressing substantially over 14 to 28 days.

3.3.2: Methodological considerations

Certain considerations need to be taken into account when analysing and discussing the data presented in this report.

Firstly, issues arise from the surgical procedure: the hemi-laminectomy will lead to some contralateral damage to the afferents innervating the vertebral muscles, the vertebrae themselves, and the skin and muscle afferents of the overlying skin, as these tissues are structurally contiguous across the spinal cord and column. Therefore some reduction in CGRP and IB4 in 1 and 14 day sham animals, and the loss contralaterally in all models, may be due to bilateral damage to dural, vertebral, and skin/muscle afferents. The dura itself is innervated by CGRP positive nociceptive primary afferents (Bove and Moskowitz, 1997;Strassman and Levy, 2006) and P2X2/3 positive nociceptor primary afferents (Staikopoulos et al., 2007) that colocalise with IB4 (Bradbury et al., 1998). The lumbar vertebral joints are also innervated by CGRP positive afferents (Morinaga et al., 1996). This may also explain the significant increase in sham astrocytic and microglial reactivity at 14 days, consistent with previous findings (Colburn et al., 1997;Hashizume et al., 2000a;Bigbee et al., 2007). Cutting the dura and prolonged disruption of the blood brain barrier, may lead to disruption of pH homeostasis in the cord that activates astrocytes bilaterally. This is shown as an increase in astrocyte GFAP-ir without hypertrophy, elongation of processes, or differentiation. Further, extensive hemi-laminectomy surgery (L5 to S1) has been shown to induce mechanical hyperalgesia up to 15 days with deformity of the spinal cord observed upon dissection (Kosta et al., 2009).

Another issue with the surgical procedure is that avulsion is the physical tearing of the roots from the cord. This may create problems with reproducibility and morphological differences in the sections of the dorsal horn between animals, with variable mechanical distortion of the cord, and variable amounts of injury to the spinal cord (Brown-Séquard Syndrome). These morphological differences were less common in rhizotomised dorsal horn as the injury is not a traction force that directly affects the spinal cord.

Secondly, issues may arise from the method of analysis of the spinal cord. The conclusions drawn from this data are based mainly on immunofluorescence analysis

only, the limitation of which is the reliance upon epitope expression. For the results that describe a reduction in antibody staining such as NeuN, it could be that injury to the dorsal horn could cause a reduction in cellular expression of the corresponding epitope within cells that may not be dead or dying, thereby giving an incorrect estimate of the number of cells lost. For this reason, the general metachromic dye, toluidine blue, that does not rely on epitope expression for staining, was employed. However this too has its limitations, as it is not specific to neurones, and can label glia and leukocytes like cresyl violet, that have hypertrophied in response to tissue damage (Sanner et al., 1993). This staining of glia was shown to increase in intensity in 14 and 28 day tissue, making it impossible to distinguish neurones or the shape of the dorsal horn. However the same trends were observed with these different methods at 1 and 2 days post injury giving strength to the notion that these injuries cause cell death.

Further issues arise in immunohistological identification with generic antibodies. The ED1 antibody, specific to the CD68 complement factor, is expressed on activated microglia as well as macrophages, making them difficult to distinguish between as they have similar morphology (Ling, 1979b). Similarly, the lectin IB4 binds to microglia, perivascular cells and group-B blood erythrocytes, albeit with a lesser efficacy, as well as a sub class of C-fibres. This overlap could potentially interfere with intensity staining analysis after injury, and this was controlled for by exclusion of randomly selected tissue sections that showed this staining within the selected area of analysis.

Limitations with TUNEL labeling also exist. The apoptotic caspase cascade takes approximately 2-4 days depending on cell type (Cooray et al., 2003). Therefore apoptotic immunohistochemical detection of cells is dependent on the point of the cascade analysed. TUNEL labelling isolates the population of cells undergoing end stage apoptosis; therefore TUNEL staining will provide only a snapshot of the total spectrum of apoptotic cells within the cord. Potentially at any time point analysed there is an underestimation of the total apoptotic population, so counts are relative and not absolute.

Thirdly, several limitations involve the flow cytometric analysis: 1) It was not possible to analyse only the dorsal horns of the spinal cord, as they could not be accurately dissected from the spinal cord. Therefore, the percentage dead cells would be of all

regions within the cord, including both white and grey matter, from L3 to L6. 2) The P1 scatter plot does not provide a clear cellular population difference between dead and alive for either PI single labelling or NeuN/DAPI colocalisation. This is due to the constituency of the dissociated tissue sample. Cells of different shapes and sizes are present in the spinal cord, some of which may have been broken down into fragments of different sizes through the titration procedure. This is shown on the scatter plot as a blended population of dead to alive, neuronal to non-neuronal, that is entirely dependent upon gating controls. These gates are generated by analysing naïve tissue and single labelled suspensions, as defined in the methodology, and then applying them to the injured tissue samples. Results from NeuN/DAPI colocalisation in naïve and sham tissue show approximately 12% and 7% dead neuronal population respectively, that is also present, but to a lesser extent in PI flow cytometric analysis. A likely explanation for this neuronal loss, is the detrimental effect to cellular integrity of the increased number of centrifuge and mechanical wash cycles most notably in NeuN/DAPI methodology. In this way a proportion of the neuronal population within all NeuN/DAPI FACs analysed groups are killed through this procedure, rather than the deafferentation surgery, overestimating the absolute loss.

3.3.3 Primary afferent terminals

Immunohistochemical analysis of the primary afferent terminals within the dorsal horn after deafferentation has shown a time dependent reduction in CGRP and IB4 levels. This begins at 1 day bilaterally, with an afferent terminal immunoreactivity loss of around 25-35% for peptidergic terminals 29-53% for non-peptidergic terminals in both deafferentation models and sham. Ipsilateral immunoreactivity shows a trend toward more loss than the respective contralateral side, but does not reach significance in any model including sham, suggesting that some reduction in terminal staining is primarily due to the laminectomy. These results are contrary to previous findings, where no contralateral effects were described using DRR or DRA models (Gibson et al., 1984;Traub et al., 1989;Muneton-Gomez et al., 2004). The differences in this work and previous literature may be due to the method of analysis, with previous literature using the contralateral side as an intrinsic control for ipsilateral effects rather than a separate group in itself. Only rhizotomy models are used in the literature, and this work has shown contralateral effects are more extensive after DRA, and therefore could have

been overlooked previously. Also, here, a more quantitative technique of primary afferent terminal density staining calculation was used. Contralateral effects are further discussed in section 3.8.

The further ipsilateral reduction of CGRP-ir and IB4-ir at 14 days in DRA and DRR is consistent with previous findings (Gibson et al., 1984;Traub et al., 1989;Tie-Jun et al., 2001;Muneton-Gomez et al., 2004). This loss is due to the degeneration of terminals distal to the injury point, which begins at 8 hours (Coimbra et al., 1984) and is complete by 7 days (Ralston, III and Ralston, 1982), as well as loss of anterogradally transported vesicles containing CGRP and the glycoprotein that binds IB4. Only isolated punctate staining of CGRP and IB4 were found after 14 days post injury in both models. This terminal labelling represents spared terminals originating from intact long range afferents arising rostrally (>L3) and caudally (<L6) to intact lumbar and sacral roots (Shortland and Wall, 1992;Muneton-Gomez et al., 2004).

The only differences in the time course of peptidergic and non-peptidergic afferent terminal loss were found at 28 days, with DRA showing significantly less immunoreactivity than DRR on the contralateral side. This suggests that ipsilaterally the mode of deafferentation does not affect the rate of terminal staining intensity loss in the spinal cord.

3.3.4: Glial activity

3.3.4.1: Microglia

Reactive gliosis occurs when resident microglia become phagocytic, enabelling removal of damaged axons, neurones, and myelin. This report shows microglia undergoing a morphological change across time after root injury, which has been shown previously in a SCI model (Popovich et al., 1997;Watanabe et al., 1999). Temporally, microglia change from a ramified form, with processes and small soma, to an activated form without such processes, identical to macrophages, but with swollen soma (amoebic-like) consistent with previous descriptions (Ling, 1979b). Importantly these changes are maintained up to 28 days in DRA where they are maximal, which is in contrast to minimal microglial activity in DRR dorsal horn.

Both deafferentation models lead to dorsal horn microglial reactivity, with ramified microglia becoming amoebic-like surrounding the injury site. This metamorphosis is observed at 1 day but significance is not reached until 2 days after injury, and directed ipsilaterally, as evidenced by an increase in Iba1 staining for both DRR and DRA, with no difference between them. Proliferation may also be a mechanism by which percentage density staining is increased (Liu et al., 2000a). A small proportion of microglia undergo apoptosis at 1 and 2 days as they begin to engulf neuronal debris; phagocytosis is a known trigger for apoptosis (Watson et al., 1996;Hacker et al., 2002;Kirschnek et al., 2005). It is likely the purpose of apoptosis is to safely remove cytotoxic phagocytic cells, preventing them from exacerbating symptoms within a lesion site.

A significant increase in microglia occurs in DRA bilaterally at 14 days, which is not present after DRR. The severity of the microglial reaction at 14 days in DRA is almost double that of DRR, both ipsilaterally and contralaterally. This is the first descriptive and quantitative comparison of microglial reactivity in these deafferentation models, and suggests the type of trauma can influence the time course and extent of the dorsal horn microglial activity. The difference in microglial reaction between injury models may be due to the direct damage to the spinal cord that occurs from root avulsion injury, whereas rhizotomy, like PNI, does not. In both deafferentation models, the response within the lesion site to the injury is similar initially, where microglia become activated and phagocytose necrotic debris. However, in the case of DRA, the microglial response is greatly increased in the lesion site from 2 to 14 days, continuing to 28 days. This suggests avulsion causes a greater autoimmune response in the later stages of injury, which is absent in rhizotomy models. Contralateral effects observed previously in SCI (Hains and Waxman, 2006), PNI (Arguis et al., 2008), and focal burn injury (Chang et al., 2010), are prominent in DRA tissue, but minimal in DRR tissue, and are likely due to a number of factors discussed separately in section 3.8.

As microglia are implicated in the maintenance of chronic neuropathic pain states in spinal cord injury (Hains and Waxman, 2006), and DRA leads to spinal cord trauma and maintained microglial activity, it could be plausible to suggest similar mechanisms involving microglia may underlie the intractability of these neuropathic pains.

Conversely rhizotomy leads to minimal microglial activity across 28 days corroborating previous data (Eriksson et al., 1993;Colburn et al., 1999), does not generally lead to neuropathic pain *in vivo* (Sheen and Chung, 1993;Yoon et al., 1996;Sukhotinsky et al., 2004), and is used to relieve peripheral nerve pain clinically (Loeser, 1972) (Chapter 4: results, for further details).

The spinal cord injury incurred after DRA, and the robust and maintained microglial activity that follows may well be the distinction between why avulsion leads to severe intractable neuropathic pain, and rhizotomy does not. The results here support the hypothesis that a rhizotomy model does not accurately represent the microglial reaction that may occur in the chronic stages of brachial plexus avulsion injury, and is important evidence when trying to ascertain the mechanisms behind neuropathic avulsion pain.

3.3.4.2: Astrocytes

The results of this chapter describe a two-step process of reactivity in both models. A significant increase in astrocytic process elongation toward the injury site can be seen at 1 day after DRA. This is earlier than the astrocytic reaction after DRR, which occurs at 2 days and is significantly less than DRA at this time point. This suggests the severity of astrocytic reactivity is dependent upon the type of deafferentation injury, once again providing contrast between these two models of brachial plexus injury.

GFAP expression continues to increase at 14 days, consistent with previous findings in SCI models (Popovich et al., 1997;Nesic et al., 2005), peripheral nerve injury models (Garrison et al., 1991;Raghavendra et al., 2003) and rhizotomy models (Beggah et al., 2005;Murray et al., 1990). It is known that astrocyte differentiation is progressive after PNI, peaking at 14 days (Echeverry et al., 2008), and it may be this differentiation that constitutes the further increase in immunofluorescence at this time point in both DRA and DRR. This may represent the change in activity of astrocytes during gliosis and their involvement in forming the non-permissive glial scar and preventing further degeneration of axons (Nomura et al., 2002). GFAP expression increases may be essential in maintaining some neuropathic pain conditions, certainly in PNI (Raghavendra et al., 2003), by taking over the role of microglia in sustaining synaptic changes within the dorsal horn of damaged and intact peripheral nerve terminals (Tanga

et al., 2004). However, although GFAP expression increases are seen in the spinal cord after SCI, coinciding with neuropathic pain behaviour (Nesic et al., 2005), astrocytes may not be responsible for the neuropathic pain perceived in this injury, as inhibition of microglial activity with minocycline at 4 weeks post SCI attenuates dorsal horn neuronal hyperresponsiveness and restored nociceptive thresholds (Hains and Waxman, 2006). A more likely role for astrocytes in the dorsal horn after dorsal root injury is in scar formation, as astrocyte morphology of interconnecting processes at 14 and 28 days may indicate. This is essential after avulsion injury to reform the barrier between CSF and the dorsal root entry zone with a greater need for scarring, and this is shown as a more substantial GFAP density than in DRR tissue at these time points.

Contralateral GFAP increase, that has been observed before in unilateral spinal nerve crush (Hatashita et al., 2008), occurs in both root injury models but is more substantial after DRA, probably due to the extent of SCI trauma inflicted in this model. These effects probably have a similar aetiology as with microglia and are discussed in section 3.8.

3.3.5 Leukocyte infiltration

3.3.5.1: Macrophages

At the early injury time points of 1 and 2 days, ED1-positive cells are small and granular in appearance, and possibly represent resident activated microglia, or tissue macrophages, or those from within the spinal cord microvasculature. Many surround the pia matter and DREZ, with only a few present in dorsal horn laminae and columns, in accordance with previous literature on root rupture and root rhizotomy at this time point (Nomura et al., 2005;George and Griffin, 1994a). The most significant increase in macrophage expression is at 14 days, especially in the dorsal columns after DRA and DRR. The macrophages are swollen, with staining principally surrounding the cell membrane, and encompass areas of vacuolisation, consistent with previous data (Fleming et al., 2006;George and Griffin, 1994a). Across later time points swollen macrophages infiltrate the dorsal column, with further vacuolization and tissue damage to this area, apparent. ‘Wallerian’ degeneration of ascending sensory fibres occurs in the dorsal columns after L4-L6 dorsal root rhizotomy, in a proximo-distal fashion, at a

rate of 3mm per hour in the rat (George and Griffin, 1994b). This data suggests that macrophages are phagocytosing damaged axons and myelin of ascending A-α/β fibres within the dorsal funiculus. Macrophages within the spinal cord are known to contain phagocytosed myelin after rhizotomy (Ling, 1979b). Secondly, the production of myeloperoxidase within macrophages, as well as neutrophils (Taoka et al., 1997), is neurotoxic, and may lead to tissue vacuolisation (Fleming et al., 2006). Surprisingly, a macrophage reaction has been shown in the ipsilateral dorsal column of ventral root avulsed rats expressing neuropathic pain behaviour (Bigbee et al., 2007), coupled with degeneration of primary afferent collaterals (Bigbee et al., 2008). This suggests that avulsion of the ventral root and therefore damage primarily to lower motor neurone axons, can detrimentally induce macrophage reactivity within ascending primary afferent fibre tracts. This may well occur through Wallerian degeneration of the transected motor axons interacting, through cytokines and inflammatory mediators, with sensory fibres within the same peripheral nerve (Bigbee et al., 2008). Interestingly, a generalized SCI, such as contusion, also leads to initial targeting of macrophages within only the dorsal columns (Carlson et al., 1998). A more diffuse ED1 expression throughout the segmental cord is found only at later time points (Carlson et al., 1998). This suggests dorsal root injury, ventral root injury, as well as spinal cord trauma, causes specific deteroriation of the ascending dorsal column sensory pathway, and is linked to macrophage extravasation and phagocytosis. However, the possibility that these ED1 cells originate from microglial populations, as shown previously after DRR injury (George and Griffin, 1994a) cannot be excluded.

In contrast to the dorsal columns, DRR and DRA macrophages within the dorsal horn have a subtle difference in appearance. They were not swollen and notably phagocytic, and did not surround regions of vacuolisation and cavities, and in the majority remained remained cellularly intact. Numbers of these smaller macrophages continue to increase across 28 days, but density staining remains substantially lower than in the dorsal column due to this separation in size. This perhaps implies a different, non-phagocytic, role of macrophages within this area of neuronal cell bodies, perhaps of a more persistent immune response similar to microglia. It is known macrophages produce reactive oxygen species, myeloperoxidase and NOS (Carlson et al., 1998), which suggests a role in neuroinflammation. As for apoptotic macrophages at 1 and 2 days post injury, similar to microglia, only a few were observed. It is likely that when

macrophages become phagocytic they also undergo a programmed cell death (Kirschnek et al., 2005). However, due to the overlap of the ED1 epitope with microglia, and the fact that only a small proportion of macrophages are colocalised with TUNEL, it is unclear whether these apoptotic macrophages are a different population to activated microglial-macrophages.

Macrophage density staining progressively increases over the course of 14-28 days after DRA and DRR, most clearly within the dorsal columns showing vastly swollen cell bodies. This increase is consistent with the findings from rat SCI (Casella et al., 2006;Trivedi et al., 2006), human SCI (Fleming et al., 2006), rat PNI (Gupta and Channual, 2006), and rat DRR (George and Griffin, 1994a). The expression of macrophages has a delayed contralateral effect at 4 weeks DRA. In this case an overspill from the increasing ipsilateral infiltration of macrophages could give rise to this contralateral effect, similar to the bilateral glial activation shown at 14 and 28 days. However, this delayed contralateral macrophage infiltration was also found in dorsal root ganglion cells after unilateral nerve ligation (Dubovy et al., 2007), where 'overspill' could not anatomically occur. This suggests either a general systemic upregulation of blood borne macrophages, targeted to specific contralateral segmental region of the cord, or perhaps a transneuronal control of macrophage infiltration (see section 3.8).

This report provides new evidence of a clear distinction between the two types of deafferentation injuries. After DRR within the dorsal horn, macrophage density remains unchanged from 2 to 28 days, at a low density, similar to previous findings (Ling, 1979b), whereas in DRA injured dorsal horn ED1 continues to rise beyond 2 days, at both 14 and 28 days, with a contralateral expression at 28 days. Within the dorsal columns both models show progressive macrophage recruitment across 2 to 28 days, but with DRA showing far greater bilateral ED1-ir than DRR. It is known that p38 MAP Kinase phosphorylation, an intracellular pathway associated with inflammation and neuropathic pain (Tikka et al., 2001), is greatly increased within macrophages after dorsal root rupture (mechanical stretch without avulsion), but only minimally after rhizotomy (Nomura et al., 2005). This suggests that a traction injury to the root and spinal cord leads to much more robust macrophage activation and infiltration into the spinal cord. Therefore the severity of deafferentation trauma, as is the case in glial

activity, is the factor behind the differential macrophage recruitment in DRA and DRR. The greater extent of spinal cord tissue damage caused by avulsion, compared to rhizotomy, increases macrophage recruitment within the dorsal horn and columns, and that this infiltration in the former injury is capable of extending across to the contralateral cord.

3.3.5.2: Neutrophils

The slow and steady increase of macrophage recruitment and activation is clearly contrasted with neutrophil infiltration. Neutrophils are apparent in the dorsal horn and columns in the acute phase of injury only, at 1 and 2 days, with very few positive cells at 14 and 28 days, consistent with previous data on SCI (Carlson et al., 1998). Original findings of this report show that DRA causes a greater neutrophil infiltration at 1 day in both dorsal horn and column of the ipsilateral cord and within the ipsilateral dorsal horn at 2 days compared to DRR. Neutrophils are recruited to the site of injury through adhesion to the surface of the vascular endothelium and transendothelial migration (Moalem and Tracey, 2006), and then targeted to the injury site by the expression of chemoattractant chemokines from inflamed tissue and immune cells such as microglia (Milner and Campbell, 2002). From here they can sensitize nociceptors through release of cytokines and reactive oxygen species (Moalem and Tracey, 2006), phagocytose foreign or native necrotic debris (Watson et al., 1996), and attract macrophages to the site of injury (Trivedi et al., 2006). This is the first time neutrophil infiltration has been shown, and quantified, in dorsal root deafferentations within the spinal cord.

The specificity of infiltration to the ipsilateral dorsal horn and dorsal column at early, but not later, time points is in parallel with the magnitude, time course, and side specificity of TUNEL expression, as well as cell loss counts from PI flow cytometry. Colocalisation reveals that, almost exclusively, TUNEL-positive nuclei are neutrophils. This result is consistent with the short life cycle of neutrophils (approximately 9 hours), regulated by apoptosis (Maianski et al., 2004), which is influenced by both intrinsic and extrinsic factors within normal and patho-physiological conditions (Trivedi et al., 2006). Neutrophil apoptosis can be accelerated both in the presence and in the absence of survival factors by activation of distinct members of the tumor necrosis factor/nerve

growth factor receptor family. A trigger for neutrophil apoptosis is phagocytosis (Watson et al., 1996) of either foreign or native debris (Popovich and Jones, 2003).

Neutrophil apoptosis in pathophysiological conditions plays an important role in the elimination of these cells from inflamed tissue without the release of hazardous intracellular contents (Simon, 2003). Macrophages phagocytose neutrophils while releasing anti-inflammatory mediators, thus controlling the extent of neutrophil mediated tissue damage (Savill et al., 2002). This explains why neutrophil infiltration and apoptosis occurs shortly after injury, within 1-2 days, before macrophage expression, whereas at 2 weeks the cord is absent of neutrophils but in an abundance of macrophages. The particulate neutrophil staining at 14 and 28 days most likely represents particles of phagocytosed neutrophil membrane.

The number of infiltrating neutrophils into the ipsilateral dorsal horn also depends on the deafferentation model. DRR resulted in fewer neutrophils in the dorsal horn than DRA, again suggesting that dorsal horn tissue damage is less severe in the former injury. The similar numbers of neutrophils in the dorsal columns at 2 days suggests similar tissue damage occurs in this area after both deafferentation models. The contralateral neutrophil count, predominantly in the dorsal columns, at 1 and 2 days are likely to occur from an ipsilateral ‘overspill’ in a similar way as observed with macrophages at 28 days. For further details refer to section 3.8.

3.3.6 Vascular loss

RECA-1 staining was used as a representation of loss of endothelial staining and microvasculature. Endothelial staining at 1 day after sham surgery was reduced in accordance with previous literature (Anderson et al., 1978), but was not maintained at 14 days suggesting a laminectomy effects the microvasculature of the dorsal horn only transiently. Endothelial reduction at 1 day post DRA and DRR may therefore be due to the cumulative effect of both transient ischemia after hemi-laminectomy as well as a result of injury to the root and radicular artery coursing with it. After 2 days vascular staining loss is maximal in both DRA and DRR dorsal horn, with vessels thin and broken within the cord. These results are consistent with SCI (Casella et al., 2006),

where RECA-1 expression is reduced after 8 hours, continuing to 2-4 days. The mechanisms behind the decrease in vascular integrity across at 2 days remain unclear.

One possibility is ischemia, through disruption of the ipsilateral posterior radicular arteries, which supply the posterior spinal artery of the spinal cord, and course along the dorsal and ventral roots and eventually supply blood to the spinal cord grey matter, as well as the single dorsal spinal vein, which overlies the posterior median sulcus in the rat, that provides venous drainage of the dorsal cord. Ligation of radicular arteries causes considerable ischemic spinal cord lesions, that are most pronounced at 7 days (Tsitsopoulos et al., 1995). Another possibility is a loss of microvascular tissue through gliosis and cytotoxicity. Nesic *et al.,* ((Nesic et al., 2005)) suggested that chronically overactivated astrocytes after SCI may cause loss of the blood brain barrier integrity within the cord. Wang *et al.,* ((Wang et al., 1996)) showed that endothelial cell necrosis could be induced through oxidative and non-oxidative mechanisms initiated after neutrophil adhesion and activation. The peak infiltration time of neutrophils and the maximal extent of vascular loss do indeed coincide in both deafferentation models; however, this unlikely to be the sole cause of vascular loss as leukocyte infiltration is strictly ipsilateral, whereas vascular loss is bilateral in the dorsal horn.

It is unclear as to the reasons why a unilateral root injury would lead to a bilateral vascular loss, and indeed so early after injury as most other contralateral effects such as glial activation, neuronal loss, and macrophage infiltration, occur much later. Contralateral vascular effects have been shown before (Sommer and Myers, 1996), with narrowing of the endoneurial lumina of the contralateral sciatic nerve 14 days after unilateral ligation. Contralateral vasculature degeneration is unlikely to be due to direct damage to arterial input to the lumbar spinal cord, which originates from a contralateral posterior spinal artery and radicular artery that would be protected from the hemi-laminectomy and the ipsilateral deafferentation. However occlusion of the single dorsal spinal vein leads to bilateral ischemia of the dorsal spinal cord incuding oedema, hemorrhage and gliosis from 1 day post injury, becoming more severe across 28 days (Zhang et al., 2001). Deafferentation, especially avulsion, may lead to damage of this major vein directly through trauma or through scar formation and expansion, as well as inflammation over the dorsal surface of the cord, and could permanently disrupt the venous drainage of the dorsal cord bilaterally.

After spinal cord hemisection (Imperato-Kalmar et al., 1997) or contusion (Casella et al., 2002;Loy et al., 2002) a potential recovery mechanism within the microvasculature can be observed after an initial vascular deterioration, beginning at 4 days and 7 days respectively as measured by RECA-1. This phenomenon is thought to be due to 'a disintegrin and metalloprotease protein 8' (ADAM8) initiation of angiogenesis (proliferation and migration of endothelial cells) (Mahoney et al., 2009). However, in the case of SCI, this angiogenesis is unable to repair the vasculature and beyond 7 days the microvascular integrity continues to decline (Imperato-Kalmar et al., 1997;Casella et al., 2002;Loy et al., 2002). New findings in this report show that after DRR a significant recovery of vascular staining occurs by 14 days, suggesting that rhizotomy does not permanently affect the vascular supply of the spinal cord, confirming previous literature (Liu et al., 1998). This recovery maybe initiated through compensatory shunting of blood supply, from other arteries such as the contralateral radicular arteries after the initial loss (Maliszewski et al., 1999), or less damage incurred by the dorsal spinal vein after rhizotomy compared to avulsion. Previous literature suggests the more likely reason for vascular recovery is angiogenesis and proliferation of endothelial cells, creating a neo-vasculature (Mahoney et al., 2009), however further studies using angiogenic markers (such as ADAM8) or neo-vascular markers (such as IB4), or markers for growth factors such as vascular endothelial growth factor (VEGF) are needed to confirm this. This angiogenic recovery has also been shown in the endoneurium of the sciatic nerve after ligation by 7 days (Sommer and Myers, 1996). Comparatively no maintained recovery of vasculature was seen in DRA up to 28 days, similarly to SCI. It is likely that the tensile stress placed on the cord through the tearing of the root, resulting in stretch and distortion of the avulsed cord, leads to permanent rupturing of the microvasculature and vasospasm (Mautes et al., 2000). The subsequent loss of tissue integrity, vast phagocytic invasion, scarring and vacuolisation in the case of avulsion overshadows any potential angiogenic recovery mechanism or blood supply diversion. This leaves this neovasculature unstable and susceptible to degeneration and phagocytosis (Imperato-Kalmar et al., 1997;Mautes et al., 2000).

There are secondary consequences to the loss of microvasculature. Vascular loss with corresponding ischemia within the lesion, may be a mechanism by which the avulsed cord could become necrotic (Mautes et al., 2000), through deposition of platelets and

formation of thrombi and mediation of multiple secondary injury inflammatory cascades (Nelson et al., 1977). Secondary neuronal loss recorded in 28 day DRA tissue may well be explained by this maintained vascular loss, as both endothelial cells and neurones deteriorate across similar time periods after SCI (Dusart and Schwab, 1994;Imperato-Kalmar et al., 1997;Casella et al., 2006), and cavity formation occurs after angiogenesis fails to re-establish neo-vasculature (Loy et al., 2002). Further, loss of vascular integrity may be a pathway by which monocyte-macrophages may enter the cord from the blood, and loss of vascular integrity after SCI coincides with macrophage infiltration, as well as glial scarring and microglial activation (Dusart and Schwab, 1994;Casella et al., 2006). This is especially evident in DRA where a maintained loss of vascular staining could facilitate further macrophage infiltration at 14 and 28 days, and also coincides with maximal astrocyte and microglial densities. Perhaps the recovery of vascular integrity in DRR by 14 days may have prevented such an increase in secondary damage at these later time points.

It is not possible to say in this report whether endothelial cells are in fact dying, as TUNEL colocalisation studies were not performed, and therefore only circumstantial evidence can be put forward to suggest a role of degenerating vasculature in the chronic stages of deafferentation injury. Indeed it is also premature to describe the vascular system as damaged, as the observations here could simply be a reduced expression of the RECA-1 epitope. However this report is the first evidence showing different microvascular effects after rhizotomy compared to avulsion. These different vascular effects suggest that rhizotomy may not give an accurate representation of the severity of the vascular loss in an avulsed spinal cord, which shows similarity to SCI.

3.3.7 Neuronal loss

This report has used immunohistochemistry, flow cytometry, and histology to investigate the effect of two different deafferentation injuries on the neuronal population of the dorsal horn. Data shows that a transneuronal loss of dorsal horn neurones occurs immediately after deafferentation, and that it is greatly increased in avulsed animals. A ‘second-wave’ of NeuN loss occurs in the case of DRA, at 28 days post injury. This data for the first time provides evidence suggesting root avulsion injury, like SCI, is a chronic, progressive trauma, and this time frame of 14-28 days of

further neurodegeneration may provide a substantial therapeutic window for chronic neuroprotective treatment clinically.

NeuN reduction after both DRR and DRA follows the pattern of downregulation found in the vasculature, and is similar in time course to previously reported findings in spinal cord hemisection (Dusart and Schwab, 1994), spinal cord contusion (Casella et al., 2006), and spinal cord compression (Huang et al., 2007). In the case of root injury, an initial reduction in NeuN in the dorsal horn at 1 day in both models is significant from both sham and naïve, and is maintained at 2 days at approximately 30% in DRA and 18% in DRR, with ipsilateral NeuN loss more severe than contralateral. This NeuN reduction at these early time points was confirmed with toluidine blue counts within the dorsal horn as well as flow cytometry analysis within the spinal cord. This death, as defined by NeuN/DAPI flow cytometry is approximately 25% after DRA and 18% after DRR at 2 days (Chew et al., 2008), and 20% in both deafferentation models in toluidine blue staining. These values represent the percentage of all neurones that have died from the moment of the injury up to 2 days, depending on the rate of neuronal phagocytosis and debris clearance of macrophages. The percentages calculated from these three different analyses are similar, with differences due to different methods of analysis. For this reason it can be concluded that death of neurones does occur rather than just a down-regulation of the NeuN epitope in injured neurones. Interestingly, this neuronal loss is, in the early injury time period, not specific to the type of deafferentation imposed on the cord, suggesting that the method of deafferentation is not a factor in early stage neuronal loss. This is in direct contrast to other spinal events such as infiltration of phagocytes, vascular disruption and glial reactivity.

The negative TUNEL-NeuN colocalisation at 1 and 2 days suggest two possibilities of the initial fate of neurones after deafferentation injury: Firstly the loss of neurons, observed by all methods, may occur through non-apoptotic mechanisms. Secondly, that cell death within the neuronal population, via apoptosis, may occur before 1 day. It is the case in spinal cord contusion injury that TUNEL positivity presents in neurones at 4 hours, peaking at 8 hours, and is absent by 24 hours (Liu et al., 1997).

The numbers of dead neurones in flow cytometric analysis at 14 days are not significantly different to naïve. This suggests two things: Firstly, the neurones that died

by 1-2 days have been cleared, most likely through phagocytosis involving the neutrophil and macrophage populations. Secondly, no further neuronal loss occurrs between 2 and 14 day time points in either model. The absence of further dead neurones at 14 days in NeuN/DAPI flow cytometry is also confirmed with NeuN immunohistochemistry, and is consistent with SCI models (Huang et al., 2007). Scarring around the lesion and the dorsal columns suggests that intrinsically the cord has prevented further neuronal loss by containing the lesion site through an astrocytic glial reaction, maintaining the integrity of the remaining intact dorsal horn. This coincides with the upregulation of GFAP in astrocytes, and the appearance of interconnected astrocytic processes in both deafferentation models.

Further analysis shows a 'second-wave' of NeuN reduction, with a significant contralateral effect, occurring by 28 days after DRA but not after DRR. Although this reduction has not been confirmed with toluidine blue or flow cytometric analysis, it could be suggested that further release of cytotoxic, free radical, and excitatory amino acids from increasing glial and phagocytic species with the injury site as well as sustained loss of vascular integrity are contributing to the secondary cell loss. This chronic neuronal reduction of approximately 56% at 28 days certainly coincides with the maximal macrophage induction, and microglia and astrocyte reactivity. Visually, tissue scarring and further cystic cavity formation have engulfed the dorsal horn and column in 28 day DRA. Interestingly, further increase in glial and macrophage species in the dorsal horn and columns of DRR animals are minimal at 28 days, coinciding with no further neuronal loss. Scarring and cavity formation has been shown to occur after SCI at 28 days accompanied with >80% neuronal loss, using NeuN (Huang et al., 2007). A neuronal loss of 20% was found after PNI (Scholz et al., 2005) in the dorsal horn over 28 days, with apoptosis implicated as the cause. As for an explanation of the 30% contralateral neuronal loss at this time point, excitotoxic effects within the ipsilateral dorsal horn, trans-neuronally or in an "over spill" mechanism may affect the contralateral dorsal horn also. Again this coincides with an increase in glial activity, macrophage recruitment, and vascular loss in the contralateral dorsal horn at 28 days. The aetiology of the neuronal loss by 28 days has not been assessed in this work, but is likely to be either necrotic, or apoptotic, at time points that have not been analysed in this report.

3.3.8 Contralateral effect

Contralateral effects were detected for primary afferent terminal loss, microglial and astrocyte reactivity, macrophage and neutrophil infilatration, and neuronal and vascular loss. These effects were usually delayed, and more severe in the DRA model compared to DRR. Contralateral effects after unilateral root injury are not observed in previous research literature. However, as mentioned above, these effects may have been missed in previous studies, as authors use the contralateral side as an internal control for ipsilateral rhizotomy comparison, rather than a naïve control. Contralateral effects in the dorsal horn, across similar time points as mentioned in this chapter, have been shown to occur in microglia (Colburn et al., 1997;Sweitzer et al., 1999;Milligan et al., 2003) and astrocytes (Colburn et al., 1997;Hatashita et al., 2008) after unilateral inflammation and PNI. Bilateral allodynia has been reported in unilateral rat injury models of dorsal root crush (Rothman et al., 2009), dorsal root ligation (Hunt et al., 2001) unilateral focal burn injury (Chang et al., 2010), spinal nerve ligation (Arguis et al., 2008), and spinal nerve crush (Hatashita et al., 2008). The ‘mirror-image’ pain in these cases was causally linked to contralateral increases in satellite cell activation and TNFα expression in the contralateral DRG (Hatashita et al., 2008); as well as activation (Chang et al., 2010) and proliferation (Rothman et al., 2009) of microglia, and astrocyte hypertrophy in the dorsal horn (Hatashita et al., 2008). In all cases the contralateral effects were delayed, always proceeded, and were of a lesser magnitude than ipsilateral. These phenomenon have two possible explanations that are clinically relevant when understanding certain contralateral pain syndromes (Sotgiu et al., 2004). Firstly, some authors suggest the spinal cord upregulation could be simply an “overspill of reactivity” from the ipsilateral side (Koltzenburg et al., 1999;Hatashita et al., 2008). Activated glia can influence nearby cells in a paracrine fashion (Milligan and Watkins, 2009), via gap junction communication as in astrocytes, or cytokines and inflammatory mediator release as in microglia. If this occurs near the grey commissure and posterior median sulcus, it is plausible that contralateral glia could be influenced and activated by ipsilateral glia. Alternatively, a transneuronal mechanism involving commissural fibre activity could be responsible for this phenomenon (Attal et al., 1990;Koltzenburg et al., 1999;Sotgiu et al., 2004). Dorsal horn neurons and interneurone axons are known to cross the cord contralaterally, such as the spinothalamic and ventral spinocerebellar tracts (Willis and Coggeshall, 1991;Willis and Westlund, 1997;Almeida et al., 2004). If

these neurons are hyperexcitable or injured and releasing excitatory amino acids, ATP, or fractalkine for example, this could also activate contralateral glia. For vascular loss, as explained previously, contralateral effects could well be due to indirect mechanisms such as ischemia through damage to the posterior venous outflow. Contralateral effects are more severe after avulsion suggesting the direct mechanical trauma, rather than deafferentation, to the spinal cord after DRA may be responsible for the magnitude of these effects.

3.3.9: Conclusion

This chapter identifies important differences in the degenerative events in the spinal cord proceeding deafferentation via root rhizotomy, used in pre-clinical root avulsion modeling, and 'true' root avulsion. When quantifying reactive processes such as microglial and astrocyte upregulation, infiltration of leukocytes or degenerative phenomena in neurones and endothelial cells, avulsion results in a more severe response than rhizotomy in all cases. A delayed contralateral effect after avulsion is prominent in primary afferent terminal, dorsal horn neuronal, and endothelial loss, as well as glial and leukocyte upregulation. This may have been overlooked in previous literature due to the use of rhizotomy models. This new evidence highlights a role for neutrophil reactivity at the early stages of injury (1-2 days), and macrophage, microglial, and astrocyte reactivity, in the later stages of avulsion injury (14-28 days). Degenerative phenomena follow these processes, with initial neuronal and vascular disruption at 1-2 days through both modes of deafferentation, but a further neurodegeneration and a maintained vascular degeneration at 28 days only after avulsion. These differences provide evidence for arguing rhizotomy, used most often for *in vivo* modeling of deafferentation, is a milder model of brachial and lumbosacral plexus avulsion injury for assessing degenerative phenomena in the spinal cord.

Neuronal loss does occur after deafferentation initially, but does not significantly change between 1 and 14 days. A second wave of neuronal loss occurs between 14 and 28 days after avulsion but not after rhizotomy. The extent and time course of dorsal horn neuronal loss after avulsion injury, with a delayed and more severe "second wave" of loss that coincides with further degenerative phenomena, may provide a therapeutic window to target and prevent exacerbation of symptoms after brachial plexus injuries.

Chapter 4: A new rodent behavioural model of avulsion pain.

4.1: Introduction

4.1.1: Neuropathic pain

The International Association for the Study of Pain (www.iasp-pain.org) defines neuropathic pain as 'pain initiated or caused by a primary lesion or dysfunction of the nervous system', different from nociceptive pain that typically results as a response to tissue damage outside of the nervous system. Neuropathic pain can be broadly described as a pathological symptom of injury, inflammation, or disease to the peripheral or central nervous system. It is usually chronic in duration, such that it lasts longer than 3 months. Various diseases can lead to neuropathic pain including trigeminal neuralgia (Cheshire, 2005), diabetic neuropathy (Veves et al., 2008), multiple sclerosis (Pollmann and Feneberg, 2008), cancer (Blumenthal, 2009), and HIV (Verma et al., 2004), to list but a few. The nature of neuropathic pain can be broadly divided into three unique sensory abnormalities or dysesthesias: 1) *Allodynia*-a painful sensation from a typically non-noxious stimulus. 2) *Hyperalgesia*- a highly exaggerated nociceptive response. 3) *Spontaneous pain*- a painful sensation from an area of anaesthetic (Anesthesia Dolorosa) tissue, which is not driven by peripheral stimulation. These characteristics may act in combination, or only one may be present. Indeed in phantom limb pain or anesthesia dolorosa where evoked sensation is not applicable, only spontaneous pain can be a symptom. These symptoms do not take into account the emotional, cognitive changes that also take place in a person with neuropathic pain, including depression and stress. Patient descriptions of neuropathic pain sensations include pricking, cold, freezing, numb and wretched, pressing and burning sensations (Herr, 2004). These dysesthesias can be continuous, such as a burning sensation, and/or paroxysmal that are likened to electric shock.

The *Neuropathic Pain Network* (www.neuropathicpainnetwork.org) estimates the prevalence of neuropathic pain in the United Kingdom at 3 million people, with similar numbers in other European countries such as France, Spain and Germany. Between the UK and the US there are estimated to be 15 million sufferers of neuropathic pain. In a recent survey across 3 UK cities the prevalence of pain of a neuropathic origin was 8%

(Torrance et al., 2006). A questionnaire sent to the general population of France recorded a prevalence of 31.7% for chronic pain, with 6.9% prevalence of neuropathic pain (Bouhassira et al., 2008). Although these studies are not ideally controlled, as they depend solely upon unblinded patient self diagnosis, they suggest an alarming number of the general population suffer from this disorder.

4.1.2: Models of neuropathic pain

Peripheral Nerve Injury (PNI)

Work in animal models has contributed greatly to our understanding of neuropathic pain mechanisms, and involve several variations of nerve injury. They have provided quick and easy tools to assess therapeutic efficacy of new drugs as pre-clinical screens. The first model of neuropathic pain, specifically spontaneous, was designed by Wall *et al.*, ((Wall et al., 1979)), with complete sciatic and saphenous nerve transection. This produced an anesthesia dolorosa in the affected limb, and resulted in atendency for the rodents to attack and mutilate the anesthetized limb which the authors described as autotomy, and a scaling system was designed to describe the extent of neuropathic pain. Many issues arise with this model, such that higher order mammals do not show self mutilation, and alternative interpretations have been proposed for autotomy (Rodin and Kruger, 1984).

Partial denervated PNI models have been designed to allow for evoked sensory testing as a more quantitative measure of neuropathic pain development (Bennett and Xie, 1988;Seltzer et al., 1990;Kim and Chung, 1992;Decosterd and Woolf, 2000;Lee et al., 2000). In these models autotomy rarely occurs, indicating a fully denervated sensory peripheral field through nerve injury is required for self mutilation. These have resulted in reproducible sensory deficits that have been typically defined as allodynia, hyperalgesia, and spontaneous pain. However they also show considerable differences in magnitude and duration of symptoms (Dowdall et al., 2005). The first model, designed by Bennett and Xie ((Bennett and Xie, 1988)) was a chronic constriction injury (CCI), accomplished by tying loose ligatures around the sciatic nerve of the rat at mid-thigh level. The ligatures evoke intraneural edema, and the nerve self-strangulates, initially leading to a loss of most A-fibres (Carlton et al., 1991;Obata et al., 2003), later

followed by C-fibres, equaling out the ratio (Coggeshall et al., 1993;Gabay and Tal, 2004). The process of Wallerian degeneration of injured motor and sensory fibres, and the corresponding secretion of inflammatory mediators, triggers spontaneous activity in non-injured fibres (Wu et al., 2002). The model results in the development of chemical and heat-evoked hyperalgesia and allodynia and spontaneous pain 2 or more days after surgery, peaking at 10-18 days, and lasting up to 2 months (Bennett and Xie, 1988;Dowdall et al., 2005), that is thought to be due to ectopic activity of A-fibres (Tal and Eliav, 1996) and central sensitization in the dorsal horn (Koltzenburg et al., 1994). Interestingly the effect of different composition of ligatures lead to different behavioural outcomes (Maves et al., 1993), with chronic gut ligatures leading to a far more severe behaviour and loss of axons than silk or plain gut, suggesting a chemical component may also play a neuropathic role. The main problem with this injury is the requirement of the nerve to become inflamed and 'strangle itself', and this can be highly variable. In most case the percentage of damaged DRG neurones, as identified by ATF3 positivity, range from 7-51% (Obata et al., 2003) as can the incidence of neuropathy 10-80%.

Seltzer *et al.*, ((Seltzer et al., 1990)) designed the partial sciatic nerve ligation model that is produced by piercing the rats sciatic nerve at the upper thigh level with a needle and suture, and tightly ligating and thus transecting about ⅓ to ½ of the nerve axons. This leads to a partial deafferenation of the rat hind paw, and induces mechanical allodynia, thermal hyperalgesia and indication of spontaneous pain, within a few hours and maintained presence for up to 7 months. Through neonatal capsaicin treatment and selective nociceptor (C and Aδ) destruction, a role of A-fibres in mechanical hypersensitivity and C-fibres mediate thermal hyperalgesia were defined in this model (Shir and Seltzer, 1990). However, the authors (Shir et al., 1998) found difficulty in replicating the neuropathic pain induced in this model, when used in different laboratories. The neuropathic behavior is greatly susceptible to changes in rat strain, vendor, age, gender, weight, diet, and personnel. There are likely to be additional conflicting factors with the extent of axonal injury (one third to half) and accuracy of surgery applied to the sciatic nerve, as well as uncontrolled co-mingeling of injured and intact axons. The sciatic nerve ligation model has recently been modified into a 'spared sciatic nerve injury' model. This involves tight ligation of only 2 of the 3 branches of the sciatic nerve, most often the tibial and common peroneal, leaving the sural intact (Decosterd and Woolf, 2000;Lee et al., 2000). In this way the co-mingling of distal

axons with degenerating axons, and the effects of Wallerian degeneration on intact axons is restricted, and enables a more reliable behavioural testing on adjacent nerve injured and 'intact' skin territories than the partial sciatic nerve injury model.

The spinal nerve ligation (SNL) otherwise known as the 'Chung' model (Kim and Chung, 1992) is perhaps the most well know and most reproducible nerve injury model, and can be modified accordingly. SNL can involve a tight ligation of the L5 and L6, L5 alone, or S1-S4 spinal nerves, close to the respective ganglia and transection without the formation of a neuroma. The hind paw or tail is therefore partially deafferented (through sciatic and sacral nerves) by 50%. Mechanical and heat-evoked hyperalgesia, and spontaneous pain, were evident immediately and maintained up to 4 months post injury (Choi et al., 1994). The neuropathic pain was shown to be sympathetically dependent (Choi et al., 1994;Kim and Chung, 1992), as lumbar sympathectomy almost completely abolishes it. Indeed after SNL injury sympathetic sprouting of noradrenergic terminals around the effected DRG has been shown to be functionally coupled and aberrantly active (McLachlan et al., 1993), a phenomenon common to all PNI models and a symptom of neuropathic pain (see section 4.1.3). The unique feature of SNL, unlike the spared sciatic injury model, is that the DRG cells of injured and intact afferents are completely separated, allowing their contribution to neuropathic pain to be separately assessed.

Several groups have tried to understand the contribution of the intact and injured spinal nerves and spinal segments in SNL neuropathic pain, and there is still much debate (Sheen and Chung, 1993;Yoon et al., 1996;Eschenfelder et al., 2000;Li et al., 2000;Sukhotinsky et al., 2004). Selective L5-L6 dorsal root rhizotomy or anaesthetic block 5 days after L5 and L6 spinal nerve ligation abolished the injury-induced evoked pain behavior (Sheen and Chung, 1993;Yoon et al., 1996;Sukhotinsky et al., 2004). This suggested afferent activity from the injured L5-L6 DRG must coordinate and maintain the neuropathic pain that is processed through the intact L3 and L4 afferent fibres and spinal segments. Ectopic discharges from the L5 and L6 DRG, perhaps mediated sympathetically (Choi et al., 1994) as peripheral targets are no longer intact, sensitize the dorsal horn neurones making them more susceptible to activation from intact adjacent afferents. Sensitization of the dorsal horn can be reversed by inhibiting these ectopic discharges with local anesthetic applied to the rhizotomised roots (Yoon et al.,

1996;Sukhotinsky et al., 2004). There is however, evidence to the contrary, where pre-emptive or delayed (5-7 days) L5 DRR does not ameliorate L5 SNL pain (Eschenfelder et al., 2000;Li et al., 2000). In both of these cases peripheral interaction between injured (L5/L6) and intact (L3/L4) nerves via Wallerian degenerative phenomena, and increased L3/L4 afferent activity were implicated as the cause for neuropathic pain after SNL. This controversy can be explained; in some cases (Colburn et al., 1999;Eschenfelder et al., 2000;Li et al., 2000) L5 DRR alone produced a robust allodynic response up to 7, 20, and 57 days post injury in respective articles, whereas in the hands of separate investigators (Sheen and Chung, 1993;Yoon et al., 1996;Sukhotinsky et al., 2004;Obata et al., 2006b) it did not produce neuropathic pain. Therefore in the hands of some investigators DRR may simply replace the L5/L6 SNL-induced neuropathic pain; however, it is still unclear which afferents, intact or injured, are most important in neuropathic pain.

Additionally, and perhaps surprisingly, rhizotomy or avulsion of the L5 ventral root can lead to glial activation in the dorsal horn (Colburn et al., 1999;Bigbee et al., 2007), increase p75 expression in satellite cells and Schwann cells of the DRG, linked to sympathetic sprouting (Zhou et al., 1996), and up-regulation of NGF, BDNF, and ED1 within the DRG, and BDNF in the dorsal horn (Obata et al., 2004). Such increase in activity and expression could be the cause of the neuropathic pain behaviours induced in this injury model (Sheth et al., 2002;Li et al., 2003;Obata et al., 2004). Prolonged treatment with NGF-antiserum attenuated ventral root-induced mechanical allodynia (Li et al., 2003). These phenomena occur most likely through Wallerian degenerative interaction between injured motor axons and intact primary afferents of the mixed nerve. However, similar to dorsal root rhizotomy, some investigators have shown no neuropathic pain responses to ventral root rhizotomy (Colburn et al., 1999). Ventral root avulsion (L6-S1), a more clinically representative model of true avulsion also leads to astrogliosis, microglial activation, macrophage infiltration, and axon degeneration, in the dorsal column and horn, with neuropathic pain behaviour maintained up to 7 weeks (Bigbee et al., 2007;Bigbee et al., 2008). Immediate reimplantation of the ventral root ameliorated these symptoms (Bigbee et al., 2007;Bigbee et al., 2008), but it is unclear what mechanism underlies this phenomenon.

The reason why dorsal or ventral root rhizotomy produces neuropathic pain in some groups but not others is unclear, as clinically (White and Sweet, 1969;Loeser, 1972;Hosobuchi, 1980;Gybels and Sweet, 1989) rhizotomy is used to relieve peripheral neuropathic pain. This may be due to a number of methodological factors (Shir et al., 1998;Sheth et al., 2002), as well as the extent of laminectomy surgery (Kosta et al., 2009). As suggested in chapter 3, because rhizotomy is unreliable at producing neuropathic pain behaviour, and does not represent the clinical condition, it is therefore an unsuitable model for the study of neuropathic pain and nerve/root injury.

Spinal Cord Injury (SCI)

Spinal cord injury also leads to the generation of neuropathic chronic pain states, and clinically has a prevalence of >65% in patients (de Miguel and Kraychete, 2009;Miladinovic, 2009). Models for spinal cord injury have been designed specifically for regenerative research rather than chronic pain, and less attention has been given to mechanism of chronic pain in SCI. The most common model is the contusion devise first described by Allen (Allen, 1911) as a simple weight that is dropped from a varying height. This crude method has now been optimized through precision controlled devises such as the Infinite Horizons Contusion (IHC) device (Precision Systems and Instrumentation, Lexington, KY) and the MASCIS/NYU impactor, designed by Wise Young, John Gruner, and Carl Mason at New York University Medical Centre in 1991. The IHC instrument enables the application of standard-force injuries through electronically controlled impaction, and force levels can be varied accordingly. The MASCIS impactor is more widely applied to studies on chronic neuropathic pain (Hulsebosch et al., 2000). It precisely measures the movement of a 10-gram rod onto the laminectomised dorsal surface of the thoracic cord. The height of the rod dropped can be accurately controlled. After impact computer readout gives information on impact trajectory, impact velocity, cord compression distance and time. In this case the intensity of impact can be varied to produce optimum hyperalgesic responses without excesses and permanent functional loss in the forepaws (‘above-lesion’), hindpaws (‘below-lesion’), and in the trunk/girdle area (‘at-level-lesion’), as well as spontaneous measures of chronic pain such as reduced activity and exploratory behavior (Siddall et al., 1995;Mills et al., 2001;Hulsebosch et al., 2000;Hulsebosch et al., 2009). In these

cases neuropathic behavior is related to the recovery of function and is therefore delayed by several weeks.

Hemi-transection injuries to the spinal cord at the thoracic level have also lead to mechanical and thermal allodynia bilaterally in forelimbs and hindlimbs after 4 weeks (Christensen and Hulsebosch, 1997a;Bennett et al., 2000). Anterolateral lesions of the spinothalamic tract in monkeys and rats resulted in excessive grooming and mechanical allodynia in the contralateral limb (Ovelmen-Levitt et al., 1995;Vierck, Jr. and Light, 2000).

Another model of chronic neuropathic pain after SCI is ischemia, involving an intravascular photochemical laser beam reaction that occludes blood vessels at the T10 vertebra (Hao et al., 1991b;Hao et al., 1991c;Hao et al., 1991a). Acute ischemia is produced at the T10 spinal cord level accompanied with transient neuropathic behavior including trunk mechanical allodynia, as determined by increased vocalization to light brushing of the flank, and spontaneous pain as determined by non-evoked vocalization, peaking at several hours and dissipating at several days (Hao et al., 1991a). This allodynia was coupled with increased sensitivity of wide dynamic range dorsal horn neurones to stimulus (Hao et al., 1991c), and behavior could be abolished with pre-treatment of NMDA antagonist MK-801 (Hao et al., 1991b).

A clip compression model in which the thoracic spinal cord is compressed by a 35 g or 50 g clip that results in mechanical hyperalgesia in the hindlimbs that coincided with a reduction in serotoninergic immunoreactivity below the level of lesion (Bruce et al., 2002), suggesting in this model below level neuropathic pain behaviour was due to loss of inhibitory tone.

Quisqualic acid injection (an AMPA/kainate and metabotropic receptor agonist) into the deep dorsal horn results in specific excitotoxic loss of deep dorsal horn neurones and produces spontaneous (excessive grooming) and evoked (mechanical allodynia and thermal hyperalgesia) neuropathic pain behaviour (Yezierski et al., 1998), with the authors suggesting, albeit without direct evidence, that loss of inhibitory neurones and hyperexcitability of spared superficial dorsal horn neurones the mechanism of neuropathic pain behaviour.

In the Hulsebosch lab, this chronic neuropathic pain behaviour in spinal cord injury models have been directly related to dorsal horn neurone hyperexcitability (Christensen and Hulsebosch, 1997a), as well as increases in CGRP immunoreactivity (Christensen and Hulsebosch, 1997b), metabotrophic glutamate transporters (Mills and Hulsebosch, 2002), and NGF (Gwak et al., 2003) have been shown in the dorsal horn. Common themes present between peripheral and central injury and the resulting neuropathic pain, such as increased excitability to peripheral stimulation and central sensitisation. Indeed the hyperalgesia and allodynia seen in these animals after either transection injuries or contusion injuries have been attenuated with CGRP receptor antagonists (Bennett et al., 2000), gabapentin (Hulsebosch et al., 2000), or anti-NGF (Gwak et al., 2003).

4.1.3: Mechanisms of neuropathic pain

Neuropathic pain can loosely be attributed to the disruption of a system 'neuromatrix'; 'a neuro-signature pattern of nerve impulses generated by widely distributed neural networks' (Melzack et al., 2001). The mechanisms by which this disruption to the nervous system leads to neuropathic pain are not entirely clear at present, but are becoming better understood in recent years. Physiological mechanisms include ectopic firing, phenotypic changes, peripheral sensory degeneration, and disinhibition that can lead to a phenomenon of central sensitisation (Woolf, 2004;Latremoliere and Woolf, 2009). Central sensitisation is the state of heightened excitability of central dorsal horn neurons and is the proposed mechanism by which allodynia and hyperalgesia develop after injury. This can be activity-dependent, caused by spontaneous firing of peripheral C- and A-fibre axons, or transcriptionally-dependent caused by increases in expression levels of BDNF, SP, NK1, COX2, cytokines and other mediators (Woolf, 2004). Extracellular recordings from the dorsal horn in various root injury, PNI, and SCI models have revealed changes in electrophysiological properties of dorsal horn neurones (Ovelmen-Levitt et al., 1984;Ovelmen-Levitt, 1988;Dalal et al., 1999;Drew et al., 2001;Hains et al., 2003b;Lampert et al., 2006). However the cellular mechanisms that occur pre- and post-synaptically, that are responsible for these physiological effects are extensive and only recently have become more clear.

Pre-synaptically

Spontaneous firing of intact C-fibre nociceptors within adjacent spinal nerves is understood to be responsible for the spontaneous pain that is experienced in neuropathic PNI and inflammatory pain states (Ali et al., 1999;Wu et al., 2001;Djouhri et al., 2006), giving further evidence for the role of the intact afferent in neuropathic pain. There is also evidence to suggest directly injured Aβ-fibres in PNI may also drive neuropathic pain of an evoked nature, such as allodynia and hyperalgesia through ectopic activity, as shown by c-Fos expression in the dorsal horn (Molander et al., 1994;Shortland and Molander, 1998;Bester et al., 2000), and shown electrophysiologically in the dorsal root (Han et al., 2000;Liu et al., 2000c) and dorsal horn (Kohno et al., 2003), suggesting both injured and adjacent intact nerves are key to the pathophysiology of central sensitisation. Ectopic activity may be caused in part by alteration in the arrangement and density of voltage gated sodium channel subunits (Dib-Hajj et al., 2009). In particular, the sodium channel subunit Nav1.3, controlling high frequency action potential firing through rapid repriming of the tetrodotoxin-sensitive (TTX-S) current and expressed at low levels in adult DRG, is upregulated in DRG cell bodies following nerve injury, leading to enhanced responses and a larger persistent current (Waxman et al., 1994;Dib-Hajj et al., 1999;Dib-Hajj et al., 2009). The tetrodotoxin-resistant (TTX-R) sodium channel subunits Nav1.8 and Nav1.9, expressed almost exclusively in rodent nociceptive neurones (Kerr et al., 2001;Djouhri et al., 2003;Silos-Santiago, 2008), are responsible for resting inactivation and hyperpolarized state of the sodium channel. These are downregulated in the injured DRG after axotomy (Dib-Hajj et al., 1999;Sleeper et al., 2000;Decosterd et al., 2002) further increasing the propensity for hyperexcitability. Sodium channel expression remains unchanged however in adjacent intact DRGs (Decosterd et al., 2002). Knock out studies for both NaV1.3 -/- mice (Nassar et al., 2006), and NaV1.8-/- mice (Kerr et al., 2001) have provided conflicting evidence for the role of these sodium channels, as the development of ‘normal’ neuropathic pain behaviour after PNI occurs up to 14 days. Interestingly NaV1.8-/- mice, show no behavioural signs of NGF-induced thermal hyperalgesia (Kerr et al., 2001), suggesting TTX-R sodium channel expression is essential in inflammatory pain but not neuropathic. An explanation for these conflicting methodologies is that sodium channel expression changes are not essential for the development and maintainence of evoked pain behaviours, but may modulate the symptoms of neuropathic pain through altering the membrane properties of injured axons. Alternatively it could be that no

single channel is responsible for the generation of neuropathic pain, and rather aberrant expression of many different sodium channel subtypes after injury may result in hyperexcitability (Nassar et al., 2006). As for root injury, after L4/5 rhizotomy (Sleeper et al., 2000) no change in NaV1.8 or 1.9 expression was found in the injured DRG at 9-12 days. However, a decrease in these sodium channels was noted in injured DRG 4-8 days in patients with brachial plexus avulsion, with recovery to naïve levels over a period of 3 months (Coward et al., 2000) suggesting time post injury or type of root injury may be a factor in sodium channel expression. An accumulation of NaV1.8 and NaV1.9 was also found across these time points post injury in developing root neuromas (Coward et al., 2000), as well as in peripheral neuromas developed 22 days after *in vivo* saphenous nerve section, with increasing ectopic activity over time (Roza et al., 2003). This suggests TTX-R channels and accumulation in the transected end of the nerve or root rather than within the DRG may be responsible for ongoing spontaneous pain.

There is debate as to whether structural changes occur after PNI, namely uninjured afferent terminal sprouting. Liu and Chambers ((LIU and CHAMBERS, 1958)) were the first to suggest the phenomenon of collateral sprouting of adjacent intact afferents in the dorsal horn after partial deafferentation. As mentioned previously, deafferented C-fibres have atrophy within lamina II after PNI (Arvidsson et al., 1986) and rhizotomy (Tessler et al., 1980;Zhang et al., 1993). As a result of C-fibre injury, Aβ-fibres sprout into laminae I and II, a region usually devoid of such afferent terminals that contains pain-sensing dorsal horn neurones, and this is corroborated extensively in the literature (Woolf et al., 1992;Lekan et al., 1996;Mannion et al., 1996;Shortland et al., 1997;Doubell et al., 1997;Nakamura and Myers, 2000;Ma and Tian, 2001;Hu et al., 2004). There is however controversy over whether the sprouting is isolated to only the injured population of A-fibres (Shortland et al., 1997) or can be induced in adjacent intact A-fibres (Mannion et al., 1996). The mechanism of intact Aβ-fibre sprouting may be due to injury-induced C-fibre transganglionic degeneration or atrophy that ‘conditions’ A-fibres into a regenerative growth state (Mannion et al., 1996). After L5 root rhizotomy, A-fibre sprouting from L4 does not occur, suggesting that simply creating synaptic space in the dorsal horn through terminal depletion is not enough stimuli to cause sprouting: rather Wallerian degenerative interaction between injured and intact afferents of the same nerve is the trigger (Mannion et al., 1998). A-fibre

sprouting after PNI is still a controversial topic however, due to recent articles questioning the selectivity of the tracer toxin used to identify 'new' terminals (Tong et al., 1999;Bao et al., 2002;Shehab et al., 2003;Shehab, 2009). C-fibres that do not normally transport cholera toxin B (CTb), taken up exclusively by A-fibres, do so after injury, and it is these C-fibre terminals that are labeled in lamina II (Tong et al., 1999). If CTb labeling is applied to the nerve before injury, some A-fibre sprouting does occur but it is much less pronounced than previously thought (Bao et al., 2002).

After multiple lumbar rhizotomies, the appearance of previously unresponsive neurones in the deafferented dorsal horn appear suggesting 'unmasking' of exsisting connections may also be a structural change associated with deafferentation and perhaps neuropathic pain (Basbaum and Wall, 1976). Disinhibition and loss of GABAergic and glycinergic inhibitory currents, possibly through excitotoxic cell death of interneurones (Scholz et al., 2005) although controversial (Polgar et al., 2003;Polgar et al., 2004;Polgar et al., 2005;Polgar and Todd, 2008) may also lead disinhibition and central sensitization. Primary afferents themselves can provide the dorsal horn with an inhibitory influence (Woolf and Wall, 1982;Woolf, 1983), and this can undergo a disinhibition after injury. Primary afferent terminals are known to send inhibitory collateral terminal branches to other primary afferent terminals, and can be 'primed', by a conditioning stimulus, to inhibit the response of primary afferents to a proceding stimulus through 'habituation'. This is A-fibre mediated inhibition of nociceptive C-fibre terminals (Woolf and Wall, 1982), but can also occur from C-fibres (Woolf, 1983). After sciatic nerve section in the rat, this A-fibre-mediated C-fibre inhibition is diminished at 7-14 days, even though afferent volleys from these transected axons can still be evoked (Woolf and Wall, 1982). This suggests another mode of synaptic reorganisation in response to nerve injury, which could exacerbate the symptoms of neuropathic pain through loss of dorsal horn inhibitory tone.

Sympathetic sprouting within the dorsal root ganglia may also occur (McLachlan et al., 1993), appearing as basket-like structures around large-diameter axotomised sensory neurones, and hypothesized to be the cause of some neuropathic pain states. Sympathetic sprouting has been shown after L5/L6 ligation linked with the development and maintanence of mechanical allodynia, as sympathectomy abolishes symptoms

(Chung et al., 1996). It is activity dependent, initiated by ectopic discharges of injured neurones (Dong et al., 2002) as well as intact neurones, as spared DRGs adjacent to spinal nerve ligated DRGs have also shown increased alpha-adrenergic sensitivity (Ali et al., 1999). Wallerian degeneration is also causally linked to sympathetic sprouting, and if both are purposefully delayed by genetic modification in mice (C57B1/wld) both CCI-induced mechanical allodynia and thermal hyperalgesia are attenuated (Ramer et al., 1997). Sympathetic sprouting contributes clinically to a condition known as complex regional pain syndrome (Seltzer and Shir, 1991), charaterised by severe pain, as well as autonomic changes such as swelling in the skin, vasospasm, and rapid nail and hair growth.

Phenotypic changes occur within the peripheral nervous system following injury. These changes in transcription lead to alterations in membrane properties, growth, excitability and transmission (Woolf, 2004;Latremoliere and Woolf, 2009). A-fibres start to express peptides characteristic of nociceptors such as substance P (SP) brain-derived neurotrophic factor (BDNF), neuropeptide Y (NPY), and galanin. BDNF is known to be a potent neuromodulator of pain, and is synthesised by small-medium sized, CGRP-+ve DRGs, within the cell body and transported to the terminals in the dorsal horn, where it is released into the dorsal horn, sensitizing neurones (Obata and Noguchi, 2006). BDNF is upregulated in medium-large diameter neurones of the injured DRG after L5 DRR and L5 VRR, and maintained up to 7-14 days, but do not show neuropathic pain behaviour (Ernfors et al., 1993;Li et al., 2006;Obata et al., 2006b). BDNF is also upregulated in both the intact L4 DRG, and injured L5 DRG, up to 28 days after selective L5 spinal nerve ligation (Fukuoka et al., 2001;Obata et al., 2006b). However, no such upregulation is found in the L4 DRG after L5 rhizotomy (Obata et al., 2006b). This suggests Wallerian degeneration in the injured nerve (absent in rhizotomy), and interaction with intact fibres within the mixed nerve, is necessary for BDNF upregulation in the intact adjacent DRG, and corresponding anterograde transport to the dorsal horn.

BDNF is also upregulated up to 28 days in the injured L4 and L5 DRG after sciatic nerve transection, coexpressed with NPY (Michael et al., 1999). NPY is not normally present in adult naïve DRG but is present in the dorsal horn with especially dense concentrations in the superficial laminae (Hokfelt et al., 2007). NPY is upregulated in

large sized myelinated neurones and in the deep dorsal horn 7-14 days after nerve injury (Wakisaka et al., 1991;Noguchi et al., 1993). NPY is released by primary afferent terminals and has pre- and post-synaptic receptor targets in the dorsal horn. The Y1 receptor can be found on primary afferent terminals and on excitatory interneurones, and activate potassium channels, thereby attenuating excitatory transmission and exerting anti-nociceptive effects (Hokfelt et al., 2007). Indeed YR1-/- mice show exaggerated evoked behavioural nociceptive responses (Hokfelt et al., 2007;Wiley et al., 2009). However, NPY also has Y2 receptors on small nociceptive primary afferents, which are upregulated in cells of all sizes after axotomy (Zheng et al., 1997), and may mediate some aspects of neuropathic pain through enhanced neuronal excitability (Abdulla and Smith, 1999;Hokfelt et al., 2007). NPY-/- mice show exaggerated spontaneous pain behaviour (autotomy) after sciatic nerve transection, although there is no difference in evoked behavioural responses from wild-type (Shi et al., 1998).

Galanin expressed in DRG and dorsal horn interneurones (Liu and Hokfelt, 2002) is also upregulated in a mixed population of DRG neurones after sciatic nerve injury (Noguchi et al., 1993), and similarly to NPY has opposing actions on pain processing depending on which receptor (GAL1 or GAL2) is activated. Upregulation of galanin in DRGs after nerve injury may result in anti-nociceptive effects in the dorsal horn via inhibitory GAL1 receptors on dorsal horn neurones, and pro-nociceptive effects via excitatory GAL2 receptors on primary afferent terminals (Liu and Hokfelt, 2002). However after nerve injury the GAL1R is downregulated, but the GAL2R less so and galanin is over expressed, perhaps shifting this balance toward pro-nociception (Liu and Hokfelt, 2002). GAL1R-/- mice do show increased evoked behavioural nociception and neuropathic pain (Wiesenfeld-Hallin et al., 2005). However the main role of galanin may well be neuroprotection and neuroregeneration after nerve injury, as GAL-/- mice show increased cell death after nerve injury, in specifically nociceptive populations of DRG neurones (Holmes et al., 2005).

Receptor expression changes also occur after nerve injury and may underlie some neuropathic pain states. The transient receptor potential channel TRPV1, previously know as vanilloid receptor 1 (VR1) is expressed primarily in small diameter sensory nociceptors and is known to drive peripherally generated thermal hyperalgesia in inflammatory injury models (Ji et al., 2002). It is upregulated by NGF-driven activation

of p38 MAPK (Ji et al., 2002) in mainly uninjured A-fibre, but also uninjured C-fibre, DRG neurones after spinal nerve injury (Hudson et al., 2001;Fukuoka et al., 2002), and partial sciatic nerve ligation (Hudson et al., 2001;Ma et al., 2008) as well as in the pre-synaptic membrane of the dorsal horn after peripheral inflammation (Luo et al., 2004), coinciding with neuropathic pain behaviour to thermal stimulation. This 'spared nerve' TRPV1 upregulation in A-fibres could be responsible for thermal allodynia, and upregulation in C-fibres responsible for thermal hyperalgesia. The receptor is downregulated in all injured DRG neurones after spinal nerve injury (Hudson et al., 2001;Fukuoka et al., 2002), sciatic nerve injury (Hudson et al., 2001;Staaf et al., 2009), and axotomy (Michael and Priestley, 1999;Hudson et al., 2001), suggesting expression is dependent apon peripheral connectivity. The purinergic receptor P2X3 is coexpressed with the TRPV1 receptor on small nociceptive primary afferents in the DRG and terminals of the dorsal horn (Wirkner et al., 2007). It is upregulated after chronic constriction injury to the sciatic nerve (Novakovic et al., 1999), but are downregulated after axotomy and rhizotomy in 50% of neurones (Bradbury et al., 1998), with a subset of small and large DRG remaining P2X3 positive, that likely provide the P2X3r-mediated component of neuropathic pain (Kage et al., 2002). Prostaglandin receptors (EP1 and EP4) have also been shown to upregulated in the injured DRG after partial sciatic nerve ligation alongside TRPV1, and correlates with neuropathic pain, and both expression and pain can be ameliorated with a selective COX2 inhibitor (Ma et al., 2008).

Recent studies have focused on the role of neurotrophins in the pathophysiology of neuropathic pain. Hyperalgesia to noxious cold has been observed in GFRα2-/- mice, alongside a 70% reduction in non-peptidergic cutaneous nerve endings (Lindfors et al., 2006), suggesting a role for GDNF in the maintenance of nociceptor subpopulations. Also, intrathecal administration of NGF lowers nociceptor thresholds in naïve animals (Ramer et al., 2003). However, intrathecal administration of GDNF does not alter nociceptive thresholds (Ramer et al., 2003). Alternatively, when administered subcutaneously, GDNF, along with neurturin (NTN) and artemin (ART) (Malin et al., 2006) each cause peripheral TRPV1 sensitisation and acute thermal hyperalgesia, suggesting some neurotrophins may have distinctly different roles centrally compared to peripherally.

Changes in non-neuronal populations such as satellite glial cells and macrophages within the DRG have been shown after nerve injury (Hu et al., 2007) and could also mediate neuropathic pain behaviour. GFAP positive satellite cells of the DRG have been shown to react to peripheral nerve injury or inflammation, by activation, proliferation, and release of mediators, and increased gap junction coupling that contribute to pain (Woodham et al., 1989;Dublin and Hanani, 2007;Xie et al., 2009). Following sciatic nerve crush or transection or DRG compression, a perineuronal satellite cell reaction in injured DRGs can be seen after 3 days (Woodham et al., 1989) and up to 7 days (Fenzi et al., 2001), that decreases sharply at 10 and 21 days but staying above control levels (Zhang et al., 2009). When quantified, 88% of neurones in the injured ganglia expressed GFAP perineuronally compared to 15% in the contralateral (Woodham et al., 1989). Ectopic sensory neurone activity after injury, with increases in levels of neuronal growth factors, has been implicated as a mechanism by which satellite cells become activated (Xie et al., 2009), and blocking sodium channel activity with TTX reduces both GFAP and NGF expression in DRG after SNL (Xie et al., 2009). CCI or transection of the sciatic nerve leads to robust macrophage infiltration around neuronal soma in the DRG (Hu et al., 2007), and mechanical and thermal hyperalgesia. The low affinity neurotrophic receptor p75 is upregulated in glia within the DRG after PNI, in close association with sympathetic nerve sprouts (Zhou et al., 1996), and cutaneous neurones (Hu and McLachlan, 2003), suggesting glial synathesis of p75 might be another mechanism of control of sympathetic sprouting, neuronal ectopic activity and neuropathic pain.

Post-synaptically

Activation of NMDA receptors within dorsal horn neurones, in response to enhanced and prolonged peripheral stimulation and pre-synaptic glutamate release is the most well know mechanism of central sensitisation. The process involves increased pre-synaptic activity, excess neurotransmitter release, maintained activation of AMPA receptors, increased post synaptic sodium influx and maintained depolarisation, voltage-dependent removal of a magnesium ion block in the NMDA channel, prolonged calcium influx through the NMDA channel, phosphorylation of the NMDA receptor via PKC, and maintained channel opening via calmodulin-dependent PKII (CaMKII) leading to dorsal horn neuronal hyperexcitation (Petrenko et al., 2003b). Postsynaptic

changes in specific subunit expression occurs in response to nerve injury; for example, the NR2A subunit expression is reduced in the dorsal horn after PNI and joint inflammation, increasing the contribution of the NR2B subunit in neuronal activity (Karlsson et al., 2002). This may play a role in neuronal hyperexcitability as NR2B shows greater sensitivity to glutamate (Karlsson et al., 2002). However, knock-out mice lacking NR2A still present similar evoked withdrawal thresholds at baseline, and after sham, PNI, and formalin injection injuries (Petrenko et al., 2003a), with the authors suggesting a developmental compensatory mechanisms from other channels may be occurring. Sodium channel subunit expression, specifically NaV1.3, has been shown to be increased in dorsal horn neurones after SCI (Hains et al., 2003a), and PNI (Hains et al., 2004) with corresponding generation of neuropathic pain behaviours. Pain is thought to be due to the increase in persistent sodium ramp currents in the dorsal horn (Lampert et al., 2006). As stated previously, delayed anti-sense knock-down of NaV1.3 reverses pain behaviours induced by PNI and SCI (Hains et al., 2003a;Hains et al., 2004), but global or nociceptive specific NaV1.3 deletion during embryo development shows no change in neuropathic phenotype upon injury (Nassar et al., 2006), leaving the relative significance of NaV1.3, as well as NR2B, as a major contributor of dorsal horn excitability and neuropathic pain, uncertain.

Similar to its generation and release from primary afferents, BDNF is also generated and released from microglia after activation via ATP-P_2X_4r signaling after PNI (Coull et al., 2005;Milligan and Watkins, 2009), coinciding with the generation of allodynic behaviour. BDNF acts on neurones by causing a membrane depolarization shift, and reversal of GABAergic currents in lamina I dorsal horn neurones into excitatory (Coull et al., 2005), intensifying central sensitization (Lu et al., 2007). This 'disinhibition' may occur through reduction in expression of Cl^--cotransporter K^+-Cl^- exporter 2 channels (KCC2) after both PNI (Coull et al., 2003) and SCI (Lu et al., 2008), that are responsible for driving chloride ions out of cells, causing normally subthreshold A and C inputs to evoke action potentials from superficial dorsal horn neurones, some of which could be nociceptive. Another mechanism of disinhibition may occur from loss of the descending opioid system (Zimmermann, 2001). For example, 4 months after dorsal root rhizotomy a 60% reduction in μ- and δ-opioid receptor binding sites occurred in the dorsal horn (Zajac et al., 1989), and the incidence of autotomy in rats after sciatic nerve section was correlated with decreased β-endorphins in the brain and

spinal cord (Panerai et al., 1987). Further, the spontaneous activity of the dorsal horn neurones of rats with multiple dorsal rhizotomies were far less sensitive to systemic morphine administration than arthritic rats (Lombard and Besson, 1989), suggesting a deafferentation neuropathy reduces opioid sensitivity in dorsal horn neurones. These results can be explained by location studies of the μ- and δ-opioid receptor binding sites, indicating 75% of which are located pre-synaptically on C-fibre terminals (Dickenson and Suzuki, 2005), and will be lost after deafferentation. A more direct loss of inhibitory tone can occur through death of GABAergic neurones or loss of GABA neurotransmitter, found after PNI (Ibuki et al., 1997;Moore et al., 2002) and SCI (Drew et al., 2004;Meisner et al., 2010).

Our understanding of pathological pain has primarily revolved around neuronal mechanisms. However more recently the involvement of spinal cord glia in central sensitization has come to light. Astrocytes and microglia have recently been recognized as powerful modulators of pain in PNI and SCI (Raghavendra et al., 2003;McMahon et al., 2005;Nesic et al., 2005;Hains and Waxman, 2006;Crown et al., 2008;Hulsebosch et al., 2009;Milligan and Watkins, 2009). Increased pre-synaptic firing in the dorsal horn after PNI, and neuronal loss in central nervous system injury within the spinal cord, leads to release of ATP, fractalkine (CX3CL1), heat shock proteins, substance P, glutamate, reactive oxygen species (ROS), cysteine-cysteine chemokine ligand 21 (CCL21), monocyte chemoattractant protein 1 (MCP-1/CCL2) (Zhang and De, 2006;Thacker et al., 2009), and many other mediators from neurones (McMahon et al., 2005;Marchand et al., 2005). This in turn results in microglial activation through the calcium-sensitive p38 MAP Kinase - CREB phosphorylation pathways via extensive neuronal-glial interactions (Tikka et al., 2001;Crown et al., 2008;Hulsebosch, 2008;Inoue and Tsuda, 2009). This intra-cellular signalling leads to surface expression of MHC class II molecules and activation of complement type receptors (e.g. CX3CR1) on the microglial cell membranes, which corresponds with a distinct change in morphology and phenotype (Popovich et al., 1997). Inhibition of this MAP Kinase phosphorylation pathway attenuates hypersensitivity post SCI (Crown et al., 2008). These neuronal-glial interactions involve such receptors as CX3CR1 (fractalkine receptor) (Milligan et al., 2004), CCR2 (CCL2 receptor), CXCR3 (MCP-1/CCL2 low affinity receptor) (Murphy et al., 2000), ATP receptors (Tsuda et al., 2003;Tsuda et al., 2005;Tsuda and Inoue, 2007), Toll-like receptors (specifically TLR3 and 4) (Tanga et

al., 2005), and matrix metalloproteinase 9 (MMP9)/Pro-IL-1β cleavage (Kawasaki et al., 2008). Receptor activation leads to microglial cell proliferation (Narita et al., 2006), increase in membrane bound receptors, and cytokine production (Crown et al., 2006;Crown et al., 2008). One major pathway of microglial activation that has been studied is via the ATP receptor P_2X_4, located on the surface of microglia, and these receptors are upregulated after nerve injury (Ulmann et al., 2008). Pharmacological blockade of the P_2X_4 receptor (Tsuda et al., 2003) and P_2X_4-/- mice lack the mechanical and thermal hyperalgesia induced by PNI (Ulmann et al., 2008;Tsuda et al., 2009), but do not exibit major defects in nociceptive pain, suggesting a role of purinergic receptors in purely neuropathic pain. Upon activation microglia release neuronal mediators, such as BDNF and NO, that hyperexcite neurones, release ROS and TNF that can lead to apoptosis of neurones, and release of inflammatory cytokines, such as IL-1β, IL-6, and TNFα, that activate neurones as well as adjacent microglia through MAPK/ERK phosphorylation and CREB intracellular signaling (Hulsebosch et al., 2009). Microglia also synthesize and released prostaglandins that directly regulate signaling between themselves and neurones via EP2 receptors shown in spinal cord contused rats, and heighten dorsal horn neurone sensitivity (Zhao et al., 2007).

The role of astrocytes in neuropathic pain is less clear. They have been shown to have an involvement in ‘at-level’ neuropathic pain after SCI (Nesic et al., 2005), and are also activated by a milieu of mediators released from injured neurones and microglia and respond by phosphorylating, and thereby activating, p38 MAPK (Crown et al., 2008). However, astrocytes do not proliferate in response to nerve injury, unlike microglia (Narita et al., 2006). Also dorsal horn astrocyte activation is slower in onset than microglia; typically taking 4 days to become apparent after L5 spinal nerve transection, and increasing over 28 days (Tanga et al., 2004;Tanga et al., 2006), compared to microglial activation at 1 day and declining after 7 days after sciatic nerve transection (Eriksson et al., 1993), with mRNA of some microglial markers expressing as early as 4 hours post L5 spinal nerve transection (Raghavendra et al., 2003;Tanga et al., 2004), associated with the development of neuropathic pain behaviours. After PNI a delayed but prolonged MMP-2/IL-1β cleavage in astrocytes maintains their activation, and corresponding neuropathic pain, whereas MMP-9 IL-1β expression in microglia is only transient (Kawasaki et al., 2008). The difference in time of activation between these glia, have been implicated in a ‘microglia-astrocyte replacement mechanism’ that

maybe essential in the maintenance of neuropathic pain in PNI (Colburn et al., 1997;Raghavendra et al., 2003;Tanga et al., 2006) by mobilization of internal calcium, release of glutamate (via GLUT1), ATP release and enhancement of synaptic signaling (Wang et al., 2009). Indeed, inhibition of microglial activity pharmacologically with minocycline pre-emptively prevents the development of PNI-induced neuropathic pain behaviour, but post-emptively has no effect in reversing it (Raghavendra et al., 2003). There is still some debate, however, to the distinct roles of microglia and astrocytes, in central verses peripherally mediated neuropathic pain (Winkelstein and DeLeo, 2002;Hains and Waxman, 2006), as well as 'at-level' and 'below-level' SCI-induced neuropathic pain (Crown et al., 2008;Gwak et al., 2009). Further, the extent of microglial reactivity has been shown to be linked to the severity of neuronal injury whereas, this is not the case for astrocytes, such that more severe nerve and root ligations produce greater dorsal horn microglial activity (Winkelstein and DeLeo, 2002), and neuropathic pain behaviour (Winkelstein et al., 2001b).

Clear role differences between microglia in the initiation of hypersensitivity after PNI, and astrocytes in the maintenance role in the longer term are not so easily defined in centrally mediated pain. For example, one month after SCI, activated microglia in the superficial and deep dorsal horn essentially control the generation and development of chronic pain, as defined behaviourally and electrophysiologically (Hains and Waxman, 2006)(Hains and Waxman, 2006), in conjunction with astrocytes (Hains and Waxman, 2006;Gwak and Hulsebosch, 2009). This is in direct comparison to the decline in microglial activity at 1 week post PNI (Eriksson et al., 1993), with a delayed but prolonged astrocyte activity (Tanga et al., 2006) maintaining neuronal hypersensitivity up to 11 days (Raghavendra et al., 2003). This is an important finding when considering brachial plexus preganglionic injuries can induce Brown-Sequard syndromes (traumatic disruption of ipsilateral spinal cord) in the avulsed segment (Stephen et al., 1997;Nordin and Sinisi, 2009). If root avulsion occurs at or within the DREZ, this may manifest in distinctly different microglial activity than would occur after a more distal avulsion or peripheral rupture. Indeed DRA injury that causes trauma to the spinal cord, leads to maintained upregulation of both astrocytes and microglia immunoreactivity in the dorsal horn across 28 days (Chapter 3), similarly to SCI (Hains and Waxman, 2006), suggesting glial activity is mediated centrally after injury to CNS tissue. However DRR that causes no trauma to the spinal cord, leads to no further increase in microglial or

astrocyte activity beyond 14 days, and in many cases no neuropathic pain behaviour (Sukhotinsky et al., 2004). Colburn *et al.*, ((Colburn et al., 1997)) showed that DRR produced less dorsal horn gliosis than even PNI, suggesting glial activity in injury models where no CNS trauma occurs, may depend upon DRG connection.

The leukocytic immune system may also have an important role in pro-nociception and central sensitization after SCI (Trivedi et al., 2006) and PNI (Thacker et al., 2007). Macrophage, neutrophil, and T-lymphocyte cells populate the dorsal horn after PNI (Hu et al., 2007;Thacker et al., 2007), DRR (Ling, 1979b;Nomura et al., 2005), SCI (Popovich et al., 1997;Carlson et al., 1998), and brain stab injury (Ling, 1979a). This occurs through mobilization of local neuronal populations and infiltration from the blood. These cells release cytokines and key inflammatory mediators, such as IFNγ, IL1β and TNFα that can influence neuropathic pain behaviour by sensitizing neurones (Thacker et al., 2007). IL1β, for example, is released from immune cells through ATP-P_2X_7 receptor interaction, and receptor knock-out reduces IL1β production in mice, abolishing hypersensitivity to mechanical and thermal stimuli after partial nerve ligation (Chessell et al., 2005). IFNγ reduces GABAergic currents through IFNγ receptor activation in the superficial dorsal horn and lateral spinal nucleus, increasing nociceptive neuronal activity (Vikman et al., 1998;Vikman et al., 2003). TNFα induces neuronal hypersensitivity via intra-cellular signaling pathways including p38-MAPK and NFκβ through its membrane receptors p55 (TNFR1) and p75 (TNFR2), that are constitutively expressed in DRG, afferent terminals, and dorsal horn neurones of laminae I and II (Holmes et al., 2004). TNFα is upregulated within the DREZ and dorsal funiculus at 48hrs post DRR and DRA, colocalising with p38 MAPK positive activated macrophages (Nomura et al., 2005). TNFR1 and R2 are upregulated in neurones, astrocytes and oligodendrocytes of the spinal cord as early as 15 minutes, peaking at 8 hours, after SCI (Yan et al., 2003), and in satellite cells, astrocytes, and DRG neurones after PNI (Ohtori et al., 2004), contributing to TNFα-mediated neuropathic pain. TNFα is notoriously involved in neuropathic and inflammatory pain, but it also has an essential role in neuroprotection and growth via activation via TNFR2 and, conversely, cell death via TNF1 activation, during both development and injury (Kraft et al., 2009). Knocking out TNFαR1 reduces inflammation and tissue injury, but inhibition of TNFα reduces functional recovery, after SCI injury (Kim et al.,

2001;Demjen et al., 2004;Genovese et al., 2008), suggesting appropriate receptor targeting of the TNFα signaling pathway is necessary to optimize recovery and ameliorate neuropathic pain after injury.

Neutrophils are the earliest inflammatory cell to infiltrate, and dominates the acute tissue inflammation process, through phagocytosis and release of cytokines and lipoxygenase products that can induce hyperalgesia (Levine et al., 1985). Substantial neutrophil extravasation into the contused spinal cord peaks at 3 hours as measured by MPO (Taoka et al., 1997), and in the injured sciatic nerve peaks between 8 and 24 hours as measured by an antibody to neutrophils (Perkins and Tracey, 2000), and may be responsible for initiating hyperalgesia in these cases. Selective cytotoxic antibody-mediated depletion of neutrophils at the time of sciatic nerve injury delayed neutrophil infiltration into the injured nerve, and delayed thermal hyperalgesia development (Perkins and Tracey, 2000). Administration of the cytotoxic antibody, 8 days post sciatic nerve injury, had no effect on pre-existing hyperalgesia, indicating neutrophils are important early in hypersensitivity development (Perkins and Tracey, 2000). Neutrophils also summon macrophages into the damaged tissue through secretion of macrophage-inflammatory protein-1 and IL-1β (Trivedi et al., 2006), which largely take over the role of prolonged immunity. IL-69-ED2 positive macrophages (MHC class II-presenting macrophages) and CD3 positive T-lymphocytes have been shown to be recruited to the dorsal and ventral horn 14 days after spinal nerve transection correlating with mechanical allodynia (Sweitzer et al., 2002). Activated macrophages may be pro-nociceptive through the release of algesic mediators such as nitric oxide, PGs, and proinflammatory cytokines like TNFα, IL-1β, and IL-6, which sensitise primary afferents and dorsal horn neurones directly (Moalem and Tracey, 2006). Conversely, the application of activated macrophages alone to the exposed peripheral nerve does not induce mechanical allodynia, and blocking macrophage activation with an antibody or depleting systemic macrophages with clodondrate 2 days prior to L5 spinal nerve transection, did not attenuate mechanical allodynia (Rutkowski et al., 2000). Other authors using partial sciatic nerve ligation have shown clodronate treatment immediately after surgery, with a follow up does 2 days later, is effective at reducing macrophages and hyperalgesia (Liu et al., 2000b), and the differing results may well be due to different dosing regimes used. On the whole, these findings suggest leukocytes

may have a role in neuropathic pain generation and maintainence, but likely act in tandem with CNS macrophages/microglia.

4.1.4: Avulsion pain

Patient descriptions of traumatic root avulsion dyesthesias are remarkably consistent, and include extreme pain detectable as burning, aching, shooting, or crushing, that is unbearable and intractable, described as 'like putting your hand in a deep fat fryer', lasting in some cases decades (Parry, 1980;Birch, 1996;Berman et al., 1998). The majority of patients (80-91%) report severe chronic pain at some point in the course of their condition (Parry, 1980;Bonnard and Narakas, 1985;Bruxelle et al., 1988;Woolf, 2004;Bertelli and Ghizoni, 2008), and certain environmental influences such as differing weather conditions and local cooling (Parry, 1980) as well as stress and illness (Berman et al., 1996) can exacerbate these symptoms. Age is another influencing factor on outcome, with younger patients much less susceptible to chronic pain and showing greater functional recovery (Anand and Birch, 2002;Bertelli and Ghizoni, 2006), most likely as greater propensity for cortical plasticity (Carlstedt et al., 2009) and lower motor neurone regeneration (Carlstedt, 2008). Pain appears within 48 hours after injury (Berman et al., 1996), and no later than 1 month (Berman et al., 1998). The pain seems to be correlated to the extent of the avulsion, such that the greater the number of roots avulsed, the greater the pain (Birch, 1996;Berman et al., 1998). The pain is hypothesized to be due to damage to the dorsal horn and/or disinhibition of neurones within the substantia gelatinosa (Loeser and Ward, Jr., 1967) and deeper laminae (Ovelmen-Levitt et al., 1984) as shown in cat experiments. Another dyesthesia is evoked border-zone hypersensitivity to thermal and mechanical stimuli, which occurs across intact and deafferented dermatomes, that increases in severity over time, with 30% of patients complaining of symptoms at 6 months (Berman et al., 1998;Htut et al., 2006;Havton and Carlstedt, 2009). Hypersensitivity is also common in adjacent intact dermatomes (Finnerup et al., 2009). Interestingly, pain occurs after ventral root avulsion both clinically (Berman et al., 1998;Htut et al., 2006), and experimentally (Bigbee et al., 2007;Bigbee et al., 2008) with noticeable degeneration of primary afferent axons in the ipsilateral dorsal column. Quite unexpectedly the pain is ameliorated with early ventral root re-implantation (Berman et al., 1996;Berman et al., 1998;Carlstedt et al., 2004;Htut et al., 2006;Kato et al., 2006;Bigbee et al., 2007). The pain relief may be linked to re-

establishing peripheral neurotrophic support (through BDNF, GDNF, and NGF) to the spinal cord via the ventral root (Bergerot et al., 2004;Carlstedt, 2008), thereby reducing neuro-degenerative and gliotic phenomenon that occur in the dorsal horn (Bigbee et al., 2007). The authors state that Wallerian degeneration of avulsed motor axons still occurs even after ventral root re-implantation (Bigbee et al., 2008), suggesting pro-nociceptive and pro-inflammatory factors, released during axon degeneration within the peripheral nerve, are unlikely to be the cause of this pain. Therefore the more likely cause of the neuropathic pain, are central mechanisms in the spinal cord (Bigbee et al., 2008).

There is controversy in the literature however about the role of the avulsed root in avulsion pain. Certainly allodynia and hyperalgesia experienced in brachial plexus avulsed patients must occur through hyper-excitability of the intact dermatomal receptive fields (Htut et al., 2006). As previously mentioned adjacent intact, and injured, afferents may acquire abnormal activity, and the corresponding spinal segment may undergo anatomical re-organisation pre- and post-synaptically, leading to evoked pain behaviours. However spontaneous pain may also originate from the same mechanisms. Bertelli and Ghizoni ((Bertelli and Ghizoni, 2008)) showed that brachial plexus injured patients complained more of spontaneous neuropathic pain if a root and DRG in the plexus remained connected to the spinal cord. Patients that had total pre-ganglionic brachial plexus avulsion had only minimal complaints of pain. This suggests that peripheral ectopic activity from the DRGs or neuroma from roots that are either avulsed post-ganglionically (a PNI), or remain intact, may also drive the spontaneous neuropathic pain in these patients, as well as central disinhibition (Loeser et al., 1968). When an anesthetic block was applied to these intact roots of brachial plexus avulsion patients, pain was ameliorated (Bertelli and Ghizoni, 2008). Alternatively if the post-ganglionically avulsed nerve was repaired through nerve grafting, then again the pain was ameliorated (Bertelli and Ghizoni, 2008). The authors suggested therefore that avulsion pain is actually mediated through DRG-intact roots and spinal segment, rather than from the directly avulsed dorsal horns (Bertelli and Ghizoni, 2008), and this is certainly the cause for evoked hypersensitivity in the adjacent intact dermatomes (Finnerup et al., 2009).

What is clear from the clinical literature (Berman et al., 1998) is that there is a need for improved modeling of neuropathic root avulsion pain. When patients present to the

clinic, immediate treatment is required and it is unethical to withhold treatment for experimental sake or provide control groups in clinical trials, as it is well known that surgical intervention after root avulsion is beneficial (Birch, 1993). From recent clinical data (Bertelli and Ghizoni, 2008) it may also be important to clearly separate studies into pre-ganglionic avulsion (proximal to the DRG) nerve-transfer and post ganglionic avulsion (distal to DRG, PNI) nerve-grafting repair. However this is clearly difficult as most patients present a mixture of preganglionic and postganglionic avulsions after brachial plexus injury (Anand and Birch, 2002;Carlstedt, 2008), and they are repaired in different ways (Berman et al., 1998;Bertelli and Ghizoni, 2008). This clinical limitation may not allow for a clear understanding of the data when defining the mechanism of avulsion induced pain as separate from PNI.

4.1.5: Modelling avulsion pain

Spontaneous pain that manifests after avulsion injury is particularly difficult to model in animals, as definition relies on patient descriptions in a verbal analogue scale, or the 'McGill Pain Questionaire' (Berman et al., 1998;Htut et al., 2006). Typically, in animal models after multiple root avulsion there is a loss of sensation in the affected limb that cannot be tested for by evoked behaviour. Semi quantitative methods for analysis of spontaneous pain *in vivo* have been used such as spontaneous foot lifting (Bennett and Xie, 1988;Djouhri et al., 2006), autotomy (Wall et al., 1979), ultrasound vocalization (Sakurada et al., 2007), nocifensive hindpaw behaviours (Kim and Chung, 1992;Choi et al., 1994;Kurvers et al., 1997;Roussy et al., 2009), and weight loss (Kurvers et al., 1997). As previously stated some models of ventral root rhizotomy have lead to evoked hyperalgesia and allodynia (Yoon et al., 1996;Sheth et al., 2002;Li et al., 2003), however others have not (Colburn et al., 1999). DRR is also unreliable (Yoon et al., 1996;Sheth et al., 2002;Sukhotinsky et al., 2004). Avulsion of the L6-S1 ventral root causes neuropathic pain behaviour, and neurodegenerative and inflammatory responses in the dorsal columns of the adjacent L5 segment (Bigbee et al., 2007). Another group has modeled a unilateral brachial plexus avulsion combined with assessment of hind paw evoked behavioural testing in rats (Rodrigues-Filho et al., 2003) and mice (Quintao et al., 2006), and acknowledged a below-level hypersensitivity to mechanical and cold stimuli occurring bilaterally that could be ameliorated with pharmacological

manipulation (Rodrigues-Filho et al., 2004). However, this ‘alternative limb pain’ is not noted in clinical literature of brachial or lumbosacral plexus avulsion.

No literature to date has determined the effect of avulsion of dorsal roots on the evoked responses in the adjacent dermatome, as well as analyzing to correlate the neuroinflammatory and neurodegenerative effects in the adjacent dorsal horn. This may be a critical gap in literature as more than 80% of brachial plexus avulsions have some intact roots (Sindou et al., 2005) and as mentioned before recent clinical evidence suggests the involvement of the adjacent intact DRG and spinal segment in certain modalities of deafferentation pain (Bertelli and Ghizoni, 2008). A new model developed in the laboratory (adapted from (He et al., 2000)) involves a single L5 spinal root avulsion. As the rat hindpaw is primarily innervated by L4 and L5 mainly (Takahashi et al., 2003), the surgery allows for testing of the L4/L5 border zone. This model is also more clinically representable, as there is no laminectomy exposure, including disruption of the dura, is required to access the roots. Indeed the laminectomy procedure has been shown recently to produce hyperalgesia (Kosta et al., 2009). The traction force on the mixed spinal root using this model will result in direct injury to the both the DRG and root, as well as the cord, better representing the clinical scenario, than previous models of DRA and DRR. In addition weight loss, an indicator of spontaneous pain, will be recorded, as well as any motor impairment and motor neurone loss accompanying the injury.

4.1.6: Possible mechanisms of avulsion pain:

There are major differences in dorsal horn histopathology between the deafferentation models of root rhizotomy and PNI, compared to true avulsion, which may underly the inconsistent and generally less severe neuropathic pain generation noted in the former (Yoon et al., 1996;Song et al., 2003;Sukhotinsky et al., 2004). For example DRR is a poor model for root avulsion with respect to the amount of cell death (Chew et al., 2008), neuroinflammation, and vascular deterioration (Chapter 3). Clinically root avulsion patients complain of excrutiating intractable pain (Parry, 1980;Berman et al., 1998) whereas rhizomtomy alleviates PNI-pain (Loeser, 1972;Gybels and Sweet, 1989). c-Fos immunoreactivity, an indirect marker of neuronal hyperactivity, is expressed in far greater quantity in the dorsal horn of root avulsed rats than nerve transected rats

(Zhao et al., 1998). Mechanical allodynia initiated by dorsal and ventral root ligation surgery is less effectively alleviated by pharmacotherapy than PNI-induced evoked pain (Winkelstein et al., 2001a). In patients 5% of PNI cases result in chronic pain, compared to 80% in brachial plexus avulsion (Bertelli and Ghizoni, 2008), and sustained long-term disability and pain was more prominent in patients with root avulsion compared to PNI (Novak et al., 2009). These differences are likely due to different basic anatomical features such as, DRG-dorsal horn connection (Winkelstein et al., 2001a), as well as central effects in the dorsal horn such as dorsal horn hyperexcitability (Ovelmen-Levitt et al., 1984) and direct damage to the spinal cord (Berman et al., 1996;Stephen et al., 1997) after avulsion. For example, maintenance of central sensitivity cannot be driven by ectopic firing of preganglionic deafferented roots, such as suggested for PNI, as DRG cell bodies are disconnected from the dorsal horn. Also Wallerian degeneration of the transected peripheral nerves may contribute to sensitization of intact adjacent fibres either at the level of the nerve, DRG, or the peripheral endings. However, after dorsal root injury, Wallerian degeneration occurs from the root stump up the dorsal columns in rats (George and Griffin, 1994b) and humans (Endo et al., 2009), begining *in vivo* after 1 day and becoming prominent at 7 days (Wroblewski et al., 2000). Retrograde Wallerian degeneration or loss of DRG neurones in the distal part of the nerve does not occur after DRA or DRR at least by 14 days (Chew et al., 2008) most likely because the neurones still maintain peripherally mediated trophic support. This suggests that peripherally mediated sensitization of adjacent uninjured nerve fibres does not occur, and is not responsible for central sensitisation.

It is not surprising that specific mechanisms of neuropathic pain in spinal root injuries are not well understood due to a complex etiology of peripheral and central injured components (Berman et al., 1998;Anand and Birch, 2002;Bertelli and Ghizoni, 2008). It is suggested that loss of inhibition of large sensory A-fibers after dorsal root damage may result in the deafferentation of nociception-transmitting neurons in the dorsal horn, and thus produce neuronal hyperactivity, hypersensitivity and abnormal spontaneous discharges with intermittent bursts of high-frequency activities (Loeser and Ward, Jr., 1967;Loeser et al., 1968;Ovelmen-Levitt et al., 1984;Ovelmen-Levitt, 1988). Pre-clinical research of brachial plexus injury models suggested the opioid endorphin system had a reduced sensitivity in a deafferented animal (Lombard and Besson, 1989), with a drastically (60%) reduced opioid receptor binding sites in the dorsal horn 4

months after DRR (Zajac et al., 1989). Recently some cellular mechanisms have been implicated in rat models of brachial plexus avulsion pain, including roles for upregulation of systemic TNFα (Quintao et al., 2006), neurotrophic factors, especially BDNF (Obata et al., 2006b;Obata and Noguchi, 2006;Quintao et al., 2008b), upregulation of central and peripheral bradykinin (B1 and B2) receptor levels (Quintao et al., 2008a) as well as cortical reorganization and CNS plasticity (Carlstedt, 2008;Carlstedt et al., 2009).

The previous chapter described glial activity, neurodegeneration, vascular degeneration, leukocyte infiltration, and cell death effects within the dorsal horn after L3-L6 dorsal root avulsion and suggested that these may contribute to the development of deafferentation pain. This chapter will attempt to corroborate these effects in a spared root avulsion model (L5 SRA) with behavioural changes indicative of neuropathic pain.

4.1.7: Aims

- The primary aim of this chapter is to determine whether hypersensitivity to stimulation can be evoked across the L4/L5 borderzone after single spinal root avulsion. More specifically it is important to establish when hypersensitivity occurs, and what type of stimulus (mechanical or thermal) can evoke this, and its duration. A surrogate measure of spontaneous pain, weight reduction, will be assessed. Motor impairment after L5 SRA will also be assessed.

- To determine the potential mechanisms of avulsion induced hypersensitivity, histology of the intact DRG should provide evidence on whether there are peripheral components including glial activity (GFAP), evidence of injury (ATF3), phenotypic change to subpopulations (CGRP, N52, and IB4), and upregulation of receptors known to be involved in evoked hypersensitivity (TRPV1). Similar histological approaches implemented in chapter 3 will be used assess central mechanisms of injury within the L4 and L5 segments of the spinal cord across 14 days. This includes glial activity (IBA1, GFAP), neuronal loss (NeuN, Tol Blue), macrophage activity (ED1), and vascular disruption (RECA-1).

4.2: Results

4.2.1: Acute behavioural effects of L5 SRA across 14 days

4.2.1.1: Motor incoordination

One day after L5 SRA, rats were able to locomote the ipsilateral limb, in a similar range of motion to sham and naïve rats, and were able to walk across the horizontal ladder. The contralateral limb was not assessed.

Total number of incorrect steps:
Naïve and sham animals presented few misplaced ipsilateral steps on the ladder rungs across 14 days, and this was not significantly different from baseline (Fig 4.1).

Across the horizontal ladder the SRA group made a significant number of incorrect paw placements (as defined in the methods) against sham and naïve levels, such that >60% of steps were misplaced on day 1 post injury (Fig 4.1). This incorrect plantar placement was maintained throughout the 14 day trial against sham, naïve and baseline values (Fig 4.1). This method of assessing plantar misplacement provided evidence for locomotor impairment after SRA, but did not assess the level of severity of the plantar deficit.

Foot fault score:
Naïve and sham animals had an average foot fault score of 1, suggesting normal plantar placement across 14 days, and this was not significantly different from baseline at any time point (Fig 4.2).

When scoring each of the misplaced ipsilateral paw steps for level of severity, rats that underwent L5 SRA had a mean misplaced ipsilateral step that was category 2 or below (see methods) (Fig 4.2). This refers to a mid-plantar placement without toe curl around the rung, the mildest foot fault on the score. Rarely did the SRA rats completely miss the rung or slip from the rung. This foot fault score was maintained across 14 days, did not increase in severity, and at every day measured, was significantly more severe than naïve and sham (Fig 4.2).

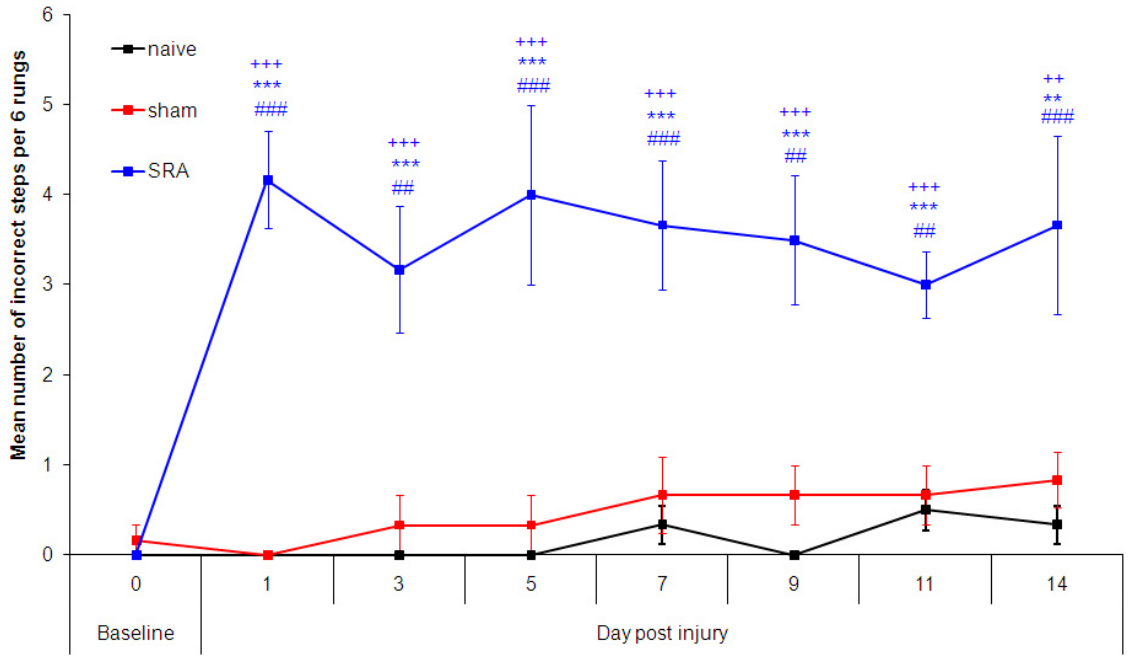

Figure 4.1: Mean number of foot faults across 6 rungs. From day 1 SRA rats develop an ipsilateral incorrect plantar paw placement across the rung. No change is detected with sham or naïve. Comparison against baseline (#), ipsilateral vs contralateral **(x)**, injury vs naïve **(*)**, and injury vs sham **(+)** are shown above respective data point. N=6 in each group.

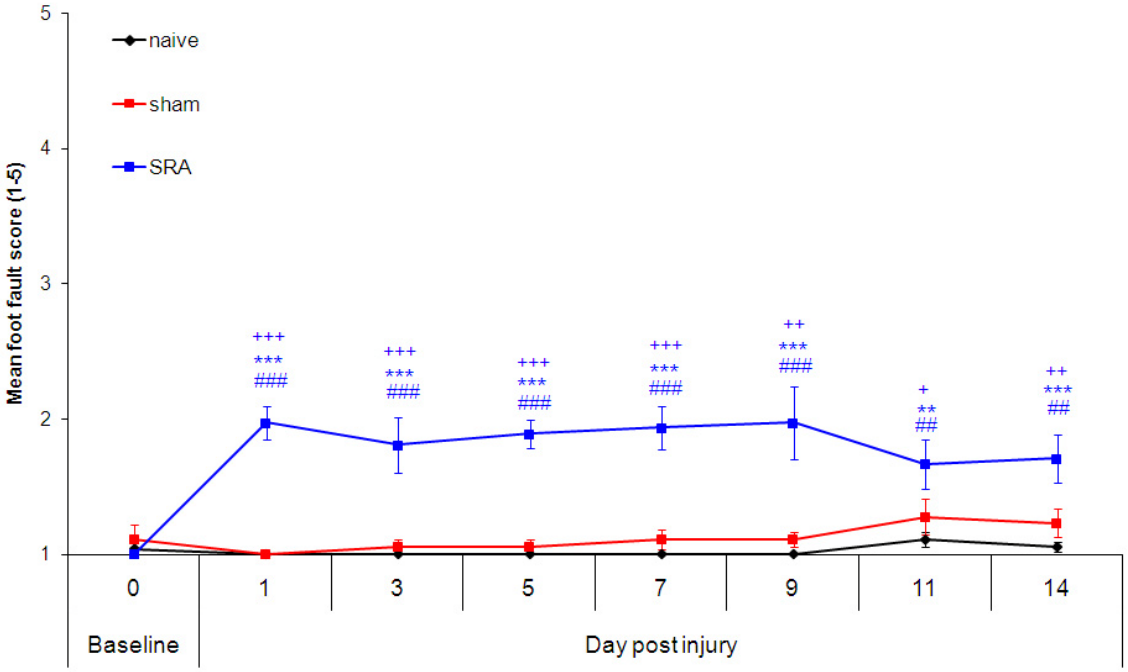

Figure 4.2: Severity of foot fault placement across 6 rungs. From day 1 SRA rats develop an inability to accurately perform plantar placement, such that mid-plantar placement without toe curl takes place on the majority of the rungs. Across 14 days no change occurs in the severity of misplaced plantar placement. No change is detected with sham or naïve. Comparison against baseline (#), ipsilateral vs contralateral **(x)**, injury vs naïve **(*)**, and injury vs sham **(+)** are shown above respective data point. N=6 in each group.

4.2.1.2: Sensory deficits

Thermal:

After 14 days of acclimatisation all rats withdrew from thermal stimulus with latency of between 7.91s (+/-0.11) and 8.30s (+/-0.24), with no significant difference between groups or paw side (Fig 4.3). Across 14 days no change in withdrawal latency occurred in naïve or sham rats against baseline or contralateral paw (Fig 4.3A and 4.3B).

After L5 SRA rats showed significant reduction in withdrawal latency against baseline values at 5, 7, 11, and 14 days (Fig 4.3D), against contralateral values at 7, 11, and 14 days (Fig 4.3C), against naive values at 3, 5, 7, 11, and 14 days (Fig 4.3D), and against sham values at 11 and 14 days (Fig 4.3D). At 14 days SRA rats showed mean withdrawal latency to thermal stimulation of 6.05s (+/-0.22) ipsilaterally, significantly less when compared to naïve [8.00s (+/-0.11)] and sham [7.57s (+/-0.17)] (Fig 4.3D).

Mechanical:

After 14 days of acclimatisation all three groups of rats bilaterally withdrew from tactile stimulation between 25.4g (+/-0.41) and 26.9g (+/-1.79), with no significant difference between groups or paw side (Fig 4.4). Across 14 days no change in withdrawal threshold occurred in naïve rats against baseline or contralateral paw (Fig 4.4A). Sham rats showed significant hypersensitivity development from 5 days maintained up to 11 days compared to naïve and baseline values (Fig 4.4D). Only at 5 days was ipsilateral significantly less than contralateral withdrawal thresholds (Fig 4.4B).

One day after L5 SRA a reduction in ipsilateral withdrawal threshold was significant from baseline, sham, and contralateral values (Fig 4.4C and 4.4D). Loss of significance from contralateral and sham values was noted at 3 days for ipsilateral SRA (Fig 4.4C and 4.4D). At 5 days [15.5g (+/-0.87)] significant difference returned, compared to contralateral [21.5g (+/-1.41)] (Fig 4.4C), naïve [25.9g (+/-0.98)] (Fig 4.4D), and baseline [25.4g (+/-0.41)] (Fig 4.4D) values. Between 5 and 14 days SRA rats showed increasingly pronounced reduction in withdrawal thresholds against all groups compared (Fig 4.4C and 4.4D). At 14 days SRA rats had a mean ipsilateral withdrawal threshold of 10.9g (+/-1.84) compared to naïve [25.2g (+/-0.86)], and sham [25.9g (+/-1.57)] (Fig 4.4D), and contralateral [25.3g (+/-1.61)].

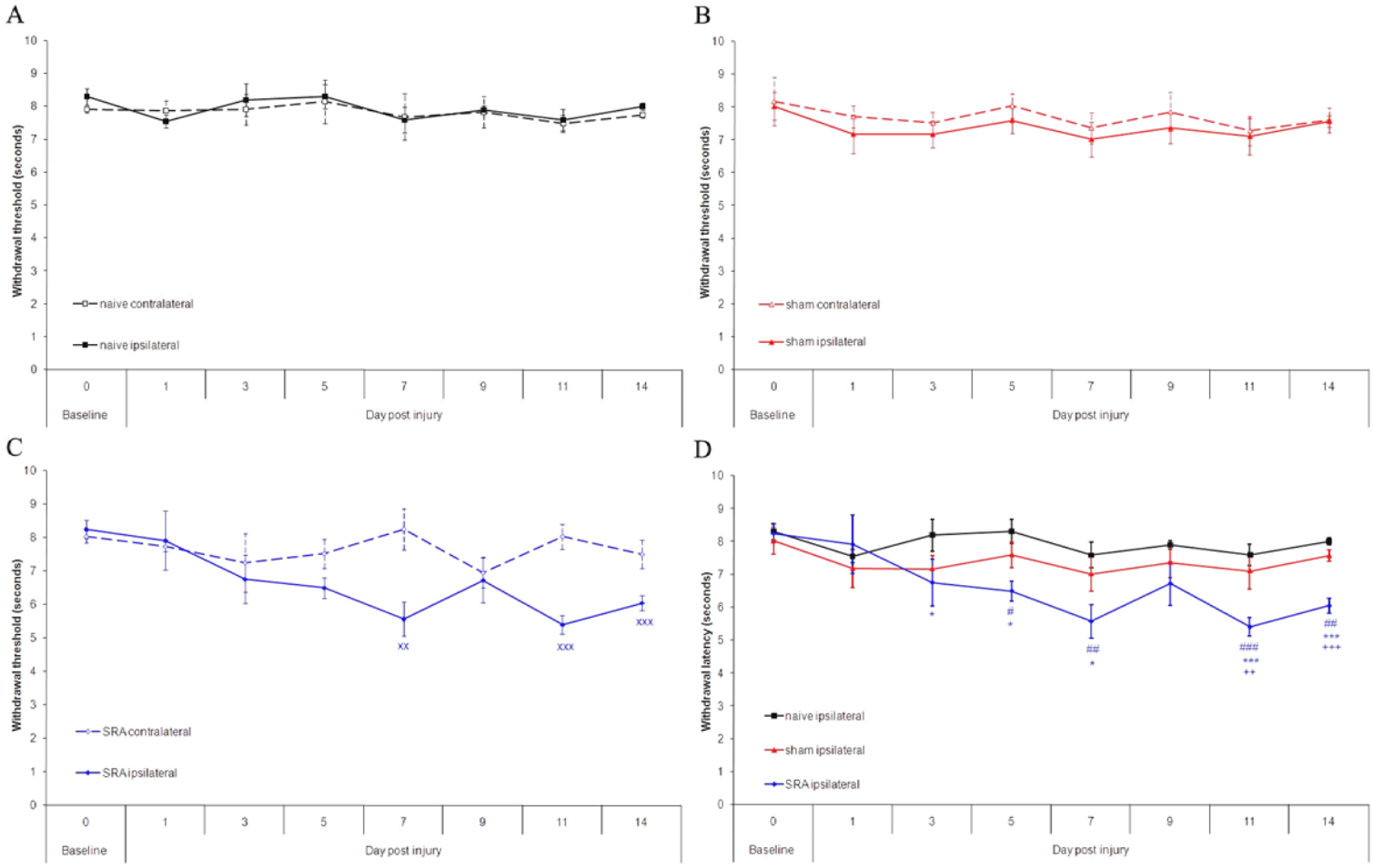

Figure 4.3: Development of thermal hypersensitivity after SRA. Over a period of 14 days no change in withdrawal was noted in naïve animals (A). Across 14 days in sham SRA animals (B) no significant development of hypersensitivity was noted. After SRA significant reduction in withdrawal threshold is noted against contralateral at 7, 11, and 14 days (C). Against sham and naïve, a significant development of hypersensitivity is noted in ipsilateral SRA at 3,5,7,9, and 14 days (D). Comparison against baseline (#), ipsilateral vs contralateral **(x)**, injury vs naïve **(*)**, and injury vs sham **(+)** are shown above respective data point. N=6 in each group.

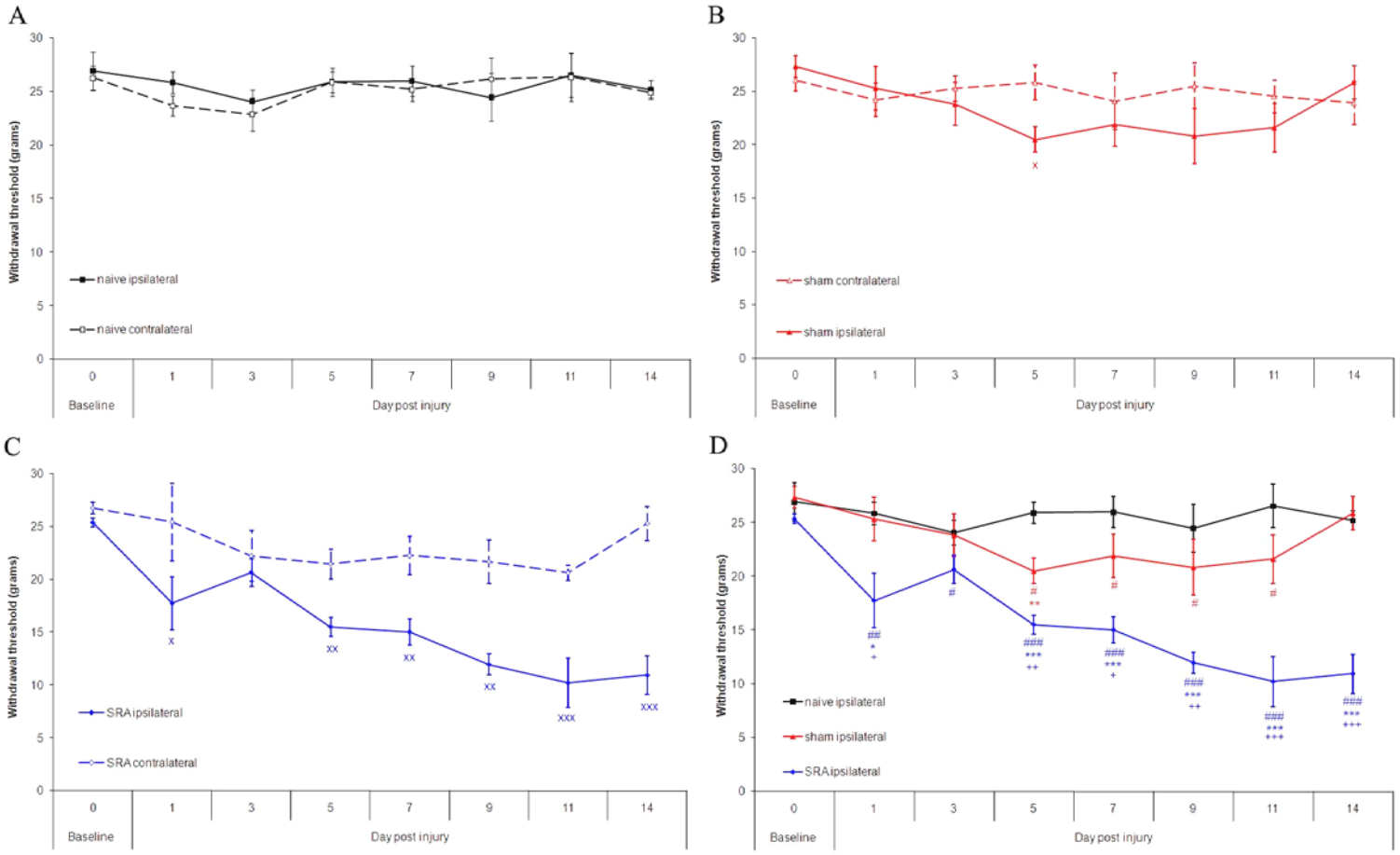

Figure 4.4: Development of mechanical hypersensitivity after SRA. Over a period of 14 days no change in withdrawal was noted in naïve animals (A). Across 14 days in sham SRA animals (B) a significant development of hypersensitivity was noted against contralateral on day 5. After SRA significant reduction in withdrawal threshold is noted against contralateral at 1, 5, 7, 9, 11, and 14 days (C). Against sham and naïve, a significant development of hypersensitivity is noted in ipsilateral SRA at 1,5,7,9, and 14 days (D). A significant reduction in withdrawal latency is noted ipsilaterally in sham SRA animals compared to baseline at 5-11 days, but is not maintained at 14 days. Comparison against baseline (#), ipsilateral vs contralateral **(x)**, injury vs naïve **(*)**, and injury vs sham **(+)** are shown above respective data point. N=6 in each group.

4.2.1.3: Reduced weight gain after SRA

Over a period of 14 days naïve male Wistar rats, with a pre-surgical baseline weight of 271.2g (+/-6.89), gain an average of 5.15 (+/-0.35) grams per day (Fig 4.5). Mean total weight gain across 14 days was 72.2 (+/-4.83) grams (Fig 4.5), which was in agreement with data from animal breeders (Charles River. Margate. UK).

Wistar rats from the same litter, with a pre-surgical baseline weight of 271.2g (+/-6.89), that underwent sham surgery gained 4.98g/day (+/-0.47) (Fig 4.5). Mean total weight gain across 14 days was 69.7g (+/-6.57), which was not significantly different to naïve rats (Fig 4.5).

However, identical Wistar litter mates, with a pre-surgical baseline weight of 266.8g (+/-10.5), that underwent L5 SRA, over the same 14 day period, gained only 3.86g (+/-0.37) (Fig 4.5). Mean total weight gain across 14 days was 54.0g (+/-5.13). This average daily weight gain is significantly lower than naive levels, but statistical significance was not achieved against sham levels (P=0.056) (Fig 4.5).

Pre-surgical baseline weights were not significantly different between groups.

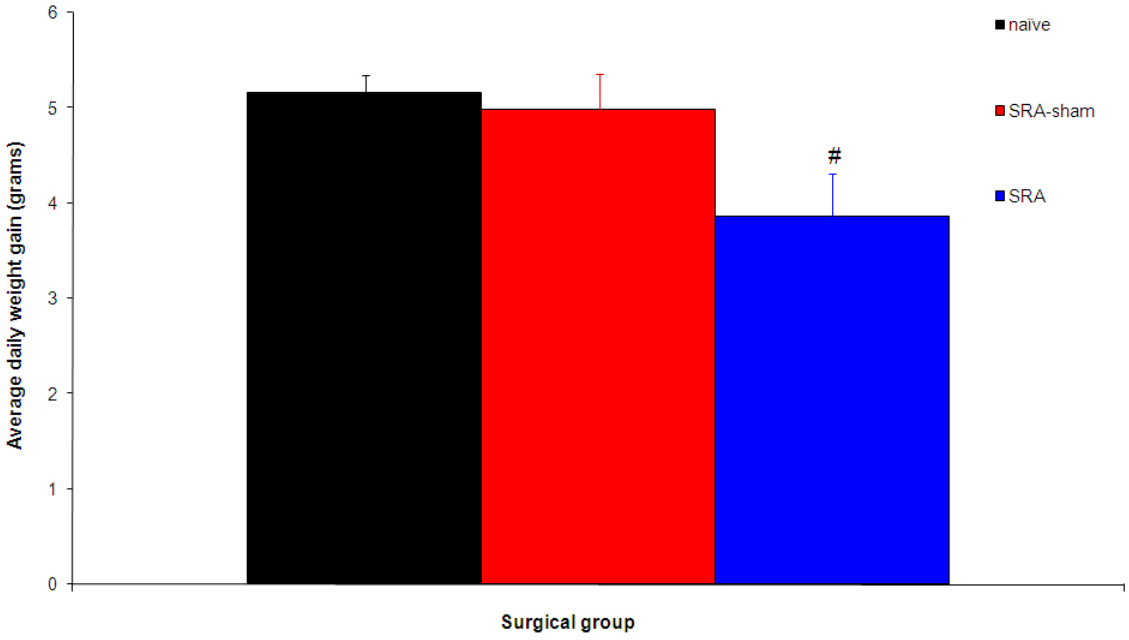

Figure 4.5: Daily weight gain in adult male Wistar rats after sham-SRA, SRA, or naïve surgery. Over a period of 14 days naïve and sham-SRA wistar rats gain 5.15g and 4.98g of weight per day respectively with no significant difference. Over the same period of assessment in SRA injured wistar rats gain only 3.86g, significantly less weight per day than their naïve litter mates. Comparison injury vs naïve **(#)** is indicated above respective data point. N=6 in each group.

4.2.2: Chronic behavioural effects of L5 SRA

After observing a significant hypersensitivity development across 14 days, it was important to assess the temporal profile of this behaviour. A 60 day trial of rats with L5 SRA, using identical thermal and tactile stimulation, was conducted in absence of sham and naïve animals, as hypersensitivity had previously been confirmed against these controls. Baseline and contralateral values were used as control values at each time point.

Before surgery, baseline thermal withdrawal thresholds were 9.57s (+/-0.38) ipsilaterally, and 9.38s (+/-0.45) contralaterally. Baseline mechanical withdrawal thresholds were 19.3g (+/-1.33) ipsilaterally, and 20.4g (+/-1.77) contralaterally. No difference was presented between cord sides and values were representative of previous data (Fig 4.3 and Fig 4.4).

By 5 days ipsilateral hypersensitivity had significantly developed to thermal stimulation [5.97s (+/-0.43)] (Fig 4.6A) compared to baseline and contralateral levels, and tactile stimulation [15.01g (+/-2.23)] (Fig 4.6B) compared only to baseline levels. By 7 days ipsilateral hypersensitivity was significantly lower than contralateral values. These withdrawal values were not significantly different to values from the previous experiment at 7 days [5.57s (+/-0.51) and 15.0g (+/-1.21g)] (Fig 4.3 and Fig 4.4).

At 25 days further significant withdrawal latency reduction was noted for tactile stimulation, such that values reached 8.42g (+/-0.59g), significantly lower than contralateral and baseline values (Fig 4.6B). This hypersensitivity was then maintained up to 60 days [8.31g (+/-0.64)] with no further change from day 25 values. Further thermal withdrawal latency reduction was not noted, and values were maintained across 60 days at 4.27s (+/-0.35) (Fig 4.6A). At no time point did contralateral values significantly fluctuate from baseline (Fig 4.6).

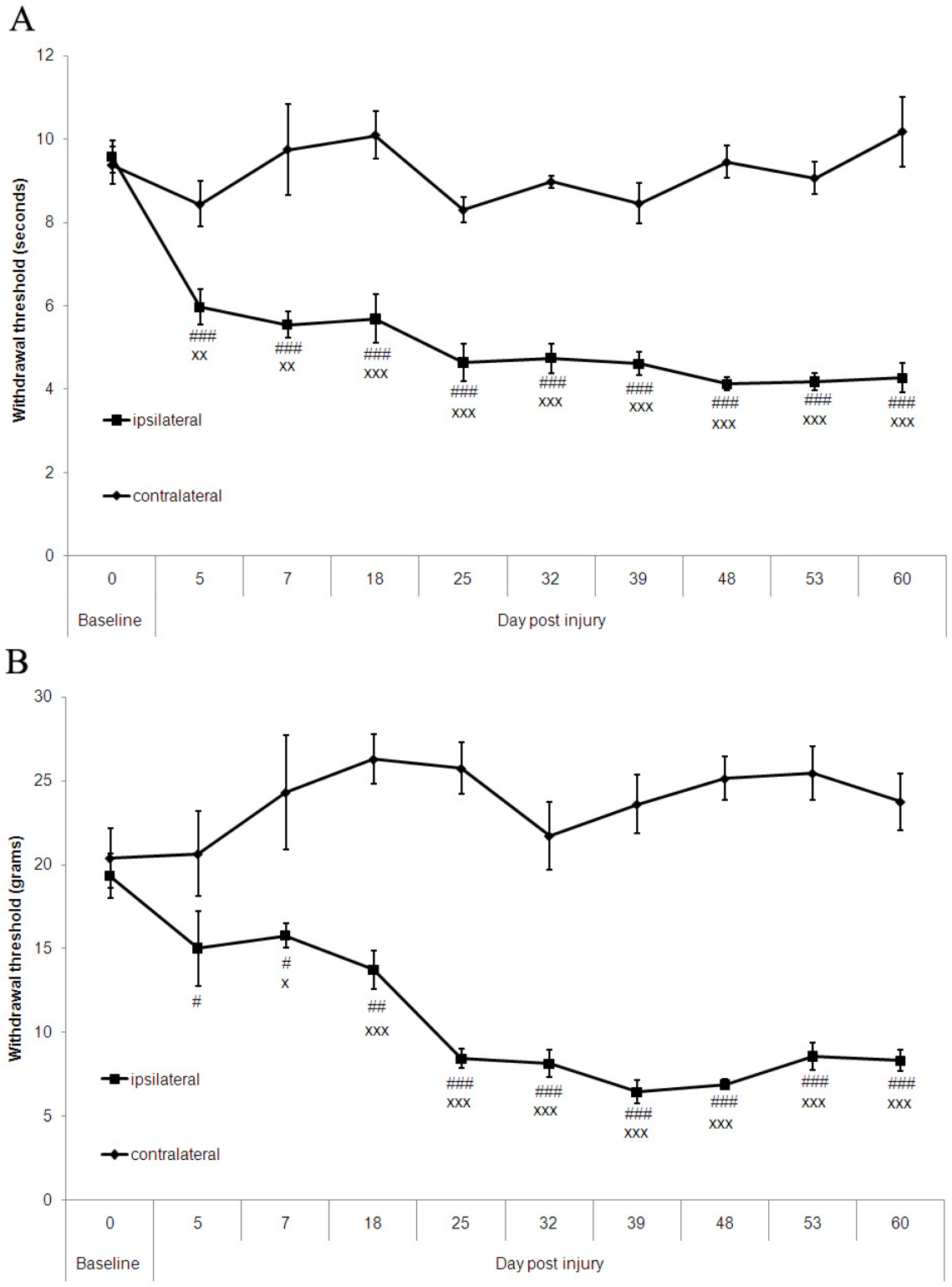

Figure 4.6: Temporal time-course of hypersensitivity after SRA. (A) Over 5 days thermal hypersensitivity develops, and is maintained up to 60 days without contralateral effect. **(B)** Over 5-7 days tactile hypersensitivity develops. Between 7 and 25 days this hypersensitivity is greatly enhanced. Between 25 days and up to 60 days this hypersensitivity is maintained. No change in contralateral withdrawal threshold is significant. Comparison ipsi vs contra **(**x**)**, and injury vs baseline levels (#) is indicated above respective data point. N= 6 in group.

4.2.3: Mechanisms of hypersensitivity development

4.2.3.1: Peripheral component of SRA induced hypersensitivity

Fourteen days after L5 SRA, quantification of phenotypic changes were made through profile counts using Neurofilament (N52), CGRP, and IB4 for the three subtypes of primary afferents within the intact ipsilateral and contralateral L4 DRG.

Analysis indicated that no significant change occurred in these subpopulations against contralateral, sham, or naïve levels. No significant difference was found with TRPV1 expression in the ipsilateral L4 DRG compared to sham, naïve, and contralateral levels. No increase in GFAP expression within satellite cells, from sham, naïve, and contralateral levels was found in the L4 DRG (Fig 4.7).

The only antibody in which there was any significant difference in the L4 DRG was the injury marker activating transcription factor 3 (ATF3) (Fig 4.8 and Fig 4.9). The percentage of L4 DRG neurones expressing ATF3 in the nucleus were greater than naive and sham bilaterally, with ipsilateral SRA expression greater than contralateral (Fig 4.9A). ATF3 colocalised with both N52 positive and N52 negative neurones (Fig 4.8E). There was also a small but significant expression compared to naïve in sham L4 ipsilateral DRG (Fig 4.9B).

All other density staining (GFAP) and counts for the ipsilateral and the contralateral DRG, were not significantly different between any of the groups (Fig 4.8 and Fig 4.9).

Quantification within the L5 DRG was not attempted for any markers mentioned above, and only pictures were taken for visual consideration (Fig 4.7). This was unavoidable due to the methodological requirement of obtaining enough viable sections for analysis. There were no animals, within the SRA group, that when cryosectioned had the minimum 400 neurones per DRG required for quantification and percentage analysis (See methods). Indeed only very few sections had recognizable DRG cells within them. However it is worth noting descriptively, that on the sections were some neurones remained, these DRG cells stained for all 3 phenotypic markers of subpopulations (Fig 4.7). TRPV1 labeling was seemingly absent in these ipsilateral L5 DRG neurones (Fig

4.7). GFAP was also highly expressed in satellite cells surrounding the remaining DRG neurones (Fig 4.7).

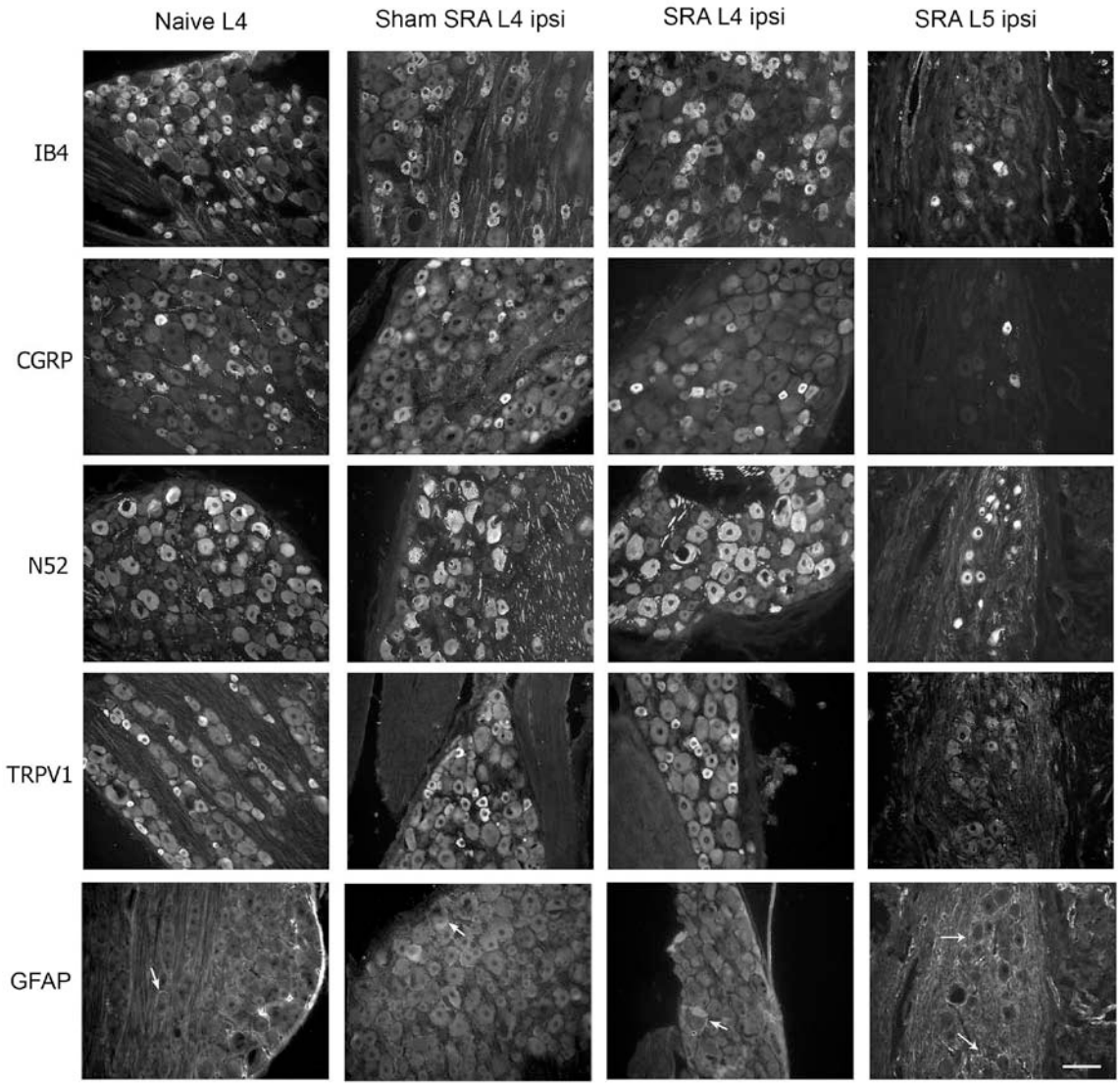

Figure 4.7: Changes in neuronal DRG subpopulations after L5 SRA. Immunolabelling with IB4, CGRP, N52, and TRPV1 shows no phenotypic changes occurring in neuronal subclasses within L4 DRG after L5 SRA. No upregulation in GFAP in satellite cells indicated little direct damage to this DRG. However, when comparing L5 DRG, a remarkable loss of neurones of all subtypes is observed. In most sections positive DRG neurones cannot be located (images not shown). TRPV1 expression is absent. Satellite cells upregulate GFAP around remaining neurones. Scale=50µm

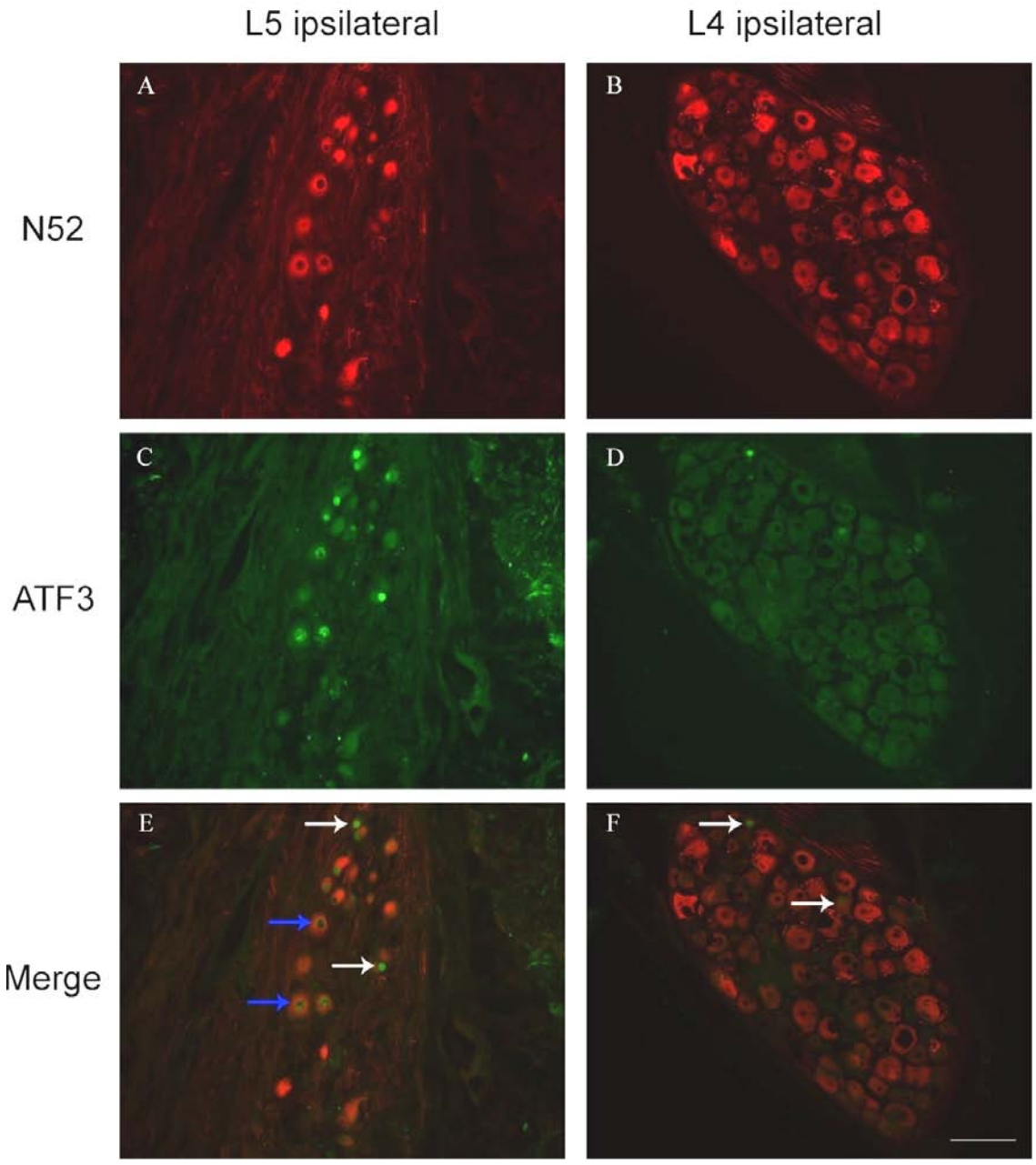

Figure 4.8: AFT3 expression in intact and avulsed DRG after L5 SRA. ATF3 is expressed in many of the remaining neurones within the ipsilateral L5 avulsed DRG. Some are large myelinated N52 positive (blue arrow), others unmyelinated N52 negative (white arrows). A few ATF3 positive neurones are found in the L4 ipsilateral intact DRG that are large, myelinated neurones (white arrows) Scale=50µm

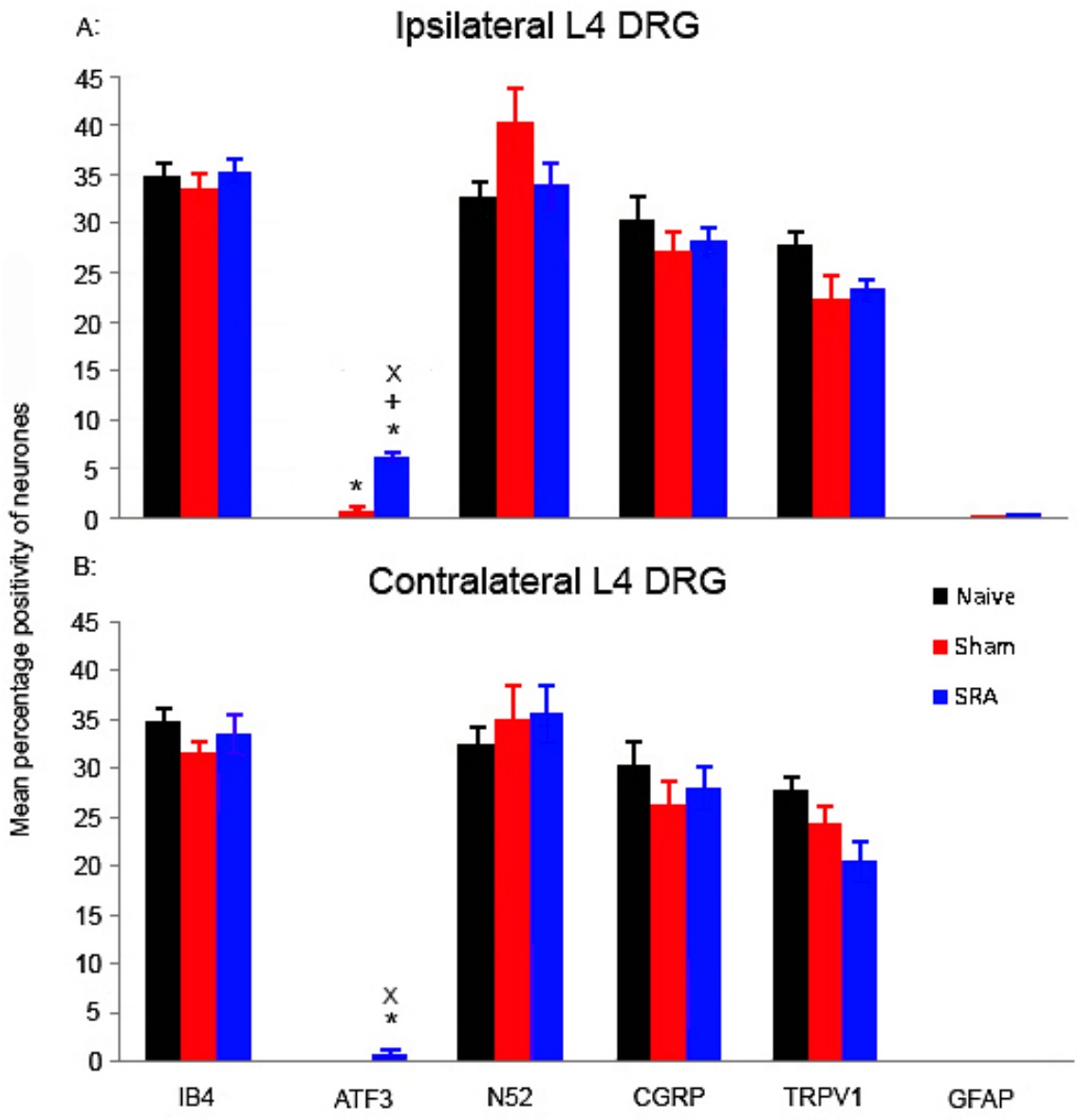

Figure 4.9: Quantification of L4 neuronal subpopulations, injury marker expression, and satellite cell expression in ipsilateral (A) and contralateral (B) DRG. No difference between naïve, sham, and SRA, and ipsilateral versus contralateral sides for small unmyelinated peptidergic neurones (CGRP), small unmyelinated non-peptidergic neurones (IB4), large neurofilament positive neurones (N52), Vanilloid receptor (TRPV1) expression, or satellite activation (GFAP). A few (5%) ATF3 positive neurones are found ipsilaterally in sham, and bilaterally in SRA DRG. Comparisons between ipsilateral and contralateral **(x),**, injury vs naïve **(*)**, and SRA vs sham **(+)** are indicated above respective data point. N=6 in each group.

4.2.3.2: Central component of SRA induced hypersensitivity

4.2.3.2.1: Dorsal horn neuronal counts

Counts in the dorsal horn for neuronal populations were quantified using the antibody NeuN as described in section 2.7 and 3.2.5.2. Toluidine staining was not applied in this case due to the observation of non-specific staining at 14 days in DRA and DRR dorsal horn (Section 3.2.5.3)

Counts of naïve dorsal horn neurones averaged 413.8 (+/-5.29) in L4 and 407.3 (+/-5.94) per section in L5 (Fig 4.11). The cytoarchitecture of the L5 dorsal horn was distinct from L4 with shorter and fatter lamina distribution and shallower dorsal fasciculus and columns (Fig 4.10). The neurones followed a distinct lamina distribution in both segments (Fig 4.10). Sham dorsal horn NeuN counts did not significantly change from naïve in any area analysed (Fig 4.11).

Fourteen days after SRA, a small but significant reduction in NeuN counts were observed in the L5 dorsal horn [376 (+/-7.72) per section] (Fig 4.11). This was significantly lower than sham, naïve, and contralateral values. NeuN loss was evident in the medial superficial laminae directly overlying Lisseaur's tract and the DREZ. Small cavities were noted in the deafferentated area around the DREZ. However lateral areas of the superficial laminae, including the lateral spinal nucleus remain intact (Fig 4.10). Contralateral NeuN counts in either deafferented or intact segments were not significantly lower than naïve levels (Fig 4.11).

Interestingly, NeuN counts also decreased in the dorsal horn of the intact L4 segment to 389.3 (+/-4.39), significantly decreased from sham, naive, and contralateral values, but not significantly different to L5 segmental loss (Fig 4.11). NeuN loss was again evident below Lisseaur's tract and DREZ, and dispersed through the deeper laminae (Fig 4.10).

Primary afferent terminal loss, determined by IB4 staining of non-peptidergic C-fibres, was distinctive in L5, with loss of staining throughout lamina II, but some residual staining remained (Fig 4.12) in accordance with results from DRA and DRR (Section 3.2.1b). A partial loss of IB4 staining in lamina II of the adjacent L4 segment was also

noted (Fig 4.12). Neuronal loss however was not anatomically correlated with primary afferent loss within either L5 or L4 segments, with NeuN+ve dorsal horn neurones present in these specific areas of deafferentation (Fig 4.12).

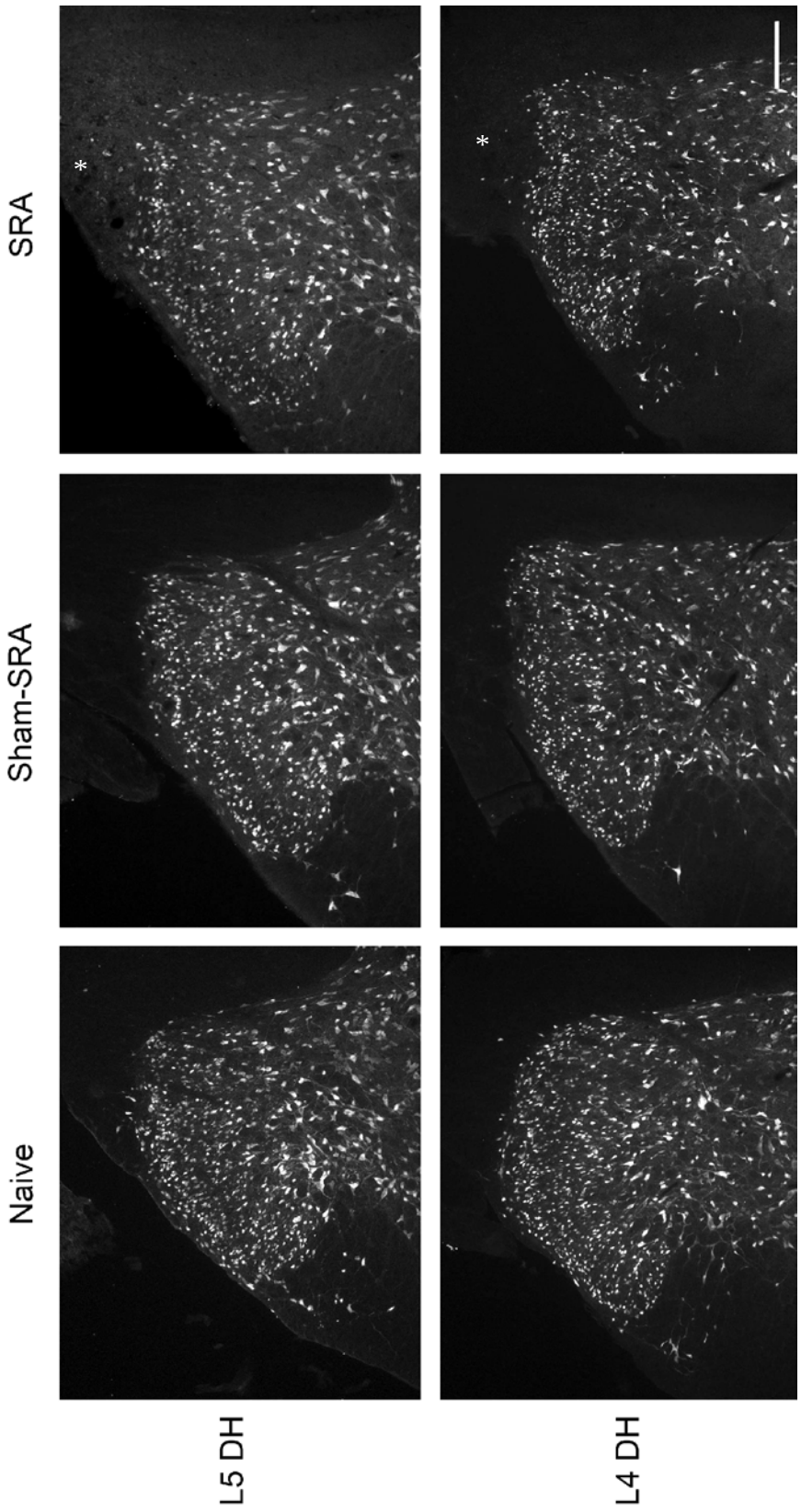

Figure 4.10: Representative images of ipsilateral dorsal horn 14 days after L5 SRA. Cavitation and NeuN loss is noticeable near DREZ and lisseaurs tract where avulsion of the L5 can be noted, in the medial aspect of the superficial dorsal horn 14 days after SRA in L5 (white asterisks). A similar NeuN loss is mirrored in L4 to a lesser extent, and absent of cavitation (white asterisks). Note the L4 root and DREZ is intact in the L$ segment. NeuN loss is not noticeable in other areas of the dorsal horn. Scale=200µm

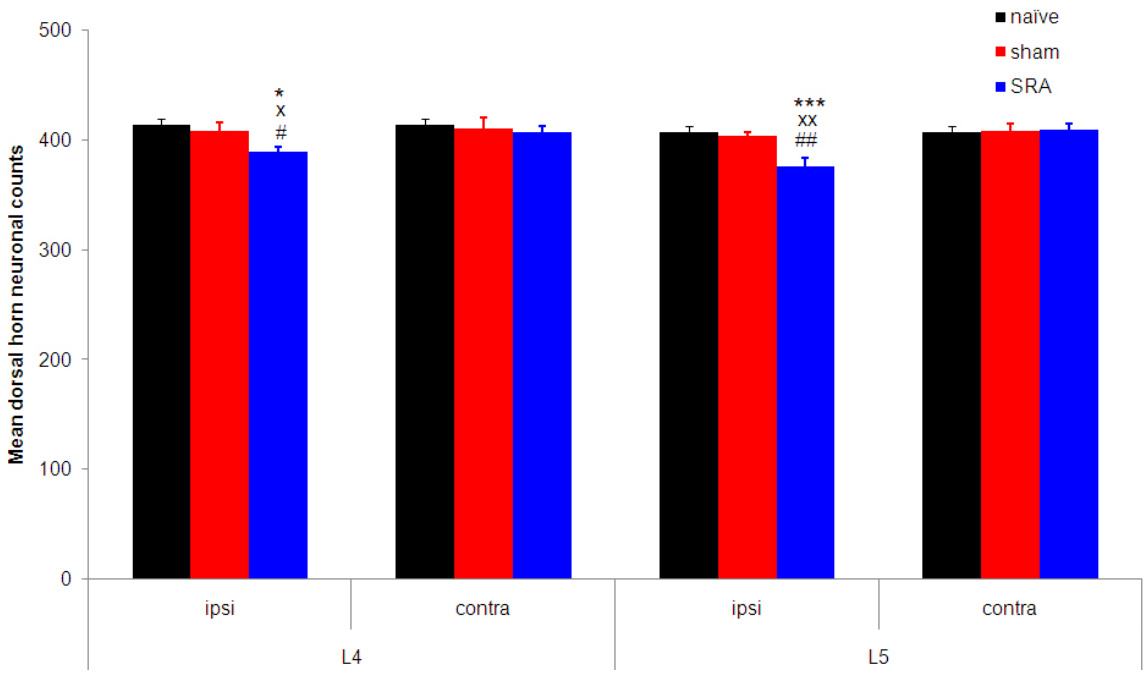

Figure 4.11: Quantification of mean number of dorsal horn neurones 14 days after SRA. A small but significant NeuN count reduction is present in both L5 and L4 segments aftr SRA injury compared to sham and naïve levels. Comparisons between ipsilateral and contralateral **(*),** injury vs naïve **(#)**, and SRA vs sham **(x)** are shown. N=6 in each group.

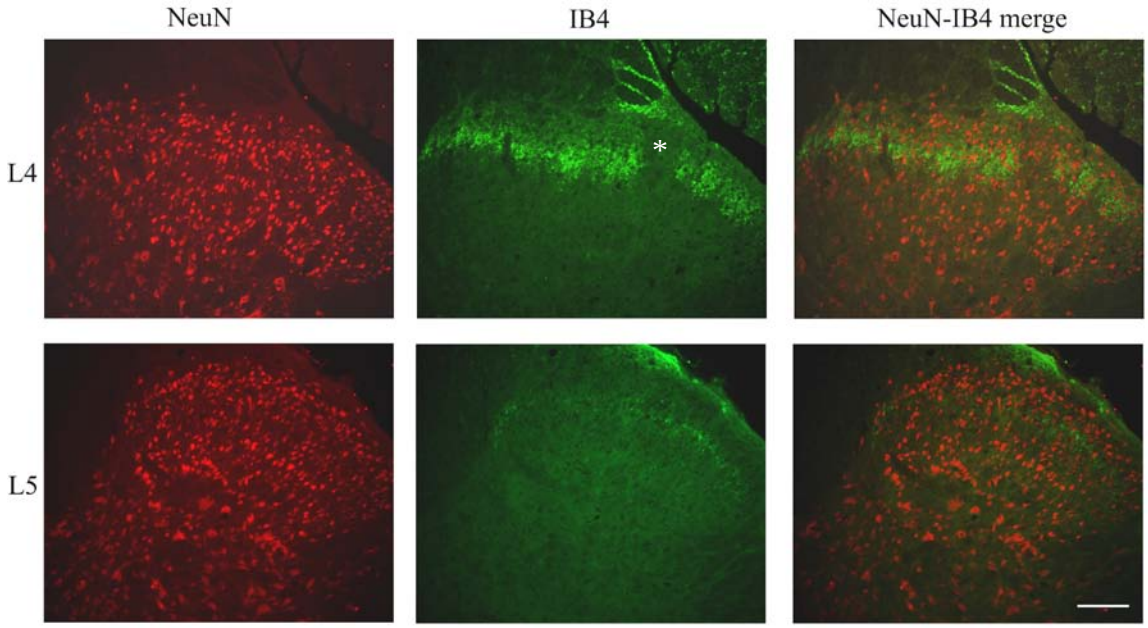

Figure 4.12: Colocalisation studies of primary afferent terminal loss and neuronal loss in L4 and L5 segments 14 days after L5 SRA. L4 IB4+ve primary afferent terminals show a decrease within the lamina II 'eyebrow' (asterisk), representing deafferented L5 fibres that branch and synapse within the adjacent segment. L5 IB4+ve staining is minimal, due to the deafferentation of L5 fibres. Residual staining does remain and may indicate adjacent overlapping from primary afferent terminals from L4 or L6. In neither segment does primary afferent loss colocalise with noticeable neuronal loss (NeuN-IB4 merge). Scale=100µm

4.2.3.2.2: Ventral horn neuronal counts

In addition to dorsal horn NeuN reduction after SRA, a prominent motor neuronal loss was found in the ipsilateral ventral horn. This was evident using either Toluidine Blue histology or NeuN immunohistochemistry (Fig 4.13 and Fig 4.14). α-motor neurones could easily be distinguished by eye using both histological methods (Fig 4.13), and the inclusion criteria has been previously described (Section 2.7). Ipsilateral values are represented as a percentage of contralateral counts (Fig 4.14). This representation of the data was preferred to actual counts due to the relatively low numbers of motor neurones per section, and the propensity for naïve motor neurone number to deviate between sections.

Sham surgery did lead to a loss of ipsilateral motor neurones, as determined by either Tol Blue or NeuN labelling (Fig 4.13 and Fig 4.14). Mean contralateral motor neurone counts in SRA ventral horn using either NeuN or Tol Blue staining was not different to contralateral sham motor neurone counts (data not shown).

After SRA the number of NeuN+ve motor neurones decreased in L5 by 69.1% (+/-6.8) of contralateral numbers. Loss was observed in three areas; dorsolateral and ventrolateral (L4 and L5), and ventromedial (caudal L5) pools (Fig 4.13 and Fig 4.14) (As described in section 2.7). NeuN+ve motor neurone percentages were also reduced in L4, and loss was 47.2% (+/-3.1) of contralateral side, but was significantly less severe than the loss in L5 (Fig 4.14). Motor neurone loss was noted in ventrolateral and dorsolateral motor neuronal pools, with greater loss in ventrolateral (Fig 4.13).

When analysing Tol Blue+ve motor neurones, a marked difference compared to NeuN immunohistochemistry was noted. Loss was limited to 42.9% (+/-4.9) in L5 and 26.6% (+/-4.0) in L4 segments, still significant from Tol Blue sham levels in both cases (Fig 4.14). The deafferented L5 ventral horn again had a greater loss of motor neurones than the intact L4 ventral horn (Fig 4.14). This loss was significantly milder than NeuN loss in similar segments (Fig 4.13). In both L4 and L5 ventral horns, some small spherical cells with faint Tol Blue staining were observed surrounding motor neurones (Fig 4.13), likely representing a glial cell population, similar to results from Tol Blue staining in the dorsal horn at 14 days after DRA and DRR (Section 3.2.5.3).

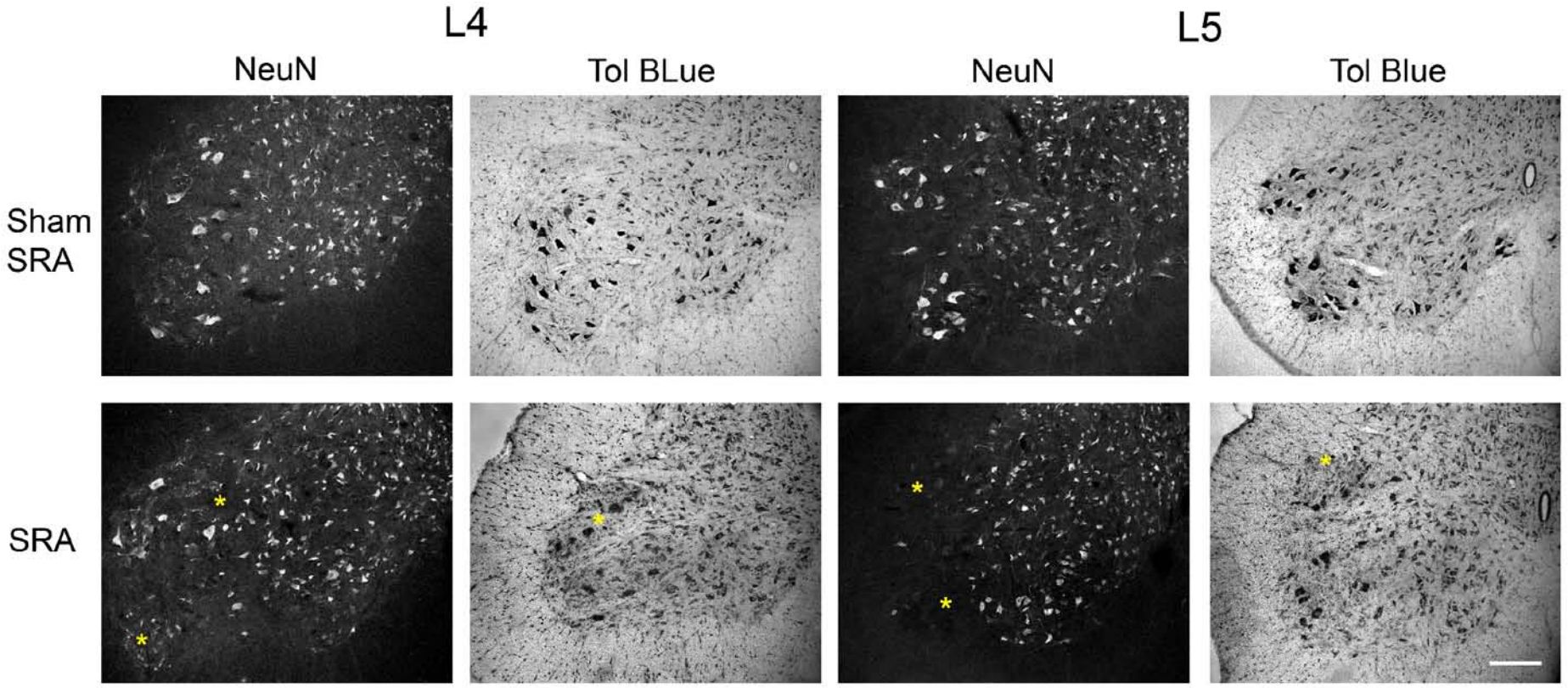

Figure 4.13: Representative images of ipsilateral ventral horn 14 days after L5 SRA. Sham injury leads to no observable motor neuronal loss (Top panel). L5 SRA injury leads to motor neuronal loss in the two motor neuronal pools in the lateral ventral areas (asterisks). This loss is noted using either a cytozolic dye (Tol Blue) or antibody to the neuronal epitope (NeuN), however is more severe in the latter stain. Tol Blue also stains smaller cells surrounding motor neurones, that likely represent glial populations upregulated in response to the injury. Scale=200µm

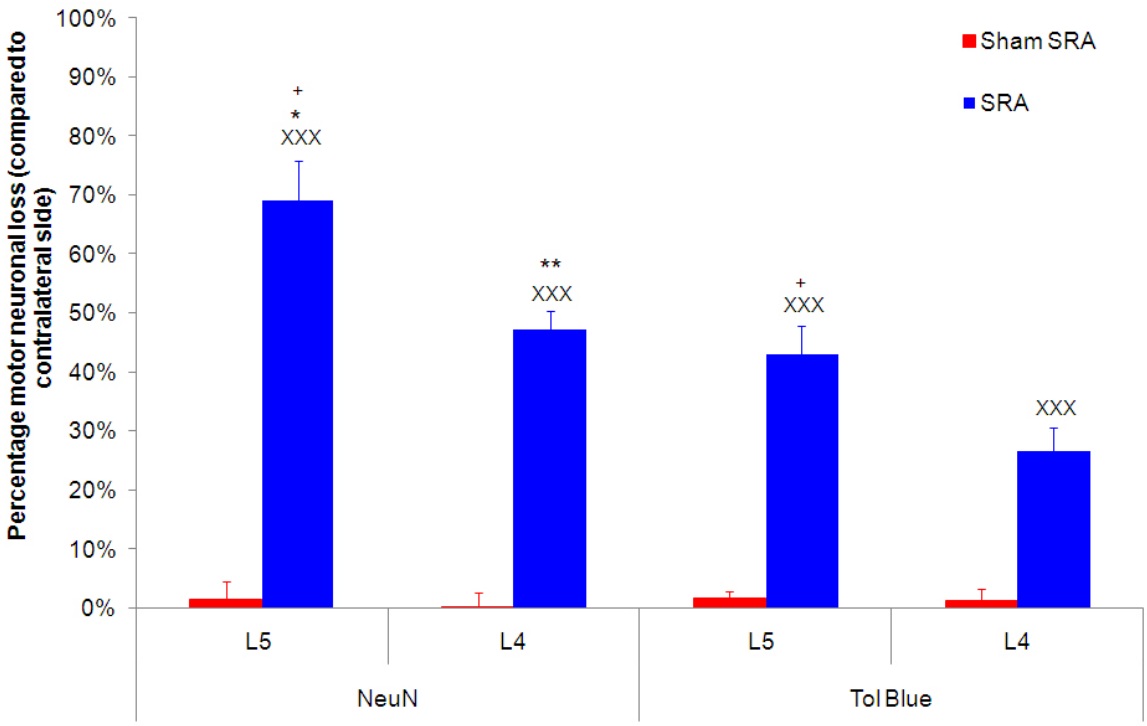

Figure 4.14: Mean motor neurone loss in ventral horn 14 days after L5 SRA. Sham ventral horn shows no loss compared to contralateral side. L5 SRA leads to significant motor neurone reduction at 14 days compared to sham in both L5 and L4 segments. When using NeuN stain, counts show a significantly greater reduction than Tol Blue in the same tissue. Comparisons between Tol Blue vs NeuN values **(*),** and SRA vs sham (x), and L4 vs L5 (+) are shown. N=6 in each group.

4.2.3.2.3: Vascular effects

Microvascular effects were assessed in naïve, sham-SRA, and SRA tissue 14 days after injury using RECA-1 density staining and quantified with the Leica Q-win program, (see section 2.3.2).

RECA-1 density staining in naïve dorsal horns was 4.45% (+/-0.51) in the L5 segment and 4.39% (+/-0.23) in the L4 segment (Fig 4.16A). In the ventral horns RECA-1 density staining was 4.67% (+/-0.45) in L5 segment and 4.87% (+/-0.46) in the L4 segment (Fig 4.16B). Sham-SRA dorsal and ventral horn vasculature staining levels were not significantly lower than naïve levels (Fig 4.16).

After 14 days in SRA, RECA-1 vasculature labelling showed a marked reduction in intensity against sham and naïve levels, in both the deafferented L5 and intact L4

segments, in both dorsal and ventral horns (Fig 4.15). The number of microvascular vessels did not seem to decrease; only the intensity of the staining of endothelial cells was reduced along with the thickness and length of the vasculature. This was not just around the lesion site of the DREZ and VREZ, but throughout the L4 and L5 segments.

Levels of RECA-1 intensity staining in the ipsilateral dorsal horn 14 days after SRA were 2.62% (+/-0.32) in the L5 segment and 2.93% (0.32) in the L4 segment, both significantly lower than naïve levels (Fig 4.16A). However only in the L5 segment dorsal horn were percentage density levels of RECA-1 significantly lower than that in the corresponding sham (Fig 4.16A).

Levels of RECA-1 intensity staining in the ipsilateral ventral horn 14 days after SRA were 2.01% (+/-0.15) in the L5 segment and 2.44% (0.26) in the L4 segment. All segments had significantly reduced RECA-1 from naïve and sham levels.

No significant difference was found in RECA-1 density staining between deafferented L5 and intact L4 segments in either ventral or dorsal horns (Fig 4.16).

A contralateral effect was significant in comparison to sham and naïve levels, and levels of RECA-1 were not significantly different to ipsilateral levels in any comparison (Fig 4.16). Contralateral RECA-1 staining, similar to ipsilateral, was more significantly reduced against corresponding naïve and sham values, in the ventral horn [L4 = 2.61% (+/-0.19), L5 = 2.28% (+/-0.24)] than in the dorsal horn [L4 = 3.28% (+/-0.34), L5 = 3.14% (+/-0.23)] (Fig 4.16).

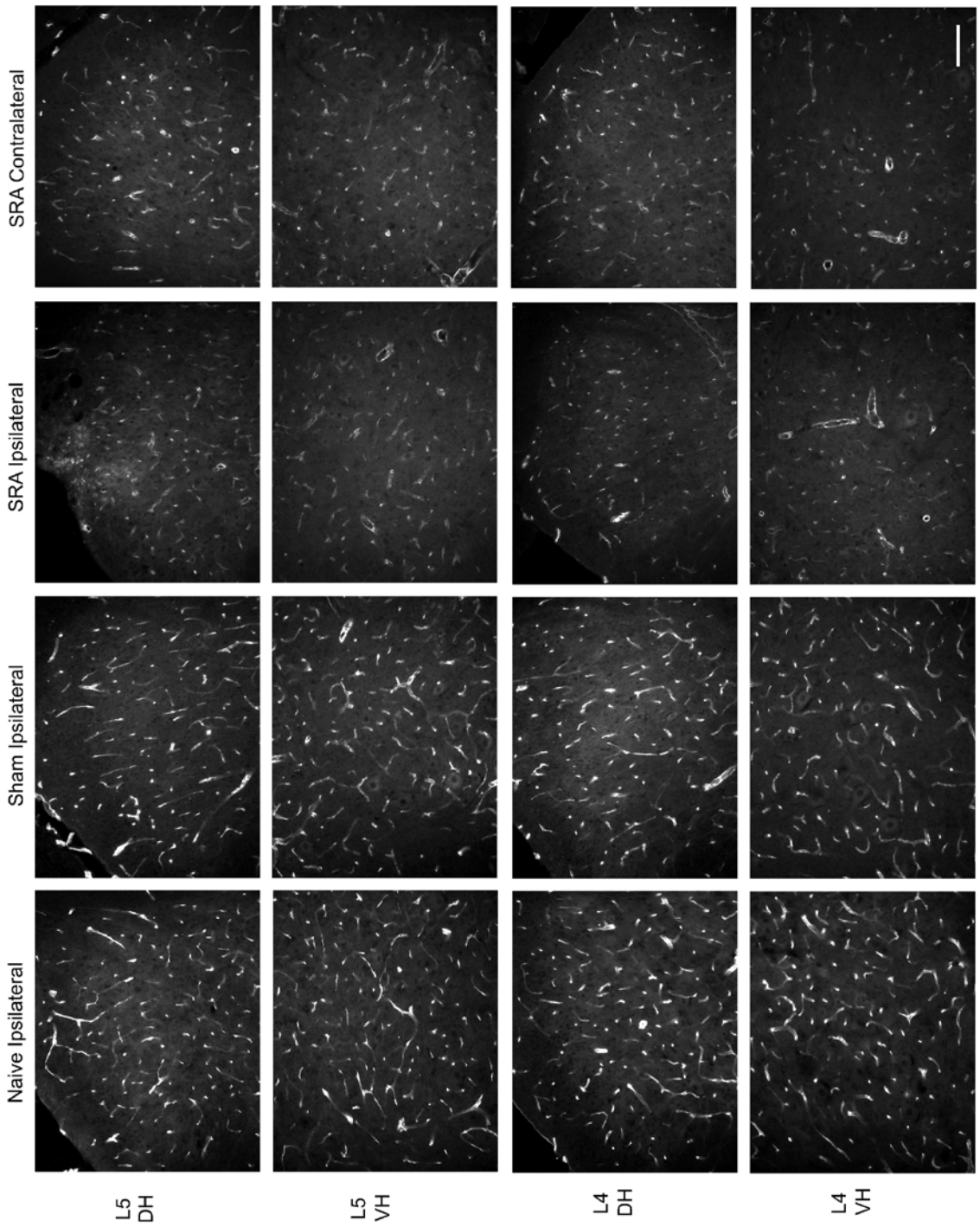

Figure 4.15: Representative images of RECA-1 staining in dorsal and ventral horns in L5 and L4 segments. Loss of vasculature labeling can be seen at 14 days after SRA in both L5 and L4 segments, bilaterally, and in both ventral and dorsal horns. The number of microvascular vessels seems unchanged, only a reduced staining of endothelial cells (RECA-1 marker) as well as shortening and thinning of vessels is noted. Scale=100μm

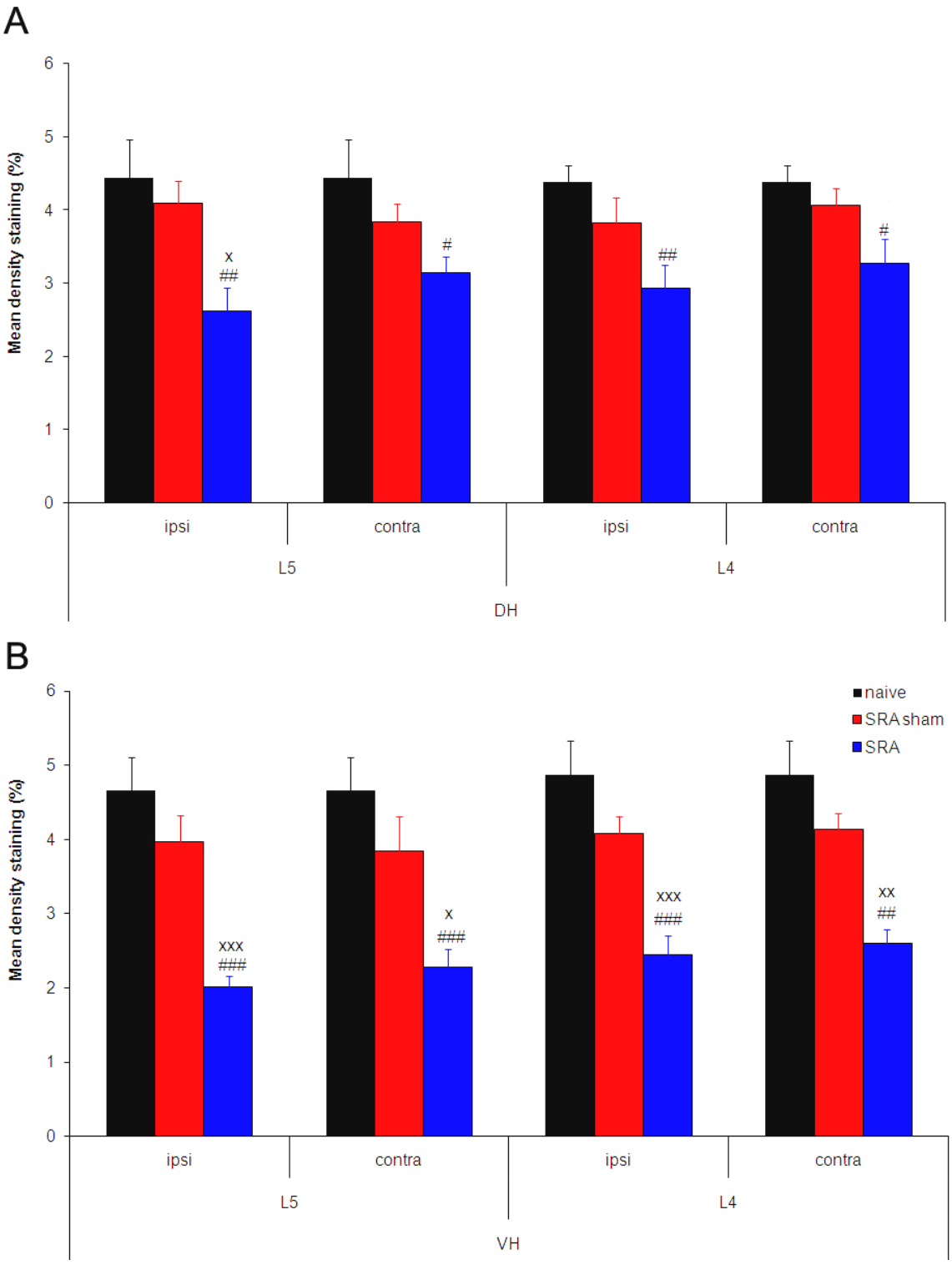

Figure 4.16: Quantification of RECA-1 staining in dorsal (A) and ventral (B) horns in deafferented (L5) and intact (L4) segments. There is no difference between naïve and sham for any area. Significant bilateral reduction in RECA-1 occurs 2 weeks after SRA in dorsal and ventral horns compared to naïve. A significant reduction from sham RECA-1 levels is apparent in ipsilateral L5 dorsal horn and bilateral L4 and L5 ventral horns. No significant differences are seen between cord sides. Comparisons between injury vs naïve **(#)**, and SRA vs sham **(x)** are shown. N=6 in each group.

4.2.3.2.4: Macrophage infiltration

Qwin analysis of naïve, sham, and contralateral SRA tissue provided no evidence of ED-1 positivity in the dorsal columns, and no ED-1 was visualised in any other areas of the L4-L5 cord in these sections (Fig 4.17 and Fig 4.18).

Fourteen days after SRA, ED-1 expression was found in the ipsilateral dorsal root entry zone and dorsal columns almost exclusively in L5 and L4 segments respectively (Fig 4.17), with no contralateral expression (results not shown). When quantified this ED-1 expression density in the DREZ and columns was significantly greater than sham levels in the dorsal columns [0.01% (+/-0.00) in L4, and 0.02% (+/-0.01) in L5], such that the L5 segment showed 3.95% (+/-1.23) and the L4 segment 1.37% (+/-0.36) density staining (Fig 4.18). However, unique to SRA injured cord, ED-1 was not significantly expressed in the dorsal horn, contrasting evidence from DRA and DRR, which show an anatomically separate macrophage population that surround the dorsal horn neurones compared to primary afferent fibres (Section 3.2.3a). A small amount of ED-1 positive staining was found in the ventral horn in both L5 and L4 segments, with some clustering around motor neurones (Fig 4.17). The presence of this ventral horn staining was inconsistent between segments and animals, and was not analysed for this reason.

Significant differences in ED-1 density expressions were seen between deafferented L5 and intact L4 segments (Fig 4.17 and Fig 4.18). In the L5 segment ED-1 macrophages are found intensely in the DREZ, with a few migrating through the ipsilateral dorsal fasiculus and column, and also into Lisseaurs tract and very few in the medial portion of superficial laminae, where dorsal horn neuronal loss was indicated. Intense ED-1 staining surrounds areas of cavitation (Fig 4.17). However in the L4 segment, dispersed ED-1 positive cells are presented in a much reduced number, and specifically within the ipsilateral dorsal column only (Fig 4.17).

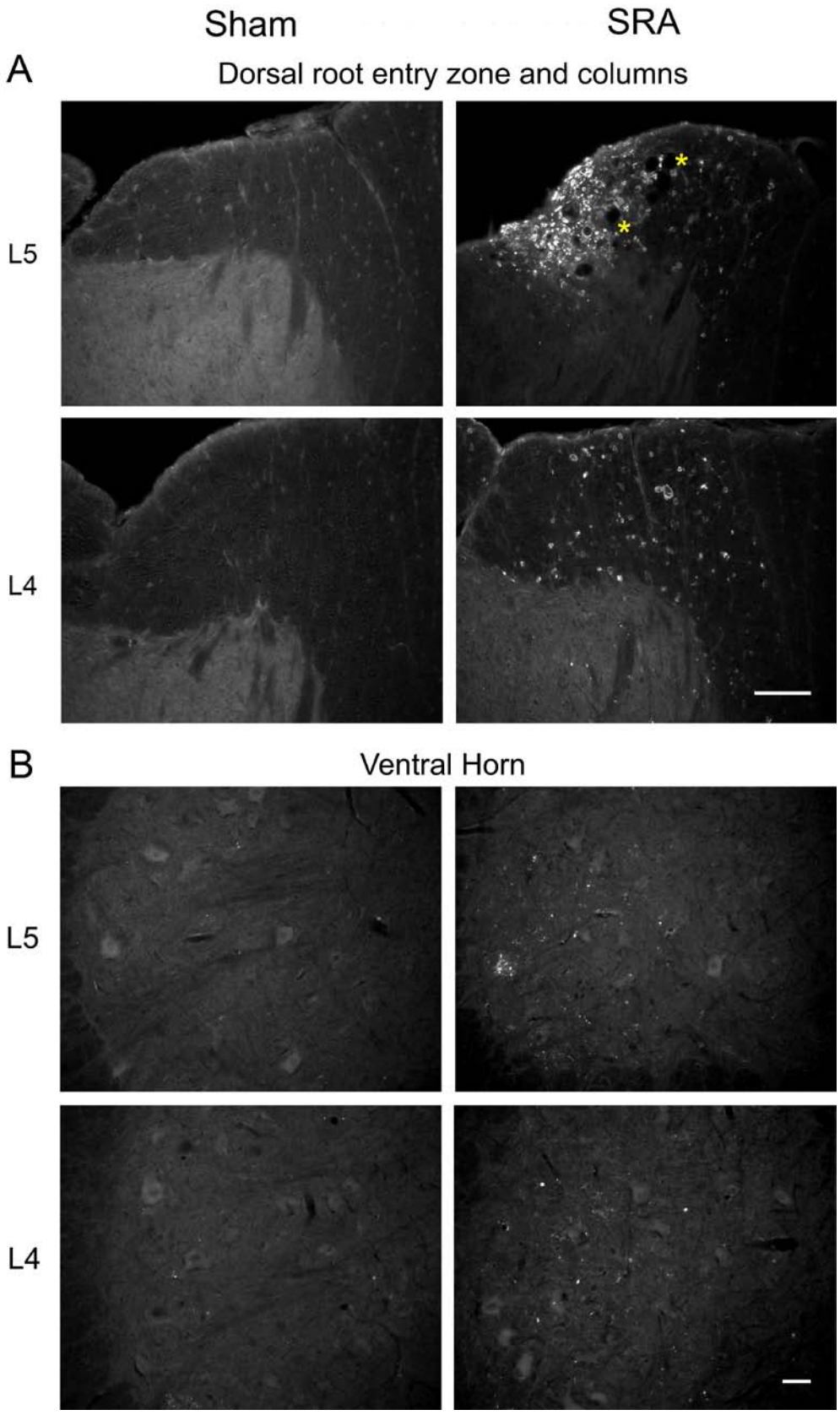

Figure 4.17: Representative images of ED1 staining in DREZ, columns, and ventral horn in deafferented-L5 (A) and intact-L4 (B) segments. ED1 positive labelling can be seen 14 days after SRA in both L5 and L4 segments. Rarely were ED1 positive cells found in sham, or naïve tissue (not shown). Some small ED-1+ve cells were present in the ventral horn in both L4 and L5 segments, with some clustering around motor neurones. Macrophages were almost exclusively located around cystic cavities and the DREZ in L5 (asterisk), whereas they are more dispersed throughout the dorsal columns in the L4 segment. Scale=50µm

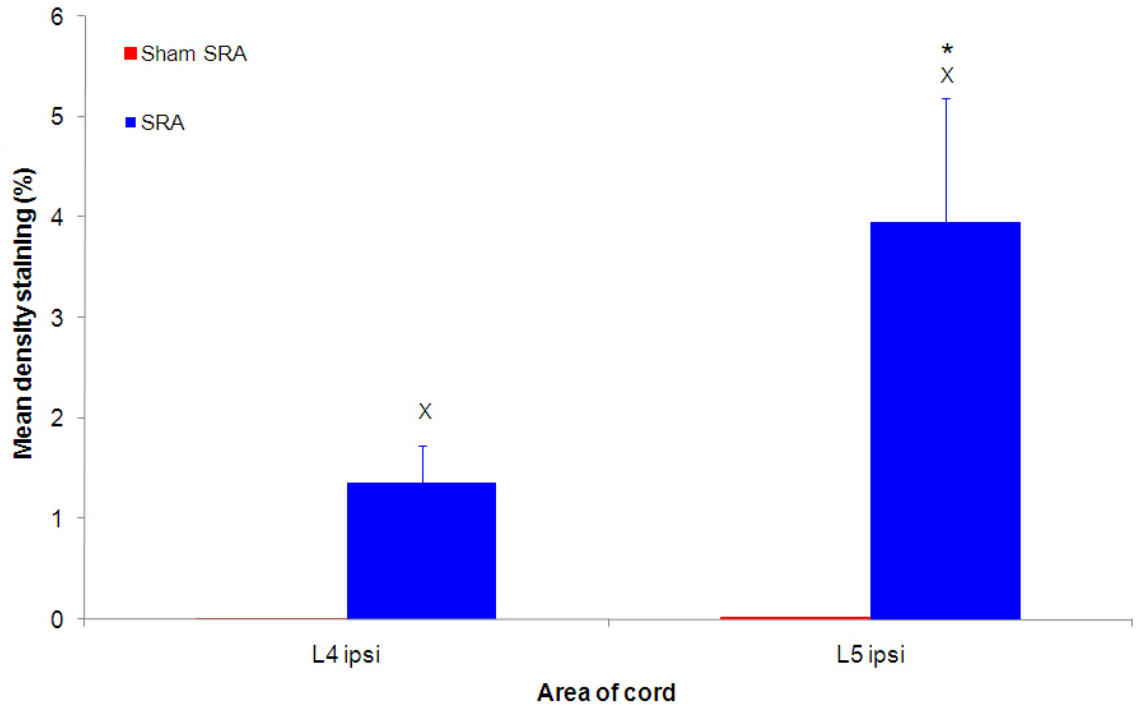

Figure 4.18: Quantification of ED-1 staining in the dorsal columns of deafferented (L5) and intact (L4) segments. ED-1 positivity was found only ipsilaterally in SRA animals. Almost no ED1 positivity was found in sham animals. Significant ED-1 density staining was found in L5 dorsal funiculus, dorsal column, and dorsal root entry zone, compared to sham ED-1 levels. ED-1 positivity was located in L4 ipsilateral dorsal columns exclusively, which was significantly less than L5 density staining. Naïve and contralateral sides not quantified. Comparisons between and SRA vs sham **(x)** and L5 vs L4 (*) are shown. N=6 in each group.

4.2.3.2.5: Astrocyte reactivity

Astrocytes were identified through immunohistochemical labelling of GFAP and quantified for density staining. Q-win analysis of naïve dorsal horns provided density staining values of 3.41% (+/-0.31) for the L4 segment and 3.39% (+/-0.23) for the L5 segment (Fig 4.20). Naïve ventral horn density staining values were 3.45% (+/-0.13) for the L4 segment and 3.76% (+/-0.29) for the L5 segment (Fig 4.20). No significant difference was found between cord sides, or segmental levels (Fig 4.20).

Fourteen days after sham surgery, a significant increase in GFAP density staining was observed bilaterally in L4 and L5 for both ventral and dorsal horns, as analysed against naïve levels (Fig 4.19 and Fig 4.20). When quantified, no significant difference was found between ipsilateral and contralateral comparisons, or between sham-injured (L5)

and intact (L4) comparisons, and density staining values fell within a range of 4.83% (+/-0.34) and 5.66% (+/-0.32) within the L4-L5 cord (Fig 4.20).

Fourteen days after SRA surgery, GFAP density staining was significantly upregulated in dorsal horn astrocytes ipsilateral to the deafferentation, in L5 as well as L4 segments, compared to sham, naïve, and contralateral levels (Fig 4.19 and Fig 4.20). Visually, a GFAP-positive network of astrocytes could be seen in the dorsal root entry zone, dorsal column of L5, with hypertrophy and increased GFAP expression in the dorsal horn of both L4 and L5 segments (Fig 4.19). Ipsilateral GFAP density staining reached 8.14% (+/-0.42) in the L4 segment and 8.11% (+/-0.40) in the L5 segment, and no significant difference was found between the deafferented L5 and intact L4 segments (Fig 4.20).

GFAP density staining was also significantly upregulated in the ventral horns of both deafferented L5 and intact L4 segments, compared to sham, naïve, and contralateral levels (Fig 4.19 and Fig 4.20). Visually in the L5 segment astroctyes were greatly upregulated around motor neurone clustering tightly in the lateral aspect of the ventral horn (Fig 4.19). Within the L4 segment, astrocytes had ‘looser’ association with motor neurones, surrounding rather than ‘blanketing’ individual cells, but each astrocyte still shows a greatly increased GFAP expression (Fig 4.19). Ipsilateral GFAP density staining reached 7.56% (+/-0.21) in the L4 segment and 7.13% (+/-0.20) in the L5 segment, and again no significant difference was found between the deafferented L5 and intact L4 segments (Fig 4.20).

A small but significant contralateral increase in GFAP density expression was found in both deafferented L5 and intact L4 segments of SRA animals compared to naïve, and in both dorsal and ventral horns, but was not significantly higher than sham levels (Fig 4.20).

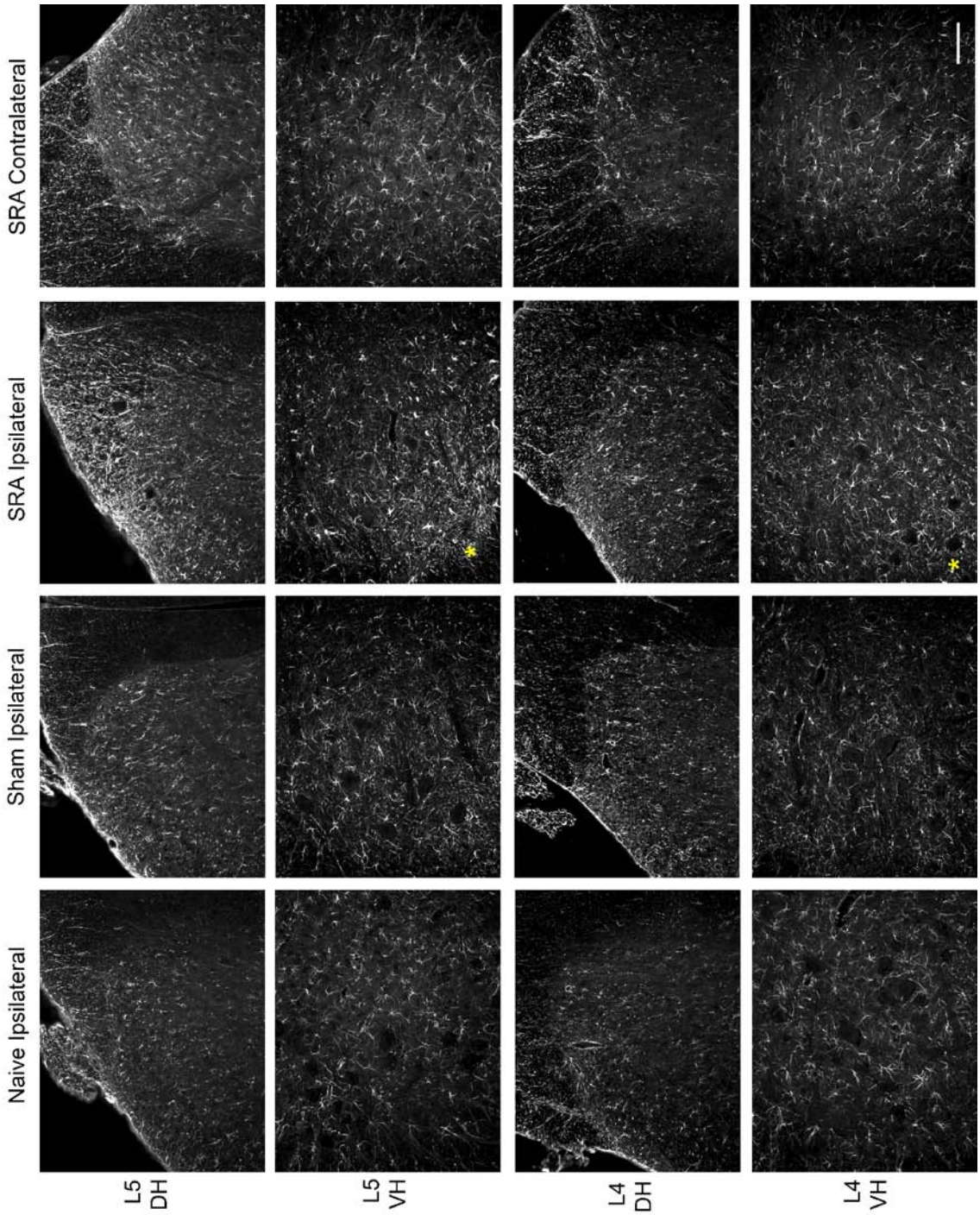

Figure 4.19: Representative images of GFAP staining in dorsal and ventral horn in deafferented-L5 and intact-L4 segments. Increase in GFAP labeling can be seen 14 days after sham surgery in the dorsal and ventral horns, in both L5 and L4 segments. Further increase in GFAP labeling can be seen 14 days after SRA, surrounding motor neurones (asterisk) and superficial dorsal horn, Lisseaur's tract, and dorsal root entry zone. There is also a contralateral increase in GFAP labeling 14 days after SRA. Scale=100µm

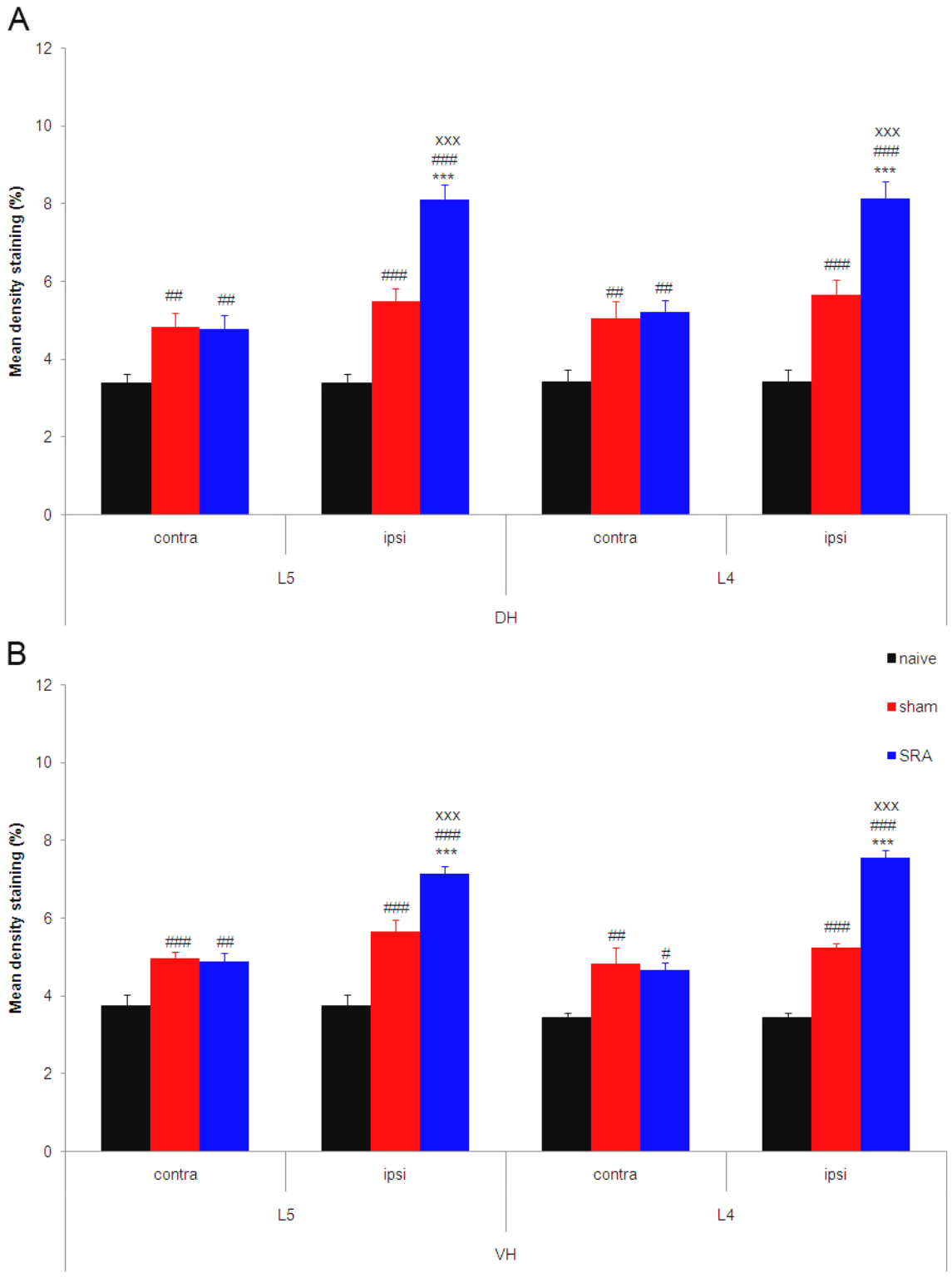

Figure 4.20: Quantification of GFAP staining in the dorsal (A) and ventral (B) horns of deafferented (L5) and intact (L4) segments. GFAP was increased in all areas, bilaterally, in sham and SRA tissue against naïve levels. Increase in GFAP in SRA from sham levels was significant in both L5 and L4 dorsal (A) and ventral (B) horns ipsilaterally. Comparisons between and injury vs naive (#), SRA vs sham **(x),** and ipsilateral vs contralateral (*) are shown. N=6 in each group.

4.2.3.2.6: Microglial reactivity

Microglia were identified through immunohistochemical labelling of ionized calcium binding adaptor molecule 1 (Iba1) and quantified for density staining. Q-win analysis of naïve tissue equated L4 density staining values of 1.60% (+/-0.35) for dorsal horn and 0.98% (+/-0.18) for ventral horn, and L5 density staining values of 1.58% (+/-0.38) for dorsal horn and 0.88% (+/-0.18) for ventral horn (Fig 4.22). No significant difference was found between cord sides, or segmental levels.

In 14 day sham tissue, a significant increase in Iba1 staining was observed bilaterally in L4 and L5 ventral horns compared to naïve, but not in the dorsal horns (Fig 4.21 and Fig 4.22). A significantly greater Iba1 density was found ipsilaterally compared to contralaterally in L5, but a similar comparison in L4 did not reach significance. No difference was found between L4 and L5 segments. Density staining values fell within a range of 2.04% (+/-0.31) and 3.57% (+/-0.67) within the L4-L5 cord for sham.

14 days after SRA, Iba1 density was significantly upregulated in dorsal horn microglia ipsilateral to the deafferentation, in L5 and L4 segments, compared to sham, naïve, and contralateral levels (Fig 4.21 and Fig 4.22A). In the L5 ipsilateral segment Iba1 expression could be seen intensely in the DREZ that spreads throughout the superficial laminae (Fig 4.21). A marked difference in Iba1 expression can be seen in the intact L4 ipsilateral segment with increased expression throughout the superficial and deep dorsal laminae and dorsal columns (Fig 4.21). Ipsilateral Iba1 density staining reached 9.01% (+/-1.11) in L4 and 10.1% (+/-1.22) in L5, with no significant difference between these segments (Fig 4.22A). In the contralateral dorsal horn of L4 and L5, a significant increase in Iba1 expression was found against naïve levels, but not against sham (Fig 4.21 and Fig 4.22A).

Iba1 expression was significantly increased in the ipsilateral ventral horns of L5 and L4 segments 14 days after SRA, compared to sham, naïve, and contralateral levels (Fig 4.21 and Fig 4.22B). In the L5 and L4 ipsilateral segments Iba1 expression was upregulated around motor neurones, clustering tightly in the lateral aspect of the ventral horn (Fig 4.21). Ipsilateral Iba1 ventral horn density staining reached 10.2% (+/-0.93) in L4 and 10.5% (+/-0.91) in L5, with no significant difference between these values (Fig

4.22B). A significant contralateral increase in Iba1 expression, against naïve, was found in L5 and L4 segments (Fig 4.21). However only in L5 [3.21% (+/-0.37)] was this Iba1 expression greater than sham levels (Fig 4.22B).

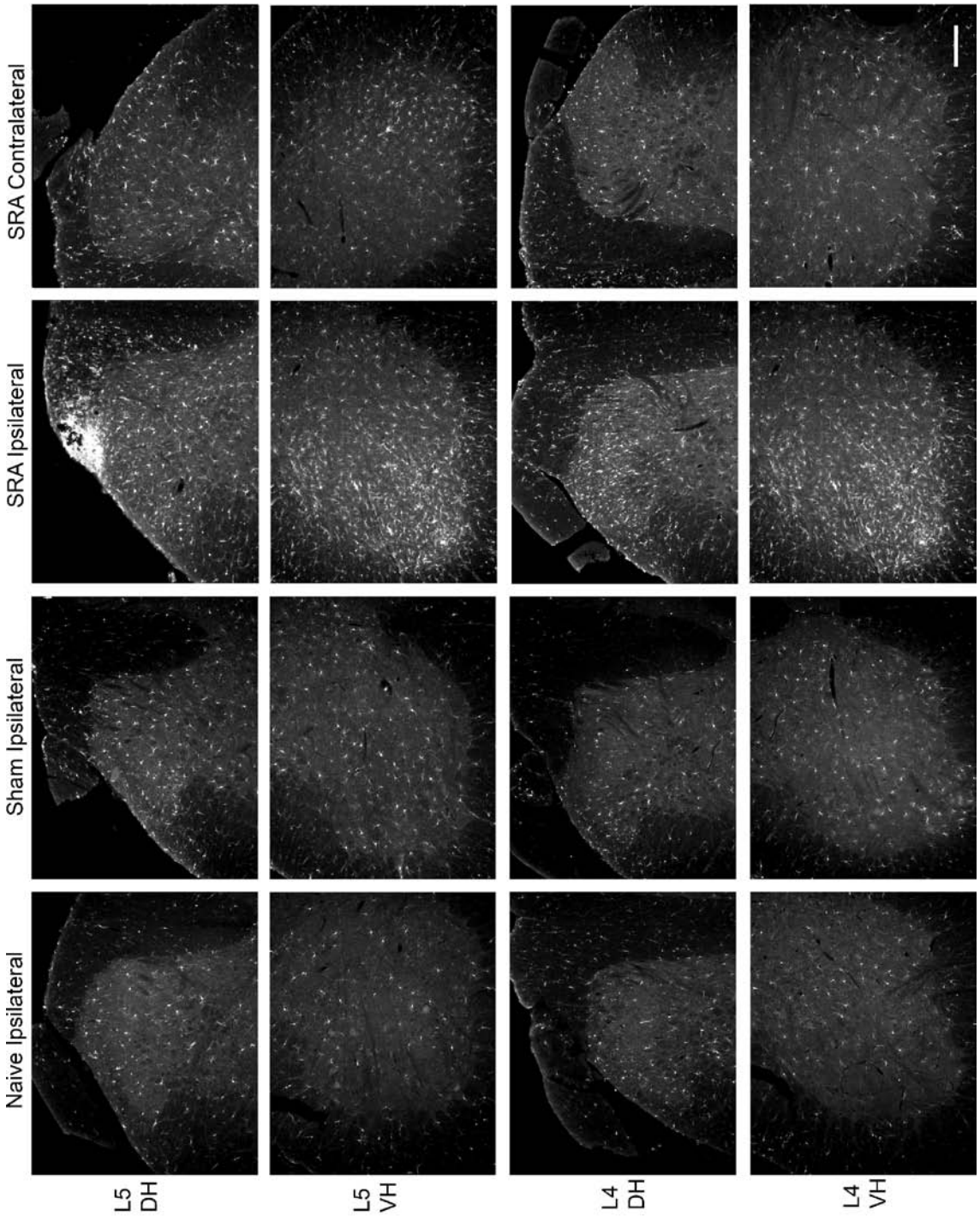

Figure 4.21: Representative images of Iba1 density staining in dorsal and ventral horn in deafferented-L5 and intact-L4 segments. Increase in Iba1 labeling can be seen in sham dorsal and ventral horns, in both L5 and L4 segments. Further increase in Iba1 labeling can be seen in SRA 14 days after SRA, surrounding motor neurones in L4 and L5 segments, and within superficial dorsal horn, Lisseaur's tract, and dorsal root entry zone in L5, and throughout the dorsal horn laminae in L4. A contralateral effect is also observed. Scale=100µm

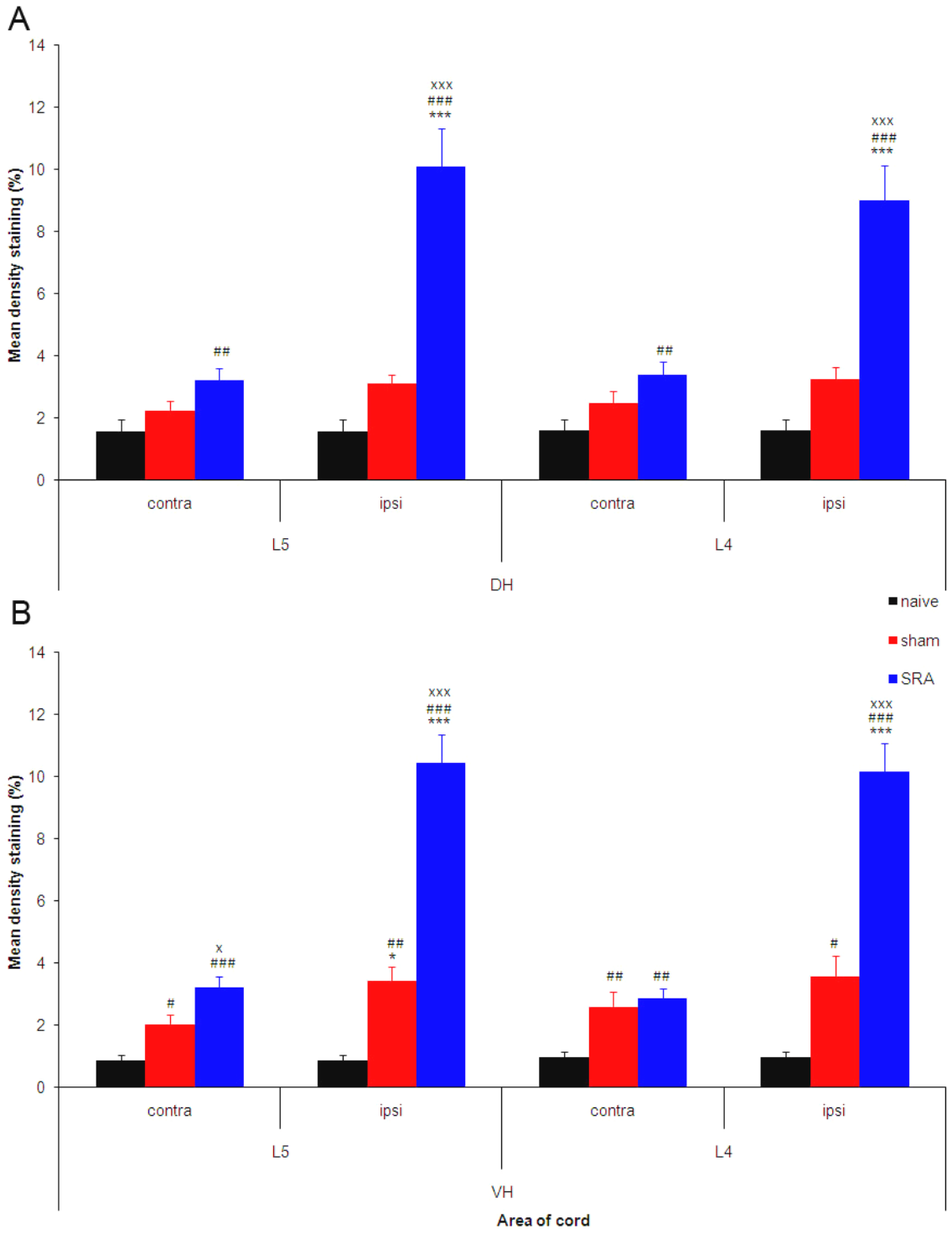

Figure 4.22: Quantification of Iba1 staining in the dorsal (A) and ventral (B) horns of deafferented (L5) and intact (L4) segments. Iba1 was increased bilaterally in the ventral horn (B) after sham surgery, compared to naïve levels. 14 days after SRA levels of Iba1 were increased in all areas of the cord investigated, compared to naïve levels. Increase in Iba1 labeling in SRA was significant from sham in both L5 and L4 dorsal (A) and ventral (B) horns ipsilaterally, with a small but significant increase in the contralateral L5 ventral horn Comparisons between and injury vs naive (#), SRA vs sham **(x),** and ipsilateral vs contralateral (*) are shown. N=6 in each group.

4.3: Discussion

4.3.1: Summary

The new findings of this study can be summarised as follows:

Avulsion of the L5 spinal root leads to only a minor incorrect plantar placement of ipsilateral paw at 1 day that does not progress in severity across 14 days. A reduced weight gain is observed across 14 days in SRA rats, suggestive of ongoing, or spontaneous, pain. Avulsion of the L5 spinal root also leads to behavioural hypersensitivity to thermal and tactile stimulation. Thermal hypersensitivity peaks by 5 days and remains unchanged thereafter. Tactile hypersensitivity develops rapidly and increases over the first month before plateauing and remaining unchanged thereafter.

Avulsion of the L5 spinal root does not lead to significant phenotypic changes in subpopulations of DRG neurones in the adjacent L4 segment, or activation of satellite glia. Expression levels of the receptor TRPV1, associated with thermal hypersensitivity, remain unchanged. An increase in ATF3 is observed in the L4 DRG, but its biological significance remains to be determined.

An ipsilateral dorsal horn neuronal loss accompanies hypersensitivity at 14 days after SRA injury; however, it is mild (~5% in L4 and ~8% in L5), associated with cavitation and trauma around the lesion site, and is not anatomically correlated with primary afferent loss in the deafferented regions. The neuronal loss in L4 may be associated with the spread of tissue damage from L5.

A more significant motor neurone loss is found in SRA animals at 14 days, but values are dependent upon the method of histological identification. NeuN labelling gives a more severe ipsilateral motor neurone loss of ~69% in L5 and ~47% in L4. Tol blue histological dye counts show only ~43% loss in L5 and ~27% loss in L4, suggesting epitope expression may well be a dependent factor in the accuracy of determining neurodegeneration. The loss of motor neurones in L4, is in accordance with the anatomical rostro-caudal spread of motor fibres from ventral horn to root, suggesting a

population of L5 motor efferents originating in the L4 segment (Nicolopoulos-Stournas and Iles, 2004).

L5 SRA leads to loss of microvascular staining in the dorsal and ventral horns of both L5 and L4 segments, bilaterally, in accordance with previous results on L3-L6 DRA studies at 14 days (see section 3.2.4).

Macrophage recruitment 14 days after SRA injury is preferentially targeted at the zone of primary trauma, i.e. the DREZ and dorsal columns. Small particulate staining is noted in the ventral horns of L4 and L5, but it is inconsistent, and biological significance remains to be indentified. L5 macrophages are primarily associated with the DREZ, and densely cluster within this region. L4 macrophages are primarily associated with the dorsal columns and are much less densely packed as noted through density analysis imaging.

Astrocytes in the L4 and L5 dorsal and ventral horns upregulate GFAP after SRA. A small but significant upregulation is noted contralaterally, as well as bilaterally in sham tissue. In the L5 segment astrocytes are intensely labelled in the DREZ around areas of cavitation, tissue trauma, and glial scarring. Astrocytes within the L4 dorsal horn are also upregulated but are less associated with tissue damage, and are spread throughout the dorsal horn. Astrocytes in the ventral horn surround motor neurones in L4, and densely cluster in the L5 region in areas that appear devoid of motor neurones.

Fourteen days after SRA microglial activity is greatly upregulated in the region of primary trauma i.e. the DREZ of L5, most likely representing activated, phagocytic microglia. This expression extends into the dorsal column and dorsal horn. Increased microglial expression is observed in both the L4 and the L5 dorsal horns, in both number of cells and intensity of Iba1 expression. Prominent microglial activation, with increased number, increased Iba1 expression intensity, and clustering is found in the ventral horn of both L5 and L4 segments, and is associated with the lateral motor neurone pools. A small but significant Iba1 upregulation is noted contralaterally in L5 and L4 dorsal and ventral horns. Iba1 expression increase is observed only in the ventral horn after sham surgery.

4.3.2: Behavioural effects of L5 SRA

4.3.2.1: L5 SRA leads to an incorrect hind paw plantar placement

Avulsion of the L5 spinal root leads immediately to an ipsilateral hind paw locomotor impairment. This impairment is maintained across 14 days, but is classified as only a mild plantar misplacement. L5 ventral root avulsion leads to a loss of fine control of plantar placement. Rats are able to successfully make a coordinated step, via swinging the affected limb and placing weight supported stance on the rung of the ladder. This suggests that loss of the L5 motor root is not sufficient at fully denervating the hind paw. The motor output from the L6 and L3 roots are capable of controlling hindlimb swing and stance phases of locomotion, with L4 compensating for the loss of L5 by maintaining plantar placement. Importantly, as each of the three joints of the hind limb are still innervated, the rat can still effectively withdraw the limb when stimulated by mechanical or thermal stimuli. It has been shown that motor neurone plasticity occurs in the adjacent spared ventral motor neurones after single ventral root rhizotomy in the cat (Holmberg and Kellerth, 2000), with monosynaptic reflexes enhanced by >200% (Holmberg and Kellerth, 1996). This motor neurone plasticity has been further characterised in rat dorsal root rhizotomy (Cuppini et al., 1999;Cuppini et al., 2002) with individual motorneurone peripheral receptive fields within the deafferented segment enlarged five to six times (Cuppini et al., 1998). This increase in synaptic density is likely to occur through activity dependency and sensory input from monosynaptic reorganisation (Holmberg and Kellerth, 1996;Cuppini et al., 2002). This plasticity may strengthen remaining monosynaptic reflex arcs and aid in locomotor compensation in the limb, which explains why only mild paresis is detected in L5 SRA.

When both L5 and L4 ventral roots are avulsed the rat is unable to flex the ankle and initiate plantar paw placement, and it scores a 5 on every rung (data not shown). However, the animal still has hip and knee flexion, and attempts to make a coordinated step. Therefore, it is indeed the L4 root that compensates for L5 motor loss of the hind paw, and that L3 and L6 roots functionally control hip and knee movement only.

4.3.2.2: L5 SRA leads to a reduced gain in weight

Reduction in weight gain has previously been used as a surrogate measure of a neuropathic pain syndrome for sciatic nerve (Willenbring et al., 1994) and trigeminal nerve injury (Imamura et al., 1997). Here, it is similarly used as a measure of spontaneous or ongoing pain after avulsion injury. A significant reduction in animal weight is found in SRA injured animals across 14 days compared to naïve with a trend against sham. It is unlikely that SRA animals undergo unique metabolic changes that lead to reduced body weight compared to sham litter mates. Loss of muscle mass in the avulsed limb, known to occur at longer time points in the range of 350-400mg across 12 weeks (Gu et al., 2005), is unlikely to play a part in gross weight changes. Access to food is unlikely to change in SRA rats, as locomotion was not significantly impared in these animals across 14 days. The most likely explanation is loss of appetite due to ongoing behavioural changes associated with SRA neuropathy, indicative of chronic pain.

4.3.2.3: L5 SRA leads to a delayed and maintained hypersensitivity

This report does not use the terms hyperalgesia or allodynia to describe the hypersensitivity developed after SRA. Hyperalgesia is defined by the International Association for the Study of Pain (IASP) as *'an increased response to a stimulus which is normally painful'*, and allodynia defined by IASP *'pain due to a stimulus which does not normally provoke pain'*. In these cases this terminology has been useful for clinicians to describe the nature of a symptom that is presented to them in the clinic. The description is defined by the patient's reaction to the question 'is this painful' rather than a withdrawal response. The rat on the other hand has no such capability, and withdrawal latency is the only quantitative measure available. Previous literature has defined an allodynic response to Von Frey hair testing as 0-1g threshold for peripheral nerve crush (Decosterd and Woolf, 2000), 1g threshold for L5/L6 spinal nerve ligation (Chaplan et al., 1994) and 2-5g threshold for chronic constriction of the sciatic nerve (Luo et al., 2002), using the 'up-and-down' analytical method (Dixon, 1980). To compare, in the case of L5 SRA minimal threshold withdrawal is a lot higher, at 6.44g across 60 days, using a slightly different tactile stimulus, the automated plantar aesthesiometer. This does not require the 'up-and-down' testing parameter to indicate a

50% response rate used for Von Frey hairs, and instead gives an exact value of hair weight and latency withdrawal. It would therefore be more appropriate to define significant lowering of threshold withdrawal as hypersensitivity, and 'suggestive' of a possible neuropathic pain state, rather than allodynia. Thermal hyperalgesia on the other hand is defined by Hargreaves *et al.*, ((Hargreaves et al., 1988)), using the nociceptive thermal plantar test as a decrease in threshold and SRA rats show on average a 25-30% decrease in threshold.

Avulsion of the L5 mixed spinal root results in delayed development of thermal hypersensitivity over 3 days, and an immediate development of mechanical hypersensitivity. This time scale is in accordance with clinical findings of avulsion pain development (Berman et al., 1996). Hypersensitivity is maintained at least up to 60 days post injury, and becomes progressively more severe in the case of tactile stimulation. The hypersensitivity is located at the borderzone of L4/L5 but it is unclear how far this spreads medially or laterally on the plantar surface. The withdrawal of the limb is usually accompanied by adverse behaviours such as lifting and licking or biting of the innervated side of the paw, and agitated movement around the testing box. This type of behaviour is in accordance with previous literature (Kim and Chung, 1992;Choi et al., 1994). Many peripheral nerve neuropathic pain models exist (Wall et al., 1979;Bennett and Xie, 1988;Seltzer et al., 1990;Kim and Chung, 1992;Decosterd and Woolf, 2000). This model is the first example of a clinically representable and reproducible hypersensitivity development after spinal root avulsion injury. No contralateral effects were noted either in thermal or mechanical withdrawal thresholds. A transient mechanical hypersensitivity is observed ipsilaterally after sham surgery. This has been shown previously by similar surgical root exposure (Hashizume et al., 2000a). As this hypersensitivity is generally observed as mild, and is reversed at 14 days, this activity is unlikely to be biologically significant in the long term.

4.3.3: Histological effects of L5 SRA

4.3.3.1: L5 SRA does not lead to phenotypic or degenerative phenomena in the intact adjacent L4 DRG

Phenotypic changes in CGRP, IB4, and N52 are not present in the intact DRG after adjacent L5 avulsion. This is consistent with previous literature on spared nerve injury (Hammond et al., 2004), and implies hypersensitivity seen in this case is not driven by changes in DRG phenotype, or selective loss of a subpopulation. However using in situ hybridization CGRP mRNA has been shown to be upregulated in the intact L4 DRG neurones after L5 spinal nerve ligation (Fukuoka et al., 1998), but without changes in overall cell size or number, or changes in any other peptides such as NPY, VIP, galanin, or SP. This previous literature, and data now provided in this thesis, suggests that peripheral nerve injury, but not a central root injury, can induce transcriptional changes to the adjacent DRG, and this is most likely linked to Wallerian degeneration in the former that is absent in the latter. However phenotypic changes cannot be excluded from the L4 DRG as marker such as BDNF, NGF, NPY, Galanin, or NOS have not been analysed.

Data in this thesis shows no change in the percentage of L4 DRG neurones expressing TRPV1 at 14 days post L5 SRA, in contrast to the upregulation of this receptor in spared DRG after PNI as a result of Wallerian degeneration and cytokine interaction with uninjured axons (Hudson et al., 2001;Fukuoka et al., 2002;Obata et al., 2006a). This result does not of course rule out possible upregulation of TRPV1 receptors in neurones already expressing this receptor, as intensity staining analysis was not performed; however, there was no obvious qualitative change by eye. It can be inferred, from these results, that the thermal hypersensitivity seen across 60 days after SRA is mediated by other means than changes in populations of TRPV1 expressing primary afferent neurones in the adjacent uninjured DRG, such as changes in the CNS.

No increase in GFAP staining was seen in the intact L4 DRG at 14 days. Satellite cell activation is believed to be a mediator of neuropathic pain after PNI (Hu and McLachlan, 2003) and inflammatory pain (Dublin and Hanani, 2007), but activity peaks early at 3-7 days then decreases after (Woodham et al., 1989;Fenzi et al., 2001;Zhang et

al., 2009), perhaps suggesting 14 days is too late to observe satellite cell activity after SRA injury. However as hypersensitivity in the SRA model is maintained for much longer periods (>60 days), and in the case of tactile hypersensitivity becomes more severe beyond 18 days, peripheral satellite cell activity is unlikely to be an essential mediator of maintained neuropathic pain behaviour after avulsion.

The ATF3 findings are of great interest as the ipsilateral L4 DRG is referred to in PNI literature as 'uninjured' (Hudson et al., 2001;Hammond et al., 2004). Sciatic nerve crush (Averill et al., 2002), and L5 spinal nerve transection (Shortland et al., 2006a), results in ATF3 expression in almost all injured DRG neurones by 1 day. Interestingly in the spared L4 DRG in the L5 spinal nerve transection, as well as the sham, ~11% ATF3 expression is found colocalised with upregulation of NOS, galanin, and NPY (Shortland et al., 2006a). These authors suspected that the surgical procedure of exposing the L5 spinal nerve caused direct damage, albeit mild, to the sensory afferents of L4. The data in this thesis shows a ~5% ATF3 expression increase in L4 DRG after L5 mixed root avulsion. Part of this small increase may be due to surgical exposure, as sham animals also expressed low levels of ATF3 (~1-2%). Furthermore, a small contralateral ATF3 expression is seen in the L4 DRG after SRA, suggesting the surgical incision and spread of the paraspinal muscle tissue with retractors during surgery may affect the primary afferents that innervate those dermatomes, bilaterally. This is not functionally significant however. It is likely both the exposure of the L5 spinal root, in sham and SRA, and the surgical disruption of overlying tissue during exposure, leads to a slight but significant increase in ATF3 expression in these cases. The ATF3 increase in these cases is unlikely to be functionally significant as it affects a small number of afferents. What is unknown, however, is the effect of surgical exposure on the L5 DRG, as this DRG was not analysed.

The reason for the discrepancy between the negative findings in L4 DRG after L5-SRA, compared to other literature on spared nerve PNI, can be explained through differences in model. Obata *et al.*, (Obata et al., 2006b) found that when comparing a 'peripheral' nerve injury model (L5 spinal nerve transection) with a 'central' root model (L5 dorsal and/or ventral root rhizotomy) markedly different levels of BDNF were found in the DRGs. 7 days after L5 DRR or L5 spinal root rhizotomy, upregulation of BDNF was found in the L5 DRG but not L4, and neuropathic pain was absent from the affected

hindpaw. L5 VRR lead to hypersensitivity, and BDNF expression only in L5 DRG. Whereas 7 days after L5 spinal nerve transection, BDNF was upregulated in both L5 and L4 DRG, and correlated with robust mechanical and thermal neuropathic behaviour (Obata et al., 2006b). The authors suggest that this discrepancy is due to the loss of direct connection of the DRG axons to the dorsal horn neurones in dorsal and spinal root rhizotomy, whereas peripheral injury and VRR maintains DRG connection. This root connection provides anterograde BDNF transport from the periphery nerve, to primary afferent terminals in the dorsal horn, where it can sensitize dorsal horn neurones. Indeed L5 DRR does reduce L5 dorsal horn BDNF-ir (Zhou and Rush, 1996), compared to L5 VRR (Obata et al., 2004) and L5 SNT (Michael et al., 1999) that leads to an increase. Upregulation of BDNF within the L4 DRG, and corresponding neuropathic pain, were proposed to be due to Wallerian degeneration of L5 sensory fibres after PNI, that is absent after dorsal root or ventral root injury (Obata et al., 2006b). Also NGF, a factor that controls the expression of many proteins such as TRPV1, CGRP, substance P, and BDNF, is upregulated in both intact and injured C-fibre DRG neurones after 'spared' PNI, but only in injured C-fibres DRG neurones and not adjacent intact afferents after rhizotomy (Obata et al., 2004). NGF is also upregulated in the spared DRG, and implicated in sprouting, 6 days after extensive adjacent lumbar ganglionectomies in the cat (Zhou et al., 2009). BDNF and NGF have been shown to increase in the L4 intact DRG after selective L5 spinal nerve ligation (Fukuoka et al., 2001;Obata et al., 2004), and coincided with the development of hypersensitivity. Selective antibody blockage of these two growth factors ameliorated the hypersensitivity. It is implied that peripherally driven hypersensitivity after spared PNI, as well as peripheral inflammatory pain, is in part mediated through decrease in NGF competition between injured and intact axons (Fukuoka et al., 2001)(Fukuoka *et al.*, 2001), increase in p38 MAPK activity through NGF, leading to BDNF expression in the intact DRG soma and terminals of the dorsal horn, modulating the processing of nociceptive information (Obata and Noguchi, 2006).

Retrograde growth factor transport occurring in the intact L4 after SRA cannot yet be ruled out, as levels of BDNF and NGF in the L4 DRG are yet to be elucidated. BDNF and NGF are clearly important markers yet to be analysed in the DRG after L5 SRA before exclusively ruling out their contribution to peripherally driven neuropathic pain behaviour.

4.3.3.2: L5 SRA leads to neurodegeneration and neuroinflammation in the intact L4 spinal segment that mirror the effects in the deafferented L5 spinal segment

Effects within the intact L4 segment significantly mirror the effects within the deafferented L5 segment, such that no difference can be quantified for dorsal horn neuronal loss, reduced endothelial labelling, and astroglial and microglial activation. This gives evidence to the argument that central neurodegenerative and neuroinflammation effects within a region adjacent to a localised deafferentation insult, could be a mechanism by which evoked neuropathic pain behaviour after SRA is generated. The effects could have 2 centrally mediated mechanisms. Firstly, a direct spread of reactive gliosis and degenerative phenomena may occur from the L5 segment that overlaps into the adjacent L4, through paracrine glial-glial activation (Milligan and Watkins, 2009). Secondly, degeneration of the L5 primary afferent terminals that terminate within the L4 segment (Shehab, 2009), and loss of avulsed L5 motor neurones that are anatomically located in the L4 ventral horn (Nicolopoulos-Stournaras and Iles, 1983) most likely lead to these histological events in the adjacent L4 segment. This is also evident when observing the caudo-rostral degeneration of primary afferent fibres that progress through spinal segments in the dorsal columns up to the dorsal column nuclei (George and Griffin, 1994b). As there is yet no evidence to suggest a phenotypic change, or primary afferent or sympathetic sprouting in the L4 DRG and terminals after L5 root injury; the gliotic events, the neurodegenerative, vascular degeneration, and macrophage infiltration in the L4 segment are likely to be due principally to the above two points.

4.3.3.2.1: Ventral horn

Motor neuronal loss

At 14 days post L5 SRA a loss of motor neurones is found in the ventral horn of the L5 avulsed ventral horn are consistent with previous literature using cresyl violet, choline acetyltransferase, SMI32, and CTB-retrograde tracing (Koliatsos et al., 1994;Hoang et al., 2003;Bergerot et al., 2004;Penas et al., 2009). Percentage cell loss varied between authors (33-80%) due to different number of roots avulsed but also different labeling techniques. Motor neurone loss is variable depending on the method of staining used to

identify the cells in this thesis. Approximately 69% of ipsilateral motor neurones were absent from the cord compared to contralateral counts using NeuN immunohistochemistry and ~43% using Tol Blue in the L5 segment. The greater loss at 14 days using NeuN staining to identify cells is likely due to loss of epitope expression in motor neurones, leading to a greater reduction in positive cell counts. Previous authors have already suggested that NeuN expression, and also with ChAT and other antibody markers, may not accurately represent the amount of cell loss, but rather reflect the physiological state of the neuron (McPhail et al., 2004a). However this may not just be a problem with antigens, as it has also been noted when using cresyl violet compared to SM132 immunohistochemistry at 28 days post avulsion (Penas et al., 2009); the former underestimates the motor neurone loss. This may be due to loss of Nissl bodies within surviving neurones after lesion that reduces cresyl violet staining. Not only is there a discrepancy with staining methods, but also with the type of transection injury, where after distal axotomy of the ventral root after an initial loss of ChAT at 7 days, most motor neurones re-express this marker and survive up to 1 month (Rende et al., 1995;Matsuura et al., 1997). It may be due to levels of phosphorylated-neurofilament from the axons that axotomised motor neurones accumulate compared to avulsed motor neurones which define the extent of cell survival (Koliatsos et al., 1989;Penas et al., 2009), this may in turn be due to proximity of injury to cell body and extent of remaining axon connected to it. In this work, the NeuN epitope may be downregulated in the injured motor neurones before they are either dead or phagocytosed from the tissue. The Toluidine Blue dye will label all cells irrespective of whether they are living, as long as there is cytosol, and the cell membrane is intact. This suggests that a large population of motor neurones ~26% (difference between values) may be present in the ventral horn after injury, but are in the process of dying or being phagocytosed, and cannot be visualized using immunohistological techniques. Indeed, there is further significant motor neurone loss between 14 and 28 days (Penas et al., 2009). The best way to represent this population of motor neurones is to use double labeling histology techniques, employing for example diaminobenzidine (DAB) visualisation of NeuN, colabelled with Tol Blue.

The surprising loss of 47% (using NeuN) and 27% (using Tol Blue) of motor neurones in the L4 segment after L5 SRA is unlikely to be due to loss of L4 motor efferent fibres. If L4 motor neurones were dying, the ipsilateral locomotor function, which is solely

reliant upon the L4 root after L5 SRA, would not be so well maintained across 14 days. This loss most likely represents the population of avulsed L5 motor neurones that are anatomically located within the L4 segment (Nicolopoulos-Stournaras and Iles, 1983). HRP labeling of the soleus muscle in neonate rats, has indicated that L5 ventral root rhizotomy leads to loss of the lumbar motor neuronal pool and transmitter concentration, throughout the L5 and L4 segments (Lowrie et al., 1985), suggesting a large rostro-caudal intermingling of L4/L5 motor efferents that are not segregated to corresponding spinal segments, at least in young animals. It may also be possible to infer that the remaining motor neurones in the L5 segment after 14 days, could actually be labeling of neurones from L6 or L4 motor efferents, rather than surviving L5 motor neurones. Therefore, one way to identify definitively the remaining 'true' population of injured L5 efferents, is to induce a delayed injury to the L4 root 1 day prior to sacrifice, and label ATF3 to identify the rostrocaudal distribution of the intact L4 motor neurone pool, as it is rapidly upregulated within 12-24 hours after injury (Tsujino et al., 2000;Shortland et al., 2006a).

Gliosis and phagocytosis

The upregulation of markers for astrocytes and microglia in the ventral horn specifically around motor neurone pools after avulsion, is consistent with previous literature (Ohlsson et al., 2006;Penas et al., 2009). Microglial cells appear to wrap up the soma of avulsed motor neurones in L5 and L4 segments. Microglial reactivity spreads over to the L5 contralateral side, and to a smaller extent in L4, in accordance with previous literature of root ligation and avulsion (Winkelstein and DeLeo, 2002;Penas et al., 2009), and this is most likely through increased commissural interneuronal activity, that coordinates bilateral locomotor function (Eide et al., 1999), or through diffusible agents such as cytokines produced in the ipsilateral spinal cord (Penas et al., 2009). Microglia presented in both ramified and amoebic form suggesting distinctly different roles, in phagocytosis of neuronal debris (Streit and Kreutzberg, 1988), neuroprotection and regeneration (Aldskogius, 2001;Streit, 2002), and conversely neurodegeneration (Brown and Neher, 2010). Phagocytic microglia have a specific NADPH oxidase called phagocytic oxidase (PHOX), that when activated by cytokines or TNFα, for example, lead to phagocytosis (Brown and Neher, 2010). Phagocytic microglia have been observed surrounding axotomised facial motor neurones (Streit and Kreutzberg,

1988;Angelov et al., 1995). Microglia transiently upregulate pro-inflammatory cytokines, such as IL-1β, IL-6, TNFα, and heat shock proteins, that as well as hyperexciting neurones (Milligan and Watkins, 2009), can also be neuroprotective to axotomised facial motor neurones (Raivich, 2001), and motor neurones after SCI (Reddy et al., 2008). However, after CNS injury or ischemia microglia also produce neurotoxic compounds such as free radicals (Boje and Arora, 1992), glutamate (Giulian et al., 1993b;Giulian et al., 1993a) and complement components (Bellander et al., 2001;Ohlsson et al., 2003) that lead to neuronal cell death (Brown and Neher, 2010). The controversy in the literature over the role of microglia in certain injury models, may be explained by different activation states of microglia that as yet cannot be physiologically characterized by histological labels such as Iba1.

There is a clear difference in the extent of microglial activity compared to astrocyte reactivity, with the former expressing higher ipsilateral levels than the latter after L5 SRA, compared to respective sham and contralateral values. Astrocyte reactivity can be seen as extensions of dendritic branching around motor neuronal pools of L5, clustering and tightly wrapping around motor neurones in accordance with previous literature (Ohlsson et al., 2006;Penas et al., 2009). This tight astrocyte-motor neurone correlation was not as obvious in the L4 segment however, rather an upregulation of GFAP expression in resident astrocytes was the key to increased density staining in this case. A small contralateral increase in GFAP is also noted in both segments similar to microglia, and in accordance with previous literature (Winkelstein and DeLeo, 2002;Penas et al., 2009), and is likely to have similar underlying mechanisms of activity that involve commissural fibres or diffusible molecules originating from the ipsilateral cord. This robust microglial activity compared to a weaker astrocyte response has been shown before in facial motor neurone pools after transection (Graeber et al., 1988b;Graeber et al., 1988a), and sciatic nerve ligation (Narita et al., 2006), and ventral root injury (Penas et al., 2009). The reason behind this inequality in activity between these glia is due to the observation that only microglial cells undergo mitosis and extensive proliferation early after motor neurone injury (Graeber et al., 1988a;Narita et al., 2006;Penas et al., 2009), and that hypertrophy and lamella process development of astrocytes is delayed, and absent of mitotic proliferative development (Graeber et al., 1988b;Penas et al., 2009). Activated astrocytes may have a role, unique from microglia, in synaptic detachment around axotomised motor neurone cell bodies (Svensson and

Aldskogius, 1993) after SRA, providing a viable perisynaptic environment for synaptogenesis (Emirandetti et al., 2006), and in this way provides structural support for avulsed motor neurones and traumatized ventral horns, and prevention of inappropriate synaptic activation. Astrocytes may therefore protect remaining motor neurones and spinal tissue during the latter scarring period after an initial axotomy, whereas microglia are involved in early debris clearance and continuing immunity. Indeed as no severe loss of motor function occurred across 14 days, these glial effects within the ventral horn do not indicate detrimental activity.

Punctate ED1 positivity was found in the L4 or L5 ventral horn at 14 days post SRA, with occasional clustering around motor neurones as observed previously (Koliatsos et al., 1994). However, the staining did not show morphology corresponding to that known to occur during phagocytosis. Interestingly, sciatic nerve CCI or transection causes an ED1 positive macrophage response in the ventral horn, without signs of typical phagocytic morphology or, strangely, cell loss (Hu et al., 2007). After extensive L5-S2 ventral root avulsion at 28 days ED1 positive macrophages were seen in the ventral horn (Ohlsson et al., 2006), and was small and punctuate, similar to the staining described in this thesis. These results suggest that macrophages have little function in phagocytosis of motor neurones themselves after injury, but more likely phagocytose degenerating sensory 1a afferent fibres synapsing with the motor neurones. The question remains however, as to how the large motor neurone cell bodies are removed from the spinal cord after they die. Perhaps this can be explained by implication of an autophagic process (Lee, 2009) of motor neurones after root avulsion, that has been shown to occur to motor neurones after ischemic injury *in vivo* (Baba et al., 2009) and glutamate excitotoxicity *in vitro* (Matyja et al., 2005). These hypotheses, however, remain to be tested.

Sham exposure of the L5 root leads to a small GFAP and Iba1 staining intensity increase in the ventral horn bilaterally. Typical structural changes of the glial cells, noted in SRA tissue, does not occur, rather an increase in epitope expression within cells is the key to increased density staining, similar perhaps to contralateral effects in SRA tissue. Increase in microglial and astroglial intensity staining in the ventral horn has been noted before in sham peripheral nerve exposure rat models as early as 3 days (Colburn et al., 1997), and also at 1-14 days after sham root exposure (Winkelstein and

DeLeo, 2002). L5 spinal root exposure could therefore be classified as a peripheral nerve injury in itself, such that it leads to increased glial reactivity in the ventral horn. However the manifestation of a mild and transient mechanical hypersensitivity in sham, is likely controlled by dorsal horn glial activity (Section 4.3.3.3.2). No ventral horn neuronal loss or locomotor impairment was noted in sham, and therefore these ventral horn glial effects are unlikely to be biologically significant.

Endothelial staining loss

Reduction of vascular integrity in the ventral horn after L5 SRA is an interesting new finding, and mirrors bilateral RECA-1 loss in the dorsal horn after L3-L6 DRA and L5 SRA. This suggests that it is not the scale of deafferentation that defines permanent endothelial degradation, but the nature of trauma, such that avulsion prevents natural recovery of the spinal cord vasculature. As described in Chapter 3, it is likely that tensile stress on the spinal cord driven through avulsion forces, damages the spinal cord leading to vasculature disruption, in a similar way to traumatic SCI. However just as dorsal root avulsion could damage the single posterior spinal vein, through direct traction trauma or scarring (Section 3.3.6) damage to the single anterior spinal artery and vein that course along the anterior median fissure, and supplies the corresponding ventral portion of the cord, may explain the loss of RECA-1 endothelial staining in the ventral horn bilaterally after L5 SRA. It also explains the effects in the intact L4 segment, as the anterior spinal artery contributes 75% of blood supply to the whole spinal cord (Grace and Mattox, 1977), and occlusion at one segment could effect the adjacent. This loss of vascular integrity could exacerbate motor neuronal loss through necrosis or secondary injury cascades (Nelson et al., 1977;Mautes et al., 2000). However as detrimental contralateral effects were not noted in either locomotor function or motor neurone loss, it is unlikely that the effects of RECA-1 immunostaining are functionally significant. Further RECA-1 staining does not give an appropriate determination of vascular integrity and ischemic effects on the ventral cord. More detailed analysis of blood flow through the arteries and veins that surround the spinal cord is required before conclusively implying trauma to the vascaular system and ischemia within neuronal tissue.

4.3.3.2.2: Dorsal horn

Neuronal loss

A small neuronal loss after L5 SRA was found in the superficial dorsal horn of L5. Neuronal loss was anatomically correlated with tissue cavitation and scarring located near the DREZ. Most neurones will be lost through this direct trauma of root avulsion in SRA similar to DRA (Chew et al., 2008). However, the loss in L4, albeit much smaller, represents perhaps transynaptic cell death within an intact segment. This could occur through caspase-dependent apoptosis initiated by ectopic activity from the spared afferents of L4, such as has been implicated for L5 spinal nerve injury (Scholz et al., 2005), however there is no evidence to suggest injury-induced changes to L4 DRG neurones. Another possibility could be that cell death is initiated by loss of L5 primary afferent terminals, that synapse with second order dorsal horn neurones in the L4 segment, though glutamate excitotoxicity from degenerating post synaptic membranes. It is well established in the rat and cat that afferent fibres enter the lumbar cord, send projections rostrally and caudally that terminate in laminae of adjacent segments, with an extensive overlap (Molander and Grant, 1985;Swett and Woolf, 1985;Smith and Bennett, 1987;Culberson and Brown, 1984;Rivero-Melian and Grant, 1990). Partial loss of the IB4 terminal 'eyebrow' in lamina II of the adjacent L4 segment indicates overlap of L5 primary afferents. However, colocalisation of NeuN and IB4 did not reveal anatomically correlated dorsal horn and primary afferent loss, suggesting that, at least with non-peptidergic terminals, terminal degeneration is unlikely to affect dorsal horn neuronal viability. A fibres and peptidergic C-fibres also need to be analysed in this way to say exclusively there is no transynaptic degenerative link between deafferented L5 terminals and dorsal horn neurones. An alternative mechanism of cell loss could be via neuroinflammatory mediators, reactive oxygen species, cytotoxins, or glutamate (Boje and Arora, 1992;Giulian et al., 1993b;Giulian et al., 1993a;Tsuda et al., 2005). This neuroinflammation, involving microglia, could occur from spread of reactivity from the L5 segment, or via degeneration of the L5 terminals in L4, activating resident L4 segment microglia (see later section on gliosis). Further work needs to be completed to ascertain whether the neuronal loss is restricted to any subpopulation of dorsal horn neurones, such as inhibitory GABAergic interneurones, and as such it is difficult to suggest the implication of this neuronal loss on evoked neuropathic behaviour.

This is the first evidence for dorsal horn neuronal loss found in the intact segment after an adjacent avulsion injury, and may have both peripherally and centrally mediated mechanisms underlying it. Further techniques, such as electrophysiology recordings from the dorsal horn (Ovelmen-Levitt et al., 1984), caspase staining (Scholz et al., 2005), TUNEL staining (Chew et al., 2008), histological dyes such as Tol Blue (Section 3.2.5.3), antibodies targeting subpopulations of dorsal horn neurones such as GABA (Drew et al., 2004), and apoptotic inhibitor administrations (Scholz et al., 2005), are required to ascertain subpopulation specific neuronal loss and assess its implications on behavioural hypersensitivity.

Gliosis and phagocytosis

After PNI, inflammation, and SCI, microglia become activated by a number of diffusible molecular pathways (Inoue and Tsuda, 2009;Marchand et al., 2005;Marchand et al., 2005;Zhang and De, 2006;Thacker et al., 2009), and is now confirmed in spinal root avulsion injury, in both spared (L4) and deafferented (L5) segments.

Similar to the avulsion model, DRA, an increase in glial activity is noted in the dorsal horn 14 days after SRA, including a small contralateral increase. However, it is clear that the greater number of dorsal roots avulsed in DRA (four) leads to a more substantial gliopathy in the dorsal horn than SRA (one). There are noticeable differences in the extent of amoebic transformation of microglia between avulsed L5 and spared L4 segmental levels, with mainly amoebic structure in the former and ramified in the latter. This is in accordance with experimental SCI models, where two different activation states of microglia are indicated (Watanabe et al., 1999). After L5 SRA the first role is most likely focussed on a phagocytic response to degenerating primary afferent fibres and/or necrotic tissue, which will be greater in the avulsed L5 segment than the L4. However, there is a potential for neurotoxicity (Tsuda et al., 2005;Brown and Neher, 2010), and a mechanism of neuronal death in the intact and avulsed dorsal horns after SRA. The second role of the microglial reaction is that of a pro-inflammatory/neuroprotective characteristic, with a ramified activated form, predominating in the L4 segment. Such microglial-neuronal interaction has been linked in previous PNI models to the synthesis and release of TNFα (Lambertsen et al., 2009), HSP (Reddy et al., 2008), cytokines (IL-6 and IL-1β) (Marchand et al., 2005), and

PGE2 (Zhao et al., 2007), that generates a hyperexcitable dorsal horn neuronal population. The prolonged microgliosis in the L4 dorsal horn at 14 days, is suggestive of a substantial role in maintained central sensitisation mechanisms in the SRA model, that is contrary to established thinking of the early 'microglial-astrocyte replacement mechanisms' in PNI (Eriksson et al., 1993;Colburn et al., 1997;Raghavendra et al., 2003), and is more reminiscent of 'microglial-maintained' pain after SCI (Hains and Waxman, 2006). This is perhaps the most important point when elucidating the etiology of avulsion pain. The reaction of microglia, within the dorsal horn L4 segment, provides evidence to suggest the neuropathic pain behaviour after avulsion injury is more closely related to central SCI-pain than PNI-pain, and perhaps treatment of this ailment should be directed at these central mechanisms.

Macrophage activity is temporally linked to the development of hyperalgesia following nerve injury. This has been shown in rats with CCI, administered with liposome-encapsulated dichloromethylene diphosphonate to deplete circulating macrophages (Liu et al., 2000b), as well as genetically modifying mice (C57BL/WLD) that have delayed macrophage recruitment and Wallerian degenerative progression and development of thermal hyperalgesia (Myers et al., 1996;Ramer et al., 1997). Shown here, 14 days after SRA, is a very specific macrophage response in the dorsal cord, with acute localisation within the dorsal white matter. This is in contrast to L3-L6 DRA where deep laminae were positive for punctate ED1 staining, suggesting multiple dorsal root avulsions lead to a greatly increased macrophage infiltration probably by increasing the surface area of the primary injury site for extravasation from the blood. This white matter localisation specificity at 14 days after single SRA suggests a limited role in phagocytosis of demyelinating primary afferents and neuronophagia in the dorsal horn at this time point, and also suggests limited role in the modulation of dorsal horn neuronal processing and the development of hypersensitivity. This finding greatly assists in the characterisation of microglial lineage within the dorsal horn after this spared root avulsion, as phagocytic microglia constitutively express ED1. These immunohistological results suggest that activated microglia within the dorsal horn (and this is also true for the ventral horn) are more likely focussed on inflammatory responses, neuroprotection and innate immunity, and as a side effect, neuronal hypersensitisation (Thacker et al., 2007) in this particular model of avulsion within the spared L4 segment. However at the site of injury in the L5 segment after SRA, and also in the deafferented cord after L3-L6 DRA,

microglial pathology may shift toward phagocytic functions, as there is considerable overlap between IBa1 and ED1 histochemistry and morphology.

Sham surgery leads to upregulation of GFAP in the dorsal horn, similar to the ventral horn. Previous nerve and root exposure surgery has been shown to lead to increased astroglial activity at 1, 3, and 7 days (Colburn et al., 1997;Winkelstein and DeLeo, 2002), and it is likely responsible for the transient hypersensitivity noted after this surgery (Colburn et al., 1997;Hashizume et al., 2000a). Astrogliosis in the ipsilateral dorsal horn after SRA, similar to microgliosis, is much less severe than that seen after a more substantial injury (L3-L6 DRA). Astrocytes increase their expression of GFAP, and form a noticeable scar in the L5 DREZ; however in the L4 segment no scar is noticeable but cellular GFAP is upregulated compared to sham and naïve levels. This suggests astrocytes are indeed active in the adjacent segment at 14 days, and may contribute to the maintenance of avulsion induced neuropathic pain, as they do in PNI (Colburn et al., 1997;Raghavendra et al., 2003) and SCI (Gwak and Hulsebosch, 2009). However, relative expression of GFAP in SRA compared to sham (approximately 8% versus 6%) is far less than for microglia (approximately 10% versus 3%), perhaps suggesting a less obvious role in the neuropathic pain behaviour. Indeed, intrathecal injections of activated spinal microglia causes thermal hyperalgesia in naive mice, that did not occur for activated astrocyte injections in identical experiments (Narita et al., 2006). Further, astrocytes caudal to a lesion to the spinal cord, do not express the typical MAP-kinase signaling cascade responsible for activation, and do not influence 'below-level' pain maintenance, whereas microglia do (Gwak et al., 2009). It may therefore be the case in SRA, that shows relatively greater microglial than astroglial reactivity, that the former cells play a more direct and important role in neuropathic avulsion pain than the latter, but by how much is difficult to say without specific cell inhibition.

Endothelial loss

Reduction of vascular integrity in the dorsal horn 14 days after L5 SRA is in accordance with the bilateral RECA-1 expression reduction in the dorsal horn after a more substantial root avulsion such as L3-L6 DRA (Section 3.2.4). The loss of endothelial staining in these two avulsion models is likely to have a similar etiology. Posterior spinal vein disruption or occlusion after L5 SRA, as well as vasospasm

resulting from mechanical trauma of the avulsion (Mautes et al., 2000), may again lead to bilateral vascular degeneration in L5 and L4 segments. It is difficult to say whether the loss of endothelial staining is likely to cause extensive ischemia, as RECA-1 immunostaining reduction was not linked to any obvious vessel depletion as was clear at 14-28 days in DRA (section 3.2.4), and it is likely that the spinal cord is still adequately perfused. In the case of SRA RECA-1 immunostaining reduction more likely represents reduced endothelial cell integrity, which could result in increased extravasation of leukocytes, elevating the inflammatory response and exacerbating hypersensitivity. However, this remains to be tested further.

Little is known about the effect of PNI or root injury on the spinal cord vasculature, whereas SCI models have been used exclusively to study detrimental effects on microvasculature (Noble and Wrathall, 1987;Noble and Wrathall, 1989;Imperato-Kalmar et al., 1997;Casella et al., 2002;Loy et al., 2002). Three to twenty four hours after contusion injury to the spinal cord extravasation is maximal within and surrounding the lesion site (Noble and Wrathall, 1989), and at 14 days it is markedly reduced, suggesting cellular extravasation plays only an acute role in pathogenesis of SCI. Disruption of the blood brain barrier in the SRA model could lead to extravasation of other inflammatory/immune cells including the lymphocytes T-cells and B-cells that play an important part in the adaptive immune response, and are found in the contused spinal cord at 3-6 hours and persist for 7 days (Popovich et al., 1997), and in the chronically constricted nerve at similar time points (Gomez-Nicola et al., 2008). The role of these immune cells in initiating or maintaining a neuropathic pain state after experimental injury is sparsely studied; however, it is well known that these cells can also generate inflammatory cytokines and chemokines and contribute to the innate immune/inflammatory response (Marchand et al., 2005) as well as further heightening dorsal horn neuronal responses. Confirmation of spinal cord vascular degeneration and leukocyte extravasation after SRA would benefit from more detailed examination of the microvasculature structural changes, as shown previously with electron-microscopy after traumatic brain injury (Dore-Duffy et al., 2000), and through intravital microscopy after SCI (Stirling et al., 2009).

4.3.3.2.3: Contralateral effects

Significant contralateral effects were seen in microglial and astroglial reactivity, and loss of endothelial staining, both dorsally and ventrally. This is similar to results from L3-L6 DRA (section 3.2), but of less magnitude. These effects most likely occur via the same mechanisms in these injuries; including inflammatory mediator overspill from one side of the cord to the other, transneuronal mediation via interneurones or sprouting, or increase in systemic circulating factors (section 3.3.8). Contralateral effects in this case are anatomically but not functionally significant, as no hypersensitivity is noted in the contralateral paw. This suggests that histological evidence of glial reactivity may not accurately portray their functional activity, such that upregulation of specific markers does not necessarily mean increase in neuronal interaction; and/or, that hypersensitivity may require a specific level of glial or neuronal activity to initiate.

4.3.4: Conclusion

This chapter has characterised a new model of lumbosacral avulsion injury, behaviourally and histologically. Avulsion of the L5 spinal mixed root leads to development of thermal and tactile hypersensitivity, reduced weight gain, but without severe locomotor impairment, across 14 days. Hypersensitivity is maintained up to 60 days. These results are suggestive of a neuropathic pain condition, and may represent the clinical scenario of root avulsion-induced pain. Histology indicated that the mechanisms of hypersensitivity are likely central in origin, specifically within the L4 dorsal horn. Significant neuronal cell loss, endothelial immunoreactivity reduction, increased microglial reactivity and to a lesser extent astrogliosis, and macrophage infiltration, similar, but with a lesser magnitude to L3-L6 DRA, is shown. Considerable differences in cellular responses between deafferented and spared segments may determine different functionality, and is especially true in the case of microglia. Results suggest that in an injury such as avulsion, where mixed trauma is widespread, cannot be defined by common doctrine of separate PNI-induced and SCI-induced central sensitization. The cellular changes characterized here, present a testable hypothesis for mechanism of action of avulsion pain, which may depend on microglial/macrophage activity or dorsal horn neuronal loss, for example, and can be investigated through therapeutic inhibition of these histological and behavioural events.

Chapter 5: Validation of the L5 SRA pain model using clinically relevant analgesics

5.1: Introduction

5.1.1: Current therapeutic treatment for avulsion pain

Current treatment for avulsion induced neuropathic pain is centered on the understanding that neuropathic pain is caused by pathologically hyperexcitable dorsal horn neurones (Loeser and Ward, Jr., 1967;Loeser et al., 1968;Ovelmen-Levitt et al., 1984). Most notably and still most effective is the coagulation procedure, DREZotomy (Nashold, Jr. and Ostdahl, 1979) of the superficial dorsal horn and root entry zone. Recently, reconstructive surgery through root grafting has had notable success at alleviating the pain (Berman et al., 1998;Terzis et al., 1999;Htut et al., 2006;Bertelli and Ghizoni, 2008), although motor functional restoration for brachial (Carlstedt et al., 2000) (Carlstedt et al., 2004;Htut et al., 2006)and lumbosacral (Lang et al., 2004;Sivaraman et al., 2008) roots is the main surgical objective. Even more recently spinal cord stimulation (SCS) above the site of lesion has shown to be effective at relieving brachial plexus pain after failed DREZotomy (Piva et al., 2003;Lai et al., 2009) perhaps through activating the descending inhibitory systems and GABAergic inhibition.

For patients that have failed to respond to DREZotomy and/or surgical repair, or have established neuropathic pain, the preferred option would be an effective pharmacological treatment regime. Additionally, for patients in the acute stages of the condition early pharmacological intervention would be used as a preventative measure for the development of neuropathic pain. So far, however, many drug types have had little therapeutic efficacy on their own (Parry, 1980;Piva et al., 2003). Recently in a rodent model of brachial plexus pain several drugs were used to characterise possible further treatment options (Rodrigues-Filho et al., 2004). These included an opioid agonist (morphine), an alpha2 adrenoceptor agonist (clonidine), an NMDA antagonist (ketamine), an anticonvulsant (gabapentin), a COX-2 inhibitor (celecoxib), a Na^{2+} channel blocker (lidocaine), a non-steriodal anti-inflammatory (diclofenac), a steroidal anti-inflammatory (dexamethasone), and an anti-depressant (imipramine). Morphine,

clonidine, ketamine and gabapentin prevented 'below level' avulsion-associated mechanical and cold allodynia suggesting many drugs currently on the market could be suitable candidates for clinical trials into avulsion pain. However this model does not accurately describe clinical avulsion pain, as patients do not complain of pain in the lower limb after brachial plexus avulsion, and therefore conclusion drawn from these results are, at best, limited.

Certainly, some conventional drugs have been shown to be at effective, at least in the short term for the treatment of avulsion pain. These include the opiate, morphine, which has had some success at alleviating avulsion pain (Schmidt and Schmidt, 2004). The μ and δ opioid receptors are found pre-synaptically in the superficial dorsal horn C-fibre terminal zone (Dickenson and Suzuki, 2005). Therefore mechanisms of action of morphine could be in pre-synaptic neurotransmitter release inhibition from ectopic adjacent intact roots (Bertelli and Ghizoni, 2008;Finnerup et al., 2009), as well as supra-spinally in the raphe nuclei, periaqueductal grey, and locus coeruleus (Dickenson and Suzuki, 2005) at the chronic stages of injury. This is however still unclear. Cannabinoids such as tetrahydrocannabinol (THC) and cannabidiol (CBD) have shown efficacy in brachial plexus injury patients (Berman et al., 2004), through reducing pain scores and improving sleep, thereby improving quality of life.

It has been the case for a long time that antidepressants (amitriptyline) and anticonvulsants/antiepileptics (carbamazepine, gabapentin, and pregabalin) have become the mainstay treatment of neuropathic pain conditions, including trigeminal neuralgia, cancer pain, diabetic and HIV neuropathy, and post operative pain (Rogawski and Loscher, 2004;Sindrup et al., 2005;Saarto and Wiffen, 2007). They are usually the first treatment regime for brachial plexus avulsed patients (Berman et al., 1998;Schmidt and Schmidt, 2004;Flores, 2006) but in most cases have only limited efficacy (Parry, 1980;Berman et al., 1996;Piva et al., 2003). When high doses are used side effects such as rash, ataxia, and sedation are common (Rapeport et al., 1984), and for this reason these drugs have to be used in conjunction with other medications (Schmidt and Schmidt, 2004). Efficacy of these drugs is increased if the patient has undergone reconstructive surgery for the avulsed root (Berman et al., 1998), however in more chronic cases of avulsion, sometimes at 10 years, these drugs show no analgesic properties (Schmidt and Schmidt, 2004).

Amitriptyline

Amitriptyline, a tricyclic antidepressant (TCA), was originally used for the treatment of depression; however the patient usually has to wait up to 2-4 weeks for effective relief. Typical adult doses for brachial plexus injured patients are 25-150mg orally daily, at night (Schmidt and Schmidt, 2004) to improve quality of sleep. Prolonged treatment is not recommended due to the propensity for its anticholinergic side effects including dry mouth, sweating, drowsiness, muscle stiffness, nausea, dizziness, constipation and urinary retention (Sindrup et al., 2005;Saarto and Wiffen, 2007). The analgesic properties of TCAs were noted more than 40 years ago and introduced as an effective treatment for painful diabetic neuropathy more than 30 years ago (Davis et al., 1977). The rational for the use of amitriptyline in neuropathic pain conditions may be due to its multimodal action at the level of the brain, brain stem, and the spinal cord, and its actions appear independent of its efficacy in depression relief (Sindrup et al., 2005;Bomholt et al., 2005).

Amitriptyline is able to effectively block both TTX-resistant and TTX-sensitive sodium channels in peripheral nerves (Brau et al., 2001;Dick et al., 2007;Leffler et al., 2007;Hur et al., 2008;Su et al., 2009), and this inhibition is likely to contribute to its analgesic effect. There are many other proposed modes of amitriptyline action for pain relief, including inhibition of NMDA receptors preventing central sensitization (Watanabe et al., 1993), NK1 receptor antagonism preventing substance P-mediated sensitization (Boselli et al., 2007), biogenic amine receptor antagonism reducing peripheral inflammation and odema (Sawynok and Reid, 2003), enhancement of endogenous adenosine tone producing antihyperalgesic effects to thermal stimulation (Esser and Sawynok, 2000), inhibition of M1 muscarinic acetylcholine receptors (Choi and Mitchelson, 1994) and nicotinic acetylcholine receptors (Freysoldt et al., 2009) implicated in C-fibre mediated nociception. There is also evidence to suggest a non-neuronal effect of amitriptyline, such that it can cause upregulation of EAA transporter channels (1 and 2) in glia after PNI, increasing glutamate clearance from dorsal horn and alleviating mechanical allodynia (Mao and Yang, 2010). All these receptors have a role in nociceptive, neuropathic or inflammatory pain. However, the effect of amitriptyline is transient in these cases, and is directly linked with the clearance properties of the drug. There is also some evidence that the analgesic properties of

amitriptyline can be permanent if the treatment is maintained. For example, amitriptyline's actions on opioid receptors, include increasing binding sites expressed in the spinal cord after prolonged (10mg/kg for 14 days) treatment (Hamon et al., 1987). Further evidence for amitriptyline's actions on the endogenous opioid system, is that CCI-induced neuropathic pain, attenuated by amitriptyline treatment, is acutely reversed with the addition of delta or kappa-opioid antagonists (Benbouzid et al., 2008).

Direct evidence for the analgesic qualities of amitriptyline come from neuropathic pain animal models, such as sciatic nerve crush, CCI, spared nerve injury, and spinal nerve ligation (Decosterd et al., 2004;De Vry et al., 2004;Bomholt et al., 2005;Song et al., 2008;Su et al., 2009;Mao and Yang, 2010). There seems to be a dose dependent action of amitriptyline as well as stimulus dependent (mechanical or thermal) amelioration in neuropathic pain models. A range of doses have been explored for efficacy between 3-30mg/kg i.p. (Decosterd et al., 2004;Bomholt et al., 2005) and 32-128mg/kg p.o. (De Vry et al., 2004) following the establishment of PNI-induced neuropathic pain. The results in these investigations showed that amitriptyline had no effect on alleviating established mechanical allodynia, but successfully attenuated thermal hyperalgesia dose dependently at 30mg/kg and above. All analgesic effects were short acting (180min maximum) corresponding to the drugs half-life and clearance qualities of these acute doses. However, amitriptyline at just 2mg/kg, delivered via intravenous injection, successfully inhibits the ectopic discharges within primary afferents after L5/L6 spinal nerve ligation, and ameliorates mechanical allodynia (Su et al., 2009). Prolonged treatment at 10mg/kg twice daily for 5 days also alleviates mechanical allodynia (Mao and Yang, 2010) suggesting analgesic effects directly depend on the type of nerve injury, dosing regimes, and mode of delivery.

Carbamazepine

Carbamazepine is an anti-convulsant drug used in the treatment of epilepsy. It is also licensed in the U.S.A. as a first line treatment for patients with trigeminal neuralgia, and is also effective in traumatic and diabetic neuropathic pain treatment, neuromuscular disorders, migraine, and psychiatric disorders (McQuay et al., 1995;Rogawski and Loscher, 2004). A typical dose for brachial plexus injured patients is 1200mg/day (Schmidt and Schmidt, 2004). The pharmacological mechanism of action of

carbamazepine is ‘cleaner’ than that of amitriptyline, and involves inhibition of sodium channel function in the periphery and centrally (Spina and Perugi, 2004). As such, carbamazepine exhibits its anti-epileptic and anti-nociceptive properties by selectively blocking high frequency TTX-resistant voltage gated sodium channels (Rogawski and Loscher, 2004;Dick et al., 2007;Hur et al., 2008).

The use of carbamazepine in the treatment of trigeminal neuralgia pain is now well established after its first introduction in 1962 (BLOM, 1962), and nowadays provides 70-80% of patients with acute pain relief; however, this figure is reduced to 50% when looking at long term efficacy (Spina and Perugi, 2004). Clinical trials have shown efficacy at doses between 100 to 1200mg per day for neuropathic pain conditions in a dose-dependent manner but, like amitriptyline, discontinuation is recommended after 2-3 months to prevent toxicity and side effects such as drowsiness, nausea, and blurred vision (Spina and Perugi, 2004). Carbamazepine exerts a central and peripheral use-dependent inhibition of sodium channels and is effective in both evoked and ectopic peripheral neuronal activity (Chapman et al., 1998). The success of carbamazepine in the treatment of trigeminal neuralgia has led to carbamazepine being tested in various, randomised, double-blind controlled trials for a range of neuropathic pain conditions, including diabetic neuropathy, post-herpatic neuralgia, stroke, and autoimmune demyelinating disorders such as Guillain-Barre syndrome (Jensen, 2002;Spina and Perugi, 2004), as well as in the treatment of brachial plexus injury pain (Berman et al., 1998;Schmidt and Schmidt, 2004;Flores, 2006).

PNI animal models have shed light on the effects of carbamazepine on behavioural neuropathic pain. After spinal nerve ligation, 22.5mg/kg subcutaneous carbamazepine treatment reversed mechanical allodynia, with its mechanism of action centred on inhibition of C- and A-fibre neuronal responses (Chapman et al., 1998). Thermal hyperalgesia was strongly attenuated, and mechanical allodynia moderately attenuated, by 32mg/kg i.p. carbamazepine treatment after CCI (De Vry et al., 2004) and mechanical allodynia was attenuated after chemotherapy-induced (vincristine administered) neuropathic pain (Lynch, III et al., 2004). However, carbamazepine has a relatively low therapeutic index (LD50/ED50) compared to other analgesics, which increases the potential for toxicity (Lynch, III et al., 2004). Like amitriptyline, a dose dependent efficacy is seen for carbamazepine, where an optimum therapeutic dose is

between 32 and 64mg/kg i.p., and maximal therapeutic efficacy at a dose of 64mg/kg i.p. for treatment of sciatic nerve ligation-induced neuropathic pain (De Vry et al., 2004). At this maximal dose however, 3/11 of the rats were unable to complete the behavioural testing due to side effects (De Vry et al., 2004). In patients drowsiness is a well recognised side effect and is the reason for prescribing the drug to be taken at night.

5.1.2: Aims

As a proof of concept of the L5 SRA as a model of avulsion injury, it was important to establish that current pain relieving drugs, in this case amitriptyline and carbamazepine, used for brachial plexus pain would have efficacy on the SRA model as previously shown in PNI models (Chapman et al., 1998;Decosterd et al., 2004;De Vry et al., 2004;Bomholt et al., 2005), and to confirm effects seen in human brachial plexus injury (Berman et al., 1998;Schmidt and Schmidt, 2004;Flores, 2006). Doses of 32mg/kg and 64mg/kg were chosen in accordance with previous literature on CCI injury and effective doses (De Vry et al., 2004;Bomholt et al., 2005). The aim was to assess the effects of a delayed, single dose treatment of i.p. administered amitriptyline and carbamazepine when behavioural hypersensitivity was already well established, following L5 spinal root avulsion. Differences in efficacy of amitriptyline and/or carbamazepine between two different doses, 32mg/kg and 64mg/kg, will be explored, against possible side effects of drowsiness and hypoalgesia. Suitable time points (3 and 6 days) between treatments would allow full clearance of the drugs from prior testing points.

5.2: Results

5.2.1: Vehicle treatment after L5 SRA

For the vehicle treated SRA group, ipsilateral thermal hypersensitivity was significantly established against both baseline values (9.57s +/- 0.38) and contralateral values (9.78 +/-0.59) by 5 days post injury (5.97s +/-0.43) (Fig 5.1A).

Ipsilateral mechanical hypersensitivity was significantly established against baseline values (20.3g +/-1.43) by 5 days (15.0g +/-2.23) and from both baseline and contralateral values (20.4g +/-1.77) at 7 days (15.8g +/-0.73) (Fig 5.1B). Withdrawal thresholds to tactile stimulation showed further reduction across the period of 25 days; where withdrawal values reached a low of 8.42g (+/- 0.59) (Fig 5.1B).

Withdrawal thresholds to thermal stimulation remained significantly lower than baseline and contralateral hindpaw withdrawal values for up to 25 days (4.64s +/-0.45) (Fig 5.1A), again consistent with previous data (section 4.2.1b).

No changes to contralateral withdrawal thresholds were recorded in this vehicle group. Importantly, i.p. vehicle injection did not cause any change in the progression of ipsilateral neuropathic pain behaviour on the day of injection or any days prior, for either thermal or tactile stimulation. This is the case for all 3 injections.

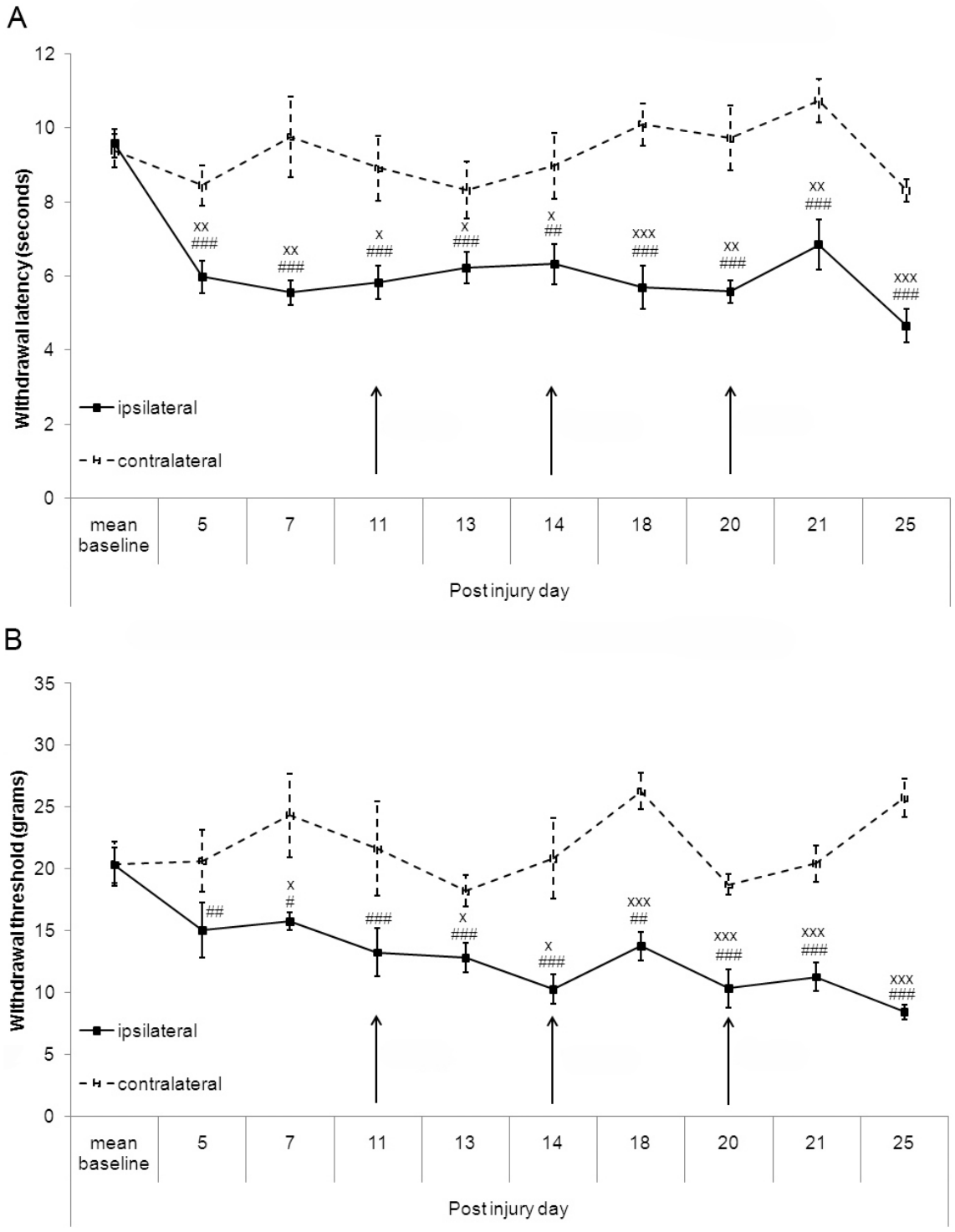

Figure 5.1: Effects of vehicle treatment on behavioural hypersensitivity. Treatment with vehicle does not ameliorate ipsilateral behavioural hypersensitivity to thermal (A) or mechanical (B) stimulation at any 3 administrations (indicated by the arrows). Significant differences are indicated for ipsi vs contra (x) and against baseline (#). N = 6/ group.

5.2.2: Amitriptyline treatment after L5 SRA

Amitriptyline treated SRA rats became hypersensitive to mechanical stimulation by 5 days (14.4g +/-1.76) compared to baseline and contralateral levels and reached 13.2s (+/-1.20) on day 7 (Fig 5.2A). Thermal hypersensitivity was apparent at 5 days (6.26s +/-0.36) compared to baseline, and maintained at 7 days (6.58s +/-0.53) (Fig 5.3A).

First treatment: On day 11, 1 hour after treatment with 32mg/kg amitriptyline, ipsilateral withdrawal responses for thermal (6.36s +/-0.96) and mechanical (17.5g +/-3.81) stimulation were not significantly difference from contralateral and baseline values (Fig 5.2A and 5.3A). No significant difference was seen against vehicle injection (Fig 5.2B and 5.3B). No contralateral change was noted. On day 13 hypersensitivity to both thermal and mechanical stimuli returned such that the ipsilateral withdrawal responses (mechanical: 11.9g +/-1.49, and thermal: 5.36s +/-0.67) were significantly lower than baseline and contralateral levels in each case (Fig 5.2A and 5.3A).

Second treatment: On day 14, 1 hour after a second treatment with 32mg/kg amitriptyline ipsilateral withdrawal responses (18.7g +/-3.01 for tactile and 9.01s +/-1.59 for thermal) were not significantly difference from contralateral and baseline values (Fig 5.2A and 5.3A). No significant difference was found between vehicle and amitriptyline for thermal hypersensitivity, but a significant amelioration of mechanical hypersensitivity against vehicle levels was found (Fig 5.2B). On day 18 both thermal and mechanical hypersensitivity again returned, such that the ipsilateral withdrawal responses (mechanical: 12.6g +/-1.03, and thermal: 5.39s +/-0.35) were significantly lower than baseline and contralateral levels in each case (Fig 5.2B and 5.3B).

Third treatment: On day 20, 1 hour after a third treatment with an increased dose of amitriptyline (64mg/kg) all significant differences from contralateral and baseline levels were again abolished and returned to 21.4g (+/-1.14) for mechanical withdrawal and 10.2s (+/-1.05) for thermal withdrawal (Fig 5.2A and 5.3A). There was a significant amelioration of ipsilateral hypersensitivity against vehicle levels (mechanical: 10.3 +/-1.54, and thermal: 5.57s +/-0.31) (Fig 5.2B and 5.3B). On day 21 and day 25 hypersensitivity, significant against all comparisons, returned to levels identical to vehicle (Fig 5.2B and 5.3B).

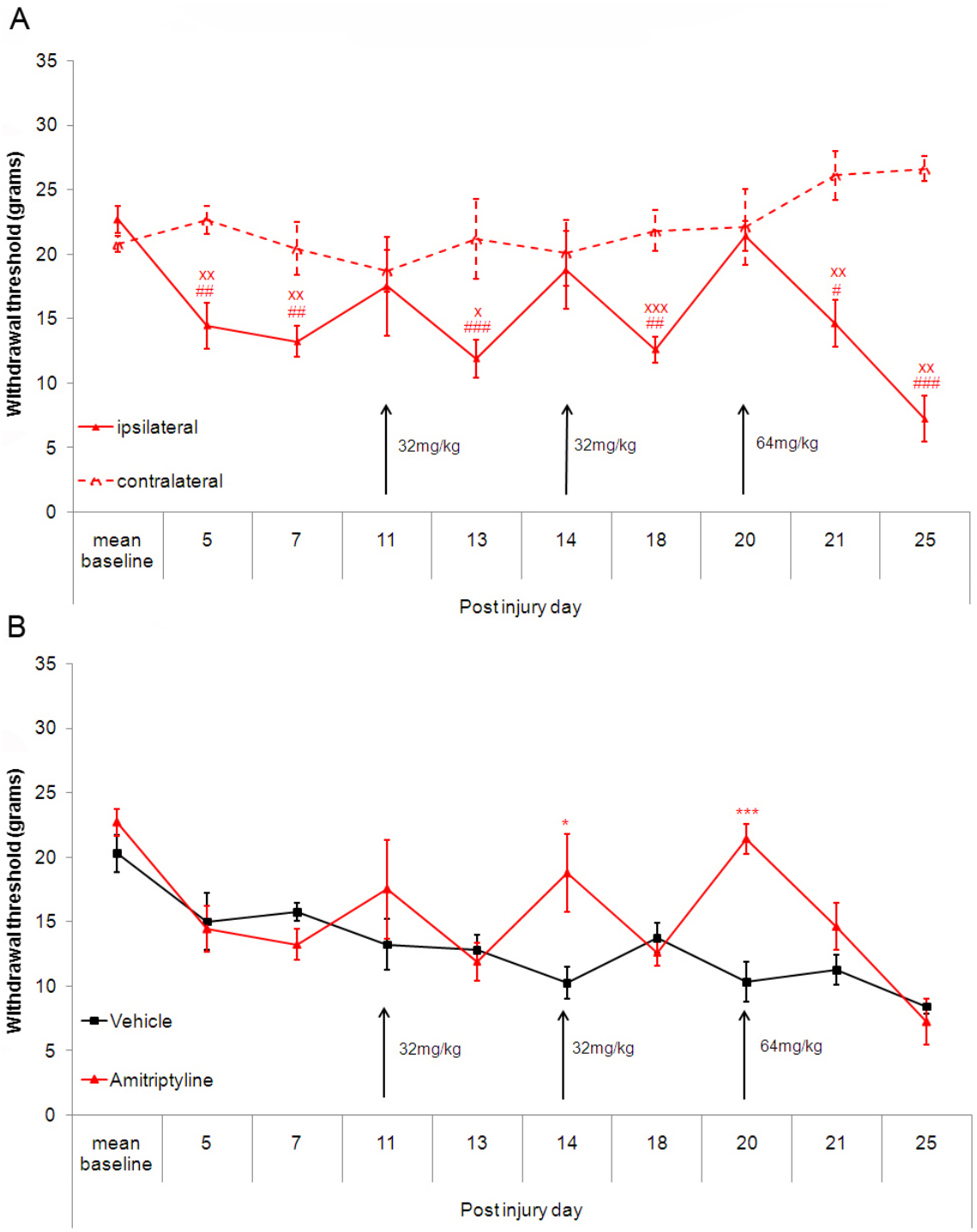

Figure 5.2: Effects of amitriptyline on mechanical hypersensitivity. Treatment with amitriptyline significantly reverses tactile hypersensitivity against contralateral and baseline values (A) and against vehicle levels (B) 1 hour post administration (indicated by the arrows). It is most effective on a repeated dose of 32mg/kg and 64mg/kg, without significant contralateral effects. Significant differences are indicated for ipsi vs contra (x), against baseline (#), and against vehicle (*). N = 6 in each group.

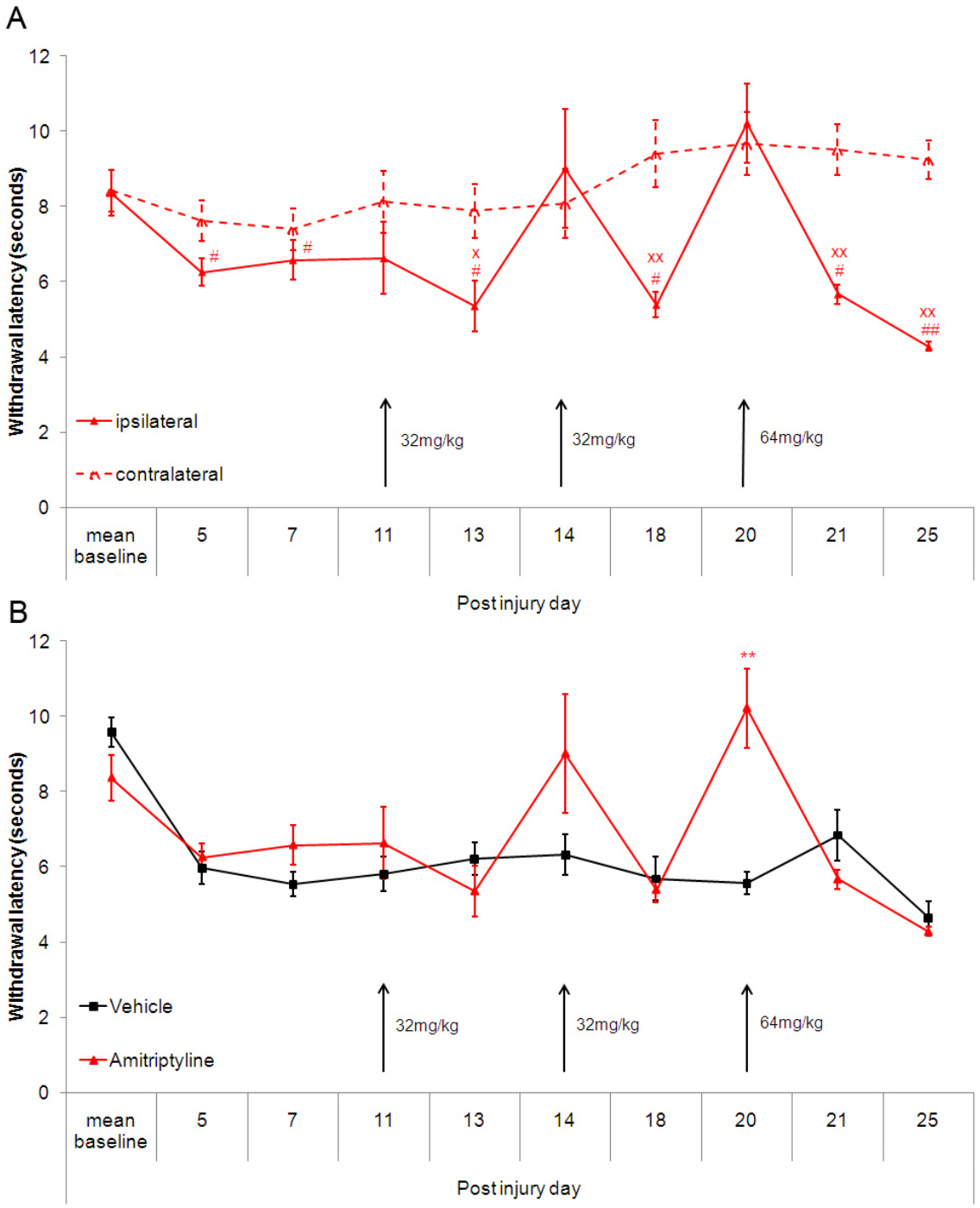

Figure 5.3: Effect of amitriptyline on thermal hypersensitivity. Treatment with amitriptyline significantly reverses thermal hypersensitivity against contralateral and baseline values (A) and against vehicle levels (B) 1 hour post administration (indicated by the arrows). It is only effective on a repeated dose of 32mg/kg and 64mg/kg, without significant contralateral effects. Significant differences are indicated for ipsi vs contra (x), against baseline (#), and against vehicle (*). N = 6 per group.

5.2.3: Carbamazepine treatment after L5 SRA

The carbamazepine-treated SRA group became significantly hypersensitive to mechanical stimulation at 7 days (15.3g +/-1.71) compared to baseline (21.5g +/-0.61) and contralateral (21.3g +/-0.64) levels (Fig 5.4A). Significant ipsilateral hypersensitivity to thermal stimulation was apparent at 5 days (6.34s +/-0.74) but only compared to baseline, and this was maintained at 7 days (6.14s +/-0.71) (Fig 5.5A). A contralateral thermal hypersensitivity was seen on days 5, 7, 13, 18, that was not present for mechanical stimulation, and was not related to drug administration (Fig 5.4A and 5.5A). This contralateral effect to thermal stimulation is anomalous as it was not seen for other groups of rats.

First dose: On day 11, 1 hour after treatment with 32mg/kg carbamazepine ipsilateral withdrawal responses (mechanical: 20.6g +/-2.15, and thermal: 7.15s +/-0.55) were not significantly different from contralateral and baseline values (Fig 5.4A and 5.5A). There was a significantly greater mechanical withdrawal threshold ipsilaterally for carbamazepine treated group compared to vehicle-treated at this time point (Fig 5.4B). However, no significant difference was noted for thermal withdrawal thresholds between treated and vehicle treated rats at this time point (Fig 5.5B). A change in contralateral levels was seen with this first treatment time point for thermal withdrawal such that it was no longer significantly different to the baseline value (Fig 5.5A). On day 13 hypersensitivity to both thermal and mechanical stimulation returned such that the ipsilateral withdrawal responses (mechanical: 15.1g +/-1.67, and thermal: 5.81s +/-0.45) were significantly lower than baseline and contralateral levels in each case (Fig 5.4A and 5.5A). For contralateral thermal withdrawal latency, this returned to significant difference from baseline (Fig 5.5A).

Second dose: On day 14, 1 hour after a second treatment with 32mg/kg carbamazepine, ipsilateral withdrawal responses (mechanical: 20.9g +/-2.45, and thermal: 7.61s +/-1.11) again were not significantly difference from contralateral and baseline values in the case of mechanical hypersensitivity, however ipsilateral responses to thermal stimulation still showed significant hypersensitivity (Fig 5.4A and 5.5A). Again there was a significantly greater mechanical withdrawal threshold ipsilaterally for carbamazepine treatment group over vehicle (Fig 5.4B). However, no significant difference was found

ipsilaterally between vehicle treatment and carbamazepine treatment for thermal withdrawal levels (Fig 5.5B). Again, a change in contralateral levels was seen with this first treatment time point for thermal withdrawal such that it was no longer significantly different to the baseline value (Fig 5.5A). On day 18 hypersensitivity to both thermal and mechanical stimulation again returned such that the ipsilateral withdrawal responses (mechanical: 13.4g +/-1.29, and thermal: 5.84s +/-0.33) were significantly lower than baseline and contralateral levels in each case (Fig 5.4A and 5.5A). For contralateral thermal withdrawal latency, this returned again to a hypersensitive level compared to baseline (Fig 5.5A).

Third dose: On day 20, 1 hour after a third treatment with an increased dose of amitriptyline (64mg/kg) all significant differences from baseline levels were again abolished and returned to 20.1g (+/-1.67) for mechanical withdrawal and 9.13 (+/-0.63) for thermal withdrawal (Fig 5.4A and 5.5A). Contralateral effects were seen for mechanical and thermal stimulation, with significantly increased withdrawal thresholds compared to baseline in both cases (Fig 5.4A and 5.5A). There was a significant amelioration of ipsilateral hypersensitivity against vehicle levels for both mechanical and thermal stimulation (Fig 5.4B and 5.5B). On day 21 and day 25 ipsilateral hypersensitivity, significant against all comparisons, returned to levels identical to vehicle, and contralateral values were not significantly different from baseline (Fig 5.4B and 5.5B).

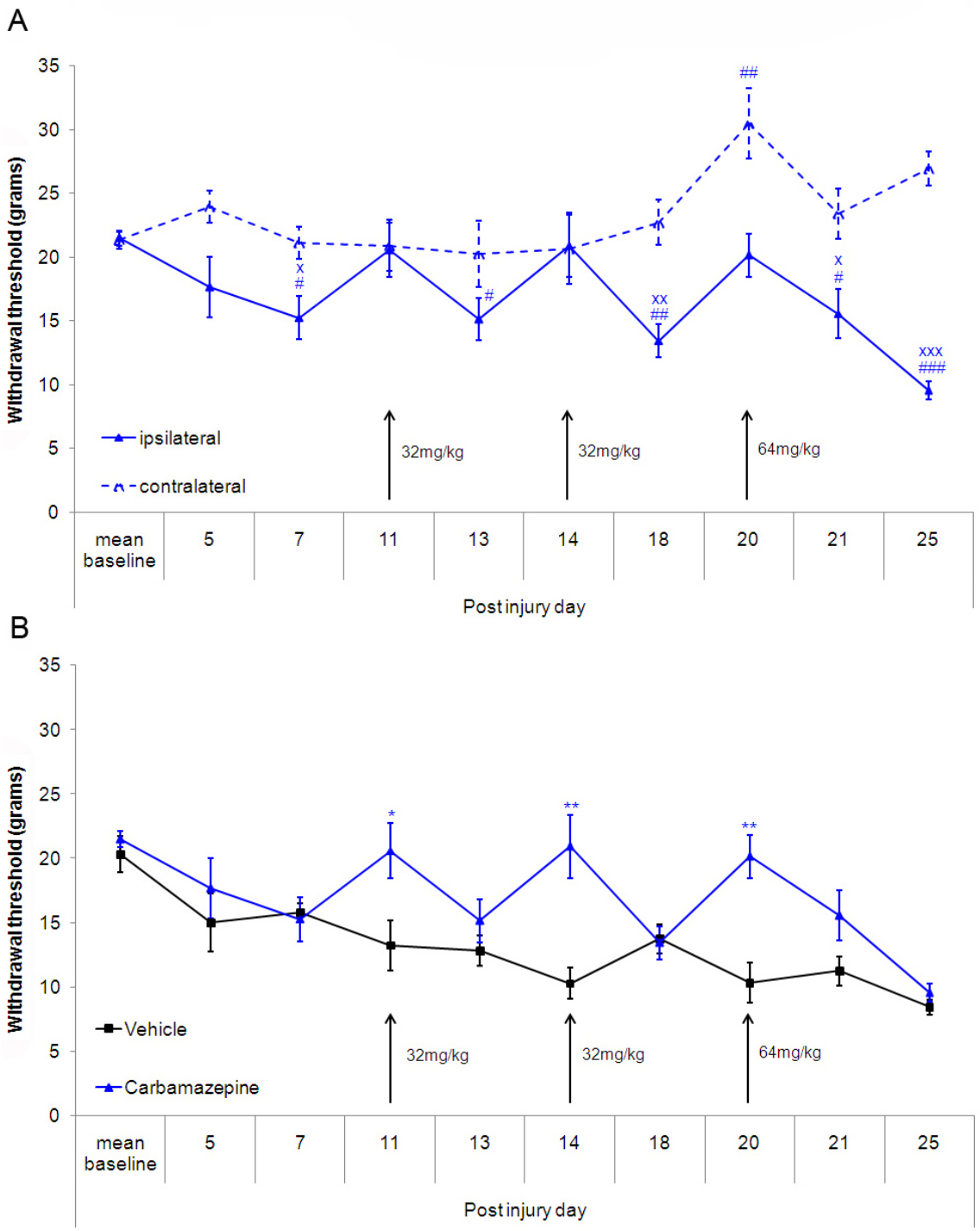

Figure 5.4: Effect of carbamazepine on mechanical hypersensivity. Treatment with carbamazepine significantly reverses tactile hypersensitivity against contralateral and baseline values (A) and against vehicle levels (B) 1 hour post administration. It is effective at all doses. A significant contralateral hyposensitivity is noted 1 hour after 64mg/kg dose but is absent 24 hours later. Significant differences are indicated for ipsi vs contra (x), against baseline (#), and against vehicle (*). N = 6 in each group.

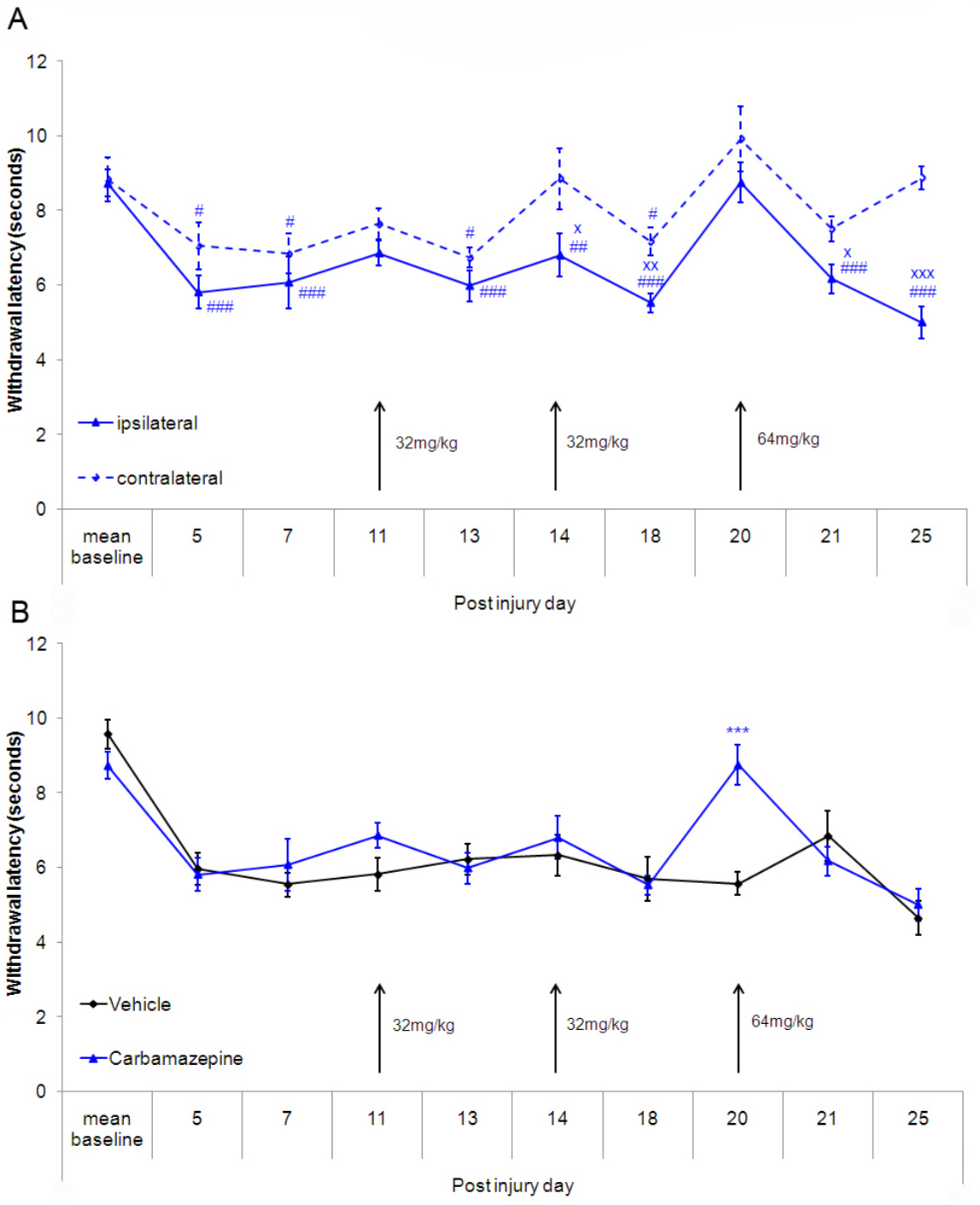

Figure 5.5: Effect of carbamazepine on thermal hypersensitivity. Treatment with carbamazepine significantly reverses thermal hypersensitivity against baseline values (A) and against vehicle levels (B) 1 hour post administration. However a contralateral hypersensitivity prevents intra-group comparison between hindpaw responses in the carbamazepine group (A). Carbamazepine is only significantly effective at ameliorating hypersensitivity on a third and increased dose of 64mg/kg. Significant differences are indicated for ipsi vs contra (x), against baseline (#), and against vehicle (*). N = 6 in each group.

5.3: Discussion

5.3.1: Effects of Amitriptyline and Carbamazepine on SRA-induced evoked neuropathic pain behaviour

In accordance with section 4.2.1b, behavioural hypersensitivity to thermal and tactile stimulation becomes significant by 5-7 days after L5 SRA injury. This has provided an opportunity to test conventional therapeutic treatment for neuropathic pain, in an animal model of root avulsion injury that reliably produces an evoked hypersensitivity.

In the case of thermal hypersensitivity, significant amelioration is found for both carbamazepine and amitriptyline in accordance with the previous literature (Decosterd et al., 2004;De Vry et al., 2004;Bomholt et al., 2005). The effective dose is 32mg/kg. This dose is higher than that which is required to ameliorate PNI-induced behavioural pain, and this observation perhaps indicates a greater severity and intractability of the neuropathy after root avulsion compared to PNI.

For the amelioration of mechanical hypersensitivity, carbamazpeine is effective on the first dose at 32mg/kg. Further increase in carbamazepine dose to 64mg/kg causes no further change in evoked hypersensitivity ipsilaterally, and leads only to contralateral hyposensitivity in accordance with previous literature suggesting a sedatory effect (De Vry et al., 2004;Lynch, III et al., 2004). The effectiveness of amitriptyline treatment at ameliorating mechanical hypersensitivity induced by SRA 1 hour post injection, is in accordance with recent literature on spared nerve injury and spinal nerve ligation rat models (Su et al., 2009;Mao and Yang, 2010), but is contradictory with earlier literature that indicates it can only alleviate thermal hypersensitivity (Decosterd et al., 2004;De Vry et al., 2004;Bomholt et al., 2005). This discrepency may be due to different injury models used, the variable methods of cutaneous mechanical stimulation, and also due to different mode of drug delivery.

In all cases the effects of the drugs are transient, lasting less than 24 hours relating to the clearance of the drugs. In man carbamazepine and amitriptyline have biological half-lives of approximately 35 hours (Bertilsson, 1978) and 24 hours (Schulz et al., 1985) respectively, when delivered orally and on the first administration. In the case of

carbamazepine this becomes shorter after repeated doses, due to enzyme ‘auto induction’ of the drug in the liver (Bertilsson, 1978), and this is one pathway to tolerance and side effects, as doses have to be increased. In rats the CNS biological half-life is much shorter, at 3.4 hours for carbamazepine (Graumlich et al., 2000) and 1.6 hours for amitriptyline (Coudore et al., 1996) after i.p administration. This is due to greater metabolisms and clearance in the kidneys, mode of administration, and magnitude of dose. This means that to maintain efficacy, drug administration would have to be performed approximately every 2 hours, as efficacy is lost after this period.

In the case of amitriptyline, significant analgesic effect requires repeated dosing at 32mg/kg, although a trend is shown on the first dose for tactile hypersensitivity amelioration. It is unclear why a second identical dose is more efficacious, as the previous dose would have been systemically cleared preventing any synergistic response between doses. Carbamazepine, on the other hand, does not require a second dose for efficacy and further signifies the difference in complexity of mechanism of action between these two drugs; with amitriptyline involved in a polymechanistic approach to analgesia, acting on a multitude of receptors, and carbamazepine specific to sodium channels. Perhaps initial dosing at 32mg/kg of amitriptyline heightens downstream signaling processes incuding receptor transcription and translocation, such as been shown it the accumulation of opioid receptors in the spinal cord (Hamon et al., 1987). This is more likely to create a permanent physiological effect, priming the spinal cord for the next dose. This may indeed be the mechanism of action of amitriptyline when used clinically for depression. Patients take low doses of these drugs (25-150mg/day representative of ~2.14mg/kg for a 70kg man) in comparison to larger doses in pre-clinical rodent models, due to the side effects, but importantly they do not experience efficacy for the first few weeks, suggesting an indirect mechanism of action of amitriptyline on the CNS, which is likely increased receptor translation and expression. This is not the case for carbamazepine, with sodium channel inhibition the primary mechanism of efficacy, and is why a similar magnitude of dose between clinical (1200mg/day representative of ~17.1mg/kg in man) and pre-clinical rodent models is seen.

Side effects

Behavioural side effects were noted at 64mg/kg doses for carbamazepine, without effects for the same volume in the vehicle treated group, or for amtriptyline. With 64mg/kg of carbamazepine a significant hypoalgesia occurred contralaterally, with an increase in withdrawal to tactile stimulation significantly above basal levels. This is in accordance with De Vry *et al.,* (De Vry et al., 2004) who showed withdrawal unresponsiveness and sedation in 3 out of 11 rats behaviorally tested at this dose for carbamazepine. This is not a systemic sedatory effect, as no hypoalgesia is noted after thermal stimulation at 64mg/kg, and may just be linked to channel inhibition associated with tactile sensation in the dorsal horn or in cutaneous receptors. This however remains to be tested. Without testing lower doses of these two drugs (e.g. 8 and 16mg/kg) obtaining a correct therapeutic index dosing for avulsion pain is difficult, but clearly a dose between 32 and 64mg/kg is effective at ameliorating the hypersensitivity.

Contralateral effect

The contralateral thermal hypersensitivity in the carbamazepine group on days 5, 7, 13, and 18, irrespective of treatment, may suggest that in some cases contralateral effects may occur with SRA similarly to PNI (Arguis et al., 2008;Hatashita et al., 2008), dorsal root injury (Hunt et al., 2001;Rothman et al., 2009), and others (Koltzenburg et al., 1999;Chang et al., 2010). The amelioration of this contralateral hypersensitivity on days 11, 14, and 20 after carbamazepine administration confirms this effect is not simply an anomaly or human sampling error. These effects are not as significant as seen ipsilaterally, and are not maintained at days 21 and 25, suggest a mild and transient contralateral effect. It is unknown why this contralateral effect is only found in this group, and only in this trial, and may be due to unrelated housing conditions and stress for these specific animals.

5.3.2: Conclusion

The analgesic effects of amitriptyline and carbamazepine in this model of avulsion injury confirms the analgesic effects seen pre-clinically in PNI (Decosterd et al., 2004;De Vry et al., 2004;Lynch, III et al., 2004;Bomholt et al., 2005;Song et al., 2008;Su et al., 2009;Mao and Yang, 2010), and clinically for many types of neuropathic pain conditions (Davis et al., 1977;Sindrup and Jensen, 2002;Rogawski and Loscher,

2004;Sindrup et al., 2005). The inability of these drugs to maintain efficacy beyond wash-out in SRA animals provides evidence for why these drugs are ineffective at alleviating root avulsion-induced neuropathic pain in the long term. Further, these effects provide a pharmacological validation of the establishment of the rodent SRA injury, as an experimentally viable model for the study of avulsion pain mechanisms. These results now enable pharmacological characterization of more experimental drugs that may potentially be of more therapeutic benefit for the treatment of avulsion injury pain.

Chapter 6: Effects of immediate and delayed minocycline and riluzole treatment of SRA-induced behavioural hypersensitivity

6.1: Introduction

6.1.1: Limitations of current neuropathic pain therapy

Drugs described as 'first line' treatment of neuropathic pain, such as anticonvulsants (e.g carbamazepine), TCAs (eg. amitriptyline), serotonin reuptake inhibitors (eg. paroxetine) and opioids (eg. morphine), that act on neurones directly through receptor and channel expression and activity, show some level of efficacy for the treatment of SCI (Baastrup and Finnerup, 2008) and PNI (Stacey, 2005) pain; however, fail to produce long lasting pain relief in plexus avulsion injury patients (Parry, 1980;Berman et al., 1996;Piva et al., 2003;Schmidt and Schmidt, 2004), or produce unacceptable side effects at efficacious doses (Berman et al., 2004). After peripheral and central neuropathy these analgesics are purposefully prescribed at low doses, and for short periods of time, due to their extensive side effects and propensity for the generation of pharmacological tolerance (Mayer et al., 1999). For example opioids, that were first prescribed to treat pain due to their inhibitory action on neurones in the spinal cord and brain-stem, are now thought to be ineffective at maintaining therapeutic efficacy, due to their activity on glia (Hutchinson et al., 2007;Mika, 2008). The actions of chronic administration of opioids such as morphine, have been shown to cause hypertrophy of astroctyes and thermal hypersensitivity (Song and Zhao, 2001), linked to activation of surface μ-3 opioid receptors on astrocytes (Dobrenis et al., 1995), and the upregulation and migration of microglia via interactions between μ-3 opioid and P_2X_4 receptors (Horvath and DeLeo, 2009). This glial-mediated neuroinflammation in the spinal cord, similar to that seen after neurotrauma, is a mechanism that antagonises the analgesic effects of morphine leading to drug tolerance. This tolerance results in the need for increased dosage to maintain physiological efficacy, culminating in drug dependency and addiction. Drug withdrawal becomes a disorder in itself, as loss of primary opioid analgesia will lead to unabated microglial-mediated neuropathic pain. This hypothesis of morphine tolerance has been clarified pre-clinically, and shown to be permanently established at 6 days in both naïve and CCI mice (Mika et al., 2009), and glial responses and cytokine expression have been shown to occur as acutely as 5 minutes after a 15ul

morphine single intrathecal injection in naïve rats, and lasts for up to 100 minutes (Hutchinson et al., 2008). This opioid-induced cytokine-mediated neuropathic behaviour can be substantially delayed by the administration of pre-emptive treatment boluses of the neuroinflammatory inhibitors minocycline (microglia), pentoxifylline (cytokine), fluorocitrate (astrocytes), and riluzole (anti-glutaminergic) (Song and Zhao, 2001;Habibi-Asl et al., 2009;Mika et al., 2009).

As described previously in chapters 3-5, there is now a shift in the understanding of neuropathic pain mechanisms, at least in pre-clinical research, that these mechanisms are at least in part due to pathologically increased glial-neuronal communication within the dorsal horn of the spinal cord, through glial activation, proliferation, and inflammatory mediator release (Raghavendra et al., 2003;McMahon et al., 2005;Hains and Waxman, 2006;Hulsebosch, 2008;Echeverry et al., 2008;Inoue and Tsuda, 2009;Milligan and Watkins, 2009). This understanding provided the rational for the use of 'non-classical' analgesic drugs to target and influence 'pre-neuronal' mechanisms such as microglial activation (Raghavendra et al., 2003;Ledeboer et al., 2005;Hains and Waxman, 2006;Marchand et al., 2009), as well as attempting to reduce extracellular glutamate (Sung et al., 2003;Coderre et al., 2007), in an attempt to indirectly modulate dorsal horn neuronal excitability. The immediate benefit in the use of these drugs assessed pre-clinically for efficacy in neuropathic pain, is that they are already marketed by pharmaceutical companies for treatment of other disorders. Two of these potential treatments may lay with the application of riluzole, an anti-glutamatergic drug, and minocycline, an anti-inflammatory drug, to target the glutaminergic system and microglia in neuropathic pain management.

6.1.2: Therapeutic potential of minocycline for neuronal injury and disease

There is now overwhelming evidence to suggest that neuroinflammation exerts an important role in the pathogenesis of several chronic neurodegenerative disorders such as Alzheimers disease, Parkinson's disease, and Huntington's disease (Glass et al., 2010), as well as acute insults such as stroke, epilepsy, ischemia (Oprica et al., 2003) and, SCI (Popovich et al., 1997) and PNI (Colburn et al., 1997;Colburn et al., 1999;Ohlsson et al., 2006). There is growing support now for therapeutic strategies

targeting inflammation as a key to prevention of neurodegeneration after neurotrauma (Popovich, 2000;Hausmann, 2003;Kim and Suh, 2009;Ankeny and Popovich, 2009).

Minocycline is a semi-synthetic second generation tetracycline derivative, effective against gram-positive and gram-negative infections, by inhibiting protein synthesis at the ribosome level (Kim and Suh, 2009). It was first introduced in 1967, and is now commonly prescribed as an antibiotic for dermatological conditions such as acne vulgaris and rosacea (Kim and Suh, 2009). It also has a profoundly anti-inflammatory property, and is used clinically for treatment of rheumatoid arthritis (O'Dell, 1999). Minocycline exerts its anti-inflammatory properties by modulating microglia, reducing immune cell activation, reducing cytokine and chemokine release, and modulating matrix metalloproteinases (MMPs) (Stirling et al., 2005). It has good pharmacokinetics being highly lipophilic in nature, easily crosses the blood brain barrier with high tissue absorption, and has a longer half-life (11-23 hours) than other tetracyclines (Langevitz et al., 2000;Kim and Suh, 2009). More recently minocycline has been implemented in the therapeutic treatment of neurodegenerative diseases due to its anti-inflammatory properties but also due to anti-apoptotic/neurotrotective properties that are distinct from its anti-microbial actions (Kim and Suh, 2009).

Minocycline was first shown to have neuroprotective qualities after ischemic stroke (Yrjanheikki et al., 1998), by increasing the survival of CA1 hippocampal neurones with treatments both pre- and post-emptively and reducing microglial activity. These therapeutic effects were causally linked to reduction of expression of inducible nitric oxide synthase (iNOS) mRNA, reduction of Il-1β-converting enzyme expression, and reduction of cyclooxygenase-2 (COX-2) and prostaglandin E2 (PGE2) production (Yrjanheikki et al., 1998;Yrjanheikki et al., 1999). Minocycline was shown to be functionally effective in rat models of thoracic contusive SCI (Lee et al., 2003;Wells et al., 2003), where immediate treatment at 45mg/kg i.p, with follow-up treatment every 12 hours, effectively reduced lesion size, increased axonal sparing, and improved locomotor scores, with corresponding reduction of apoptotic markers such as TUNEL and caspase-3, and decreasing TNFα expression. Many authors have shown similar effects *in vivo* and *in vitro* (He et al., 2001;Tikka et al., 2001;Stirling et al., 2004;Festoff et al., 2006). The primary mechanism of minocycline's anti-apoptotic action is the direct inhibition of cytochrome-C release from mitochondria, shown initially in

Huntington's disease models (Chen et al., 2000), but also in contusive SCI (Teng et al., 2004). Minocycline has been shown to reduce NMDA mediated excitotoxicity and microglial proliferation via inhibition of p38 MAP-Kinase in animal models of SCI, stroke, and Huntington's disease (Hains and Waxman, 2006;Crown et al., 2008;Tikka et al., 2001;Tikka and Koistinaho, 2001). Minocycline administration for 2 weeks in experimental autoimmune encephalitis (EAE) ameliorates clinical severity by downregulation of MHC-2 expression on microglia and reactivity inhibition (Nikodemova et al., 2007). Minocycline's actions are cell specific, having been shown to attenuate microglial but not astroglial activity after cerebellar focal lesions (Viscomi et al., 2008). Minocycline treatment has also been shown to be a potent macrophage inhibitor after dorsal column crush injury (McPhail et al., 2004b), reducing axonal dieback (Stirling et al., 2004), as well as alleviating the cell death of oligodendrocytes (Stirling et al., 2004;Yune et al., 2007). More specifically for root injury, minocycline has been shown to protect motor neurones from cell death after ventral L6 root avulsion injury (Hoang et al., 2008).

There is, however, much controversy in the literature over the effectiveness of minocycline in SCI therapy, as well as the emergence of toxicity, with the inability to replicate initial BBB locomotor and histological observations of improvement after contusive thoracic SCI from the labs in Seoul (Lee et al., 2003) and Alberta (Wells et al., 2003), and at the Miami Project in Florida (Pinzon et al., 2008). Positive observations do not cross over into different models of injury either, such that minocycline has limited neuroprotection after balloon-compression SCI (Saganova et al., 2008), fails to mitigate neuronal degeneration after focal cerebellar lesion (Viscomi et al., 2008), and worsens both hypoxic-ischemic brain injury in neonatal mouse models (Tsuji et al., 2004), and dopaminergic neurone loss in mouse models of Parkinson's and Huntingtons disease (Yang et al., 2003;Diguet et al., 2004a;Stefanova et al., 2004). Minocycline also has rare but significant side-effects at high and prolonged dosing regimens clinically, when used for acne vulgaris in patients, with terminal fulminant hepatic failure requiring liver transplantation (Losanoff et al., 2007), life-threatening hypersensitivity and autoimmune reactions (Shapiro et al., 1997;Ramakrishna et al., 2009), as well as demineralization and discoloration of tooth enamel (Good and Hussey, 2003) and skin pigmentation (Geria et al., 2009). There are now calls in the literature for

the establishment of a forum of negative results and side effects due to the overhelming controversy with minocycline efficacy in neuroprotection (Diguet et al., 2004b).

With the emergence of microglia as a target for neuropathic pain treatment (Milligan and Watkins, 2009;Inoue and Tsuda, 2009) there is now a rationale for the use of minocycline as a potential analgesic treatment for neuropathic pain (Raghavendra et al., 2003;Ledeboer et al., 2005;Hains and Waxman, 2006;Marchand et al., 2009). Preemptive minocycline treatment, 1 hour before PNI in animal models, attenuates the development of behavioural hypersensitivity and is essentially linked to microglial inhibition (Raghavendra et al., 2003) through inhibition of p38 MAPK, preventing activation and proliferation (Tikka et al., 2001;Tikka and Koistinaho, 2001). A similar, if not identical, mechanism exists in spinal cord injury, where p38 MAPK expression is upregulated just rostrally or caudally to the lesion site, and has been causally linked to the occurrence of 'at-level' (Crown et al., 2008) and 'below-level' neuropathic pain (Hains and Waxman, 2006) respectively. Although astroctyes, as well as microglia, show upregulation of p38 MAPK after contusive SCI (Crown et al., 2008), minocycline is yet to be shown effective at ameliorating astrocyte reactivity (Tikka and Koistinaho, 2001;Viscomi et al., 2008). As previously mentioned delayed minocycline treatment, although effectively reduces microglial reactivity at 5-7 days post PNI, is ineffective at ameliorating allodynia and hyperalgesia at this time point, which is attributed to the increasing contribution of astrocytes (but not microglia) in the maintenance of peripheral neuropathic pain (Raghavendra et al., 2003;Ledeboer et al., 2005). Whereas delayed intrathecal minocycline treatment 4 weeks after thoracic SCI, time point of established neuropathic behaviour, ameliorates hyperactivity of dorsal horn neurones and restored nociceptive thresholds, and microglial cells revert back to quiescent morphology (Hains and Waxman, 2006). The beneficial effects of minocycline may therefore be related to the level of involvement of microglia compared to astrocytes in neuropathic pain maintenance, and minocycline may therefore only be effective as a delayed treatment after more central nerve injuries. These therapeutic behavioural effects are attributed to the inhibition of IL-1β, TNFα and other cytokine mediators and their respective converting enzymes (Ledeboer et al., 2005), as well as endocannabinoid reduction (Guasti et al., 2009). Interestingly minocycline treatment in rats does not affect the basal threshold levels of nociceptive pain sensitivity (Padi and Kulkarni, 2008) or post operative pain sensitivity (Ito et al., 2009), or effect lamina I/II neuronal

c-Fos induction in uninjured animals after noxious stimulation (Marchand et al., 2009). It does, however, reduce microglial activity and the level of neuronal c-Fos induction in the hemisected dorsal horn after thermal noxious stimulation to the periphery (Marchand et al., 2009). This suggests firstly, that there is an essential role for microglia in neuropathic pain generation that is not apparent in nociceptive pain; and secondly, but more importantly, advocates that the effectiveness of minocycline's analgesic qualities are dependent on the presence of neurotrauma.

The question relative to this thesis is two fold; firstly, can immediate minocycline treatment ameliorate neuropathic pain behaviour and microglial activity after root injury, a trauma with both central and peripheral consequences? Secondly, does a delayed minocycline administration effectively relieve established avulsion pain?

6.1.3: Therapeutic potential of riluzole for neuronal injury and disease

Riluzole (2-amino-6-trifluoro-methoxy-benzothiazole), or Rilutek™ (Sanofi-Aventis), is an anticonvulsant which has been licensed for patients with the fatal neurological disease, amyotrophic lateral sclerosis (ALS) for over 10 years. A double-blind, placebo-controlled, multicentre and international clinical trial was performed across 18 months (Lacomblez et al., 1996), and at doses of 100mg/day, riluzole was shown to delay the need for tracheostomy surgery, prolonging the life of the patient by 2-3 months (Miller et al., 2007). It has a small beneficial effect on bulbar and limb function, but shows no improvement on muscle strength. Riluzole has also been implicated as a potential anti-depressant due to its positive activity on glial reuptake of excitatory amino-acids (Valentine and Sanacora, 2009).

The neuroprotective effects of riluzole that have been shown are attributed to antagonism of presynaptic calcium dependent glutamate release (Cheramy et al., 1992) and enhancement of glutamate re-uptake via the glutmate transporters GLAST (glial), GLT1 (glial) and EAAC1 (neuronal) (Sung et al., 2003;Fumagalli et al., 2008). These effects pharmacologically are due to inactivation of voltage-sensitive sodium channels (Benoit and Escande, 1991), activation of G-protein-dependent signal transduction processes, as well as non-competitive NMDA blockade (Doble, 1996), and in this way can be described as anti-excitototoxic. Riluzole may also have indirect trophic

mechanisms of neuronal support, by increasing neurotrophic factors (BDNF, NGF, and GDNF) or cytokine production by non-neuronal cells such as astrocytes and schwann cells, improving motor neuronal survival, and dorsal root ganglion neuronal survival, neuritogenesis, and sprouting, as observed in adult and neonatal rat cell culture (Peluffo et al., 1997;Mizuta et al., 2001;Shortland et al., 2006b).

Riluzole, administered at 4 or 8mg/kg i.p, also reduces lesion size and necrosis in rat striatum, in an excitotoxicity model of Huntington's disease, with a proposed indirect mechanism of action of NMDA antagonism (Mary et al., 1995). More specifically to root injury, riluzole has been shown to provide acute neuroprotection for avulsed motor neurones, as well as promoting enhanced neurite formation and outgrowth in avulsed dorsal root ganglion neurones (Shortland et al., 2006b), but has greatest efficacy when administered i.p. in conjunction with reimplantation and GDNF i.p. administration, and shows improved functional recovery on the BBB scale (Bergerot et al., 2004). When retrogradely labelling motor axons in the L4 ventral root after avulsion and reimplantation, and corresponding delayed i.p. treatment with riluzole, motor neuronal pools were labelled in the spinal cord to the same extent as immediate treatment, even after treatment delays of up to 10 days (Nogradi et al., 2007). Muscle wasting of the extensor digitorum longus and tibialis anterior was also reduced in delayed riluzole administration after avulsion/reimplantation (Nogradi et al., 2007). However at 14 days and later, motor neurone survival is not accomplished through riluzole treatment, and is related to the irreversible loss of motor neurones around this time point (Nogradi et al., 2007). This information gives a suitable time window of effective therapeutic intervention in the clinic, of <14 days after an avulsion injury to ventral roots.

Riluzole, like minocycline, has an additional therapeutic target; in neuropathic pain treatment. When riluzole is administered at 1, 4, 6, or 12mg/kg immediately, twice daily for 4 days following CCI in rats, it effectively ameliorates the development of mechanical and thermal hypersensitivity (Sung et al., 2003;Coderre et al., 2007). Riluzole is different to minocycline, in that it has the ability to affect nociceptive thresholds and attenuate anxiety behaviour in naive animals (Coderre et al., 2007;Munro et al., 2007), and at high doses such as 23.3-32.2mg/kg shows general anaesthetic properties in rats with loss of righting reflex, movement and nociceptive responses (Irifune et al., 2007). Nociceptive withdrawal thresholds in naïve and formalin-injected

rats were increased with riluzole treatment and this effect was linked to prolonged reductions in spinal glutamate and aspartate levels (Coderre et al., 2007) and increased glutamate transporter function (Sung et al., 2003).

However, there is some debate as to the effectiveness of riluzole, as when administered clinically at 100mg/day and 200mg/day, in a randomized, placebo-controlled study for peripheral neuropathic pain and at 100mg/kg in a burn pain trial, and patients did not note on a pain intensity visual analogue scale to tactile and thermal stimulation any alleviation (Hammer et al., 1999;Galer et al., 2000), but this may have been due to collating data from mixed pathologies and small cohert sizes. Like minocycline, side effects are apparent clinically at doses of 200mg/kg (recommended dose of riluzole is 50mg twice daily). Common symptoms include vertigo, diarrhea, nausea, and paresthesias around the face, but these are reversible (Siniscalchi, 2004). High concentrations of riluzole (100-300µM) *in vivo* are able to induce cortical neuronal casapase-dependent apoptosis (Koh et al., 1999).

6.1.4: Aims

The positive effects of both riluzole and minocycline in pre-clinical animal models across a range of neurological disorders and diseases, as well as tolerable side effects, have lead to these two drugs entering clinical trials organised in University of Toronto Phase I, and Calgary Phase II respectively, for assessment of functional recovery after SCI (Hawryluk et al., 2008).

The aim of this final chapter is to ascertain if neuropathic pain after avulsion injury is mediated in part by glial and inflammatory mechanisms as well as neuronal loss and disinhibition within the spinal cord, and whether these detrimental processes can be modulated to prevent the development of, or reverse established avulsion pain. The two drugs minocycline and riluzole when administered in the SRA model and analysed behaviourally and histologically will provide an opportunity to test ‘proof of principle’; that inflammatory responses and neuronal loss in the spinal cord after avulsion lead to neuropathic pain.

This shall be accomplished in three ways:

- The behavioural assessment of the efficacy of riluzole (i.p. 4mg/kg) and minocycline (i.p. 40mg/kg) in an immediate treatment strategy, across a 14 day vehicle controlled trial, will ascertain whether the prevention of thermal and mechanical hypersensitivity development after L5 SRA is possible.

- The histological effects of riluzole (i.p. 4mg/kg) and minocycline (i.p. 40mg/kg) treatment on glial, inflammatory, and neuronal populations compared to a vehicle treated group, at 14 days post SRA will be examined and correlated with the behaviour at this time point.

- The efficacy of delayed administration of riluzole (i.p. 4mg/kg) and minocycline (i.p. 40mg/kg) after establishment of SRA-induced thermal and mechanical hypersensitivity will be assessed behaviourally. Drug administration will be from 7-13 days post operatively, once a day, and then from 14-21 days, once every two days.

If efficacy is proven in this model, it may provide a rationale for the application of these drugs in multiple pre-clinical models of neuropathic pain, and perhaps more importantly clinically for brachial and lumbosacral plexus avulsion injured patients. Treatment can be applied to future patients as a preventative measure, and perhaps more immediately needed is treatment for an already pre-established intractable avulsion-pain for current sufferers. Both riluzole and minocycline are already approved and licensed for medical use, and currently available for clinical testing for neuropathic pain treatment.

6.2: Results

6.2.1: Immediate and maintained treatment of L5 SRA-induced hypersensitivity across 14 days

6.2.1.1: Vehicle treatment

Vehicle (0.1M HCl) treatment immediately after L5 SRA, and maintained across 14 days, did not prevent, or reverse at any time point assessed, the development of hypersensitivity to tactile or thermal stimulation. Preoperative baseline values for both thermal and tactile stimulation were in accordance with values from SRA untreated groups (Chapter 4), and again did not differ when compared to ipsilateral and contralateral sides.

Mechanical

Significant ipsilateral mechanical hypersensitivity was established against both baseline values (21.8g +/- 1.00) and contralateral values (22.0 +/-1.01) by 1 day (15.9g +/-1.98) post operatively. This mechanical hypersensitivity was maintained for 14 days where final values were recorded at 11.6g (+/-1.41) withdrawal threshold (Fig 6.1A). No change was found in contralateral values compared to baseline (Fig 6.1A).

Thermal

Significant ipsilateral thermal hypersensitivity was established against baseline values (8.45s +/-0.34) by 5 days (6.79s +/-0.09) and from contralateral values (8.22s +/-0.64) by 9 days (5.83s +/-0.75) post operatively. This is maintained up to 14 days where final values were recorded at 6.01s (+/-0.32) withdrawal latency (Fig 6.1B). No change was found in contralateral values compared to baseline (Fig 6.1B).

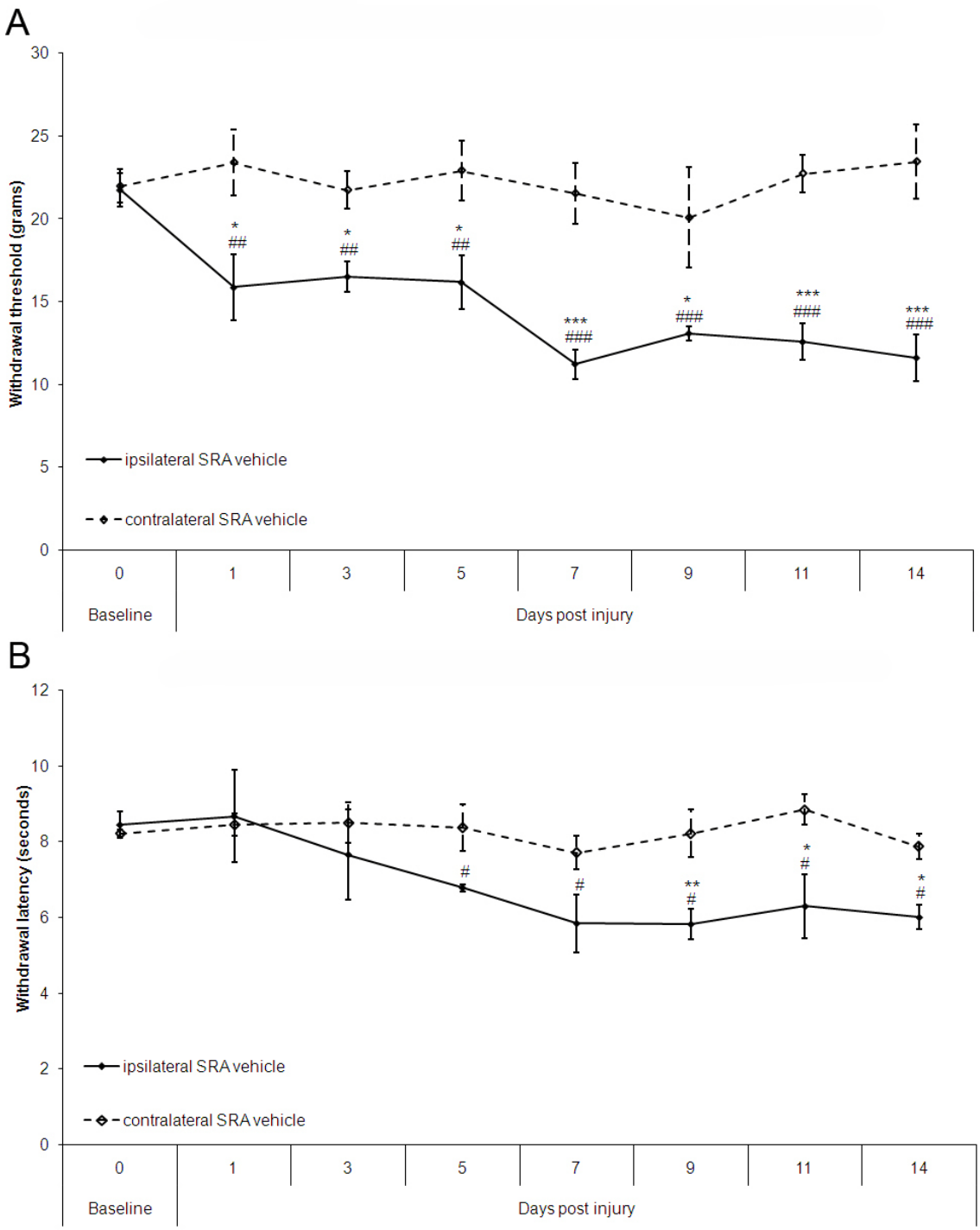

Figure 6.1: Effects of vehicle treatment on mechanical (A) and thermal (B) thresholds after L5 SRA. Administration of vehicle does not prevent the development of ipsilateral behavioural hypersensitivity to tactile (A) or thermal (B) stimulation. Tactile hypersensitivity is established by 1 day compared to baseline and contralateral. Thermal hypersensitivity is established by 5 days. Significant differences are indicated for ipsi vs contra (*) and against baseline (#). N = 6.

6.2.1.2: Riluzole treatment

Riluzole treatment immediately after L5 SRA for 14 days, delayed the development of hypersensitivity to mechanical and thermal stimulation, but did not prevent its establishment by the end of the treatment period. Preoperative baseline values for both thermal (8.75s +/-0.79) and mechanical (21.1 +/- 0.88) stimulation were not significantly different to vehicle treated (Fig 6.2B and 6.3B), and again did not differ when compared bilaterally (Fig 6.2A and 6.3A).

Mechanical

Significant ipsilateral mechanical hypersensitivity was established against contralateral values (21.1g +/-0.92) by 3 days (16.7g +/-2.68). However on days 5, 7, and 9, ipsilateral mean withdrawal threshold values were increased such that no significant difference to contralateral values was found (Fig 6.2A). Further, on day 7 (17.7g +/-1.17) and day 9 (20.1g +/-1.53) withdrawal threshold values were significantly higher than mean vehicle withdrawal levels (Fig 6.2B). However by day 11 ipsilateral withdrawal threshold values (15.6s +/-1.21) returned to vehicle levels representative of hypersensitivity, and were significantly lower than contralateral values. Only on the final day were ipsilateral values (12.9g +/-2.21) significantly lower than baseline values. No change was found in contralateral values compared to baseline (Fig 6.2A).

Thermal

Significant ipsilateral thermal hypersensitivity was established against contralateral values (9.53s +/-0.52) only at 5 days (7.44s +/-0.49). However, at all other time points, mean ipsilateral withdrawal latencies were not significantly different to contralateral values (Fig 6.3A). On days 7-11 riluzole treated thermal withdrawal thresholds were significantly higher than compared to vehicle ipsilateral withdrawal latencies (Fig 6.3B). However, by day 14 riluzole-treated thermal withdrawal threshold values (6.61s +/-1.28) returned to vehicle levels. At no time point ipsilateral values (12.9g +/-2.21) significantly lower than baseline values. No change was found in contralateral values compared to baseline (Fig 6.3A).

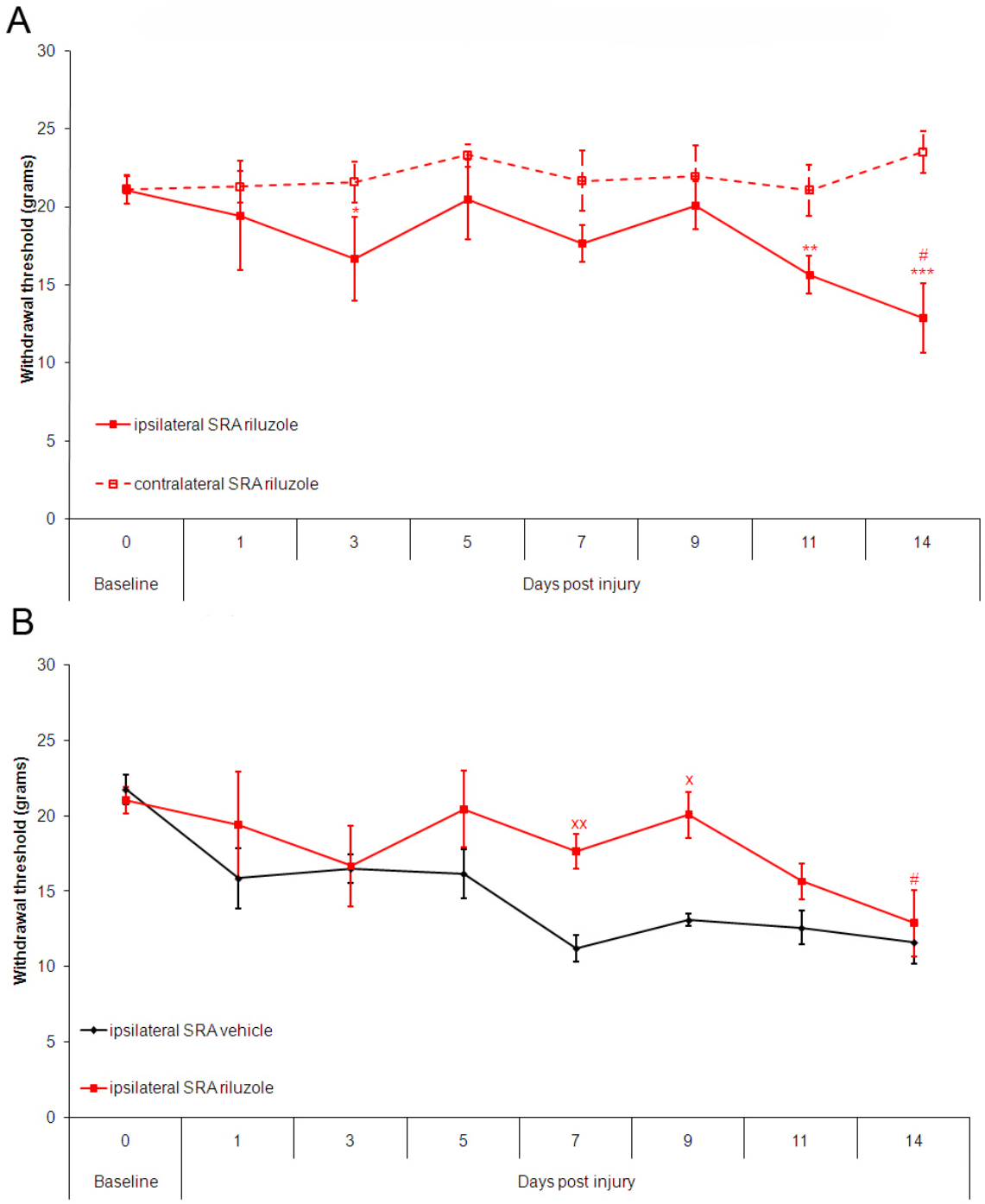

Figure 6.2: Effects of riluzole on mechanical thresholds after L5 SRA. Riluzole treatment delays the development of tactile hypersensitivity against contralateral and baseline values (A) and against vehicle levels (B) on days 5, 7, and 9. This effect is not maintained at 11 and 14 days. Significant differences are indicated for ipsi vs contra (*), against baseline (#), and against vehicle (x). N = 6 in each group.

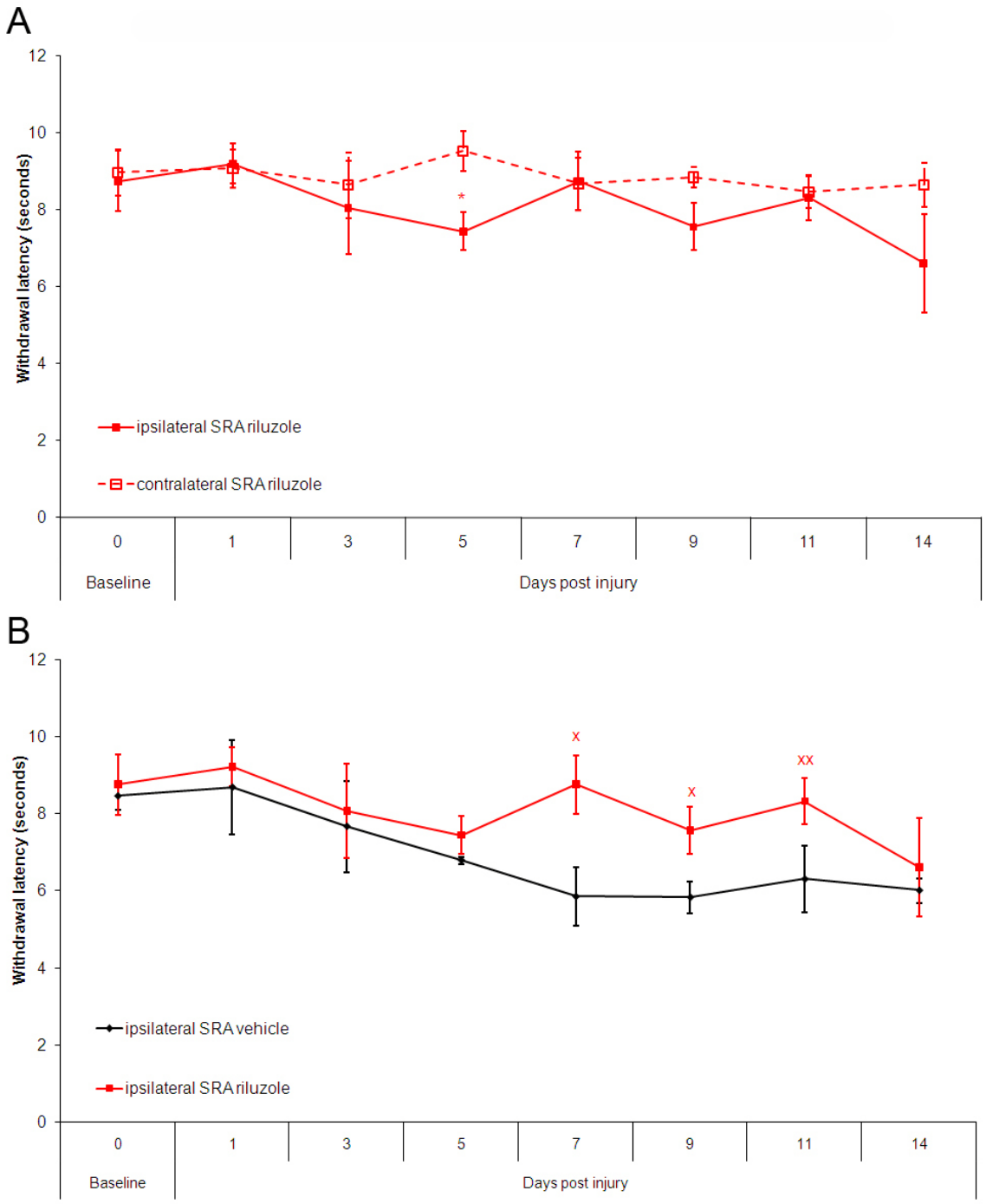

Figure 6.3: Effects of riluzole on thermal thresholds after L5 SRA. Riluzole treatment prevents the development of thermal hypersensitivity against contralateral and baseline values (A) and against vehicle levels (B) on all days, except day 5 and 14. Significant differences are indicated for ipsi vs contra (*), against baseline (#), and against vehicle (x). N = 6 in each group

6.2.1.3: Minocycline treatment

Minocycline treatment that started immediately after L5 SRA for 14 days prevented the development of thermal and mechanical hypersensitivity compared to baseline levels and vehicle treatment, but on several days contralateral effects were noted. Preoperative baseline values for both thermal (9.36s +/-0.27) and mechanical (19.9g +/- 0.71) stimulation were not significantly different to vehicle levels (Fig 6.4B and 6.5B), and did not differ when compared bilaterally (Fig 6.4A and 6.5A).

Mechanical

No mechanical hypersensitivity was seen compared to baseline values at any time point (Fig 6.4A). Minocycline treatment significantly raised ipsilateral mechanical withdrawal thresholds compared to vehicle levels from 3 days onwards (Fig 6.4B). However, there was development of an intermittent contralateral hyposensitivity, such that ipsilateral mechanical withdrawal thresholds were significantly lower than contralateral values (24.5g +/-1.17) on day 1 (17.6g +/-2.23), with contralateral values significantly increased over baseline. On days 3, 7 and 9, contralateral withdrawal thresholds returned to baseline, and were not significantly greater than ipsilateral levels (Fig 6.4A). However, contralateral hyposensitivity again developed against baseline on day 5 (10.6s +/-1.21), day 11 (25.0g +/-1.83) and day 14 (24.4g +/-0.98), with withdrawal threshold values significantly higher than ipsilateral withdrawal levels at 11 and 14 days (Fig 6.4A). However, across the 14 day time course, contralateral hyposensitivity did not increase beyond that noted initially on day 1.

Thermal

No thermal hypersensitivity was established against contralateral or baseline values at any time point assessed across 14 days (Fig 6.5A). Minocycline treatment significantly maintained ipsilateral thermal withdrawal latency values from day 5-14 compared to vehicle treated animals where the threshold began to fall during this time frame (Fig 6.5B). A contralateral thermal hyposensitivity only developed on day 9 (12.0s +/-0.59), and was significantly higher than baseline withdrawal latencies, but was not significantly different to ipsilateral values (Fig 6.5A).

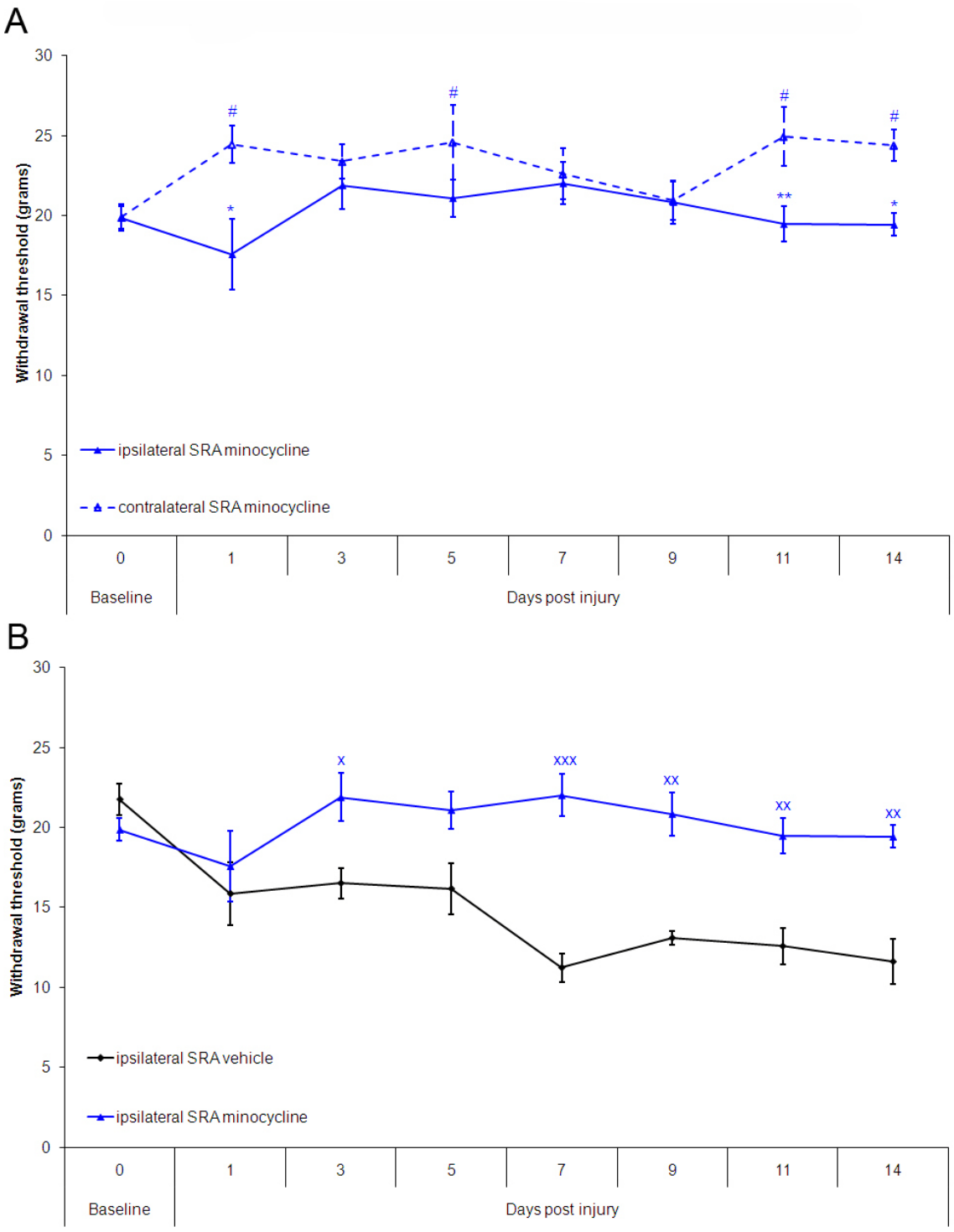

Figure 6.4: Effects of minocycline on mechanical thresholds after L5 SRA. Minocycline treatment prevents the development of tactile hypersensitivity against contralateral and baseline values (A) and against vehicle treatment (B) over 14 days. Significant differences are indicated for ipsi vs contra (*), against baseline (#), and against vehicle (x). N = 6 in each group.

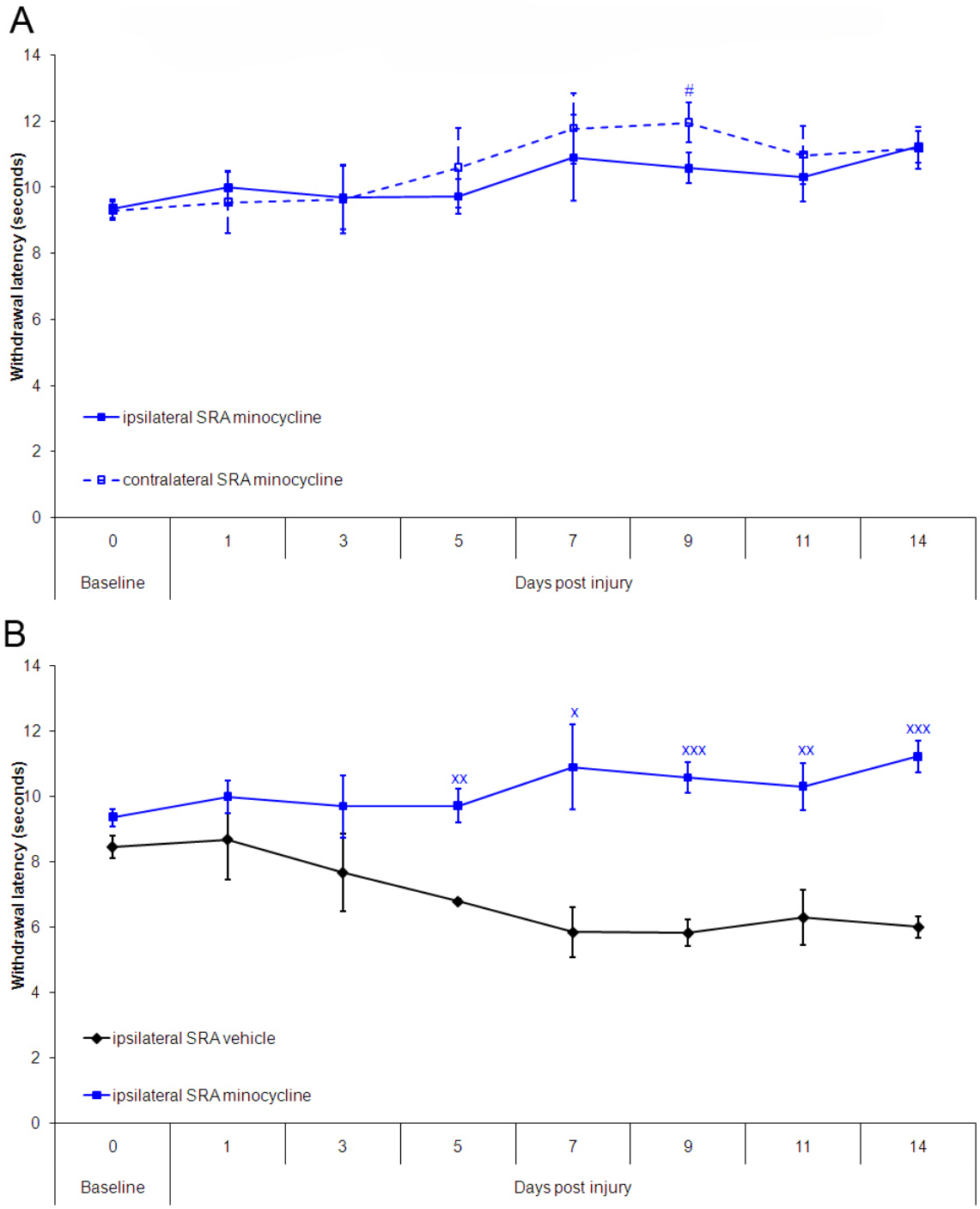

Figure 6.5: Effects of minocycline on thermal thresholds after L5 SRA. Minocycline treatment prevents the development of thermal hypersensitivity against contralateral and baseline values (A) and against vehicle levels (B) across 14 days. Significant differences are indicated for ipsi vs contra (*), against baseline (#), and against vehicle (x). N = 6 in each group.

6.2.1.4: Effect of treatment on weight gain after L5 SRA.

Male Wistar rats underwent SRA+vehicle treatment with a pre-surgical baseline weight of 234.8g (+/-4.06). Daily weight gain across 14 days was 5.35g/day (+/-0.37) (Fig 6.6). Total weight gain across 14 days was 74.8g (+/-5.24).

Age matched male Wistar rats underwent SRA+riluzole treatment with a pre-surgical baseline weight of 233.7g (+/-6.06). Daily weight gain across 14 days was 5.61g/day (+/-0.37), which was not significantly different to vehicle treatment (Fig 6.6). Total weight gain across 14 days was 78.5g (+/-5.18).

Age matched male Wistar rats underwent SRA+minocycline treatment with a pre-surgical baseline weight of 234.7g (+/-7.42). Daily weight gain across 14 days was 3.75g/day (+/-0.21), which was significantly lower than vehicle treatment (Fig 6). Total weight gain across 14 days was 52.5g (+/-2.93).

Pre-surgical baseline weights were not significantly different between groups.

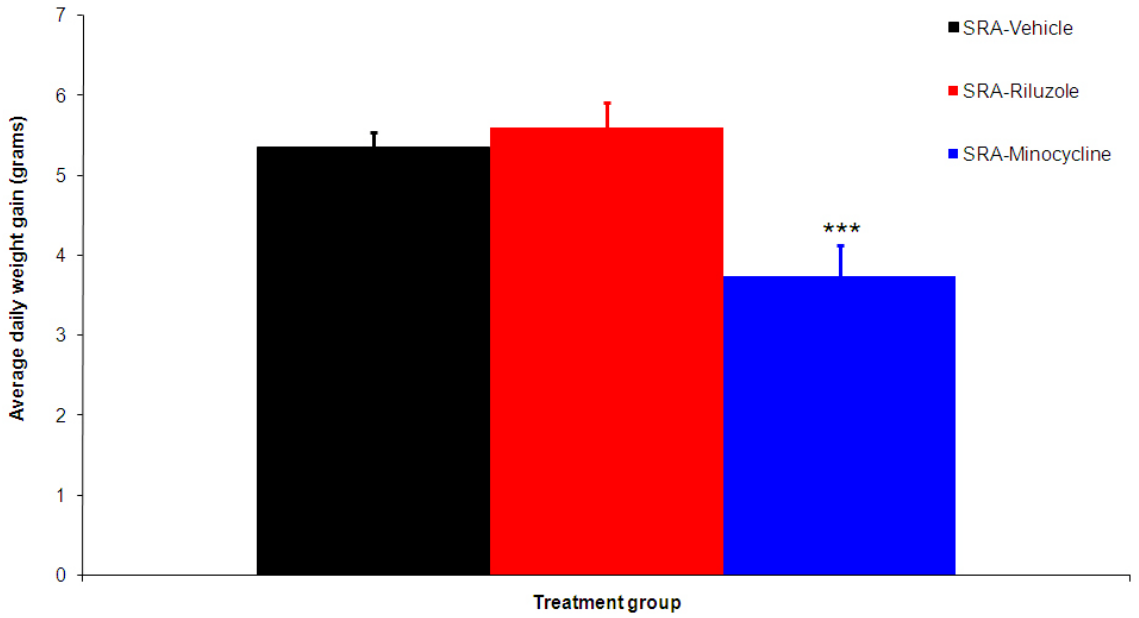

Figure 6.6: Mean daily weight gain in adult male Wistar rats after SRA, and different drug treatments. Over a period of 14 days vehicle and riluzole treated rats gain a similar amount of weight. However, over the same period of assessment with minocycline treatment, SRA injured rats gain significantly less weight than SRA-vehicle treated animals. Comparison for treatment vs vehicle **(*)** is indicated. N = 6 in each group.

6.2.2: Immunohistological analysis of L4 and L5 spinal cord in riluzole, minocycline, and vehicle treated rats

6.2.2.1: Dorsal horn neuronal counts

Fourteen days after SRA-vehicle treatment, similar to SRA-untreated (Chapter 4) animals, L5 segmental NeuN loss was seen in the superficial lamina directly underlying Lisseaur's tract and dorsal root entry zone and lateral superficial areas, with small cystic cavities within the area of deafferentation (Fig 6.7A). NeuN loss in the adjacent L4 segment was seen similar to SRA-untreated (Chapter 4), but to a lesser extent than that found caudally in L5, but was seen in the superficial lamina underlying Lisseaur's tract (Fig 6.7A).

When quantified spinal cord tissue from 14 day SRA-vehicle treatment, mean dorsal horn neuronal counts per section were 351.7 (+/-15.5) for the L5, and 375.7 (+/-10.4) for the L4 segments, with counts significantly lower than contralateral values (L5: 387.9 +/-11.3 and L4: 404.5 +/-9.60) (Fig 6.7B).

Fourteen day SRA treatment with riluzole (4mg/kg) lead to no significant improvement in NeuN mean number of cells per section (Fig 7A) in deafferented (L5 = 344 +/-15.7) or intact (L4 = 373.5 +/-11.4) dorsal horn against vehicle treated cords (Fig 6.7B).

Fourteen day SRA treatment with minocycline (40mg/kg) lead to no significant improvement in mean NeuN number per section in the deafferented L5 segment (355.3 +/-10.9). However, the mean number of neurones in the L4 dorsal horn (390.8 +/-6.94), was not significantly different to the contralateral side. No significant difference was found between ipsilateral dorsal horns of vehicle and minocycline treated (Fig 6.7B).

No significant difference was found between contralateral cords of any treatment group (Fig 6.7B).

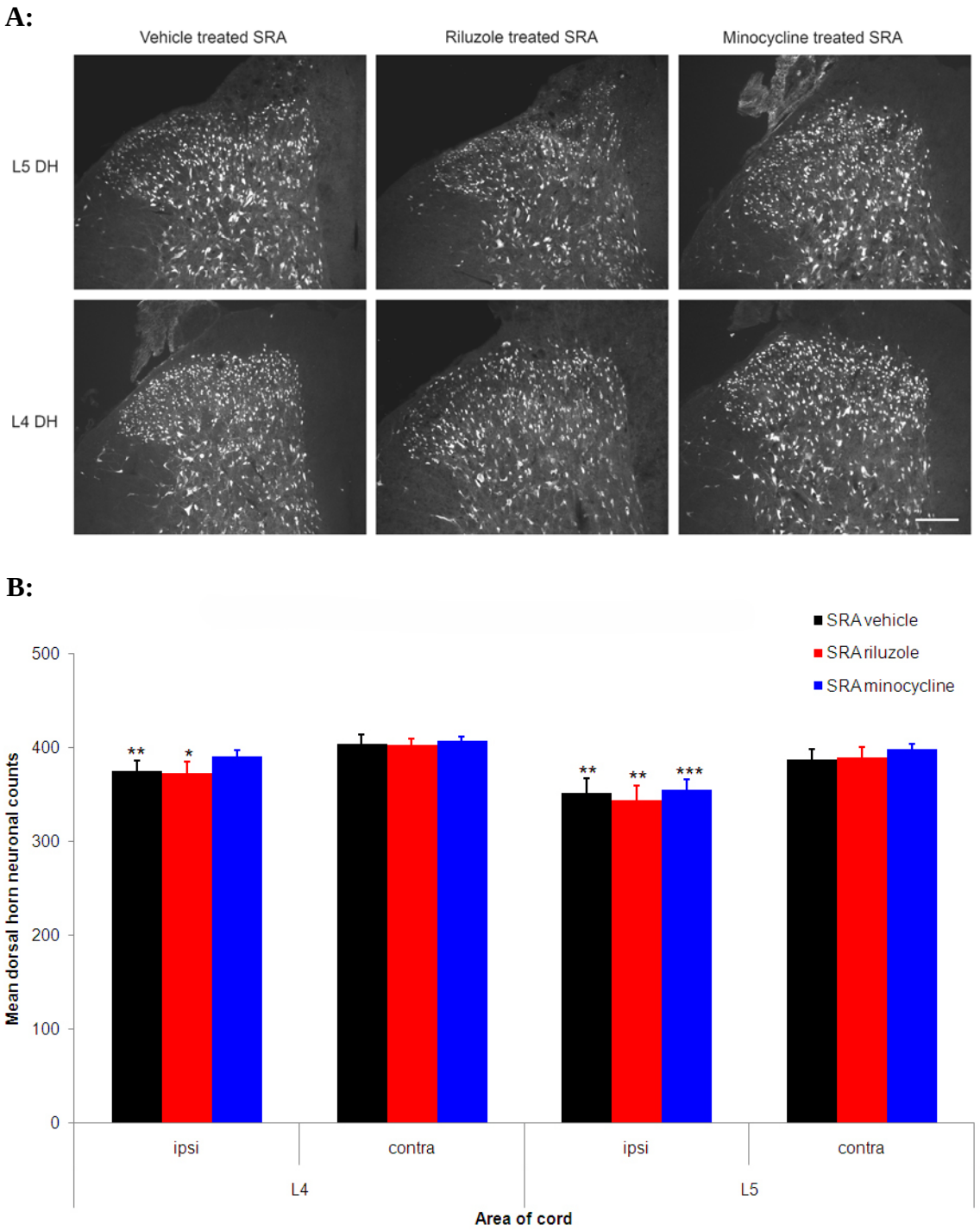

Figure 6.7: Photomicrographs of effects of drug treatment on dorsal horn neuronal staining (A) and quantification of total dorsal horn neurones per section (B) 14 days after L5 SRA, in L4 and L5 segments. A: Cavitation and neuronal reduction is noticeable near DREZ and Lisseaur's tract 2 weeks after SRA in vehicle, riluzole and minocycline treated animals. B: NeuN number was similar in the L4 dorsal horns, ipsilaterally versus contralaterally, but this was not the case in the L5 segment, with minocycline treatment. Riluzole had no effect on NeuN counts. Significant differences for ipsi vs contra (*) are shown. N = 6 in each group. Scale=100µm

6.2.2.2: Ventral horn neuronal counts

Similarly to SRA-untreated animals (chapter 2), a prominent motor neuronal loss was found in the ipsilateral ventral horn 14 days after SRA with vehicle treatment, using both Toluidine Blue histology and NeuN immunohistochemistry. Again a greater percentage reduction using immunohistochemistry, rather than histological dye, was visually apparent (Fig 6.8) and quantifiable (Fig 6.9).

Using NeuN immunohistochemistry 14 days after SRA plus vehicle treatment, motor neurone loss was seen in L5 (69.3% +/-3.8) and L4 (50.3% +/-4.7) segments compared to contralateral sides (Fig 6.9).

When analysing Tol Blue histology for neuronal counts in SRA-vehicle treated rats, a marked difference in percentage reduction from NeuN immunohistochemistry was noted. Mean reduction was limited to 39.6% (+/-4.5) in L5 and 26.6% (+/-7.4) in L4 (Fig 6.9).

Treatment with riluzole did not produce significant improvements in the number of NeuN or Toluidine Blue stained motor neurones in the ipsilateral cord 14 days after SRA (Fig 6.8) in the deafferented (L5 = 68.6% +/-3.4) or intact (L4 = 46.5% +/-1.7) ventral horn compared to vehicle treated cords (Fig 6.8). Toluidine Blue histological analysis also showed no significant difference between riluzole treated (L5 = 44.5% +/-6.0 and L4 = 26.6% +/-6.1) and vehicle treated animals (Fig 6.9).

Likewise, treatment with minocycline did not produce significant neuroprotection of NeuN or Toluidine Blue stained cells in the ipsilateral cord 14 days after SRA (Fig 6.8) in the deafferented L5 (71.1% +/-4.8) or the intact L4 (42.6% +/-10.9) segments compared to vehicle treated animals (Fig 6.9). Toluidine Blue histological analysis also showed no significant difference between minocycline treated (L5 = 41.7% +/-5.3 and L4 = 31.3% +/-6.5) and vehicle percentage motor neurone ratios (Fig 6.9).

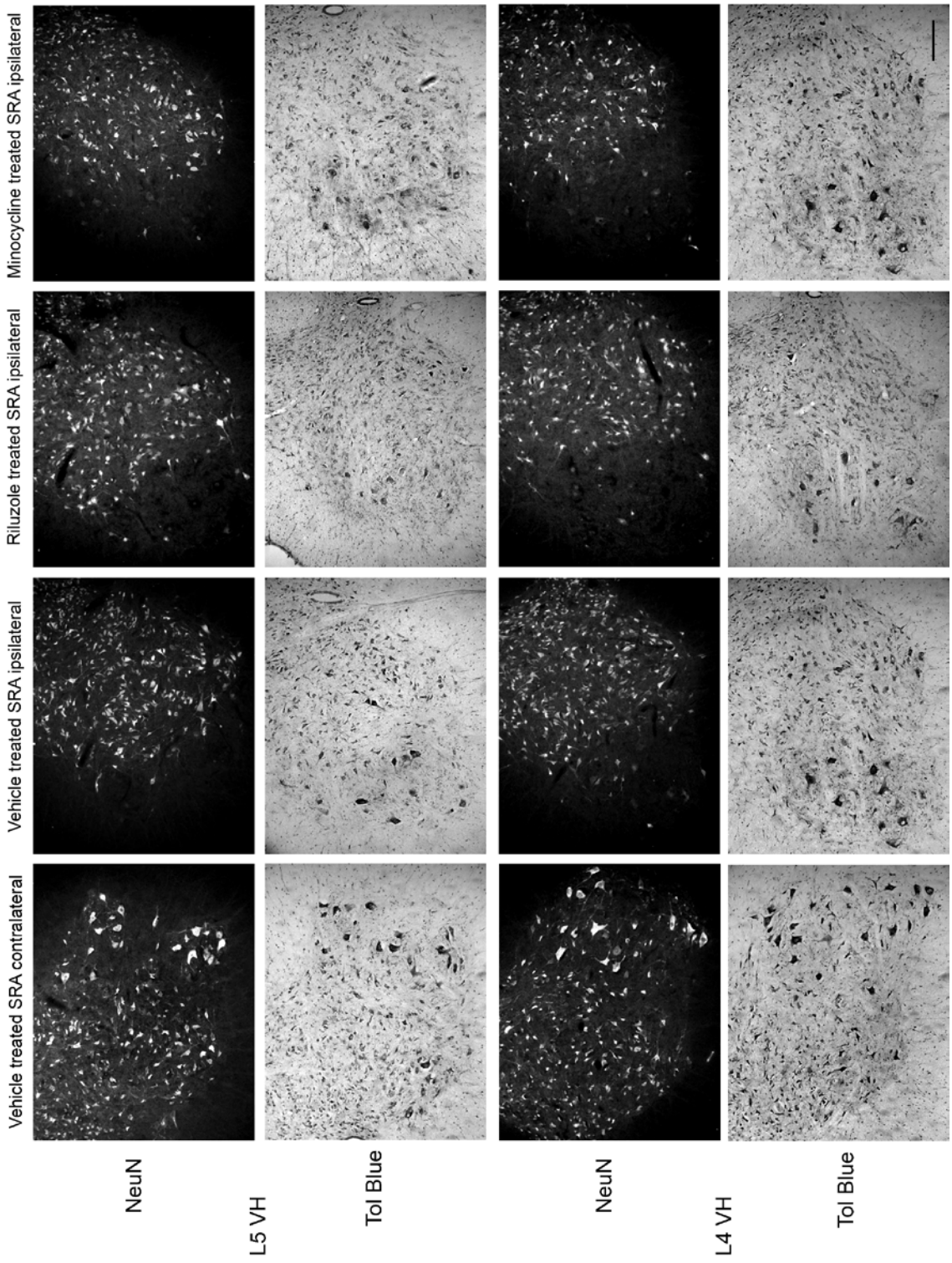

Figure 6.8: Photomicrographs of effects of drug treatments on motor neurone number 14 days after SRA as assessed by NeuN or toluidine blue staining, in L4 and L5 segments. Treatment with either riluzole or minocycline does not prevent the loss of motor neurones after SRA, shown with vehicle treatment, in either L5 or L4 segments, compared to contralateral numbers. Scale=100µm

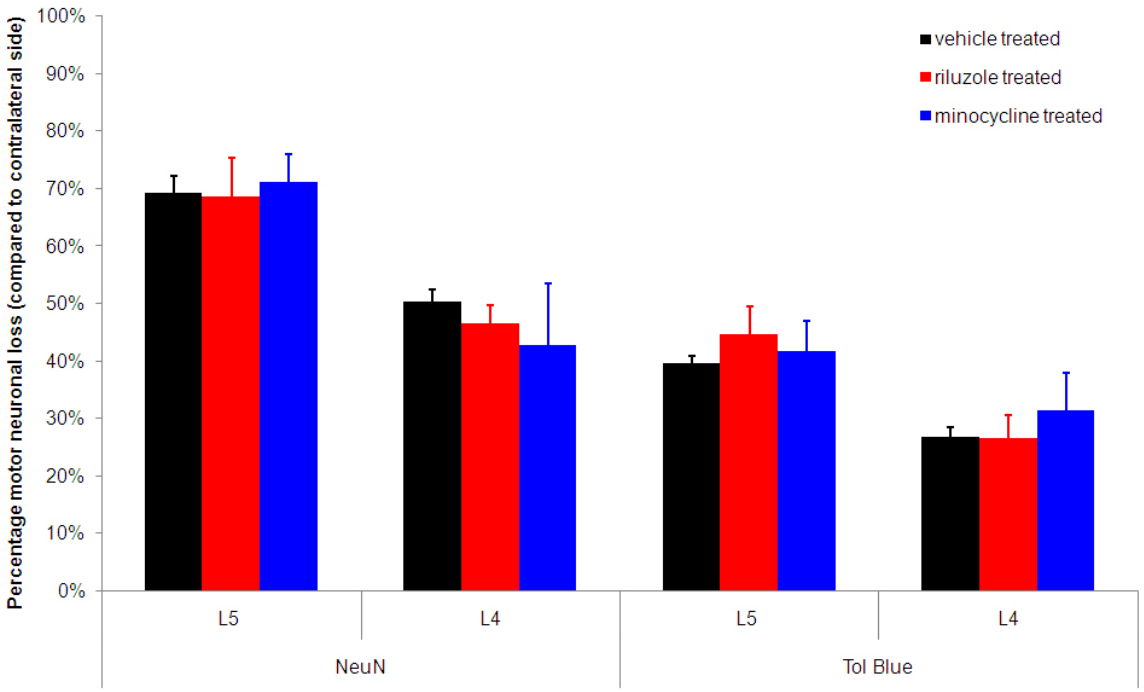

Figure 6.9: Quantitative effects of drug treatment on mean number of motor neurones using toluidine blue or NeuN labelling 14 days after SRA, in L4 and L5 segments. No significant difference is found for either riluzole or minocycline compared to the loss found with vehicle treatment, using either Tol Blue or NeuN counts in L4 or L5 ventral horn segments. The loss of motor neurones compared to contralateral sides was much less using Tol Blue histology than NeuN immunohistochemistry to perform counts. N = 6 per group.

6.2.2.3: Microglial reactivity in the dorsal and ventral horns

Fourteen days after SRA with vehicle treatment, Iba1 density was significantly upregulated in the dorsal horn microglia ipsilateral to the deafferentation, in L5 as well as L4 segments, compared to contralateral levels (Fig 6.10). Within the deafferented L5 ipsilateral segments Iba1 expression could be seen intensely in the DREZ that spreads throughout the superficial laminae (Fig 6.10). Iba1 expression increase is confined to the grey matter in the L4 cord, but is present in both grey and white matter in L5, notably around the DREZ (Fig 6.10). Mean ipsilateral Iba1 density staining reached 8.85% (+/-0.88) in L4 and 9.39% (+/-0.69) in L5 dorsal horns (Fig 6.11A). No significant difference was found between microglial density staininig between the deafferented L5 and intact L4 dorsal horns (Fig 6.11A).

Iba1 expression in SRA tissue was also significantly upregulated in the ipsilateral ventral horns of both deafferented L5 and intact L4 segments, compared contralateral levels (Fig 6.11B). Visually, in the L5 ipsilateral segment as well as the L4 segment, Iba1 positive microglia were greatly upregulated around motor neurone pools, clustering tightly in the lateral aspect of the ventral horn (Fig 10). Mean ipsilateral Iba1 ventral density staining reached 8.95% (+/-0.66) in L4 and 9.34% (+/-0.47) in L5, and again no significant difference was found between the deafferented L5 and intact L4 segments (Fig 6.11B).

Treatment with riluzole visibly reduced Iba1 staining in the L5 and L4 ipsilateral dorsal horn and L4 ventral horn 14 days after SRA (Fig 6.10). Quantitative analysis showed mean dorsal horn Iba1 staining per section was significantly reduced to 5.67% (+/-0.59) in L5 and 5.12% (+/-0.55) in L4 cord (Fig 6.11A). In the ventral horn only L4 showed significant reduction in mean Iba1 density staining per section (6.43% +/-0.41) (Fig 6.11B).

Treatment with minocycline reduced microglial staining in all areas of the ipsilateral cord, and the pockets of intense staining shown in SRA-vehicle, were absent in this tissue (Fig 6.10). When quantified, mean Iba1 staining per section was significantly reduced compared to SRA-vehicle in the intact adjacent L4 (DH=3.86% +/-0.80 and VH=4.55% +/-0.93) and deafferented L5 (DH=3.94% +/-0.61 and VH=4.14% +/-0.94) spinal cord segments. Values of SRA-minocycline were successfully reduced to sham levels in all cases (Fig 6.11).

Mean contralateral Iba1 reduction with minocycline treatment was significant in L4 ventral horn (1.97% +/-0.21) against SRA-vehicle contralateral values (2.89% +/-0.29) (Fig 6.11B). However, no significant contralateral increase in Iba1 expression was found after SRA-vehicle, in either deafferented L5 or intact L4 segments, dorsally or ventrally (Fig 6.11).

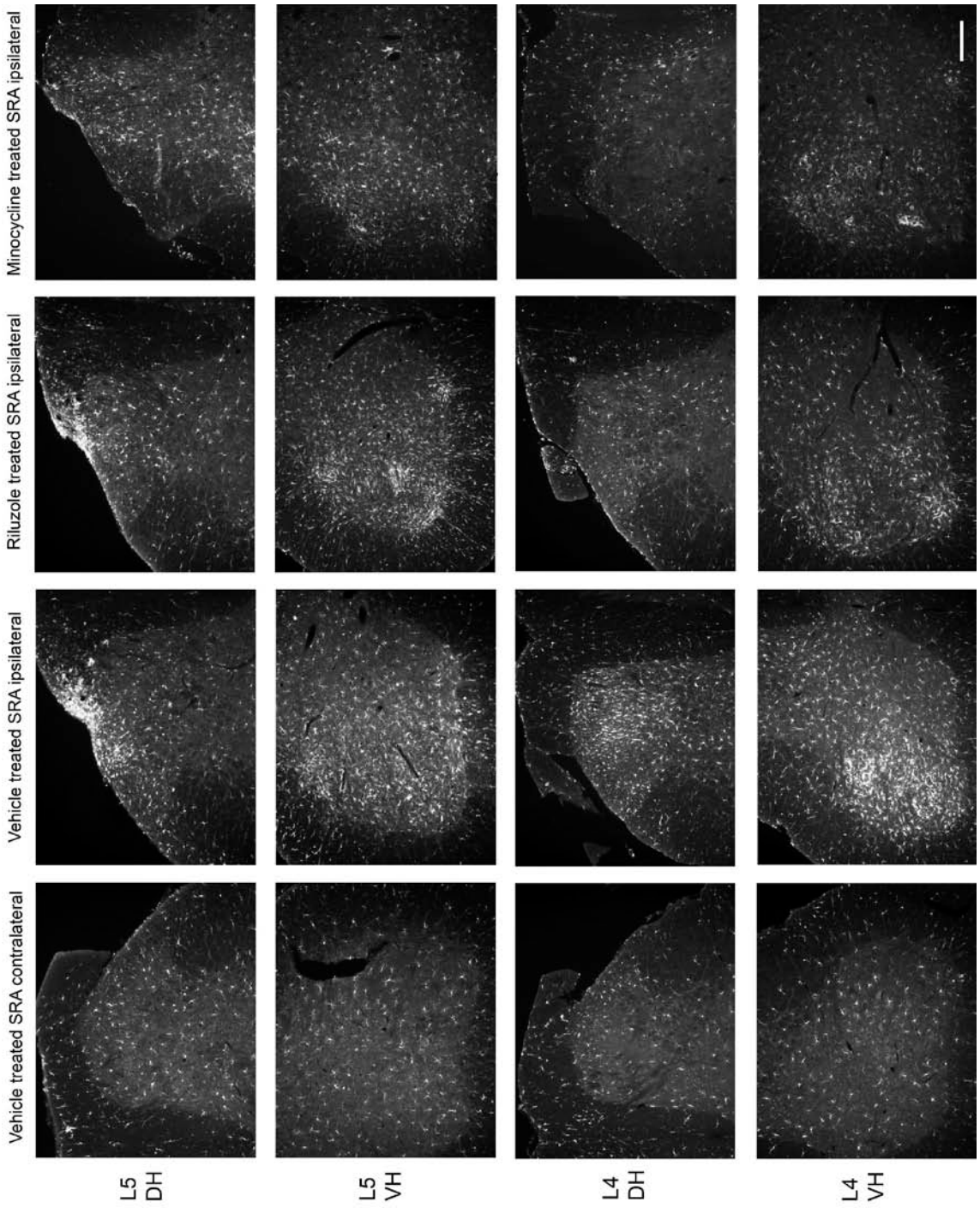

Figure 6.10: Photomicrographs of effects of drug treatment on dorsal horn (DH) and ventral horn (VH) Iba1 labelling 14 days after L5 SRA in L4 and L5 segments. Increase in Iba1 labeling can be seen in the superficial dorsal and lateral ventral horns, in both L5 and L4 ipsilateral segments, compared to contralateral. Riluzole reduces Iba1 staining in the dorsal and ventral horns of L4 and the dorsal horn of L5, but this is not evident in the ventral horn of L5. Minocycline reduces Iba1 staining in all areas shown. Scale=100μm

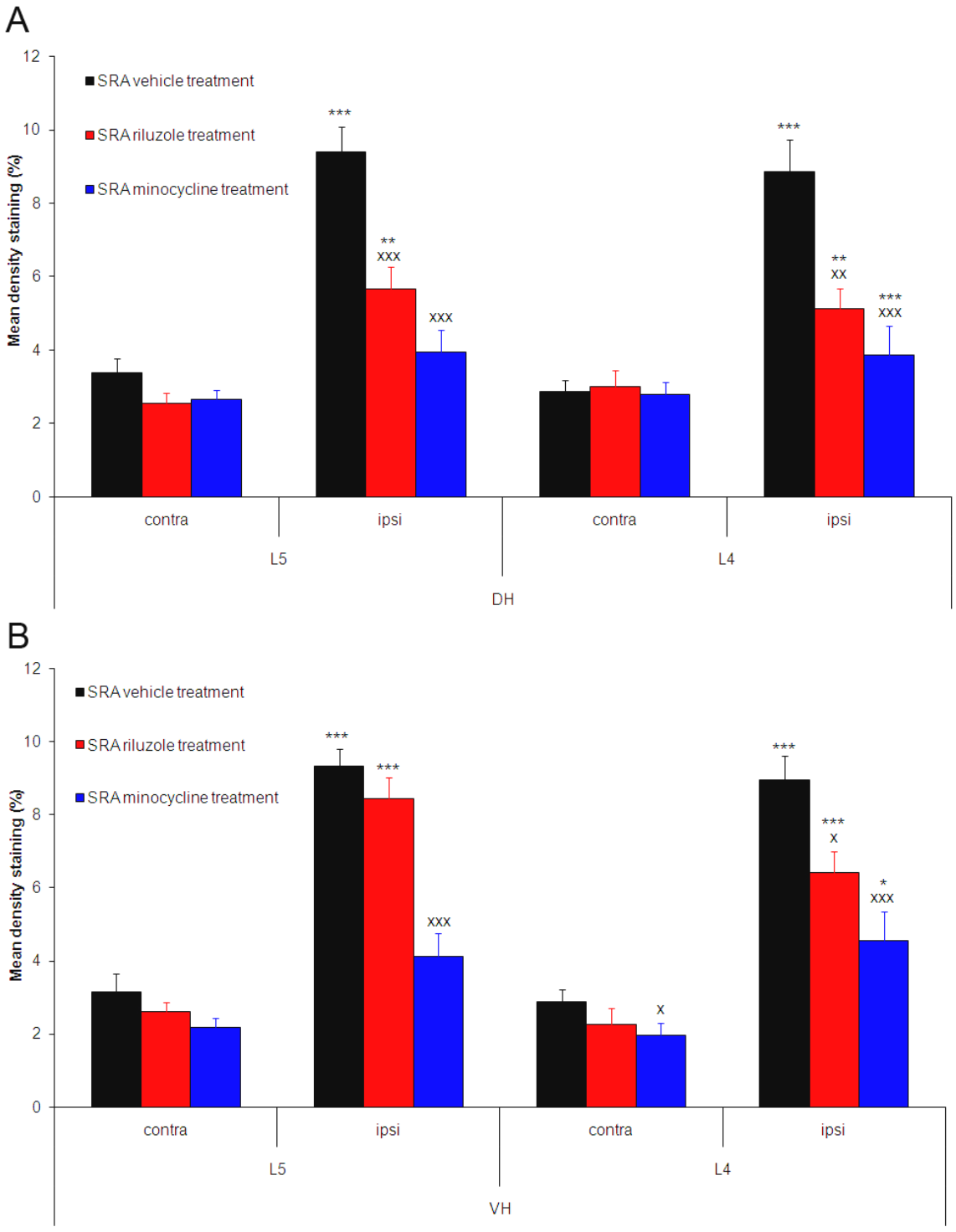

Figure 6.11: Quantitative effects of drug treatment on dorsal horn (A) and ventral horn (B) Iba1 labelling 14 days after L5 SRA in L4 and L5 segments. SRA-vehicle shows significant upregulation of Iba1 staining in all areas analysed. Riluzole treatment leads to a significant Iba1 reduction in L5 and L4 dorsal horns and L4 ventral horn, but not in L5 ventral horn, compared to vehicle. Minocycline treatment leads to a significant staining reduction in all areas analysed compared to vehicle (B). Significant differences are indicated for, ipsi vs contra (#), and treatment vs vehicle (*). N = 6 per group.

6.2.2.4: Astrocyte reactivity in the dorsal and ventral horns

Fourteen days after SRA with vehicle treatment, GFAP density was significantly upregulated in the dorsal horn astrocytes ipsilateral to the deafferentation, in L5 as well as L4 segments, compared to contralateral levels (Fig 6.12 and 6.13). A network of GFAP-positive astrocytes could be seen in the dorsal root entry zone and dorsal column of L5, with hypertrophy and increased GFAP expression in the superficial and deep dorsal laminae of both L4 and L5 spinal cord (Fig 6.12). Mean ipsilateral GFAP density staining per section reached 8.97% (+/-0.80) in L4 and 8.87% (+/-0.81) in L5 dorsal horns (Fig 6.13). No significant difference in density staining was found between the L5 and L4 dorsal horns (Fig 6.13).

GFAP expression in SRA tissue was also significantly upregulated in the ipsilateral ventral horns of both L5 and L4 segments, compared contralateral levels (Fig 6.13). In the L5 segment, GFAP density staining was upregulated around motor neuronal pools. Within the L4 segment, astrocytes had 'looser' association with motor neurones, surrounding rather than 'blanketing' individual cells, but each astrocyte still shows a greatly increased GFAP expression (Fig 6.12). Mean ipsilateral GFAP density staining per section in the ventral horn reached 7.76% (+/-0.40) in L4 and 7.93% (+/-0.48) in L5, and again no significant difference in density was found between the L5 and L4 segments (Fig 6.13).

Treatment with riluzole showed only a trend toward reduction of GFAP density staining in the dorsal and ventral horns after SRA compared to vehicle treated animals (Fig 6.12 and 6.13). Mean density staining levels per section were 8.40% (+/-0.48) in L5 and 7.73% (+/-0.41) in L4 (Fig 6.13). Ventral horn GFAP levels were 7.01% (+/-0.46) in L5 and 7.32% (+/-0.68) in L4 (Fig 6.13).

Treatment with minocycline visibly reduced GFAP staining in all areas of the ipsilateral cord (Fig 6.12). When quantified, mean GFAP staining per section was significantly reduced compared to SRA-vehicle in the ventral horns of L4 (6.64% +/-0.25) and L5 (6.07% +/-0.24) segments (Fig 6.13). However, only a trend in GFAP staining reduction was found in the dorsal horns in L4 (7.83% +/-0.30) and L5 (7.23% +/-0.53) segments (Fig 6.13).

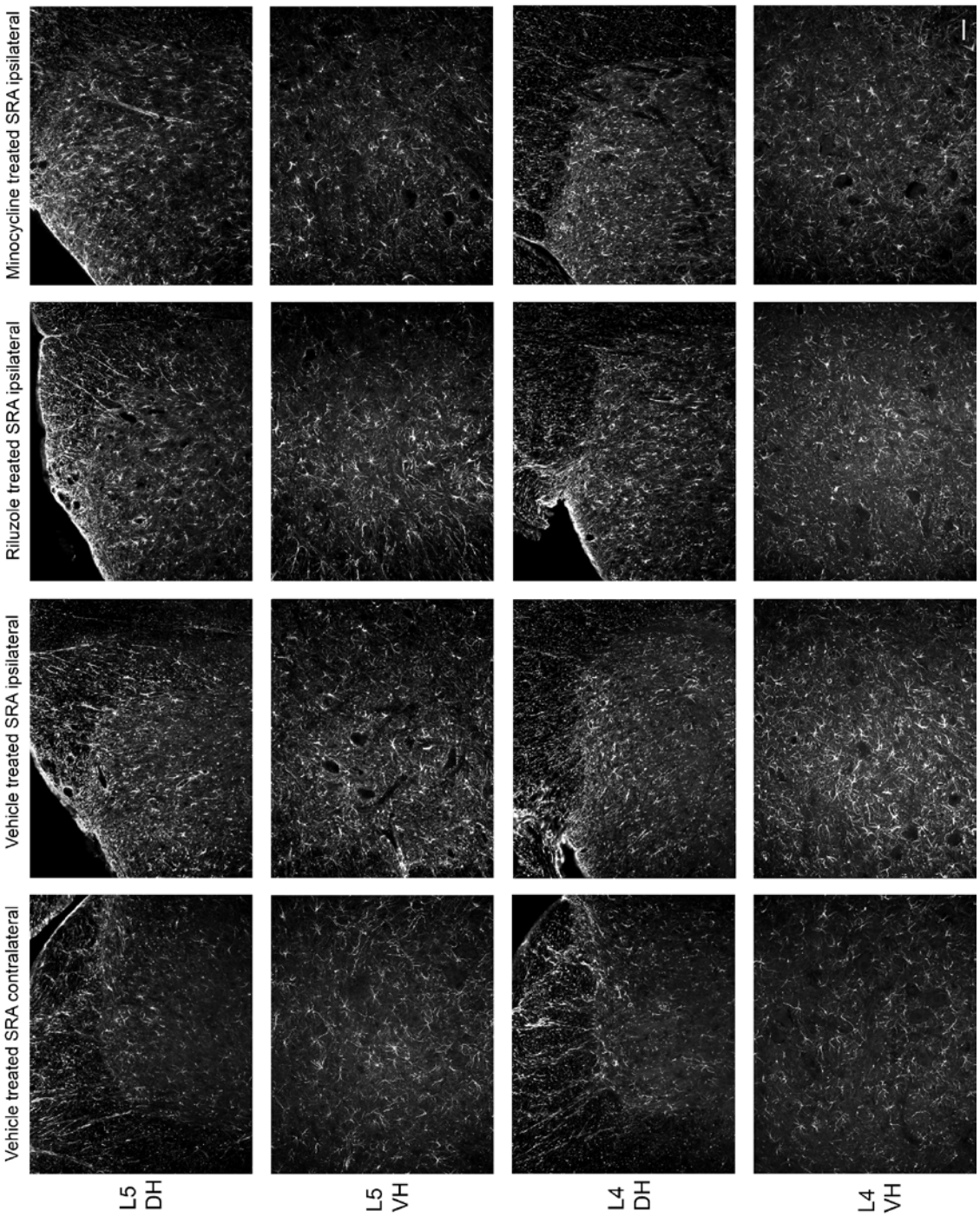

Figure 6.12: Photomicrographs of effects of drug treatment on dorsal horn (DH) and ventral horn (VH) GFAP labelling 14 days after L5 SRA, in L4 and L5 segments. GFAP labeling can be seen in SRA-vehicle 14 days after SRA, surrounding motor neurones and superficial dorsal horn, Lisseaur's tract, and the dorsal root entry zone, greatly increased from contralateral levels. Riluzole treatment has little effect on GFAP staining in the dorsal and ventral horns of L4 and L5. Minocycline treatment reduces GFAP staining in the ventral horns of L4 and L5, with no significant effect in the dorsal horns. Scale=100µm

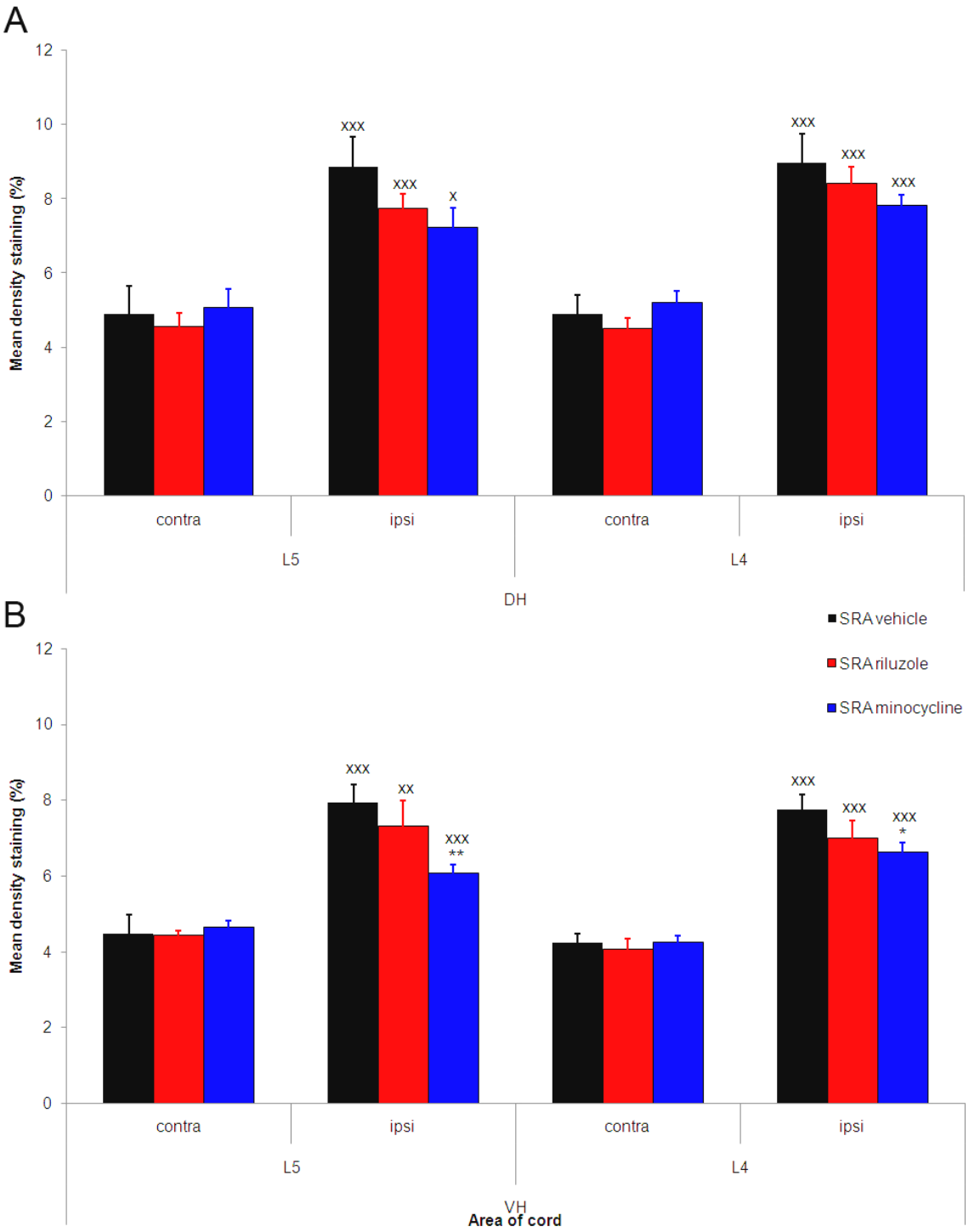

Figure 6.13: Quantitative effects of drug treatment on dorsal horn (A) and ventral horn (B) GFAP staining 14 days after L5 SRA, in L4 and L5 segments. SRA-vehicle shows significant upregulation of GFAP staining in all areas. Riluzole treatment leads to a trend in GFAP staining reduction in all areas analysed compared to vehicle. Minocycline treatment leads to a trend in GFAP staining reduction in the L5 and L4 dorsal horns (A), and a significant staining reduction in the L5 and L4 ventral horns (B). Significant differences are indicated for, ipsi vs contra (#) and treatment vs vehicle (*). N = 6 per group.

6.2.2.5: Macrophage infiltration in the dorsal horn

Fourteen days after SRA with vehicle treatment, ED-1 expression was found exclusively in the ipsilateral dorsal root entry zone and dorsal columns of L5 and L4 segments respectively (Fig 6.14), with different ED-1 expression patterns between L5 and L4 segments. Macrophages are seen clustered tightly around the DREZ of L5, and were spread more loosely throughout the dorsal columns in the L4 segment (Fig 6.14). When quantified this density staining reached 4.34% (+/-0.95) in L5 and 2.06% (+/-0.41) in L4 (Fig 6.15).

Fourteen days of treatment with riluzole after SRA significantly increased the density of ED1 staining in the dorsal columns of L4 (3.72% +/-0.70) and showed a trend in increase in L5 (5.12% +/-1.09) (Fig 6.15).

In contrast to riluzole treatment, 14 days of treatment with minocycline after SRA, significantly reduced the density of ED1 staining in the dorsal columns of L5 (1.49% +/-0.29), and showed a trend toward a reduction in L4 (1.13% +/-0.50) (Fig 6.15).

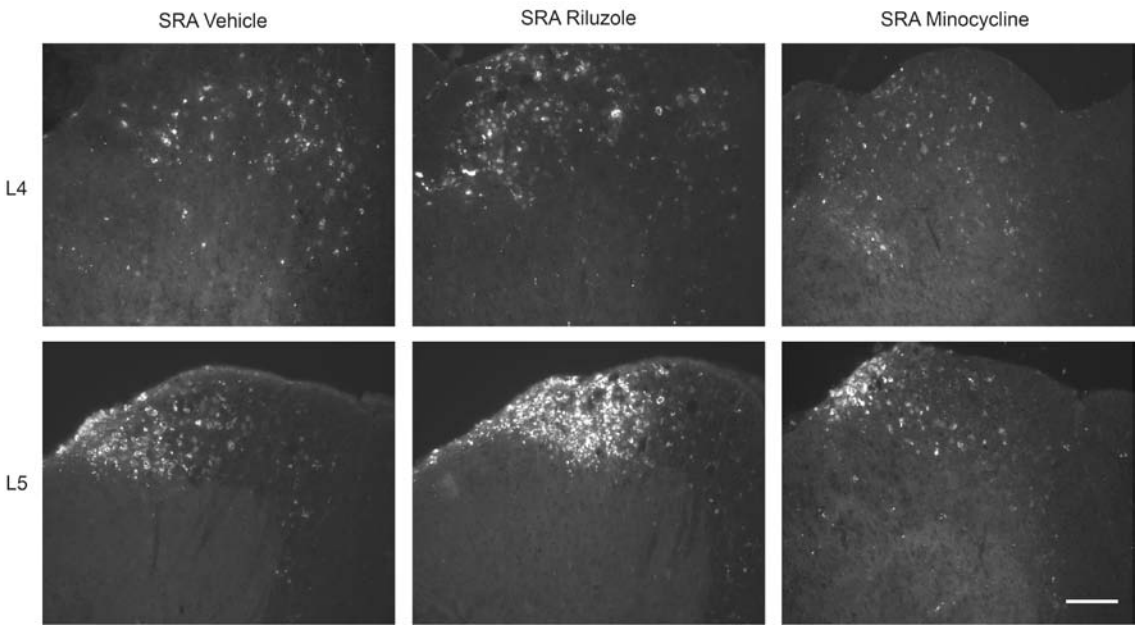

Figure 6.14: Photomicrographs of effects of drug treatment on dorsal horn ED1 labelling 14 days after L5 SRA, in L4 and L5 segments. ED1 positive labelling can be seen at 14 days after SRA-vehicle in both L5 and L4 ipsilateral segments. Similarly to SRA-untreated animals, macrophages were located around cystic cavities and dorsal root entry zone in L5, whereas they were dispersed throughout the dorsal columns in L4. Riluzole treatment increased the staining of ED1, whereas minocycline treatment reduced macrophage recruitment. Scale=50µm

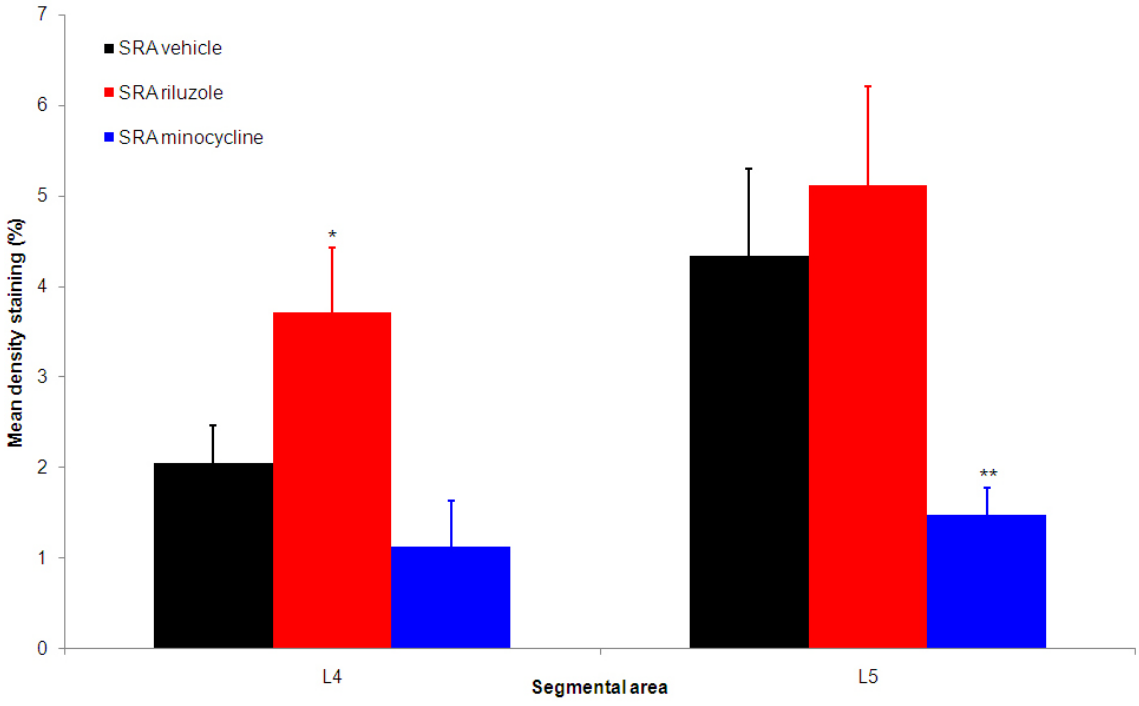

Figure 6.15: Quantitative effects of drug treatment on dorsal horn (A) and ventral horn (B) ED1 staining 14 days after L5 SRA, in L4 and L5 segments. Riluzole treatment significantly increased the staining of ED1 in L4, with a trend in L5. Minocycline treatment significantly reduced ED1 staining in L5 with a trend toward reduction in L4. Significant differences are shown for, SRA treatment group vs SRA vehicle (*). N = 6 per group.

6.2.3: Effects of a delayed drug treatment regime on L5 SRA-induced hypersensitivity

6.2.3.1: Riluzole delayed treatment

Riluzole treatment (4mg/kg), given daily from 7-13 days, and every other day from 14-21 days, significantly reverses thermal and tactile hypersensitivity but the effects are transient and delayed across a 14 day period, and are not maintained after withdrawal of treatment (Fig 6.16).

Mechanical:

Pre-surgical acclimatisation and training produced a mean baseline withdrawal threshold of 20.0g (+/-0.78) to mechanical stimulation (Fig 6.16A), similar to previous baselines assessed (Section 4.2 and 5.2).

Significant ipsilateral mechanical hypersensitivity was reached against the contralateral side by day 3 [15.8g (+/-3.78)], and against both contralateral and baseline values by day 7 [11.1g (+/-1.24)] (Fig 6.16A).

Riluzole treatment produced a significant decrease in mechanical hypersensitivity over days 15-19 (Fig 6.16A). However, after the withdrawal of treatment on day 21, withdrawal thresholds to mechanical stimulation again became hypersensitive [11.2g (+/-1.21) on day 21], and remained unchanged thereafter (Fig 6.16A).

Contralateral hyposensitivity to mechanical stimulation, significant from baseline values, was noted on day 17 [25.8g (+/-2.22)] only (Fig 6.16A).

Thermal:

Pre-surgical acclimatisation and training produced a mean baseline withdrawal threshold of 7.31s (+/-0.34) to thermal stimulation (Fig 6.16B), similar to previous baselines assessed (Section 4.2 and 5.2).

Significant ipsilateral thermal hypersensitivity was reached against baseline and contralateral levels by 3 days post operatively, such that withdrawal thresholds were reduced to 5.74s (+/-0.56), and this was maintained thereafter (5.09s +/-0.24) (Fig 6.16B).

Apart from day 15 (6.45s +/-0.48), riluzole treatment did not produce a significant amelioration of thermal hypersensitivity compared to contralateral and baseline values (Fig 6.16B). Final withdrawal thresholds were recorded on day 27 as; 5.10s (+/-0.92), significantly lower than both baseline and contralateral values. (Fig 6.16B).

Transient contralateral hyposensitivity to thermal stimulation was seen only on days 7 (8.57s +/-0.33) and 21 (8.86s +/-0.51) (Fig 6.16B).

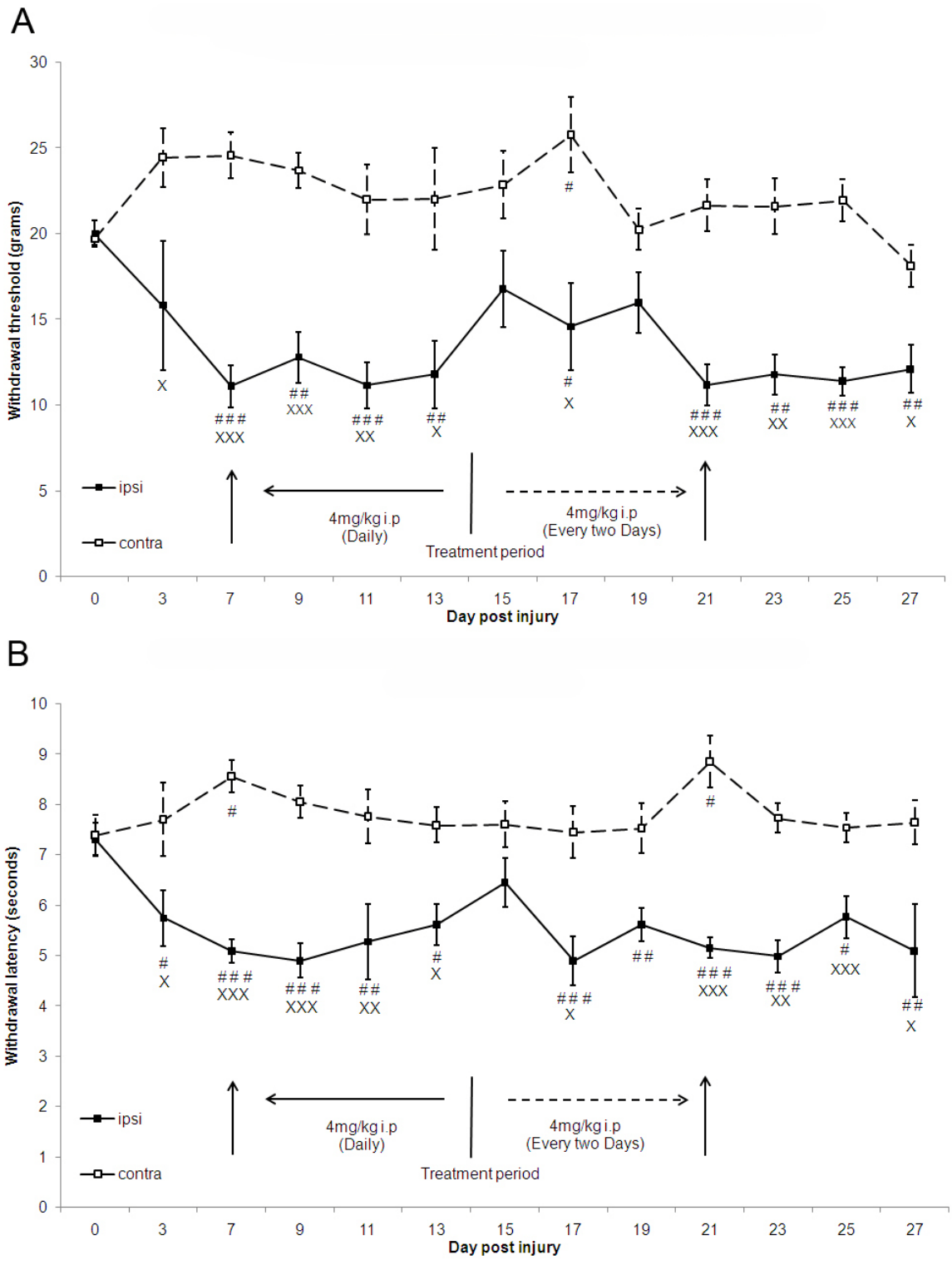

Figure 6.16: Effects of delayed riluzole treatment on established mechanical (A) and thermal (B) hypersensitivity after L5 SRA. Delayed riluzole treatment transient reverses mechanical hypersensitivity (A). Delayed riluzole treatment has little effect on thermal hypersensitivity, apart from day 15. Significant difference is indicated for ipsi vs baseline (#), and ipsi vs contra (X). N = 6 per group.

6.2.3.2: Minocycline delayed treatment

Minocycline treatment (40mg/kg), given daily from 7-13 days, and every other day from 14-21 days, significantly reverses an established ipsilateral hypersensitivity to both thermal and tactile stimulation. After cessation of treatment this analgesic effect was maintained for a further 7 days (21-27 days) (Fig 6.17).

Mechanical:

Pre-surgical acclimatisation and training produced a mean baseline withdrawal threshold of 21.6g (+/-0.70), to mechanical stimulation (Fig 6.17A), similar to previous baselines assessed (Section 4.2 and 5.2).

Significant ipsilateral mechanical hypersensitivity was reached against contralateral levels by day 3 [15.3g (+/-2.22)], and against both contralateral and baseline values by day 7 [11.6g (+/-0.66)] (Fig 6.17A).

Minocycline treatment reversed mechanical hypersensitivity by day 9 [17.4g (+/-2.52)] (Fig 6.17A) and persisted for the entirety of the treatment period up to day 19 [21.6g (+/-2.29)] (Fig 6.17A). Uniquely, after cesation of minocycline treatment after day 19, the analgesic effect was maintained up to day 27 [20.5g (+/-2.39)] (Fig 6.17A).

No significant change occurred in withdrawal threshold levels contralaterally for tactile stimulation before, during, or after minocycline treatment (Fig 6.17A).

Thermal:

Pre-surgical acclimatisation and training produced a mean thermal withdrawal threshold baseline of 7.64s (+/-0.62) (Fig 6.17B), similar to previous baselines assessed (Section 4.2 and 5.2).

Significant ipsilateral thermal hypersensitivity was reached against baseline and contralateral levels by 7 days, such that withdrawal thresholds were reduced to 5.37s (+/-0.42) (Fig 6.17B).

Minocycline treatment produced a significant amelioration of thermal hypersensitivity by day 9 [5.93 (+/-0.52)] compared to contralateral and baseline values, and this is maintained up to 15 days (Fig 6.17B). Although thermal hypersensitivity returned on days 17 [5.96s (+/-0.39)] and 19 [6.31s (+/-0.37)] compared to the contralateral side, these latencies were not significantly lower than baseline (Fig 6.17B). After the cessation of treatment, the reversal of thermal hypersensitivity was maintained up to the final day [7.44s (+/-0.87) day 27] (Fig 6.17B).

No significant change occurred in withdrawal threshold levels contralaterally for thermal stimulation before, during, or after minocycline treatment (Fig 6.17B).

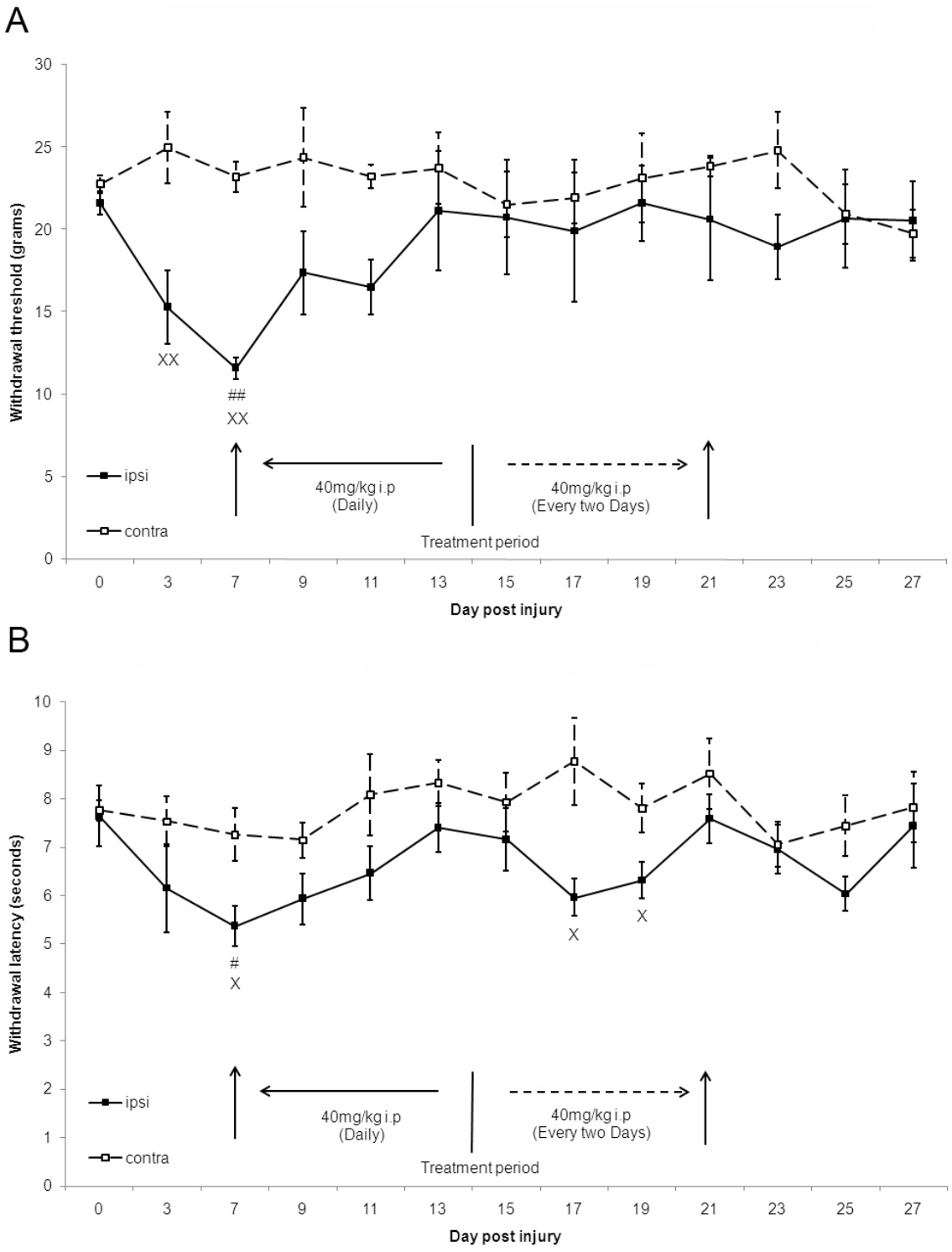

Figure 6.17: Effects of delayed minocycline treatment on established mechanical (A) and thermal (B) hypersensitivity after L5 SRA. Delayed minocycline treatment permanently reverses established tactile hypersensitivity by day 9, and this is maintained across the treatment period (A). Delayed minocycline treatment also reverses thermal hypersensitivity by day 9, compared to baseline values. After cessation of treatment on day 19, the analgesic effect is still apparent for both modalities. Significant difference is indicated for ipsi vs baseline (#), and ipsi vs contra (X). N = 6 per group.

6.3: Discussion

6.3.1: Summary

Immediate and prolonged treatment with riluzole is able to transiently reverse hypersensitivity to both mechanical and thermal stimulation. Immediate and prolonged treatment with minocycline effectively prevents the development of tactile and thermal hypersensitivity across 14 days.

Immediate and prolonged riluzole treatment has no effect on average weight gain across 14 days compared to vehicle treatment; however, immediate and prolonged minocycline treatment has significant detrimental effects on weight compared to vehicle treatment.

Immediate and prolonged riluzole treatment reduces microglial reactivity in the dorsal horn, and increases macrophage expression in the adjacent (L4) segment with a trend for increase in the injured (L5) segment. Minocycline effectively reduces ipsilateral microglial reactivity in the dorsal and ventral horns, and reduces macrophage recruitment in injured (L5) and adjacent (L4) segments. Neither riluzole nor minocycline treatment shows significant neuroprotective qualities in dorsal or ventral horns.

Delayed riluzole treatment, after the establishment of behavioural hypersensitivity, produced a transient amelioration of both thermal and mechanical hypersensitivity during the treatment period, but this was not maintained after treatment withdrawal.

Delayed minocycline treatment, after the establishment of behavioural hypersensitivity, effectively reversed both thermal and mechanical hypersensitivity, with ameliorative effects maintained after withdrawal of treatment.

6.3.2: Riluzole

Immediate and maintained treatment with riluzole after L5 SRA injury transiently reverses thermal hypersensitivity on days 7-11, and transiently reverses mechanical

hypersensitivity on days 7 and 9. This amelioration therefore shows a delay in efficacy, which is not maintained in the long term (at 14 days). This amelioration of hypersensitivity could be via anaesthetic properties of the drug acting on multiple channels and pathways in the nervous system. Indeed riluzole does directly block excitatory glutamatergic nerve fibers in CA1 hippocampal cortical slice preparations, producing potent depression of population spike amplitude and excitatory postsynaptic potential responses (MacIver et al., 1996). However, at clinical relevant doses, used for ALS treatment (100mg/kg/day), riluzole was an ineffective anaesthetic for pre-emptive treatment of acute burn-induced hypersensitivity, or in normal subjects (Hammer et al., 1999). Indeed no change in contralateral withdrawal latencies was noted at any time point after SRA injury with riluzole treatment, suggesting no anaesthetic behavioural properties. The transient efficacy must therefore be through an analgesic action, corroborated with previous nerve injury models. Immediate riluzole treatment of CCI-induced and formalin-induced hypersensitivity at 6 and 12mg/kg/day (Coderre et al., 2007) and 1-4mg/kg/day (Sung et al., 2003), effectively reduced mechanical and cold allodynia on three days analysed post injury, and was causally linked to the reduction in glutamate and aspartate in the spinal cord dorsal horn. Intracerebroventricular (ICV) administration of riluzole also delays morphine-induced tolerance and thermal hyperalgesia in rats by 5 days (Habibi-Asl et al., 2009). This suggests that neuropathic pain after avulsion, peripheral nerve, cutaneous damage, and opioid-tolerance can all be treated with riluzole; however the maintained effectiveness of riluzole in avulsion injury is less apparent. This may be due to more complex trauma to the spinal cord after root avulsion, and corresponding gliosis/inflammation within the dorsal horn. Alternatively, the dosing regimen in this case is too low to produce maintained efficacy in the SRA model compared to PNI (Sung et al., 2003;Coderre et al., 2007). This is clear during the second week of administration, where the dose was halved, and this may have lead to loss of therapeutic efficacy. The dosing regime was chosen based on positive neuroprotective results in avulsion injury (Bergerot et al., 2004), perhaps continuing the daily administration of 4mg/kg throughout the second week of L5 SRA treatment could yield better analgesic efficacy for riluzole. Further experiments are required to determine this.

Analysis of spinal cord tissue from immediate riluzole-treated SRA showed reduced microglial reactivity in the injured (L5) and adjacent (L4) dorsal horn, in the adjacent

(L4) ventral horn, and a trend for reduction in the injured (L5) ventral horn, but none of these values were reduced to sham levels. Riluzole was, however, ineffective in reducing astrogliosis, as determined by GFAP staining levels, in all areas analysed, showing only a trend in reduction of expression. These effects are difficult to substantiate, as very little work has focused on the effects of riluzole on glia. Riluzole has been shown to reverse stress-induced amino acid metabolism in glia (Valentine and Sanacora, 2009) and reduce stress-induced GFAP mRNA expression in the prefrontal cortex (Banasr et al., 2008). However, this work has centred on antidepressant activity of riluzole through glutaminergic modulation for mood disorder therapy and not effects on neurotrauma. Chronic and high dose (40mg/kg/day for 1 month) riluzole treatment in Wobbler mice, a model of motor neurone disease, after establishment of symptoms, reduces both GFAP-astrocyte and Cd11b-microglial immunoreactivity in the ventral horn, distinct from its anti-glutaminergic effects (Fumagalli et al., 2006). The intracellular downstream pathways of glial activation may be influenced by riluzole at certain levels. In *in vitro* experiments riluzole administration has been shown to be a direct PKC inhibitor (Noh et al., 2000), and downregulation of PKC leads to a decrease in cAMP in microglial cultures, that controls MHC-II expression, differentiation and cytokine production (Patrizio et al., 1997). Interestingly, inhibition of PKC-cAMP regulation has no effect on astrocyte reactivity in culture, suggesting different intracellular signaling pathways of activation of these two glial populations (Patrizio et al., 1997). This may explain the significant reversal of microglial reactivity but not astroglial activity in SRA injured rats, when treated with riluzole. However, the involvement of PKC signalling in these glial cells after injury is again quite different to naïve levels in culture. Indeed after PNI the mitogen-activating protein kinase (MAPK) pathways, such as ERK, are phosphorylated and activated (Zhuang et al., 2005;Ji et al., 2009), and are important in the establishment of immediate microglial activation (initiation of neuropathic pain) and delayed astrocyte activation (maintainence of neuropathic pain) (Raghavendra et al., 2003). However, after L3 and L4 DRR (Cheng et al., 2003) and SCI (Hains and Waxman, 2006;Gwak et al., 2009) MAPK and ERK are upregulated in microglia, but interestingly not within astrocytes. Very recently riluzole has been shown to block MAPK/pERK expression in murine melanocytes (Yip et al., 2009), and this may be the intracellular mechanism of microglial, but not astroglial inhibition, in the case of SRA. The ineffectiveness of riluzole to produce a significant reduction in astrogliosis dorsally and ventrally, and microgliosis ventrally may also be

dependent upon dosage, similarly to only transient effective analgesia. The dose used in this report, 4mg/kg, was based on previous evidence in ventral root avulsion models (Nogradi and Vrbova, 2001;Bergerot et al., 2004;Nogradi et al., 2007), however with the combination of both dorsal and ventral root avulsion in SRA, the additional trauma may have compounded the gliotic effects in the spinal cord, requiring a higher dose of riluzole to relieve it.

The actions of riluzole on macrophage recruitment are in direct contrast to its ameliorative effects on microglial activation. The mechanisms behind the macrophage expression increase in the L4 dorsal column, and the trend toward increase in the L5 dorsal column after riluzole treatment are unclear. Several possibilities include increased extravasation of monocytes, prevention of phagocytosis-induced apoptosis of macrophages, or increased microglial-macrophage activity. One mechanism may be anti-apoptotic, as riluzole reduces normal lymphocyte apoptosis and HIV-1 induced lymphocyte apoptosis in blood plasma (Achour et al., 2009). In these patients the cytokines, IL1-β and IL-6, that are notably involved in inflammation and neuropathic pain (Milligan and Watkins, 2009), were also reduced. Conversely however, riluzole has also been shown to reduce lymphocyte recruitment in the spinal cords of MOG-induced EAE mice models along with reducing demyelination and axonal damage (Gilgun-Sherki et al., 2003). Further confusion arises in clinical studies of ALS patients, where continued riluzole treatment actually produces no change in expression levels of macrophage/monocyte markers CCR2 and MCP-1 in blood plasma compared to untreated ALS patients (Zhang et al., 2006). One reason for the discrepancy may be due to the injury model used, and the macrophage increase shown here for SRA-riluzole treatment may be trauma dependent. Perhaps a similar immunomodulatory capacity of riluzole after avulsion injury may be present for macrophages as in lymphocytes, through increasing their number by anti-apoptotic mechanisms. What is unclear is the identity of the macrophage lineage that is being increased in the dorsal columns and root entry zone. Activated macrophages can fall into 3 categories: classically activated (M1) monocytes, alternatively activated (M2) monocytes, and microglial derived. The M1 macrophage lineage activated by IFN-γ and TNF-α is associated with inflammation, phagocytosis, cytokine production, and cell death (Kigerl et al., 2009), processes implicated in neuropathic pain. The M2 lineage, activated by IL-4, is associated with promoting angiogenesis, matrix remodelling and repair (Kigerl et al., 2009). Many

activated microglia develop into macrophages in response to injury (Graeber et al., 1998), express the ED1 marker, are morphologically identical to monocyte-derived macrophages, and as such are indistinguishable at the light microscopic level (Guillemin and Brew, 2004). As yet there are no immunohistological markers capable of determining macrophage lineage, and without defining what subpopulations of macrophages are being upregulated in the dorsal columns, it is impossible to accurate predict what effect this has behaviourally. At first glance, these results suggest detrimental effects on the management of neuropathic pain in SRA-riluzole animals, as macrophages play a key role. Depletion (Liu et al., 2000b;Mert et al., 2009) and genetic manipulation (Myers et al., 1996) of the endogenous circulating macrophage population have lead to exacerbated diabetic neuropathic pain (Mert et al., 2009) and PNI-induced pain (Myers et al., 1996;Liu et al., 2000b;Barclay et al., 2007). However riluzole-induced upregulation of macrophages is centred solely in the DREZ and dorsal column, rather than the dorsal horn grey matter, and is most likely associated with the degeneration of ascending primary afferents and subsequent phagocytosis of myelin. Therefore, this phenomenon is unlikely to have a direct effect on dorsal horn hypersensitivity, but is more likely related to phagocytosis debris clearance and remodeling of the dorsal column pathway.

The ineffectiveness of immediate and prolonged riluzole treatment in reproducing the neuroprotective effects in motor neurones shown in previous studies of root avulsion models (Bergerot et al., 2004), ventral root reimplantation models (Bergerot et al., 2004;Nogradi et al., 2007), ischemic injury models (Lips et al., 2000), and mouse models of MS (Fumagalli et al., 2006) suggests that the trauma of dorsal root injury in SRA may compound to further exacerbate the injury, such that riluzole is ineffective at preventing cell loss. The combination of the dorsal and ventral root avulsion may increase the severity of the trauma from that seen in a single root avulsion, such that a greater gliosis and inflammatory reaction occurs in the spinal cord that overwhelms the neuroprotective effects of riluzole. Loss of monosynaptic or polysynaptic (via interneurones) connection between dorsal afferents and motor neurones may also contribute to their fate. DRR has been shown to induce motor neurone plasticity (Cuppini et al., 1999), suggesting transneuronal mechanisms in the ventral horn can be manipulated through primary afferent degeneration. However, directly initiating cell death of motor neurones through transneuronal mechanisms is unlikely, leaving the

mechanism unclear. In addition, only one investigation, previously, looked at neuroprotection with riluzole without combining re-implantation therapy (Bergerot et al., 2004), and a different treatment dosing regimen was used. The dosing regimen was a daily i.p. 4mg/kg administration of riluzole from Tockris Cookson Ltd. (UK) for 14 days. In this thesis riluzole was obtained from Sigma (UK), and was administered at half dose during the second week. Therefore not only could the SRA injury be more severe trauma than VRA, the dosing regimen is clearly different. Clearly defining motor neuronal loss is a crucial point. Tract tracing from ventral roots in the SRA model may more accurately locate L5 and L4 motor neuronal pools, to assess motor neuronal loss and the potential for neuroprotection. Alternatively, and as previously eluded to (Section 4.3.3.3.1), a lesion of the ipsilateral L4 ventral root 12-24 hours prior to sacrifice would provide ATF3 identification of this population of motor neurones, distinct from L5 motor neurones.

When riluzole treatment is delayed by 7 days post SRA, after hypersensitivity has been established, there is a transient amelioration of both thermal and mechanical hypersensitivity. This is also seen after a 5 day delayed treatment of riluzole after CCI (Sung et al., 2003). However, after SRA, riluzole is ineffective at maintaining efficacy after cessation of treatment, which is similar to clinical peripheral neuropathic pain studies (Galer et al., 2000) where a 14 day treatment with a 14 day washout resulted in no change in pain scores compared to placebo. However, in animal models of CCI, after 4 days of riluzole treatment and withdrawal, there was still effective alleviation of hyperalgesia and allodynia in two independent experiments; up to 6 and 10 days (Sung et al., 2003;Coderre et al., 2007). In these CCI models the ameliorative action of riluzole on neuropathic pain behaviour was attributed to increased glutamate reuptake, and length of effect due to repeated administration every 12 hours, representative of half-life in humans (Wokke, 1996); however the plasma half-life of riluzole in the rat is approximately 2 hours after i.p. administration (Milane et al., 2009). After repeated administration in humans, half-life is greatly increased to 40.3 - 49 hours (Le Liboux et al., 1999). It is unclear however, what effect repeated administration has on the half-life of riluzole in rats. If therapeutic efficacy is dependent on blood plasma levels, this administration regime may be too infrequent in the rat to maintain adequate drug concentration. There are clear differences in methodology with previous investigations on the action of riluzole on pre-clinical neuropathic pain models (Sung et al.,

2003;Coderre et al., 2007), and the results presented here. Firstly CCI is a PNI that induces inflammatory pain, which results in different hypersensitivity responses than noted in neuropathic pain (Jabakhanji et al., 2006). The SRA-riluzole treatment dosage was less and more infrequent compared to previous literature (Sung et al., 2003); i.t. 10µg twice daily; (Coderre et al., 2007); i.p. 6 and 12mg/kg twice daily). In addition these CCI models rarely presented data suggesting riluzole treatment could ameliorate neuropathic pain behaviour to baseline levels, and contralateral levels were not assessed; both a prerequisite for clarification of significant effects in this SRA model. These methodological constraints may shadow potential positive effects of riluzole seen in previous models of neuropathic pain (Sung et al., 2003;Coderre et al., 2007).

Perhaps higher and more frequent doses *in vivo* may produce earlier more stable ameliorative properties for the treatment of SRA-induced hypersensitivity. However the prospective benefits of riluzole treatment for root avulsion patients may not be as robust as shown pre-clinically. The ineffectiveness of riluzole in the SRA model suggests that excess glutamate and hyperexcitability, are not be the only mechanisms responsible for the generation and maintenance of avulsion pain. The contribution of microglial activation in neuropathic pain, a central topic of this report, has been implicated extensively in both peripheral nerve, ventral root, and spinal cord injury pain (Raghavendra et al., 2003;McMahon et al., 2005;Nesic et al., 2005;Hains and Waxman, 2006;Ohlsson et al., 2006;Hulsebosch et al., 2009;Milligan and Watkins, 2009;Penas et al., 2009). Riluzole therefore, with only a limited effect on glia, may not be the most suitable candidate for drug trials in avulsion pain clinically.

6.3.3: Minocycline

Immediate treatment with minocycline after L5 SRA effectively prevents the development of tactile and thermal hypersensitivity. Evidence of minocycline's effectiveness for treatment of neuropathic pain conditions is extensive in the literature. Across many different factors such as rat strain, surgical procedure, dosing concentration, testing period post administration, mode of administration, and sensory testing parameters, immediate or pre-emptive minocycline treatment has been shown to successfully reduce, or prevents, the development of trauma-induced hypersensitivity

(Raghavendra et al., 2003;Ledeboer et al., 2005;Hains and Waxman, 2006;Lin et al., 2007;Guasti et al., 2009;Marchand et al., 2009;Mika et al., 2009). The data presented in this thesis is the first to show that minocycline treatment prevents the development of avulsion-induced hypersensitivity. The positive results of minocyline treatment for neuropathic pain relief, across a broad range of injury models, suggest similar neuropathic mechanisms may exist between avulsion (presented here), SCI (Hains and Waxman, 2006;Marchand et al., 2009) and PNI (Raghavendra et al., 2003;Ledeboer et al., 2005;Lin et al., 2007;Guasti et al., 2009;Mika et al., 2009) in the induction of neuropathic pain. This is most likely due to the ubiquitous action of microglia in these pathologies (Milligan and Watkins, 2009). However, some conflicting evidence comes from the significant reduction in weight gain observed over 14 days using prolonged minocycline treatment. At first slight, this suggests minocycline is reducing appetite in these animals indicative of ongoing pain. However, a variety of reasons could explain this result, as minocycline-induced weight loss is also found in a rodent model of Parkinson's disease (Yang et al., 2003). Firstly, the drug could well be showing toxic qualities; indeed after sacrifice, discolouration of bone, yellow deposits in the liver and peritoneum, liver sclerosis, were noted in some animals, corroborated with previous pre-clinical (Light et al., 1994;Fagan et al., 2004) and clinical literature (Good and Hussey, 2003;Losanoff et al., 2007), suggesting poor absorbtion, excessive deposition, and liver toxicity. In previous animal studies minocycline, at doses higher than 20mg/kg, results in pleurodesis and morbidity in rabbits, such is the potential toxicity of this drug (Light et al., 1994). If minocycline hydrochloride (Sigma-Aldrich) is disoolved from the initial powder through heating the saline, and administered immediately, these toxic effects are not apparent (Teng et al., 2004), and neuroprotective effects are pronounced, suggesting poor dissolving may be a contributing factor to increased risk of toxicity and reduced efficacy. Using alternative administration methods, such as intravenous or intrathecal catheterization can avoid these issues and improve plasma concentrations (Fagan et al., 2004;Hains and Waxman, 2006).

This thesis is the first evidence to indicate the effectiveness of minocycline treatment in microglial reactivity amelioration after avulsion injury. Such is the potency of this minocycline treatment, that ipsilateral microglial reactivity to levels similar to contralateral, in the ventral and dorsal horns of both the adjacent L4 and avulsed L5 segments. The correlation of this finding with the prevention of hypersensitivity

development across the same time period provides direct evidence to implicate dorsal horn microglia reactivity, specifically in the adjacent segment to the injury (L4), in the pathology of avulsion-pain, as evoked hypersensitivity is mediated through the 'spared' L4 root/segment. The action of minocycline on microglia via inhibition of p38-MAPK phosphorylation (Tikka et al., 2001;Tikka and Koistinaho, 2001;Hains and Waxman, 2006), is the likely candidate for pharmacokinetics. A contralateral effect with minocycline treatment was noted. Immediate treatment with minocycline has also been shown to reduce OX42 expression bilaterally after a unilateral rat spinal cord hemisection at T13 (Marchand et al., 2009). In some cases this contralateral effect in SRA-minocycline treated tissue is functionally significant, contradictory to literature on minocycline treatment of nociceptive pain (Padi and Kulkarni, 2008), but this again may be an issue of injury models.

Minocycline treatment shows a small but significant reduction in astrocyte reactivity in the ventral horn. The GFAP reduction may be due to direct inhibition of p38 MAPK phosphorylation pathways that have been shown to be activated in astrocytes within and around the lesion site after moderate SCI (Crown et al., 2008). Little information exists on the mechanisms of astrocyte activation after neuropathy. Minocycline treatment has no effect in the dorsal horn astrocyte response; and so there may be multiple activation pathways at play after SRA injury. With the successful prevention of hypersensitivity development in SRA-minocycline treated animals, it can be suggested that astrocyte activity is not a key player in hypersensitivity production and maintenance after root avulsion, again similar to SCI models of neuropathic pain (Hains and Waxman, 2006;Gwak et al., 2009). Certainly there is now a shift in understanding of the role of astrocytes in neuropathic pain from original thought (Raghavendra et al., 2003), with microglia becoming the main culprits at least after injury to the spinal cord. Recently, it has been shown that the astrocyte inhibitor fluorocitrate, when administered i.p. twice daily, reduces astrogliosis 7 days after CCI, but does not ameliorate tactile and cold hypersensitivity, whereas minocycline does, alongside reducing microgliosis (Mika et al., 2009). Sciatic nerve ligation leads to a greater spinal cord microglial response including proliferation at 7 days, that is absent in the astrocyte population (Narita et al., 2006). Notably intrathecal injection of PKC-activated astrocytes into naïve spinal cord does not lead to hypersensitivity, whereas PKC-activated microglia injection does (Narita et al., 2006). The results from immediate minocycline treatment on the reduction

of microglial activity and neuropathic pain, suggests that microglial activity is the essential mediator in avulsion pain.

In contrast to riluzole, minocycline treatment effectively reduces macrophage recruitment in the dorsal columns significantly in L5 with a trend in L4, and this is in accordance with previous literature, using a SCI model (Ritfeld et al., 2010), dorsal column crush injury model (McPhail et al., 2004b), cerebral ischemic models (Wasserman and Schlichter, 2007) and EAE models (Nikodemova et al., 2007). P38 MAPK plays a key role in monocyte/macrophage inflammatory responses (Hulsebosch, 2008). After dorsal root rupture, p38 MAPK is increased in macrophages within 48 hours in the ipsilateral DREZ and root (Nomura et al., 2005), and both macrophage recruitment and activation is dependent upon the extent of traction injury to the root and DREZ (Nomura et al., 2005), shown in Section 3.2.3a. Vascular adhesion molecule-1 (VCAM-1) on endothelia controls the extent of macrophage adhesion to endothelial cell membranes and subsequent extravasation into a lesion site, through interaction with α4-β1 integrin on the surface of leukocytes (Mabon et al., 2000). VCAM-1 surface expression is in turn controlled by the cytokines IL-1β and TNFα (Mabon et al., 2000). Minocycline could therefore have a 'two-pronged' inhibitory action on macrophages; through inhibition of infiltration, via suppression of cytokine release from microglia (Ledeboer et al., 2005), as well as reduction of activity via p38 MAPK inhibition (Tikka et al., 2001;Tikka and Koistinaho, 2001;Hains and Waxman, 2006) leading to the reduced ED1 expression shown in the L4 and L5 dorsal columns. The 'double-edged sword' debate on the consequences of increased macrophage activity, suggests that reduction of macrophages in these areas could have either a detrimental effect on neuronal tissue regeneration (Thacker et al., 2007;Gensel et al., 2009), or a beneficial effect on matrix reformation and prevention of axonal dieback (McPhail et al., 2004b;McPhail et al., 2004b); as well as, consequently, reducing the propensity for neuropathic pain (Myers et al., 1996;Liu et al., 2000b;Barclay et al., 2007), depending on the lineages being activated and targeted (Kigerl et al., 2009). It is also unclear whether these macrophages are infact distinct from microglial cells. As described previously, the function of these 'white matter' macrophages is more likely focused on phagocytosis and matrix remodelling of the lesion area after SRA, and the decrease in ED-1 expression seen with minocycline is unlikely linked to the prevention of hypersensitivity development.

The neuroprotective qualities of minocycline showed only a trend toward amelioration of dorsal horn neuronal loss in L4. If this trend is indeed biologically significant, it could be attributable to the neuroprotective quality of minocycline through inhibition of mitochondrial cytochrome C release (Teng et al., 2004), and prevention of caspase-3 activation (Stirling et al., 2004) in neurones, or indirectly via p38 MAPK inhibition in microglia (Tikka et al., 2001) preventing inflammation-mediated cell death. As TUNEL studies in DRA (Section 3.2.5.4) could not confirm neuronal apopotic cell death, it may be the inhibition of microglia/macrophages that tends toward a neuroprotective mechanism, and may also substantiate why this neuroprotective quality was not present with riluzole that showed limited efficacy on gliosis. Then again, it is not surprising significant neuroprotection was absent, such is the controversy over minocycline's ability to prevent neurodegeneration in numerous models of neurotrauma and CNS disease (Yang et al., 2003;Diguet et al., 2004a;Stefanova et al., 2004;Tsuji et al., 2004;Pinzon et al., 2008;Saganova et al., 2008;Viscomi et al., 2008).

Further, the absence of neuroprotective qualities is mirrored in the ventral horn. No prevention of motor neurone loss was found, and this is directly contrary to data from L6 VRA models (Hoang et al., 2008). However, differences in dosing regimen (50mg/kg halved in second week) and injury model, as well as method of motor neurone identification and analysis may contribute to this discrepency. The large variation in neuronal counts, between methodologies in this report (Section 4.2.3.2b), is also found in the literature between different investigators (Koliatsos et al., 1994;Bergerot et al., 2004;Hoang et al., 2008;Penas et al., 2009), and this variation could shadow small neuroprotective effects of drugs such as minocycline.

It is rather contradictory as to why minocycline shows efficacy in reducing microgliosis but not neurodegeneration, although these two processes may be linked. Minocycline robustly reduce microglial activation induced by MPTP neurotoxin administration in a model of Parkinson's disease (Yang et al., 2003). Conversely, it exacerbated the loss of dopaminergic neurones. The authors speculated that the reduction of microglial activity may subsequently lead to reduction in cytokine expression needed for neuronal survival (Yang et al., 2003). Activated microglia have the capacity for aiding neuroregeneration (Aldskogius, 2001), remyelination and functional recovery (Yaguchi et al., 2008), and the loss of the protective aspect of microglial activity through minocycline

administration may be the reason why neuroprotection is absent in the SRA model. Further, the dependence on correct dose and mode of administration may determine the expression of neuroprotective effects from exacerbation of symptoms, such that 20mg/kg is neuroprotective but 100mg/kg exacerbates symptoms in brain ischemic models (Matsukawa et al., 2009). Intraperitoneal administration route may not be the best method, due to incomplete and erratic absorbtion of minocycline from the peritoneal cavity and deposition in the liver (Fagan et al., 2004). Intravenous administration has been shown to produce more reliable plasma and tissue concentration levels (Fagan et al., 2004), and correct preparation of the minocycline solution may also be an overlooked but essential factor (Teng et al., 2004). Further research to carefully assess minocycline pharmacokinetics and phamacodynamics is required both pre-clinically and, more importantly with caution, clinically for the treatment of neuropathic pain.

Minocycline, for the first time, has been shown to be effective at reversing established neuropathic hypersensitivity, contrary to previous literature in peripheral nerve injury models (Raghavendra et al., 2003;Ledeboer et al., 2005). Moreover, it is the first time that minocycline has been shown to maintain efficacy outside the washout period, contrary to previous literature (Ledeboer et al., 2005). The biological half life of minocycline, when administered orally is on average 18-23 hours in humans (Langevitz et al., 2000). In rats this is much shorter, averaging 2.8 hours after intravenous administration, and more variable after intraperitoneal administration (Fagan et al., 2004). This suggests the drug effects will be washed-out before the next testing day (day 21). Differences seen here are yet to be correlated with immunohistological analysis; but these results suggest, that if microglial activity is indeed responsible for avulsion pain, pharmacological inhibition may persist for at least 7 days after drug cessation. It is unclear how effective this treatment regimen could be for multiple root avulsion, or indeed in the human condition, or whether neuropathic pain is ameliorated beyond 7 days. However, these are encouraging results, and provide a potentially new therapeutic intervention to further study avulsion injury and neuropathic pain therapy in humans.

6.3.4: Conclusion

The evidence presented here gives weight to advocate minocycline as a suitable drug candidate for preventating and reversing avulsion-pain, as long as side effects are minimised. The potential for neuroprotection is currently being assessed in clinical trials for SCI (ClinicalTrials.gov Identifier: NCT00559494), traumatic brain injury (ClinicalTrials.gov Identifier: NCT01058395), and stroke (ClinicalTrials.gov Identifier: NCT00930020). Riluzole was less effective at treating established avulsion-induced pain in this model, with only partial anti-glial effects. However, it was effective at delaying the onset of thermal hyperalgesia, suggesting some rationale for use. There was an inability to confirm neuroprotective effects of either drug; however, this may well be an issue of dosing, mode of administration, or different injury models. Potentially a combinatorial treatment approach may produce more beneficial effects when assessing neuronal sparing, as the drugs have shown synergistic qualities (Milane et al., 2009). They have been used recently in ALS treatment (Pontieri et al., 2005;Gordon et al., 2007), but caution is warranted as the potential for toxicity and symptom exacerbation is increased at doses of 400mg/kg of minocycline (Gordon et al., 2007;Milane et al., 2009). Combinatorial treatment with minocycline and riluzole in focal cerebral ischemia, ameliorates both inflammation and excitotoxicity; studies show reduced microglial/macrophage reactivity, reduced caspase-3 positivity and decreased size of infarction, far beyond the effects of the single treatments alone (Weng and Kriz, 2007). As ventral root reimplantation strategies are still the most effectively therapy for maintaining the motor neurone pool, and promoting functional recovery after brachial plexus avulsion (Bergerot et al., 2004;Nogradi et al., 2007;Havton and Carlstedt, 2009); a combinatorial reimplantation strategy with minocycline may increase the potential for motor neuronal survival and recovery, whilest alleviating or preventing neuropathic pain.

Chapter 7: General discussion

7.1: Introduction

This thesis has aimed to provide greater insight into the underlying mechanisms that contribute to the generation and maintenance of intractable neuropathic pain experienced by a large majority of people with spinal root avulsion. A clear, histological characterisation of the temporal degenerative events within the avulsed spinal cord is lacking in current literature, and in addition, there is no established animal model of avulsion injury that mirrors the human condition, that can be used to test drug efficacy or to explore the underlying mechanisms. The current *in vivo* model used for histological studies within spinal cord and dorsal root ganglia to mimic avulsion is a rhizotomy, and inferences of the clinical condition are based on these findings. However, rhizotomy is an artificial surgical lesion and not a 'traction injury', so therefore does not injure the dorsal horn, as is sometimes the case in avulsion. Furthermore, most research has focussed on understanding motor functional deficits after avulsion injury (Carlstedt et al., 1986;Koliatsos et al., 1994;Bergerot et al., 2004;Nogradi et al., 2007;Hoang et al., 2008), rather than neuropathic pain. A model of below-level (hind-limb) avulsion-pain induced after brachial plexus avulsion has been used to characterise potential pharmacotherapy for avulsion pain (Rodrigues-Filho et al., 2003), without any clear proof of concept on the model or its clinical relevance. A ventral root avulsion model (Bigbee et al., 2007) produces neuropathic pain behaviour correlated with primary afferent degeneration, this is however in the absence of direct injury to dorsal roots. In the clinic brachial plexus and lumbosacral plexus injuries typically present both dorsal and ventral root avulsion injuries.

This thesis has aimed to develop a new model of avulsion pain that mirrors the clinical aetiology, and to provide a platform for pharmacological testing. Establishment of this model has enabled the testing of established drugs that have shown clinical efficacy for neuropathic pain treatment, and for ameliorating PNI- induced pain *in vivo*, and to assess whether these drugs have any therapeutic efficacy for treatment of avulsion pain. Clinically, conventional drugs for neuropathic pain treatment such as anticonvulsants and antidepressants have poor efficacy for the treatment of avulsion pain (Parry, 1980;Berman et al., 1996;Piva et al., 2003). Therefore registered drugs, that are not

currently in use for analgesia but have shown potential *in vivo* for treatment of neuropathic pain in spinal cord and peripheral nerve injury models, have also been assessed for preventative therapy and treatment of SRA-induced neuropathic pain behaviour.

7.2: DRA leads to a progression of gliosis, inflammation, and degeneration within the dorsal spinal cord, and is quantitatively more severe than rhizotomy

Loss of inhibitory tone has been implicated as a mechanism of neuropathic pain development (Loeser et al., 1968;Ovelmen-Levitt, 1988), and this has been shown to occur, in the dorsal horn after PNI and SCI, through neurodegeneration of GABAergic interneurones (Ibuki et al., 1997;Moore et al., 2002;Drew et al., 2004;Meisner et al., 2010) and a microglial controlled shift in anion gradients in neurones via BDNF (Coull et al., 2003;Coull et al., 2005;Lu et al., 2007;Lu et al., 2008). Dorsal horn sensitisation is also a mechanism by which neuropathic pain can occur, through activation of glia (Milligan and Watkins, 2009), and inflammatory cells (Thacker et al., 2007). However, a full characterisation of these events in the avulsed dorsal horn has not taken place, and neuronal cell death, or loss of GABAergic tone, after PNI is controversial (Polgar et al., 2003;Polgar et al., 2004;Polgar et al., 2005;Polgar and Todd, 2008). This chapter provides quantification of these events within the dorsal horn at early and late time points post injury in a model of lumbosacral plexus avulsion (L3-L6 DRA). The model produces a gradual loss of immunostaining in primary afferent terminals in the superficial dorsal horn, with maximal reduction by 14 days using CGRP and IB4 antibodies for C-fibre identification, which is similar to DRR and the previous literature (Gibson et al., 1984;Traub et al., 1989;Tie-Jun et al., 2001;Muneton-Gomez et al., 2004). Afferent terminal degeneration coincides with increase in phagocytic cell infiltration, neuroinflammation, and neurodegeneration. A two stage trans-synaptic loss of dorsal horn neurones occurs firstly within 1 to 2 days, and a second loss from 14 to 28 days. This loss of the neuronal epitope NeuN could not be linked at these time points to apoptotic mechanisms; the only substantial apoptosis involved the neutrophil population, after their acute infiltration at 1-2 days. The initial loss of NeuN is likely due to the direct trauma of the avulsion, but the reduction in NeuN number at later time points is linked closely with a rise in astrogliosis, microgliosis, and macrophage recruitment. This suggests that avulsion is not just an acute lesion, but has a chronic

progressive stage of secondary cell death, similar to SCI (Totoiu and Keirstead, 2005;Huang et al., 2007). Encouragingly, this potentially provides an accessible therapeutic window for neuroprotective intervention. The continued increase in microglial and macrophage activity up to 14-28 days after DRA coincides with secondary neuronal loss, and is contradictory to the the decrease in microglial activity in PNI at 7 days (Eriksson et al., 1993), and is more reminiscent of SCI gliosis (Hains and Waxman, 2006;Gwak and Hulsebosch, 2009). Vascular endothelial staining was reduced followed this neuronal loss across 28 days, resembling vascular deterioration in SCI (Imperato-Kalmar et al., 1997). However, it is uncertain whether reduction in endothelial staining links to loss of vascular integrity and therefore ischemia.

This spatial and temporal assessment gives an insight into possible mechanisms of neuropathic pain. Microglia/macrophages and astrocytes heighten dorsal horn neurone activity, through expression of TNFα and cytokines (IL6 and IL1-β) (Milligan and Watkins, 2009). Microglia and astrocytes have been shown to contribute to SCI-induced neuropathic pain maintenance (Hains and Waxman, 2006;Gwak and Hulsebosch, 2009), with the latter glial cell contributing to the maintenance of PNI-induced pain (Eriksson et al., 1993;Colburn et al., 1997;Raghavendra et al., 2003).

Quantitative analysis of DRA and DRR showed that rhizotomy is a less severe form of avulsion injury. This is most likely due to the neuropathological consequences of direct trauma to the spinal cord after avulsion injury that does not occur after rhizotomy. This is important to distinguish, as 70% of brachial plexus injuries incorporate direct avulsion of at least one root from the spinal cord, and brachial plexus avulsion leads to a partial Brown-Séquard SCI syndrome (Berman et al., 1996;Carlstedt, 2009). Indeed, DRA causes direct injury to the ipsilateral DREZ, dorsal column, and dorsal horn, presenting as cavitations and some tissue deformation, with a progressive, ~56%, loss of NeuN over 28 days, which does not occur in rhizotomized tissue. Vascular staining, that has not been studied in root avulsion models, recovers at 14 days post rhizotomy, in comparison with a maintained reduction after avulsion up to 28 days. DRA produces a quicker and more pronounced astroglial response than DRR, and is bilateral at 28 days, unlike DRR injury. DRA produces a progressive bilateral microglia reaction across 28 days, greater than DRR at each time point, with DRR showing a decreased microglial reactivity after 14 days. This unique finding is important evidence when attempting to

determined the conflicting roles of microglia in PNI and SCI pain maintenance (Eriksson et al., 1993;Raghavendra et al., 2003;Hains and Waxman, 2006), suggesting perhaps that the neuropathology of DRR is similar to PNI, whereas DRA is reminiscent of SCI. Bilateral astroglial and microglial responses have been seen before in PNI and focal burn injury models (Milligan et al., 2003;Hatashita et al., 2008;Chang et al., 2010), and is that to be associated with contralateral and 'extra-territorial' hypersensitivity (Seltzer and Shir, 1991;Tal and Bennett, 1994;Arguis et al., 2008). Clinically mirror pain is rare, but is cited in literature concerning causalgia (Seltzer and Shir, 1991), atypical facial pain (Woda and Pionchon, 1999) and reflex sympathetic dystrophy (Maleki et al., 2000), however it is not reported in the root avulsion literature.

These differences in the severity of the dorsal horn neuropathology may explain why rhizotomy pre-clinically does not produce a neuropathic behaviour (Sheen and Chung, 1993;Yoon et al., 1996;Sukhotinsky et al., 2004), and is clinically used to relieve peripheral neuropathic limb pain (White and Sweet, 1969;Loeser, 1972;Gybels and Sweet, 1989;Hosobuchi, 1980), whereas clinical avulsion injury almost always results in the most severe pain (Parry, 1980;Berman et al., 1998;Piva et al., 2003;Htut et al., 2006).

7.3: SRA leads to neuropathic pain behaviour

A recent model of brachial plexus avulsion (Rodrigues-Filho et al., 2003) produces a bilateral hindlimb hypersensitivity, which has neither a clear mechanistic cause nor is it representative of the clinical condition, as pain is not experienced by patients in unaffected limbs. Ventral or dorsal root rhizotomy as a model has conflicting evidence for neuropathic pain behaviour (Sheen and Chung, 1993;Colburn et al., 1999;Eschenfelder et al., 2000;Li et al., 2000;Sukhotinsky et al., 2004). Ventral root avulsion pain may be due to the influence of degenerating motor axons influencing adjacent intact primary afferents within the same peripheral nerve (Bigbee et al., 2007;Bigbee et al., 2008) akin to that seen in SNL injury models. This thesis has developed a reproducible, and clinically relevant avulsion model, as it involves both ventral and dorsal root components (Havton and Carlstedt, 2009), for the study of evoked neuropathic pain behaviour in the border zone of the avulsed and adjacent intact dermatomes. It negates the need for laminectomy, a surgical injury in itself that

produces histological (Colburn et al., 1997;Winkelstein and DeLeo, 2002;Bigbee et al., 2007;Huang et al., 2007), and behavioural effects (Hashizume et al., 2000a;Hashizume et al., 2000b). The neuropathic behaviour induced by SRA is both evoked, through stimulation with tactile and thermal probes, and has a spontaneous modality, inferred by a reduced weight gain. However a limitation of the model is that it is difficult to measure other surrogate methods of spontaneous pain measurements such as autotomy, due to the fact the the limb is not fully denervated. The evoked behaviour is not fully established until 3-5 days post injury, and is maintained for at least 60 days. The locomotor impairment of the ventral root avulsion is minimal.

Phenotypic changes in peptide expression in subpopulations of primary afferents (Fukuoka et al., 1998), upregulation in expression of certain receptors, such as TRPV1 (Hudson et al., 2001;Fukuoka et al., 2002), and activation of satellite glia (Hu and McLachlan, 2003;Dublin and Hanani, 2007), all contribute to the generation of PNI pain. However, after SRA no obvious change in phenotypic expression occurs in the L4 DRG cells, through which the evoked behavioural responses must occur. Satellite cells show no increase in GFAP expression, notable after activation, and ATF3 expression, a ubiquitous marker for neuronal injury (Averill et al., 2002;Shortland et al., 2006a) is minimal in the L4 DRG neurones. This suggests neuropathic pain may not be attributable to peripheral plasticity within the neurones of L4 DRG, although many other peptides and growth factors that are expressed in injured and adjacent DRG neurones, after PNI and root injury, such as NPY, NGF, BDNF, NOS, and Galanin (Shortland et al., 2006a;Fukuoka et al., 2001;Obata et al., 2004;Zhou et al., 2009) are associated with neuropathic pain. These peptides and growth factors have not been assessed in this thesis, and would need to be quantified before conclusively saying the L4 DRG does not mediate the hypersensitivity seen after SRA to the L5 root.

Degenerative, glial, and inflammatory mechanisms within the spinal cord similar to that seen after DRA are also found in the avulsed (L5) segment as a consequence of SRA; however not as severe, as the number of roots avulsed determines extent of pathology and pain (Berman et al., 1998). Neuronal loss is minimal (8%) in the avulsed dorsal horn after SRA compared to DRA (31%) at 14 days. The more substantial ‘secondary’ neurodegeneration seen between 14 and 28 days after DRA, has not been assessed in SRA. Motor neuronal loss (43-69%) by 14 days is consistent with previous observations

(Koliatsos et al., 1994;Hoang et al., 2003;Bergerot et al., 2004;Nogradi et al., 2007;Penas et al., 2009), but the quanitification varies due to the staining method, with immunohistochemistry revealing greater loss than histological dye. This suggests that some neurones may well be present at a certain time point post injury, only the epitope of interest (in this instance NeuN) is no longer expressed within them, and they cannot be viewed through certain methodological staining procedures. Vascular integrity is also compromised in the L5 dorsal and ventral horns at 14 days post SRA, bilaterally, but it is unclear whether this is a consequence of secondary degenerative phenomena, or occlusion of the arterioles and venuoles that supply the spinal cord from the primary lesion. Macrophage recruitment is restricted to the dorsal root entry zone and columns at 14 days post SRA, in stark contrast to the robust and deep infiltration shown in the dorsal horn of DRA at the same time point. The most pronounced inflammatory reaction within the avulsed L5 dorsal horn is gliosis, microglial especially, an important finding given their substantial role in the generation and maintainence of neuropathic pain in PNI and SCI (Hains and Waxman, 2006;Hulsebosch, 2008;Gwak and Hulsebosch, 2009;Hulsebosch et al., 2009;Inoue and Tsuda, 2009;Milligan and Watkins, 2009).

Avulsion of the L5 root leads to similar, but less severe, neurodegenerative phenomena within the adjacent L4 segment (47% [NeuN] and 27% [Tol blue] motor neuronal loss, and 5% dorsal horn loss). Similar magnitudes of microglial and astrocyte reactivity were quantified in the adjacent L4 and avulsed L5 spinal cord. The overlap of L5 and L4 afferent collaterals within the L4 segment is well known (Molander and Grant, 1985;Molander and Grant, 1986;Rivero-Melian and Grant, 1990;Shehab et al., 2008;Shehab, 2009). The degeneration of L5 terminals within the L4 intact segment is the likely mechanism that leads to these histological responses, and therefore leads to the hypothesis for the mechanism of this evoked neuropathic pain generation: the neuropathic pain behaviour induced by L5 SRA could be generated at and/or processed through the adjacent L4 segment. Clinically, 80% of plexus avulsions have a least one intact root (Sindou et al., 2005) for signalling between periphery and dorsal horn, and this root and the corresponding segment has been shown to mediate neuropathic avulsion-pain (Bertelli and Ghizoni, 2008). This thesis therefore provides, for the first time, a model that represents these clinical findings, with a hypothesis that substantiates the evoked behaviour, and enables the testing of pharmacological agents for treatment of this pain.

7.4: SRA-induced hypersensitivity can be acutely modulated with the conventional analgesics amitriptyline and carbamazepine

Current pharmacological treatments for neuropathic pain, include the antidepressant, amitriptyline, and the anticonvulsant, carbamazepine, but these have limited efficacy in treating root avulsion pain (Parry, 1980;Berman et al., 1996;Piva et al., 2003). However, these drugs have improved efficacy in the long term, when combined with ventral root reimplantation surgery (Berman et al., 1998), most likely due to the compounding effect of the pain relief that follows motor functional recovery after surgical reimplantation (Htut et al., 2006). Amitriptyline and carbamazepine have shown analgesic efficacy in PNI rodent models (Chapman et al., 1998;Decosterd et al., 2004;De Vry et al., 2004). Effects were short lasting with single bolus administrations of these drugs. This chapter has shown that the behavioural hypersensitivity induced by SRA, can be relieved, albeit transiently, by administering boluses of amitriptyline and carbamazepine. The positive results also validate this model suitable for pre-clinical screening of noval drugs for treatment in avulsion pain.

Amitriptyline had no analgesic effect on hypersensitivity at first dose, but carbamazapine effectively ameliorated tactile hypersensitivity. A repeated dose leads to amelioration of tactile hypersensitivity with both amitriptyline and carbamazepine, without relief from thermal hypersensitivity. Increasing efficacy on the third administration (double dose) lead to amelioration of both thermal and tactile hypersensitivity; however side effects became apparent. The mechanism of action is likely related to direct inhibition of voltage gated sodium channels in dorsal horn and perhaps supraspinally (Dick et al., 2007;Hur et al., 2008). It is unclear why these drugs show more therapeutic efficacy when treating mechanical hypersensitivity compared to thermal, as this is converse to established literature on PNI-induced neuropathic pain behaviour (De Vry et al., 2004;Bomholt et al., 2005), where mechanical allodynia is intractable and thermal hyperalgesia is effectively treated at similar doses. However, this is evidence again for different mechanisms of action between PNI-induced and avulsion-induced behavioural hypersensitivity. The ineffectiveness of these drugs to maintain efficacy beyond 24 hours, is related to the drugs biological half-life and clearance, which is reached in the rodent CNS by approximately 1.6 hours for amitriptyline and 3.4 hours for carbamazepine (Coudore et al., 1996;Graumlich et al.,

2000), and the reversal of sodium channel blockade. The drugs ineffectiveness at maintaining efficacy beyond drug washout is in agreement with their mode of action as reversible sodium channel blockers, as well as the clinical findings; that these drugs have poor long term therapeutic efficacy in avulsion pain (Parry, 1980;Berman et al., 1996;Piva et al., 2003). Pharmacologically targeting the cause of neuronal hyperexcitability, such as the neuroinflammatory cascade, gliosis, and cell death, rather than trying to manipulate it directly with sodium channel blockers, may yield a more substantial and maintained pain relief in the SRA model.

7.5: Minocycline prevents the establishment of, and can reverse, SRA-induced neuropathic pain behaviour through microglial inhibition. Rilzuole was less effective for treatment of avulsion pain behaviour

It is now well established that neuropathic pain can be induced and maintained through pathologically increased glial activity in the spinal cord (McMahon et al., 2005;Hains and Waxman, 2006;Echeverry et al., 2008;Hulsebosch, 2008;Milligan and Watkins, 2009;Inoue and Tsuda, 2009). This glial reactivity is pronounced after SRA injury within the L5 and L4 segments, surrounding deafferented dorsal horn neurones and avulsed motor neurones, leading to the hypothesis that avulsion pain could be mediated by overactive microglia. This histological finding has lead to the rational in this thesis for the application of minocycline to directly target and inhibit microglial activity. In contrast, riluzole, an anti-excitotoxic drug, was administered and assessed separately to assess therapeutic efficacy of direct inhibition of glutaminergic activity within the spinal cord. If these treatments show efficacy *in vivo*, the immediate benefit for the treatment of neuropathic pain is that they are already marketed by pharmaceutical companies for treatment of other disorders, and can be applied to clinical trials immediately if successful.

Immediate minocycline treatment prevented the development of evoked behaviour. However, the treatment displayed some side effects including reduced weight gain and contralateral hyposensitivity. The prevention of neuropathic pain behaviour corresponded histologically with robust amelioration of microglial/macrophage staining in the avulsed and adjacent dermatomes, with partial amelioration of astrocyte reactivity. This shows that glial activity, most notably microglial, is important in

mediating SRA-induced neuropathic behaviour. Increased microglial reactivity in L5, and importantly L4, may lead to central sensitization of dorsal horn neurones, increasing their responsiveness to peripheral input from the spared L4 primary afferents. The effective prevention by minocycline of the induction of neuropathic pain behaviour in rats with L5 SRA may provide rational for this drug to be administered to patients with root avulsion. Neuropathic pain symptoms begin to appear 48 hours after avulsion injury (Berman et al., 1996) providing a therapeutic window of opportunity for these patients. However people who already suffer from excruciating neuropathic avulsion pain will have missed this therapeutic window. Encouragingly, delayed minocycline treatment can fully reverse established avulsion-induced hypersensitivity to baseline levels, at least at 7 days post operatively. Furthermore, the analgesic effects of the drug extend well beyond its biological half-life (Fagan et al., 2004) by at least 7 days, suggesting long lasting changes to sensory processing. This needs to be assessed at much longer time points post operatively, as well as post drug-withdrawal, to see if this is a permanent effect. Most importantly, it remains to be seen if these effects are causally linked to reversal of microglial activity. If this is indeed the case, this would provide conclusive evidence for minocycline as an irreversible potent inhibitor and ameliorator of microglial activity. Clinically, this would have implications for the treatment of many neuropathic pain conditions that are derived through pathological microglial activity, such as PNI (Raghavendra et al., 2003), SCI (Hains and Waxman, 2006), diabetic neuropathy (Tsuda et al., 2008), focal burn pain (Chang et al., 2010), and now root avulsion. Additionally a reevaluation of dosing regimes would be needed to see if a single administration would be sufficient to prevent/reverse the behavioural effects.

Immediate riluzole treatment delayed the onset of mechanical and thermal hypersensitivity. Histologically, it produced partial reduction in glial staining. This suggests that the dosing regimen was sub-optimal. An increase in macrophage reactivity was present in riluzole treated animals. However the lineage of either neuro-inflammatory (M1) or neuro-reparatory (M2) orientated macrophages is not presently clear to substantiate their role. Riluzole has only limited effects on reversing neuropathic pain behaviour; again the most likely reason is a suboptimal dosing regime.

Neither drug showed significant neuroprotection of motor or dorsal horn neurones, contrary to prior evidence in ventral root avulsion models (Bergerot et al., 2004;Hoang et al., 2008). This inconsistancy may be due to the cumulative trauma induced on the cord by the dorsal root avulsion. The loss of interneuronal and monosynaptic connections between primary afferents and motor neurones is known to induced physiological adjustments of the reflex pathways, but does not indicate cell loss (Holmberg and Kellerth, 1996;Cuppini et al., 1999). Perhaps the cumulative effect of ventral and dorsal gliosis within the ipsilateral cord may overwhelm the effectiveness of the treatment and propensity for motor and sensory neuronal survival. These effects are yet to be analysed in DRA and VRA models, to corroborate this finding, leaving the reasons for this discrepancy in the potential for neuroprotection unclear.

7.6: Summary of thesis findings

This thesis has provided a descriptive and quantitative analysis of the progressive events that occur in neuronal, vascular, glial, and inflammatory cell types in the deafferented dorsal horn after multiple dorsal root avulsion and rhizotomy. Dorsal root rhizotomy, used as the classical model for root avulsion injury, is not representative of such, showing less severe consequences compared to dorsal root avulsion, and should be replaced with animal models that more closely mimic the clinical condition. Evidence here supports the use of an L5 spinal root avulsion as a model of avulsion pain. Maintained neuropathic pain behaviour can be elicited from the rat hind-paw, as well as behavioural responses suggestive of spontaneous pain. This behaviour is correlated at 14 days post injury with neuropathological changes within the avulsed L5 segment, but also within the adjacent L4 segment, suggesting the hypersensitivity is mediated through central changes involving input from the adjacent spared root that innervates the hind-paw. This pathological behaviour can be prevented through treatment with minocycline, and to a lesser extent riluzole, through inhibition of microglia/macrophage reactivity. Importantly, minocycline shows promise when administered as treatment for established pain behaviour, as it is able to reverse, and prevent the return of, hypersensitivity after drug withdrawal. The evidence put forth in this thesis advocates the use of SRA as a suitable model to explore further mechanisms involved in avulsion pain, and as a model for the validation of more experimental drugs in the treatment of avulsion injury pain.

Reference List

Abdulla FA, Smith PA (1999) Nerve injury increases an excitatory action of neuropeptide Y and Y2-agonists on dorsal root ganglion neurons. Neuroscience 89:43-60.

Achour A, M'Bika JP, Biquard JM (2009) Enhanced endogenous type I interferon cell-driven survival and inhibition of spontaneous apoptosis by Riluzole. Virology 386:160-167.

Aldskogius H (2001) Microglia in neuroregeneration. Microsc Res Tech 54:40-46.

Aldskogius H, Kozlova EN (1998) Central neuron-glial and glial-glial interactions following axon injury. Prog Neurobiol 55:1-26.

Ali Z, Ringkamp M, Hartke TV, Chien HF, Flavahan NA, Campbell JN, Meyer RA (1999) Uninjured C-fiber nociceptors develop spontaneous activity and alpha-adrenergic sensitivity following L6 spinal nerve ligation in monkey. J Neurophysiol 81:455-466.

Allen A (1911) Surgery of experimental lesion of spinal cord equivalent to crush injury or fracture dislocation of spinal column. A preliminary report. J Am Med Assoc 57:870-880.

Almeida TF, Roizenblatt S, Tufik S (2004) Afferent pain pathways: a neuroanatomical review. Brain Res 1000:40-56.

Alvarez FJ, Morris HR, Priestley JV (1991) Sub-populations of smaller diameter trigeminal primary afferent neurons defined by expression of calcitonin gene-related peptide and the cell surface oligosaccharide recognized by monoclonal antibody LA4. J Neurocytol 20:716-731.

Anand P, Birch R (2002) Restoration of sensory function and lack of long-term chronic pain syndromes after brachial plexus injury in human neonates. Brain 125:113-122.

Anderson CM, Swanson RA (2000) Astrocyte glutamate transport: review of properties, regulation, and physiological functions. Glia 32:1-14.

Anderson DK, Nicolosi GR, Means ED, Hartley LE (1978) Effects of laminectomy on spinal cord blood flow. J Neurosurg 48:232-238.

Andrew D, Krout KE, Craig AD (2003) Differentiation of lamina I spinomedullary and spinothalamic neurons in the cat. J Comp Neurol 458:257-271.

Angelov DN, Gunkel A, Stennert E, Neiss WF (1995) Phagocytic microglia during delayed neuronal loss in the facial nucleus of the rat: time course of the neuronofugal migration of brain macrophages. Glia 13:113-129.

Ankeny DP, Popovich PG (2009) Mechanisms and implications of adaptive immune responses after traumatic spinal cord injury. Neuroscience 158:1112-1121.

Arguis MJ, Perez J, Martinez G, Ubre M, Gomar C (2008) Contralateral neuropathic pain following a surgical model of unilateral nerve injury in rats. Reg Anesth Pain Med 33:211-216.

Arvidsson J, Ygge J, Grant G (1986) Cell loss in lumbar dorsal root ganglia and transganglionic degeneration after sciatic nerve resection in the rat. Brain Res 373:15-21.

Asato F, Butler M, Blomberg H, Gordh T (2000) Variation in rat sciatic nerve anatomy: implications for a rat model of neuropathic pain. J Peripher Nerv Syst 5:19-21.

Attal N, Jazat F, Kayser V, Guilbaud G (1990) Further evidence for 'pain-related' behaviours in a model of unilateral peripheral mononeuropathy. Pain 41:235-251.

Averill S, Davis DR, Shortland PJ, Priestley JV, Hunt SP (2002) Dynamic pattern of reg-2 expression in rat sensory neurons after peripheral nerve injury. J Neurosci 22:7493-7501.

Averill S, McMahon SB, Clary DO, Reichardt LF, Priestley JV (1995) Immunocytochemical localization of trkA receptors in chemically identified subgroups of adult rat sensory neurons. Eur J Neurosci 7:1484-1494.

Ayata C, Ayata G, Hara H, Matthews RT, Beal MF, Ferrante RJ, Endres M, Kim A, Christie RH, Waeber C, Huang PL, Hyman BT, Moskowitz MA (1997) Mechanisms of reduced striatal NMDA excitotoxicity in type I nitric oxide synthase knock-out mice. J Neurosci 17:6908-6917.

Azkue JJ, Zimmermann M, Hsieh TF, Herdegen T (1998) Peripheral nerve insult induces NMDA receptor-mediated, delayed degeneration in spinal neurons. Eur J Neurosci 10:2204-2206.

Baastrup C, Finnerup NB (2008) Pharmacological management of neuropathic pain following spinal cord injury. CNS Drugs 22:455-475.

Baba H, Sakurai M, Abe K, Tominaga R (2009) Autophagy-mediated stress response in motor neuron after transient ischemia in rabbits. J Vasc Surg 50:381-387.

Banasr M, Chowdhury GM, Terwilliger R, Newton SS, Duman RS, Behar KL, Sanacora G (2008) Glial pathology in an animal model of depression: reversal of stress-induced cellular, metabolic and behavioral deficits by the glutamate-modulating drug riluzole. Mol Psychiatry.

Bao L, Wang HF, Cai HJ, Tong YG, Jin SX, Lu YJ, Grant G, Hokfelt T, Zhang X (2002) Peripheral axotomy induces only very limited sprouting of coarse myelinated afferents into inner lamina II of rat spinal cord. Eur J Neurosci 16:175-185.

Baptiste DC, Fehlings MG (2006) Pharmacological approaches to repair the injured spinal cord. J Neurotrauma 23:318-334.

Barclay J, Clark AK, Ganju P, Gentry C, Patel S, Wotherspoon G, Buxton F, Song C, Ullah J, Winter J, Fox A, Bevan S, Malcangio M (2007) Role of the cysteine protease cathepsin S in neuropathic hyperalgesia. Pain 130:225-234.

Basbaum AI, Wall PD (1976) Chronic changes in the response of cells in adult cat dorsal horn following partial deafferentation: the appearance of responding cells in a previously non-responsive region. Brain Res 116:181-204.

Beggah AT, Dours-Zimmermann MT, Barras FM, Brosius A, Zimmermann DR, Zurn AD (2005) Lesion-induced differential expression and cell association of Neurocan, Brevican, Versican V1 and V2 in the mouse dorsal root entry zone. Neuroscience 133:749-762.

Beggs S, Salter MW (2007) Stereological and somatotopic analysis of the spinal microglial response to peripheral nerve injury. Brain Behav Immun 21:624-633.

Bellander BM, Singhrao SK, Ohlsson M, Mattsson P, Svensson M (2001) Complement activation in the human brain after traumatic head injury. J Neurotrauma 18:1295-1311.

Benbouzid M, Choucair-Jaafar N, Yalcin I, Waltisperger E, Muller A, Freund-Mercier MJ, Barrot M (2008) Chronic, but not acute, tricyclic antidepressant treatment alleviates neuropathic allodynia after sciatic nerve cuffing in mice. Eur J Pain 12:1008-1017.

Bennett AD, Chastain KM, Hulsebosch CE (2000) Alleviation of mechanical and thermal allodynia by CGRP(8-37) in a rodent model of chronic central pain. Pain 86:163-175.

Bennett GJ, Seltzer Z, Lu GW, Nishikawa N, Dubner R (1983) The cells of origin of the dorsal column postsynaptic projection in the lumbosacral enlargements of cats and monkeys. Somatosens Res 1:131-149.

Bennett GJ, Xie YK (1988) A peripheral mononeuropathy in rat that produces disorders of pain sensation like those seen in man. Pain 33:87-107.

Benoit E, Escande D (1991) Riluzole specifically blocks inactivated Na channels in myelinated nerve fibre. Pflugers Arch 419:603-609.

Benton RL, Maddie MA, Minnillo DR, Hagg T, Whittemore SR (2008a) Griffonia simplicifolia isolectin B4 identifies a specific subpopulation of angiogenic blood vessels following contusive spinal cord injury in the adult mouse. J Comp Neurol 507:1031-1052.

Benton RL, Maddie MA, Worth CA, Mahoney ET, Hagg T, Whittemore SR (2008b) Transcriptomic screening of microvascular endothelial cells implicates novel molecular regulators of vascular dysfunction after spinal cord injury. J Cereb Blood Flow Metab 28:1771-1785.

Bergerot A, Shortland PJ, Anand P, Hunt SP, Carlstedt T (2004) Co-treatment with riluzole and GDNF is necessary for functional recovery after ventral root avulsion injury. Exp Neurol 187:359-366.

Berman D, Rodin BE (1982) The influence of housing condition on autotomy following dorsal rhizotomy in rats. Pain 13:307-311.

Berman J, Anand P, Chen L, Taggart M, Birch R (1996) Pain relief from preganglionic injury to the brachial plexus by late intercostal nerve transfer. J Bone Joint Surg Br 78:759-760.

Berman JS, Birch R, Anand P (1998) Pain following human brachial plexus injury with spinal cord root avulsion and the effect of surgery. Pain 75:199-207.

Berman JS, Symonds C, Birch R (2004) Efficacy of two cannabis based medicinal extracts for relief of central neuropathic pain from brachial plexus avulsion: results of a randomised controlled trial. Pain 112:299-306.

Bertelli JA, Ghizoni MF (2006) Concepts of nerve regeneration and repair applied to brachial plexus reconstruction. Microsurgery 26:230-244.

Bertelli JA, Ghizoni MF (2008) Pain after avulsion injuries and complete palsy of the brachial plexus: the possible role of nonavulsed roots in pain generation. Neurosurgery 62:1104-1113.

Bertilsson L (1978) Clinical pharmacokinetics of carbamazepine. Clin Pharmacokinet 3:128-143.

Bester H, Beggs S, Woolf CJ (2000) Changes in tactile stimuli-induced behavior and c-Fos expression in the superficial dorsal horn and in parabrachial nuclei after sciatic nerve crush. J Comp Neurol 428:45-61.

Bigbee AJ, Hoang TX, Havton LA (2007) At-level neuropathic pain is induced by lumbosacral ventral root avulsion injury and ameliorated by root reimplantation into the spinal cord. Exp Neurol 204:273-282.

Bigbee AJ, Hoang TX, Havton LA (2008) Reimplantation of avulsed lumbosacral ventral roots in the rat ameliorates injury-induced degeneration of primary afferent axon collaterals in the spinal dorsal columns. Neuroscience 152:338-345.

Birch R (1993) Surgery for brachial plexus injuries. J Bone Joint Surg Br 75:346-348.

Birch R (1996) Brachial plexus injuries. J Bone Joint Surg Br 78:986-992.

Blits B, Carlstedt TP, Ruitenberg MJ, de WF, Hermens WT, Dijkhuizen PA, Claasens JW, Eggers R, van der Sluis R, Tenenbaum L, Boer GJ, Verhaagen J (2004) Rescue and sprouting of motoneurons following ventral root avulsion and reimplantation combined with intraspinal adeno-associated viral vector-mediated expression of glial cell line-derived neurotrophic factor or brain-derived neurotrophic factor. Exp Neurol 189:303-316.

BLOM S (1962) Trigeminal neuralgia: its treatment with a new anticonvulsant drug (G-32883). Lancet 1:839-840.

Blumenthal DT (2009) Assessment of neuropathic pain in cancer patients. Curr Pain Headache Rep 13:282-287.

Boje KM, Arora PK (1992) Microglial-produced nitric oxide and reactive nitrogen oxides mediate neuronal cell death. Brain Res 587:250-256.

Bomholt SF, Mikkelsen JD, Blackburn-Munro G (2005) Antinociceptive effects of the antidepressants amitriptyline, duloxetine, mirtazapine and citalopram in animal models of acute, persistent and neuropathic pain. Neuropharmacology 48:252-263.

Bonnard C, Narakas A (1985) [Pain syndromes and post-traumatic lesions of the brachial plexus. Study of the effect of surgical repair on the pain syndrome in 211 operated patients with post-traumatic lesions caused by avulsion or rupture of the brachial plexus]. Helv Chir Acta 52:621-632.

Boselli C, Barbone MS, Lucchelli A (2007) Older versus newer antidepressants: substance P or calcium antagonism? Can J Physiol Pharmacol 85:1004-1011.

Bouhassira D, Lanteri-Minet M, Attal N, Laurent B, Touboul C (2008) Prevalence of chronic pain with neuropathic characteristics in the general population. Pain 136:380-387.

Bove GM, Moskowitz MA (1997) Primary afferent neurons innervating guinea pig dura. J Neurophysiol 77:299-308.

Bradbury EJ, Burnstock G, McMahon SB (1998) The expression of P2X3 purinoreceptors in sensory neurons: effects of axotomy and glial-derived neurotrophic factor. Mol Cell Neurosci 12:256-268.

Bradbury EJ, Moon LD, Popat RJ, King VR, Bennett GS, Patel PN, Fawcett JW, McMahon SB (2002) Chondroitinase ABC promotes functional recovery after spinal cord injury. Nature 416:636-640.

Brau ME, Dreimann M, Olschewski A, Vogel W, Hempelmann G (2001) Effect of drugs used for neuropathic pain management on tetrodotoxin-resistant Na(+) currents in rat sensory neurons. Anesthesiology 94:137-144.

Brodal P (2004) The central nervous system
structure and function. Oxford: Oxford University Press.

Brown AG (1981) The spinocervical tract. Prog Neurobiol 17:59-96.

Brown AG, Rose PK, Snow PJ (1977) The morphology of spinocervical tract neurones revealed by intracellular injection of horseradish peroxidase. J Physiol 270:747-764.

Brown GC, Neher JJ (2010) Inflammatory Neurodegeneration and Mechanisms of Microglial Killing of Neurons. Mol Neurobiol.

Brown PB, Culberson JL (1981) Somatotopic organization of hindlimb cutaneous dorsal root projections to cat dorsal horn. J Neurophysiol 45:137-143.

Bruce JC, Oatway MA, Weaver LC (2002) Chronic pain after clip-compression injury of the rat spinal cord. Exp Neurol 178:33-48.

Brumovsky P, Watanabe M, Hokfelt T (2007) Expression of the vesicular glutamate transporters-1 and -2 in adult mouse dorsal root ganglia and spinal cord and their regulation by nerve injury. Neuroscience 147:469-490.

Bruxelle J, Travers V, Thiebaut JB (1988) Occurrence and treatment of pain after brachial plexus injury. Clin Orthop Relat Res87-95.

Cafferty WB, Bradbury EJ, Lidierth M, Jones M, Duffy PJ, Pezet S, McMahon SB (2008) Chondroitinase ABC-mediated plasticity of spinal sensory function. J Neurosci 28:11998-12009.

Cameron B, Landreth GE (2010) Inflammation, microglia, and Alzheimer's disease. Neurobiol Dis 37:503-509.

Carlson SL, Parrish ME, Springer JE, Doty K, Dossett L (1998) Acute inflammatory response in spinal cord following impact injury. Exp Neurol 151:77-88.

Carlstedt T (2008) Root repair review: basic science background and clinical outcome. Restor Neurol Neurosci 26:225-241.

Carlstedt T (2009) Nerve root replantation. Neurosurg Clin N Am 20:39-50, vi.

Carlstedt T, Anand P, Hallin R, Misra PV, Noren G, Seferlis T (2000) Spinal nerve root repair and reimplantation of avulsed ventral roots into the spinal cord after brachial plexus injury. J Neurosurg 93:237-247.

Carlstedt T, Anand P, Htut M, Misra P, Svensson M (2004) Restoration of hand function and so called "breathing arm" after intraspinal repair of C5-T1 brachial plexus avulsion injury. Case report. Neurosurg Focus 16:E7.

Carlstedt T, Cullheim S (2000) Spinal cord motoneuron maintenance, injury and repair. Prog Brain Res 127:501-514.

Carlstedt T, Grane P, Hallin RG, Noren G (1995) Return of function after spinal cord implantation of avulsed spinal nerve roots. Lancet 346:1323-1325.

Carlstedt T, Hultgren T, Nyman T, Hansson T (2009) Cortical activity and hand function restoration in a patient after spinal cord surgery. Nat Rev Neurol 5:571-574.

Carlstedt T, Linda H, Cullheim S, Risling M (1986) Reinnervation of hind limb muscles after ventral root avulsion and implantation in the lumbar spinal cord of the adult rat. Acta Physiol Scand 128:645-646.

Carlstedt TP, Hallin RG, Hedstrom KG, Nilsson-Remahl IA (1993) Functional recovery in primates with brachial plexus injury after spinal cord implantation of avulsed ventral roots. J Neurol Neurosurg Psychiatry 56:649-654.

Carlton SM, Dougherty PM, Pover CM, Coggeshall RE (1991) Neuroma formation and numbers of axons in a rat model of experimental peripheral neuropathy. Neurosci Lett 131:88-92.

Caroni P (1997) Intrinsic neuronal determinants that promote axonal sprouting and elongation. Bioessays 19:767-775.

Carr PA, Yamamoto T, Karmy G, Nagy JI (1991) Cytochemical relationships and central terminations of a unique population of primary afferent neurons in rat. Brain Res Bull 26:825-843.

Carr PA, Yamamoto T, Nagy JI (1990) Calcitonin gene-related peptide in primary afferent neurons of rat: co-existence with fluoride-resistant acid phosphatase and depletion by neonatal capsaicin. Neuroscience 36:751-760.

Casella GT, Bunge MB, Wood PM (2006) Endothelial cell loss is not a major cause of neuronal and glial cell death following contusion injury of the spinal cord. Exp Neurol 202:8-20.

Casella GT, Marcillo A, Bunge MB, Wood PM (2002) New vascular tissue rapidly replaces neural parenchyma and vessels destroyed by a contusion injury to the rat spinal cord. Exp Neurol 173:63-76.

Cavaliere C, Cirillo G, Rosaria BM, Rossi F, De N, V, Maione S, Papa M (2007) Gliosis alters expression and uptake of spinal glial amino acid transporters in a mouse neuropathic pain model. Neuron Glia Biol 3:141-153.

Cervero F, Iggo A, Molony V (1977) Responses of spinocervical tract neurones to noxious stimulation of the skin. J Physiol 267:537-558.

Cervero F, Iggo A, Ogawa H (1976) Nociceptor-driven dorsal horn neurones in the lumbar spinal cord of the cat. Pain 2:5-24.

Cervero F, Tattersall JE (1986) Somatic and visceral sensory integration in the thoracic spinal cord. Prog Brain Res 67:189-205.

Chang YW, Tan A, Saab C, Waxman S (2010) Unilateral focal burn injury is followed by long-lasting bilateral allodynia and neuronal hyperexcitability in spinal cord dorsal horn. J Pain 11:119-130.

Chaplan SR, Bach FW, Pogrel JW, Chung JM, Yaksh TL (1994) Quantitative assessment of tactile allodynia in the rat paw. J Neurosci Methods 53:55-63.

Chapman V, Suzuki R, Chamarette HL, Rygh LJ, Dickenson AH (1998) Effects of systemic carbamazepine and gabapentin on spinal neuronal responses in spinal nerve ligated rats. Pain 75:261-272.

Chen HJ, Tu YK (2006) Long term follow-up results of dorsal root entry zone lesions for intractable pain after brachial plexus avulsion injuries. Acta Neurochir Suppl 99:73-75.

Chen M, Ona VO, Li M, Ferrante RJ, Fink KB, Zhu S, Bian J, Guo L, Farrell LA, Hersch SM, Hobbs W, Vonsattel JP, Cha JH, Friedlander RM (2000) Minocycline inhibits caspase-1 and caspase-3 expression and delays mortality in a transgenic mouse model of Huntington disease. Nat Med 6:797-801.

Cheng XP, Wang BR, Liu HL, You SW, Huang WJ, Jiao XY, Ju G (2003) Phosphorylation of extracellular signal-regulated kinases 1/2 is predominantly enhanced in the microglia of the rat spinal cord following dorsal root transection. Neuroscience 119:701-712.

Cheramy A, Barbeito L, Godeheu G, Glowinski J (1992) Riluzole inhibits the release of glutamate in the caudate nucleus of the cat in vivo. Neurosci Lett 147:209-212.

Cheshire WP (2005) Trigeminal neuralgia: diagnosis and treatment. Curr Neurol Neurosci Rep 5:79-85.

Chessell IP, Hatcher JP, Bountra C, Michel AD, Hughes JP, Green P, Egerton J, Murfin M, Richardson J, Peck WL, Grahames CB, Casula MA, Yiangou Y, Birch R, Anand P, Buell GN (2005) Disruption of the P2X7 purinoceptor gene abolishes chronic inflammatory and neuropathic pain. Pain 114:386-396.

Chew DJ, Leinster VH, Sakthithasan M, Robson LG, Carlstedt T, Shortland PJ (2008) Cell death after dorsal root injury. Neurosci Lett 433:231-234.

Chierzi S, Ratto GM, Verma P, Fawcett JW (2005) The ability of axons to regenerate their growth cones depends on axonal type and age, and is regulated by calcium, cAMP and ERK. Eur J Neurosci 21:2051-2062.

Choi A, Mitchelson F (1994) Variation in the affinity of amitriptyline for muscarine receptor subtypes. Pharmacology 48:293-300.

Choi Y, Yoon YW, Na HS, Kim SH, Chung JM (1994) Behavioral signs of ongoing pain and cold allodynia in a rat model of neuropathic pain. Pain 59:369-376.

Chong MS, Woolf CJ, Haque NS, Anderson PN (1999) Axonal regeneration from injured dorsal roots into the spinal cord of adult rats. J Comp Neurol 410:42-54.

Christensen MD, Hulsebosch CE (1997a) Chronic central pain after spinal cord injury. J Neurotrauma 14:517-537.

Christensen MD, Hulsebosch CE (1997b) Spinal cord injury and anti-NGF treatment results in changes in CGRP density and distribution in the dorsal horn in the rat. Exp Neurol 147:463-475.

Chung K, Coggeshall RE (1979) Primary afferent axons in the tract of Lissauer in the cat. J Comp Neurol 186:451-463.

Chung K, Langford LA, Applebaum AE, Coggeshall RE (1979) Primary afferent fibers in the tract of Lissauer in the rat. J Comp Neurol 184:587-598.

Chung K, Lee BH, Yoon YW, Chung JM (1996) Sympathetic sprouting in the dorsal root ganglia of the injured peripheral nerve in a rat neuropathic pain model. J Comp Neurol 376:241-252.

Cizkova D, Lukacova N, Marsala M, Marsala J (2002) Neuropathic pain is associated with alterations of nitric oxide synthase immunoreactivity and catalytic activity in dorsal root ganglia and spinal dorsal horn. Brain Res Bull 58:161-171.

Coderre TJ, Kumar N, Lefebvre CD, Yu JS (2007) A comparison of the glutamate release inhibition and anti-allodynic effects of gabapentin, lamotrigine, and riluzole in a model of neuropathic pain. J Neurochem 100:1289-1299.

Coderre TJ, Melzack R (1986) Procedures which increase acute pain sensitivity also increase autotomy. Exp Neurol 92:713-722.

Coggeshall RE, Carlton SM (1997) Receptor localization in the mammalian dorsal horn and primary afferent neurons. Brain Res Brain Res Rev 24:28-66.

Coggeshall RE, Dougherty PM, Pover CM, Carlton SM (1993) Is large myelinated fiber loss associated with hyperalgesia in a model of experimental peripheral neuropathy in the rat? Pain 52:233-242.

Coggeshall RE, Lekan HA, White FA, Woolf CJ (2001) A-fiber sensory input induces neuronal cell death in the dorsal horn of the adult rat spinal cord. J Comp Neurol 435:276-282.

Coimbra A, Ribeiro-da-Silva A, Pignatelli D (1984) Effects of dorsal rhizotomy on the several types of primary afferent terminals in laminae I-III of the rat spinal cord. An electron microscope study. Anat Embryol (Berl) 170:279-287.

Colburn RW, DeLeo JA, Rickman AJ, Yeager MP, Kwon P, Hickey WF (1997) Dissociation of microglial activation and neuropathic pain behaviors following peripheral nerve injury in the rat. J Neuroimmunol 79:163-175.

Colburn RW, Rickman AJ, DeLeo JA (1999) The effect of site and type of nerve injury on spinal glial activation and neuropathic pain behavior. Exp Neurol 157:289-304.

Conrath M, Taquet H, Pohl M, Carayon A (1989) Immunocytochemical evidence for calcitonin gene-related peptide-like neurons in the dorsal horn and lateral spinal nucleus of the rat cervical spinal cord. J Chem Neuroanat 2:335-347.

Cooray S, Best JM, Jin L (2003) Time-course induction of apoptosis by wild-type and attenuated strains of rubella virus. J Gen Virol 84:1275-1279.

Coudore F, Besson A, Eschalier A, Lavarenne J, Fialip J (1996) Plasma and brain pharmacokinetics of amitriptyline and its demethylated and hydroxylated metabolites after one and six half-life repeated administrations to rats. Gen Pharmacol 27:215-219.

Coull JA, Beggs S, Boudreau D, Boivin D, Tsuda M, Inoue K, Gravel C, Salter MW, De KY (2005) BDNF from microglia causes the shift in neuronal anion gradient underlying neuropathic pain. Nature 438:1017-1021.

Coull JA, Boudreau D, Bachand K, Prescott SA, Nault F, Sik A, De KP, De KY (2003) Trans-synaptic shift in anion gradient in spinal lamina I neurons as a mechanism of neuropathic pain. Nature 424:938-942.

Coward K, Plumpton C, Facer P, Birch R, Carlstedt T, Tate S, Bountra C, Anand P (2000) Immunolocalization of SNS/PN3 and NaN/SNS2 sodium channels in human pain states. Pain 85:41-50.

Crown ED, Gwak YS, Ye Z, Johnson KM, Hulsebosch CE (2008) Activation of p38 MAP kinase is involved in central neuropathic pain following spinal cord injury. Exp Neurol 213:257-267.

Crown ED, Ye Z, Johnson KM, Xu GY, McAdoo DJ, Hulsebosch CE (2006) Increases in the activated forms of ERK 1/2, p38 MAPK, and CREB are correlated with the expression of at-level mechanical allodynia following spinal cord injury. Exp Neurol 199:397-407.

Culberson JL, Brown PB (1984) Projections of hindlimb dorsal roots to lumbosacral spinal cord of cat. J Neurophysiol 51:516-528.

Cuppini R, Ambrogini P, Sartini S (1998) Enlargement of motoneuron peripheral field following partial denervation with or without dorsal rhizotomy. Neuroscience 84:151-161.

Cuppini R, Ambrogini P, Sartini S, Bruno C, Lattanzi D, Rocchi MB (2002) The role of sensory input in motor neuron sprouting control. Somatosens Mot Res 19:279-285.

Cuppini R, Sartini S, Ambrogini P, Fulgenzi G, Graciotti L (1999) Rat motor neuron plasticity induced by dorsal rhizotomy. Neurosci Lett 275:29-32.

Dalal A, Tata M, Allegre G, Gekiere F, Bons N, Albe-Fessard D (1999) Spontaneous activity of rat dorsal horn cells in spinal segments of sciatic projection following transection of sciatic nerve or of corresponding dorsal roots. Neuroscience 94:217-228.

Davis JL, Lewis SB, Gerich JE, Kaplan RA, Schultz TA, Wallin JD (1977) Peripheral diabetic neuropathy treated with amitriptyline and fluphenazine. JAMA 238:2291-2292.

de Miguel M, Kraychete DC (2009) Pain in patients with spinal cord injury: a review. Rev Bras Anestesiol 59:350-357.

De Vry J, Kuhl E, Franken-Kunkel P, Eckel G (2004) Pharmacological characterization of the chronic constriction injury model of neuropathic pain. Eur J Pharmacol 491:137-148.

Decosterd I, Allchorne A, Woolf CJ (2004) Differential analgesic sensitivity of two distinct neuropathic pain models. Anesth Analg 99:457-63, table.

Decosterd I, Ji RR, Abdi S, Tate S, Woolf CJ (2002) The pattern of expression of the voltage-gated sodium channels Na(v)1.8 and Na(v)1.9 does not change in uninjured primary sensory neurons in experimental neuropathic pain models. Pain 96:269-277.

Decosterd I, Woolf CJ (2000) Spared nerve injury: an animal model of persistent peripheral neuropathic pain. Pain 87:149-158.

Demjen D, Klussmann S, Kleber S, Zuliani C, Stieltjes B, Metzger C, Hirt UA, Walczak H, Falk W, Essig M, Edler L, Krammer PH, Martin-Villalba A (2004) Neutralization of CD95 ligand promotes regeneration and functional recovery after spinal cord injury. Nat Med 10:389-395.

Dib-Hajj SD, Black JA, Waxman SG (2009) Voltage-gated sodium channels: therapeutic targets for pain. Pain Med 10:1260-1269.

Dib-Hajj SD, Fjell J, Cummins TR, Zheng Z, Fried K, LaMotte R, Black JA, Waxman SG (1999) Plasticity of sodium channel expression in DRG neurons in the chronic constriction injury model of neuropathic pain. Pain 83:591-600.

Dick IE, Brochu RM, Purohit Y, Kaczorowski GJ, Martin WJ, Priest BT (2007) Sodium channel blockade may contribute to the analgesic efficacy of antidepressants. J Pain 8:315-324.

Dickenson AH, Suzuki R (2005) Opioids in neuropathic pain: clues from animal studies. Eur J Pain 9:113-116.

Diguet E, Fernagut PO, Wei X, Du Y, Rouland R, Gross C, Bezard E, Tison F (2004a) Deleterious effects of minocycline in animal models of Parkinson's disease and Huntington's disease. Eur J Neurosci 19:3266-3276.

Diguet E, Gross CE, Tison F, Bezard E (2004b) Rise and fall of minocycline in neuroprotection: need to promote publication of negative results. Exp Neurol 189:1-4.

Dixon WJ (1980) Efficient analysis of experimental observations. Annu Rev Pharmacol Toxicol 20:441-462.

Djouhri L, Fang X, Okuse K, Wood JN, Berry CM, Lawson SN (2003) The TTX-resistant sodium channel Nav1.8 (SNS/PN3): expression and correlation with membrane properties in rat nociceptive primary afferent neurons. J Physiol 550:739-752.

Djouhri L, Koutsikou S, Fang X, McMullan S, Lawson SN (2006) Spontaneous pain, both neuropathic and inflammatory, is related to frequency of spontaneous firing in intact C-fiber nociceptors. J Neurosci 26:1281-1292.

Djouhri L, Lawson SN (2004) Abeta-fiber nociceptive primary afferent neurons: a review of incidence and properties in relation to other afferent A-fiber neurons in mammals. Brain Res Brain Res Rev 46:131-145.

Doble A (1996) The pharmacology and mechanism of action of riluzole. Neurology 47:S233-S241.

Dobrenis K, Makman MH, Stefano GB (1995) Occurrence of the opiate alkaloid-selective mu3 receptor in mammalian microglia, astrocytes and Kupffer cells. Brain Res 686:239-248.

Dolan S, Nolan AM (2007) Blockade of metabotropic glutamate receptor 5 activation inhibits mechanical hypersensitivity following abdominal surgery. Eur J Pain 11:644-651.

Dong C, Xie Z, Fan J, Xie Y (2002) Ectopic discharges trigger sympathetic sprouting in rat dorsal root ganglia following peripheral nerve injury. Sci China C Life Sci 45:191-200.

Dore-Duffy P, Owen C, Balabanov R, Murphy S, Beaumont T, Rafols JA (2000) Pericyte migration from the vascular wall in response to traumatic brain injury. Microvasc Res 60:55-69.

Doubell TP, Mannion RJ, Woolf CJ (1997) Intact sciatic myelinated primary afferent terminals collaterally sprout in the adult rat dorsal horn following section of a neighbouring peripheral nerve. J Comp Neurol 380:95-104.

Dowdall T, Robinson I, Meert TF (2005) Comparison of five different rat models of peripheral nerve injury. Pharmacol Biochem Behav 80:93-108.

Drew GM, Siddall PJ, Duggan AW (2001) Responses of spinal neurones to cutaneous and dorsal root stimuli in rats with mechanical allodynia after contusive spinal cord injury. Brain Res 893:59-69.

Drew GM, Siddall PJ, Duggan AW (2004) Mechanical allodynia following contusion injury of the rat spinal cord is associated with loss of GABAergic inhibition in the dorsal horn. Pain 109:379-388.

Dublin P, Hanani M (2007) Satellite glial cells in sensory ganglia: their possible contribution to inflammatory pain. Brain Behav Immun 21:592-598.

Dubovy P, Tuckova L, Jancalek R, Svizenska I, Klusakova I (2007) Increased invasion of ED-1 positive macrophages in both ipsi- and contralateral dorsal root ganglia following unilateral nerve injuries. Neurosci Lett 427:88-93.

Durrenberger PF, Facer P, Gray RA, Chessell IP, Naylor A, Bountra C, Banati RB, Birch R, Anand P (2004) Cyclooxygenase-2 (Cox-2) in injured human nerve and a rat model of nerve injury. J Peripher Nerv Syst 9:15-25.

Dusart I, Schwab ME (1994) Secondary cell death and the inflammatory reaction after dorsal hemisection of the rat spinal cord. Eur J Neurosci 6:712-724.

EARLE KM (1952) The tract of Lissauer and its possible relation to the pain pathway. J Comp Neurol 96:93-111.

Echeverry S, Shi XQ, Zhang J (2008) Characterization of cell proliferation in rat spinal cord following peripheral nerve injury and the relationship with neuropathic pain. Pain 135:37-47.

Eide AL, Glover J, Kjaerulff O, Kiehn O (1999) Characterization of commissural interneurons in the lumbar region of the neonatal rat spinal cord. J Comp Neurol 403:332-345.

Emirandetti A, Graciele ZR, Sabha M, Jr., de Oliveira AL (2006) Astrocyte reactivity influences the number of presynaptic terminals apposed to spinal motoneurons after axotomy. Brain Res 1095:35-42.

Endo K, Suzuki N, Misu T, Aoki M, Itoyama Y (2009) Dorsal-roots enhancement and Wallerian degeneration of dorsal cord in the patient of acute sensory ataxic neuropathy. J Neurol 256:1765-1766.

Eriksson NP, Persson JK, Svensson M, Arvidsson J, Molander C, Aldskogius H (1993) A quantitative analysis of the microglial cell reaction in central primary sensory projection territories following peripheral nerve injury in the adult rat. Exp Brain Res 96:19-27.

Ernfors P, Rosario CM, Merlio JP, Grant G, Aldskogius H, Persson H (1993) Expression of mRNAs for neurotrophin receptors in the dorsal root ganglion and spinal cord during development and following peripheral or central axotomy. Brain Res Mol Brain Res 17:217-226.

Eschenfelder S, Habler HJ, Janig W (2000) Dorsal root section elicits signs of neuropathic pain rather than reversing them in rats with L5 spinal nerve injury. Pain 87:213-219.

Esser MJ, Sawynok J (2000) Caffeine blockade of the thermal antihyperalgesic effect of acute amitriptyline in a rat model of neuropathic pain. Eur J Pharmacol 399:131-139.

Fagan SC, Edwards DJ, Borlongan CV, Xu L, Arora A, Feuerstein G, Hess DC (2004) Optimal delivery of minocycline to the brain: implication for human studies of acute neuroprotection. Exp Neurol 186:248-251.

Faulkner JR, Herrmann JE, Woo MJ, Tansey KE, Doan NB, Sofroniew MV (2004) Reactive astrocytes protect tissue and preserve function after spinal cord injury. J Neurosci 24:2143-2155.

Fawcett JW (2006) The glial response to injury and its role in the inhibition of CNS repair. Adv Exp Med Biol 557:11-24.

Fawcett JW, Asher RA (1999) The glial scar and central nervous system repair. Brain Res Bull 49:377-391.

Fawcett JW, Keynes RJ (1990) Peripheral nerve regeneration. Annu Rev Neurosci 13:43-60.

Fenzi F, Benedetti MD, Moretto G, Rizzuto N (2001) Glial cell and macrophage reactions in rat spinal ganglion after peripheral nerve lesions: an immunocytochemical and morphometric study. Arch Ital Biol 139:357-365.

Feria M, Sanchez A, Abad F, Abreu P (1992) Effects of selective neurotoxic lesion of lumbosacral serotonergic and noradrenergic systems on autotomy behaviour in rats. Pain 51:101-109.

Festoff BW, Ameenuddin S, Arnold PM, Wong A, Santacruz KS, Citron BA (2006) Minocycline neuroprotects, reduces microgliosis, and inhibits caspase protease expression early after spinal cord injury. J Neurochem 97:1314-1326.

Finnerup NB, Norrbrink C, Fuglsang-Frederiksen A, Terkelsen AJ, Hojlund AP, Jensen TS (2009) Pain, referred sensations, and involuntary muscle movements in brachial plexus injury. Acta Neurol Scand.

Fleming JC, Norenberg MD, Ramsay DA, Dekaban GA, Marcillo AE, Saenz AD, Pasquale-Styles M, Dietrich WD, Weaver LC (2006) The cellular inflammatory response in human spinal cords after injury. Brain 129:3249-3269.

Flores LP (2006) [Epidemiological study of the traumatic brachial plexus injuries in adults]. Arq Neuropsiquiatr 64:88-94.

Franson P, Ronnevi LO (1989) Myelin breakdown in the posterior funiculus of the kitten after dorsal rhizotomy. A qualitative and quantitative light and electron microscopic study. Anat Embryol (Berl) 180:273-280.

Freysoldt A, Fleckenstein J, Lang PM, Irnich D, Grafe P, Carr RW (2009) Low concentrations of amitriptyline inhibit nicotinic receptors in unmyelinated axons of human peripheral nerve. Br J Pharmacol 158:797-805.

Fukuoka T, Kondo E, Dai Y, Hashimoto N, Noguchi K (2001) Brain-derived neurotrophic factor increases in the uninjured dorsal root ganglion neurons in selective spinal nerve ligation model. J Neurosci 21:4891-4900.

Fukuoka T, Tokunaga A, Kondo E, Miki K, Tachibana T, Noguchi K (1998) Change in mRNAs for neuropeptides and the GABA(A) receptor in dorsal root ganglion neurons in a rat experimental neuropathic pain model. Pain 78:13-26.

Fukuoka T, Tokunaga A, Tachibana T, Dai Y, Yamanaka H, Noguchi K (2002) VR1, but not P2X(3), increases in the spared L4 DRG in rats with L5 spinal nerve ligation. Pain 99:111-120.

Fumagalli E, Bigini P, Barbera S, De PM, Mennini T (2006) Riluzole, unlike the AMPA antagonist RPR119990, reduces motor impairment and partially prevents motoneuron death in the wobbler mouse, a model of neurodegenerative disease. Exp Neurol 198:114-128.

Fumagalli E, Funicello M, Rauen T, Gobbi M, Mennini T (2008) Riluzole enhances the activity of glutamate transporters GLAST, GLT1 and EAAC1. Eur J Pharmacol 578:171-176.

Gabay E, Tal M (2004) Pain behavior and nerve electrophysiology in the CCI model of neuropathic pain. Pain 110:354-360.

Galer BS, Twilling LL, Harle J, Cluff RS, Friedman E, Rowbotham MC (2000) Lack of efficacy of riluzole in the treatment of peripheral neuropathic pain conditions. Neurology 55:971-975.

Garrison CJ, Dougherty PM, Kajander KC, Carlton SM (1991) Staining of glial fibrillary acidic protein (GFAP) in lumbar spinal cord increases following a sciatic nerve constriction injury. Brain Res 565:1-7.

Gavrieli Y, Sherman Y, Ben-Sasson SA (1992) Identification of programmed cell death in situ via specific labeling of nuclear DNA fragmentation. J Cell Biol 119:493-501.

Genovese T, Mazzon E, Crisafulli C, Di PR, Muia C, Esposito E, Bramanti P, Cuzzocrea S (2008) TNF-alpha blockage in a mouse model of SCI: evidence for improved outcome. Shock 29:32-41.

Gensel JC, Nakamura S, Guan Z, van RN, Ankeny DP, Popovich PG (2009) Macrophages promote axon regeneration with concurrent neurotoxicity. J Neurosci 29:3956-3968.

George R, Griffin JW (1994a) Delayed macrophage responses and myelin clearance during Wallerian degeneration in the central nervous system: the dorsal radiculotomy model. Exp Neurol 129:225-236.

George R, Griffin JW (1994b) The proximo-distal spread of axonal degeneration in the dorsal columns of the rat. J Neurocytol 23:657-667.

Geria AN, Tajirian AL, Kihiczak G, Schwartz RA (2009) Minocycline-induced skin pigmentation: an update. Acta Dermatovenerol Croat 17:123-126.

Gibson SJ, Polak JM, Bloom SR, Sabate IM, Mulderry PM, Ghatei MA, McGregor GP, Morrison JF, Kelly JS, Evans RM, . (1984) Calcitonin gene-related peptide immunoreactivity in the spinal cord of man and of eight other species. J Neurosci 4:3101-3111.

Giesler GJ, Jr., Cliffer KD (1985) Postsynaptic dorsal column pathway of the rat. II. Evidence against an important role in nociception. Brain Res 326:347-356.

Gilgun-Sherki Y, Panet H, Melamed E, Offen D (2003) Riluzole suppresses experimental autoimmune encephalomyelitis: implications for the treatment of multiple sclerosis. Brain Res 989:196-204.

Giulian D, Corpuz M, Chapman S, Mansouri M, Robertson C (1993a) Reactive mononuclear phagocytes release neurotoxins after ischemic and traumatic injury to the central nervous system. J Neurosci Res 36:681-693.

Giulian D, Vaca K, Corpuz M (1993b) Brain glia release factors with opposing actions upon neuronal survival. J Neurosci 13:29-37.

Glass CK, Saijo K, Winner B, Marchetto MC, Gage FH (2010) Mechanisms underlying inflammation in neurodegeneration. Cell 140:918-934.

Gomez-Nicola D, Valle-Argos B, Suardiaz M, Taylor JS, Nieto-Sampedro M (2008) Role of IL-15 in spinal cord and sciatic nerve after chronic constriction injury: regulation of macrophage and T-cell infiltration. J Neurochem 107:1741-1752.

Good ML, Hussey DL (2003) Minocycline: stain devil? Br J Dermatol 149:237-239.

Gordon PH, Moore DH, Miller RG, Florence JM, Verheijde JL, Doorish C, Hilton JF, Spitalny GM, MacArthur RB, Mitsumoto H, Neville HE, Boylan K, Mozaffar T, Belsh JM, Ravits J, Bedlack RS, Graves MC, McCluskey LF, Barohn RJ, Tandan R (2007) Efficacy of minocycline in patients with amyotrophic lateral sclerosis: a phase III randomised trial. Lancet Neurol 6:1045-1053.

Grace RR, Mattox KL (1977) Anterior spinal artery syndrome following abdominal aortic aneurysmectomy. Case report and review of the literautre. Arch Surg 112:813-815.

Graeber MB, Lopez-Redondo F, Ikoma E, Ishikawa M, Imai Y, Nakajima K, Kreutzberg GW, Kohsaka S (1998) The microglia/macrophage response in the neonatal rat facial nucleus following axotomy. Brain Res 813:241-253.

Graeber MB, Streit WJ, Kreutzberg GW (1988a) Axotomy of the rat facial nerve leads to increased CR3 complement receptor expression by activated microglial cells. J Neurosci Res 21:18-24.

Graeber MB, Streit WJ, Kreutzberg GW (1988b) The microglial cytoskeleton: vimentin is localized within activated cells in situ. J Neurocytol 17:573-580.

GrandPre T, Nakamura F, Vartanian T, Strittmatter SM (2000) Identification of the Nogo inhibitor of axon regeneration as a Reticulon protein. Nature 403:439-444.

Graumlich JF, McLaughlin RG, Birkhahn D, Shah N, Burk A, Jobe PC, Dailey JW (2000) Subcutaneous microdialysis in rats correlates with carbamazepine concentrations in plasma and brain. Epilepsy Res 40:25-32.

Gray H, Williams PL, Warwick R (1980) Gray's anatomy. 36th ed.

Gris D, Marsh DR, Oatway MA, Chen Y, Hamilton EF, Dekaban GA, Weaver LC (2004) Transient blockade of the CD11d/CD18 integrin reduces secondary damage after spinal cord injury, improving sensory, autonomic, and motor function. J Neurosci 24:4043-4051.

Gu HY, Chai H, Zhang JY, Yao ZB, Zhou LH, Wong WM, Bruce IC, Wu WT (2005) Survival, regeneration and functional recovery of motoneurons after delayed reimplantation of avulsed spinal root in adult rat. Exp Neurol 192:89-99.

Guasti L, Richardson D, Jhaveri M, Eldeeb K, Barrett D, Elphick MR, Alexander SP, Kendall D, Michael GJ, Chapman V (2009) Minocycline treatment inhibits microglial activation and alters spinal levels of endocannabinoids in a rat model of neuropathic pain. Mol Pain 5:35.

Guenot M, Bullier J, Rospars JP, Lansky P, Mertens P, Sindou M (2003) Single-unit analysis of the spinal dorsal horn in patients with neuropathic pain. J Clin Neurophysiol 20:143-150.

Guenot M, Bullier J, Sindou M (2002) Clinical and electrophysiological expression of deafferentation pain alleviated by dorsal root entry zone lesions in rats. J Neurosurg 97:1402-1409.

Guillemin GJ, Brew BJ (2004) Microglia, macrophages, perivascular macrophages, and pericytes: a review of function and identification. J Leukoc Biol 75:388-397.

Gupta R, Channual JC (2006) Spatiotemporal pattern of macrophage recruitment after chronic nerve compression injury. J Neurotrauma 23:216-226.

Gwak YS, Hulsebosch CE (2009) Remote astrocytic and microglial activation modulates neuronal hyperexcitability and below-level neuropathic pain after spinal injury in rat. Neuroscience 161:895-903.

Gwak YS, Nam TS, Paik KS, Hulsebosch CE, Leem JW (2003) Attenuation of mechanical hyperalgesia following spinal cord injury by administration of antibodies to nerve growth factor in the rat. Neurosci Lett 336:117-120.

Gwak YS, Unabia GC, Hulsebosch CE (2009) Activation of p-38alpha MAPK contributes to neuronal hyperexcitability in caudal regions remote from spinal cord injury. Exp Neurol 220:154-161.

Gybels J, Sweet WH (1989) Neurosurgical treatment of persistent pain
physiological and pathological mechanisms of human pain. Basel: Karger.

Habibi-Asl B, Hassanzadeh K, Charkhpour M (2009) Central administration of minocycline and riluzole prevents morphine-induced tolerance in rats. Anesth Analg 109:936-942.

Hacker H, Furmann C, Wagner H, Hacker G (2002) Caspase-9/-3 activation and apoptosis are induced in mouse macrophages upon ingestion and digestion of Escherichia coli bacteria. J Immunol 169:3172-3179.

Hagg T, Oudega M (2006) Degenerative and spontaneous regenerative processes after spinal cord injury. J Neurotrauma 23:264-280.

Hains BC, Klein JP, Saab CY, Craner MJ, Black JA, Waxman SG (2003a) Upregulation of sodium channel Nav1.3 and functional involvement in neuronal hyperexcitability associated with central neuropathic pain after spinal cord injury. J Neurosci 23:8881-8892.

Hains BC, Saab CY, Klein JP, Craner MJ, Waxman SG (2004) Altered sodium channel expression in second-order spinal sensory neurons contributes to pain after peripheral nerve injury. J Neurosci 24:4832-4839.

Hains BC, Waxman SG (2006) Activated microglia contribute to the maintenance of chronic pain after spinal cord injury. J Neurosci 26:4308-4317.

Hains BC, Willis WD, Hulsebosch CE (2003b) Temporal plasticity of dorsal horn somatosensory neurons after acute and chronic spinal cord hemisection in rat. Brain Res 970:238-241.

Hammer NA, Lilleso J, Pedersen JL, Kehlet H (1999) Effect of riluzole on acute pain and hyperalgesia in humans. Br J Anaesth 82:718-722.

Hammond DL, Ackerman L, Holdsworth R, Elzey B (2004) Effects of spinal nerve ligation on immunohistochemically identified neurons in the L4 and L5 dorsal root ganglia of the rat. J Comp Neurol 475:575-589.

Hamon M, Gozlan H, Bourgoin S, Benoliel JJ, Mauborgne A, Taquet H, Cesselin F, Mico JA (1987) Opioid receptors and neuropeptides in the CNS in rats treated chronically with amoxapine or amitriptyline. Neuropharmacology 26:531-539.

Han HC, Lee DH, Chung JM (2000) Characteristics of ectopic discharges in a rat neuropathic pain model. Pain 84:253-261.

Hao JX, Xu XJ, Aldskogius H, Seiger A, Wiesenfeld-Hallin Z (1991a) Allodynia-like effects in rat after ischaemic spinal cord injury photochemically induced by laser irradiation. Pain 45:175-185.

Hao JX, Xu XJ, Aldskogius H, Seiger A, Wiesenfeld-Hallin Z (1991b) The excitatory amino acid receptor antagonist MK-801 prevents the hypersensitivity induced by spinal cord ischemia in the rat. Exp Neurol 113:182-191.

Hao JX, Xu XJ, Yu YX, Seiger A, Wiesenfeld-Hallin Z (1991c) Hypersensitivity of dorsal horn wide dynamic range neurons to cutaneous mechanical stimuli after transient spinal cord ischemia in the rat. Neurosci Lett 128:105-108.

Hargreaves K, Dubner R, Brown F, Flores C, Joris J (1988) A new and sensitive method for measuring thermal nociception in cutaneous hyperalgesia. Pain 32:77-88.

Hashizume H, DeLeo JA, Colburn RW, Weinstein JN (2000a) Spinal glial activation and cytokine expression after lumbar root injury in the rat. Spine (Phila Pa 1976) 25:1206-1217.

Hashizume H, Rutkowski MD, Weinstein JN, DeLeo JA (2000b) Central administration of methotrexate reduces mechanical allodynia in an animal model of radiculopathy/sciatica. Pain 87:159-169.

Hatashita S, Sekiguchi M, Kobayashi H, Konno S, Kikuchi S (2008) Contralateral neuropathic pain and neuropathology in dorsal root ganglion and spinal cord following hemilateral nerve injury in rats. Spine (Phila Pa 1976) 33:1344-1351.

Hausmann ON (2003) Post-traumatic inflammation following spinal cord injury. Spinal Cord 41:369-378.

Havton LA, Carlstedt T (2009) Repair and rehabilitation of plexus and root avulsions in animal models and patients. Curr Opin Neurol.

Hawryluk GW, Rowland J, Kwon BK, Fehlings MG (2008) Protection and repair of the injured spinal cord: a review of completed, ongoing, and planned clinical trials for acute spinal cord injury. Neurosurg Focus 25:E14.

He JW, Hirata K, Kuraoka A, Kawabuchi M (2000) An improved method for avulsion of lumbar nerve roots as an experimental model of nitric oxide-mediated neuronal degeneration. Brain Res Brain Res Protoc 5:223-230.

He JW, Hirata K, Wang S, Kawabuchi M (2003) Expression of nitric oxide synthase and 27-kD heat shock protein in motor neurons of ventral root-avulsed rats. Arch Histol Cytol 66:83-93.

He Y, Appel S, Le W (2001) Minocycline inhibits microglial activation and protects nigral cells after 6-hydroxydopamine injection into mouse striatum. Brain Res 909:187-193.

Herr K (2004) Neuropathic pain: a guide to comprehensive assessment. Pain Manag Nurs 5:9-18.

Hesselgard K, Reinstrup P, Stromblad LG, Unden J, Romner B (2007) Selective dorsal rhizotomy and postoperative pain management. A worldwide survey. Pediatr Neurosurg 43:107-112.

Hoang TX, Akhavan M, Wu J, Havton LA (2008) Minocycline protects motor but not autonomic neurons after cauda equina injury. Exp Brain Res 189:71-77.

Hoang TX, Nieto JH, Tillakaratne NJ, Havton LA (2003) Autonomic and motor neuron death is progressive and parallel in a lumbosacral ventral root avulsion model of cauda equina injury. J Comp Neurol 467:477-486.

Hodge CJ, Jr., Apkarian AV (1990) The spinothalamic tract. Crit Rev Neurobiol 5:363-397.

Hodgkinson I, Berard C, Jindrich ML, Sindou M, Mertens P, Berard J (1997) Selective dorsal rhizotomy in children with cerebral palsy. Results in 18 cases at one year postoperatively. Stereotact Funct Neurosurg 69:259-267.

Hoeksma AF, Wolf H, Oei SL (2000) Obstetrical brachial plexus injuries: incidence, natural course and shoulder contracture. Clin Rehabil 14:523-526.

Hoffmann CF, Choufoer H, Marani E, Thomeer RT (1993) Ultrastructural study on avulsion effects of the cat cervical moto-axonal pathways in the spinal cord. Clin Neurol Neurosurg 95 Suppl:S39-S47.

Hokfelt T, Brumovsky P, Shi T, Pedrazzini T, Villar M (2007) NPY and pain as seen from the histochemical side. Peptides 28:365-372.

Holmberg P, Kellerth JO (1996) Physiological adjustments in a reflex pathway following partial loss of target neurons. Brain Res 731:155-160.

Holmberg P, Kellerth JO (2000) Do synaptic rearrangements underlie compensatory reflex enhancement in spinal motoneurons after partial cell loss? Synapse 38:384-391.

Holmes FE, Mahoney SA, Wynick D (2005) Use of genetically engineered transgenic mice to investigate the role of galanin in the peripheral nervous system after injury. Neuropeptides 39:191-199.

Holmes GM, Hebert SL, Rogers RC, Hermann GE (2004) Immunocytochemical localization of TNF type 1 and type 2 receptors in the rat spinal cord. Brain Res 1025:210-219.

Holtzer CA, Marani E, de PW, Thomeer RT (1998) The process of decompaction and myelin removal after C7 ventral root avulsion in the cat. Arch Physiol Biochem 106:116-127.

Horvath RJ, DeLeo JA (2009) Morphine enhances microglial migration through modulation of P2X4 receptor signaling. J Neurosci 29:998-1005.

Hosobuchi Y (1980) The majority of unmyelinated afferent axons in human ventral roots probably conduct pain. Pain 8:167-180.

Htut M, Misra P, Anand P, Birch R, Carlstedt T (2006) Pain phenomena and sensory recovery following brachial plexus avulsion injury and surgical repairs. J Hand Surg Br 31:596-605.

Hu J, Mata M, Hao S, Zhang G, Fink DJ (2004) Central sprouting of uninjured small fiber afferents in the adult rat spinal cord following spinal nerve ligation. Eur J Neurosci 20:1705-1712.

Hu P, Bembrick AL, Keay KA, McLachlan EM (2007) Immune cell involvement in dorsal root ganglia and spinal cord after chronic constriction or transection of the rat sciatic nerve. Brain Behav Immun 21:599-616.

Hu P, McLachlan EM (2003) Selective reactions of cutaneous and muscle afferent neurons to peripheral nerve transection in rats. J Neurosci 23:10559-10567.

Huang WL, George KJ, Ibba V, Liu MC, Averill S, Quartu M, Hamlyn PJ, Priestley JV (2007) The characteristics of neuronal injury in a static compression model of spinal cord injury in adult rats. Eur J Neurosci 25:362-372.

Hudson LJ, Bevan S, Wotherspoon G, Gentry C, Fox A, Winter J (2001) VR1 protein expression increases in undamaged DRG neurons after partial nerve injury. Eur J Neurosci 13:2105-2114.

Huittinen VM (1972) Lumbosacral nerve injury in fracture of the pelvis. A postmortem radiographic and patho-anatomical study. Acta Chir Scand Suppl 429:3-43.

Hulsebosch CE (2008) Gliopathy ensures persistent inflammation and chronic pain after spinal cord injury. Exp Neurol.

Hulsebosch CE, Hains BC, Crown ED, Carlton SM (2009) Mechanisms of chronic central neuropathic pain after spinal cord injury. Brain Res Rev 60:202-213.

Hulsebosch CE, Xu G, Perez-Polo J, Westlund KN, Taylor C, McAdoo DJ (2000) Rodent model of chronic central pain after spinal cord contusion injury and effects of gabapentin. J Neurotrauma 17:1205-1217.

Hunt JL, Winkelstein BA, Rutkowski MD, Weinstein JN, DeLeo JA (2001) Repeated injury to the lumbar nerve roots produces enhanced mechanical allodynia and persistent spinal neuroinflammation. Spine (Phila Pa 1976) 26:2073-2079.

Hur YK, Choi IS, Cho JH, Park EJ, Choi JK, Choi BJ, Jang IS (2008) Effects of carbamazepine and amitriptyline on tetrodotoxinresistant Na+ channels in immature rat trigeminal ganglion neurons. Arch Pharm Res 31:178-182.

Hutchinson MR, Bland ST, Johnson KW, Rice KC, Maier SF, Watkins LR (2007) Opioid-induced glial activation: mechanisms of activation and implications for opioid analgesia, dependence, and reward. ScientificWorldJournal 7:98-111.

Hutchinson MR, Coats BD, Lewis SS, Zhang Y, Sprunger DB, Rezvani N, Baker EM, Jekich BM, Wieseler JL, Somogyi AA, Martin D, Poole S, Judd CM, Maier SF, Watkins LR (2008) Proinflammatory cytokines oppose opioid-induced acute and chronic analgesia. Brain Behav Immun 22:1178-1189.

Ibrahim AG, Kirkwood PA, Raisman G, Li Y (2009a) Restoration of hand function in a rat model of repair of brachial plexus injury. Brain 132:1268-1276.

Ibrahim AG, Raisman G, Li Y (2009b) Permanent loss of fore-paw grasping requires complete deprivation of afferent input from a minimum of four dorsal roots of the rat brachial plexus. Exp Neurol 215:142-145.

Ibuki T, Hama AT, Wang XT, Pappas GD, Sagen J (1997) Loss of GABA-immunoreactivity in the spinal dorsal horn of rats with peripheral nerve injury and promotion of recovery by adrenal medullary grafts. Neuroscience 76:845-858.

Imamura Y, Kawamoto H, Nakanishi O (1997) Characterization of heat-hyperalgesia in an experimental trigeminal neuropathy in rats. Exp Brain Res 116:97-103.

Imperato-Kalmar EL, McKinney RA, Schnell L, Rubin BP, Schwab ME (1997) Local changes in vascular architecture following partial spinal cord lesion in the rat. Exp Neurol 145:322-328.

Inman DM, Steward O (2003a) Ascending sensory, but not other long-tract axons, regenerate into the connective tissue matrix that forms at the site of a spinal cord injury in mice. J Comp Neurol 462:431-449.

Inman DM, Steward O (2003b) Physical size does not determine the unique histopathological response seen in the injured mouse spinal cord. J Neurotrauma 20:33-42.

Inoue K, Koizumi S, Kataoka A, Tozaki-Saitoh H, Tsuda M (2009) P2Y(6)-Evoked Microglial Phagocytosis. Int Rev Neurobiol 85:159-163.

Inoue K, Tsuda M (2009) Microglia and neuropathic pain. Glia 57:1469-1479.

Irifune M, Kikuchi N, Saida T, Takarada T, Shimizu Y, Endo C, Morita K, Dohi T, Sato T, Kawahara M (2007) Riluzole, a glutamate release inhibitor, induces loss of righting reflex, antinociception, and immobility in response to noxious stimulation in mice. Anesth Analg 104:1415-21, table.

Ito N, Obata H, Saito S (2009) Spinal microglial expression and mechanical hypersensitivity in a postoperative pain model: comparison with a neuropathic pain model. Anesthesiology 111:640-648.

Jabakhanji R, Foss JM, Berra HH, Centeno MV, Apkarian AV, Chialvo DR (2006) Inflammatory and neuropathic pain animals exhibit distinct responses to innocuous thermal and motoric challenges. Mol Pain 2:1.

Jackowski A (1995) Neural injury repair: hope for the future as barriers to effective CNS regeneration become clearer. Br J Neurosurg 9:303-317.

Jensen TS (2002) Anticonvulsants in neuropathic pain: rationale and clinical evidence. Eur J Pain 6 Suppl A:61-68.

Ji RR, Gereau RW, Malcangio M, Strichartz GR (2009) MAP kinase and pain. Brain Res Rev 60:135-148.

Ji RR, Samad TA, Jin SX, Schmoll R, Woolf CJ (2002) p38 MAPK activation by NGF in primary sensory neurons after inflammation increases TRPV1 levels and maintains heat hyperalgesia. Neuron 36:57-68.

Johnson EO, Zoubos AB, Soucacos PN (2005) Regeneration and repair of peripheral nerves. Injury 36 Suppl 4:S24-S29.

Jones TB, McDaniel EE, Popovich PG (2005) Inflammatory-mediated injury and repair in the traumatically injured spinal cord. Curr Pharm Des 11:1223-1236.

Kage K, Niforatos W, Zhu CZ, Lynch KJ, Honore P, Jarvis MF (2002) Alteration of dorsal root ganglion P2X3 receptor expression and function following spinal nerve ligation in the rat. Exp Brain Res 147:511-519.

Karlsson U, Sjodin J, Angeby MK, Johansson S, Wikstrom L, Nasstrom J (2002) Glutamate-induced currents reveal three functionally distinct NMDA receptor populations in rat dorsal horn - effects of peripheral nerve lesion and inflammation. Neuroscience 112:861-868.

Kato N, Htut M, Taggart M, Carlstedt T, Birch R (2006) The effects of operative delay on the relief of neuropathic pain after injury to the brachial plexus: a review of 148 cases. J Bone Joint Surg Br 88:756-759.

Kauppila T (1998) Correlation between autotomy-behavior and current theories of neuropathic pain. Neurosci Biobehav Rev 23:111-129.

Kauppila T, Pertovaara A (1991) Effects of different sensory and behavioral manipulations on autotomy caused by a sciatic lesion in rats. Exp Neurol 111:128-130.

Kawasaki Y, Xu ZZ, Wang X, Park JY, Zhuang ZY, Tan PH, Gao YJ, Roy K, Corfas G, Lo EH, Ji RR (2008) Distinct roles of matrix metalloproteases in the early- and late-phase development of neuropathic pain. Nat Med 14:331-336.

Keilhoff G, Fansa H, Wolf G (2002) Neuronal nitric oxide synthase is the dominant nitric oxide supplier for the survival of dorsal root ganglia after peripheral nerve axotomy. J Chem Neuroanat 24:181-187.

Keilhoff G, Fansa H, Wolf G (2003) Nitric oxide synthase, an essential factor in peripheral nerve regeneration. Cell Mol Biol (Noisy -le-grand) 49:885-897.

Keirstead HS, Blakemore WF (1999) The role of oligodendrocytes and oligodendrocyte progenitors in CNS remyelination. Adv Exp Med Biol 468:183-197.

Kerr BJ, Souslova V, McMahon SB, Wood JN (2001) A role for the TTX-resistant sodium channel Nav 1.8 in NGF-induced hyperalgesia, but not neuropathic pain. Neuroreport 12:3077-3080.

Kevetter GA, Haber LH, Yezierski RP, Chung JM, Martin RF, Willis WD (1982) Cells of origin of the spinoreticular tract in the monkey. J Comp Neurol 207:61-74.

Kigerl KA, Gensel JC, Ankeny DP, Alexander JK, Donnelly DJ, Popovich PG (2009) Identification of two distinct macrophage subsets with divergent effects causing either neurotoxicity or regeneration in the injured mouse spinal cord. J Neurosci 29:13435-13444.

Kim GM, Xu J, Xu J, Song SK, Yan P, Ku G, Xu XM, Hsu CY (2001) Tumor necrosis factor receptor deletion reduces nuclear factor-kappaB activation, cellular inhibitor of apoptosis protein 2 expression, and functional recovery after traumatic spinal cord injury. J Neurosci 21:6617-6625.

Kim HS, Suh YH (2009) Minocycline and neurodegenerative diseases. Behav Brain Res 196:168-179.

Kim SH, Chung JM (1992) An experimental model for peripheral neuropathy produced by segmental spinal nerve ligation in the rat. Pain 50:355-363.

Kingwell SP, Curt A, Dvorak MF (2008) Factors affecting neurological outcome in traumatic conus medullaris and cauda equina injuries. Neurosurg Focus 25:E7.

Kirschnek S, Ying S, Fischer SF, Hacker H, Villunger A, Hochrein H, Hacker G (2005) Phagocytosis-induced apoptosis in macrophages is mediated by up-regulation and activation of the Bcl-2 homology domain 3-only protein Bim. J Immunol 174:671-679.

Koh JY, Kim DK, Hwang JY, Kim YH, Seo JH (1999) Antioxidative and proapoptotic effects of riluzole on cultured cortical neurons. J Neurochem 72:716-723.

Kohno T, Moore KA, Baba H, Woolf CJ (2003) Peripheral nerve injury alters excitatory synaptic transmission in lamina II of the rat dorsal horn. J Physiol 548:131-138.

Koliatsos VE, Applegate MD, Kitt CA, Walker LC, DeLong MR, Price DL (1989) Aberrant phosphorylation of neurofilaments accompanies transmitter-related changes in rat septal neurons following transection of the fimbria-fornix. Brain Res 482:205-218.

Koliatsos VE, Price WL, Pardo CA, Price DL (1994) Ventral root avulsion: an experimental model of death of adult motor neurons. J Comp Neurol 342:35-44.

Koltzenburg M, Torebjork HE, Wahren LK (1994) Nociceptor modulated central sensitization causes mechanical hyperalgesia in acute chemogenic and chronic neuropathic pain. Brain 117 (Pt 3):579-591.

Koltzenburg M, Wall PD, McMahon SB (1999) Does the right side know what the left is doing? Trends Neurosci 22:122-127.

Kondziolka D, Lunsford LD, Bissonette DJ (1994) Long-term results after glycerol rhizotomy for multiple sclerosis-related trigeminal neuralgia. Can J Neurol Sci 21:137-140.

Kosta V, Kojundzic SL, Sapunar LC, Sapunar D (2009) The extent of laminectomy affects pain-related behavior in a rat model of neuropathic pain. Eur J Pain 13:243-248.

Kraft AD, McPherson CA, Harry GJ (2009) Heterogeneity of microglia and TNF signaling as determinants for neuronal death or survival. Neurotoxicology 30:785-793.

Kriz N, Rokyta R (2000) Effect of unilateral deafferentation on extracellular potassium concentration levels in rat thalamic nuclei. Neuroscience 96:101-108.

Kumazawa T (1990) Functions of the nociceptive primary neurons. Jpn J Physiol 40:1-14.

Kurvers HA, Tangelder GJ, De Mey JG, Slaaf DW, Beuk RJ, van den Wildenberg FA, Kitslaar PJ, Reneman RS, Jacobs MJ (1997) Skin blood flow abnormalities in a rat model of neuropathic pain: result of decreased sympathetic vasoconstrictor outflow? J Auton Nerv Syst 63:19-29.

Lacomblez L, Bensimon G, Leigh PN, Guillet P, Meininger V (1996) Dose-ranging study of riluzole in amyotrophic lateral sclerosis. Amyotrophic Lateral Sclerosis/Riluzole Study Group II. Lancet 347:1425-1431.

Lai HY, Lee CY, Lee ST (2009) High cervical spinal cord stimulation after failed dorsal root entry zone surgery for brachial plexus avulsion pain. Surg Neurol 72:286-289.

Lambertsen KL, Clausen BH, Babcock AA, Gregersen R, Fenger C, Nielsen HH, Haugaard LS, Wirenfeldt M, Nielsen M, Dagnaes-Hansen F, Bluethmann H, Faergeman NJ, Meldgaard M, Deierborg T, Finsen B (2009) Microglia protect neurons against ischemia by synthesis of tumor necrosis factor. J Neurosci 29:1319-1330.

LaMotte C (1977) Distribution of the tract of Lissauer and the dorsal root fibers in the primate spinal cord. J Comp Neurol 172:529-561.

Lampert A, Hains BC, Waxman SG (2006) Upregulation of persistent and ramp sodium current in dorsal horn neurons after spinal cord injury. Exp Brain Res 174:660-666.

Lang EM, Borges J, Carlstedt T (2004) Surgical treatment of lumbosacral plexus injuries. J Neurosurg Spine 1:64-71.

Langevitz P, Livneh A, Bank I, Pras M (2000) Benefits and risks of minocycline in rheumatoid arthritis. Drug Saf 22:405-414.

Latremoliere A, Woolf CJ (2009) Central sensitization: a generator of pain hypersensitivity by central neural plasticity. J Pain 10:895-926.

Lawson SN, Crepps BA, Perl ER (1997) Relationship of substance P to afferent characteristics of dorsal root ganglion neurones in guinea-pig. J Physiol 505 (Pt 1):177-191.

Lawson SN, Harper AA, Harper EI, Garson JA, Anderton BH (1984) A monoclonal antibody against neurofilament protein specifically labels a subpopulation of rat sensory neurones. J Comp Neurol 228:263-272.

Le Liboux A, Cachia JP, Kirkesseli S, Gautier JY, Guimart C, Montay G, Peeters PA, Groen E, Jonkman JH, Wemer J (1999) A comparison of the pharmacokinetics and tolerability of riluzole after repeat dose administration in healthy elderly and young volunteers. J Clin Pharmacol 39:480-486.

Ledeboer A, Sloane EM, Milligan ED, Frank MG, Mahony JH, Maier SF, Watkins LR (2005) Minocycline attenuates mechanical allodynia and proinflammatory cytokine expression in rat models of pain facilitation. Pain 115:71-83.

Lee BH, Won R, Baik EJ, Lee SH, Moon CH (2000) An animal model of neuropathic pain employing injury to the sciatic nerve branches. Neuroreport 11:657-661.

Lee JA (2009) Autophagy in neurodegeneration: two sides of the same coin. BMB Rep 42:324-330.

Lee SM, Yune TY, Kim SJ, Park DW, Lee YK, Kim YC, Oh YJ, Markelonis GJ, Oh TH (2003) Minocycline reduces cell death and improves functional recovery after traumatic spinal cord injury in the rat. J Neurotrauma 20:1017-1027.

Leffler A, Reiprich A, Mohapatra DP, Nau C (2007) Use-dependent block by lidocaine but not amitriptyline is more pronounced in tetrodotoxin (TTX)-Resistant Nav1.8 than in TTX-sensitive Na+ channels. J Pharmacol Exp Ther 320:354-364.

Lekan HA, Carlton SM, Coggeshall RE (1996) Sprouting of A beta fibers into lamina II of the rat dorsal horn in peripheral neuropathy. Neurosci Lett 208:147-150.

Levine JD, Gooding J, Donatoni P, Borden L, Goetzl EJ (1985) The role of the polymorphonuclear leukocyte in hyperalgesia. J Neurosci 5:3025-3029.

Levine JM, Nishiyama A (1996) The NG2 chondroitin sulfate proteoglycan: a multifunctional proteoglycan associated with immature cells. Perspect Dev Neurobiol 3:245-259.

Li L, Xian CJ, Zhong JH, Zhou XF (2003) Lumbar 5 ventral root transection-induced upregulation of nerve growth factor in sensory neurons and their target tissues: a mechanism in neuropathic pain. Mol Cell Neurosci 23:232-250.

Li L, Xian CJ, Zhong JH, Zhou XF (2006) Upregulation of brain-derived neurotrophic factor in the sensory pathway by selective motor nerve injury in adult rats. Neurotox Res 9:269-283.

Li Y, Carlstedt T, Berthold CH, Raisman G (2004) Interaction of transplanted olfactory-ensheathing cells and host astrocytic processes provides a bridge for axons to regenerate across the dorsal root entry zone. Exp Neurol 188:300-308.

Li Y, Dorsi MJ, Meyer RA, Belzberg AJ (2000) Mechanical hyperalgesia after an L5 spinal nerve lesion in the rat is not dependent on input from injured nerve fibers. Pain 85:493-502.

Li Y, Yamamoto M, Raisman G, Choi D, Carlstedt T (2007) An experimental model of ventral root repair showing the beneficial effect of transplanting olfactory ensheathing cells. Neurosurgery 60:734-740.

Light AR, Perl ER (1977) Differential termination of large-diameter and small-diameter primary afferent fibers in the spinal dorsal gray matter as indicated by labeling with horseradish peroxidase. Neurosci Lett 6:59-63.

Light AR, Perl ER (1979) Spinal termination of functionally identified primary afferent neurons with slowly conducting myelinated fibers. J Comp Neurol 186:133-150.

Light AR, Perl ER (2003) Unmyelinated afferent fibers are not only for pain anymore. J Comp Neurol 461:137-139.

Light AR, Trevino DL, Perl ER (1979) Morphological features of functionally defined neurons in the marginal zone and substantia gelatinosa of the spinal dorsal horn. J Comp Neurol 186:151-171.

Light RW, Wang NS, Sassoon CS, Gruer SE, Vargas FS (1994) Comparison of the effectiveness of tetracycline and minocycline as pleural sclerosing agents in rabbits. Chest 106:577-582.

Lin CS, Tsaur ML, Chen CC, Wang TY, Lin CF, Lai YL, Hsu TC, Pan YY, Yang CH, Cheng JK (2007) Chronic intrathecal infusion of minocycline prevents the development of spinal-nerve ligation-induced pain in rats. Reg Anesth Pain Med 32:209-216.

Lindfors PH, Voikar V, Rossi J, Airaksinen MS (2006) Deficient nonpeptidergic epidermis innervation and reduced inflammatory pain in glial cell line-derived neurotrophic factor family receptor alpha2 knock-out mice. J Neurosci 26:1953-1960.

Ling EA (1979a) Electron microscopic study of macrophages appearing in a stab wound of the brain of rats following intravenous injection of carbon particles. Arch Histol Jpn 42:41-50.

Ling EA (1979b) Evidence for a haematogenous origin of some of the macrophages appearing in the spinal cord of the rat after dorsal rhizotomy. J Anat 128:143-154.

Ling LJ, Honda T, Shimada Y, Ozaki N, Shiraishi Y, Sugiura Y (2003) Central projection of unmyelinated (C) primary afferent fibers from gastrocnemius muscle in the guinea pig. J Comp Neurol 461:140-150.

Lips J, de HP, Bodewits P, Vanicky I, Dzoljic M, Jacobs MJ, Kalkman CJ (2000) Neuroprotective effects of riluzole and ketamine during transient spinal cord ischemia in the rabbit. Anesthesiology 93:1303-1311.

LIU CN, CHAMBERS WW (1958) Intraspinal sprouting of dorsal root axons; development of new collaterals and preterminals following partial denervation of the spinal cord in the cat. AMA Arch Neurol Psychiatry 79:46-61.

Liu HX, Hokfelt T (2002) The participation of galanin in pain processing at the spinal level. Trends Pharmacol Sci 23:468-474.

Liu L, Persson JK, Svensson M, Aldskogius H (1998) Glial cell responses, complement, and clusterin in the central nervous system following dorsal root transection. Glia 23:221-238.

Liu L, Rudin M, Kozlova EN (2000a) Glial cell proliferation in the spinal cord after dorsal rhizotomy or sciatic nerve transection in the adult rat. Exp Brain Res 131:64-73.

Liu T, van RN, Tracey DJ (2000b) Depletion of macrophages reduces axonal degeneration and hyperalgesia following nerve injury. Pain 86:25-32.

Liu X, Eschenfelder S, Blenk KH, Janig W, Habler H (2000c) Spontaneous activity of axotomized afferent neurons after L5 spinal nerve injury in rats. Pain 84:309-318.

Liu XZ, Xu XM, Hu R, Du C, Zhang SX, McDonald JW, Dong HX, Wu YJ, Fan GS, Jacquin MF, Hsu CY, Choi DW (1997) Neuronal and glial apoptosis after traumatic spinal cord injury. J Neurosci 17:5395-5406.

Loeser JD (1972) Dorsal rhizotomy for the relief of chronic pain. J Neurosurg 36:745-750.

Loeser JD, Ward AA, Jr. (1967) Some effects of deafferentation on neurons of the cat spinal cord. Arch Neurol 17:629-636.

Loeser JD, Ward AA, Jr., White LE, Jr. (1968) Chronic deafferentation of human spinal cord neurons. J Neurosurg 29:48-50.

Loeser JD, Bonica JJ (2001) Bonica's management of pain. Philadelphia, PA: Lippincott Williams & Wilkins.

Lombard MC, Besson JM (1989) Attempts to gauge the relative importance of pre- and postsynaptic effects of morphine on the transmission of noxious messages in the dorsal horn of the rat spinal cord. Pain 37:335-345.

Lombard MC, Nashold BS, Jr., Albe-Fessard D, Salman N, Sakr C (1979) Deafferentation hypersensitivity in the rat after dorsal rhizotomy: a possible animal model of chronic pain. Pain 6:163-174.

Losanoff JE, Holder-Murray JM, Ahmed EB, Cochrane AB, Testa G, Millis JM (2007) Minocycline toxicity requiring liver transplant. Dig Dis Sci 52:3242-3244.

Lowrie MB, O'Brien RA, Vrbova G (1985) The effect of altered peripheral field on motoneurone function in developing rat soleus muscles. J Physiol 368:513-524.

Loy DN, Crawford CH, Darnall JB, Burke DA, Onifer SM, Whittemore SR (2002) Temporal progression of angiogenesis and basal lamina deposition after contusive spinal cord injury in the adult rat. J Comp Neurol 445:308-324.

Lu VB, Ballanyi K, Colmers WF, Smith PA (2007) Neuron type-specific effects of brain-derived neurotrophic factor in rat superficial dorsal horn and their relevance to 'central sensitization'. J Physiol 584:543-563.

Lu Y, Zheng J, Xiong L, Zimmermann M, Yang J (2008) Spinal cord injury-induced attenuation of GABAergic inhibition in spinal dorsal horn circuits is associated with down-regulation of the chloride transporter KCC2 in rat. J Physiol 586:5701-5715.

Luo H, Cheng J, Han JS, Wan Y (2004) Change of vanilloid receptor 1 expression in dorsal root ganglion and spinal dorsal horn during inflammatory nociception induced by complete Freund's adjuvant in rats. Neuroreport 15:655-658.

Luo ZD, Calcutt NA, Higuera ES, Valder CR, Song YH, Svensson CI, Myers RR (2002) Injury type-specific calcium channel alpha 2 delta-1 subunit up-regulation in rat neuropathic pain models correlates with antiallodynic effects of gabapentin. J Pharmacol Exp Ther 303:1199-1205.

Lynch JJ, III, Wade CL, Zhong CM, Mikusa JP, Honore P (2004) Attenuation of mechanical allodynia by clinically utilized drugs in a rat chemotherapy-induced neuropathic pain model. Pain 110:56-63.

Ma QP, Tian L (2001) A-fibres sprouting from lamina I into lamina II of spinal dorsal horn after peripheral nerve injury in rats. Brain Res 904:137-140.

Ma S, Cornford ME, Vahabnezhad I, Wei S, Li X (2000) Responses of nitric oxide synthase expression in the gracile nucleus to sciatic nerve injury in young and aged rats. Brain Res 855:124-131.

Ma W, Chabot JG, Vercauteren F, Quirion R (2008) Injured nerve-derived COX2/PGE2 contributes to the maintenance of neuropathic pain in aged rats. Neurobiol Aging.

Mabon PJ, Weaver LC, Dekaban GA (2000) Inhibition of monocyte/macrophage migration to a spinal cord injury site by an antibody to the integrin alphaD: a potential new anti-inflammatory treatment. Exp Neurol 166:52-64.

MacIver MB, Amagasu SM, Mikulec AA, Monroe FA (1996) Riluzole anesthesia: use-dependent block of presynaptic glutamate fibers. Anesthesiology 85:626-634.

Mahoney ET, Benton RL, Maddie MA, Whittemore SR, Hagg T (2009) ADAM8 is selectively up-regulated in endothelial cells and is associated with angiogenesis after spinal cord injury in adult mice. J Comp Neurol 512:243-255.

Maianski NA, Maianski AN, Kuijpers TW, Roos D (2004) Apoptosis of neutrophils. Acta Haematol 111:56-66.

Maier IC, Baumann K, Thallmair M, Weinmann O, Scholl J, Schwab ME (2008) Constraint-induced movement therapy in the adult rat after unilateral corticospinal tract injury. J Neurosci 28:9386-9403.

Maikos JT, Shreiber DI (2007) Immediate damage to the blood-spinal cord barrier due to mechanical trauma. J Neurotrauma 24:492-507.

Maillard JC, Zouaoui A, Bencherif B, Bouayed N, Chedid G, Marsault C (1992) Imaging in the exploration of lumbosacral plexus avulsion. Two cases. J Neuroradiol 19:38-48.

Maleki J, LeBel AA, Bennett GJ, Schwartzman RJ (2000) Patterns of spread in complex regional pain syndrome, type I (reflex sympathetic dystrophy). Pain 88:259-266.

Malin SA, Molliver DC, Koerber HR, Cornuet P, Frye R, Albers KM, Davis BM (2006) Glial cell line-derived neurotrophic factor family members sensitize nociceptors in vitro and produce thermal hyperalgesia in vivo. J Neurosci 26:8588-8599.

Maliszewski M, Ladzinski P, Aleksandrowicz R, Majchrzak H, Bierzynska-Macyszyn G, Wolanska-Karut J (1999) Occlusion of radicular arteries - reasons, consequences and anastomotic substitution pathways. Spinal Cord 37:710-716.

Mann MD (1973) Clarke's column and the dorsal spinocerebellar tract: a review. Brain Behav Evol 7:34-83.

Mannion RJ, Doubell TP, Coggeshall RE, Woolf CJ (1996) Collateral sprouting of uninjured primary afferent A-fibers into the superficial dorsal horn of the adult rat spinal cord after topical capsaicin treatment to the sciatic nerve. J Neurosci 16:5189-5195.

Mannion RJ, Doubell TP, Gill H, Woolf CJ (1998) Deafferentation is insufficient to induce sprouting of A-fibre central terminals in the rat dorsal horn. J Comp Neurol 393:135-144.

Mao QX, Yang TD (2010) Amitriptyline upregulates EAAT1 and EAAT2 in neuropathic pain rats. Brain Res Bull 81:424-427.

Marchand F, Perretti M, McMahon SB (2005) Role of the immune system in chronic pain. Nat Rev Neurosci 6:521-532.

Marchand F, Tsantoulas C, Singh D, Grist J, Clark AK, Bradbury EJ, McMahon SB (2009) Effects of Etanercept and Minocycline in a rat model of spinal cord injury. Eur J Pain 13:673-681.

Martin LJ, Kaiser A, Price AC (1999) Motor neuron degeneration after sciatic nerve avulsion in adult rat evolves with oxidative stress and is apoptosis. J Neurobiol 40:185-201.

Mary V, Wahl F, Stutzmann JM (1995) Effect of riluzole on quinolinate-induced neuronal damage in rats: comparison with blockers of glutamatergic neurotransmission. Neurosci Lett 201:92-96.

Matsukawa N, Yasuhara T, Hara K, Xu L, Maki M, Yu G, Kaneko Y, Ojika K, Hess DC, Borlongan CV (2009) Therapeutic targets and limits of minocycline neuroprotection in experimental ischemic stroke. BMC Neurosci 10:126.

Matsuura J, Ajiki K, Ichikawa T, Misawa H (1997) Changes of expression levels of choline acetyltransferase and vesicular acetylcholine transporter mRNAs after transection of the hypoglossal nerve in adult rats. Neurosci Lett 236:95-98.

Matyja E, Taraszewska A, Naganska E, Rafalowska J (2005) Autophagic degeneration of motor neurons in a model of slow glutamate excitotoxicity in vitro. Ultrastruct Pathol 29:331-339.

Mautes AE, Weinzierl MR, Donovan F, Noble LJ (2000) Vascular events after spinal cord injury: contribution to secondary pathogenesis. Phys Ther 80:673-687.

Maves TJ, Pechman PS, Gebhart GF, Meller ST (1993) Possible chemical contribution from chromic gut sutures produces disorders of pain sensation like those seen in man. Pain 54:57-69.

Mayer DJ, Mao J, Holt J, Price DD (1999) Cellular mechanisms of neuropathic pain, morphine tolerance, and their interactions. Proc Natl Acad Sci U S A 96:7731-7736.

McKeon RJ, Schreiber RC, Rudge JS, Silver J (1991) Reduction of neurite outgrowth in a model of glial scarring following CNS injury is correlated with the expression of inhibitory molecules on reactive astrocytes. J Neurosci 11:3398-3411.

McLachlan EM, Janig W, Devor M, Michaelis M (1993) Peripheral nerve injury triggers noradrenergic sprouting within dorsal root ganglia. Nature 363:543-546.

McMahon SB, Cafferty WB, Marchand F (2005) Immune and glial cell factors as pain mediators and modulators. Exp Neurol 192:444-462.

McNeill DL, Carlton SM, Hulsebosch CE (1991) Intraspinal sprouting of calcitonin gene-related peptide containing primary afferents after deafferentation in the rat. Exp Neurol 114:321-329.

McPhail LT, McBride CB, McGraw J, Steeves JD, Tetzlaff W (2004a) Axotomy abolishes NeuN expression in facial but not rubrospinal neurons. Exp Neurol 185:182-190.

McPhail LT, Plunet WT, Das P, Ramer MS (2005) The astrocytic barrier to axonal regeneration at the dorsal root entry zone is induced by rhizotomy. Eur J Neurosci 21:267-270.

McPhail LT, Stirling DP, Tetzlaff W, Kwiecien JM, Ramer MS (2004b) The contribution of activated phagocytes and myelin degeneration to axonal retraction/dieback following spinal cord injury. Eur J Neurosci 20:1984-1994.

McQuay H, Carroll D, Jadad AR, Wiffen P, Moore A (1995) Anticonvulsant drugs for management of pain: a systematic review. BMJ 311:1047-1052.

Meisner JG, Marsh AD, Marsh DR (2010) Loss of GABAergic interneurons in Laminae I-III of the spinal cord dorsal horn contributes to reduced GABAergic tone and neuropathic pain following spinal cord injury. J Neurotrauma.

Melzack R, Coderre TJ, Katz J, Vaccarino AL (2001) Central neuroplasticity and pathological pain. Ann N Y Acad Sci 933:157-174.

Menetrey D, Giesler GJ, Jr., Besson JM (1977) An analysis of response properties of spinal cord dorsal horn neurones to nonnoxious and noxious stimuli in the spinal rat. Exp Brain Res 27:15-33.

Mert T, Gunay I, Ocal I, Guzel AI, Inal TC, Sencar L, Polat S (2009) Macrophage depletion delays progression of neuropathic pain in diabetic animals. Naunyn Schmiedebergs Arch Pharmacol 379:445-452.

Metz GA, Whishaw IQ (2002) Cortical and subcortical lesions impair skilled walking in the ladder rung walking test: a new task to evaluate fore- and hindlimb stepping, placing, and co-ordination. J Neurosci Methods 115:169-179.

Michael GJ, Averill S, Shortland PJ, Yan Q, Priestley JV (1999) Axotomy results in major changes in BDNF expression by dorsal root ganglion cells: BDNF expression in large trkB and trkC cells, in pericellular baskets, and in projections to deep dorsal horn and dorsal column nuclei. Eur J Neurosci 11:3539-3551.

Michael GJ, Priestley JV (1999) Differential expression of the mRNA for the vanilloid receptor subtype 1 in cells of the adult rat dorsal root and nodose ganglia and its downregulation by axotomy. J Neurosci 19:1844-1854.

Michaelis M, Habler HJ, Jaenig W (1996) Silent afferents: a separate class of primary afferents? Clin Exp Pharmacol Physiol 23:99-105.

Mika J (2008) Modulation of microglia can attenuate neuropathic pain symptoms and enhance morphine effectiveness. Pharmacol Rep 60:297-307.

Mika J, Wawrzczak-Bargiela A, Osikowicz M, Makuch W, Przewlocka B (2009) Attenuation of morphine tolerance by minocycline and pentoxifylline in naive and neuropathic mice. Brain Behav Immun 23:75-84.

Miladinovic K (2009) [Spinal cord injury and chronic pain]. Med Arh 63:106-107.

Milane A, Tortolano L, Fernandez C, Bensimon G, Meininger V, Farinotti R (2009) Brain and plasma riluzole pharmacokinetics: effect of minocycline combination. J Pharm Pharm Sci 12:209-217.

Miller KE, Seybold VS (1987) Ultrastructure of the central gray region (lamina X) in cat spinal cord. Neuroscience 22:1057-1066.

Miller RG, Mitchell JD, Lyon M, Moore DH (2007) Riluzole for amyotrophic lateral sclerosis (ALS)/motor neuron disease (MND). Cochrane Database Syst RevCD001447.

Milligan ED, Twining C, Chacur M, Biedenkapp J, O'Connor K, Poole S, Tracey K, Martin D, Maier SF, Watkins LR (2003) Spinal glia and proinflammatory cytokines mediate mirror-image neuropathic pain in rats. J Neurosci 23:1026-1040.

Milligan ED, Watkins LR (2009) Pathological and protective roles of glia in chronic pain. Nat Rev Neurosci 10:23-36.

Milligan ED, Zapata V, Chacur M, Schoeniger D, Biedenkapp J, O'Connor KA, Verge GM, Chapman G, Green P, Foster AC, Naeve GS, Maier SF, Watkins LR (2004) Evidence that exogenous and endogenous fractalkine can induce spinal nociceptive facilitation in rats. Eur J Neurosci 20:2294-2302.

Mills CD, Grady JJ, Hulsebosch CE (2001) Changes in exploratory behavior as a measure of chronic central pain following spinal cord injury. J Neurotrauma 18:1091-1105.

Mills CD, Hulsebosch CE (2002) Increased expression of metabotropic glutamate receptor subtype 1 on spinothalamic tract neurons following spinal cord injury in the rat. Neurosci Lett 319:59-62.

Milner R, Campbell IL (2002) The integrin family of cell adhesion molecules has multiple functions within the CNS. J Neurosci Res 69:286-291.

Mizuta I, Ohta M, Ohta K, Nishimura M, Mizuta E, Kuno S (2001) Riluzole stimulates nerve growth factor, brain-derived neurotrophic factor and glial cell line-derived neurotrophic factor synthesis in cultured mouse astrocytes. Neurosci Lett 310:117-120.

Moalem G, Tracey DJ (2006) Immune and inflammatory mechanisms in neuropathic pain. Brain Res Rev 51:240-264.

Molander C, Grant G (1985) Cutaneous projections from the rat hindlimb foot to the substantia gelatinosa of the spinal cord studied by transganglionic transport of WGA-HRP conjugate. J Comp Neurol 237:476-484.

Molander C, Grant G (1986) Laminar distribution and somatotopic organization of primary afferent fibers from hindlimb nerves in the dorsal horn. A study by transganglionic transport of horseradish peroxidase in the rat. Neuroscience 19:297-312.

Molander C, Hongpaisan J, Persson JK (1994) Distribution of c-fos expressing dorsal horn neurons after electrical stimulation of low threshold sensory fibers in the chronically injured sciatic nerve. Brain Res 644:74-82.

Molander C, Xu Q, Grant G (1984) The cytoarchitectonic organization of the spinal cord in the rat. I. The lower thoracic and lumbosacral cord. J Comp Neurol 230:133-141.

Molander C, Xu Q, Rivero-Melian C, Grant G (1989) Cytoarchitectonic organization of the spinal cord in the rat: II. The cervical and upper thoracic cord. J Comp Neurol 289:375-385.

Montana V, Ni Y, Sunjara V, Hua X, Parpura V (2004) Vesicular glutamate transporter-dependent glutamate release from astrocytes. J Neurosci 24:2633-2642.

Moore KA, Kohno T, Karchewski LA, Scholz J, Baba H, Woolf CJ (2002) Partial peripheral nerve injury promotes a selective loss of GABAergic inhibition in the superficial dorsal horn of the spinal cord. J Neurosci 22:6724-6731.

Morganti-Kossmann MC, Rancan M, Stahel PF, Kossmann T (2002) Inflammatory response in acute traumatic brain injury: a double-edged sword. Curr Opin Crit Care 8:101-105.

Morinaga T, Takahashi K, Yamagata M, Chiba T, Tanaka K, Takahashi Y, Nakamura S, Suseki K, Moriya H (1996) Sensory innervation to the anterior portion of lumbar intervertebral disc. Spine (Phila Pa 1976) 21:1848-1851.

Muneton-Gomez V, Taylor JS, Averill S, Priestley JV, Nieto-Sampedro M (2004) Degeneration of primary afferent terminals following brachial plexus extensive avulsion injury in rats. Biomedica 24:183-193.

Munro G, Erichsen HK, Mirza NR (2007) Pharmacological comparison of anticonvulsant drugs in animal models of persistent pain and anxiety. Neuropharmacology 53:609-618.

Murphy PM, Baggiolini M, Charo IF, Hebert CA, Horuk R, Matsushima K, Miller LH, Oppenheim JJ, Power CA (2000) International union of pharmacology. XXII. Nomenclature for chemokine receptors. Pharmacol Rev 52:145-176.

Murray M, Goldberger ME (1986) Replacement of synaptic terminals in lamina II and Clarke's nucleus after unilateral lumbosacral dorsal rhizotomy in adult cats. J Neurosci 6:3205-3217.

Murray M, Wang SD, Goldberger ME, Levitt P (1990) Modification of astrocytes in the spinal cord following dorsal root or peripheral nerve lesions. Exp Neurol 110:248-257.

Myers RR, Heckman HM, Rodriguez M (1996) Reduced hyperalgesia in nerve-injured WLD mice: relationship to nerve fiber phagocytosis, axonal degeneration, and regeneration in normal mice. Exp Neurol 141:94-101.

Nakamura SI, Myers RR (2000) Injury to dorsal root ganglia alters innervation of spinal cord dorsal horn lamina involved in nociception. Spine (Phila Pa 1976) 25:537-542.

Narita M, Yoshida T, Nakajima M, Narita M, Miyatake M, Takagi T, Yajima Y, Suzuki T (2006) Direct evidence for spinal cord microglia in the development of a neuropathic pain-like state in mice. J Neurochem 97:1337-1348.

Nashold BS, Jr., Ostdahl RH (1979) Dorsal root entry zone lesions for pain relief. J Neurosurg 51:59-69.

Nassar MA, Baker MD, Levato A, Ingram R, Mallucci G, McMahon SB, Wood JN (2006) Nerve injury induces robust allodynia and ectopic discharges in Nav1.3 null mutant mice. Mol Pain 2:33.

Nelson E, Gertz SD, Rennels ML, Ducker TB, Blaumanis OR (1977) Spinal cord injury. The role of vascular damage in the pathogenesis of central hemorrhagic necrosis. Arch Neurol 34:332-333.

Nesic O, Lee J, Johnson KM, Ye Z, Xu GY, Unabia GC, Wood TG, McAdoo DJ, Westlund KN, Hulsebosch CE, Regino Perez-Polo J (2005) Transcriptional profiling of spinal cord injury-induced central neuropathic pain. J Neurochem 95:998-1014.

Nicholas AP, Zhang X, Hokfelt T (1999) An immunohistochemical investigation of the opioid cell column in lamina X of the male rat lumbosacral spinal cord. Neurosci Lett 270:9-12.

Niclou SP, Franssen EH, Ehlert EM, Taniguchi M, Verhaagen J (2003) Meningeal cell-derived semaphorin 3A inhibits neurite outgrowth. Mol Cell Neurosci 24:902-912.

Nicolopoulos-Stournaras S, Iles JF (1983) Motor neuron columns in the lumbar spinal cord of the rat. J Comp Neurol 217:75-85.

Nikodemova M, Watters JJ, Jackson SJ, Yang SK, Duncan ID (2007) Minocycline down-regulates MHC II expression in microglia and macrophages through inhibition of IRF-1 and protein kinase C (PKC)alpha/betaII. J Biol Chem 282:15208-15216.

Noble LJ, Wrathall JR (1987) The blood-spinal cord barrier after injury: pattern of vascular events proximal and distal to a transection in the rat. Brain Res 424:177-188.

Noble LJ, Wrathall JR (1989) Distribution and time course of protein extravasation in the rat spinal cord after contusive injury. Brain Res 482:57-66.

Nogradi A, Szabo A, Pinter S, Vrbova G (2007) Delayed riluzole treatment is able to rescue injured rat spinal motoneurons. Neuroscience 144:431-438.

Nogradi A, Vrbova G (1996) Improved motor function of denervated rat hindlimb muscles induced by embryonic spinal cord grafts. Eur J Neurosci 8:2198-2203.

Nogradi A, Vrbova G (2001) The effect of riluzole treatment in rats on the survival of injured adult and grafted embryonic motoneurons. Eur J Neurosci 13:113-118.

Noguchi K, De LM, Nahin RL, Senba E, Ruda MA (1993) Quantification of axotomy-induced alteration of neuropeptide mRNAs in dorsal root ganglion neurons with special reference to neuropeptide Y mRNA and the effects of neonatal capsaicin treatment. J Neurosci Res 35:54-66.

Noh KM, Hwang JY, Shin HC, Koh JY (2000) A novel neuroprotective mechanism of riluzole: direct inhibition of protein kinase C. Neurobiol Dis 7:375-383.

Nomura H, Furuta A, Iwaki T (2002) Dorsal root rupture injury induces extension of astrocytic processes into the peripheral nervous system and expression of GDNF in astrocytes. Brain Res 950:21-30.

Nomura H, Furuta A, Tanaka Y, Iwaki T (2005) Forced retraction of spinal root injury enhances activation of p38 MAPK cascade in infiltrating macrophages. Neuropathology 25:37-47.

Nordin L, Sinisi M (2009) Brachial plexus-avulsion causing Brown-Sequard syndrome: a report of three cases. J Bone Joint Surg Br 91:88-90.

Novak CB, Anastakis DJ, Beaton DE, Katz J (2009) Patient-reported outcome after peripheral nerve injury. J Hand Surg Am 34:281-287.

Novakovic SD, Kassotakis LC, Oglesby IB, Smith JA, Eglen RM, Ford AP, Hunter JC (1999) Immunocytochemical localization of P2X3 purinoceptors in sensory neurons in naive rats and following neuropathic injury. Pain 80:273-282.

Novikov L, Novikova L, Kellerth JO (1995) Brain-derived neurotrophic factor promotes survival and blocks nitric oxide synthase expression in adult rat spinal motoneurons after ventral root avulsion. Neurosci Lett 200:45-48.

O'Dell JR (1999) Is there a role for antibiotics in the treatment of patients with rheumatoid arthritis? Drugs 57:279-282.

Oatway MA, Chen Y, Bruce JC, Dekaban GA, Weaver LC (2005) Anti-CD11d integrin antibody treatment restores normal serotonergic projections to the dorsal, intermediate, and ventral horns of the injured spinal cord. J Neurosci 25:637-647.

Obata K, Katsura H, Miyoshi K, Kondo T, Yamanaka H, Kobayashi K, Dai Y, Fukuoka T, Akira S, Noguchi K (2008) Toll-like receptor 3 contributes to spinal glial activation and tactile allodynia after nerve injury. J Neurochem.

Obata K, Katsura H, Sakurai J, Kobayashi K, Yamanaka H, Dai Y, Fukuoka T, Noguchi K (2006a) Suppression of the p75 neurotrophin receptor in uninjured sensory neurons reduces neuropathic pain after nerve injury. J Neurosci 26:11974-11986.

Obata K, Noguchi K (2006) BDNF in sensory neurons and chronic pain. Neurosci Res 55:1-10.

Obata K, Yamanaka H, Dai Y, Mizushima T, Fukuoka T, Tokunaga A, Yoshikawa H, Noguchi K (2004) Contribution of degeneration of motor and sensory fibers to pain behavior and the changes in neurotrophic factors in rat dorsal root ganglion. Exp Neurol 188:149-160.

Obata K, Yamanaka H, Fukuoka T, Yi D, Tokunaga A, Hashimoto N, Yoshikawa H, Noguchi K (2003) Contribution of injured and uninjured dorsal root ganglion neurons to pain behavior and the changes in gene expression following chronic constriction injury of the sciatic nerve in rats. Pain 101:65-77.

Obata K, Yamanaka H, Kobayashi K, Dai Y, Mizushima T, Katsura H, Fukuoka T, Tokunaga A, Noguchi K (2006b) The effect of site and type of nerve injury on the expression of brain-derived neurotrophic factor in the dorsal root ganglion and on neuropathic pain behavior. Neuroscience 137:961-970.

Ohlsson M, Bellander BM, Langmoen IA, Svensson M (2003) Complement activation following optic nerve crush in the adult rat. J Neurotrauma 20:895-904.

Ohlsson M, Hoang TX, Wu J, Havton LA (2006) Glial reactions in a rodent cauda equina injury and repair model. Exp Brain Res 170:52-60.

Ohlsson M, Mattsson P, Svensson M (2004) A temporal study of axonal degeneration and glial scar formation following a standardized crush injury of the optic nerve in the adult rat. Restor Neurol Neurosci 22:1-10.

Ohtori S, Takahashi K, Moriya H, Myers RR (2004) TNF-alpha and TNF-alpha receptor type 1 upregulation in glia and neurons after peripheral nerve injury: studies in murine DRG and spinal cord. Spine (Phila Pa 1976) 29:1082-1088.

Oprica M, Eriksson C, Schultzberg M (2003) Inflammatory mechanisms associated with brain damage induced by kainic acid with special reference to the interleukin-1 system. J Cell Mol Med 7:127-140.

Ovelmen-Levitt J (1988) Abnormal physiology of the dorsal horn as related to the deafferentation syndrome. Appl Neurophysiol 51:104-116.

Ovelmen-Levitt J, Gorecki J, Nguyen KT, Iskandar B, Nashold BS, Jr. (1995) Spontaneous and evoked dysesthesias observed in the rat after spinal cordotomies. Stereotact Funct Neurosurg 65:157-160.

Ovelmen-Levitt J, Johnson B, Bedenbaugh P, Nashold BS, Jr. (1984) Dorsal root rhizotomy and avulsion in the cat: a comparison of long term effects on dorsal horn neuronal activity. Neurosurgery 15:921-927.

Padi SS, Kulkarni SK (2008) Minocycline prevents the development of neuropathic pain, but not acute pain: possible anti-inflammatory and antioxidant mechanisms. Eur J Pharmacol 601:79-87.

Panerai AE, Sacerdote P, Brini A, Bianchi M, Mantegazza P (1987) Autotomy and central nervous system neuropeptides after section of the sciatic nerve in rats of different strains. Pharmacol Biochem Behav 28:385-388.

Parry CB (1980) Pain in avulsion lesions of the brachial plexus. Pain 9:41-53.

Parsadanian A, Pan Y, Li W, Myckatyn TM, Brakefield D (2006) Astrocyte-derived transgene GDNF promotes complete and long-term survival of adult facial motoneurons following avulsion and differentially regulates the expression of transcription factors of AP-1 and ATF/CREB families. Exp Neurol 200:26-37.

Patrizio M, Slepko N, Levi G (1997) Opposite regulation of adenylyl cyclase by protein kinase C in astrocyte and microglia cultures. J Neurochem 69:1267-1277.

Patwardhan RV, Minagar A, Kelley RE, Nanda A (2006) Neurosurgical treatment of multiple sclerosis. Neurol Res 28:320-325.

Peluffo H, Estevez A, Barbeito L, Stutzmann JM (1997) Riluzole promotes survival of rat motoneurons in vitro by stimulating trophic activity produced by spinal astrocyte monolayers. Neurosci Lett 228:207-211.

Penas C, Casas C, Robert I, Fores J, Navarro X (2009) Cytoskeletal and activity-related changes in spinal motoneurons after root avulsion. J Neurotrauma 26:763-779.

Perkins NM, Tracey DJ (2000) Hyperalgesia due to nerve injury: role of neutrophils. Neuroscience 101:745-757.

Perry MJ, Lawson SN, Robertson J (1991) Neurofilament immunoreactivity in populations of rat primary afferent neurons: a quantitative study of phosphorylated and non-phosphorylated subunits. J Neurocytol 20:746-758.

Petrenko AB, Yamakura T, Baba H, Sakimura K (2003a) Unaltered pain-related behavior in mice lacking NMDA receptor GluRepsilon 1 subunit. Neurosci Res 46:199-204.

Petrenko AB, Yamakura T, Baba H, Shimoji K (2003b) The role of N-methyl-D-aspartate (NMDA) receptors in pain: a review. Anesth Analg 97:1108-1116.

Pinzon A, Marcillo A, Quintana A, Stamler S, Bunge MB, Bramlett HM, Dietrich WD (2008) A re-assessment of minocycline as a neuroprotective agent in a rat spinal cord contusion model. Brain Res 1243:146-151.

Pioli EY, Gross CE, Meissner W, Bioulac BH, Bezard E (2003) The deafferented nonhuman primate is not a reliable model of intractable pain. Neurol Res 25:127-129.

Piva B, Shaladi A, Saltari R, Phd GG (2003) Spinal cord stimulation in the management of pain from brachial plexus avulsion. Neuromodulation 6:27-31.

Polgar E, Gray S, Riddell JS, Todd AJ (2004) Lack of evidence for significant neuronal loss in laminae I-III of the spinal dorsal horn of the rat in the chronic constriction injury model. Pain 111:144-150.

Polgar E, Hughes DI, Arham AZ, Todd AJ (2005) Loss of neurons from laminas I-III of the spinal dorsal horn is not required for development of tactile allodynia in the spared nerve injury model of neuropathic pain. J Neurosci 25:6658-6666.

Polgar E, Hughes DI, Riddell JS, Maxwell DJ, Puskar Z, Todd AJ (2003) Selective loss of spinal GABAergic or glycinergic neurons is not necessary for development of thermal hyperalgesia in the chronic constriction injury model of neuropathic pain. Pain 104:229-239.

Polgar E, Todd AJ (2008) Tactile allodynia can occur in the spared nerve injury model in the rat without selective loss of GABA or GABA(A) receptors from synapses in laminae I-II of the ipsilateral spinal dorsal horn. Neuroscience 156:193-202.

Polikov VS, Block ML, Fellous JM, Hong JS, Reichert WM (2006) In vitro model of glial scarring around neuroelectrodes chronically implanted in the CNS. Biomaterials 27:5368-5376.

Polistina DC, Murray M, Goldberger ME (1990) Plasticity of dorsal root and descending serotoninergic projections after partial deafferentation of the adult rat spinal cord. J Comp Neurol 299:349-363.

Pollmann W, Feneberg W (2008) Current management of pain associated with multiple sclerosis. CNS Drugs 22:291-324.

Pontieri FE, Ricci A, Pellicano C, Benincasa D, Buttarelli FR (2005) Minocycline in amyotrophic lateral sclerosis: a pilot study. Neurol Sci 26:285-287.

Popovich PG (2000) Immunological regulation of neuronal degeneration and regeneration in the injured spinal cord. Prog Brain Res 128:43-58.

Popovich PG, Jones TB (2003) Manipulating neuroinflammatory reactions in the injured spinal cord: back to basics. Trends Pharmacol Sci 24:13-17.

Popovich PG, Longbrake EE (2008) Can the immune system be harnessed to repair the CNS? Nat Rev Neurosci 9:481-493.

Popovich PG, Wei P, Stokes BT (1997) Cellular inflammatory response after spinal cord injury in Sprague-Dawley and Lewis rats. J Comp Neurol 377:443-464.

Priestley JV, Michael GJ, Averill S, Liu M, Willmott N (2002) Regulation of nociceptive neurons by nerve growth factor and glial cell line derived neurotrophic factor. Can J Physiol Pharmacol 80:495-505.

Qin H, Zhou X, Zhang W, Chen S (2004) Expressional change of nitric oxide synthase in dorsal root ganglia of cats after selective dorsal rhizotomy. Journal of Sichuan University Medical science edition 35:29-31.

Quintao NL, Balz D, Santos AR, Campos MM, Calixto JB (2006) Long-lasting neuropathic pain induced by brachial plexus injury in mice: Role triggered by the pro-inflammatory cytokine, tumour necrosis factor alpha. Neuropharmacology 50:614-620.

Quintao NL, Passos GF, Medeiros R, Paszcuk AF, Motta FL, Pesquero JB, Campos MM, Calixto JB (2008a) Neuropathic pain-like behavior after brachial plexus avulsion in mice: the relevance of kinin B1 and B2 receptors. J Neurosci 28:2856-2863.

Quintao NL, Santos AR, Campos MM, Calixto JB (2008b) The role of neurotrophic factors in genesis and maintenance of mechanical hypernociception after brachial plexus avulsion in mice. Pain 136:125-133.

Raghavendra V, Tanga F, DeLeo JA (2003) Inhibition of microglial activation attenuates the development but not existing hypersensitivity in a rat model of neuropathy. J Pharmacol Exp Ther 306:624-630.

Raivich G (2001) Microglial response in the axotomized facial motor nucleus. In: Microglia in the regenerating and degenerating central nervous system (Streit WJ, ed), New York: Springer-Verlag.

Ralston HJ, III, Ralston DD (1982) The distribution of dorsal root axons to laminae IV, V, and VI of the Macaque spinal cord: a quantitative electron microscopic study. J Comp Neurol 212:435-448.

Ralston HJ, III, Ralston DD (1992) The primate dorsal spinothalamic tract: evidence for a specific termination in the posterior nuclei (Po/SG) of the thalamus. Pain 48:107-118.

Ramakrishna J, Johnson AR, Banner BF (2009) Long-term minocycline use for acne in healthy adolescents can cause severe autoimmune hepatitis. J Clin Gastroenterol 43:787-790.

Ramer MS, Bradbury EJ, Michael GJ, Lever IJ, McMahon SB (2003) Glial cell line-derived neurotrophic factor increases calcitonin gene-related peptide immunoreactivity in sensory and motoneurons in vivo. Eur J Neurosci 18:2713-2721.

Ramer MS, French GD, Bisby MA (1997) Wallerian degeneration is required for both neuropathic pain and sympathetic sprouting into the DRG. Pain 72:71-78.

Ramer MS, Priestley JV, McMahon SB (2000) Functional regeneration of sensory axons into the adult spinal cord. Nature 403:312-316.

Ramon YC, May RM (1928) Degeneration & regeneration of the nervous system.

Rapeport WG, Rogers KM, McCubbin TD, Agnew E, Brodie MJ (1984) Treatment of intractable neurogenic pain with carbamazepine. Scott Med J 29:162-165.

Reddy SJ, La MF, Park P (2008) The role of heat shock proteins in spinal cord injury. Neurosurg Focus 25:E4.

Rende M, Giambanco I, Buratta M, Tonali P (1995) Axotomy induces a different modulation of both low-affinity nerve growth factor receptor and choline acetyltransferase between adult rat spinal and brainstem motoneurons. J Comp Neurol 363:249-263.

Reuss MH, Reuss S (2001) Nitric oxide synthase neurons in the rodent spinal cord: distribution, relation to Substance P fibers, and effects of dorsal rhizotomy. J Chem Neuroanat 21:181-196.

REXED B (1952) The cytoarchitectonic organization of the spinal cord in the cat. J Comp Neurol 96:414-495.

REXED B (1954) A cytoarchitectonic atlas of the spinal cord in the cat. J Comp Neurol 100:297-379.

Rigaud M, Gemes G, Barabas ME, Chernoff DI, Abram SE, Stucky CL, Hogan QH (2008) Species and strain differences in rodent sciatic nerve anatomy: implications for studies of neuropathic pain. Pain 136:188-201.

Ritfeld GJ, Tewarie RD, Rahiem ST, Hurtado A, Roos RA, Grotenhuis A, Oudega M (2010) Reducing macrophages to improve bone marrow stromal cell survival in the contused spinal cord. Neuroreport 21:221-226.

Rivero-Melian C, Grant G (1990) Distribution of lumbar dorsal root fibers in the lower thoracic and lumbosacral spinal cord of the rat studied with choleragenoid horseradish peroxidase conjugate. J Comp Neurol 299:470-481.

Rock RB, Gekker G, Hu S, Sheng WS, Cheeran M, Lokensgard JR, Peterson PK (2004) Role of microglia in central nervous system infections. Clin Microbiol Rev 17:942-64, table.

Rodin BE, Kruger L (1984) Deafferentation in animals as a model for the study of pain: an alternative hypothesis. Brain Res 319:213-228.

Rodrigues-Filho R, Campos MM, Ferreira J, Santos AR, Bertelli JA, Calixto JB (2004) Pharmacological characterisation of the rat brachial plexus avulsion model of neuropathic pain. Brain Res 1018:159-170.

Rodrigues-Filho R, Santos AR, Bertelli JA, Calixto JB (2003) Avulsion injury of the rat brachial plexus triggers hyperalgesia and allodynia in the hindpaws: a new model for the study of neuropathic pain. Brain Res 982:186-194.

Rogawski MA, Loscher W (2004) The neurobiology of antiepileptic drugs for the treatment of nonepileptic conditions. Nat Med 10:685-692.

Rosson JW (1987) Disability following closed traction lesions of the brachial plexus sustained in motor cycle accidents. J Hand Surg Br 12:353-355.

Rothman SM, Guarino BB, Winkelstein BA (2009) Spinal microglial proliferation is evident in a rat model of painful disc herniation both in the presence of behavioral hypersensitivity and following minocycline treatment sufficient to attenuate allodynia. J Neurosci Res 87:2709-2717.

Rothman SM, Kreider RA, Winkelstein BA (2005) Spinal neuropeptide responses in persistent and transient pain following cervical nerve root injury. Spine (Phila Pa 1976) 30:2491-2496.

Roussy G, Dansereau MA, Baudisson S, Ezzoubaa F, Belleville K, Beaudet N, Martinez J, Richelson E, Sarret P (2009) Evidence for a role of NTS2 receptors in the modulation of tonic pain sensitivity. Mol Pain 5:38.

Roza C, Laird JM, Souslova V, Wood JN, Cervero F (2003) The tetrodotoxin-resistant Na+ channel Nav1.8 is essential for the expression of spontaneous activity in damaged sensory axons of mice. J Physiol 550:921-926.

Rubinstein RE, Deem KC, Jensen J, Mackinnon SE, Tung TH (2003) Strain differences in autotomy in mice after peripheral nerve transection or repair. Microsurgery 23:363-368.

Rutkowski MD, Pahl JL, Sweitzer S, van RN, DeLeo JA (2000) Limited role of macrophages in generation of nerve injury-induced mechanical allodynia. Physiol Behav 71:225-235.

Saarto T, Wiffen PJ (2007) Antidepressants for neuropathic pain. Cochrane Database Syst RevCD005454.

Saganova K, Orendacova J, Cizkova D, Vanicky I (2008) Limited minocycline neuroprotection after balloon-compression spinal cord injury in the rat. Neurosci Lett 433:246-249.

Sakurada T, Komatsu T, Kuwahata H, Watanabe C, Orito T, Sakurada C, Tsuzuki M, Sakurada S (2007) Intrathecal substance P (1-7) prevents morphine-evoked spontaneous pain behavior via spinal NMDA-NO cascade. Biochem Pharmacol 74:758-767.

Sampson JH, Cashman RE, Nashold BS, Jr., Friedman AH (1995) Dorsal root entry zone lesions for intractable pain after trauma to the conus medullaris and cauda equina. J Neurosurg 82:28-34.

Sanner CA, Murray M, Goldberger ME (1993) Removal of dorsal root afferents prevents retrograde death of axotomized Clarke's nucleus neurons in the cat. Exp Neurol 123:81-90.

Savill J, Dransfield I, Gregory C, Haslett C (2002) A blast from the past: clearance of apoptotic cells regulates immune responses. Nat Rev Immunol 2:965-975.

Sawynok J, Reid A (2003) Peripheral interactions between dextromethorphan, ketamine and amitriptyline on formalin-evoked behaviors and paw edema in rats. Pain 102:179-186.

Schmidt AP, Schmidt SR (2004) Treatment of refractory neuropathic pain related to a brachial plexus injury. Injury 35:528-530.

Scholz J, Broom DC, Youn DH, Mills CD, Kohno T, Suter MR, Moore KA, Decosterd I, Coggeshall RE, Woolf CJ (2005) Blocking caspase activity prevents transsynaptic neuronal apoptosis and the loss of inhibition in lamina II of the dorsal horn after peripheral nerve injury. J Neurosci 25:7317-7323.

Scholz J, Woolf CJ (2007) The neuropathic pain triad: neurons, immune cells and glia. Nat Neurosci 10:1361-1368.

Schulz P, Dick P, Blaschke TF, Hollister L (1985) Discrepancies between pharmacokinetic studies of amitriptyline. Clin Pharmacokinet 10:257-268.

Seltzer Z, Beilin BZ, Ginzburg R, Paran Y, Shimko T (1991) The role of injury discharge in the induction of neuropathic pain behavior in rats. Pain 46:327-336.

Seltzer Z, Dubner R, Shir Y (1990) A novel behavioral model of neuropathic pain disorders produced in rats by partial sciatic nerve injury. Pain 43:205-218.

Seltzer Z, Shir Y (1991) Sympathetically-maintained causalgiform disorders in a model for neuropathic pain: a review. J Basic Clin Physiol Pharmacol 2:17-61.

Senter HJ, Venes JL (1978) Altered blood flow and secondary injury in experimental spinal cord trauma. J Neurosurg 49:569-578.

Shapiro LE, Knowles SR, Shear NH (1997) Comparative safety of tetracycline, minocycline, and doxycycline. Arch Dermatol 133:1224-1230.

Shapiro S (1997) Neurotransmission by neurons that use serotonin, noradrenaline, glutamate, glycine, and gamma-aminobutyric acid in the normal and injured spinal cord. Neurosurgery 40:168-176.

Sheen K, Chung JM (1993) Signs of neuropathic pain depend on signals from injured nerve fibers in a rat model. Brain Res 610:62-68.

Shehab SA (2009) Acute and chronic sectioning of fifth lumbar spinal nerve has equivalent effects on the primary afferents of sciatic nerve in rat spinal cord. J Comp Neurol 517:481-492.

Shehab SA, Al-Marashda K, Al-Zahmi A, Abdul-Kareem A, Al-Sultan MA (2008) Unmyelinated primary afferents from adjacent spinal nerves intermingle in the spinal dorsal horn: a possible mechanism contributing to neuropathic pain. Brain Res 1208:111-119.

Shehab SA, Spike RC, Todd AJ (2003) Evidence against cholera toxin B subunit as a reliable tracer for sprouting of primary afferents following peripheral nerve injury. Brain Res 964:218-227.

Sheth RN, Dorsi MJ, Li Y, Murinson BB, Belzberg AJ, Griffin JW, Meyer RA (2002) Mechanical hyperalgesia after an L5 ventral rhizotomy or an L5 ganglionectomy in the rat. Pain 96:63-72.

Shi TJ, Zhang X, Berge OG, Erickson JC, Palmiter RD, Hokfelt T (1998) Effect of peripheral axotomy on dorsal root ganglion neuron phenotype and autonomy behaviour in neuropeptide Y-deficient mice. Regul Pept 75-76:161-173.

Shir Y, Ratner A, Raja SN, Campbell JN, Seltzer Z (1998) Neuropathic pain following partial nerve injury in rats is suppressed by dietary soy. Neurosci Lett 240:73-76.

Shir Y, Seltzer Z (1990) A-fibers mediate mechanical hyperesthesia and allodynia and C-fibers mediate thermal hyperalgesia in a new model of causalgiform pain disorders in rats. Neurosci Lett 115:62-67.

Shortland P, Kinman E, Molander C (1997) Sprouting of A-fibre primary afferents into lamina II in two rat models of neuropathic pain. Eur J Pain 1:215-227.

Shortland P, Molander C (1998) The time-course of abeta-evoked c-fos expression in neurons of the dorsal horn and gracile nucleus after peripheral nerve injury. Brain Res 810:288-293.

Shortland P, Wall PD (1992) Long-range afferents in the rat spinal cord. II. Arborizations that penetrate grey matter. Philos Trans R Soc Lond B Biol Sci 337:445-455.

Shortland P, Woolf CJ, Fitzgerald M (1989) Morphology and somatotopic organization of the central terminals of hindlimb hair follicle afferents in the rat lumbar spinal cord. J Comp Neurol 289:416-433.

Shortland PJ, Baytug B, Krzyzanowska A, McMahon SB, Priestley JV, Averill S (2006a) ATF3 expression in L4 dorsal root ganglion neurons after L5 spinal nerve transection. Eur J Neurosci 23:365-373.

Shortland PJ, Leinster VH, White W, Robson LG (2006b) Riluzole promotes cell survival and neurite outgrowth in rat sensory neurones in vitro. Eur J Neurosci 24:3343-3353.

Siddall P, Xu CL, Cousins M (1995) Allodynia following traumatic spinal cord injury in the rat. Neuroreport 6:1241-1244.

Silos-Santiago I (2008) The role of tetrodotoxin-resistant sodium channels in pain states: are they the next target for analgesic drugs? Curr Opin Investig Drugs 9:83-89.

Simon HU (2003) Neutrophil apoptosis pathways and their modifications in inflammation. Immunol Rev 193:101-110.

Sindou M, Mertens P, Wael M (2001) Microsurgical DREZotomy for pain due to spinal cord and/or cauda equina injuries: long-term results in a series of 44 patients. Pain 92:159-171.

Sindou M, Quoex C, Baleydier C (1974) Fiber organization at the posterior spinal cord-rootlet junction in man. J Comp Neurol 153:15-26.

Sindou MP, Blondet E, Emery E, Mertens P (2005) Microsurgical lesioning in the dorsal root entry zone for pain due to brachial plexus avulsion: a prospective series of 55 patients. J Neurosurg 102:1018-1028.

Sindrup SH, Jensen TS (2002) Pharmacotherapy of trigeminal neuralgia. Clin J Pain 18:22-27.

Sindrup SH, Otto M, Finnerup NB, Jensen TS (2005) Antidepressants in the treatment of neuropathic pain. Basic Clin Pharmacol Toxicol 96:399-409.

Siniscalchi A (2004) [Tolerability of riluzole: a review of the literature]. Clin Ter 155:25-28.

Sivaraman A, Altaf F, Carlstedt T, Noordeen H (2008) Intradural repair of lumbar nerve roots for traumatic paraparesis leading to functional recovery. J Spinal Disord Tech 21:553-556.

Sleeper AA, Cummins TR, Dib-Hajj SD, Hormuzdiar W, Tyrrell L, Waxman SG, Black JA (2000) Changes in expression of two tetrodotoxin-resistant sodium channels and their currents in dorsal root ganglion neurons after sciatic nerve injury but not rhizotomy. J Neurosci 20:7279-7289.

Smith KJ, Bennett BJ (1987) Topographic and quantitative description of rat dorsal column fibres arising from the lumbar dorsal roots. J Anat 153:203-215.

Snider WD, Zhou FQ, Zhong J, Markus A (2002) Signaling the pathway to regeneration. Neuron 35:13-16.

Sommer C, Myers RR (1996) Vascular pathology in CCI neuropathy: a quantitative temporal study. Exp Neurol 141:113-119.

Song L, Yang B, Kang X, Xiao H, Yang F, Liu H (2008) [Peripheral anti-hyperalgesic effect of amitriptyline for sciatic nerve blockade on neuropathic pain of rats]. Zhongguo Xiu Fu Chong Jian Wai Ke Za Zhi 22:1339-1343.

Song P, Zhao ZQ (2001) The involvement of glial cells in the development of morphine tolerance. Neurosci Res 39:281-286.

Song XJ, Vizcarra C, Xu DS, Rupert RL, Wong ZN (2003) Hyperalgesia and neural excitability following injuries to central and peripheral branches of axons and somata of dorsal root ganglion neurons. J Neurophysiol 89:2185-2193.

Sotgiu ML, Brambilla M, Valente M, Biella GE (2004) Contralateral input modulates the excitability of dorsal horn neurons involved in noxious signal processes. Potential role in neuronal sensitization. Somatosens Mot Res 21:211-215.

Spina E, Perugi G (2004) Antiepileptic drugs: indications other than epilepsy. Epileptic Disord 6:57-75.

Sroga JM, Jones TB, Kigerl KA, McGaughy VM, Popovich PG (2003) Rats and mice exhibit distinct inflammatory reactions after spinal cord injury. J Comp Neurol 462:223-240.

Staaf S, Oerther S, Lucas G, Mattsson JP, Ernfors P (2009) Differential regulation of TRP channels in a rat model of neuropathic pain. Pain 144:187-199.

Stacey BR (2005) Management of peripheral neuropathic pain. Am J Phys Med Rehabil 84:S4-16.

Staikopoulos V, Sessle BJ, Furness JB, Jennings EA (2007) Localization of P2X2 and P2X3 receptors in rat trigeminal ganglion neurons. Neuroscience 144:208-216.

Stefanova N, Mitschnigg M, Ghorayeb I, Diguet E, Geser F, Tison F, Poewe W, Wenning GK (2004) Failure of neuronal protection by inhibition of glial activation in a rat model of striatonigral degeneration. J Neurosci Res 78:87-91.

Stephen AB, Stevens K, Craigen MA, Kerslake RW (1997) Brown-Sequard syndrome due to traumatic brachial plexus root avulsion. Injury 28:557-558.

Stevanato G, Vazzana L, Daramaras S, Trincia G, Saggioro GC, Squintani G (2007) Lumbosacral plexus lesions. Acta Neurochir Suppl 100:15-20.

Stirling DP, Khodarahmi K, Liu J, McPhail LT, McBride CB, Steeves JD, Ramer MS, Tetzlaff W (2004) Minocycline treatment reduces delayed oligodendrocyte death, attenuates axonal dieback, and improves functional outcome after spinal cord injury. J Neurosci 24:2182-2190.

Stirling DP, Koochesfahani KM, Steeves JD, Tetzlaff W (2005) Minocycline as a neuroprotective agent. Neuroscientist 11:308-322.

Stirling DP, Liu S, Kubes P, Yong VW (2009) Depletion of Ly6G/Gr-1 leukocytes after spinal cord injury in mice alters wound healing and worsens neurological outcome. J Neurosci 29:753-764.

Stoll G (2002) Inflammatory cytokines in the nervous system: multifunctional mediators in autoimmunity and cerebral ischemia. Rev Neurol (Paris) 158:887-891.

Strassman AM, Levy D (2006) Response properties of dural nociceptors in relation to headache. J Neurophysiol 95:1298-1306.

Streit WJ (2002) Microglia as neuroprotective, immunocompetent cells of the CNS. Glia 40:133-139.

Streit WJ, Kreutzberg GW (1988) Response of endogenous glial cells to motor neuron degeneration induced by toxic ricin. J Comp Neurol 268:248-263.

Streit WJ, Schulte BA, Balentine JD, Spicer SS (1986) Evidence for glycoconjugate in nociceptive primary sensory neurons and its origin from the Golgi complex. Brain Res 377:1-17.

Su X, Liang AH, Urban MO (2009) The effect of amitriptyline on ectopic discharge of primary afferent fibers in the L5 dorsal root in a rat model of neuropathic pain. Anesth Analg 108:1671-1679.

Sugiura Y, Terui N, Hosoya Y (1989) Difference in distribution of central terminals between visceral and somatic unmyelinated (C) primary afferent fibers. J Neurophysiol 62:834-840.

Sukhotinsky I, Ben-Dor E, Raber P, Devor M (2004) Key role of the dorsal root ganglion in neuropathic tactile hypersensibility. Eur J Pain 8:135-143.

Sung B, Lim G, Mao J (2003) Altered expression and uptake activity of spinal glutamate transporters after nerve injury contribute to the pathogenesis of neuropathic pain in rats. J Neurosci 23:2899-2910.

Svensson M, Aldskogius H (1993) Synaptic density of axotomized hypoglossal motorneurons following pharmacological blockade of the microglial cell proliferation. Exp Neurol 120:123-131.

Sweitzer SM, Colburn RW, Rutkowski M, DeLeo JA (1999) Acute peripheral inflammation induces moderate glial activation and spinal IL-1beta expression that correlates with pain behavior in the rat. Brain Res 829:209-221.

Sweitzer SM, Hickey WF, Rutkowski MD, Pahl JL, DeLeo JA (2002) Focal peripheral nerve injury induces leukocyte trafficking into the central nervous system: potential relationship to neuropathic pain. Pain 100:163-170.

Swett JE, Woolf CJ (1985) The somatotopic organization of primary afferent terminals in the superficial laminae of the dorsal horn of the rat spinal cord. J Comp Neurol 231:66-77.

Takahashi Y, Chiba T, Kurokawa M, Aoki Y (2003) Dermatomes and the central organization of dermatomes and body surface regions in the spinal cord dorsal horn in rats. J Comp Neurol 462:29-41.

Takahashi Y, Takahashi K, Moriya H (1995) Mapping of dermatomes of the lower extremities based on an animal model. J Neurosurg 82:1030-1034.

Tal M, Bennett GJ (1994) Extra-territorial pain in rats with a peripheral mononeuropathy: mechano-hyperalgesia and mechano-allodynia in the territory of an uninjured nerve. Pain 57:375-382.

Tal M, Eliav E (1996) Abnormal discharge originates at the site of nerve injury in experimental constriction neuropathy (CCI) in the rat. Pain 64:511-518.

Tandrup T, Woolf CJ, Coggeshall RE (2000) Delayed loss of small dorsal root ganglion cells after transection of the rat sciatic nerve. J Comp Neurol 422:172-180.

Tanga FY, Nutile-McMenemy N, DeLeo JA (2005) The CNS role of Toll-like receptor 4 in innate neuroimmunity and painful neuropathy. Proc Natl Acad Sci U S A 102:5856-5861.

Tanga FY, Raghavendra V, DeLeo JA (2004) Quantitative real-time RT-PCR assessment of spinal microglial and astrocytic activation markers in a rat model of neuropathic pain. Neurochem Int 45:397-407.

Tanga FY, Raghavendra V, Nutile-McMenemy N, Marks A, DeLeo JA (2006) Role of astrocytic S100beta in behavioral hypersensitivity in rodent models of neuropathic pain. Neuroscience 140:1003-1010.

Taoka Y, Okajima K, Uchiba M, Murakami K, Kushimoto S, Johno M, Naruo M, Okabe H, Takatsuki K (1997) Role of neutrophils in spinal cord injury in the rat. Neuroscience 79:1177-1182.

Tasaki I (1939) The electro-saltatory transmission of the nerve impulse and the effect of narcosis upon the nerve fiber. American Journal of Physiology 127:211-227.

Teixeira MJ, Fonoff ET, Montenegro MC (2007) Dorsal root entry zone lesions for treatment of pain-related to radiation-induced plexopathy. Spine (Phila Pa 1976) 32:E316-E319.

Teng YD, Choi H, Onario RC, Zhu S, Desilets FC, Lan S, Woodard EJ, Snyder EY, Eichler ME, Friedlander RM (2004) Minocycline inhibits contusion-triggered mitochondrial cytochrome c release and mitigates functional deficits after spinal cord injury. Proc Natl Acad Sci U S A 101:3071-3076.

Terzis JK, Vekris MD, Soucacos PN (1999) Outcomes of brachial plexus reconstruction in 204 patients with devastating paralysis. Plast Reconstr Surg 104:1221-1240.

Terzis JK, Vekris MD, Soucacos PN (2001) Brachial plexus root avulsions. World J Surg 25:1049-1061.

Tessler A, Glazer E, Artymyshyn R, Murray M, Goldberger ME (1980) Recovery of substance P in the cat spinal cord after unilateral lumbosacral deafferentation. Brain Res 191:459-470.

Tessler A, Himes BT, Artymyshyn R, Murray M, Goldberger ME (1981) Spinal neurons mediate return of substance P following deafferentation of cat spinal cord. Brain Res 230:263-281.

Thacker MA, Clark AK, Bishop T, Grist J, Yip PK, Moon LD, Thompson SW, Marchand F, McMahon SB (2009) CCL2 is a key mediator of microglia activation in neuropathic pain states. Eur J Pain 13:263-272.

Thacker MA, Clark AK, Marchand F, McMahon SB (2007) Pathophysiology of peripheral neuropathic pain: immune cells and molecules. Anesth Analg 105:838-847.

Tie-Jun SS, Xu Z, Hokfelt T (2001) The expression of calcitonin gene-related peptide in dorsal horn neurons of the mouse lumbar spinal cord. Neuroreport 12:739-743.

Tikka T, Fiebich BL, Goldsteins G, Keinanen R, Koistinaho J (2001) Minocycline, a tetracycline derivative, is neuroprotective against excitotoxicity by inhibiting activation and proliferation of microglia. J Neurosci 21:2580-2588.

Tikka TM, Koistinaho JE (2001) Minocycline provides neuroprotection against N-methyl-D-aspartate neurotoxicity by inhibiting microglia. J Immunol 166:7527-7533.

Tilton A (2009) Management of spasticity in children with cerebral palsy. Semin Pediatr Neurol 16:82-89.

Tong YG, Wang HF, Ju G, Grant G, Hokfelt T, Zhang X (1999) Increased uptake and transport of cholera toxin B-subunit in dorsal root ganglion neurons after peripheral axotomy: possible implications for sensory sprouting. J Comp Neurol 404:143-158.

Torrance N, Smith BH, Bennett MI, Lee AJ (2006) The epidemiology of chronic pain of predominantly neuropathic origin. Results from a general population survey. J Pain 7:281-289.

Totoiu MO, Keirstead HS (2005) Spinal cord injury is accompanied by chronic progressive demyelination. J Comp Neurol 486:373-383.

Traub RJ, Mendell LM (1988) The spinal projection of individual identified A-delta- and C-fibers. J Neurophysiol 59:41-55.

Traub RJ, Solodkin A, Ruda MA (1989) Calcitonin gene-related peptide immunoreactivity in the cat lumbosacral spinal cord and the effects of multiple dorsal rhizotomies. J Comp Neurol 287:225-237.

Trivedi A, Olivas AD, Noble-Haeusslein LJ (2006) Inflammation and Spinal Cord Injury: Infiltrating Leukocytes as Determinants of Injury and Repair Processes. Clin Neurosci Res 6:283-292.

Tsitsopoulos PD, Tsonidis CA, Tsoleka KD, Tavridis GN (1995) The effect of radicular arteries ligation on the spinal cord blood supply in cats. Br J Neurosurg 9:227-232.

Tsuda M, Inoue K (2007) [Neuropathic pain and ATP receptors in spinal microglia]. Brain Nerve 59:953-959.

Tsuda M, Inoue K, Salter MW (2005) Neuropathic pain and spinal microglia: a big problem from molecules in "small" glia. Trends Neurosci 28:101-107.

Tsuda M, Kuboyama K, Inoue T, Nagata K, Tozaki-Saitoh H, Inoue K (2009) Behavioral phenotypes of mice lacking purinergic P2X4 receptors in acute and chronic pain assays. Mol Pain 5:28.

Tsuda M, Shigemoto-Mogami Y, Koizumi S, Mizokoshi A, Kohsaka S, Salter MW, Inoue K (2003) P2X4 receptors induced in spinal microglia gate tactile allodynia after nerve injury. Nature 424:778-783.

Tsuda M, Ueno H, Kataoka A, Tozaki-Saitoh H, Inoue K (2008) Activation of dorsal horn microglia contributes to diabetes-induced tactile allodynia via extracellular signal-regulated protein kinase signaling. Glia 56:378-386.

Tsuji M, Wilson MA, Lange MS, Johnston MV (2004) Minocycline worsens hypoxic-ischemic brain injury in a neonatal mouse model. Exp Neurol 189:58-65.

Tsujino H, Kondo E, Fukuoka T, Dai Y, Tokunaga A, Miki K, Yonenobu K, Ochi T, Noguchi K (2000) Activating transcription factor 3 (ATF3) induction by axotomy in sensory and motoneurons: A novel neuronal marker of nerve injury. Mol Cell Neurosci 15:170-182.

Tubbs RS, Golden B, Doyle S, Grabb PA, Oakes WJ (2006) Lap-belt injury with complete avulsion of the spinal cord and cauda equina. Clin Anat 19:665-668.

Tung TH, Martin DZ, Novak CB, Lauryssen C, Mackinnon SE (2005) Nerve reconstruction in lumbosacral plexopathy. Case report and review of the literature. J Neurosurg 102:86-91.

Uetani M, Hayashi K, Hashmi R, Nakahara N, Aso N, Ito N (1997) Traction injuries of the brachial plexus: signal intensity changes of the posterior cervical paraspinal muscles on MRI. J Comput Assist Tomogr 21:790-795.

Ulmann L, Hatcher JP, Hughes JP, Chaumont S, Green PJ, Conquet F, Buell GN, Reeve AJ, Chessell IP, Rassendren F (2008) Up-regulation of P2X4 receptors in spinal microglia after peripheral nerve injury mediates BDNF release and neuropathic pain. J Neurosci 28:11263-11268.

Vaculin S, Franek M, Andrey L, Rokyta R (2005) Self-mutilation in young rats after dorsal rhizotomy. Neuro Endocrinol Lett 26:25-28.

Valentine GW, Sanacora G (2009) Targeting glial physiology and glutamate cycling in the treatment of depression. Biochem Pharmacol 78:431-439.

Vargas ME, Barres BA (2007) Why is Wallerian degeneration in the CNS so slow? Annu Rev Neurosci 30:153-179.

Verma P, Chierzi S, Codd AM, Campbell DS, Meyer RL, Holt CE, Fawcett JW (2005) Axonal protein synthesis and degradation are necessary for efficient growth cone regeneration. J Neurosci 25:331-342.

Verma S, Estanislao L, Mintz L, Simpson D (2004) Controlling neuropathic pain in HIV. Curr HIV /AIDS Rep 1:136-141.

Vestergaard S, Tandrup T, Jakobsen J (1997) Effect of permanent axotomy on number and volume of dorsal root ganglion cell bodies. J Comp Neurol 388:307-312.

Veves A, Backonja M, Malik RA (2008) Painful diabetic neuropathy: epidemiology, natural history, early diagnosis, and treatment options. Pain Med 9:660-674.

Vierck CJ, Jr., Light AR (2000) Allodynia and hyperalgesia within dermatomes caudal to a spinal cord injury in primates and rodents. Prog Brain Res 129:411-428.

Vikman K, Robertson B, Grant G, Liljeborg A, Kristensson K (1998) Interferon-gamma receptors are expressed at synapses in the rat superficial dorsal horn and lateral spinal nucleus. J Neurocytol 27:749-759.

Vikman KS, Hill RH, Backstrom E, Robertson B, Kristensson K (2003) Interferon-gamma induces characteristics of central sensitization in spinal dorsal horn neurons in vitro. Pain 106:241-251.

Viscomi MT, Latini L, Florenzano F, Bernardi G, Molinari M (2008) Minocycline attenuates microglial activation but fails to mitigate degeneration in inferior olive and pontine nuclei after focal cerebellar lesion. Cerebellum 7:401-405.

Vissers K, De Jongh R, Hoffmann V, Heylen R, Crul B, Meert T (2003) Internal and External Factors Affecting the Development of Neuropathic Pain in Rodents. Is It All About Pain? Pain Practice 3:326-342.

Vizzard MA (1997) Increased expression of neuronal nitric oxide synthase in bladder afferent and spinal neurons following spinal cord injury. Dev Neurosci 19:232-246.

Vos BP, Strassman AM, Maciewicz RJ (1994) Behavioral evidence of trigeminal neuropathic pain following chronic constriction injury to the rat's infraorbital nerve. J Neurosci 14:2708-2723.

Wakisaka S, Kajander KC, Bennett GJ (1991) Increased neuropeptide Y (NPY)-like immunoreactivity in rat sensory neurons following peripheral axotomy. Neurosci Lett 124:200-203.

Wall PD, Devor M, Inbal R, Scadding JW, Schonfeld D, Seltzer Z, Tomkiewicz MM (1979) Autotomy following peripheral nerve lesions: experimental anaesthesia dolorosa. Pain 7:103-111.

Wang JH, Redmond HP, Watson RW, Duggan S, McCarthy J, Barry M, Bouchier-Hayes D (1996) Mechanisms involved in the induction of human endothelial cell necrosis. Cell Immunol 168:91-99.

Wang SD, Goldberger ME, Murray M (1991) Plasticity of spinal systems after unilateral lumbosacral dorsal rhizotomy in the adult rat. J Comp Neurol 304:555-568.

Wang W, Wang W, Mei X, Huang J, Wei Y, Wang Y, Wu S, Li Y (2009) Crosstalk between spinal astrocytes and neurons in nerve injury-induced neuropathic pain. PLoS One 4:e6973.

Wasserman JK, Schlichter LC (2007) Neuron death and inflammation in a rat model of intracerebral hemorrhage: effects of delayed minocycline treatment. Brain Res 1136:208-218.

Watanabe T, Yamamoto T, Abe Y, Saito N, Kumagai T, Kayama H (1999) Differential activation of microglia after experimental spinal cord injury. J Neurotrauma 16:255-265.

Watanabe Y, Saito H, Abe K (1993) Tricyclic antidepressants block NMDA receptor-mediated synaptic responses and induction of long-term potentiation in rat hippocampal slices. Neuropharmacology 32:479-486.

Watkins LR, Maier SF (2003) Glia: a novel drug discovery target for clinical pain. Nat Rev Drug Discov 2:973-985.

Watkins LR, Milligan ED, Maier SF (2001) Glial activation: a driving force for pathological pain. Trends Neurosci 24:450-455.

Watson RW, Redmond HP, Wang JH, Condron C, Bouchier-Hayes D (1996) Neutrophils undergo apoptosis following ingestion of Escherichia coli. J Immunol 156:3986-3992.

Waxman SG, Kocsis JD, Black JA (1994) Type III sodium channel mRNA is expressed in embryonic but not adult spinal sensory neurons, and is reexpressed following axotomy. J Neurophysiol 72:466-470.

Wells JE, Hurlbert RJ, Fehlings MG, Yong VW (2003) Neuroprotection by minocycline facilitates significant recovery from spinal cord injury in mice. Brain 126:1628-1637.

Weng YC, Kriz J (2007) Differential neuroprotective effects of a minocycline-based drug cocktail in transient and permanent focal cerebral ischemia. Exp Neurol 204:433-442.

White JC, Sweet WH (1969) Pain and the neurosurgeon
a forty-year experience. Springfield, Ill: C. C. Thomas.

Wiesenfeld-Hallin Z, Xu X, Crawley J, Hokfelt T (2005) Galanin and spinal nociceptive mechanisms: recent results from transgenic and knock-out models. Neuropeptides 39:207-210.

Wiley RG, Lemons LL, Kline RH (2009) Neuropeptide Y receptor-expressing dorsal horn neurons: role in nocifensive reflex responses to heat and formalin. Neuroscience 161:139-147.

Willenbring S, DeLeo JA, Coombs DW (1994) Differential behavioral outcomes in the sciatic cryoneurolysis model of neuropathic pain in rats. Pain 58:135-140.

Willis WD, Coggeshall RE (1991) Sensory mechanisms of the spinal cord. New York: Plenum Press.

Willis WD, Westlund KN (1997) Neuroanatomy of the pain system and of the pathways that modulate pain. J Clin Neurophysiol 14:2-31.

Winkelstein BA, DeLeo JA (2002) Nerve root injury severity differentially modulates spinal glial activation in a rat lumbar radiculopathy model: considerations for persistent pain. Brain Res 956:294-301.

Winkelstein BA, Rutkowski MD, Sweitzer SM, Pahl JL, DeLeo JA (2001a) Nerve injury proximal or distal to the DRG induces similar spinal glial activation and selective cytokine expression but differential behavioral responses to pharmacologic treatment. J Comp Neurol 439:127-139.

Winkelstein BA, Rutkowski MD, Weinstein JN, DeLeo JA (2001b) Quantification of neural tissue injury in a rat radiculopathy model: comparison of local deformation, behavioral outcomes, and spinal cytokine mRNA for two surgeons. J Neurosci Methods 111:49-57.

Wirkner K, Sperlagh B, Illes P (2007) P2X3 receptor involvement in pain states. Mol Neurobiol 36:165-183.

Woda A, Pionchon P (1999) A unified concept of idiopathic orofacial pain: clinical features. J Orofac Pain 13:172-184.

Wokke J (1996) Riluzole. Lancet 348:795-799.

Woodham P, Anderson PN, Nadim W, Turmaine M (1989) Satellite cells surrounding axotomised rat dorsal root ganglion cells increase expression of a GFAP-like protein. Neurosci Lett 98:8-12.

Woolf CJ (1983) C-primary afferent fibre mediated inhibitions in the dorsal horn of the decerebrate-spinal rat. Exp Brain Res 51:283-290.

Woolf CJ (2004) Dissecting out mechanisms responsible for peripheral neuropathic pain: implications for diagnosis and therapy. Life Sci 74:2605-2610.

Woolf CJ, Fitzgerald M (1986) Somatotopic organization of cutaneous afferent terminals and dorsal horn neuronal receptive fields in the superficial and deep laminae of the rat lumbar spinal cord. J Comp Neurol 251:517-531.

Woolf CJ, Shortland P, Coggeshall RE (1992) Peripheral nerve injury triggers central sprouting of myelinated afferents. Nature 355:75-78.

Woolf CJ, Wall PD (1982) Chronic peripheral nerve section diminishes the primary afferent A-fibre mediated inhibition of rat dorsal horn neurones. Brain Res 242:77-85.

Wroblewski R, Roomans GM, Kozlova EN (2000) Effects of dorsal root transection on morphology and chemical composition of degenerating nerve fibers and reactive astrocytes in the dorsal funiculus. Exp Neurol 164:236-245.

Wu G, Ringkamp M, Hartke TV, Murinson BB, Campbell JN, Griffin JW, Meyer RA (2001) Early onset of spontaneous activity in uninjured C-fiber nociceptors after injury to neighboring nerve fibers. J Neurosci 21:RC140.

Wu G, Ringkamp M, Murinson BB, Pogatzki EM, Hartke TV, Weerahandi HM, Campbell JN, Griffin JW, Meyer RA (2002) Degeneration of myelinated efferent fibers induces spontaneous activity in uninjured C-fiber afferents. J Neurosci 22:7746-7753.

Wu W (1993) Expression of nitric-oxide synthase (NOS) in injured CNS neurons as shown by NADPH diaphorase histochemistry. Exp Neurol 120:153-159.

Wu W, Li L (1993) Inhibition of nitric oxide synthase reduces motoneuron death due to spinal root avulsion. Neurosci Lett 153:121-124.

Wu W, Li L, Yick LW, Chai H, Xie Y, Yang Y, Prevette DM, Oppenheim RW (2003) GDNF and BDNF alter the expression of neuronal NOS, c-Jun, and p75 and prevent motoneuron death following spinal root avulsion in adult rats. J Neurotrauma 20:603-612.

Xie W, Strong JA, Zhang JM (2009) Early blockade of injured primary sensory afferents reduces glial cell activation in two rat neuropathic pain models. Neuroscience 160:847-857.

Xin WJ, Weng HR, Dougherty PM (2009) Plasticity in expression of the glutamate transporters GLT-1 and GLAST in spinal dorsal horn glial cells following partial sciatic nerve ligation. Mol Pain 5:15.

Yaguchi M, Ohta S, Toyama Y, Kawakami Y, Toda M (2008) Functional recovery after spinal cord injury in mice through activation of microglia and dendritic cells after IL-12 administration. J Neurosci Res 86:1972-1980.

Yan P, Liu N, Kim GM, Xu J, Xu J, Li Q, Hsu CY, Xu XM (2003) Expression of the type 1 and type 2 receptors for tumor necrosis factor after traumatic spinal cord injury in adult rats. Exp Neurol 183:286-297.

Yang L, Sugama S, Chirichigno JW, Gregorio J, Lorenzl S, Shin DH, Browne SE, Shimizu Y, Joh TH, Beal MF, Albers DS (2003) Minocycline enhances MPTP toxicity to dopaminergic neurons. J Neurosci Res 74:278-285.

Yezierski RP, Liu S, Ruenes GL, Kajander KJ, Brewer KL (1998) Excitotoxic spinal cord injury: behavioral and morphological characteristics of a central pain model. Pain 75:141-155.

Yip D, Le MN, Chan JL, Lee JH, Mehnert JA, Yudd A, Kempf J, Shih WJ, Chen S, Goydos JS (2009) A phase 0 trial of riluzole in patients with resectable stage III and IV melanoma. Clin Cancer Res 15:3896-3902.

Yiu G, He Z (2006) Glial inhibition of CNS axon regeneration. Nat Rev Neurosci 7:617-627.

Yoon YW, Na HS, Chung JM (1996) Contributions of injured and intact afferents to neuropathic pain in an experimental rat model. Pain 64:27-36.

Yrjanheikki J, Keinanen R, Pellikka M, Hokfelt T, Koistinaho J (1998) Tetracyclines inhibit microglial activation and are neuroprotective in global brain ischemia. Proc Natl Acad Sci U S A 95:15769-15774.

Yrjanheikki J, Tikka T, Keinanen R, Goldsteins G, Chan PH, Koistinaho J (1999) A tetracycline derivative, minocycline, reduces inflammation and protects against focal cerebral ischemia with a wide therapeutic window. Proc Natl Acad Sci U S A 96:13496-13500.

Yune TY, Lee JY, Jung GY, Kim SJ, Jiang MH, Kim YC, Oh YJ, Markelonis GJ, Oh TH (2007) Minocycline alleviates death of oligodendrocytes by inhibiting pro-nerve growth factor production in microglia after spinal cord injury. J Neurosci 27:7751-7761.

Zajac JM, Lombard MC, Peschanski M, Besson JM, Roques BP (1989) Autoradiographic study of mu and delta opioid binding sites and neutral endopeptidase-24.11 in rat after dorsal root rhizotomy. Brain Res 477:400-403.

Zhang B, Goldberger ME, Murray M (1993) Proliferation of SP- and 5HT-containing terminals in lamina II of rat spinal cord following dorsal rhizotomy: quantitative EM-immunocytochemical studies. Exp Neurol 123:51-63.

Zhang B, Goldberger ME, Wu LF, Murray M (1995) Plasticity of complex terminals in lamina II in partially deafferented spinal cord: the cat spared root preparation. Exp Neurol 132:186-193.

Zhang H, Mei X, Zhang P, Ma C, White FA, Donnelly DF, Lamotte RH (2009) Altered functional properties of satellite glial cells in compressed spinal ganglia. Glia 57:1588-1599.

Zhang J, De KY (2006) Spatial and temporal relationship between monocyte chemoattractant protein-1 expression and spinal glial activation following peripheral nerve injury. J Neurochem 97:772-783.

Zhang R, Gascon R, Miller RG, Gelinas DF, Mass J, Lancero M, Narvaez A, McGrath MS (2006) MCP-1 chemokine receptor CCR2 is decreased on circulating monocytes in sporadic amyotrophic lateral sclerosis (sALS). J Neuroimmunol 179:87-93.

Zhang XH, Li YJ, Hu YS, Tao W, Zheng Z (2008) Dorsal root entry zone coagulation for treatment of deafferentation pain syndromes. Chin Med J (Engl) 121:1089-1092.

Zhang Z, Nonaka H, Nagayama T, Hatori T, Ihara F, Zhang L, Akima M (2001) Circulatory disturbance of rat spinal cord induced by occluding ligation of the dorsal spinal vein. Acta Neuropathol 102:335-338.

Zhao P, Waxman SG, Hains BC (2007) Extracellular signal-regulated kinase-regulated microglia-neuron signaling by prostaglandin E2 contributes to pain after spinal cord injury. J Neurosci 27:2357-2368.

Zhao S, Pang Y, Beuerman RW, Thompson HW, Kline DG (1998) Expression of c-Fos protein in the spinal cord after brachial plexus injury: comparison of root avulsion and distal nerve transection. Neurosurgery 42:1357-1362.

Zheng J, Zhang P, Toews M, Hexum TD (1997) Neuropeptide Y enhances ATP-induced formation of inositol phosphates in chromaffin cells. Biochem Biophys Res Commun 239:287-290.

Zhou LH, Wu W (2006) Survival of injured spinal motoneurons in adult rat upon treatment with glial cell line-derived neurotrophic factor at 2 weeks but not at 4 weeks after root avulsion. J Neurotrauma 23:920-927.

Zhou X, Yang JW, Zhang W, Ou KQ, Zhou HL, Ma YQ, Chen SX, Li LY, Wang TH (2009) Role of NGF in spared DRG following partial dorsal rhizotomy in cats. Neuropeptides 43:363-369.

Zhou XF, Rush RA (1996) Endogenous brain-derived neurotrophic factor is anterogradely transported in primary sensory neurons. Neuroscience 74:945-953.

Zhou XF, Rush RA, McLachlan EM (1996) Differential expression of the p75 nerve growth factor receptor in glia and neurons of the rat dorsal root ganglia after peripheral nerve transection. J Neurosci 16:2901-2911.

Zhuang ZY, Gerner P, Woolf CJ, Ji RR (2005) ERK is sequentially activated in neurons, microglia, and astrocytes by spinal nerve ligation and contributes to mechanical allodynia in this neuropathic pain model. Pain 114:149-159.

Zimmermann M (2001) Pathobiology of neuropathic pain. Eur J Pharmacol 429:23-37.